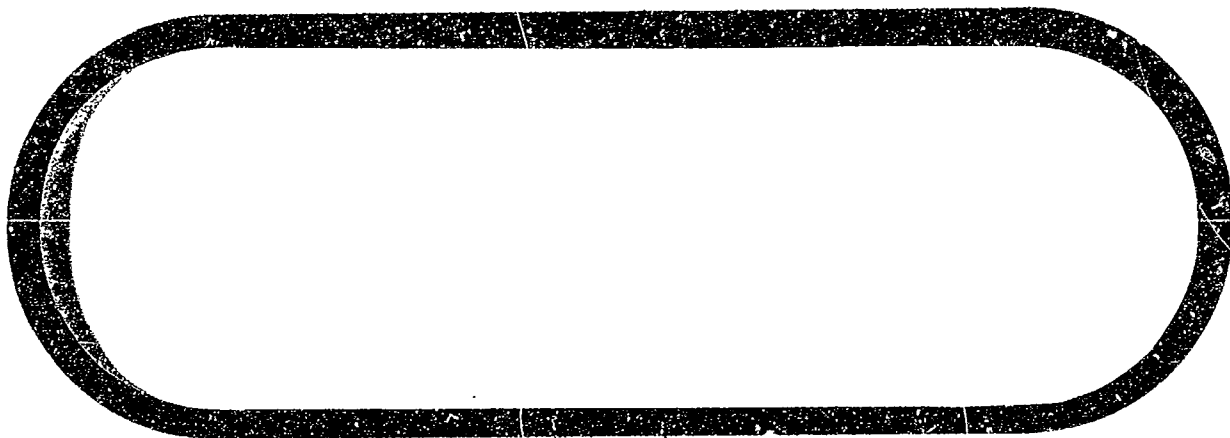


BOEING



FACILITY FORM 602

N66 26689
(ACCESSION NUMBER)
387
(PAGES)
CR-66047
(NASA CR OR TMX OR AD NUMBER)

(THRU)
1
(CODE)
31
(CATEGORY)

GPO PRICE \$ _____

CFSTI PRICE(S) \$ _____

Hard copy (HC) 7.00

Microfiche (MF) 2.00

ff 653 July 65

SEATTLE, WASHINGTON

Rd 35280

THE **BOEING** COMPANY

CODE IDENT. NO. 81205

DOCUMENT NO. D2-84042-1

TITLE. A SYSTEM STUDY OF A MANNED ORBITAL TELESCOPE

MODEL _____ CONTRACT NO. NAS-1-3968

ISSUE NO.

ISSUED TO

SEE DISTRIBUTION LIMITATIONS PAGE

PREPARED BY Aerospace Group

SUPERVISED BY *N. J. Bogdanoff* 11-12-65
David Bogdanoff

APPROVED BY _____

APPROVED BY _____

APPROVED BY _____

BOEING

NO. D2-84042-1

SH. 1

ACTIVE PAGE RECORD

SECTION	ORIG REL PAGE NO.	REV SYM	ADDED PAGES				SECTION	ORIG REL PAGE NO.	REV SYM	ADDED PAGES				REV SYM
			PAGE NO.	REV SYM	PAGE NO.	REV SYM				PAGE NO.	REV SYM	PAGE NO.	REV SYM	
	1							42						
	2							43						
	3							44						
	4							45						
	5							46						
	6							47						
	7							48						
	8							49						
	9							50						
	10							51						
	11							52						
	12							53						
	13							54						
	14							55						
	15							56						
	16							57						
	17							58						
	18							59						
	19							60						
	20							61						
	21							62						
	22							63						
	23							64						
	24							65						
	25							66						
	26							67						
	27							68						
	28							69						
	29							70						
	30							71						
	31							72						
	32							73						
	33							74						
	34							75						
	35							76						
	36							77						
	37							78						
	38							79						
	39							80						
	40							81						
	41							82						

BOEING

REV SYM _____

NO. D2-84042-1

SECT _____

PAGE 11

ACTIVE PAGE RECORD													
SECTION	ORIG REL PAGE NO.	REV SYM	ADDED PAGES				SECTION	ORIG REL PAGE NO.	REV SYM	ADDED PAGES			
			PAGE NO.	REV SYM	PAGE NO.	REV SYM				PAGE NO.	REV SYM	PAGE NO.	REV SYM
	83							124					
	84							125					
	85							126					
	86							127					
	87							128					
	88							129					
	89							130					
	90							131					
	91							132					
	92							133					
	93							134					
	94							135					
	95							136					
	96							137					
	97							138					
	98							139					
	99							140					
	100							141					
	101							142					
	102							143					
	103							144					
	104							145					
	105							146					
	106							147					
	107							148					
	108							149					
	109							150					
	110							151					
	111							152					
	112							153					
	113							154					
	114							155					
	115							156					
	116							157					
	117							158					
	118							159					
	119							160					
	120							161					
	121							162					
	122							163					
	123							164					

REV SYM _____

BOEING

NO. D2-84042-1
SECT PAGE 111

ACTIVE PAGE RECORD

SECTION	ORIG REL PAGE NO.	REV SYM	ADDED PAGES			SECTION	ORIG REL PAGE NO.	REV SYM	ADDED PAGES			SECTION	ORIG REL PAGE NO.	REV SYM
			PAGE NO.	REV SYM	PAGE NO.				PAGE NO.	REV SYM	PAGE NO.			
	165						206							
	166						207							
	167						208							
	168						209							
	169						210							
	170						211							
	171						212							
	172						213							
	173						214							
	174						215							
	175						216							
	176						217							
	177						218							
	178						219							
	179						220							
	180						221							
	181						222							
	182						223							
	183						224							
	184						225							
	185						226							
	186						227							
	187						228							
	188						229							
	189						230							
	190						231							
	191						232							
	192						233							
	193						234							
	194						235							
	195						236							
	196						237							
	197						238							
	198						239							
	199						240							
	200						241							
	201						242							
	202						243							
	203						244							
	204						245							
	205						246							

BOEING

NO.

D2-84042-1

SECT

PAGE

1v

REV SYM

ACTIVE PAGE RECORD

SECTION	ORIG REL PAGE NO.	REV SYM	ADDED PAGES				SECTION	ORIG REL PAGE NO.	REV SYM	ADDED PAGES			
			PAGE NO.	REV SYM	PAGE NO.	REV SYM				PAGE NO.	REV SYM	PAGE NO.	REV SYM
	247							288					
	248							289					
	249							290					
	250							291					
	251							292					
	252							293					
	253							294					
	254							295					
	255							296					
	256							297					
	257							298					
	258							299					
	259							300					
	260							301					
	261							302					
	262							303					
	263							304					
	264							305					
	265							306					
	266							307					
	267							308					
	268							309					
	269							310					
	270							311					
	271							312					
	272							313					
	273							314					
	274							315					
	275							316					
	276							317					
	277							318					
	278							319					
	279							320					
	280							321					
	281							322					
	282							323					
	283							324					
	284							325					
	285							326					
	286							327					
	287							328					

BOEING

NO. D2-84042-1

REV SYM _____

SECT. PAGE v

ACTIVE PAGE RECORD

SECTION	ORIG REL PAGE NO.	REV SYM	ADDED PAGES				SECTION	ORIG REL PAGE NO.	REV SYM	ADDED PAGES			
			PAGE NO.	REV SYM	PAGE NO.	REV SYM				PAGE NO.	REV SYM	PAGE NO.	REV SYM
	329							370					
	330							371					
	331							372					
	332							373					
	333							374					
	334							375					
	335												
	336												
	337												
	338												
	339												
	340												
	341												
	342												
	343												
	344												
	345												
	346												
	347												
	348												
	349												
	350												
	351												
	352												
	353												
	354												
	355												
	356												
	357												
	358												
	359												
	360												
	361												
	362												
	363												
	364												
	365												
	366												
	367												
	368												
	369												

BOEING

NO.

D2-84042-1

REV SYM _____

SECT

PAGE vi

[illegible]

2-5142-2

BOEING | NO. D2-84042-1

ABSTRACT

The broad objective of the overall NASA program of investigation is to establish the feasibility of designing, fabricating, launching, and operating a manned astronomical observatory. Within this framework the specific objectives of the systems study of a Manned Orbital Telescope are to:

- Investigate the possible operational modes of such an observatory with special emphasis on the way in which man will be used to support the observatory;
- Accomplish the necessary engineering studies, analyses, design, and planning required to select the best operational mode and observatory design;
- Indicate areas of technology where state-of-the-art advances are necessary

KEY WORDS

Manned Orbital Telescope (MOT)

Manned Orbital Research Laboratory (MORL)

Diffraction Limited Optics

Telescope Thermal Analysis

Orbital Optics Structures

Cassegrainian Telescope

Orbital Telescope Operations

Orbital Telescope Attitude Control and Stability

USE FOR TYPEWRITTEN MATERIAL ONLY

**A SYSTEM STUDY OF A
MANNED ORBITAL TELESCOPE**

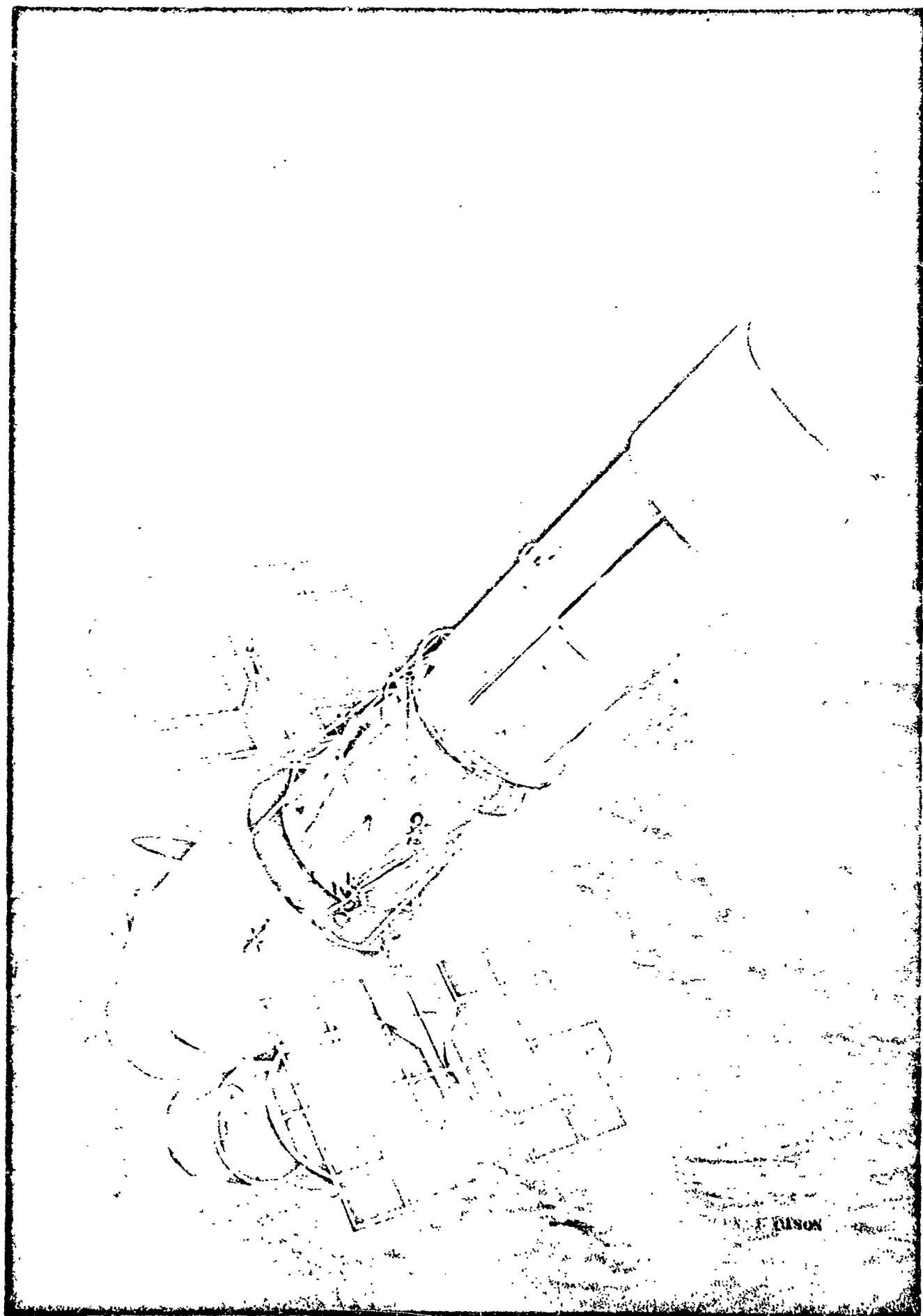
D2-840-12-1

October, 1965

**Prepared for
National Aeronautics and Space Administration
Langley Research Center
Hampton, Virginia**

**Under Contract
NAS1-3968**

**Prepared by
Aerospace Group
THE BOEING COMPANY
Seattle, Washington**



CONTENTS

	<u>Page</u>
1.0 INTRODUCTION	1
2.0 SUMMARY	5
3.0 ASTRONOMY AND OPTICS	9
3.1 APPROACH	10
3.2 Discussion of Astronomical Studies	13
3.3 Definition of observation Requirements	19
3.4 Telescope Optics	19
3.5 Definition of Instrumentation and Systems Performance	27
3.6 Problem Areas	50
3.7 Discussion of Results	59
4.0 OPERATIONAL ANALYSIS	63
4.1 Basic Telescope Concept	63
4.2 Approach and Study Development	67
4.3 Operational Description of the Two Final Modes	71
4.4 Timeline Analysis	88
4.5 Definition of Logistics Requirements	96
4.6 Definition of Shuttle Requirements	98
4.7 Crew Requirements	99
4.8 Evaluation of Two Final Concepts	101
4.9 Summary of Problem Areas	112
5.0 DESIGN AND SUBSYSTEM INTEGRATION	113
5.1 Approach and Design Development	113
5.2 Configurations	114
5.3 Structures	168
5.4 Attitude Control	240

CONTENTS (Cont.)

5.5 Thermal Control	<u>Page</u> 330
5.6 Other Subsystems	356
6.0 BIBLIOGRAPHY	375

1.0 INTRODUCTION

Previous NASA studies have made it apparent that one of the principal reasons for developing a manned orbital space station is the opportunity to perform astronomical observations of a scope far beyond anything possible from the ground or with unmanned systems such as the OAO. The capabilities of such an orbital observatory, as compared with ground-based telescopes, form an important part of the background of such a study. These capabilities are illustrated in Figure 1-1. The main limitation for spectrographic, photoelectric, and thermoelectric work is the presence of the atmosphere which acts as a filter for all but some narrow bands (in the visible and IR ranges) in the frequency spectrum to be covered by the MOT. This range has been assumed to be from the Lyman limit (912 Å) to approximately one millimeter. Astronomic work and planetary photographs in ground-based telescopes are restricted by the phenomenon of "seeing", which limits the average resolution to 1 second of arc or slightly better. In the case of the MOT, a performance very nearly approaching the full diffraction limit of 0.05 seconds of arc should be attainable.

NASA has instituted a broad program of investigation into the various problems associated with the performance of such observations. To explore experiments possible with such an observatory and to define its general design characteristics, a study was performed by Dr. L. W. Fredrick of the University of Virginia. In addition, a study was undertaken by the J. W. Pecker Division of the American Optical Company to establish, in a preliminary sense, the design feasibility of the telescope and a possible design configuration. These studies provided baselines in their respective areas for the present study.

The broad objective of the overall NASA program of investigation is to establish the feasibility of designing, fabricating, launching, and operating a manned astronomical observatory. Within this framework the specific objectives of the systems study of a Manned Orbital Telescope are to:

- Investigate the possible operational modes of such an observatory with special emphasis on the way in which man will be used to support the observatory;
- Accomplish the necessary engineering studies, analyses, design, and planning required to select the best operational mode and observatory design;
- Indicate areas of technology where state-of-the-art advances are necessary.

The study constraints and scope of the work are defined as follows:

- The telescope aperture is to be 120 inches and diffraction-limited performance for the basic optics at the midpoint of the visible light spectrum is required;
- The telescope is to be launched unmanned and is to rendezvous and operate in conjunction with the NASA MORL space station as defined by the Douglas MORL studies. A circular orbit of 250 NMi and 28.7° inclination is used;

FIGURE 1-1

OBSERVATION	COMPARISON	GROUND-BASED TELESCOPES	NOT
HIGH-DISPERSION SPECTRA VISIBLE & UV		VISIBLE SPECTRUM RANGE	LIMITED BY CUMULATIVE EXPOSURE TIME
LOW-DISPERSION SPECTRA		VISIBLE SPECTRUM RANGE	LIMITED BY CUMULATIVE EXPOSURE TIME
PHOTOELECTRIC PHOTOMETRY		VISIBLE SPECTRUM RANGE	<ul style="list-style-type: none"> • GREATER RESOLUTION • FAINTER SOURCES
PHOTOGRAPHIC, ASTROMETRIC, & ASTROPHYSICAL		LIMITED BY SEEING CONDITIONS (1 ARC SEC) AND ABSORPTION OF IR & UV	<ul style="list-style-type: none"> • ASTROMETRIC - 0.06 ARC SEC RESOLUTION • COMPLETE SPECTRUM
HIGH-DISPERSION IR SPECTRA		ONLY THROUGH NARROW WINDOWS (8 - 13 μ)	LIMITED ONLY BY EXPOSURE TIME
THERMOELECTRIC MEASUREMENTS		ONLY THROUGH NARROW WINDOWS (8 - 13 μ)	LIMITED ONLY BY SOURCE INTENSITY
PHOTOGRAPHIC (PLANETARY)		LIMITED BY SEEING CONDITIONS (1 ARC SEC OR SLIGHTLY BETTER)	0.06 ARC SEC RESOLUTION

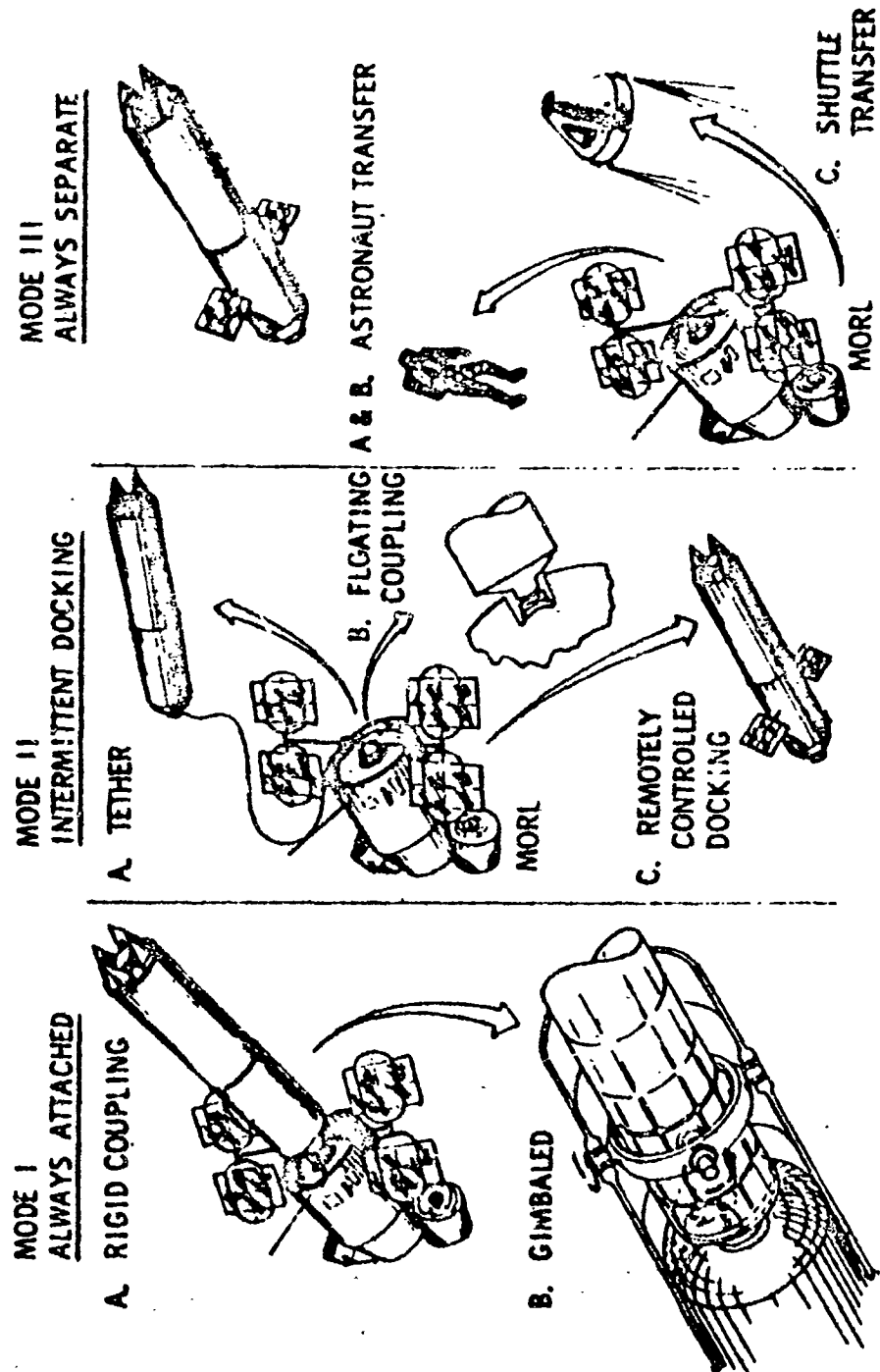
SCIENTIFIC CAPABILITY COMPARISON

- The scientific studies defined by Dr. Fredrick, with certain noted exceptions, are to form a basis for the scientific objectives of the MOT;
- Three basic modes of operation of the telescope that were considered are telescope docked and permanently coupled to the MORL, telescope coupled to the MORL for experiment setup but decoupled for operation, and telescope and laboratory completely decoupled;
- Special attention is to be given to selecting the best mode of operation, the role of man, structural configuration, attitude control & stabilization, and the thermal/optical problem;
- Indication is to be made of the areas where state-of-the-art advancement may be necessary;
- Sufficient design and operational analysis is to be accomplished to select the best mode of operation and to verify the design feasibility of the observatory.

The scientific objectives defined by NASA, and the development of an observational plan in sufficient detail to determine the optical system specification and the scientific instrumentation necessary to accomplish the program were reviewed. The study determined the types of scientific instrumentation, sizes, weights, performance, and problem areas. Layouts were made to determine an efficient arrangement for operating the scientific instruments and the supporting subsystems. This information, together with an analysis of thermal and structural problems, determined the basic telescope design. The attitude stability requirements dictated by the precision of the experimental data and the methods used in attaining this precision were used in synthesizing the attitude stabilization & control system. Three basic modes of operation were expanded into eight variants, as shown in Figure 1-2. These eight modes were evaluated against technical risk, operational capability, and MORL interface constraints and requirements prior to the midterm review. Mode IIB (Floating Socket) and a hybrid of Modes IIIC and IIC were selected for further study during the balance of the program. As a result of the midterm review, in which questions were raised concerning the technical risk associated with the floating socket, a soft gimbal mode (IC) was developed and substituted for the floating socket. The balance of the program was devoted to developing data for the definition and evaluation of these modes. Design concepts were finalized for these two modes, operational descriptions were developed, an evaluation of the attitude stability & control problems for the soft gimbal was made, and a final evaluation of these modes was performed.

Throughout the study, General Electric was retained as attitude stability & control subcontractor. In addition, the consultant services of Dr. Zdenek Kopal, Chairman of the Department of Astronomy of the University of Manchester (England) and Dr. James G. Baker of Harvard College Observatory were utilized in the fields of astronomy and optics.

FIGURE 1-2 MODES OF OPERATION



2.0 SUMMARY

Principal results of the study reported in this document are summarized in the following discussion:

Astronomy and Optics - A review was made of the astronomical studies in and beyond the solar system that would be performed by the MOT, which resulted in the conclusion that the advantages to astronomy would be inestimable. This review also established the planetary observation requirements in the fields of photography, thermoelectric measurements, and high dispersion IR spectroscopy as well as the stellar observation requirements in the fields of high and low dispersion spectroscopy, photometry, and photography.

The basic optical configuration selected was a Cassegrainian type with two alternate secondary mirrors and two flat folding mirrors. The two secondary mirrors permit operation of the telescope at $ef/15$ and $ef/30$. The Ritchey-Chretien modification of the pure Cassegrainian system was selected and an $f/4$ primary mirror was recommended. Tolerances for the positioning of the secondary with respect to the primary were computed. Scientific instruments to be used for the various experiments were defined and their performance requirements were established. These instruments would be mounted on a large platen in the MOT cabin and operated at $ef/15$ or $ef/30$ focal ratios. The results of the performance study indicated that the observation requirements of the MOT as determined from the review of the astronomical studies could be met. However, the telescope would not be diffraction limited unless problems of manufacture and control of the figure of the primary mirror to $\lambda/32$ at 5000 \AA can be met and an attitude stability of 0.01 seconds of arc can be achieved.

Operations Analysis - Significant problem areas concerning the role of man in the MOT operations were identified to compare the advantages and disadvantages of the various operational modes. Further evaluation included the comparison of man's ability to perform the necessary tasks and the comparisons of timeline analyses for each of the various modes. Much data was also generated in the area of technical risk, operational capability, and constraints on MORL to allow valid comparisons.

These studies narrowed the field of investigation in the latter half of the program to Mode IIID (a detached mode, capable of docking with MORL, but employing a shuttle for normal operations) and Mode IC (the soft gimbal mode, which is a closely-associated mode employing a soft suspension for the telescope gimbal axes). Operational descriptions for these modes were developed, together with a more detailed timeline analysis. Final evaluation of these modes indicated the soft gimbal mode to be preferred. Logistic and shuttle requirements were defined. The analysis indicated the telescope would be available for observation approximately 80 percent of the night hours.

Configurations - Through successive iterations telescope baseline design was developed, which incorporated all the optical elements, scientific instruments, and the associated structural support. Modifications were incorporated to satisfy the varying design requirements for the different operational modes considered.

Launch and orbital configurations for the two final modes of operation were developed. Scientific instrumentation and cabin arrangement for the MOT were defined. Special areas, such as the support of the primary mirror and the support and tolerance adjustment for the secondaries, were defined in greater detail. None of the design problems which could be identified at this level of detail were considered insurmountable or beyond feasible engineering solutions.

Structures - The primary structural design was based on the boost condition. Structural concepts and materials, however, were employed to optimize the four requirements of structural stiffness, thermal isolation, optical alignment, and stress level. Special investigations were made of primary mirror stresses during boost and docking, the dynamics of the soft gimbal mode, thermal distortions of the primary mirror during operation, and meteoroids and radiation.

Analysis of the primary mirror stresses indicated that large margins of safety exist during boost and in operation. Investigation of the soft gimbal indicated that it is a feasible system. Thermal distortions of the primary mirror during telescope operation were analyzed and results indicated the RMS deviations of the mirror surface ($\lambda/36.3$ at 5000 \AA) could be achieved without active control, provided certain design and operational features were incorporated. Meteoroid damage posed no problem; however, the radiation investigation indicated that special precautions must be taken with sensitive film.

Attitude Stability and Control - The observational requirements were used to synthesize an attitude control system for the MOT. This system makes maximum utilization of the experience obtained from the OAO program and the advanced concepts resulting from it. Stellar reference would be acquired through a programmed roll search procedure, to establish the coarse pointing mode, in which attitude reference would be obtained from star trackers, and control torques. During coarse, intermediate, and fine pointing, the MOT would be controlled by torques generated by control moment gyros. The results of fine-pointing sensor study were incorporated into an overall performance evaluation which included the elastic response of the MOT bending modes of vibration. The study showed that it would be feasible to stabilize the telescope to within 0.01 seconds of arc. Examination of the soft gimbal concept indicated a pointing error of about 0.003 arc seconds greater than the detached mode, indicating a high degree of feasibility for this mode.

Thermal Analysis - Mirror temperature gradients were determined, using computerized thermal analysis technique, for the finite difference solution of time dependent heat transfer problems. Temperature gradients were determined in the telescope structure and in the primary and secondary mirrors. Three cases were examined; with the telescope axis normal to the solar vector, with the telescope axis parallel to the solar vector but pointing away from the Sun, and the transient case when the telescope attitude changes from parallel to perpendicular to the solar vector. Results indicated that no objectionable gradients would occur if the telescope doors were closed during the times which the telescope would be viewing Earth. These doors would have to be maintained in an isothermal environment; this would be accomplished by the employment of an earthshade.

General Conclusions and Recommendations - The general conclusions were that within the scope of the present investigation, the MOT would be a feasible system,

the soft gimbal operational concept would be preferred, and the following special problems would require further investigation; manufacture of the primary mirror and the investigation of its long term stability, attitude stability and control, and radiation protection of the more sensitive films.

The following actions were recommended: More thorough investigation and definition of the soft gimbal concept; breadboard fabrication of the fine-pointing sensors and control moment gyros; an investigation into problems associated with the design and fabrication of a large primary mirror; and institution of an intermediate sized telescope program to check out the feasibility of the solutions to the technological problem areas and to establish the role of man.

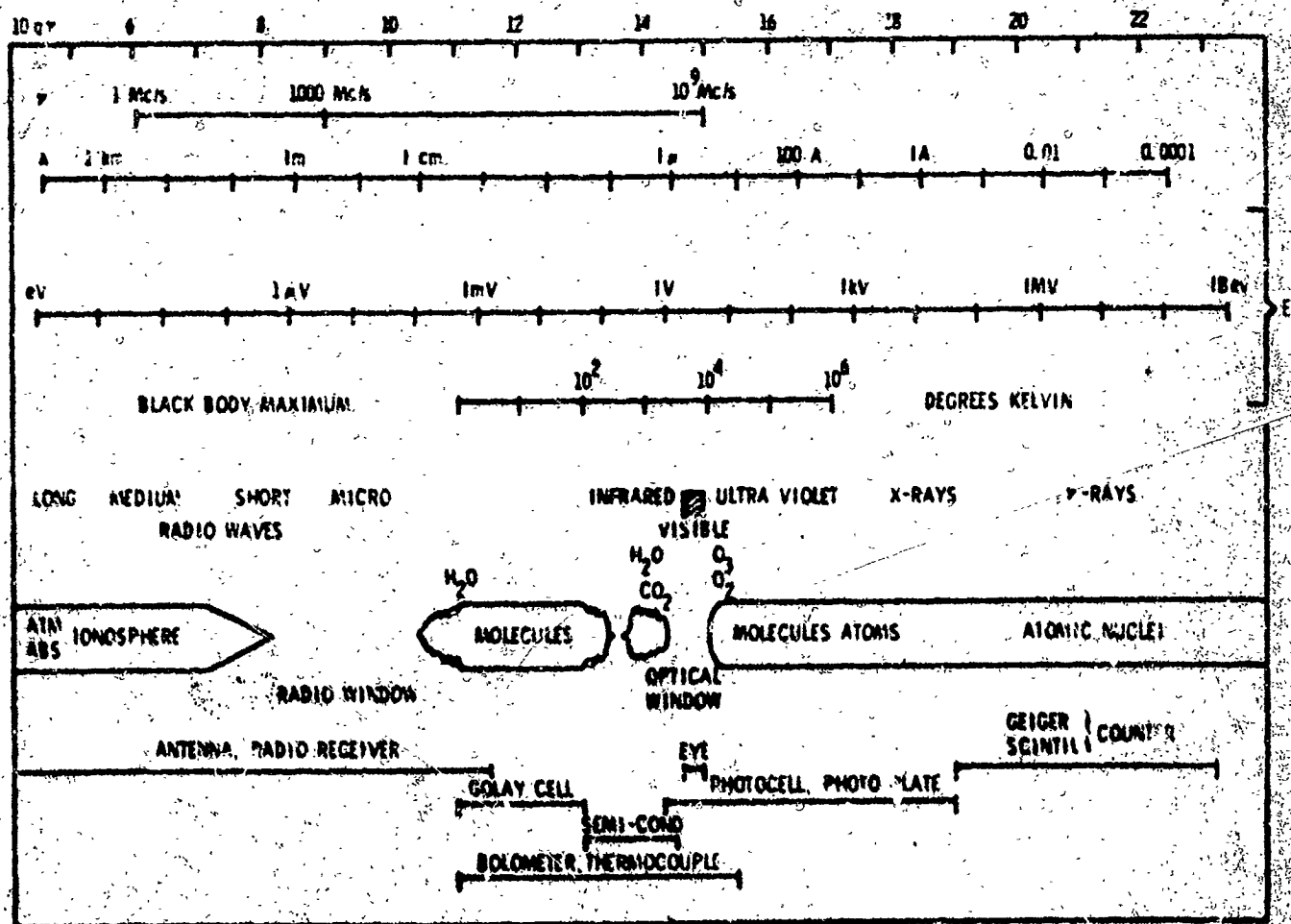
BLANK PAGE 8

3.0 ASTRONOMY & OPTICS

Astronomical advantages of operating a large telescope in space over similar ground-based operations are overwhelming, and are summarized as follows.

The bulk of astronomical observations have been restricted to the radio window extending from a wavelength of 1 cm to a few meters and the optical window from 0.3μ to 1μ . This restriction is due to the absorption of the atmosphere. Many astronomical studies involve the detection, identification, determination of the state of excitation or ionization, and the amounts of the elements constituting a celestial body. The state of excitation or ionization results in radiation characteristics observed by the astronomer. Figure 3-1 shows that the optical window corresponds to radiative energy levels of 1 to 10 eV. Many, but not all, of the atomic transitions occur in this region. In fact, the resonance lines of the very important elements of hydrogen and helium are in the far ultraviolet. On the other side of the optical window, the majority of the molecular transitions occur in the infrared. Likewise, the radiation from cool bodies, such as late-type stars, planets, and interstellar dust, is in the infrared. The radiation from the "hot" stars of the early-type A, B, and classifications emit in the ultraviolet, whereas the "middle-age" G and F type emit in the visible. Studies of all of these types are important in confirming the unified theories of the universe.

Figure 3 - 1: Relation of Energy Units and Detectors as a Function of Frequency



Refraction anomalies due to atmospheric turbulence, which are the reason for "bad seeing" experienced on the ground, would be absent, a fact which would limit the resolution attainable by spaceborne telescopes largely to the quality of their optics alone. On the ground, atmospheric conditions prevalent over most sites seldom allow the diffraction limit to be attained for apertures in excess of 12 to 15 inches; from space, this limit could probably be increased at least tenfold.

The virtual absence of any atmosphere above an orbiting telescope would also reduce considerably the residual sky brightness, and thus enable the observer to prolong the duration of useful exposures and increase the limiting stellar magnitude recorded on the plates. The exact amount of the gain arising from this source would depend on the mean altitude of the orbiting spacecraft; but it should come close to a factor two. Moreover, not only would the sky background, as seen from the orbiting telescope, be reduced by a factor of two, but fluctuations in the residual brightness (due, on the ground, to scintillation and auroral activities) would be also diminished; thus bringing the background noise down to the statistical noise of the detectors.

The absence of gravity aboard an orbiting vehicle would ease the problem of the control of the flexure of the optical surface of the primary mirror, as well as of the supporting structure designed to keep the entire optical system in alignment.

3.1 APPROACH

The approach taken in the MOT feasibility study was to develop very early in the program the astronomical observation requirements using the consulting services of Dr. Z. Kopal. The requirements were then used as guidelines in developing the telescope optics and the scientific instruments. As the study progressed, further iterations were performed using the works of Code and Fredrick and the consultant services of Dr. J. G. Baker. The object of these iterations was to arrive at operational and performance criteria that were as definitive as possible.

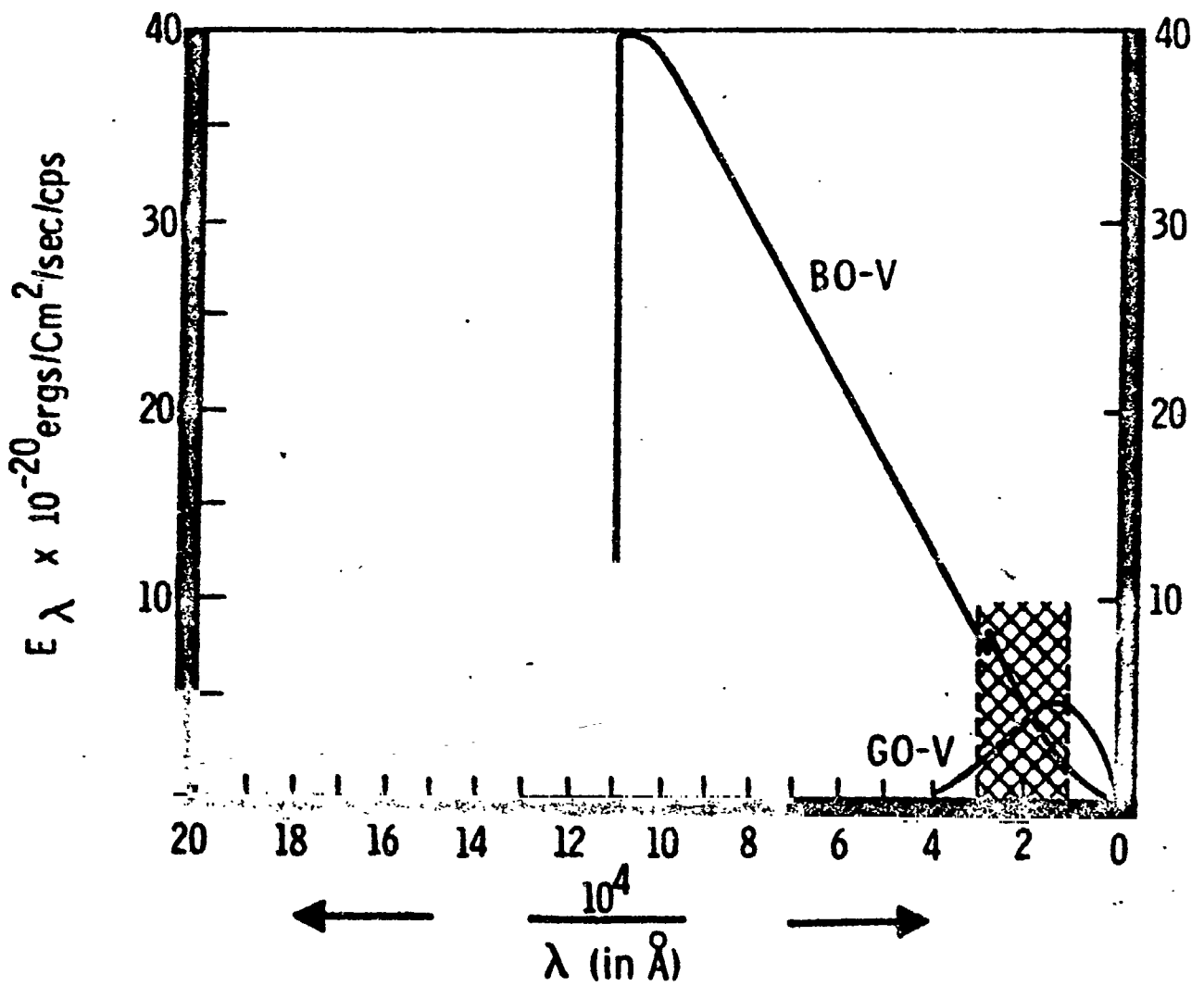
3.1.1 Selection of Research Studies

A review of astronomical research studies which either require the advantages of space astronomy or could greatly benefit from them indicate that the capabilities of the MOT must be very flexible. In addition, the MOT should be prepared to observe the unexpected, not only from the aspect of improved resolution, but also from its ability to observe all radiant. Many astronomical phenomena may be observed only from certain Earth-based observatories at present.

The MOT should be prepared to perform observations that may even appear at present to be overlapping those of the OAO programs. This would provide a good followup capability for studies utilizing OAO-acquired data.

At present, studies to determine the process of stellar evolution involve the use of a theoretical model of the atmospheres surrounding the stars. The early type B0 stars have their energy peaks in the ultraviolet. The only verification to the theoretical models of these stellar atmospheres has been as the result of measurement of the radiation transmitted through the Earth's atmosphere. Figure 3-2 illustrates

Figure 3 - 2: Energy Distribution for Bo and Go Stars



the small portion of the total radiation that is now measurable. Code also states that spectra line profile observations of the wings of the Lyman lines and the lines of such elements as NI at 1200 Å, OI at 1302 Å, CI at 1657 Å, and SiI at 2515 Å should be made for stellar evolution studies.

Also, spectra studies should be made of the resonance lines in the ultraviolet of hydrogen, helium, carbon, oxygen, and nitrogen.

On the other end of the spectrum, Code recommends the study of cool stars to obtain further data to fit into the stellar evolution puzzle. It is expected that cool stars should have an atmosphere containing H_2O and/or CO_2 . These would be detected by their infrared spectra studies.

In addition to those already mentioned, galactic nebulae and the stars within the nebulae will need further study to understand the evolution of the universe.

3.1.2 Selection of Astronomical Observations

From the observational point of view, priority should be given to those tasks which cannot be done from ground-based facilities. Some of these have already been mentioned in Section 3.0, i.e., those tasks which utilize the UV and IR regions of the spectrum. This does not mean that observations at wavelengths which are visible from ground should not be included in the MOT observational capability. The advantage of the MOT in superior resolution, limited by the aperture rather than "seeing", would justify including observations in the visual region of the spectrum.

3.1.3 Operational Criteria

The operational approach taken may be summarized as follows:

- 1) The major instruments will be permanently mounted on a common reference plate.
- 2) A change of observing instrument will be made by rotationally indexing a folding mirror.
- 3) The instrumentation will be arranged to permit observation of the same celestial body with different instruments using remote control.
- 4) Parametric changes in observations should be remotely controlled.
- 5) Critical alignment parameters should be remotely monitored, continuously or at will.
- 6) Man will not be in the instrumentation cabin during observations.

3.1.4 Performance Criteria

The principal technical advantage of the MOT should be the ability to perform at (or near) the diffraction limit for sustained periods. This capability should increase the resolving power approximately five to tenfold. Baker suggests a resolution threshold of 0.05 arc seconds for the MOT, compared to the best planetary results of 0.25 to 0.50 arc seconds for a ground-based telescope.

Not all tasks will require such high resolution. It would be quite superfluous for most aspects of nebular photography because of the poor definition of the objects themselves, or in some cases of photoelectric photometry of single light sources. On the other hand, astrometric or planetary photography and high dispersion spectra work require the highest resolution attainable.

3.2 DISCUSSION OF ASTRONOMICAL STUDIES

The opportunities for unique contributions to astronomical research, which could not be approached at all from the ground or could be done vastly better from space, would tax to capacity, not one, but several MOT's for many years to come. Limitations of space allow only a brief outline of tasks be enumerated. These will be developed primarily in accordance with the similarity of the objects of study (with their increasing distance in space), and secondly with respect to the similarity of study techniques.

3.2.1 Solar System Observations (Planets, Satellites, and Comets)

The objects of interest in the solar system (excepting, of course, the sun) can be classed in two groups; the planets and their satellites, characterized by continuous radiation and absorption spectra; and the comets (with weak continua and emission spectra). Important tasks to be undertaken by MOT should include lunar and planetary (high resolution) photography, photometry, and high dispersion spectroscopy.

Photography - To begin with the nearest natural celestial object, a diffraction-limited 120-inch MOT should resolve a linear separation of 93 meters at 5000 Å and 37 meters at 2000 Å on the Moon (at its mean distance from the Earth). Of the principal planets of the solar system, only Mercury will be permanently inaccessible to the MOT because of its close proximity to the sun. For Venus (observable by MOT for some time around maximum elongation), the theoretical resolution would be 15 Kms on its surface in the ultraviolet region, while for Mars, Jupiter, and Saturn, the corresponding resolutions at the time of their oppositions are 9, 86, and 176 Kms, respectively. Thermal problems rule out the observation of Venus. The extent of the limitation on this observation has not been determined to date.

Within the above limits, the MOT could be regarded as a very powerful camera for investigation of specific details on the surfaces of these celestial bodies. Transient diurnal (or seasonal) variations on their surfaces, as well as their atmospheres (such as cloud formations), could be studied. Planets surrounded by atmospheres which are optically thick (such as those of Jupiter, Saturn, Uranus, and Neptune) could be photographed through narrow-passband filters centered on their principal atmospheric absorption bands (NH_3 , CH_4). This type of data should furnish valuable insight into the stratification of different atmospheric constituents of these planets.

Photometry - One of the most important tasks in astrophysics of the solar system to be observed with the MOT should be photoelectric photometry and polarimetry of the occultations of planetary satellites during the eclipse stage. Unless the planet in question (Jupiter, Saturn) happens to be exactly in opposition, the ingress (or egress) of a satellite into (or from) the planet's shadow will occur at a certain

angular distance from the planet's limb. The disappearance (or reappearance) of the satellite during such an eclipse is not sudden, and is due to increasing extinction of illuminating sunlight which passes through progressively lower and denser atmospheric layer. Monochromatic light curves of such phenomena observed through filters centered at the principal atmospheric absorption bands could furnish very important data concerning the stratification of different molecules with altitude. Any variations in polarization of the reflected sunlight during the ingress or egress stage of the eclipse could add important information concerning solid particles (frozen crystals) which may be present at different layers.

Observational studies of this type cannot be successfully pursued from ground-based facilities, because such photometric measurements would be largely vitiated by the bright light of the nearby planetary disk scattered in the terrestrial atmosphere; nor could they be pursued in space with telescopes of much smaller aperture than that of the MOT.

Another task which falls in this category would be thermoelectric photometry of planetary or satellite heat radiation in the infrared, which could provide a more complete picture of diurnal as well as seasonal variations of the emitting surface. As the actual temperatures are generally low ($< 400^\circ\text{K}$ except for Mercury which will be inaccessible to MOT), thermal radiation of the planetary surfaces will not begin to emerge from the background of scattered sunlight until at wavelengths in excess of a few microns. The maxima of the Planckian emission of the surfaces of the major planets (from Jupiter to Neptune), or of the lunar night hemisphere, lie between 20-30 μ 's. Radiation at these wavelengths is almost entirely absorbed by our atmosphere (or incompletely transmitted through it in certain relatively narrow passbands); so that the MOT should again offer immeasurable advantages over ground-based possibilities. Its full aperture would be needed not only to collect enough energy to activate the detectors, but also to retain sufficient resolving power, since at wavelengths between 20-30 μ 's, the Rayleigh diffraction limit would be close to 0.08 inch. This would correspond to the diameters of the largest satellites of Jupiter or Saturn, to half the diameter of Neptune, or to about 1.5 miles on lunar ground at its average distance from the Earth.

Spectroscopy - Tasks in the area of planetary spectroscopy would be confined largely to the visible and infrared parts of the spectrum, because relatively little of major interest is to be expected in the UV, apart from possible fluorescent bands excited by solar activity, or such special problems as the backscattering of the solar Lyman α -radiation on planetary hydrogen "geocorona", in particular of Jupiter

Infrared spectroscopy should be concerned primarily with molecular bands. These are of interest in studies of the reflection spectra of Martian ice caps, with spectroscopic indications of the presence of organic molecules in seasonal spectra of Martian dark markings, or with a search for absorption spectra of the molecules of free radicals (NH_2 , CH_3 , etc.) in the atmospheres of major planets (primarily Jupiter), whose Zeeman splitting could reveal the presence and measure the strength of the planetary magnetic fields.

Cometary Observations - The inability to point the MOT close to the sun would largely restrict its use for the studies of cometary tails because these do not fully develop until at relatively short heliocentric distances. However, photometric as well as spectroscopic studies of transient phenomena exhibited by cometary nuclei and heads at heliocentric distances above about one astronomical unit, should receive an appropriate place in the observing program.

3.2.2 Stellar Observations

Photographic - The stellar photography which will be undertaken with the MOT can be technically divided into narrow field and wide field photography. Narrow field photography will be used largely for astrometric purposes, i.e., to obtain data for the measurement of stellar parallaxes and proper motions. Sustained investigations of the latter may, in turn, lead to discovery of faint companions of nearby stars from the nonlinearity of proper motions; or in case of resolvable close binaries, to determine the elements of their visual orbits. "Astrometric" binaries known to possess invisible companions are listed in Figure 3-3. The orbital period of most of the binaries listed is long in comparison to the lifetime of the MOT; hence, interest would be centered primarily on the discovery of binary systems of shorter periods. The scientific yield is greater when a larger portion of the period is observed. In determinations of stellar parallaxes, the fundamental period of observation is one year; so that valuable fundamental measurement of the distances of nearby stars could be accomplished even if the period of its activity was no longer than one year.

All astrometric work on close binaries, visual or unresolved, will pose certain problems which may require special treatment. On the ground, the principal limitation to resolution of objects, as seen through the atmosphere, is the difference in brightness and, by implication of masses, of the two components. In the sense observational selection operates strongly against the discovery of pairs in which the disparity in mass-ratio is large. In space, limits of discovery will be clearly given only by the resolution of overlapping diffraction patterns of point sources of light. For stars differing greatly in brightness, the problem will be to discern the first Airy's disk of the image of the weaker source through the diffraction pattern of the brighter component. Since the scale of the diffraction pattern is a linear function of the wavelength (for a given aperture), monochromatic photography through suitable filters can be employed to bring out any point of the region surrounding the bright star in between the latter's consecutive diffraction rings. Actually, the detection of faint companions to nearby stars will not come into its own until a telescope of the class of the MOT is in operation.

The measurement of the relative displacements of the position of the components of such systems in the course of time should eventually make it possible to establish the elements of their visual orbits, and by combining these with the parallax of the system, to determine the absolute masses of such stars. An extension of the mass-luminosity relation of such objects to the domain of very faint stars, possible only from the work with a space telescope, should constitute an invaluable contribution to astrophysics.

Another important task using high-resolution large scale photography would be to photograph the central portion of globular clusters. The stars in such clusters cannot be resolved with ground-based telescopes due to the effects of "seeing." High-resolution observations will provide important data regarding the distribution of stars close to the center in dense clusters. An analysis of the spatial distribution of stars in different magnitude ranges will provide data for the determination of stellar masses. Such studies will contribute to understanding cluster dynamics and the connection between the formation of such cluster and dwarf galaxies.

Apart from the astrometric (large scale) photography to provide the basis for investigations outlined in the foregoing paragraphs, many other tasks in stellar astronomy

Figure 3 - 3: Stars with Invisible Components of Small Mass

STAR	RA	DECL
η Cas A	0 ^h 46 ^m 03 ^s	+57°33.'1
σ^2 Eri A	4 12 58	- 7 43. 8
Ross 434	9 41 29	+76 17.3
Wolf 358	10 48 19	+ 7 05.1
Lalande 21185	11 00 37	+36 18.3
BD + 11°2625	14 10 05	+11 01.4
Proxima Cen	14 26 19	-62 28.1
ϵ Boo A	14 49 05	+19 18.4
ADS 10598 A	17 27 49	- 1 01.4
μ Her A	17 44 30	+27 44.9
Barnard's Star	17 55 23	+ 4 33.3
70 Oph A	18 02 56	+ 2 30.6
Ci 1244	19 20 37	-59 55.1
δ Aql	19 22 59	+ 3 00.8
61 Cyg A	21 04 40	+38 30.0

call for the use of wide-angle photography for astrophysical purposes. Special techniques may have to be used outside the atmospheric optical window. The systematic search for faint but very hot stars (supernova remnants, blue subdwarfs, or white dwarfs) in the UV is an example of such a technique. Another application would be the search for nascent cool stars in the IR (the "Hayashi objects"); this search could be pursued effectively through the intermediary of an IR image converter or a mosaic of IR detectors.

Photographic search for extended nebula emissions in the light of specific spectral lines may require very narrow-passband photography, and should represent a field of research eminently suitable for MOT. The virtual absence of night-sky emission of atmospheric origin should permit recording of much fainter nebular objects than accessible from the ground (the only limit, apart from instrumental noise, being imposed by the back-scattering of sunlight on interplanetary dust). Moreover, as work of this kind does not call for maximum angular resolution, exposures could be resumed after successive periods of daylight and their cumulative total would add up to many hours.

A word of explanation may be in order concerning the focal ratios to be used in such work for MOT. As the prime focus of the main mirror is not readily accessible, the shorter of the two Cassegrainian foci (i.e., $f/15$) would generally be much too slow for this type of work. However, this constitutes only an apparent limitation, for one can convert the $f/15$ focus into much a faster one by purely optical means; namely, by collimating the beam of light past the $f/15$ focal plane by the use of an auxiliary concave mirror and rephotographing the field with the aid of a fast Schmidt camera. The f -number determines the speed of the system. Moreover, the fact that the beam intercepted by the Schmidt plate has been collimated permits one to place a narrow-passband interference filter in this beam. In this way, it should be possible to use the 120-inch telescope as a camera with an effective focal ratio of $f/1$ or faster with the only penalty being a reduction in angular size of the field of view.

Photometric - A large part of routine photometric surveys of the stars in those parts of the spectrum which are not accessible from ground are scheduled to be performed by the CAO before the advent of the MOT. MOT programs should be those which could not be undertaken by the CAO because of the latter's lack of resolving power or programming flexibility. Such programs should embrace photometric observations of transient luminous phenomena which occur at particular times, and photometric observations of objects requiring high angular resolution for their success.

A few examples of the first category are rapid variations of light exhibited by explosive variables or flare stars, or totally eclipsing systems around the times of their second and third contacts of the eclipses. Under the second category, systematic observations, both photometric and astrometric, of physical variables which occur as components of visual binary systems, should be mentioned. In such systems, the absolute masses of the variable components could be determined, providing data which are at present lacking.

Spectroscopic - Stellar spectroscopy with MOT will give rise to a new set of problems, both theoretical and instrumental. With the exception of certain special tasks concerned with studies of intrinsically faint stars (subdwarfs and white dwarfs, for instance, or nova remnants) when low dispersion may be forced upon the user by lack of light, it is probable that a large fraction of stellar spectroscopy work will be for high dispersion of the order of 5 \AA/mm , and spectral resolution on the order

of 0.01-0.1 Å. Not all spectrographic work should, however, call for complete coverage of wide spectral regions; for as our knowledge increases, an increasing number of problems will require detailed surveys of specific parts of the spectrum, and/or of transient phenomena exhibited in them. This should be true, for example, of most phenomena exhibited by variable stars at different phases of their cycles--in particular, of the periodic line broadening, reversal from absorption to emission or appearance of emission bands in explosive variables. It is also true of the "flash spectra" in the hydrogen Balmer or Lyman lines of eclipsing variables just before and after a total eclipse of their early-type components. Such phenomena can best be recorded by scanning spectrographs with photoelectric registration, or tunable Fabry-Perot etalons.

3.2.3 Extragalactic Studies

An important field of studies to be undertaken by MOT should be extragalactic studies to extend the present limits of the observable universe by photography, photometry, spectrometry, and polarimetry of the light of distant spiral nebulae and quasi-stellar radio sources.

It is probable that, comparison with similar telescopes on ground, MOT should gain approximately a factor of +0.7 in limiting magnitude by being above the atmospheric extinction, and a further factor of 2.6 magnitude by virtue of better definition of the images unimpaired by atmospheric turbulence. The total gain of four magnitude should increase the limiting photographic magnitude for detection of faint objects in optical frequencies to +27; and for photoelectric detectors (available so far for registration of point sources rather than finite areas) this could be further increased to +29.

Under these conditions, direct photography should permit extension of the present nebular counts to a distance of a factor of ten greater than attainable by the 120-inch telescope of the Lick Observatory (which outperforms the 200-inch telescope at Mount Palomar, because of better optics and superior seeing). Low-dispersion spectroscopy, with cumulative exposures over many orbits, should permit the present knowledge of the nebular red shift versus apparent magnitude to be extended in a similar manner.

Photoelectric photometry, with its linear response, should permit extension of a reliable magnitude scale to distant objects; and also the measurement of the extent of the general reddening of such objects down to the limiting magnitudes attainable with MOT. Such data should represent invaluable observational checks of various cosmological models (explosive, evolutionary, steady-state, etc.) which should permit better discrimination than is now possible from the ground. In doing so, MOT should provide a more meaningful idea of the structure, the past as well as the future, of the universe.

3.3 DEFINITION OF OBSERVATION REQUIREMENTS

A summary of the observational requirements expected from MOT is diagrammatically given on the accompanying Figures 3-4, 3-5, and 3-6. Figure 3-4 surveys the expected capabilities of MOT for the entire field of astronomical studies as regards wavelength range, limiting magnitude, and resolution. The requirements have been particularized for planetary and stellar observations on Figures 3-5 and 3-6.

3.4 TELESCOPE OPTICS

This section discusses optical configuration, operational aspects of the telescope, full field of view, alignment of the secondary mirror, and focus, presenting the recommended systems and the associated requirements. Further details may be obtained from Boeing Document D2-84041-1.

3.4.1 Optical Configuration

The optical configuration recommended is a Cassegrainian-type with an aperture of 120 inches. The system consists of a 120-inch primary mirror with two alternate secondary mirrors and two flat folding mirrors as shown in Figures 3-7a and 3-7b.

The two secondary mirrors permit the telescope to be used at two equivalent focal ratios, $ef/15$ and $ef/30$.

The two flat folding mirrors result from the packaging requirement of the instrumentation in the cabin. The folding mirror M_4 serves two purposes; for $ef/15$ operation, mirror M_4 redirects the light radially at indexed positions to the $ef/15$ instrumentation and the telescope alignment fixture; for $ef/30$ operation, mirror M_4 is used in a fixed position and directs the light to mirror M_5 . Mirror M_5 is rotationally indexed to direct the light to $ef/30$ instrumentation.

3.4.2 Field of View

Field of view is the angular subtend of the celestial object. This is an important consideration in the MOT program because celestial objects are not all singular point sources. They may be an extended continuum or a group of point sources extending over an appreciable angle.

When extended objects are observed with a pure Cassegrainian optical system, the off-axis portion of the image will be degraded by coma and astigmatism. If the off-axis angle is great enough, curvature of field becomes a problem.

There are a number of modifications that can be made to this system to correct for coma and astigmatism. The modification recommended for the MOT is called the Ritchey-Chretien design. This design corrects coma, leaving only astigmatism and curvature of field to affect resolution, by making the primary mirror hyperbolic (under-corrected) and the secondary mirror more hyperbolic than the pure Cassegrainian (over-corrected). Curvature of field may also be corrected or the photographic film or plate bent to conform.

FIGURE 3-4

ASTRONOMICAL STUDY REQUIREMENTS

STUDY	OBSERVATION	WAVELENGTH	MAGNITUDE	RESOLUTION		
				PHOTOGRAPHY	PHOTOMETRIC	SPECTRAL
<u>SOLAR SYSTEM</u> LUNAR	PHOTOGRAPHIC	2000Å-8000Å		93M AT 5000Å	PHOTO. APERTURE 0.1MM-500M	
	PHOTOMETRIC	2000Å-40 μ				
PLANETARY						
MARS			-2.6	9 KM		
JUPITER	PHOTOGRAPHIC	3000Å-7000Å	-2.5	86 KM		
SATURN	PHOTOMETRIC	3000Å-40 μ	-0.4	176 KM	0"2-2"0	
URANUS	POLARIMETRIC		5.7			2 Å
NEPTUNE	SPECTROSCOPIC	3000Å-13 μ	8.0		5"0-1"0 (COMETS)	1-100 Å
COMETS						
<u>STELLAR</u> <u>ASTROMETRIC</u> BINARIES	PHOTOGRAPHIC	3000Å-8000Å	AT LEAST TO 14	0"07		
	PHOTOMETRIC	912Å-8000Å	AT LEAST TO 14			
	SPECTROSCOPIC	912Å-8000Å	AT LEAST TO 10			
	PHOTOGRAPHIC	3000Å-8000Å				
NEBULAE, SUB-	PHOTOMETRIC	912Å-3 μ	TO 27			
DWARFS, WHITE	SPECTROSCOPIC	912Å-3 μ				
DWARFS, & NOVA				0"07		2 Å
REMNANTS, "HAYASHI"						
OBJECTS						
<u>EXTRAGALACTIC</u> <u>SPIRAL NEBULAE</u> ,	PHOTOGRAPHIC	3000Å-8000Å	27			
QUASI-STELLAR	PHOTOMETRIC	912Å-8000Å	28			1000 Å
RADIO SOURCES	(POLARIMETRIC) SPECTROSCOPIC	912Å-8000Å	HOPEFULLY 20			

FIGURE 3-5
PLANETARY OBSERVATION REQUIREMENTS

	1	2	3
TYPE OF OBSERVATION	HIGH DISPERSION IR SPECTRA	THERMOELECTRIC MEASUREMENTS	PHOTOGRAPHIC
EQUIPMENT REQUIREMENTS	SPECTROMETER (WITH INTERFEROMETER AT TIMES)	SEMI-CONDUCTOR RECORDING DEVICE (PHOTOMETER)	CAMERA & FILTERS
FORM OF DATA (FILM, SPECTROGRAPH)	PEN-RECORDER CHARTS OF DIRECT OUTPUT ON MAGNETIC TAPE	PEN-RECORDER CHARTS OR DIRECT OUTPUT ON MAGNETIC TAPE	FILMS
DURATION OF OBSERVATION (EXPOSURE TIME)	SELDOM LESS THAN 1/2 REVOLUTION; OFTEN SEVERAL TIMES AS LONG	CONTINUOUS FOR APPROX. 10 ORBITS (INTERRUPTIONS PERMISSIBLE)	OF THE ORDER OF A SECOND OR LESS FOR EACH FRAME. SEVERAL HUNDRED, MAYBE 1000 FRAMES REQUIRED.
ATTITUDE STABILITY ACCURACY REQUIREMENTS	ATTITUDE STABILITY OF APPROX. $\pm 1/2$ SLIT-WIDTH	ATTITUDE STABILITY OF APPROX. $\pm 1/2$ DETECTOR DIA. HIGH GUIDING ACCURACY REQ'D	ATTITUDE STABILITY OF APPROX. $\pm 1/2$ AIRY DISK DIA.
f-NUMBER	f-NUMBER LARGEST ONE CAN GET ($f/30-f/60$);	f-NUMBER LARGEST ONE CAN GET ($f/30-f/60$);	LARGEST f-NUMBERS ATTAINABLE ($f/30-f/60$);
FIELD OF VIEW	FIELD OF VIEW $< 1^\circ$	FIELD OF VIEW $< 1^\circ$	FIELD GENERALLY LESS THAN 1°

FIGURE 3-6
STELLAR OBSERVATION REQUIREMENTS

	1	2	3	4
TYPE OF OBSERVATION	HIGH DISPERSION SPECTRA	LOW DISPERSION SPECTRA	PHOTOELECTRIC PHOTOMETRY	PHOTOGRAPHIC
EQUIPMENT REQUIREMENTS	GRATING SPECTROGRAPH, SPECTROMETER, OR INTERFEROMETER	LOW DISPERSION SPECTROGRAPH, SPECTROMETER	PHOTOMETER (WITH POLARIMETER ATTACHMENT)	CAMERA & FILTERS
FORM OF DATA (FILM, SPECTROGRAPH)	FILM AND/OR PHOTOELECTRIC SCANNING	FILM AND PHOTOELECTRIC SCANNING	PEN-RECORDER CHARTS OR DIRECT OUTPUT ON MAGNETIC TAPE	FILMS OR PLATES
DURATION OF OBSERVATION (EXPOSURE TIME)	SELDOM LESS THAN 1/2 ORBIT AND OFTEN SEVERAL TIMES AS LONG (10 MAX., 5 AVG.)	SELDOM LESS THAN 1/2 ORBIT AND OFTEN SEVERAL TIMES AS LONG (10 MAX., 5 AVG.)	CONTINUOUS FOR APPROX. 10 ORBITS (INTERRUPTIONS PERMISSIBLE)	UP TO 1/2 ORBIT; CANNOT BE CONTINUED FROM CYCLE TO CYCLE
ATTITUDE STABILITY ACCURACY REQUIREMENTS f-NUMBER, FIELD OF VIEW	ATTITUDE STABILITY OF APPROX. $\pm 1/2$ SLIT WIDTH $f/15-f/30$ LIGHT FIELD OF VIEW: POINT	ATTITUDE STABILITY OF APPROX. $\pm 1/2$ SLIT WIDTH SMALLEST f-NUMBER POSSIBLE ($f/4-f/15$) FIELD OF VIEW: POINT	f-NUMBER MODERATE ($\sim f/15$); FAIRLY HIGH GUIDING ACCURACY; FIELD OF VIEW: POINT	ACCURACY OF THE ORDER OF 0".01 IN GUIDING ESSENTIAL; $f/4$ ASTRO-PHYSICAL FIELD OF VIEW 1/2 DEG. OR LARGER; $f/15$ FIELD OF VIEW 1 MIN. (FOR ASTROMETRIC PURPOSE)

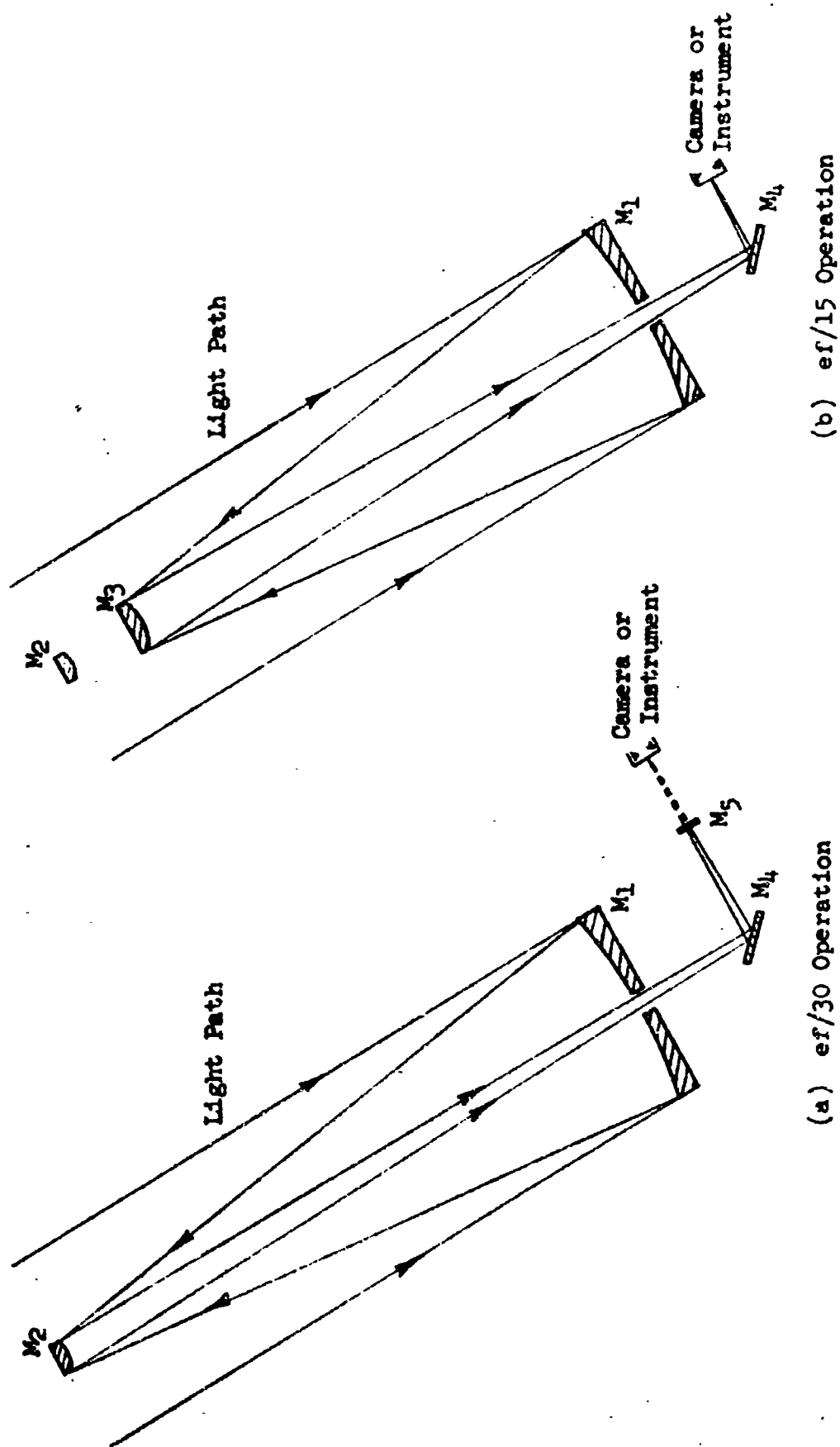


FIGURE 3-7 - ALTERNATE EQUIVALENT FOCAL RATIO OPERATION OF TELESCOPE

The observation program calls for a field of view of 0.5 degree at $ef/15$ and one minute at $ef/30$. Computation of astigmatism as a function of field angle reveals that a correction lens would be required for the $ef/15$ operation but not for the $ef/30$.

For this situation where two alternate secondary mirrors are used for the same uncorrected primary, it is necessary to make a choice of which secondary to correct for the Ritchey-Chretien design. The $ef/15$ system has to operate over a much wider field; therefore, it should be the Ritchey-Chretien design. The $ef/30$ system operates over such a small field that it will be no problem to correct it by aspherizing the secondary. No corrector lens will be required. Details of the optical configuration are listed in Figure 3-8.

3.4.3 Alignment Tolerances of the Secondary Mirror

A study was made to determine the alignment tolerances of the secondary mirror of a pure Cassegrainian telescope. These tolerances are a function of the equivalent focal ratio, with systems having different primary mirror focal ratios. The alignment tolerances were determined for systems having primary mirrors with focal ratios of $f/2$, $f/3$, and $f/4$, with each of the primary mirrors being used at equivalent focal ratios of $ef/8$, $ef/15$, $ef/30$, and $ef/60$. The details of this study are reported in Boeing Document D2-84041-1.

Alignment tolerances were defined as the limit of tilt or lateral displacement of the secondary mirror permitted before the transverse aberration becomes equal to the diameter of the visual spurious disk, or the limit of resolution. The condition for the tolerance on transverse aberration is given by the formula

$$Y_K < (ef/n) \lambda$$

where Y_K = transverse aberration
 ef/n = equivalent focal ratio
 λ = wavelength

The alignment tolerances were determined by evaluating coma and astigmatism as a function of alignment error. In geometrically pure systems, the aberration which first appears in the off-axis condition is coma. This is because there is a slight variation in the equivalent focal length of various rays throughout the aperture of the telescope. This variation is such that the magnification is greater for rays through the outer zones than for those through the inner zones. The superposition of the images slightly displaced from the various zones produces the aberration coma.

The procedure used to determine the alignment tolerances was as follows:

- 1) Determine the field angle equivalent to a given tilt of the secondary mirror.
- 2) Perform third order aberration computation on the IBM 1620 computer for each field angle.
- 3) Extract the coma and astigmatism aberrations contributed by the secondary mirror from the computer output.
- 4) Insert these contributions into the third order off-axis polynomial equations to determine the coma and astigmatism as a function of tilt.

Coma and astigmatism may be made a function of lateral displacement by the relationship

$$\delta = \phi L_2$$

where δ = linear displacement

ϕ = tilt angle of the mirror

L_2 = axial distance from the prime focus to the secondary mirror surface

Figure 3-9 illustrates the definition of alignment and presents the tolerance values which resulted from this study.

FIGURE 3-8

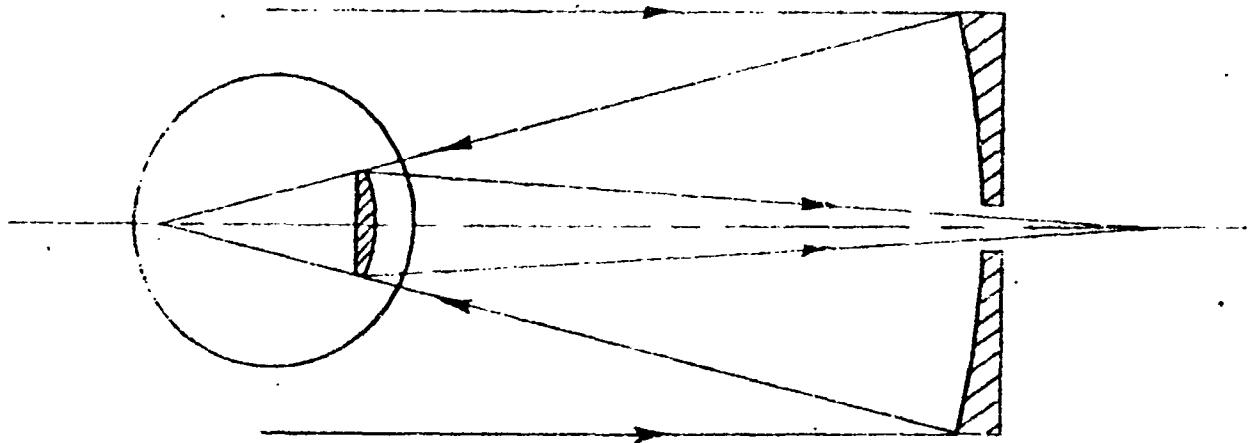
OPTICAL SYSTEM SPECIFICATIONS

	ef/15 OPERATION	ef/30 OPERATION
APERTURE	120 INCHES	120 INCHES
PRIMARY F/NUMBER	F/4	F/4
EF/N (EFFECTIVE)	EF/15	EF/30
PRIMARY-TO-SECONDARY DISTANCE	354 INCHES	400 INCHES
BACK FOCAL DISTANCE	118 INCHES	193 INCHES
PLATE SCALE	4.38 SEC/MM	2.19 SEC/MM
FIELD OF VIEW	3.9' (WITHOUT CORRECTOR) 1/2° (WITH CORRECTOR)	2' (WITHOUT CORRECTOR)
FORMAT	16 x 16 INCHES	2 x 2 INCHES
RESOLUTION	47 ℓ /MM*	36 ℓ /MM*
LIMITING MAGNITUDE	26**	27**
* $\lambda = 5000 \text{ \AA}$		
**TYPE 103 FILM		

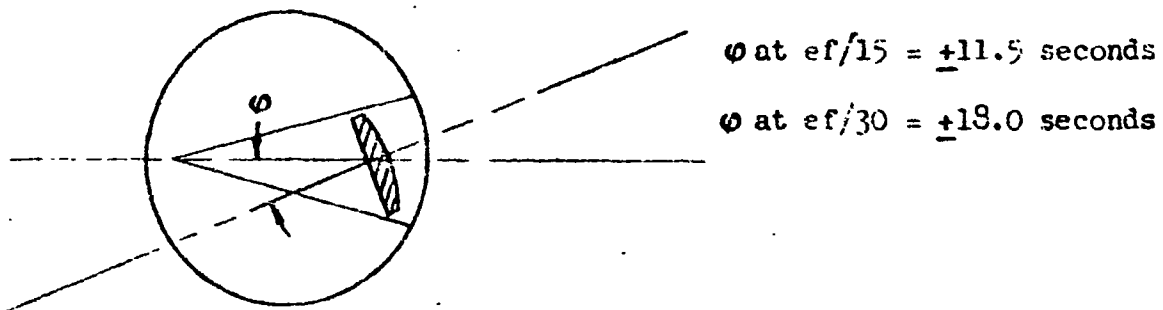
Several considerations should be kept in mind regarding the tolerances presented. It is very unlikely that the tilt error will appear without an error in displacement also, as these errors will probably be coupled mechanically. In such a case, it

FIGURE 3-9

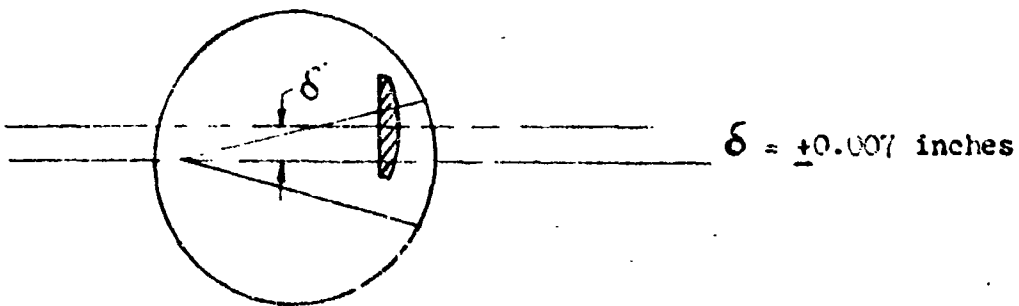
TILT AND LATERAL DISPLACEMENT TOLERANCE OF SECONDARY MIRROR



a) Telescope Aligned



b) Tilt



c) Lateral Displacement

will become necessary to divide the tolerances into those contributed by the two parameters. The division of the tolerance should be weighed according to the difficulty of sensing and correcting the corresponding parametric error.

The tolerances presented were determined for pure Cassegrainian systems. In modifying this system from a pure Cassegrainian to a Ritchey-Chretien, coma has been corrected. However, this correction is only valid for an aligned system. When the secondary mirror is misaligned, coma and astigmatism will appear. Therefore, it is recommended that the alignment tolerances determined by coma using the pure Cassegrainian system, be used.

3.4.4 Focus Tolerance

Focus of astronomical telescopes is not dependent on the object distance as all celestial objects are at infinity focus. However, an out-of-focus condition can occur due to a changing of three initial conditions: the distance between the primary and secondary mirror; the mechanical back focal distance; and the equivalent focal length due to figure change at the primary mirror.

An out-of-focus condition produces an aberration similar to spherical aberration. The limit of this aberration is put in terms of the longitudinal shift in focus in one direction and may be determined by the formula

$$\Delta f' = 2\lambda (ef/n)^2$$

where $\Delta f'$ = shift in focus
 λ = wavelength of light
 ef/n = equivalent focal ratio

One concern of the telescope study is the amount of longitudinal movement permitted for the secondary mirror with respect to the primary mirror. Longitudinal movement of the secondary mirror causes the image to move out of focus. The amount the image moves per unit movement of the secondary mirror is a function of the magnification.

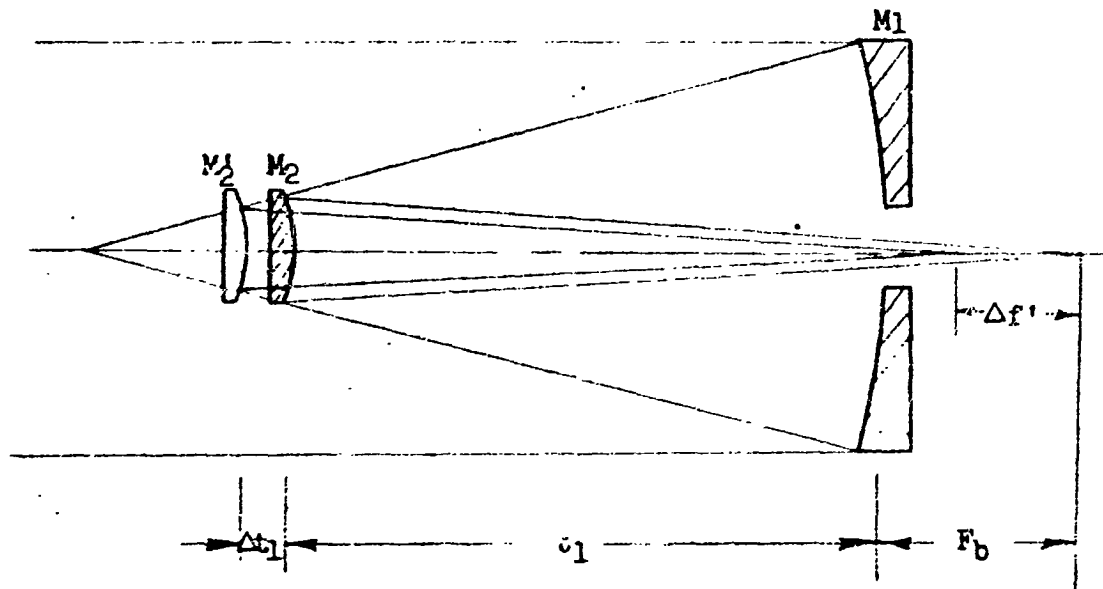
Computations were performed on the IBM 1620 computer where the movement of this image was determined as a function of the incremental movements of the secondary mirror. Figure 3-10 illustrates the tolerances. Computations were also performed for equivalent focal ratios of $ef/8$ and $ef/60$. In all cases, the computations were performed using a primary mirror of $f/2$ and $f/3$ as well as $f/4$. These results and details are given in Boeing Document D2-84041-1.

3.5 DEFINITION OF INSTRUMENTATION AND SYSTEMS PERFORMANCE

In this section the arrangement and theoretical performance of the scientific instruments in the cabin is presented, whereas the functional aspects of the instrumentation are discussed in Section 4.3. In order to cover many observations, the classic instruments of astronomy have been considered in this study. No attempt has been made to optimize these instruments, but they have been defined sufficiently to show feasibility.

FIGURE 3-10

LONGITUDINAL DISPLACEMENT TOLERANCE OF SECONDARY MIRROR



$$\Delta t_1 \text{ at } ef/15 = \pm 0.00062 \text{ inch}$$

$$\Delta t_1 \text{ at } ef/30 = \pm 0.00064 \text{ inch}$$

Figures 3-11a and 3-11b illustrate the arrangement of the scientific instrumentation in the MOT cabin. The instruments are located at either of two equivalent focal ratios, $ef/15$ and $ef/30$.

Considerations when determining whether the instrument was to be located at $ef/15$ or $ef/30$ were the performance requirement, size and shape, and simplicity of operation. Further details of these considerations are presented in Boeing Document D2-84041-1.

The instruments as shown in Figure 3-11 will perform the following types of observations; photography, wide and narrow field, high- and low-dispersion spectroscopy covering the spectrum from the ultraviolet into the far infrared, and photometry from the ultraviolet into the far infrared. The instrumentation will be discussed in this order.

3.5.1 Photography

For the purposes of this study, wide angle photography is defined as that requiring close to 0.5-degree field of view. The narrow field photography is defined as that with less than 10 minutes.

A study was made to determine the angular resolution as a function of equivalent focal ratios for spectrographic films. Results of this study, as shown in Figure 3-12, are useful in comparison of the theoretical resolution to that required for different astronomical studies.

3.5.1.1 Wide Angle Photography

Wide angle photography will be performed at $ef/15$. Figure 3-13 contains graphs of the telescope camera system modulation transfer functions (MTF) using four types of spectrographic film at $\lambda = 5000 \text{ \AA}$. The assumed obscuration ratio is $\eta = 0.25$. Optical quality of the telescope system was assumed to have an average modulation transmission factor of 0.9. The attitude stability was assumed to be $\alpha = +0.01$ arc seconds. Results of the MTF calculations in terms of granularity limited resolution may be seen by the intersection of the detectivity curve for each of the films and the corresponding MTF.

Results of the MTF computation were used to determine the photographic disk diameter. Using the computed diameter, it is possible to determine the limiting stellar magnitude of the telescope with the particular film, using the formula given by Selwyn

$$m_L = m_{\text{sky}} + 5 \log f - 2.5 \log d - 16.1$$

where m_L = limiting detectable stellar magnitude
 m_{sky} = equivalent brightness of sky in magnitude
 f = focal length in inches
 d = diameter of the photographic disk in millimeters

The value used for the sky brightness is $m_{\text{sky}} = 23.75$ as given by Fredrick.

The limiting magnitude which may be photographed, assuming a maximum exposure of 40 minutes, was determined from the formula referenced by Fredrick and Selwyn

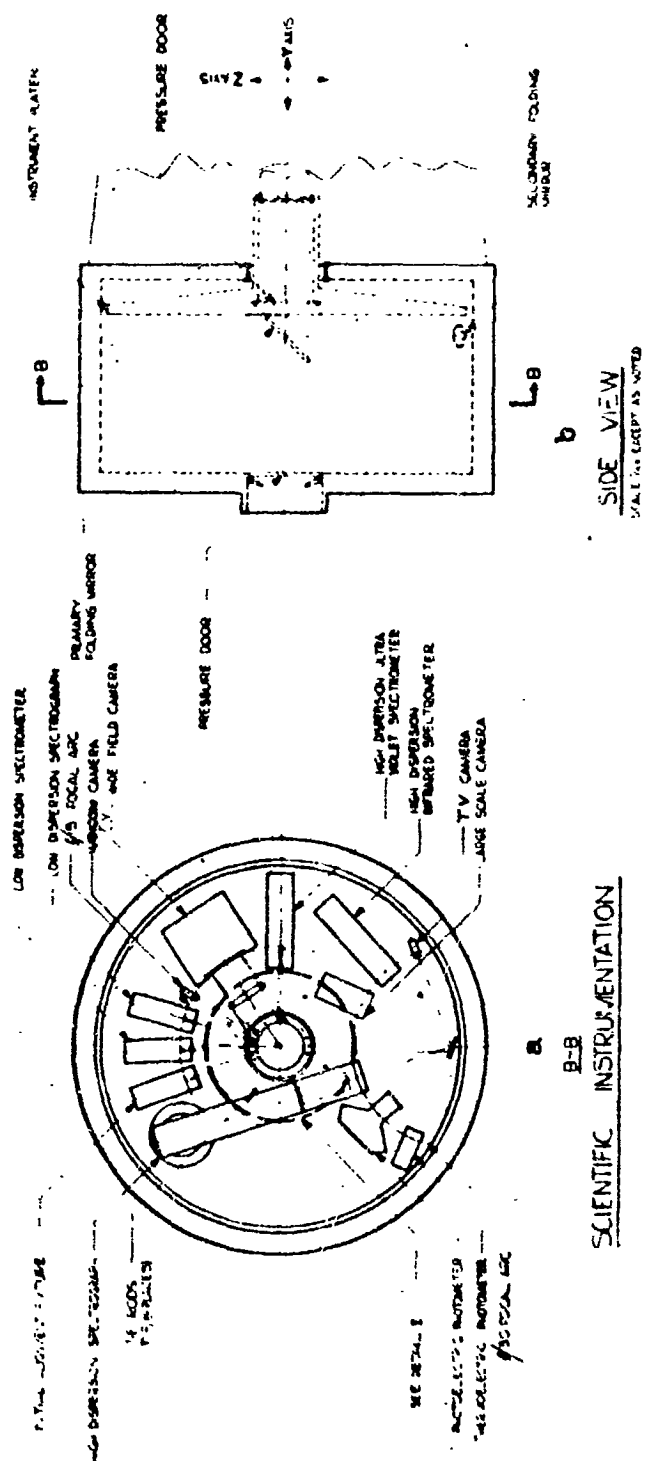
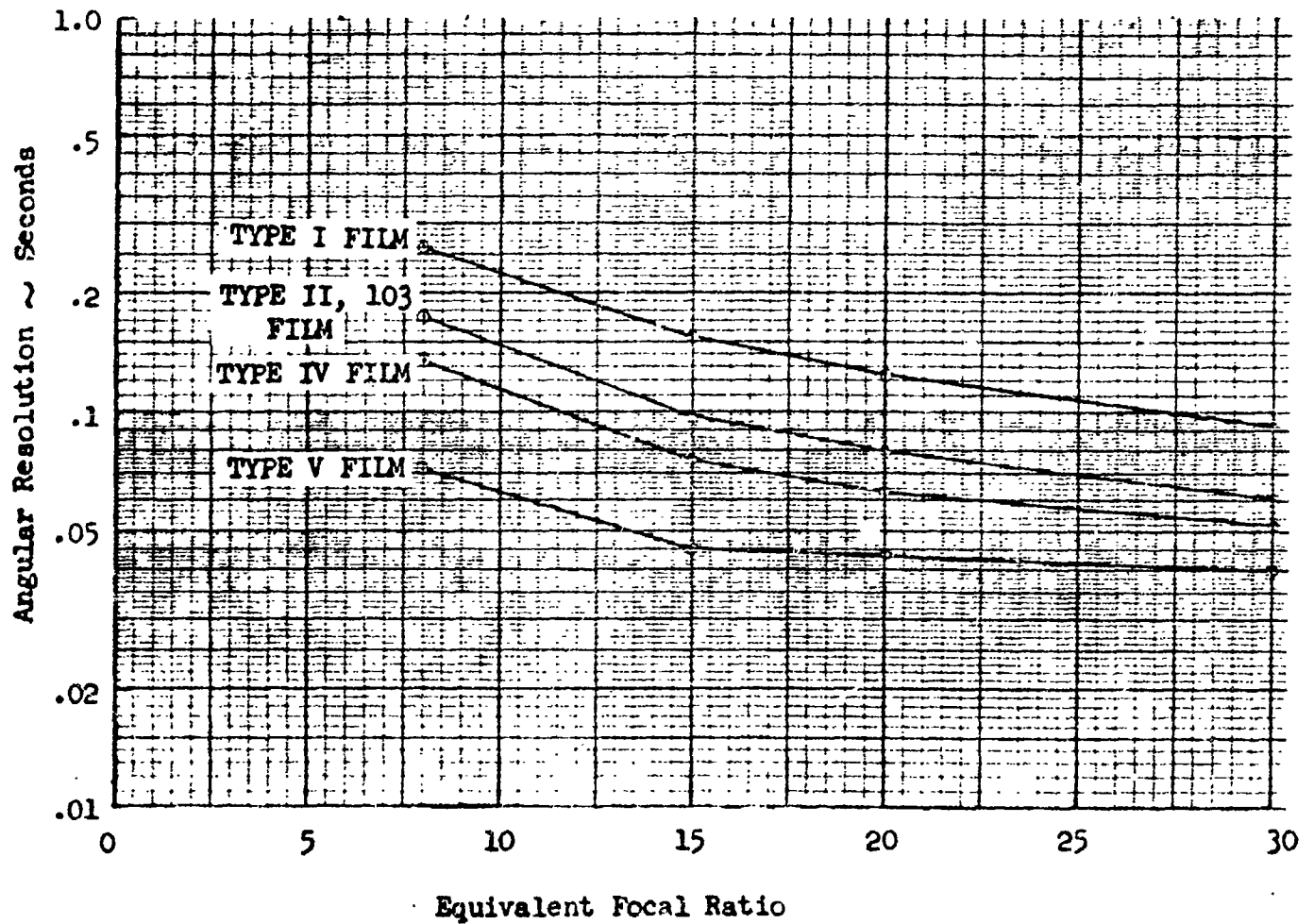


FIGURE 3-11

FIGURE 3-12

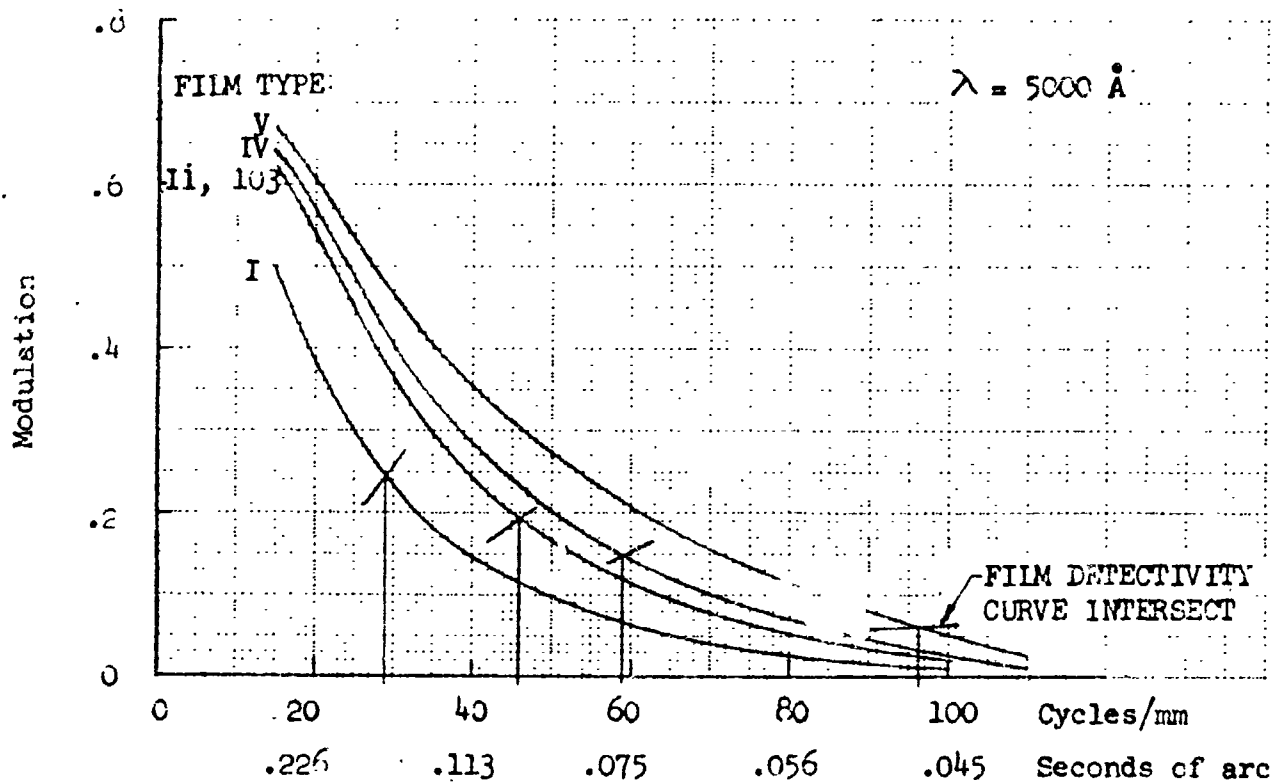
ANGULAR RESOLUTION AS A FUNCTION OF
EQUIVALENT FOCAL RATIO FOR SPECTROGRAPHIC FILMS



D2-84042-1

FIGURE 3-13

MODULATION TRANSFER FUNCTIONS
FOR SPECTROGRAPHIC FILM AT $ef/15$



$$T = \frac{8(ef/n)^2}{\text{antilog } 0.4 (m_L - pg^m_L)} \text{ minutes}$$

where ef/n = equivalent focal ratio

m_L = limiting magnitude

pg^m_L = limiting magnitude desired to photograph

This formula may be rearranged into the form

$$pg^m_L = m_L - 2.5 \log \frac{8(ef/n)^2}{T}$$

This formula is based on a fast, blue-sensitive film; presumably E.K. Type 103.

Making suitable corrections for different film sensitivities and reciprocity failures, the limiting photographic magnitude pg^m_L is computed for two of the spectrographic films used for the MTF curve.

FIGURE 3-14

LIMITING PHOTOGRAPHIC MAGNITUDE AT $ef/15$

FILM TYPE	ONE ORBIT	TEN ORBITS
103	22.8	23.8
II	20.5	22.1

The exposure time as a function of magnitude may be determined by

$$T = \frac{8 (ef/n)^2}{\text{antilog } 0.4(m_L - pg^m_L - \Delta pg^m_s - \Delta pg^m_R)} \text{ minutes}$$

The results shown in Figures 3-14 and 3-15 are computations of photographic magnitude as a function of total exposure time, assuming 40 minutes of exposure per orbit

3.5.1.2 Narrow Field Photography

Narrow field photography is planned for $ef/30$. In this section the theoretical performance that is expected photographically will be presented. Figure 3-16 shows the MTF curves of the telescope camera system at $ef/30$ for the four types of spectrographic film.

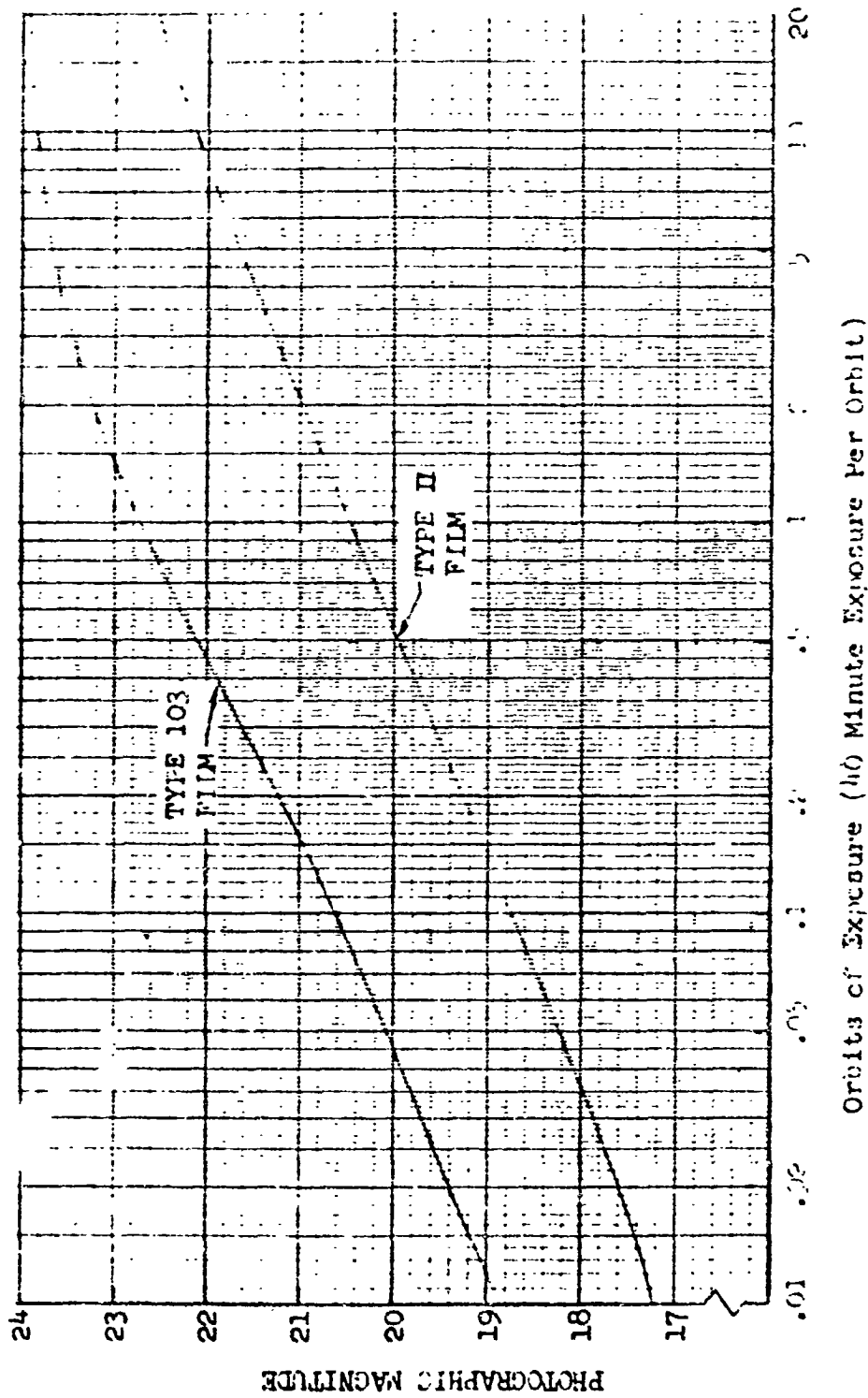
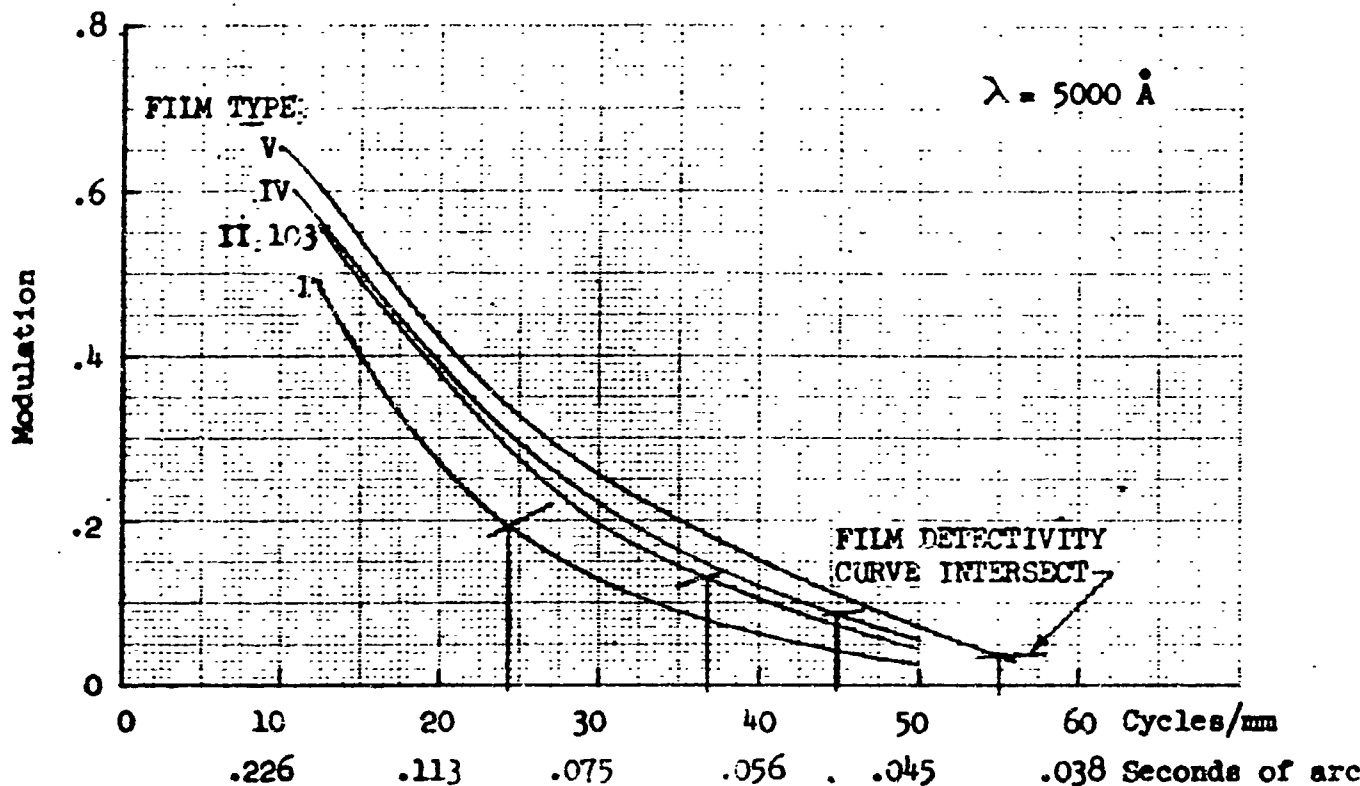


FIGURE 3-15 LIMITING PHOTOGRAPHIC MAGNITUDE AT 40/1
AS A FUNCTION OF EXPOSURE TIME

FIGURE 3-16

MODULATION TRANSFER FUNCTIONS FOR SPECTROGRAPHIC FILM
AT $ef/30$



The results of the MTF curves are again used to determine the photographic disk for each type of film and the limiting magnitude computed as before.

The exposure time as a function of stellar magnitude for two types of film used at $ef/30$ is presented in Figures 3-17 and 3-18.

FIGURE 3-17

LIMITING PHOTOGRAPHIC MAGNITUDE AT $ef/30$

FILM TYPE	ONE ORBIT	TEN ORBITS
103	22.5	23.8
II	20.3	21.9

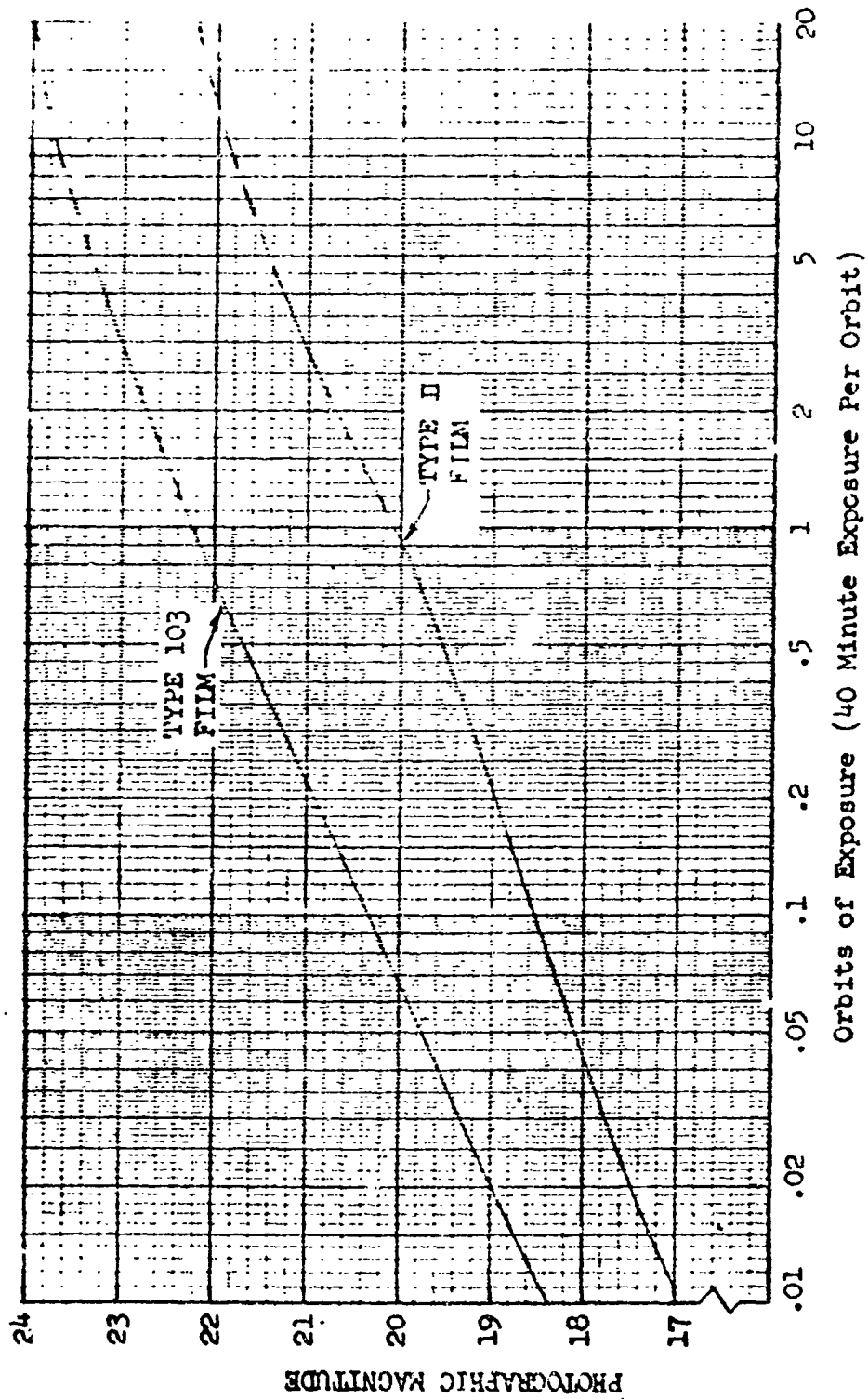
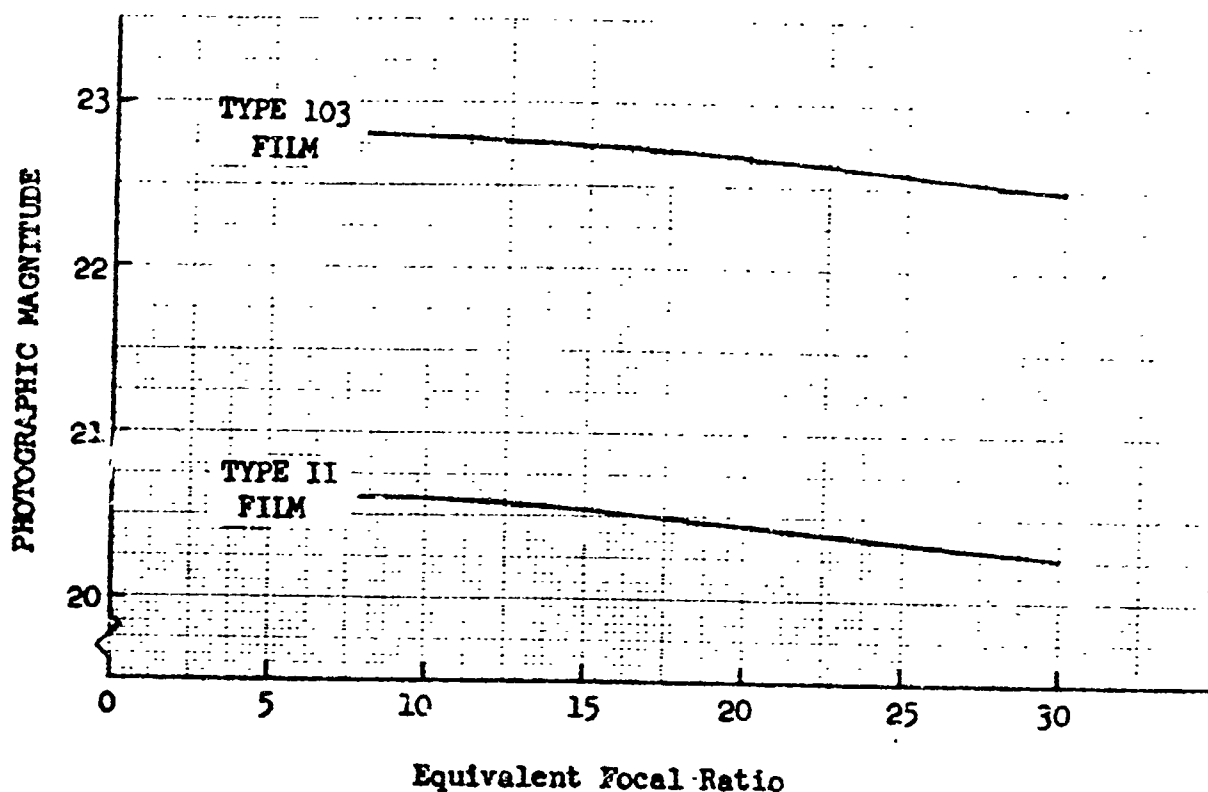


FIGURE 3-18 LIMITING PHOTOGRAPHIC MAGNITUDE AT $ef/30$
AS A FUNCTION OF EXPOSURE TIME

FIGURE 3-19

LIMITING PHOTOGRAPHIC MAGNITUDE FOR 40-MINUTE EXPOSURE AS A FUNCTION OF EQUIVALENT FOCAL RATIO FOR SPECTROGRAPHIC FILMS



The performance presented has been for equivalent focal ratios of $ef/15$ and $ef/30$. In the process of optical configuration studies, three equivalent focal ratios were considered. In an effort to simplify the optical system, consideration was given to the effect of performing wide angle photography at $ef/15$ rather than $ef/8$. The effect may be seen by computing resolution and limiting magnitude as a function of equivalent focal ratios. Figure 3-12 (presented previously) showed considerable gain in resolution by performing wide angle photography at $ef/15$ rather than $ef/8$. Now the results shown in Figure 3-19 indicate there was negligible loss in the magnitude star that could be photographed within the maximum 40-minute exposure at $ef/15$ compared to $ef/8$. However, when there is a closer match between the telescope resolution and the film resolution, such as when using Type V film, the photographic speed becomes more significant.

3.5.2.1 High-Dispersion Ultraviolet Spectrometer

The spectrometer shown in Figure 3-20 is in principal recommended by Dr. J. G. Baker. Liller also describes Baker's application of this type of mount using a concave grating and a fast Schmidt spectral camera.

The instrument consists of a concave reflective grating G used as a collimator for the entrance slit S_1 , an off-axis paraboloidal collecting mirror M, and the exit slit in front of the detector. The concave grating, collecting mirror, slit, and detector rotate about the point of intersection of the optical axis and the grating normal. Rotation in this manner maintains a stigmatic image.

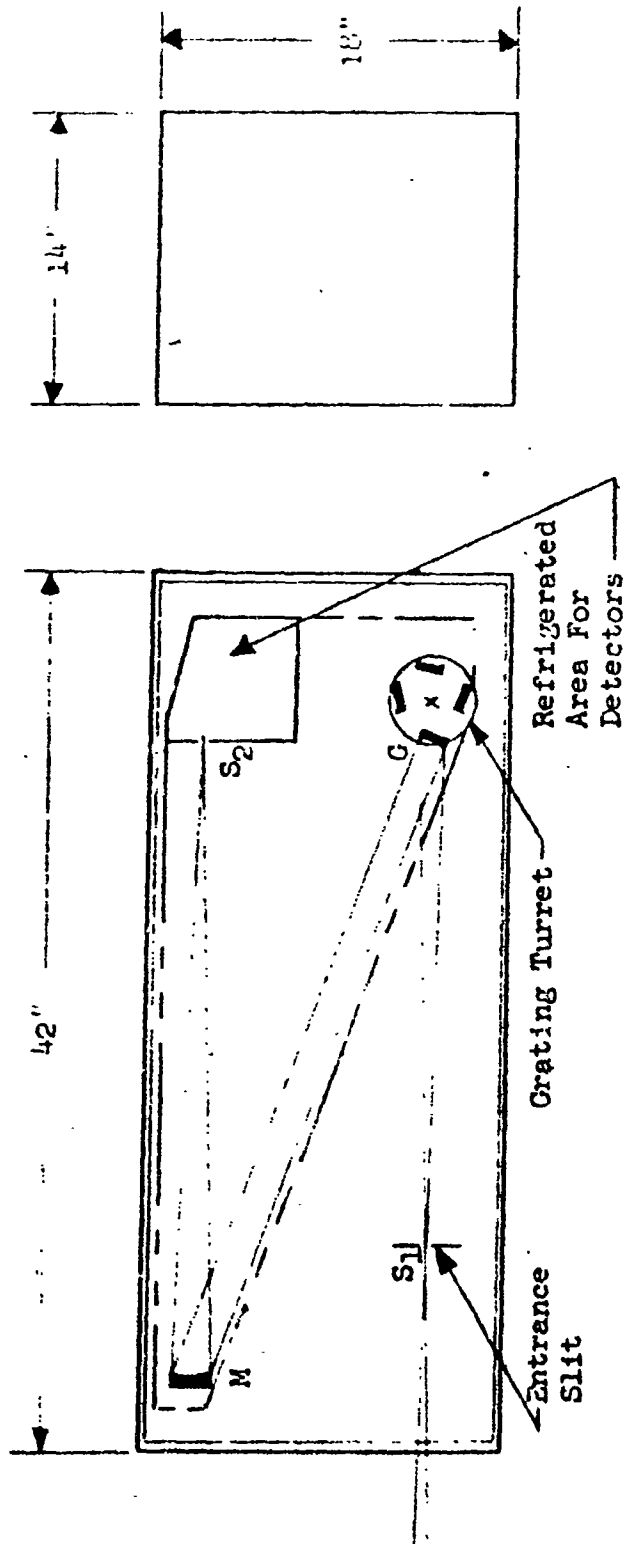


FIGURE 3-20
HIGH DISPERSION UV SPECTROMETER
(900-4500 Å)

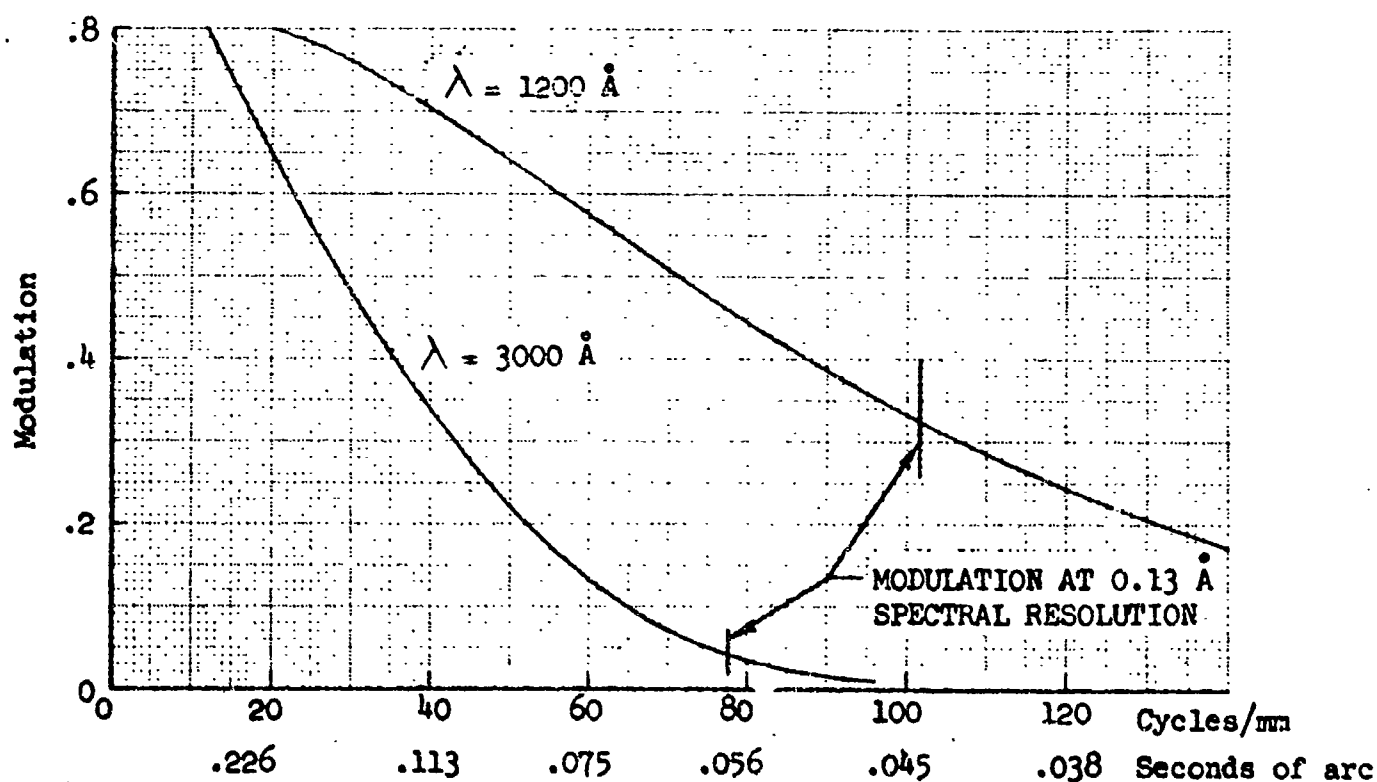
The operational specifications of the high dispersion UV spectrometer may be listed as follows:

Focal Length G	=	24 inches	
Radius of Curvature of Grating	=	48 inches	
Focal Length M	=	30 inches	
Grating & Blaze Wavelength	=	1200 $\text{\AA}/\text{mm}$; 1200 \AA , 3000 \AA	
		600 $\text{\AA}/\text{mm}$; 1200 \AA , 3000 \AA	
Linear Reciprocal Dispersion	At	$\lambda = 1200 \text{\AA}$	$\lambda = 3000 \text{\AA}$
With 1200 $\text{\AA}/\text{mm}$ Grating	=	10.2 $\text{\AA}/\text{mm}$	11.1 $\text{\AA}/\text{mm}$
With 600 $\text{\AA}/\text{mm}$ Grating	=	20.4 $\text{\AA}/\text{mm}$	20.6 $\text{\AA}/\text{mm}$

The theoretical performance of the spectrometer is illustrated by the system modulation transfer functions shown in Figure 3-21. When the spectrometer slit is adjusted to a width equal to the Airy disk, the modulation would be 0.04 at $\lambda = 3000 \text{\AA}$ and 0.32 at $\lambda = 1200 \text{\AA}$. This would be the modulation at a spectral resolution of 0.13 \AA .

FIGURE 3-21

MODULATION TRANSFER FUNCTIONS
FOR HIGH DISPERSION UV SPECTROMETER



3.5.2.2 High-Dispersion Spectrograph

The high-dispersion spectrograph covering the visual and ultraviolet range is shown in Figure 3-22 and consists of an off-axis folded collimator, a turret of reflection gratings, and an off-axis spectral camera.

The off-axis collimator permits folding without an obscuration due to the secondary mirror. The off-axis spectral camera is a folded Schmidt-type system, with the aspheric correction on the reflection gratings. This permits a close fold of the system with no obscuration due to a secondary mirror.

The collimator utilizes a $f/4$ primary to obtain an equivalent focal length of 80 inches. Four 8-inch-diameter gratings blazed at 4000, 5000, 6000, and 7500 Å are used. The gratings have 15,000 grooves per inch and are mounted on an indexed turret. This design permits replacing the turret with gratings blazed for the ultraviolet region, as there are no transmission optics except the window in the film cassette. In such a case, a cassette would be designed for UV work and would have the appropriate window transmission characteristics.

The spectral camera is a Schmidt system corrected for a 15-degree field. The system has an equivalent focal ratio of $ef/10$ with the chosen gratings, to produce a linear reciprocal dispersion of 3.67 to 4.05 Å/mm in the second order spectra. Figure 3-2 shows the system modulation transfer functions for the several spectrographic films. The intersect points of the granularity-limited detectivity curves are shown along with the required resolution to obtain the required 0.1 Å spectral resolution.

The exposure time required to observe a 10th magnitude star with a spectrograph was determined by the formula

$$T = \frac{8(ef/n)^2}{\text{antilog } 0.4(A_{mL} - S^m - \Delta S^m - \Delta m_S - \Delta p_{gR}^m)}$$

where ef/n = equivalent focal ratio

A_{mL} = magnitude limit determined by the Airy disk diameter

S^m = the magnitude of the star to be observed

ΔS^m = the loss in magnitude because the observation is by spectrograph

Δm_S = the change in magnitude due to different film sensitivity

Δp_{gR}^m = the loss in magnitude due to reciprocity failure

The loss in magnitude caused by the dispersion of the spectrograph may be computed by the formula

$$\Delta_{SP^m} = \frac{5}{2} \log \frac{W(\lambda_2 - \lambda_1)}{K d^2}$$

where

W = width of spectrum in millimeters

$(\lambda_2 - \lambda_1)$ = wavelength range of plate used in Å

K = linear reciprocal dispersion in Å/mm

d = diameter of photographic disk in mm

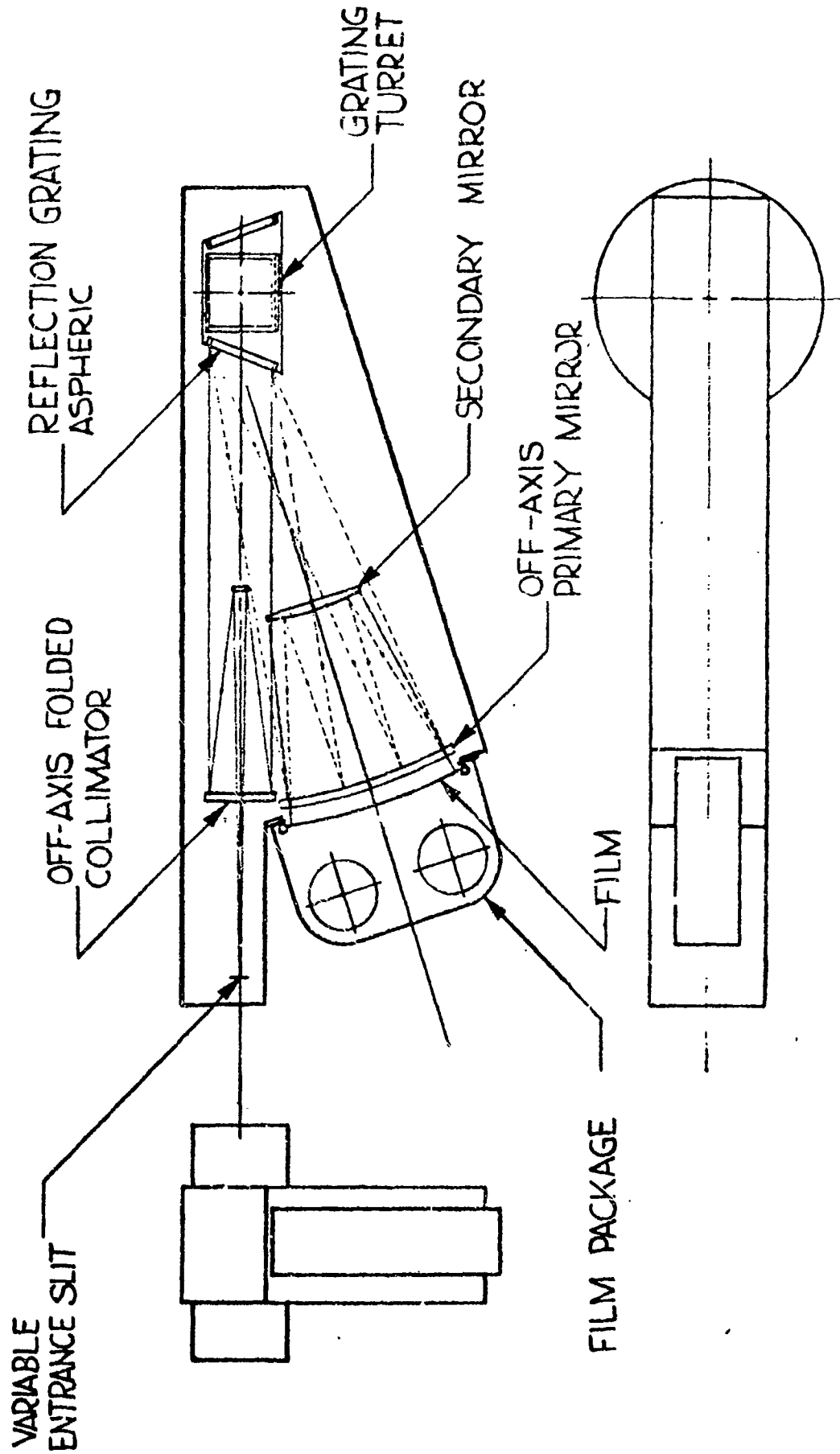
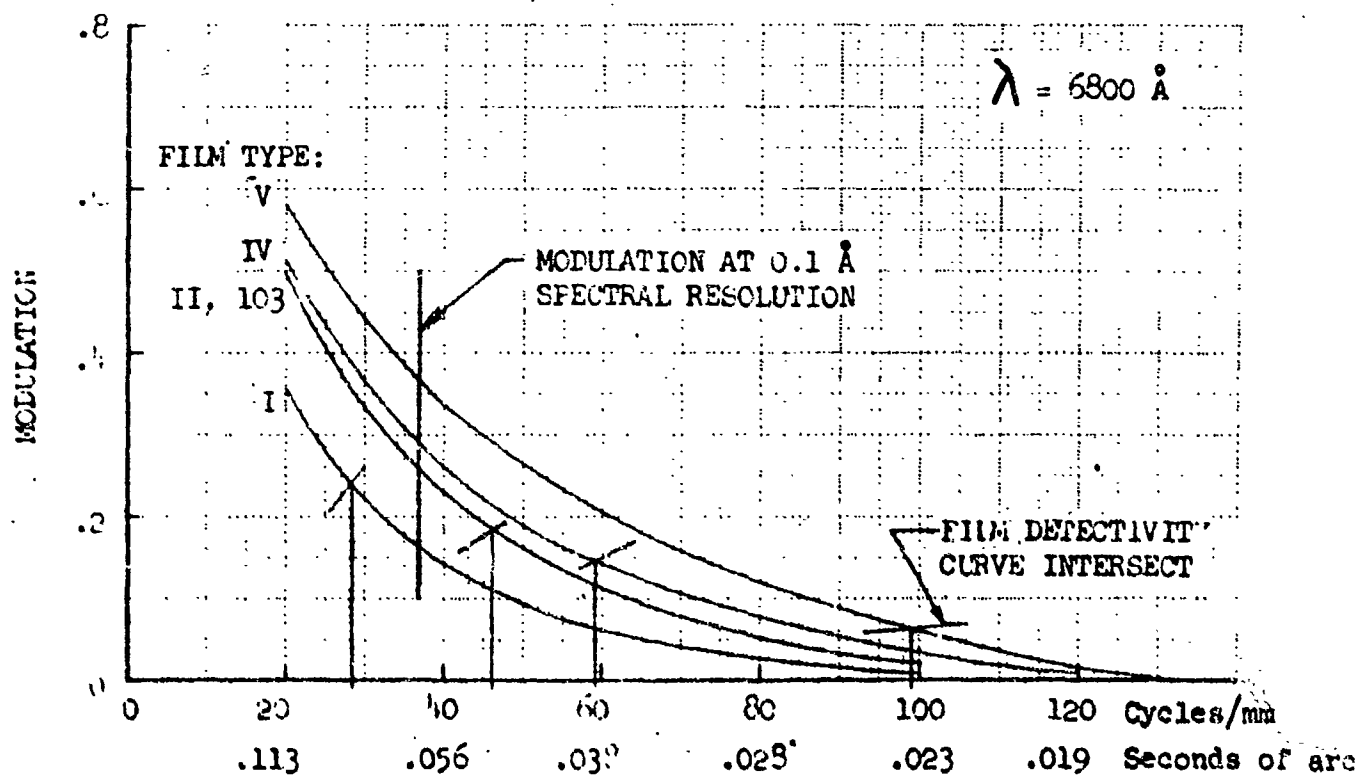
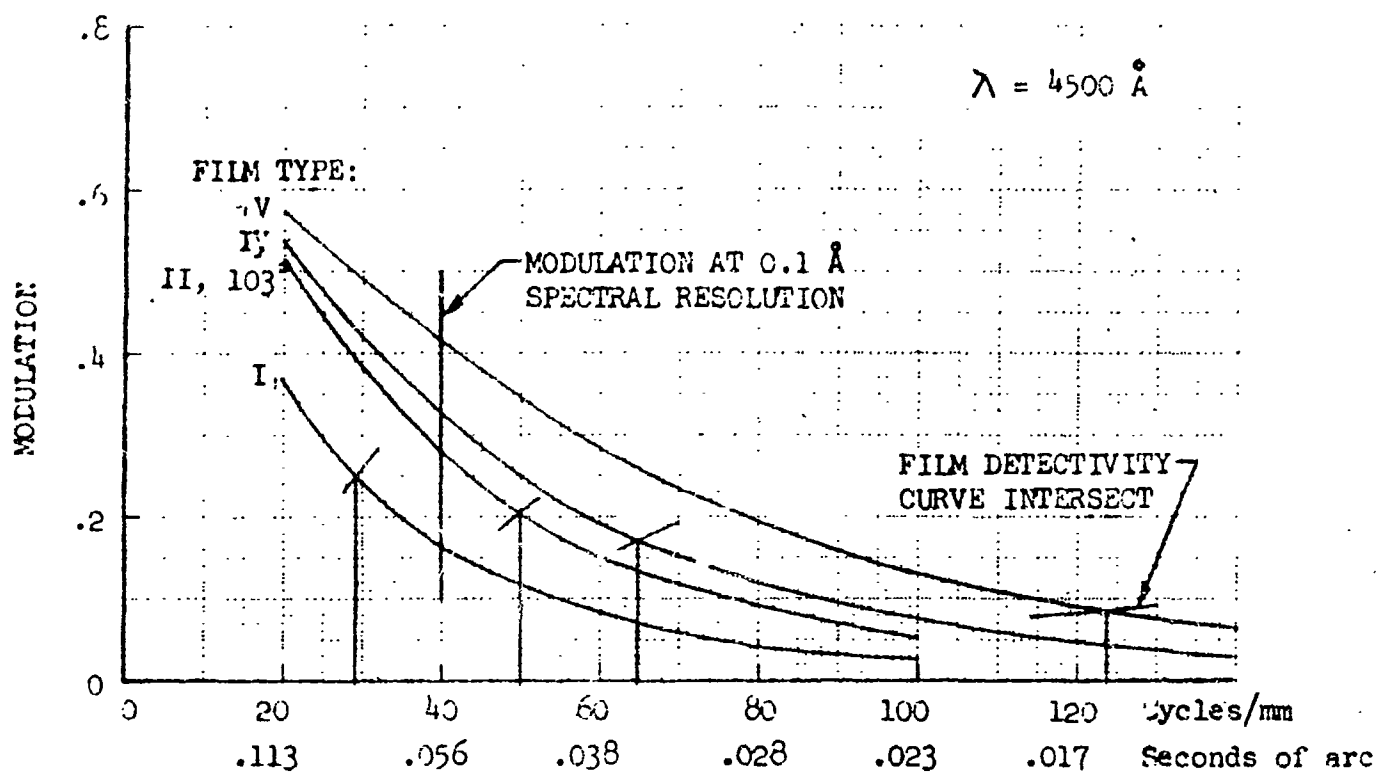


FIGURE 3-22
HIGH DISPERSION SPECTROGRAPH
 (3000-8900 Å)

FIGURE 3-23

MODULATION TRANSFER FUNCTIONS
FOR HIGH DISPERSION SPECTROGRAPH



Spectrographic magnitude limits SP^m_L were determined for Type 103 film to bring out problems connected with the operational aspects of MOT. Results of these computations are shown below.

FIGURE 3-24

SPECTROGRAPHIC MAGNITUDE LIMIT FOR TYPE 103 FILM

λ	K	W	ΔSP^m	SP^m_L
4500 Å	4.4	0.1 mm	12.64	16.33
		0.2	13.39	15.58
		0.4	14.14	14.83
6800 Å	4.4	0.1	12.99	15.96
		0.2	13.75	15.20
		0.4	14.50	14.45

The observation requirements for high dispersion spectra require observing as dim a star as 10th magnitude. Computations were made for the exposure time required to reach such a star at a wavelength of 4500 Å. These computations were made using the same linear reciprocal dispersion and spectrum widening values as in Figure 3-24. In addition, the attitude stability α was allowed to vary by values of $\pm 0''.01$, $\pm 0''.02$, and $\pm 0''.04$. The results of these computations are presented in the following table.

FIGURE 3-25

EXPOSURE TIME (NUMBER OF ORBITS) REQUIRED FOR 10TH MAGNITUDE STAR AS A FUNCTION OF ATTITUDE STABILITY FOR DIFFERENT VALUES OF SPECTRUM WIDENING*

W	$\alpha = 0''.00$	$\alpha = \pm 0''.01$	$\alpha = \pm 0''.02$	$\alpha = \pm 0''.04$
0.1 mm	0.528	1.83	2.53	4.82
0.2 mm	1.055	3.67	5.06	9.65
0.4 mm	2.106	7.33	10.12	19.29

*Assuming Type 103 Film, $\lambda = 4500 \text{ Å}$

3.5.2.3 High-Dispersion IR Spectrometer

The spectrometer feasibility model for the infrared region, 0.79 to 13 microns, shown in Figure 3-26 consists of a $f/30$ Cassegrainian collimator with an equivalent focal length of 168 inches; a mosaic of four echelette gratings or a 10-inch etchelette grating; an $f/6$ off-axis paraboloidal collector mirror; and exit slit followed by the infrared detectors.

D2-24042-1

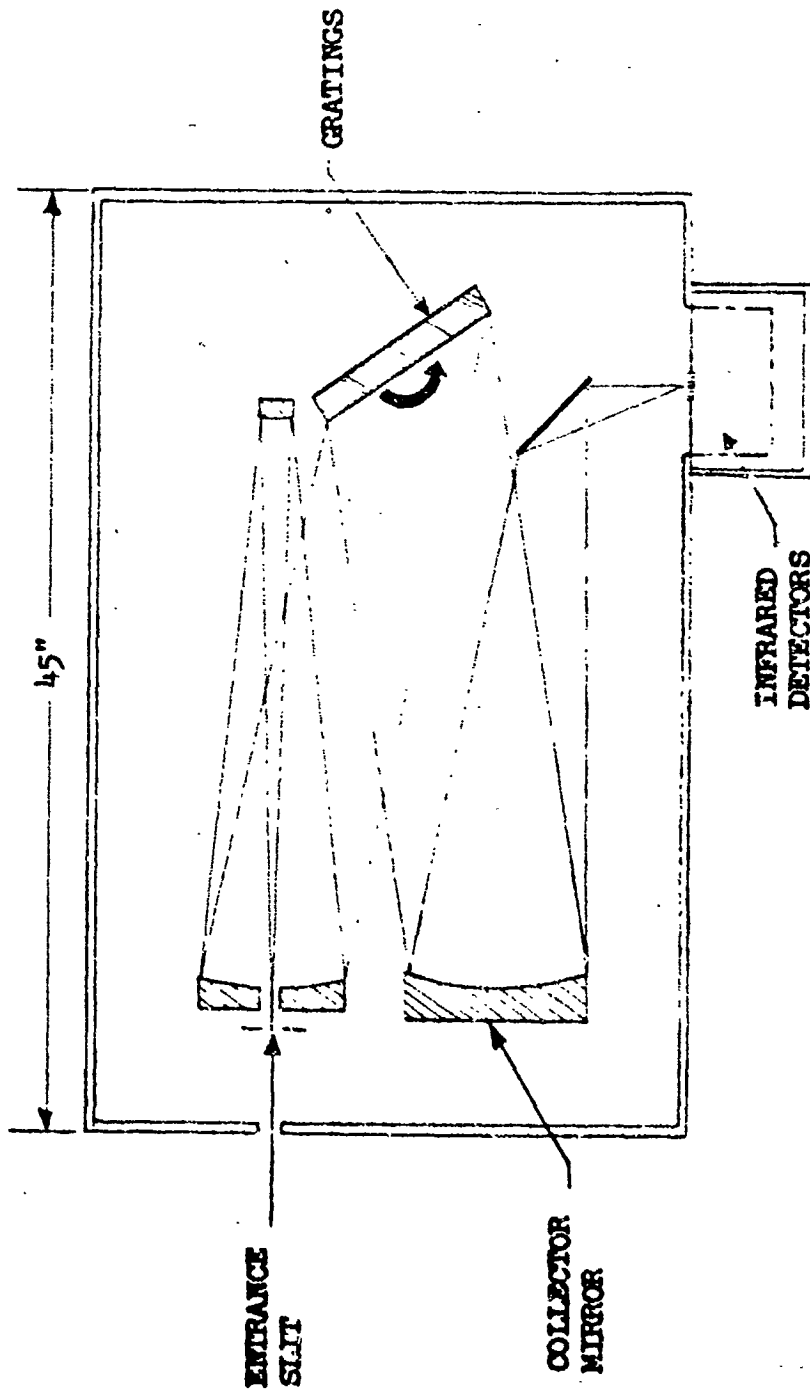
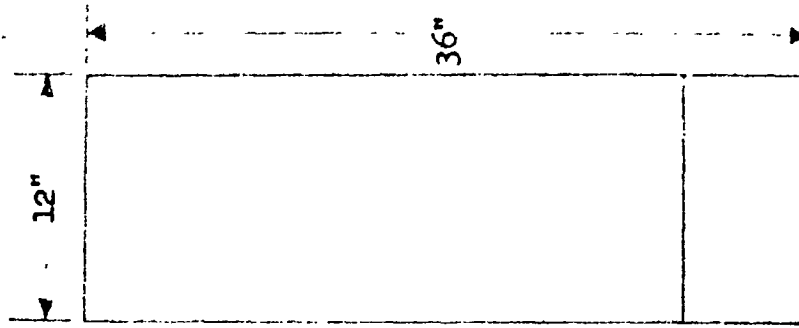


FIGURE 3-26
HIGH DISPERSION IR SPECTROMETER
(.79-15 MICRONS)

The grating would be precisely rotated to produce a spectral scan at the exit slit. The grating would consist of a mosaic of four echelette gratings or could be a single grating. If the mosaic was used, the four component gratings would be blazed for 0.85, 1.7, 4.5, and 10 microns with two having 600 ℓ/mm and one each 250 ℓ/mm and 100 ℓ/mm , respectively. If the single 10-inch echelette grating was used for the 2.5 to 15 micron region, the grating would be 94 ℓ/mm and blazed at 10 microns in the first order. The spectral region and the order observed would be: 2.5-3 μ (fourth order), 3-4 μ (third order), 4-7 μ (second order), and 7-15 μ (first order).

The collecting mirror would be an $f/6$ off-axis paraboloidal mirror with several slits in the focal plane. These slits would be followed by the appropriate infrared detectors array. This would provide simultaneous scan of several portions of the spectrum. The resolution expected would be one or two waves per centimeter.

3.5.2.4 Low-Dispersion Ultraviolet Spectrometer

The low-dispersion UV spectrometer in Figure 3-27 is based on the same optical principles as the high-dispersion UV spectrometer. The system becomes smaller but more complicated because of the variety of observational parameters required of the instrument. The spectrometer operates from 900 \AA to 4500 \AA with linear reciprocal dispersions of 60, 200, and 1000 $\text{\AA}/\text{mm}$. A concave reflective grating (G) is again used as a collimator. This collimator disperses the radiation into any one of three off-axis paraboloidal collecting mirrors $M_1 - M_3$. The collecting mirrors are rotationally mounted about an axis N. Rotation of shaft N will alternately position the mirrors correctly with the proper detector. The indexed shaft, mirrors, detectors, and grating are mounted on a common mount which pivots about the point of intersection of the grating normal and the optical axis. The four gratings are mounted on an indexed turret to obtain the following operational capability:

Concave Gratings	600 ℓ/mm	300 ℓ/mm
Radius of Curvature	40 inches	40 inches
Collimator Focal Length	20 inches	20 inches
Diameter Grating	>1.33 inches	>1.33 inches
Blazed Wavelength	1500 \AA	1500 \AA
	3000 \AA	3000 \AA
Focal Length of Collecting Mirrors	$f_s = 11.5$ inches	
	3.5 inches	
	1.2 inches	
Linear Reciprocal Dispersion	60 $\text{\AA}/\text{mm}$ with $f_s = 11.5$ inches	
	200 $\text{\AA}/\text{mm}$ with $f_s = 3.5$ inches	
	1000 $\text{\AA}/\text{mm}$ with $f_s = 1.2$ inches	

The 600 ℓ/mm gratings are used for the 60 $\text{\AA}/\text{mm}$ and 200 $\text{\AA}/\text{mm}$ operation. For a linear reciprocal dispersion of 1000 $\text{\AA}/\text{mm}$, 300 ℓ/mm gratings are used.

3.5.2.5 Low-Dispersion Spectrograph

The low-dispersion spectrograph shown in Figure 3-28 will provide linear reciprocal dispersions of 60, 200, and 1000 $\text{\AA}/\text{mm}$. The following operational specification should permit studies from 4000 to 7000 \AA .

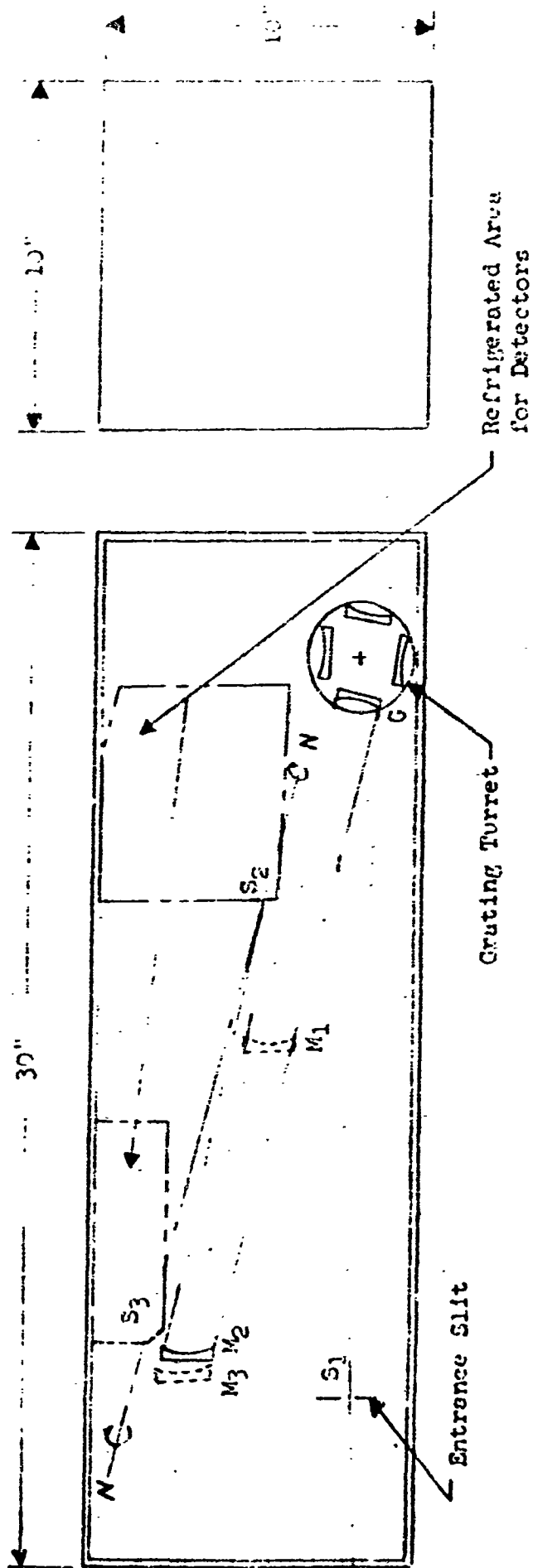


FIGURE 3-27
LOW DISPERSION UV SPECTROMETER
(900-4500 Å)

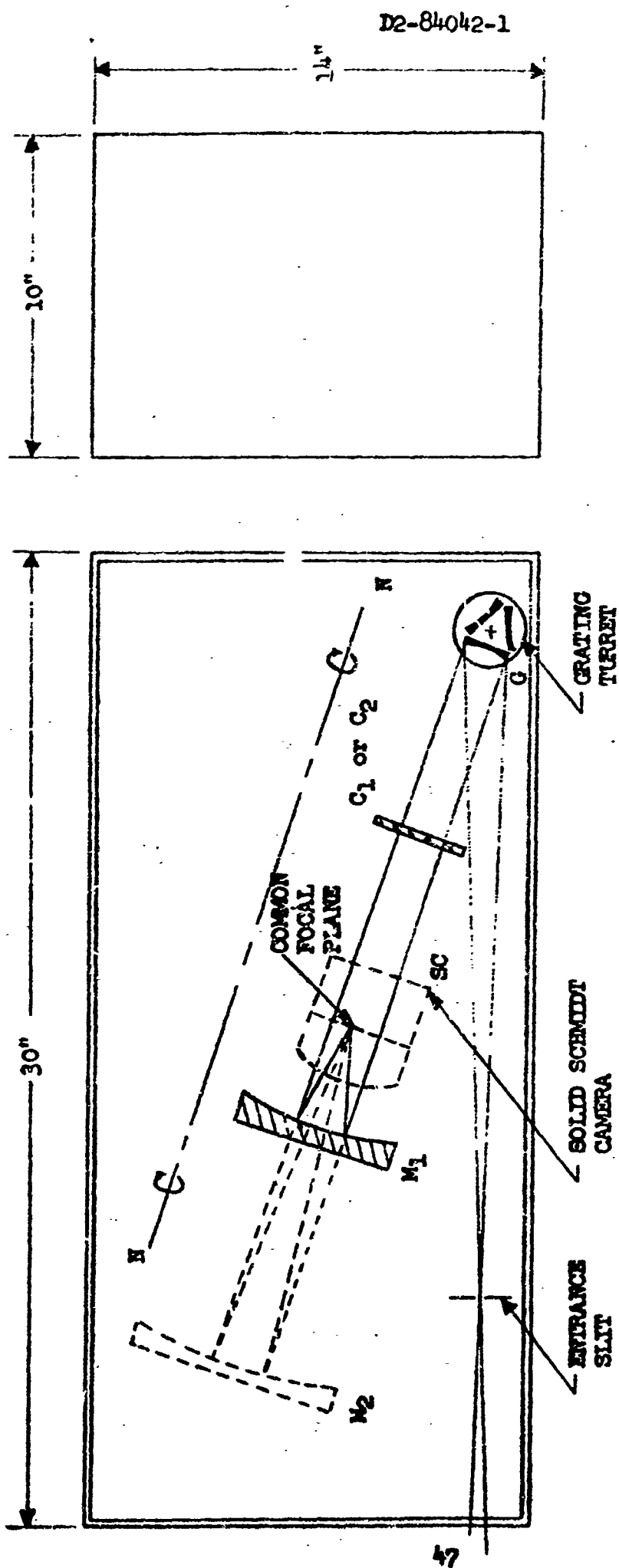


FIGURE 3-28
LOW DISPERSION SPECTROGRAPH (4000-7000 Å)

SPECTRAL CAMERA		GRATING	BLAZE	LINEAR RECIPROCAL DISPERSION
FOCAL LENGTH	F-RATIO			
11.0 inches	8.2	600 ℓ/mm	5000 Å	60 Å/mm
3.2	2.4	600	5000	200
1.3	0.98	300	5000	1000

In this type of mounting, the optical axes of the grating and the camera coincide. The cameras would be the Schmidt type with the fastest being a solid Schmidt. The spectral cameras are designed to alternately use a common film plane. The cameras are positioned by rotation of shaft N. The mirror M_1 and its corrector C_1 along with the solid Schmidt and corrector C_2 are mounted on shaft N. The components are mounted radially about shaft N in such a way that corrector C_2 would be in position at midpoint of the shaft rotation. Further rotation would move corrector C_2 out and bring the solid Schmidt into position. Reversing the rotation would bring mirror M_1 and corrector C_1 into position. This permits remotely changing the spectra' cameras without changing the film cassette.

3.5.3.1 Photoelectric Photometry

The photoelectric photometer shown in Figure 3-29 will operate in the ultraviolet and visual regions of the spectrum. Basically the photometer would consist of finding guidance, focal plane diaphragm turret, field mirror, filter turret, detector, and signal processor. The photometer will be used at an equivalent focal ratio of $ef/30$ to reduce the effect of sky background.

The feasibility model photometer is a two-channel photometer; one channel measures the brightness of the star, while the other measures the brightness of the sky adjacent to the star.

The field stop aperture and filters would be calibrated and mounted on separately controlled turrets.

3.5.3.2 Thermoelectric Photometry

Thermoelectric photometry will be accomplished with an infrared radiometer as shown in Figure 3-30. This instrument will be located at $ef/30$ and will consist of a chopper, detector, comparison IR source, preamplifier, and a data processing unit. The chopper will be a rotating butterfly mirror to alternately reflect the comparison source into the detector.

This unit would be designed as a module for easy replacement by a thermoelectric radiometer which would employ a mosaic of detectors to be used for search of low temperature stars.

FIGURE 3-29

PHOTOELECTRIC PHOTOMETER - DOUBLE CHANNEL

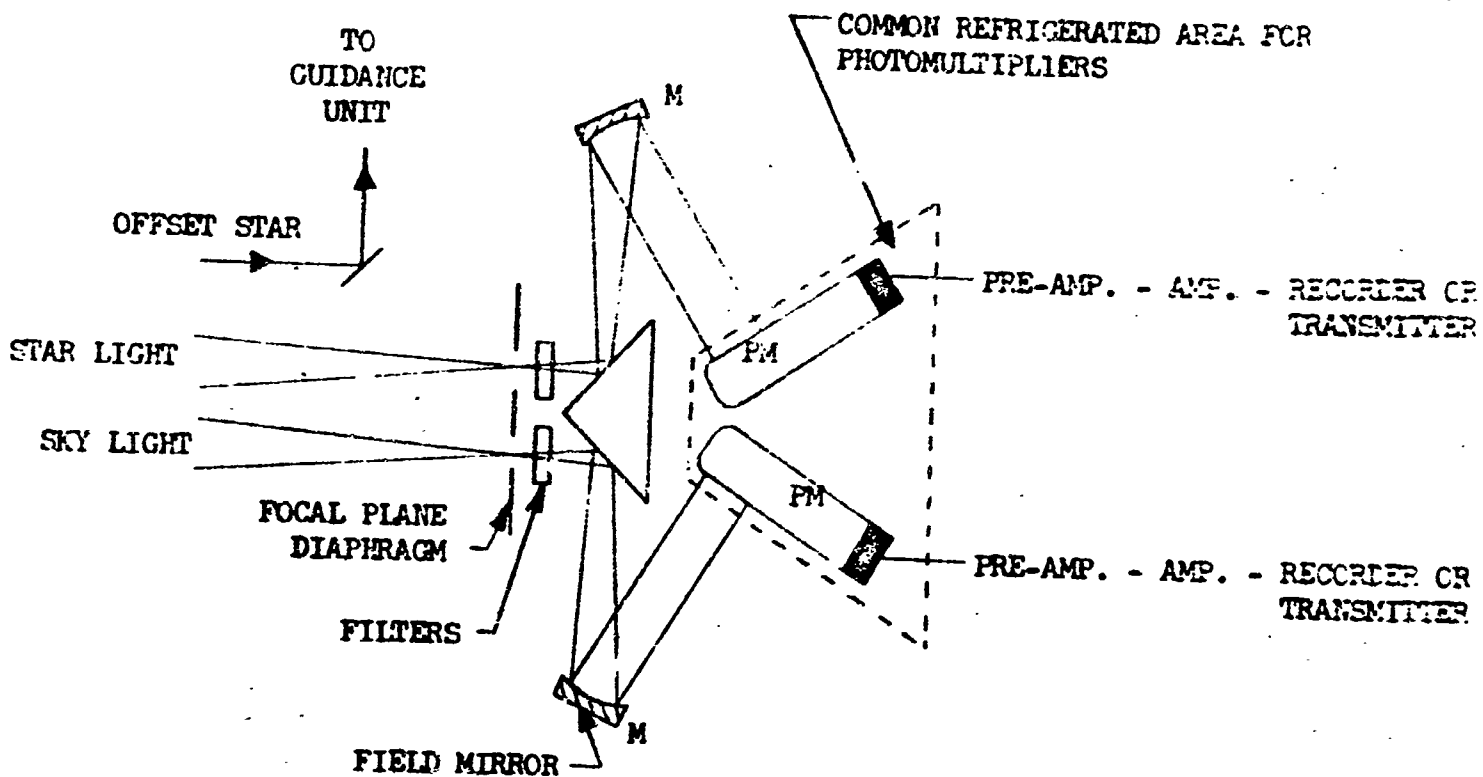
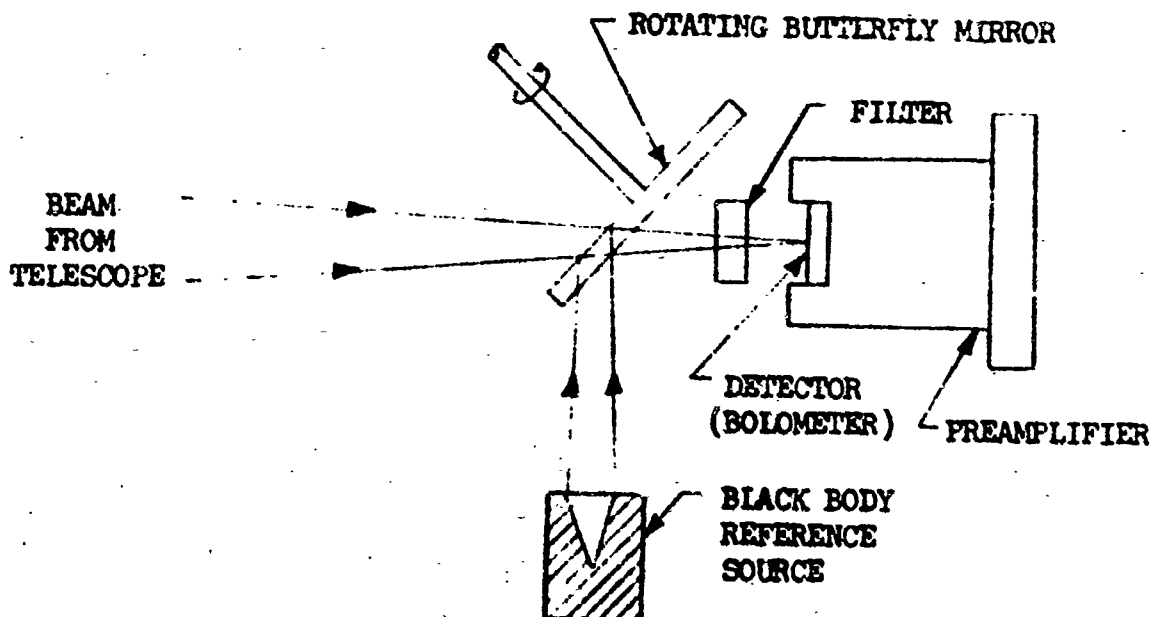


FIGURE 3-30

INFRARED RADIOMETER



3.6 PROBLEM AREAS

The problem areas discussed in this section are optical in relation to the telescope and the instrumentation, and are presented in terms of the optical requirements, optical quality, optical alignment, and attitude stability.

3.6.1 Optical Quality

A perfect optical system would image a star as a bright central condensation surrounded by diffraction rings. The central condensation would contain 85 percent of the image light with the remaining 15 percent in the diffraction rings. Irregularities in the optical surfaces will cause a reduction of this central condensation by scattering some of this light into the diffraction ring area. When the light is scattered in this manner, the fine detail is lost if it is not of high contrast.

At the Rayleigh limit (commonly termed diffraction limit), 68 percent of the light is in the central condensation with an additional 17 percent scattered into the diffraction ring area.

Hufnagel has published a method of incorporating the effects of random wavefront deformations into the modulation transfer function. Using this method, it is possible to determine the percentage of light in the central condensation as a function of the RMS surface deformations of an optical system. It is also possible to estimate the optical performance of a system as a function of the RMS surface deformation.

The following formula is used to determine the modulation transmission factor M or the percentage of possible light in the central condensation:

$$M = \exp \left[-(4 \pi^2 / \lambda^2) (\text{RMS wavefront variation})^2 \right]$$

M = modulation transmission factor
exp [] is to the base e

The net M value for light passing through several optics is just the product of the M value of each optic. Then the M_s of each optic is $M_s = M^{1/n}$ where n is the number of the surfaces (if all surfaces are weighted equally). If the optic is a mirror surface, the RMS deformation of the surface is one-half the RMS wavefront variation.

A value of $M = 0.90$ has been used in the modulation transfer function computations. To obtain this value, it was estimated that the secondary and folding mirror modulation transmission factor M_s , M_1 , and M_2 , would each be equal to 0.985 or a maximum surface deformation of $\sim 1/20$ of a wavelength or an RMS of $1/100$ wavelength. This means the primary mirror will have a value of $M_p = .95$. The primary mirror would be required to have surface deformations less than $\sim 1/10$ wavelength and an RMS of $1/53$ wavelength.

If all the surfaces were weighted equally, the surfaces would have to be made to an RMS surface variation of $< 1/80$ wavelength, to expect the same performance. This would be easier for the smaller mirror but much more difficult for the primary mirror. If all mirrors were made to an RMS surface variation of $1/53$ wavelength, the overall performance would drop to a value of $M = 0.8$.

Assuming that the problem of meeting the optical requirement is much greater with the primary mirror, the telescope performance has been computed as a function of the primary mirror optical quality. Figure 3-31 is a plot of the percent of light in the central condensation as a function of the primary mirror RMS surface deformations. Figure 3-32 illustrates the effect of changing the modulation transmission factor of the telescope system by a change in M_p .

3.6.2 Optical Alignment

The tolerances for optical alignment of the secondary mirror were given in Section 3.4.3. The problem reviewed here is the technique that should be used for alignment.

There are two basic approaches to the alignment problem, which for discussion purposes will be labeled "the functional approach" and "the positional approach."

Functional Approach - The functional approach involves a systematic reduction of aberrations by visual interpretation of the image and performing mechanical alignment operations in a reiterative process.

There are two factors which make this technique objectionable for space telescopes; the image quality is dependent upon the initial pointing accuracy, and the parameters causing the aberration are not decoupled from each in the image pattern. Because of these two factors, it takes a highly skilled technician to perform the alignment. Even then, the whole process can be highly frustrating and subjective under laboratory conditions. Figure 3-33 illustrates the type of star image that may be encountered for various alignment conditions. These simulated star images were produced by an $f/18$, 12-inch-diameter Cassegrainian telescope in connection with a comparison study of the functional and positional methods of alignment. Study details are reported in Boeing Document D2-36209-1.

Positional Approach - The positional approach is to position the secondary mirror with regard to tilt, lateral, and longitudinal displacement by means of decoupled optical sensors.

The optical sensors are instruments based on the principles of autocollimation, auto-alignment, and interferometry. The auto-collimator senses tilt, the auto-aligner senses lateral displacement, and the interferometer senses the longitudinal displacement of the secondary mirror. The signal from all three of these devices may be monitored continuously in the MORL without interrupting the observations.

In addition to the monitoring alignment sensors, it would be advisable to have an initial alignment fixture based on the same principles. The alignment fixture would perhaps have larger operating ranges at some sacrifice of precision.

As each parameter is aligned, the respective monitoring sensor is switched into the servo loop.

Upon alignment of tilt and lateral displacement, the folding mirror is rotated to the wide-field camera position. The telescope is then slewed to bring a star within the acceptance cone of the automatic focus sensor. Position of best focus is determined by longitudinal movement of the secondary mirror. Upon completion of the focus operation, the interferometer sensor for longitudinal displacement is "zeroed" and switched into the servo loop. The purpose of this servo loop is to keep the

FIGURE 3-31

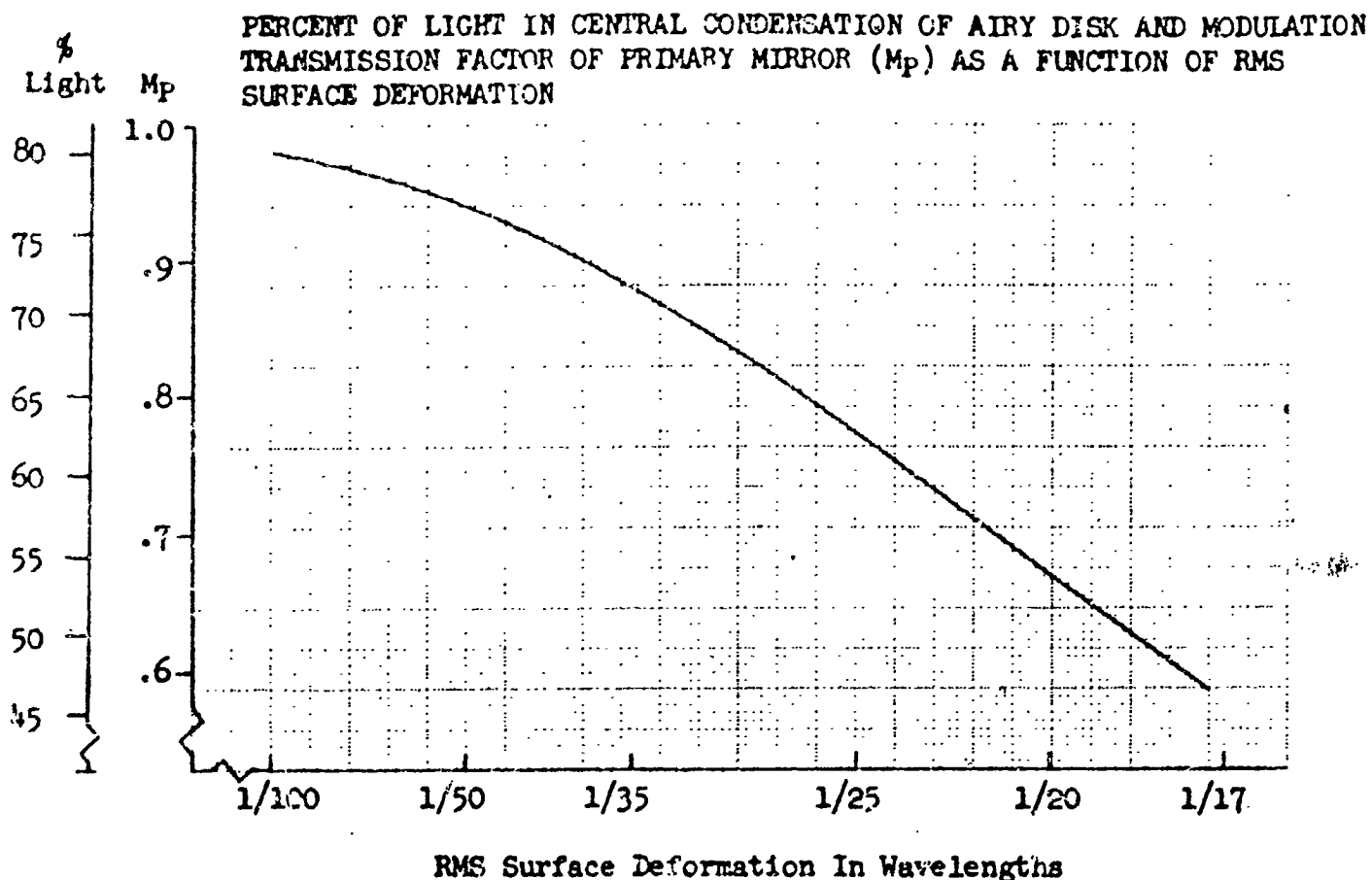
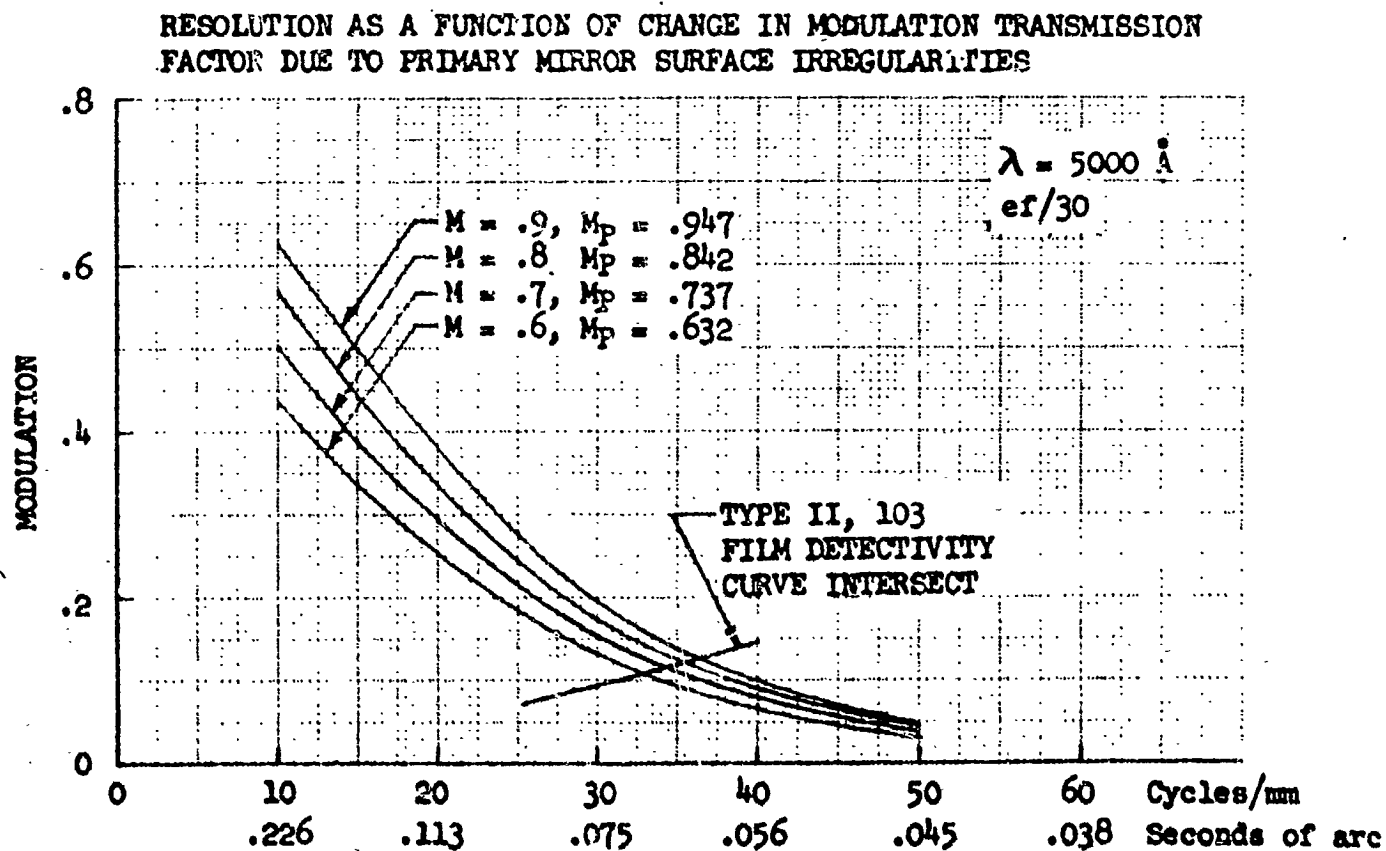
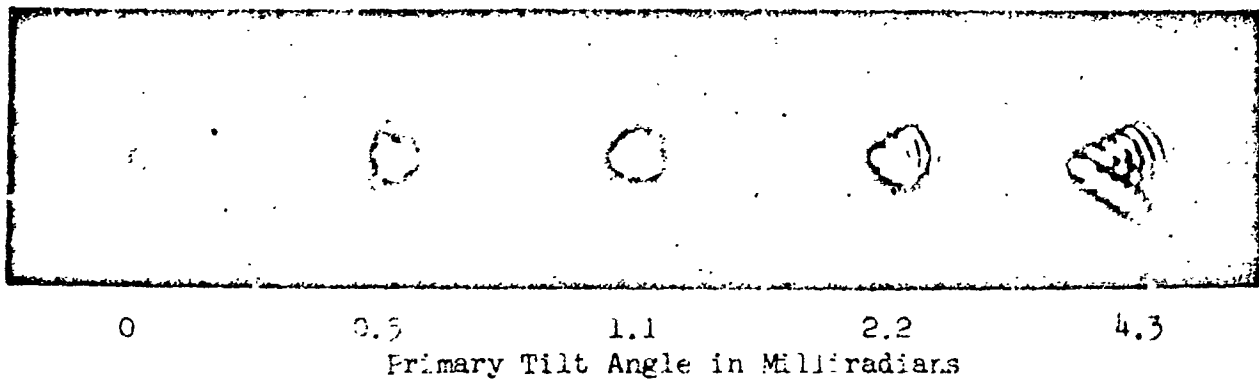
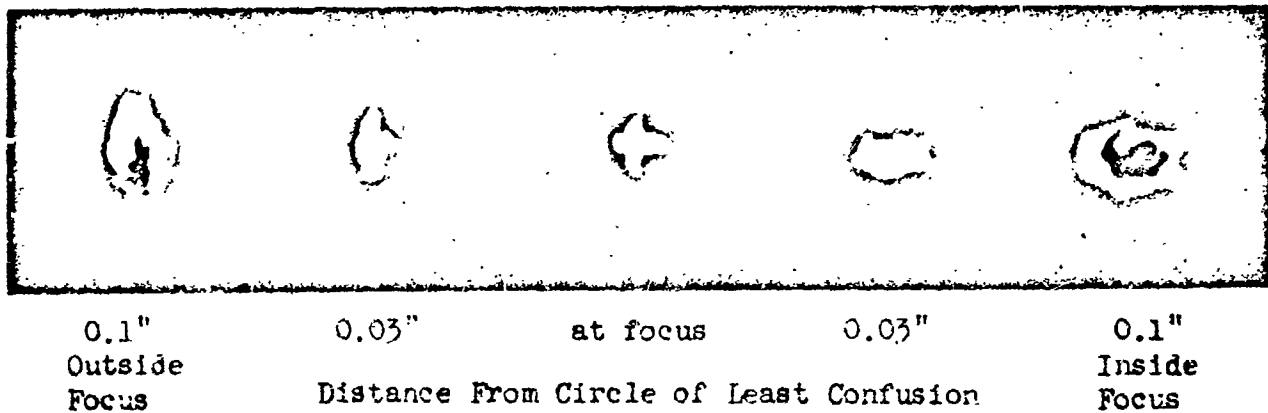


FIGURE 3-32





(a) Comatic image resulting from tilted primary mirror.



(b) Astigmatic image resulting from tilting secondary mirror 3.25 milliradian. This sequence shows how the image changes as the eyepiece tube is drawn through focus.



(c) Combination of 4.3 milliradian primary tilt and 3.25 milliradian secondary tilt as eyepiece tube is drawn through focus.

STAR IMAGES FOR VARIOUS ALIGNMENT CONDITIONS

Figure 3-33

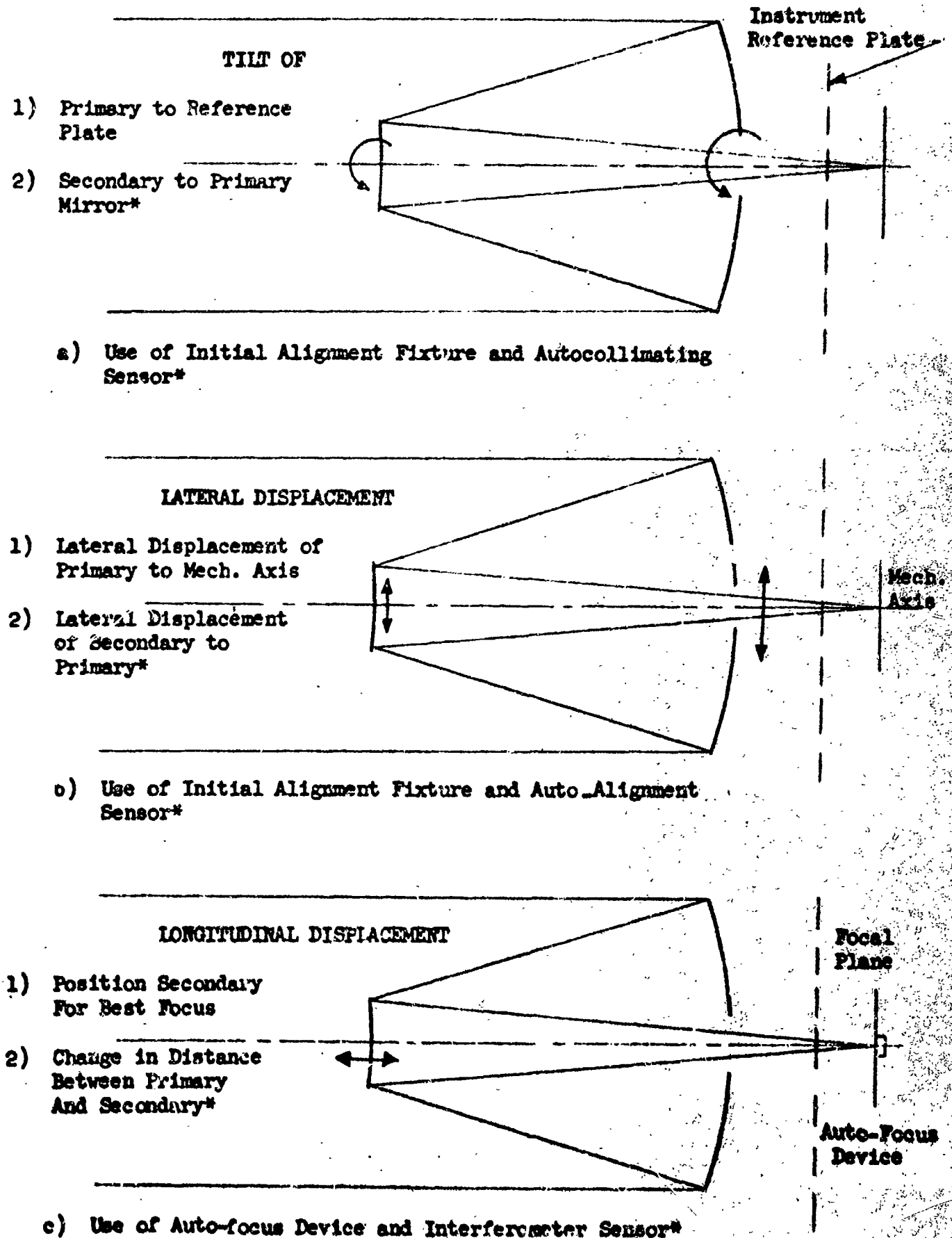
proper spacing between the primary and secondary mirror. Figure 3-34 illustrates the techniques and application of the alignment sensors.

Assuming the telescope has been successfully aligned and the monitoring sensors are completing the servo loop to maintain alignment, there is a remaining problem. This is the possibility of an out-of-focus condition arising from a change in the back focal distance (the optical distance from the surface of the primary mirror back to the focal plane). Since the tolerance on focus is ± 0.009 inches at $ef/15$ and ± 0.036 inches at $ef/30$, either of two methods would appear feasible. Auto-focus devices will be located on the most critical instruments for focus, such as the cameras.

3.6.3 Limits of Attitude Stability

Image motion arising from uncompensated angular rates will have three effects; small amounts of image reduce the contrast of fine detail, larger amounts will reduce the resolution; the exposure time required will be lengthened; and the magnitude limit will be changed due to enlargement of the photographic disk. Figure 3-35 illustrate the change in modulation and resolution as a function of attitude stability.

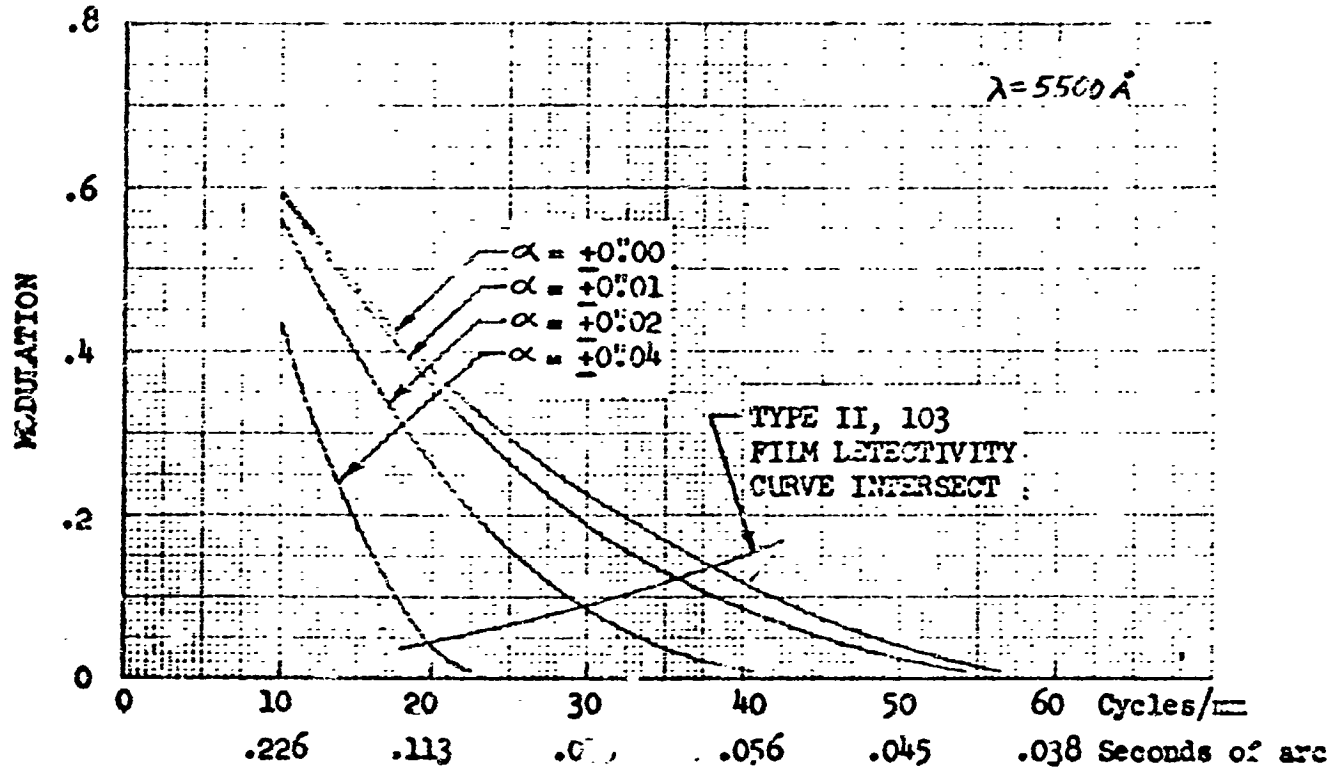
FIGURE 3-34 OPTICAL ALIGNMENT OF TELESCOPE



D2-84042-1

FIGURE 3-35

RESOLUTION AND MODULATION FOR VARIOUS VALUES OF
ATTITUDE STABILITY



The loss in magnitude as a result of attitude instability may be computed by the formula

$$\Delta m_{\alpha} = -2.5 \log \left(\frac{\pi d + 4 d_g}{\pi d} \right)$$

where Δm_{α} = change in magnitude

d = photographic disk diameter (mm)

d_g = linear image smear (mm)

Insertion of this term in the formulas for determining exposure time and limiting magnitude permits a parametric study of attitude stability. Figure 3-36 illustrates such a study for large scale photography at $ef/30$, chosen because it represents the most stringent resolution requirement. For example, astrometric photography requires a resolution of 0.07 arc seconds according to Fredrick. From the plot it appears that a movement greater than ± 0.02 arc seconds per exposure time would degrade the photographic quality to an unacceptable level.

The frequency and amplitude tolerances of such an oscillation is a function of the magnitude being observed. Short exposure times would permit larger instability amplitudes or, conversely, long exposures permit small amplitude at high frequency

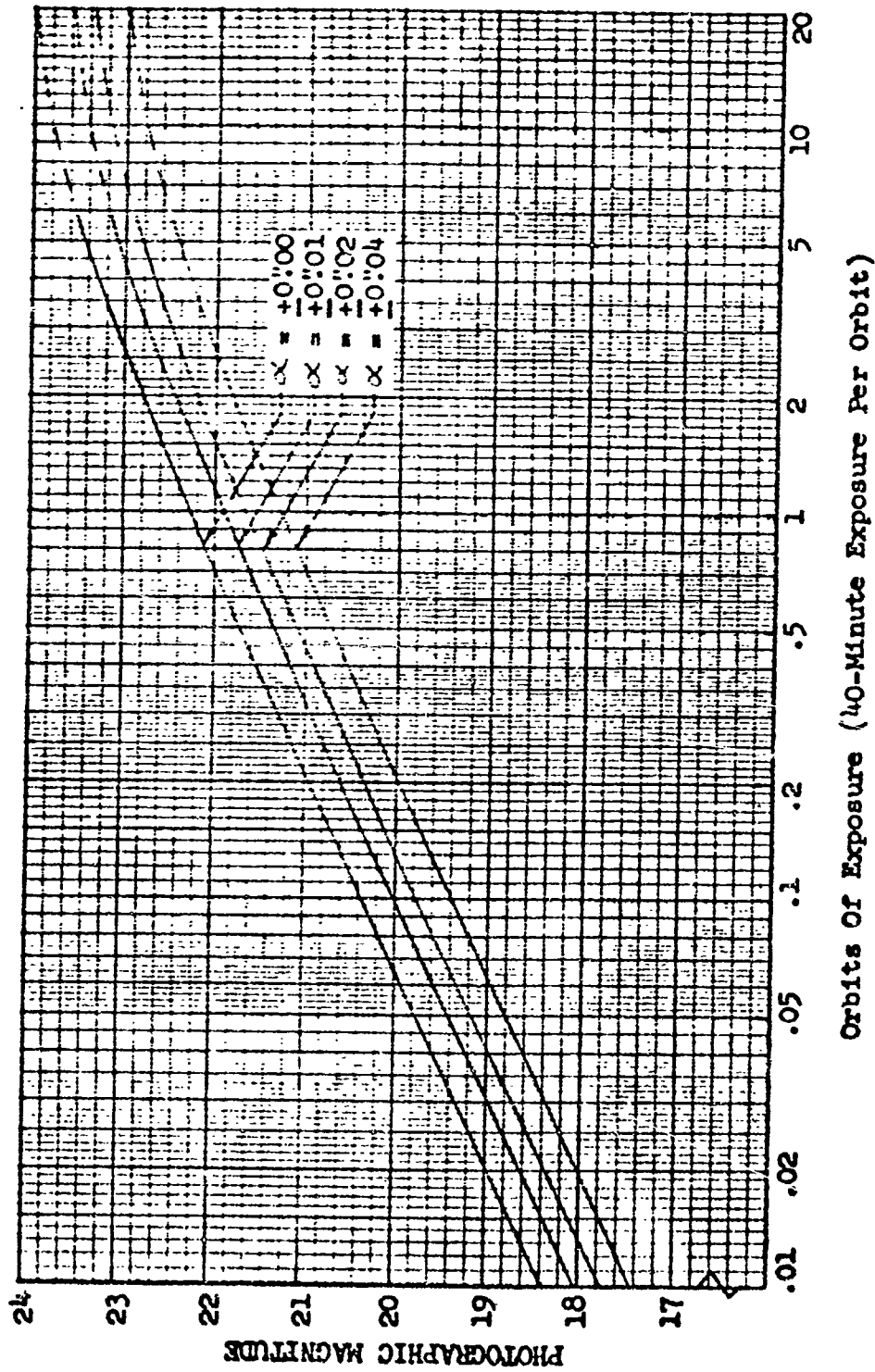


FIGURE 3-36 LIMITING PHOTOGRAPHIC MAGNITUDE AT $\epsilon_f/30$
 AS A FUNCTION OF EXPOSURE TIME FOR TYPE
 103 FILM WITH VARIOUS VALUES OF ATTITUDE
 STABILITY

3.7 DISCUSSION OF RESULTS.

Various aspects of the study will be presented in this section. These aspects influenced the selection of the optical system and the instrumentation, but for clarification purposes were omitted previously.

3.7.1 Optical System

Very early in the program the significance of selecting the focal ratio of the primary mirror became evident. An $f/2$ versus $f/4$ trade study was undertaken with the assumption that the most feasible focal ratio would fall within this range. This would also be sufficient to illuminate the problems associated with the selection. The problem was reviewed with respect to astronomical objectives, optical engineering, optical manufacture, structural design, and geometrical stability. Details of this study are presented in Boeing Document D2-84041-1. The results are summarized in Figure 3-37. As a result of this study, a decision was made to use an $f/4$ primary mirror in the configuration studies.

3.7.2 Optical Quality

The modulation transfer functions were computed in most cases using a value of $M = 0.9$ corresponding to 76 percent of the light falling in the central condensation of the Airy disk. This is the limit recommended by Conrady (P139). To obtain such performance would require the primary mirror to have RMS surface deviations of $\lambda/53$ or less. In view of the fact this is a very stringent requirement, it should be reviewed from the standpoint of manufacturing capabilities and the effect of coarser tolerances.

As to manufacture, the 84-inch Kitt Peak Telescope mirror is cited as reference. Schulte, in describing the test patterns of the 84-inch mirror, states, "Figure 4 is a set of four reproductions of knife-edge photographs through the null tester, showing progressive improvement of the figure on the indicated dates. For scale reference, the measured amplitude of the small ripples near the edge, as they appear on the second photograph, was not more than $1/8$ wave." Photographs of tests taken after further polishing had been done on the mirror indicated considerable smoothing but with some of the $1/8$ wave ripples ($RMS \sim 1/40$ wavelength) remaining.

This mirror is evidently close to the ultimate MOT surface quality. However, the Kitt Peak mirror is solid quartz whereas the one anticipated in the MOT is a lightweight beryllium type. Dr. Baker believes that for a mirror of this type, it would be more realistic to expect an $RMS \sim 1/20$ of mercury green wavelength.

How does this affect the performance? Review of Figure 3-31 indicates an $RMS \sim \lambda/20$ of the primary would give ~ 53 percent light in the Airy disk, which is a modulation ~ 0.6 . Using Figure 3-32, the resolution is estimated at ~ 0.07 arc seconds. Now the detectivity curve shown in Figure 3-32 is for objects with a contrast ratio of 100 or 5 magnitudes. Assuming the sky background to be equal to 23.75 magnitude would indicate resolution of 0.07 arc seconds could be expected for stars of 18.75 magnitude or brighter. Since most of the astrometric photography will be 14th magnitude or brighter, this optical quality would be usable.

For planetary photography the contrast ratio is in the order of three. The effect of this is to change the detectivity curve to a value approximately twice what it

FIGURE 3-37 - $f/2$ VERSUS $f/4$ PRIMARY MIRROR TRADE STUDY SUMMARY

<u>TECHNICAL AREAS</u>	<u>TRADE FACTORS</u>	
	<u>$f/2$</u>	<u>$f/4$</u>
1. Astronomical Observation Requirements	Not dependent on primary mirror focal ratio	
2. Optical Alignment Tolerance - Secondary Mirror		
Tilt		$3 \times f/2$
Lateral Displacement		$10 \times f/2$
Longitudinal Displacement		$4 \times f/2$
3. Optical Manufacture		
Difficulty to Manufacture	$8 \times f/4$	
Cost	$3 \times f/4$	
Time	$3-6$ yrs	$1-3$ yrs
(All-out, cost-doesn't-count-effort)	$2-4$ yrs	
4. Structural Design		
Complexity	Slightly less	
Length	571 in.	650 in 670 in (telescope design)
5. Geometrical Stability		
Temperature Distribution		
Deep space observation along inner tube radially	$2 \times f/4$ (gradients) (no significant difference)	
Venus observation along inner tube		
sunlit side	$4 \times f/4$ (gradients)	
cold side	$7 \times f/4$	
Radially		
sunlit side	$1.3 \times f/4$	
cold side		
Temperature Gradient Limit	In all cases, higher for $f/4$	
Primary Mirror Thermal Distortion	$464 \times$ limit	$528 \times$ limit

is now. This in turn increases the angle that can be resolved by a factor of ~ 2 .

3.7.3 Summary of Recommended Telescope and Instrumentation

In summary of the results of this section, the observational requirements can be met by the following telescope system and scientific instrumentation:

Telescope System

Aperture	120 inches
Primary f/number	f/4
Effective f/number	f/15 and f/30
Ritchey-Chretien Type	

Wide Field Photography (at ef/15)

Plate scale	4.38 sec/mm
Field of View	3.9' (without corrector) - 1/2° (with corrector)
Format	16 x 16 inches
Limiting Magnitude	26
Resolution	0''.1

Narrow Field Photography (at ef/30)

Plate Scale	2.19 sec/mm
Field of View	2' (without corrector)
Format	2 x 2 inches
Limiting Magnitude	27
Resolution	0''.06

High Dispersion Ultraviolet Spectrometer (at ef/15)

Grating and Blaze Wavelength	= 1200 $\text{\AA}/\text{mm}$; 1200 \AA , 3000 \AA
	= 600 $\text{\AA}/\text{mm}$; 1200 \AA , 3000 \AA
Linear Reciprocal Dispersion	at $\lambda = 1200 \text{\AA}$ $\lambda = 3000 \text{\AA}$
with 1200 $\text{\AA}/\text{mm}$ grating	$K = 10.2 \text{\AA}/\text{mm}$ $K = 11.1 \text{\AA}/\text{mm}$
with 600 $\text{\AA}/\text{mm}$ grating	$K = 20.4 \text{\AA}/\text{mm}$ $K = 20.6 \text{\AA}/\text{mm}$

Spectral resolution

Modulation of 0.04 for resolution of 0.13 \AA at 3000 \AA

Modulation of 0.32 for resolution of 0.13 \AA at 1200 \AA

High Dispersion Spectrograph (at ef/30)

Grating and Blaze Wavelength	= 600 $\text{\AA}/\text{mm}$; 4000 \AA , 5000 \AA , 6000 \AA , 7500 \AA
Linear Reciprocal Dispersion	$K = 3.67$ to $4.05 \text{\AA}/\text{mm}$
Spectral Resolution	$< 0.1 \text{\AA}$
Limiting Magnitude	~ 16

High Dispersion IR Spectrometer (ef/30)

Grating	Mosaic of four echelette gratings; two with 600 ℓ/mm and a 250 ℓ/mm , a 100 ℓ/mm
Blaze Wavelengths	0.85, 1.7, 4.5, and 10 μ
Spectral Resolution	1-2 waves/centimeter

Low Dispersion Ultraviolet Spectrometer (ef/15)

Concave Grating	600 ℓ/mm and 300 ℓ/mm
Blazed Wavelength	1500 \AA and 3000 \AA
Linear Reciprocal Dispersion	60 $\text{\AA}/\text{mm}$, 200 $\text{\AA}/\text{mm}$ and 1000 $\text{\AA}/\text{mm}$

Low Dispersion Spectrograph (ef/15)

Concave Grating	600 ℓ/mm and 300 ℓ/mm
Blazed Wavelength	5000 \AA
Linear Reciprocal Dispersion	60 $\text{\AA}/\text{mm}$, 200 $\text{\AA}/\text{mm}$ and 1000 $\text{\AA}/\text{mm}$

Photoelectric Photometry (ef/30)

<u>Wavelength</u>	<u>Photometer Aperture</u>	<u>Angular Resolution</u>
5000 \AA	0.001 inch	0.'' 05
10 μ	0.02	1.'' 0

4.0 OPERATIONAL ANALYSIS

4.1 BASIC TELESCOPE CONCEPT

The basic approach used to examine methods of operation and design problems was first, to generate a telescope baseline configuration which included all the basic optical and experiment subsystems and associated structural support and then, to incorporate modifications as required to satisfy the varying functions and design requirements defined for the different operational concepts being considered. Conceptual design work was tailored to generate the technical data required to conduct engineering and operational analyses. These analyses provided the basis for establishing design feasibility and for evaluating the alternate conceptual candidates.

Major design factors include requirements and constraints associated with the telescope optical systems, experiment equipment, crew accommodations, launch vehicle, and orbital operations. Orbital operation requirements cover vehicle rendezvous and docking, maintenance; space environments, such as temperature, micrometeoroids, and radiation; and the vehicle performance needed for astronomical observations. The two requirements associated with vehicle performance that were considered critical feasibility problem areas are the thermal control necessary to maintain the precise optical geometry of the telescope, and the attitude stability needed to attain the diffraction limited performance of a 120-inch telescope.

The telescope optical geometry and the cabin for housing the experiment equipment at the Cassegrainian focus are the dominating design requirements which govern the shape and size of the basic MOT configuration. Launch loads, thermal control requirements, and the servo elastic requirements are the most critical items governing structural design. Both the long operational life for the MOT (3-5 years) and the desired versatility for conducting various types of optical experiments impose many requirements for men to set up experiments and to perform maintenance while in orbit. These requirements call for unique design and installations due to man's limitations while working in zero gravity and in a spacecraft.

Most of the study effort covering subsystems was devoted to the two systems related to the critical feasibility problem areas, which are the thermal balance and control and the attitude stability and control. The other subsystems, such as electrical power, communications, and propulsion, were reviewed and were found to have requirements compatible with those systems which are being considered for space flight in the time period prior to operation of the MOT. Study effort on these systems was therefore limited to identifying a typical system and installation which may be required for the MOT operational concepts. These data were primarily needed for weight statements, installation volume requirements, and for defining electrical power requirements.

The original baseline telescope configuration used in the initial phase of the MOT study utilized the f/2 primary mirror design previously developed by the Fecker division of the American Optical Company. This baseline is depicted by Configuration A of Figure 4-1. The only significant changes to the Fecker design are the addition of the pressurized cabin to house the experiment equipment at the Cassegrainian focus and the addition of the telescope doors.

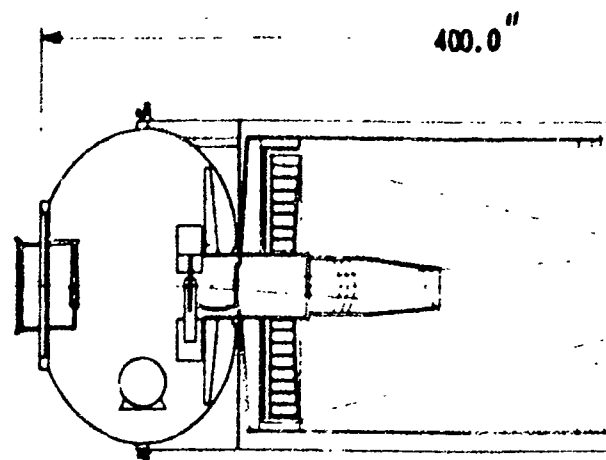
Configuration B is the initial baseline of an $f/4$ primary mirror telescope generated by Boeing, which is very similar to the $f/2$ concept, except for the additional length. An extendable or telescoping-type structure supporting the secondary mirrors was used to attain the additional length in the orbit configuration while retaining a minimum height in the launch configuration. This configuration was used to initiate thermal and attitude stability control analyses and to generate conceptual designs for examining the alternate methods in which the telescope can be operated with the MCR.

Configuration C was generated midway in the study and the geometry and mass characteristics of this design were used for the completion of the attitude stability control analysis and associated structural servo elastic analysis, plus the completion of the thermal analysis. The major change in this design, compared to Configuration B, is a fixed support structure for the secondary mirrors. This change was initiated to eliminate the telescoping or erection of the secondary mirror section in orbit and to drop the requirement to conduct experiments at the prime focus. The latter requirement change, plus the use of pyramid-type doors located adjacent to the secondary mirror support, made it possible to keep the overall height of the $f/4$ telescope within acceptable limits without using an extendable-type structure for support of the secondaries.

Configuration D depicts the final design study iteration of the MCT, which incorporates conceptual designs developed in the following subsystem areas:

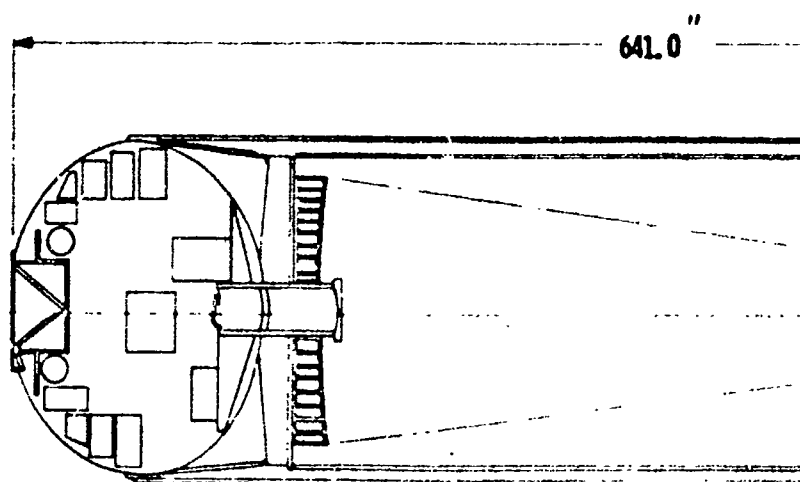
1. Cabin arrangement and experiment installation requirements
2. Secondary mirror installation and alignment control systems
3. Thermal control
4. Miscellaneous subsystem equipment installation, such as star tracker, reaction control jets, solar panels, communication antennas, etc.

Major design changes which affected the configuration geometry are the altered cabin and addition of an earthshade. Installation of large pieces of experiment equipment, such as the high dispersion visual spectograph, led to the selection of a cabin design consisting of a cylinder with flat bulkheads, rather than the elliptical pressure dome design used on the initial baseline. The earthshade, which is an extendable cylindrical structure at the open end of the telescope, was incorporated to stabilize temperatures in the area of the secondary mirrors, the primary mirror, and the telescope doors. Detail descriptions of the final baseline telescope configuration and conceptual operational designs for the final two modes of operation are presented in Section 5.



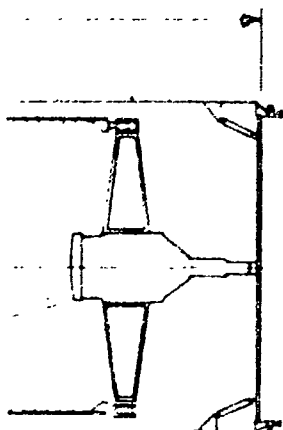
A

f-2 PRIMARY MIRROR INITIAL COI

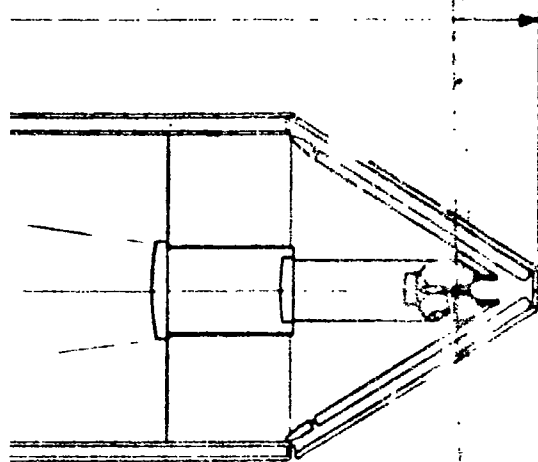


C

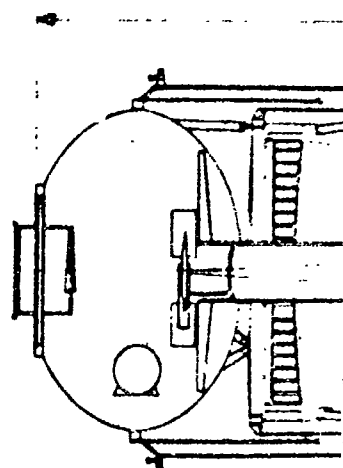
f-4 PRIMARY MIRROR FIXED OF
SYSTEM STRUCTURE - PYRAMID



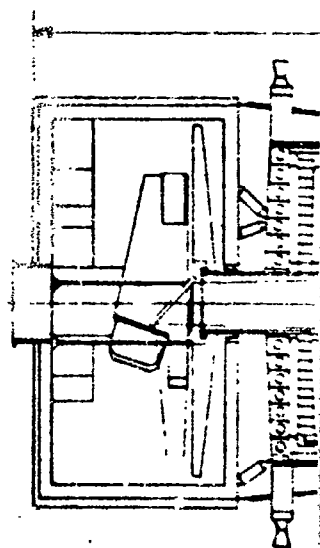
FIGURATION



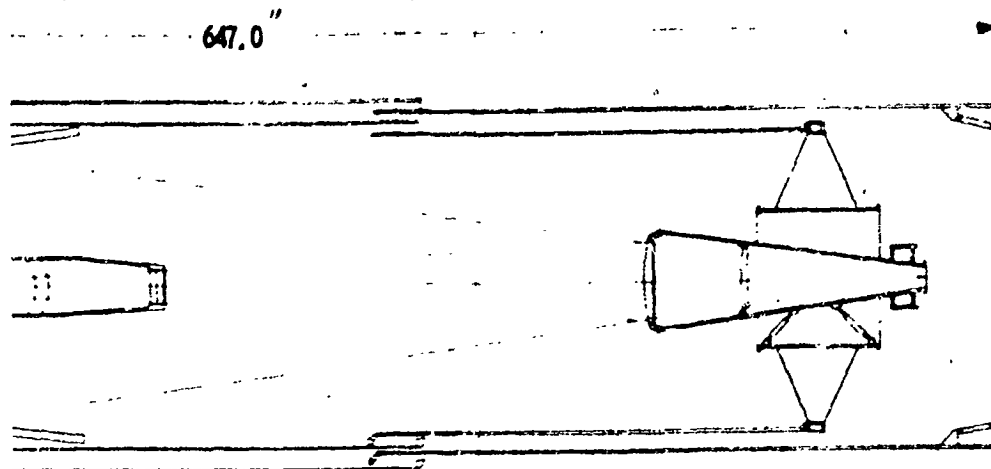
TICAL
DOORS



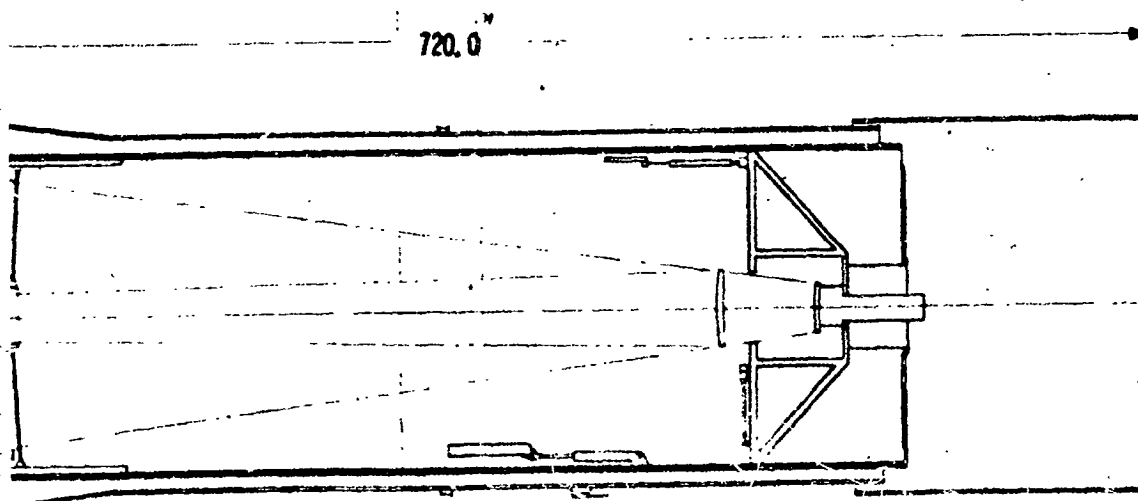
B



D



1-4 PRIMARY MIRROR EXTENDABLE
OPTICAL SYSTEM STRUCTURE



1-4 PRIMARY MIRROR FIXED OPTICAL
SYSTEM STRUCTURE - EXTENDABLE EARTH SHADE

FIGURE 4-1
EVOLUTION OF 120 INCH MOT CONFIGURATIONS

4.2 APPROACH & STUDY DEVELOPMENT

The approach used in this operational analysis was to identify the significant problem areas concerning the role of man in the MOT operations and to compare the relative advantages or disadvantages of the various operational modes. Consideration was given to man's capabilities and limitations in the space environment and their effect or constraints on the laboratory equipment and telescope design. Further evaluation included the comparison of man's ability to perform the necessary tasks and the comparisons of timeline analyses for each of the various modes. In addition to evaluation of man's role and the timeline analyses, sufficient data was generated in the areas of technical risk, operational capability, and constraints on the MORL, to allow valid comparisons.

The study was conducted for three basic modes of operation, with variations of each of these modes as depicted on Figure 4-2 and described below.

MODE I - The telescope is docked and then permanently attached to the laboratory for all subsequent operations. The rigid couple and the gimballed couple were considered as alternate designs in this mode.

MODE IA - Rigid Couple - The telescope is launched separately and, after docking to the MORL, is permanently coupled to the laboratory for all operations. Attitude positioning and stabilization is accomplished by the entire MORL/MOT combination. Environmental control and electrical power is provided by augmented MORL subsystems.

MODE IB - Gimballed Couple - This approach retained a rigid attachment to the MORL, yet partially decoupled MORL disturbances from the telescope optical systems through the use of a two-axis gimbal support. The angular travel within the gimbal is limited to ± 0.5 degrees which is compatible to the MORL attitude control subsystem. For large angular changes of the telescope, the gimbals are locked and the MORL/MOT combination slewed to the desired attitude. For this mode, too, electrical power and environmental control are supplied from the MORL.

MODE II - The telescope is docked and rigidly attached to the laboratory for experiment setup and maintenance functions, but decoupled for those operations associated with astronomical observations. Mode II alternate system approaches included the tether system, the floating socket, and intermittent remote controlled docking without a physical attachment.

MODE IIA - Tether System - This approach was simply the attachment of an umbilical tether when the telescope is decoupled from the MORL. Electrical power and environmental control are supplied by the MORL.

MODE IIB - This approach to intermittent coupling utilizes a floating socket mechanism as the inter-connection. This mechanism permits complete separation from the MORL disturbances during observations but prevents separation beyond the confines of the socket. During observations the MORL is maneuvered to stay clear of the telescope.

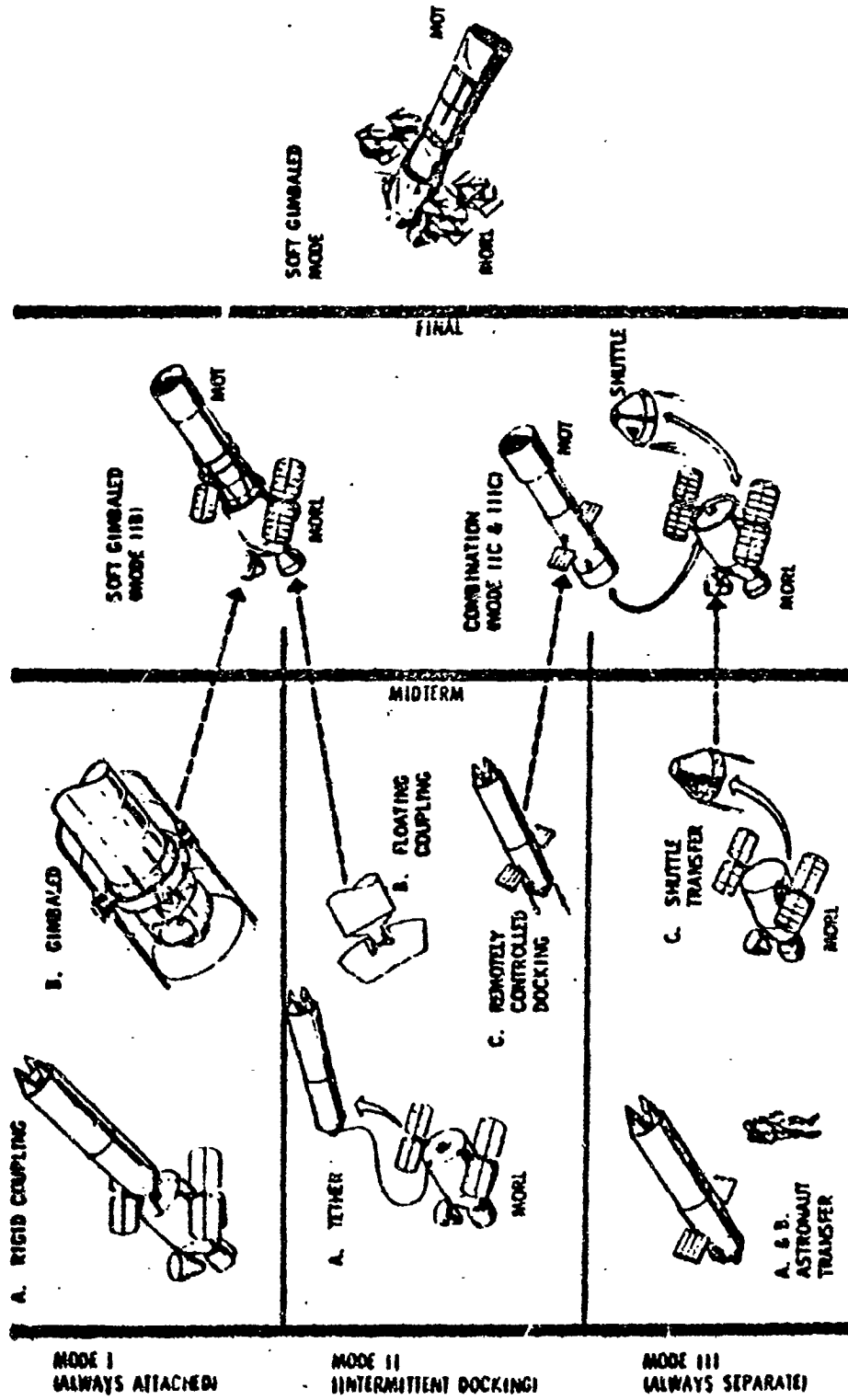


Figure 4 - 2: Evolution of Operational Modes

MODE IIC - Remote Controlled - In this mode, the telescope is completely decoupled from the MORL with no physical restrictions to limit the separation distance. A remote control system in the MORL is used for initial rendezvous and docking, as well as the repetitive dockings required before and after the observation functions. Electrical power and environmental control are provided by the MORL when coupled, but the telescope is also provided with an independent electrical and environmental system for its uncoupled operation.

MODE III - The telescope is placed in orbit near the laboratory and is operated in a separated position at all times.

MODE IIA - Astronaut Transfer - Man travels to the telescope and performs all functions in a pressurized spacesuit. The MOT contains its own electrical power and orbit keeping systems.

MODE IIIB - Astronaut Transfer - Man travels to the telescope in a pressurized spacesuit but works within a pressurized cabin in a shirtsleeve environment. The MOT contains its own electrical power, environmental control, and orbit-keeping systems.

MODE IIIC - Shuttle Vehicle - The MOT remains in the vicinity of the MORL and man utilizes a shuttle vehicle for transfer. The shuttle vehicle provides a shirtsleeve environment during transfer and also provides MOT cabin pressurization and orbit keeping when docked. The MOT contains its own electrical power and thermal control systems.

The first phase of the study, up to the midterm report, was devoted primarily to generating sufficient data to conduct a comparative evaluation and rating of these eight modes of operation to provide a basis for a selection of the two most promising approaches. The principle weighing factors considered were:

- o Technical Risk - The probability of systems not meeting design or operational requirements in the specified environment by the specified time period.
- o Operational Capability - The assessment of relative observation time, reliability and safety, flexibility and versatility, and man's ability to perform the assigned tasks.
- o MORL Interface Constraints & Requirements - The consideration of the constraints imposed on the MORL by the MOT for each mode of operation in the areas of design, function, subsystems, and man's operation.

Further discussion of the evaluation criteria, the considerations affecting the ratings, and the conclusions are included in Document D2-84041-1. At the midterm of the study, the two recommended modes were IIB, the floating socket as an attached concept, and a hybrid between Modes IIC and IIIC, which considered the shuttle vehicle for frequent short duration trips in conjunction with the capability of docking the MOT to the MORL for longer duration maintenance requirements.

The hybrid mode was considered to be an acceptable concept for the remote or detached operation, but continued design study was deemed necessary to resolve

the problems associated with the floating socket concept. At the midterm review, the relative rating for technical risk assigned to the floating socket was considered to be optimistic. The attitude control and reaction jet and propulsion subsystems would be required to operate often to keep the MOT within the floating coupling and maintain the stationkeeping limits. Because of this constraint and the addition of complexity to the MORL subsystems, further design study of a close couple mode resulted in the "soft gimbal" concept, which provided sufficient attenuation of the MORL disturbance forces to overcome the technical risk associated with the conventional gimbal designs.

These two modes were then evaluated to arrive at the final selection for the final phase of the study.

4.3 OPERATIONAL DESCRIPTION OF THE TWO FINAL MODES

4.3.1 Soft Gimbal Mode (Boeing Model No. 946-41C)

4.3.1.1 Launch

The launch vehicle for the MOT will be the Saturn IB. The MOT will be mounted within an adapter and fairing similar to the Apollo LEM adapter. Access to the MOT cabin area on the launch pad will be provided through an access door in the adapter and a door in the side of the MOT cabin, which will be bolted and sealed prior to launch. These doors are sufficiently large to permit removal of the high dispersion spectrograph, which is the largest single piece of equipment in the cabin.

In order to withstand the severe vibration environment during boost, inflatable bladders will be used for supporting the primary mirror, to prevent the introduction of stresses.

During the launch of the MOT, the outer fairing will be jettisoned to maximize the payload capability in orbit. The nose cone and the outer fairing will be separated and jettisoned after the end of first stage burnout. The vehicle will remain in this configuration through burnout of the S-IVB stage, after which separation will occur. Figure 4-3, launch profile, illustrates the parts jettisoned and the general sequence of operations through the boost profile.

The MOT is launched into an elliptical orbit of 250 nautical miles apogee and 80 nautical miles perigee. This type of orbit permits the use of a Hohman transfer for purposes of rendezvous with the MORL. The orbit injection engine, guidance and control equipment, and associated propulsion systems on the MOT are used to perform the transfer. Ground control will be in command of the MOT during the catchup orbit and will initiate the final Hohmann transfer. After the MOT is placed within approximately ten to fifteen nautical miles of the MORL, control will be transferred to the MORL crew for final rendezvous and docking.

4.3.1.2 Rendezvous & Docking

After the MORL crew acquires control of the MOT, the MOT reaction control propulsion system will be used for making the final orbital adjustments prior to docking. Visual as well as radar systems can be used to aid in making the final maneuvers. Docking will be accomplished at the large end of the MORL near the 3-man airlock. The MORL must be modified in this area to provide a transfer tunnel, an Apollo-type docking receptacle, and attach points for the supports from the MOT gimbal. The initial rendezvous and docking operation is the same as for the remote mode, and is discussed in Section 4.3.2.2.

4.3.1.3 Deployment

After the MOT and MORL have docked, a permanent attachment is made between the MOT and MORL. Figure 5.2-3 illustrates the orbital arrangement and Figure 4-4 the struts being attached by the MORL crew. These struts provide a rigid connection between the MORL and the MOT gimbal support structure. In addition, boost support structure

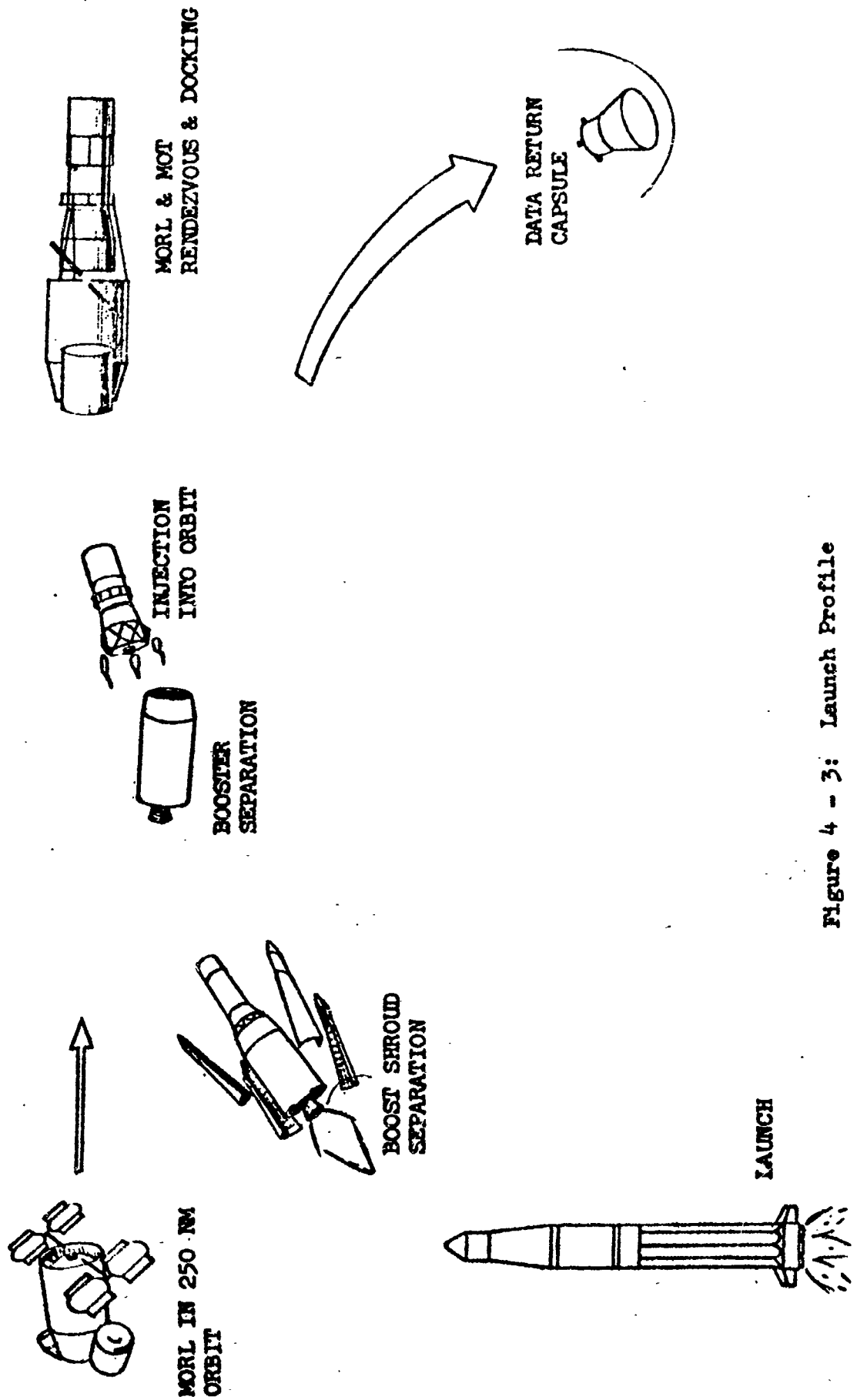


Figure 4 - 3: Launch Profile

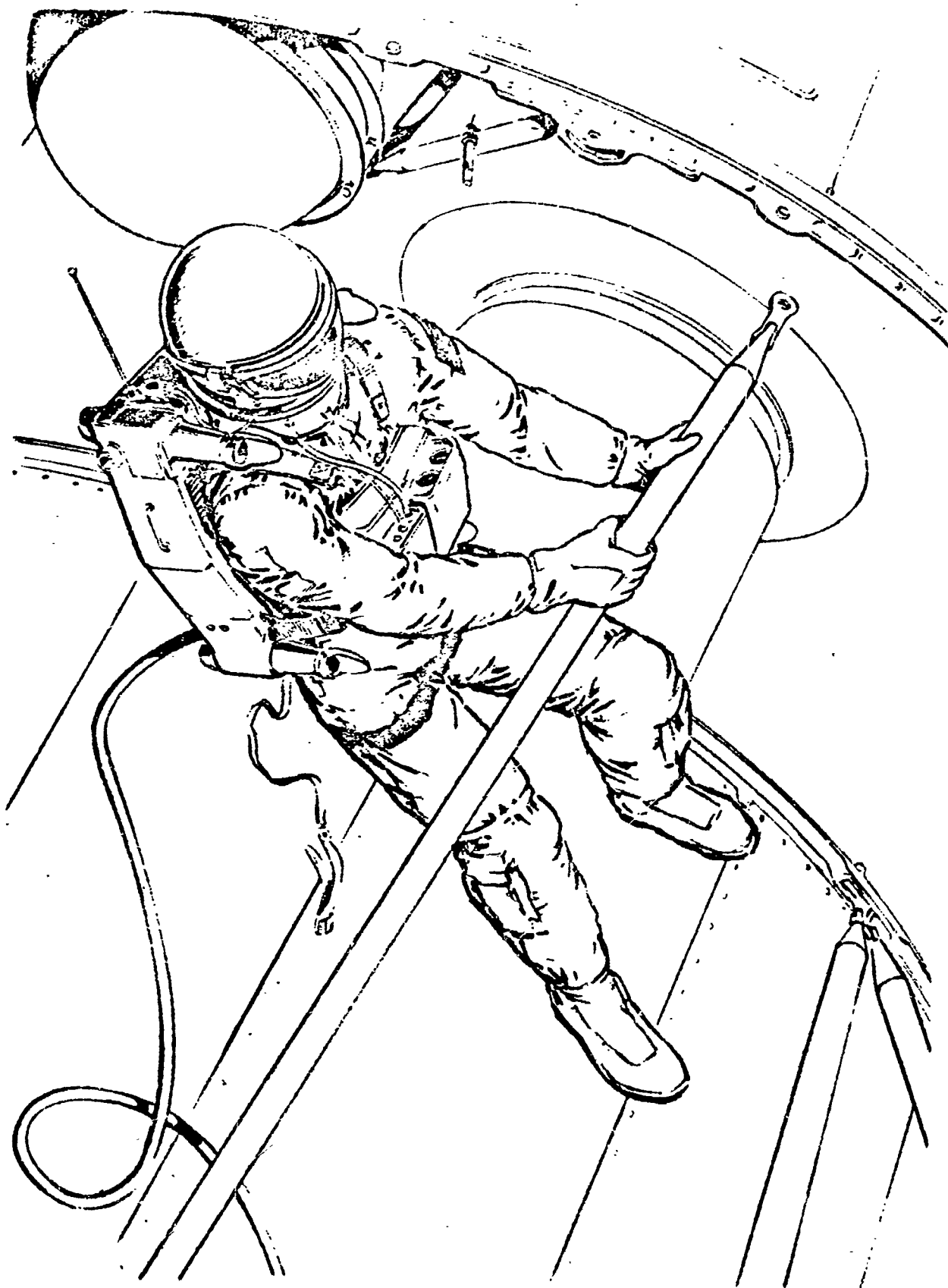


Figure 4 - 4: Extravehicular Assembly Operations

used to support and stabilize the gimbals and spring suspension system during launch must be removed. A mechanism used for making rigid the MOT/MORL during orbit will then be actuated.

The telescoping crew tunnel on the MORL is sealed at the MOT cabin interface, the docking cone removed, and umbilicals connected in the tunnel. The cabin is then pressurized from the MORL systems, allowing shirtsleeve entry into the MOT cabin.

4.3.1.4 Setup, Checkout, & Alignment

Setting up the telescope to its orbital configuration from the launch configuration is begun after the MOT is docked to the MORL. This conversion involves the participation of man and requires operations extravehicular as well as within the pressurized MOT cabin. Removal of boost structure and supports, installation of orbital supports, alignment and checkout of the mirrors, checkout of all actuation sensors, etc. are activities which will be accomplished in the space environment. Man restraint provisions will be located at those areas where manual tasks are to be conducted.

The highly critical nature of the optical elements requires special supports and restraints to withstand the severe boost environment. These supports will be removed and orbital supports attached. The inflatable restraint bladders installed around the primary mirror during boost will be depressurized and allowed to contract as described in Section 5.

After the boost supports are removed, the primary mirror will be attached to the three point tangent bar supports. If possible, this function will be done automatically; however, man must be able to back up the automatic system. If a crewman is required to accomplish this attachment it will be necessary for him to work inside the telescope and in front of the mirror. A similar task is required in the area of the secondary mirror cell where boost support structure must be removed for the mirror as well as the servo positioners which are used for optical control. Figure 4-5 illustrates man working on the telescope in space.

Scientific instrumentation in the cabin is aligned on the ground prior to launch. This is mounted in place on an instrument mounting base or platen which is rigidly connected to the primary optics. In orbit, the man must make a final adjustment of these elements so that an optical alignment can be accomplished. Figure 4-6 shows the cabin arrangement and arrangement of the scientific optical equipment. Autocollimating type alignment units are used for both initial alignment and for checking the alignment of the entire optical system. Two folding mirrors, shown on Figure 4-6, are used to allow the use of both the $f/30$ equipment and $f/15$ equipment. The first mirror is used for folding the $f/15$ light directly into the instrument package. The $f/30$ light is folded to a rotating mirror which in turn folds the light to the applicable instrument.

Optical checkout and alignment must be accomplished for the telescope in thermal equilibrium at operational temperature. The autocollimating and alignment unit will be carefully aligned to the primary mirror itself. A check of this will be made in orbit. Once it is verified that the autocollimating unit is aligned with the primary mirror, it will be used through the folding mirror to align the secondary mirror. Using the autocollimating unit, the secondary mirror will be positioned vertically and laterally to the correct position. This will serve to zero the positioners used for maintaining the secondaries in the correct position. After vertical

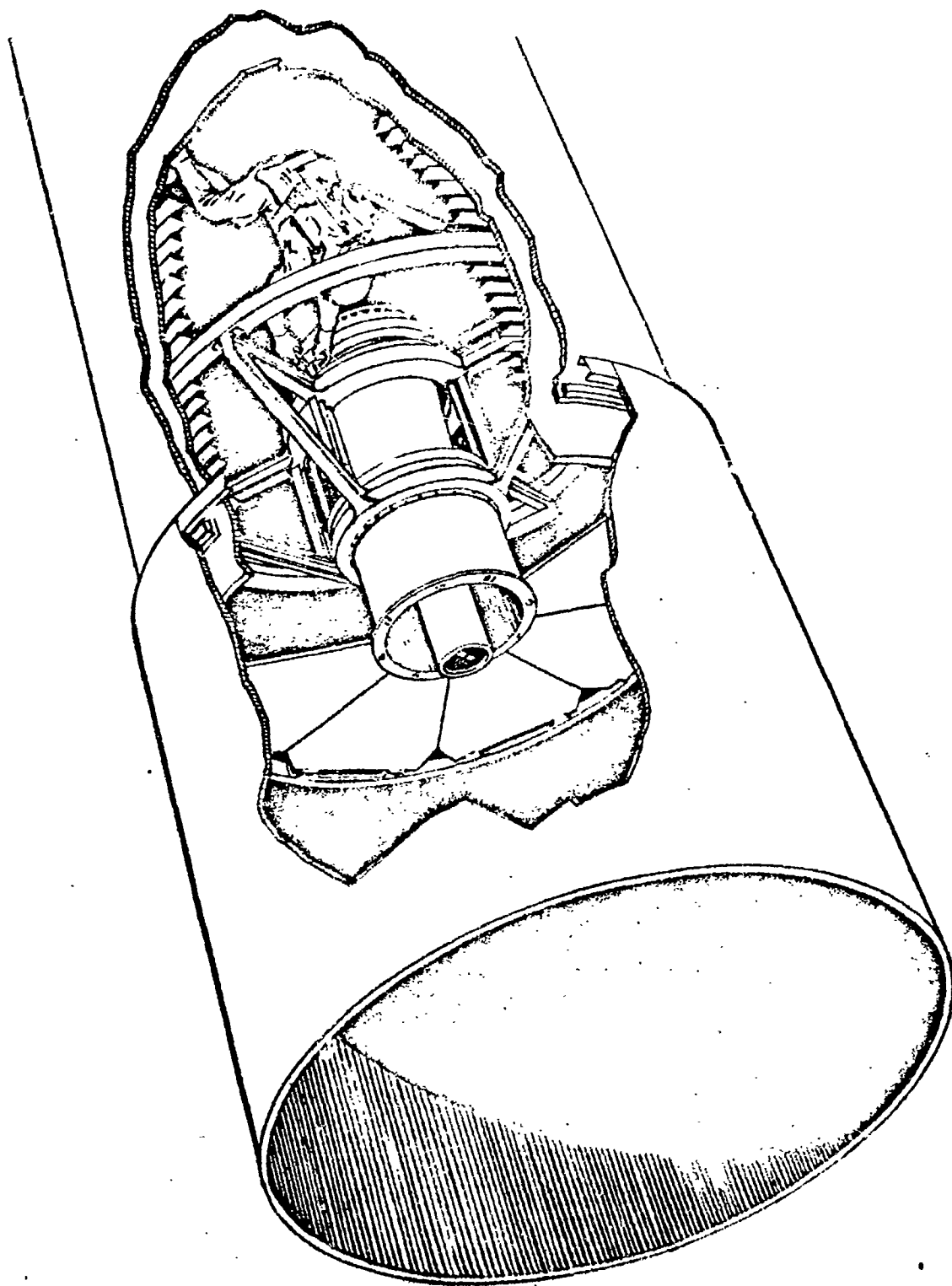


Figure 4 - 5: Extravehicular Checkout Operations

and lateral positioning, the tilt of the secondary mirror will be checked with the autocollimator in a similar manner. The remaining axis to be checked is the longitudinal position of the secondary, which determines whether or not the system is in focus. Figure 4-6 illustrates the man at the display console which will include those controls and displays required for optical and subsystem checkout readings. In addition, much of the information from the MOT will be displayed and checked out remotely from the MORL. Electrical power for the soft gimbal mode will be provided by the MORL systems. The MOT is operated normally with the cabin depressurized. MOT cabin atmosphere is pumped into a low pressure tank and stored until later pressurization is desired to conserve expendables.

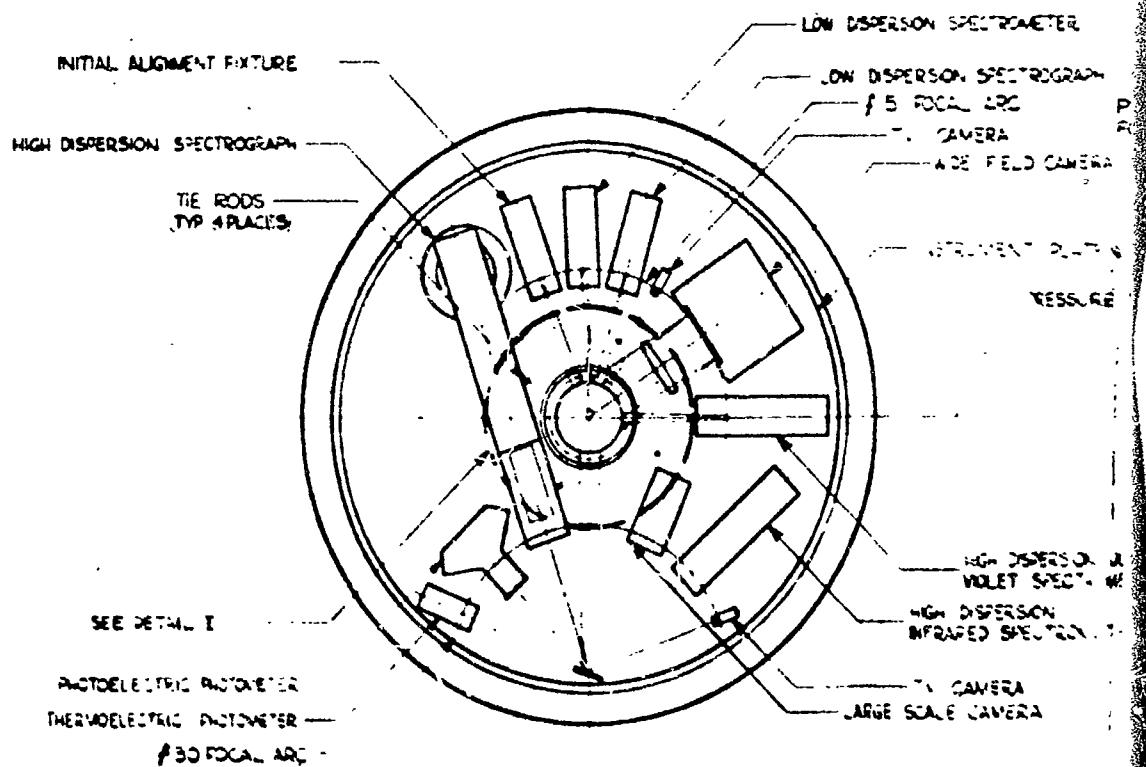
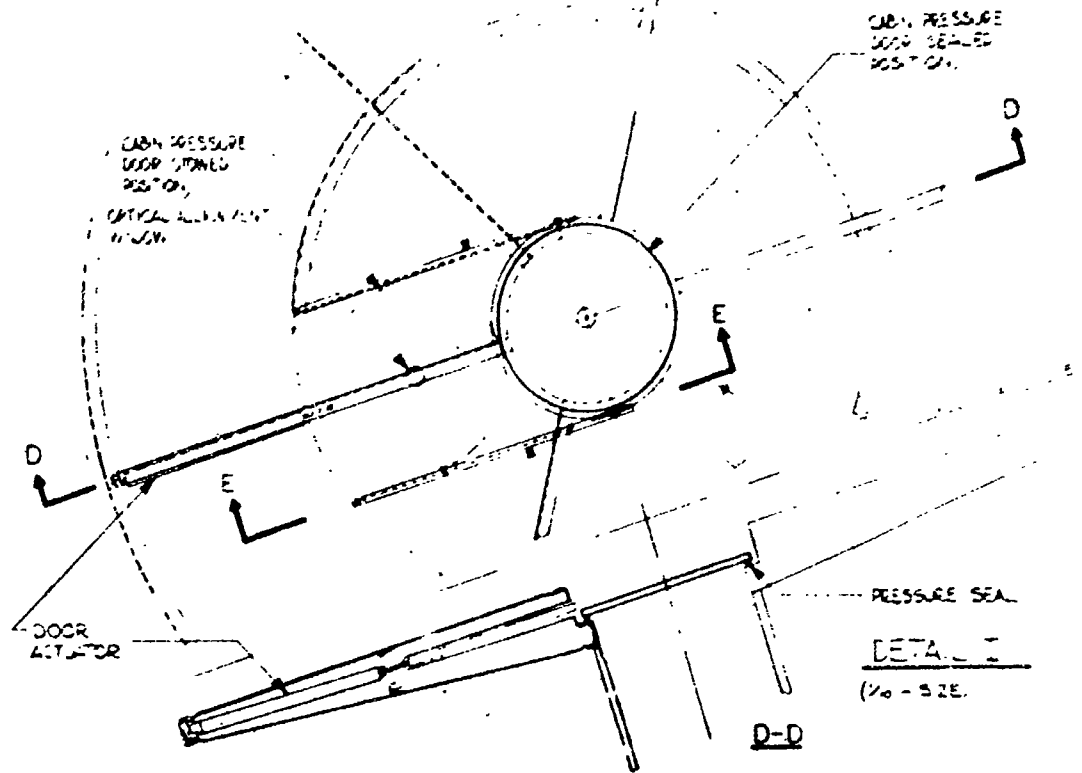
4.3.1.5 Operation

The operation of the MOT in the soft gimbal mode requires that the MORL basically assume the orientation of the telescope. There is a rigid coupling between the MOT soft gimbal support structure and the MORL. A spring suspension and a two-axis gimbal allows approximately $\pm 1/2$ degrees angular travel. In order to position the MOT for observation, the MORL crew will remotely lock out the MOT gimbal and spring suspension system and slew the combination of MORL and MOT into the desired inertial attitude. When the combination of MOT and MORL is positioned to the target area within a range of $1/2$ degree, the tunnel is retracted, the MOT gimbal is released, and the fine stabilization and guidance system of the MOT perform the final attitude positioning of the MOT.

For normal operation, the telescope will always point 90 degrees or greater to sunline, which means that the telescope will be looking into deep space. The telescope doors are closed to prevent the telescope from viewing the Earth's surface or atmosphere during the daytime periods of each orbit. The door actuators must be very reliable since they may be operated approximately 16 times per day for between 3 and 5 years. Access to the main part of the telescope by man will be made by using one of the telescope doors for entry and exit. Once inside, optical surfaces will be covered and the telescope doors will be closed to provide a controlled environment and protection for man. These doors serve as meteoroid and radiation shielding for the man and permit a controlled lighting environment.

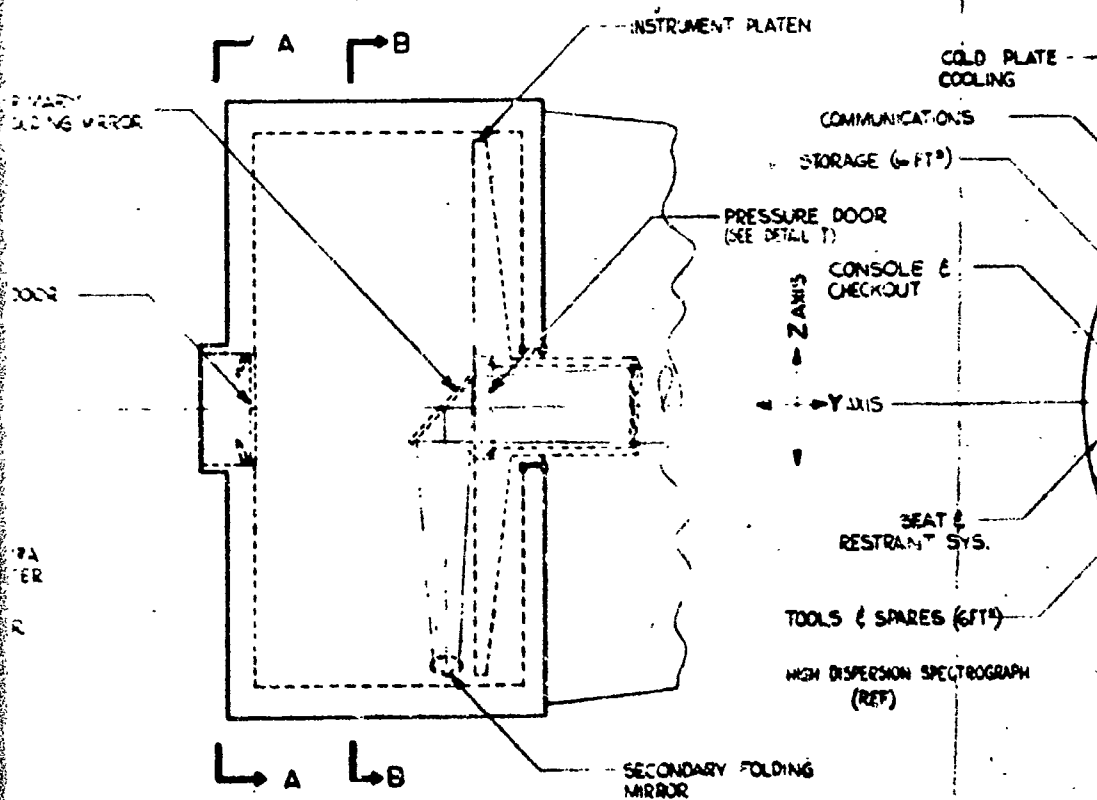
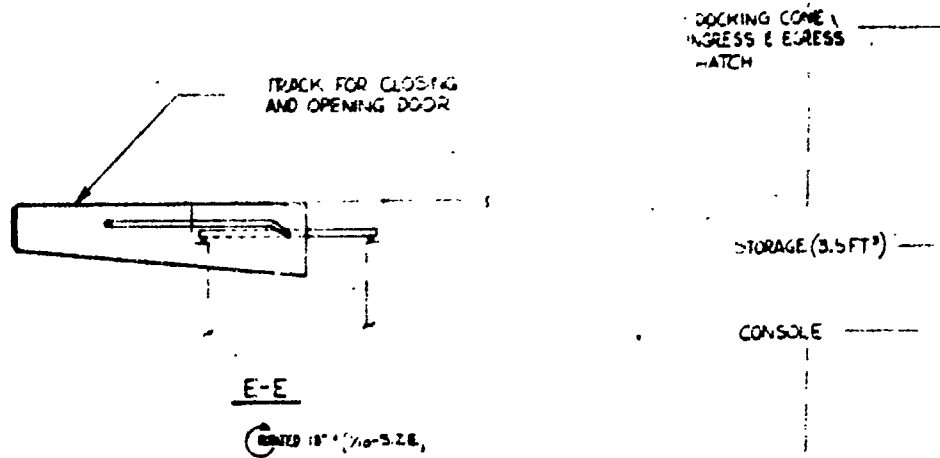
Using reference stars, the MOT/MORL will be slewed to the proper orientation. This gross positioning can be done using the MOT coarse mode reference system to command both the MOT and MORL control torques. With the MOT/MORL pointed at the target area well within the $1/2$ degree, the MOT/MORL soft gimbal system is activated. The man in the MORL could then use a TV monitor to observe the telescope stellar pattern. He could select the target star or offset guidance star from the pattern using a map-matching technique, and remotely command the MOT to position the guiding star in the proper orientation. When the target or guiding star is positioned as accurately as possible in this manner, it would automatically fall within the range of the fine guidance sensor. The attitude control system would subsequently provide the stabilization and pointing to the target.

Figure 4-6 shows the light path and the method of selecting any one of the $f/15$ or $f/30$ pieces of equipment. The elliptical folding mirror is mounted in a motor driven head and indexes from one instrument to the next. Exact alignment must be maintained in the new position. Stc's will be provided and indexed, but final adjustments will be required. The size of the elliptical folding mirror is dictated



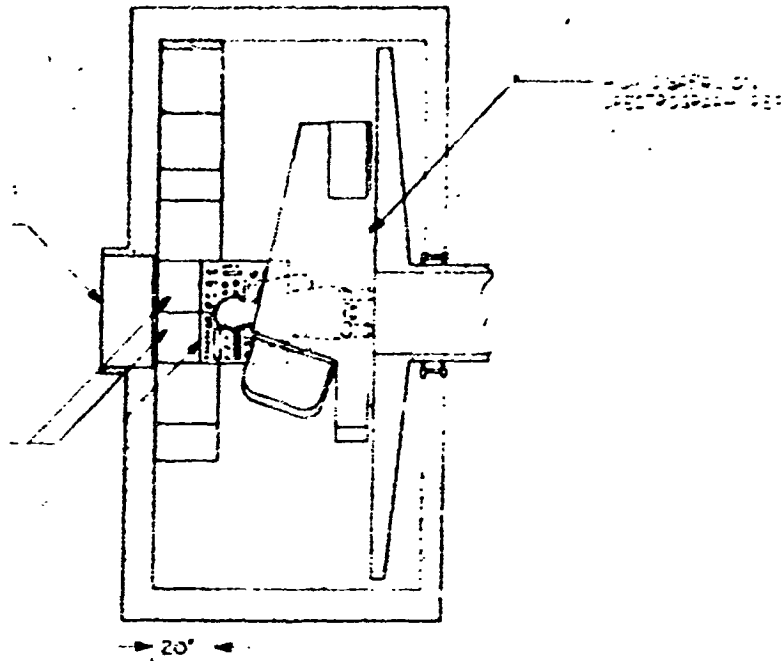
B-B
SCIENTIFIC INSTRUMENTATION

770

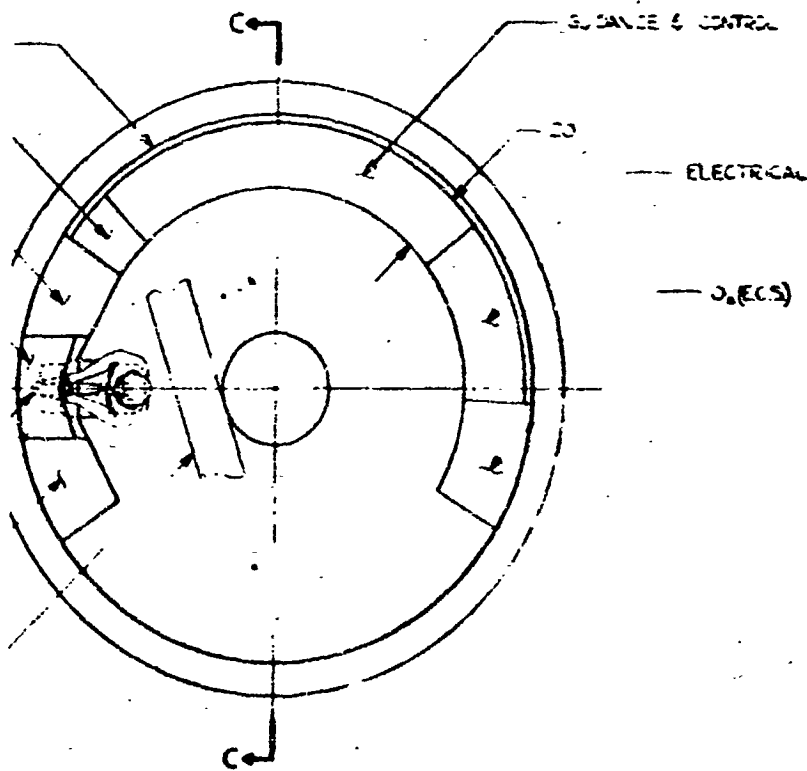


SIDE VIEW
SCALE 1/16" EXCEPT AS NOTED

SCIENTIFIC INSTRUMENTS



C-C



A-A

VEHICLE SUB/SYSTEMS

AND CABIN ARRANGEMENT
FIGURE 4-6

by the format for astrophysical photography which is approximately 16 x 16 inches. A high degree of remote control is required in the MOT operation. With the capability of remotely selecting various optical instruments, the number of trips required by man to the MOT cabin can be minimized. Remote commands will be utilized to advance the film from one frame to the next for such items as astrophysical photography, advancement of the film in the high and low dispersion spectrographs, and changing from one slide to another for astrometric photography. Manual operations in the cabin are anticipated to be primarily that of installing and removing film modules or packages and checkout of a new film package for proper functioning prior to automatic or remote controlled operation. Equipment, such as the photoelectric photometer and the spectrometers which utilize photoelectric sensing, must be turned on remotely from the MORL. The data from this equipment will be monitored and recorded in the MORL, then telemetered to the ground.

A remotely operated pressure hatch, shown on Figure 4-6, is provided between the cabin and telescope to allow pressurization of the cabin. The hatch includes a 3.0 inch-diameter optically flat window located in the center to permit a beam of light to penetrate into the cabin when the hatch is in the closed position. This capability allows for preliminary optical alignment checks of the folding mirrors and experiment equipment while the crewman is in the cabin. For normal telescope operation, the hatch is retracted and stowed. Final alignment and adjustments for astronomical observations will be accomplished by the man in his pressurized suit after the cabin is depressurized and the hatch retracted.

Figure 5.2-2 illustrates arrangement of the secondary mirrors and the method considered for changing from f/15 to f/30 operation. The f/15 secondary mirror is mounted on a hinged support to allow it to be folded out of the way and stowed along the inner surface of the telescope tube. After removal of the f/15 mirror, the f/30 mirror must be adjusted and its alignment checked before use. This function can be accomplished manually by the crewmen working in pressurized space-suits. Access to the inner telescope tube is accomplished through the doors at the open end. Hand holds, assist bars, and restraint devices will be provided to assure maximum protection for the crewman, the mirrors, and associated equipment within the telescope.

4.3.1.6 Maintenance

The conduct of maintenance is one of the important considerations in the role of man for the MOT system and is essential in orbit to maintain the telescope operation for the 3 to 5 year period. Equipment located both internal and external to the cabin will require periodic inspection and maintenance. Maintenance requirements have been considered at a gross level and time has been allocated for scheduled maintenance at reasonable intervals in addition to approximately 15 percent of the total time reserved for the unscheduled maintenance requirements.

Maintenance in the MOT cabin will normally be done in a shirtsleeve environment, although in event of a failure of the environmental control system or meteoroid puncture, it will be necessary for the crewmen to conduct the required repair in a pressurized suit. This places a constraint on the design and arrangement of the equipment. The approach will be to modularize the electronics and other subsystem components to various levels to make replacement of spare modules relatively easy.

Obviously all parts cannot be spared in orbit. More critical items such as electronic components, actuators, automatic servo positioners, and other items which require high frequency of use will be made as standardized units and adequate spares provided. When a module has been replaced, it will be taken to the MORL for repair and test.

Much of the optical equipment such as mirrors, gratings, filters, etc. are passive elements and not subject to wear. Items such as motors, solenoids, drive mechanisms, etc. are subject to failure and wearout and are more critical items. Actual hours of operation considered for the optical sensors is not large, therefore, reasonable periodic preventative maintenance should result in a low spares requirement.

Checkout will be possible from the MORL by means of the telemetry link. In addition, a display console in the MOT cabin will include monitoring displays and controls necessary for checkout and fault isolation.

When maintenance is required outside the MOT cabin, the crewman's activities will be monitored and assistance made available from within the cabin. Equipment items such as the star trackers, reaction control modules, door actuators, secondary mirror positioners, interferometers used for maintaining secondary mirror alignment, etc. require periodic servicing and maintenance and necessitate crew activity in the space environment. Provisions are required for crew locomotion and restraint. One concept of such equipment is illustrated in Figure 4-5. This is a movable seat and stirrup restraint device that is motor-driven and actuated to position the man in various attitudes in the area of the secondary mirror for maintenance purposes. The seat and stirrup provides three reaction points for taking out applied torques. The unit is mounted on a telescoping arm which has two pivots and is mounted in a 360 degree track. Electric motors with conveniently located slewing switches are used to move the man in a wide range of positions and attitudes. Four degrees of freedom are provided, and the unit may be locked in any desired position. Attachments such as containers for tools, spare parts, and other maintenance items can be attached to the side of the seat. This restraint and positioning device will be removable for repair or replacement and stowed out of the optical path when not in use.

4.3.2 Operational Description of Shuttle Mode (Boeing Model No. 948-43D)

The shuttle mode of operation, one of the two selected for further study, is the detached concept in which the MOT is maintained separate from the MORL for the astronomical observations. For this approach, a shuttle vehicle is used for the frequent short duration trips required between the MORL and the telescope and allows shirt-sleeve environment during the transfer. It includes the same docking provisions and mechanism as the Apollo logistics vehicle and can dock with both the MORL and MOT in the same manner. Stowage provisions for the shuttle are required on the MORL.

In this mode, the MOT will be launched unmanned and rendezvous and dock with the MORL for initial setup and preparation of the telescope for the astronomical program. When the MOT is ready for use, it will be separated from the MORL and will remain detached for extended periods of time. When crew activities, such as replacement of film or changing from one piece of optical equipment to another, are required, a shirtsleeve crew transfer into the shuttle is accomplished. After

checkout of the subsystems, the shuttle traverses to the MOT and docks. The MOT cabin pressurization is provided by the shuttle. When the cabin has been pressurized the entry hatch is removed and the crewmen can then conduct the required task. If egress to space is necessary, the shuttle serves as an airlock in the loop.

For the shuttle mode of operation, the MOT requires its own electrical power source. Therefore, solar panels are included, as shown on the orbital configuration, Figure 5.2-5.

When requirements for longer stay times or extended activities such as maintenance on the telescope become necessary, the MOT will be remotely docked to the MORL. A rigid attachment is made and an interconnecting crew transfer tunnel becomes the mode of entry to and exit from the MOT cabin. In this configuration, electrical power, environment control, and orbitkeeping are provided by the MORL.

4.3.2.1 Launch

The launch requirements for the shuttle mode are basically the same as for the soft gimbal mode. The primary difference, however, is the addition of solar panels which would be deployed after separation from the booster.

It is desirable to include the shuttle vehicle as part of an Apollo ferry vehicle launch. The scope of this study did not include the design of a shuttle; however, the incorporation of a shuttle into the Apollo logistics module is considered feasible. The shuttle vehicle would be launched prior to the MOT so that it would be available for immediate use, if necessary, in the activation of the telescope in orbit.

4.3.2.2 Rendezvous, Docking, and Orbitkeeping

For the shuttle mode the rendezvous and docking procedures are identical to that for the soft gimbal mode. Even though the shuttle mode utilizes the MOT separated from the MORL, it will be docked initially for setup and alignment.

The operation orbital flight performance analysis for the MORL-MOT mission with respect to rendezvous, stationkeeping and orbitkeeping have been made under the following ground rules:

- 1) Time average atmospheric density at 250 N Mi; attitude, $(3.246)(10^{-13})$ lbs/ft³.
- 2) Representative weight of MORL plus two logistics vehicles plus two shuttle vehicles 83,600 pounds.
- 3) Representative weight of MOT, 24,000 pounds.
- 4) Effective I_{sp} of propulsion system(s), 300 lbs/lb/sec.
- 5) Stationkeeping performed by that vehicle which has the greater orbit decay rate.

The atmospheric density is based on an operational time period of 1980 for which the mean 10.7 cm solar flux is projected to be in the vicinity of $240 (10^{-22}) \text{ watts/M}^2\text{-cps}$ based on the eleven-year solar cycle. This density is twice that of the U.S. Standard Atmosphere, 1962, at 250 N Mi attitude.

The ballistic coefficient of the MORL varies with attitude orientation from 14 to 35 psf with long-term average estimated to be 25 psf. The ballistic coefficient of the MOT varies with attitude orientation from 15 to 48 psf with long-term average estimated to be 17.5 psf. As a result, the rates of orbital decay of these two configurations will vary with time so that sometimes the MOT orbit is decaying faster than the MORL orbit and at other times the roles are reversed. When not constrained by experimental or operational requirements, it may be possible to orient the MORL so as to modulate the separation of the vehicles.

To minimize the orbitkeeping requirements, the vehicle having the larger orbit decay rate (lowest ballistic coefficient) will perform the stationkeeping maneuvers. Both the MORL and MOT will be required to perform stationkeeping operations, thus partially meeting the orbitkeeping requirements.

The most unfavorable possible combination of ballistic coefficients ($W/C_d A$) occurs when the MOT is at minimum drag attitude, $W/C_d A = 48 \text{ psf}$, and the MORL is at maximum drag attitude, $W/C_d A = 14 \text{ psf}$. This combination occurs only briefly since the MOT is inertially stabilized and only occasionally will its longitudinal axis coincide with the flight path. However, it is possible for the MOT to be inertially oriented with its longitudinal axis normal to its orbit plane so that for extended periods of time it will be at maximum drag attitude, $W/C_d A = 15 \text{ psf}$. It is also possible for the MORL to remain at minimum drag ($W/C_d A = 35 \text{ psf}$) during this time. For any extended period of time the most unfavorable combination of ballistic coefficients is 15 and 35 psf for the MOT and MORL, respectively. In this combination, the MOT orbit will decay faster than the MORL orbit. In order to keep the MOT within the vicinity of the MORL, it will be necessary to periodically apply a minute reboost to the MOT. Propellant requirements and procedures for these stationkeeping operations are discussed below.

Based on the long-term average values of ballistic coefficient, the propellant required for orbit keeping by the MOT is 575 pounds per year, and the propellant required by the MORL is 1500 pounds per year with perfect systems.

These propellant allotments represent reserves of only 25 percent for uncertainties in drag coefficient, atmospheric density fluctuations, guidance and control errors. These minimal reserves are justified in that, with logistic support systems as integral parts of the MORL-MOT operation, an unfavorable combination of uncertainties can be met with resupply.

Since stationkeeping operations are performed by perturbing the vehicle with the lower ballistic coefficient, the frequency of orbitkeeping is determined by the decay rate of the higher ballistic coefficient vehicle. In the worst possible case, this ballistic coefficient would be 15 psf and the time required for the orbit attitude to decay from 250 to 247.5 N Mi would be 15 days. Consequently, orbitkeeping operations will be required so infrequently, even with a narrow attitude tolerance, that such operations need not be scheduled outside of the stationkeeping operations schedule.

Figure 4-7 shows the time required for the two vehicles to separate by one N Mi along the trajectory for various combinations of ballistic coefficients, beginning with the two vehicles adjacent at zero relative velocity and independent of each other with respect to drag. Under the most unfavorable long-term combination of ballistic coefficients, it takes almost nine hours for the vehicles to separate by one N Mi, so that even under the worst conditions the frequency of stationkeeping should not introduce an operational problem such as would occur if the time interval was something like two hours or less. A stationkeeping operation scheduled every nine hours is more than adequate to meet both station and orbit-keeping requirements and will be accomplished during the daylight period. Such a schedule should be considered representative and not optimum with regard to operations integration or propellant requirements. As the curves of Figure 4-7 show, the time required approaches infinity as the ballistic coefficients of the two vehicles become identical.

On the basis of average ballistic coefficients, the MOT requires 137 pounds of propellant per year to match the decay rate of the MORL with perfect sensors and controls. However, in matching the MORL's decay rate, the MOT is partially fulfilling its orbitkeeping requirements so that the propellant requirements for orbit-keeping will cover this stationkeeping requirement.

When altitude of the MOT decreases faster than the MORL, and after an initial transient condition of less than half an orbit, the tangential separation increases proportional to the square of the time from separation. When the separation reaches 1 N Mi a minute reboost impulse is applied to the MOT. The MOT is now in an orbit which results in the MOT lagging behind its undisturbed position with separation proportional to time. These motions are graphed in Figure 4-8 ignoring minute cyclic variations, for the most unfavorable long-term combination of ballistic coefficients (15 and 35 psf). The impulse applied is of such magnitude as to cause the MOT to slow down relative to the MORL and go behind it by no more than 1 N Mi before overtaking it again. The next impulse is then applied when the MOT again leads the MORL by 1 N Mi. For the most unfavorable ballistic coefficient combination, a retro impulse of 0.29 fps is applied to the MORL at 8.97 hours after separation (Figure 4-8). The MORL catches up to the MOT at 12.5 hours, is 1 N Mi ahead of 21.45 hours, and is 1 N Mi behind the MOT again at 34.7 hours. The second MOT reboost is applied at MOT apogee passage just prior to 34.7 hours so as to keep the attitude separation reasonable while cycling through another catchup operation.

For the initial rendezvous operation, where the MORL is in orbit and the MOT is launched from the Earth, the ΔV allowance for rendezvous should be 125 fps over simple orbit injection so that the total maneuver ΔV at 250 N Mi is 380 fps. This allowance is necessary to cover tracking, guidance, and control errors and finite thrust-to-weight and burn-time effects. The allowance is perhaps conservative, but more exact values require detailed definition of all the pertinent subsystems (tracking, guidance, control and propulsion) and detailed simulation of the rendezvous operation incorporating the characteristics of these subsystems.

The ΔV required to rendezvous with the MOT from a distance of 1 N Mi along the orbit varies inversely with the time taken to rendezvous; however, rendezvous times of more than several orbit periods are not always possible nor practical.

FIGURE 4-7
TIME REQUIRED FOR TANGENTIAL SEPARATION OF ONE NAUTICAL MILE

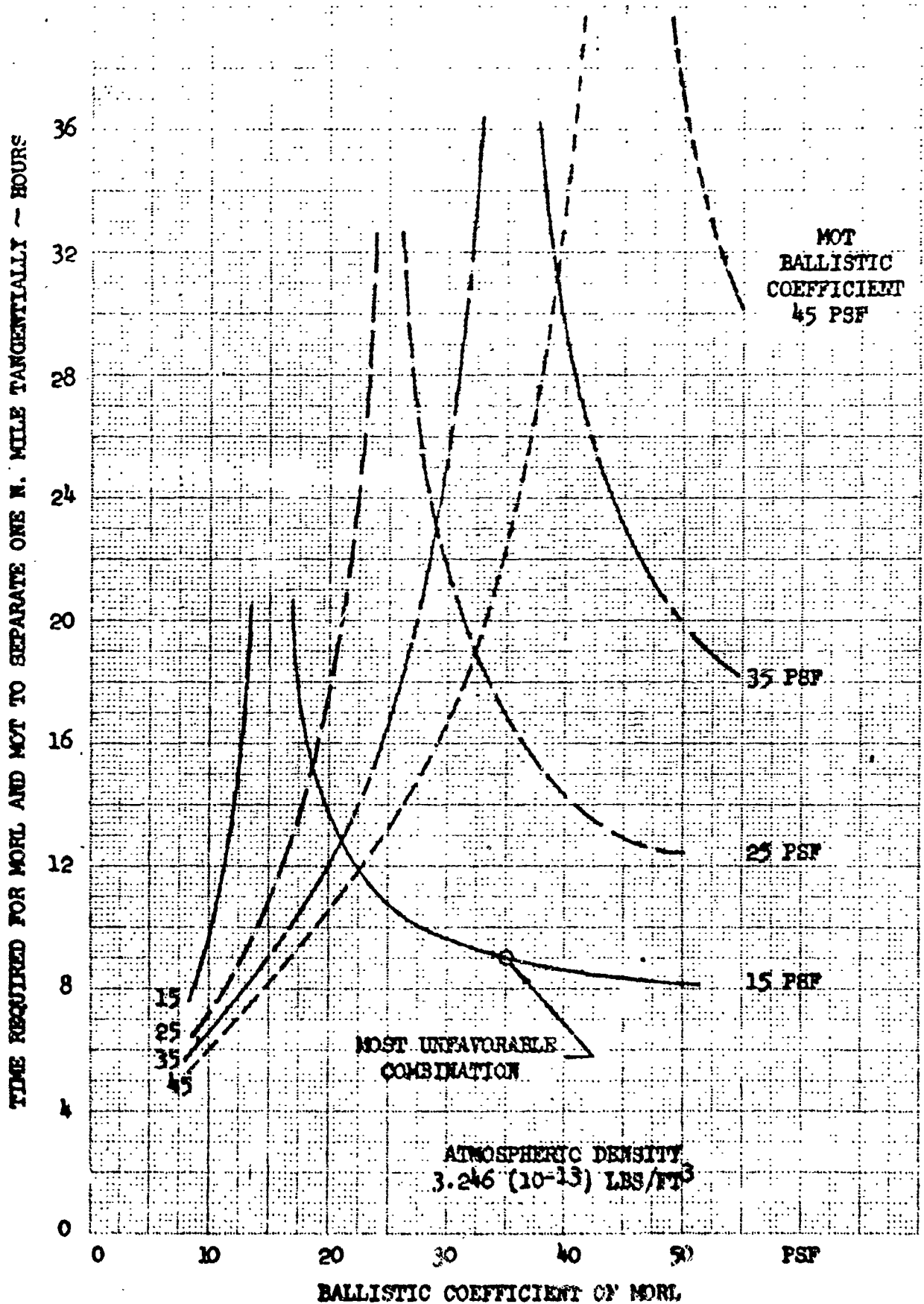
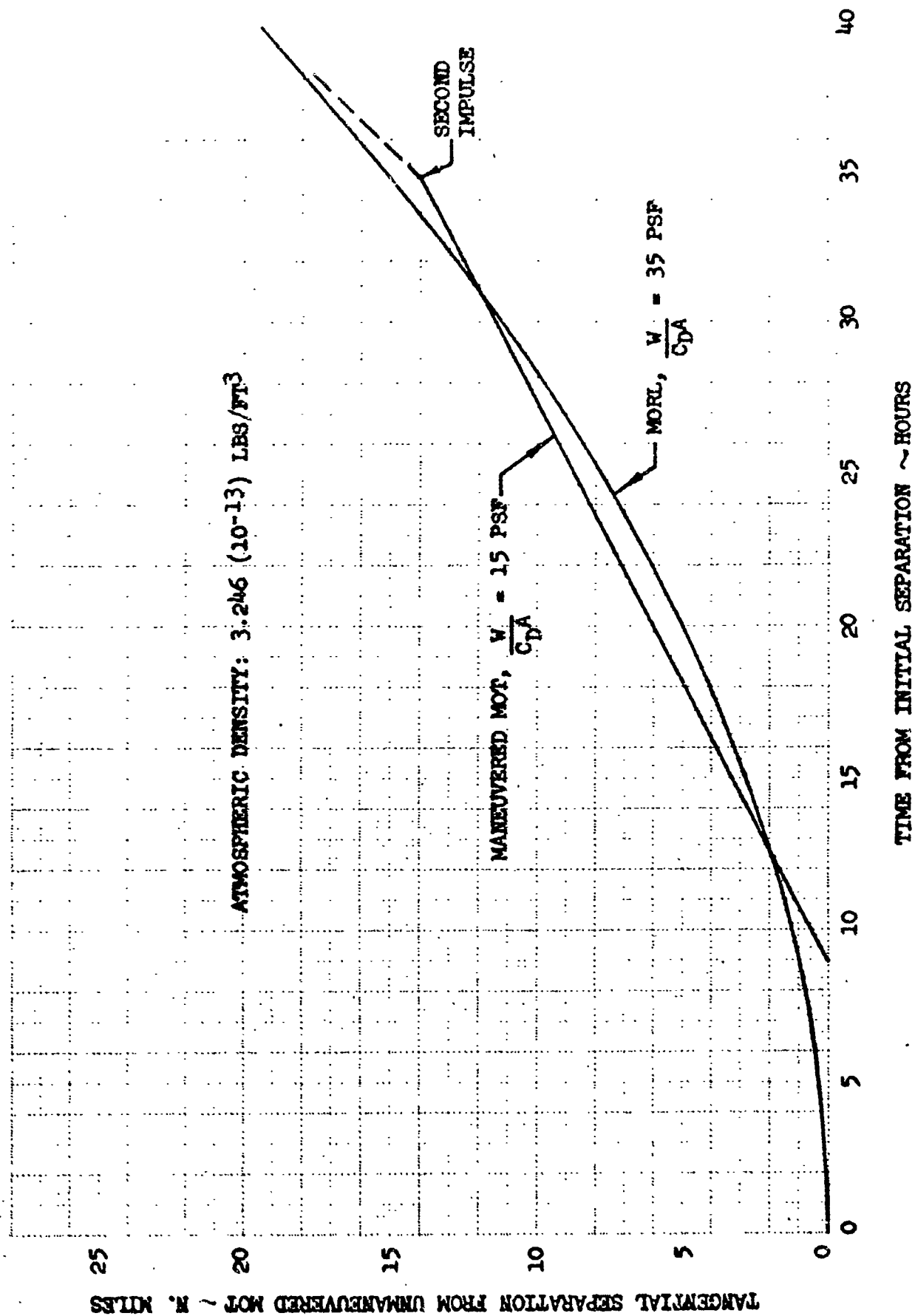


FIGURE 4-8 RELATIVE MOTION OF MOT AND MORL
(MOST UNFAVORABLE COMBINATION OF BALLISTIC COEFFICIENTS)



The ΔV required to catch up and reduce the relative velocity in one orbit period is one foot per second with perfect systems. The altitude difference can be reduced in a separate maneuver in one half-orbit at a rate of 0.3 N Mi per foot per second. Then the ΔV required to rendezvous from 1 N Mi along the orbit in one to two orbital periods is about the ΔV penalty introduced by system errors. To reduce the horizontal and vertical separation in a single maneuver generally requires slightly more ΔV .

A ΔV allowance of 20 fps for rendezvous and docking from one N Mi will provide for flexible rendezvous operation. With highly sophisticated system, routine rendezvous in about one orbit period should be possible with less than 10 fps, making available more than 20 fps for rendezvous in 10 to 20 minutes when required. (With a thrust-to-weight ratio of 0.03, the fastest rendezvous possible would be about 3 minutes and would require 170 fps.)

Orbitkeeping, stationkeeping, and rendezvous requirements introduce no serious constraint on propellant requirements or operations of the MOT mission.

4.3.2.3 Deployment

The shuttle vehicle is normally stowed on the MORL and can be activated and positioned by the deployment arms in the same manner that the Apollo logistics vehicles are stowed and manipulated on the MORL. Once the MOT has been docked to the MORL, the telescope can be converted to its orbital configuration.

4.3.2.4 Setup, Checkout, & Alignment

With the MOT initially docked to the MORL, the telescope will be changed to its orbital configuration in a procedure similar to that used with the soft gimbal mode. The one function which is eliminated is the requirement for setting up the soft gimbal interconnection. During this period the MORL will provide electrical power and MOT cabin atmosphere.

In this case, the shuttle vehicle also requires a setup and checkout operation, which consists of checkout of environmental control, electrical power (batteries), propulsion, and communication systems. As required, expendables such as oxygen and propellants will be installed or filled. In addition to a structural inspection, the operating controls and mechanisms such as the docking and entry hatches will be checked.

4.3.2.5 Operation

For operation of the shuttle mode, the MOT will be separated from the MORL. It has its own solar panels for electrical power and independent attitude and positioning capability and will be remotely slewed to the proper target. Its solar panels are adjustable, but will be locked in a fixed position during the observation periods to eliminate possible disturbances.

When it becomes necessary for the crew to transfer to the MOT, they will activate and enter the shuttle and maneuver to the MOT, which maintains its inertial attitude. Once docked, the cabin will be pressurized from the shuttle system and the crew will enter in a shirtsleeve environment. Upon completion of their tasks, the crewmen will re-enter the shuttle, depressurize the cabin, and return to the MORL.

with the film, plates, or other equipment.

4.3.2.6 Maintenance

The maintenance requirements for the MOT are much the same for the shuttle mode as discussed under the soft gimbal mode. For the shuttle mode there are additional maintenance requirements for the solar panels and solar panel actuators on the MOT. Also, the shuttle vehicle will require periodic inspection, maintenance, and replacement of defective parts. Maintenance required for the shuttle vehicle will be accomplished at the MORL and will be somewhat independent from the operational requirements of the MOT.

4.4 TIMELINE ANALYSIS

During the study it was recognized that it was necessary to establish a one-year astronomical program in order to estimate telescope operation time and resulting man's participation. For example, the various experiment observations have varying requirements for monitoring, film replacement, exposure times, quantities of exposures per target, and optics. To obtain maximum utilization of the telescope, each experiment was evaluated on an individual requirement basis and considered as blocks of time with specific operational requirements. The approach was then to develop a typical experiment program conducting all experiments in a logical order. Conducting all of the f/15 observations before changing the secondary mirrors for the f/30 observations increases the useful telescope time as it is estimated that this change may require as much as four days. The number of crew-transfer trips and their frequency results in a means of determining shuttle logistics requirements used to accomplish a mode evaluation.

Two modes of operations were studied in developing the accompanying charts:

- o MOT soft gimbaled to the MORL - servicing via tunnel from MORL;
- o MOT in parallel orbit with the MORL - servicing via shuttle from MORL and/or docked with MOT.

For the purpose of this study, it has been assumed that time expenditures for film replacement, scheduled and unscheduled maintenance, film processing and transmittal will be the same in either mode of operation. This is based on the assumption that the shuttle travel time between MORL and the MOT will be time-sequenced in parallel with the concluding portion of the previous MOT experiment, and assumes the same time function allocation for the docking and pressurization sequence of either mode, allowing the same time analysis to be used.

Timeline analyses were made for each of the astronomical observation experiments and integrated into a timeline analysis for a one-year period. These analyses cover only the operational period of the telescope and do not include the launch, orbit insertion, docking, readjustment and alignment time periods.

The following figures depict the development of the timeline analysis for the photographic experiments for a one-year period:

Figure 4-9 Wide Field Photography (f/15),

Figure 4-10 Low Dispersion Spectra (f/15),

Figure 4-11 Large Scale Photography (f/30),

Figure 4-12 High Dispersion Spectra - Visible (f/30).

The detailed analyses for the various types of astronomical observations have been organized as a baseline from which other programs can be generated. In each case, the time for film, slides, or tape changes has been allocated as 2 orbits (3 hours). Each observation, therefore, incorporates a block of time for which a predetermined

ORBIT NO	1	2	3	4	5	6	7	8	9	10	11	12	13	14	15	16
1 DAY			TARGET #1 3 EXPOSURES/TARGET	SLEW & STABILIZE TO NEW TARGET	TARGET #2	SLEW & STABILIZE TO NEW TARGET	TARGET #3	SLEW & STABILIZE TO NEW TARGET	TARGET #4	SLEW & STABILIZE TO NEW TARGET	TARGET #5	SLEW & STABILIZE TO NEW TARGET				SLEW & STABILIZE TO NEW TARGET

ORBIT NO	1	2	3	4	5	6	7	8	9	10	11	12	13	14	15	16
2 DAYS		TARGET #6	SLEW & STABILIZE TO NEW TARGET	TARGET #7	SLEW & STABILIZE TO NEW TARGET	TARGET #8	SLEW & STABILIZE TO NEW TARGET	TARGET #9	SLEW & STABILIZE TO NEW TARGET	TARGET #10	SLEW & STABILIZE TO NEW TARGET	TARGET #11	SLEW & STABILIZE TO NEW TARGET			

ORBIT NO	1	2	3	4	5	6	7	8	9	10	11	12	13	14	15	16
3 DAYS		SLEW & STABILIZE TO NEW TARGET	TARGET #12	SLEW & STABILIZE TO NEW TARGET	TARGET #13	SLEW & STABILIZE TO NEW TARGET	TARGET #14	SLEW & STABILIZE TO NEW TARGET	TARGET #15	SLEW & STABILIZE TO NEW TARGET						SECURE & MAKE PRESSURE SEAL CABIN & CHECKOUT REPLACE FILM EXIT & PUMPDOWN MOT CABIN DISENGAGE STABILIZE TO TARGET

FIGURE 4-9: Wide Field Photography (f/15)

ORBIT NO	1	2	3	4	5	6	7	8	9	10	11	12	13	14	15	16
1 DAY	STABILIZE TO TARGET			SPECTROGRAPH EXPOSURE #1			EXPOSURE #2			EXPOSURE #3						

ORBIT NO	1	2	3	4	5	6	7	8	9	10	11	12	13	14	15	16
2 DAYS	REMOTE SELECT SPECTROMETER			SPECTROMETER RECORDING #1			SECURE & MAKE PRESSURE SEAL PRESSURIZE MOT CABIN & CHECKOUT REPLACE FILM EXIT & PUMPDOWN MOT CABIN DISBARGE			SPECTROGRAPH EXPOSURE #1			EXPOSURE #2			

ORBIT NO	1	2	3	4	5	6	7	8	9	10	11	12	13	14	15	16
3 DAYS	EXPOSURE #3			REMOTE SELECT SPECTROMETER									SPECTROMETER RECORDING #1			

FIGURE 4-10: Low Dispersion Spectra (f/15)

ORBIT NO	1	2	3	4	5	6	7	8	9	10	11	12	13	14	15	16					
1 DAY	STABILIZE TO TARGET	STABILIZE TO TARGET	STABILIZE TO TARGET	STABILIZE TO TARGET	TARGET #5	TARGET #6	TARGET #7	TARGET #8	TARGET #9	TARGET #10	SECURE & MAKE PRESSURE SEAL	PRESSURIZE MOT CABIN & CHECKOUT	REPLACE FILM	EXIT & PUMPDOWN	MOT CABIN	DISENGAGE	STABILIZE TO TARGET	TARGET #1	TARGET #2	TARGET #3	TARGET #4

ORBIT NO	1	2	3	4	5	6	7	8	9	10	11	12	13	14	15	16
2 DAYS	TARGET #5	TARGET #6	TARGET #7	TARGET #8	TARGET #9	TARGET #10	TARGET #11	TARGET #12	TARGET #13	TARGET #14	TARGET #15	TARGET #16	TARGET #17	TARGET #18	TARGET #19	TARGET #20

ORBIT NO	1	2	3	4	5	6	7	8	9	10	11	12	13	14	15	16			
3 DAYS	TARGET #21	TARGET #22	TARGET #23	TARGET #24	TARGET #25	TARGET #26	TARGET #27	TARGET #28	TARGET #29	TARGET #30	SECURE & MAKE PRESSURE SEAL	PRESSURIZE MOT CABIN & CHECKOUT	REPLACE FILM EXIT & PUMPDOWN	MOT CABIN DISENGAGE	STABILIZE TO TARGET	TARGET #1	TARGET #2	TARGET #3	TARGET #4

FIGURE 4-11: Large Scale Photography - Stellar & Planetary (f/30)

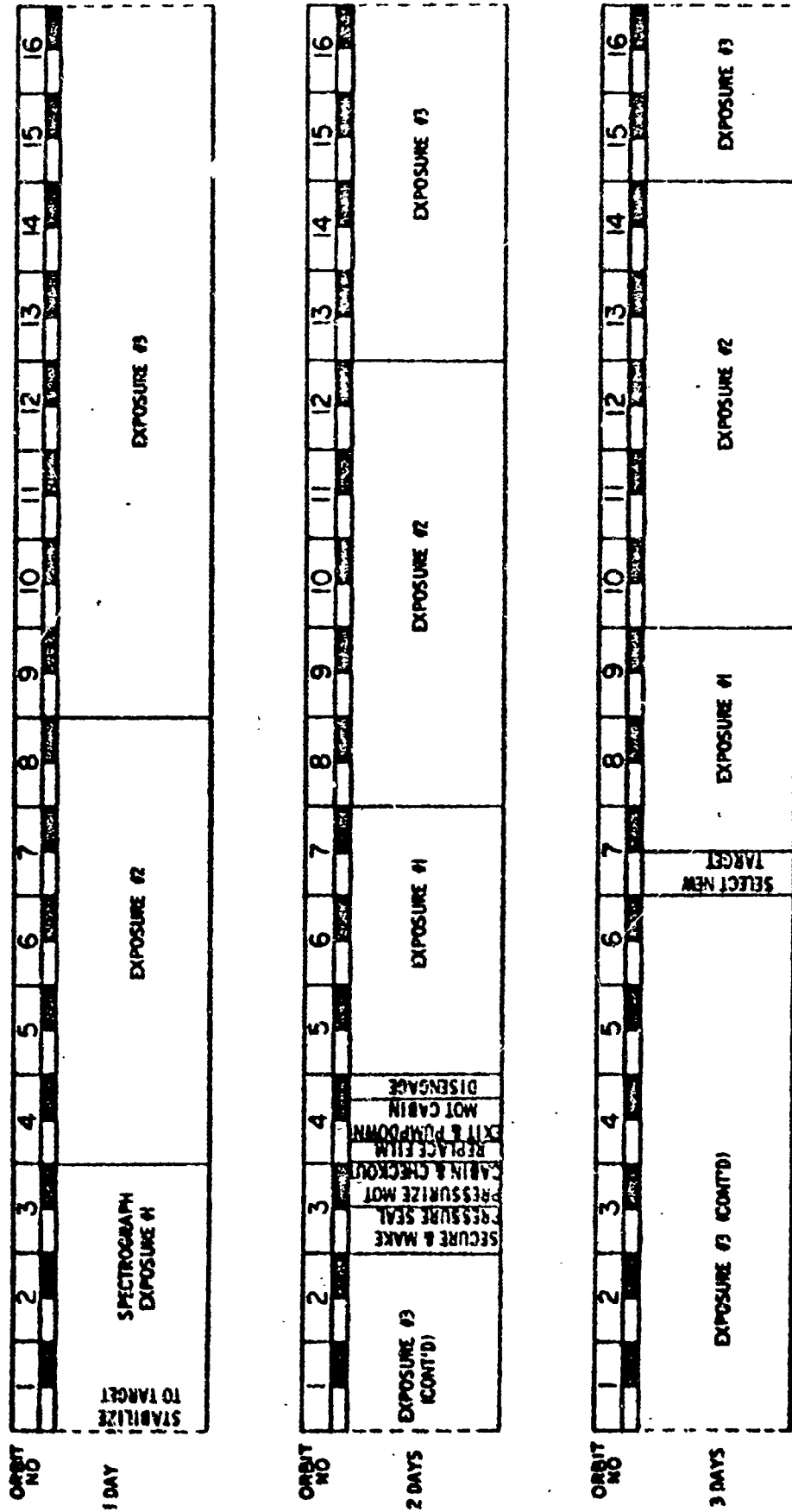


FIGURE 4-12: High Dispersion Spectra (f/30)

number of targets can be acquired before the recording media requires changing. Each block of time further lists the number of exposures, recordings, and targets acquired for each of the astronomical observation experiments.

The MOT one-year program, Figure 4-13, integrates the blocks of time for each observation into a total program, incorporating the scheduled and unscheduled maintenance periods, and the times for changing mirrors into a planned sequence of events. In this manner, each series of observations relative to mirror settings is provided a degree of flexibility commensurate with divergence of opinion of observation priority among astronomers. The time required to set up and check out the equipment for each observation experiment is 5 orbits, (7.5 hours) and provides a 3-orbit penalty if this option is exercised. Based on consultation with Dr. Z. Kopal, the program presented represents the best utilization of time for the percentage allocation of telescope use.

Scheduled maintenance periods, based on 3 percent of total time, have been allocated in accordance with equipment reliability values and establish those periods of a one-year schedule where this type of maintenance will be required.

Unscheduled maintenance, based on 15 percent of total time, has been allocated in block periods of time for simplicity, recognizing that the occurrence of these requirements could be highly diversified within the total program. The blocks of unscheduled maintenance, however, could occur at any time during one type of astronomical observation experiment without significantly degrading the planned program.

A program summary chart, Figure 4-14, based on the one year program, indicates the resulting number of possible targets for each scientific experiment after deducting the time required to replace film and accomplish experiment setup and checkout.

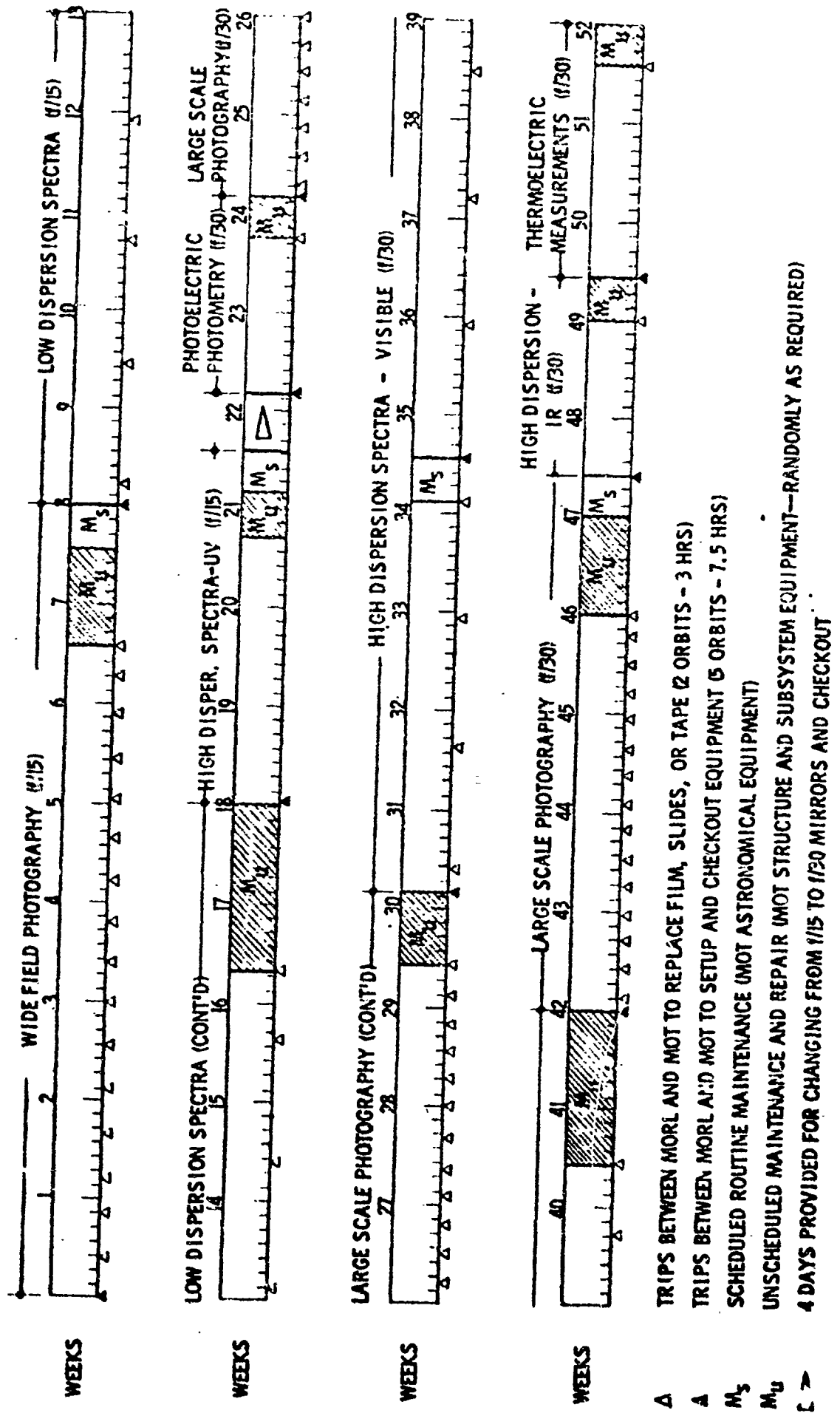


Figure 4 - 13: MOT One-Year Astronomical Program

	EXP. NO.	TDS	OBSERVATION SIDE		NUMBER OF TRIPS		USEFUL ORBITS	ORBITS PER TARGET	NUMBER OF EXPOSURES OR RECORDING PER TARGET	APPROX. NO. OF TARGETS	NOTES
			NO. OF DAYS	NO. OF ORBITS	SETUP, CHECKOUT EQUIPMENT & MAINTENANCE	REPLACE FILM					
WIDE FIELD PHOTOGRAPHY	15	13	47	750	1	16	720	1	3	240	o Slewing and fine stabilization for each new target--
LARGE DISPERSION SPECTRA	15	16	58	928	1	8	909	5 23 16	1 4 3	39	o Trip to replace film, slides or tape--3 hrs (2 orbits)
SPECTROMETER SPECTROGRAPH											
HIGH DISPERSION SPECTRA ULTRAVIOLET	15	5	19	304	1	1	297	5	1	61	o Trip to setup and checkout equipment--8 hrs (5 orbits)
PHOTOELECTRIC PHOTOMETRY	30	3	11	176	1	1	171	10	1	17	o Routine maintenance--3 days approximately every 3 months
LARGE SCALE PHOTOGRAPHY	30	18	65	1040	2	34	966	1	5	966	
HIGH DISPERSION SPECTRA VISIBLE	30	19	69	1104	2	9	1080	12	3	60	
HIGH DISPERSION IR	30	3	11	176	1	1	171	1	1	171	RECYCLE MODE ONLY
PHOTOCHEMICAL MEASUREMENT	30	4	15	240	1	1	235	10	1	23	o Stationkeeping (to be accomplished during daylight phase of orbit)--Every 9 hrs average
TOTALS		81	295	4718	10	71	4549			1577	o Orbitkeeping (in parallel with a stationkeeping operation) As required
MAINTENANCE & REPAIR REQUIREMENTS											
SCHEDULED											
ASTRONOMICAL EQUIPMENT		3	12	192							
CHANGE SECONDARY MIRROR		1	4	64							
UNRECORDED		25	54	864							
TOTALS		19	70	1190							

Figure 4 - 14: MOT One-Year Astronomical Program Summary

4.5 DEFINITION OF LOGISTICS REQUIREMENTS

The logistics requirements for the MOT consist of scientific experiment expendables, subsystem expendables, and equipment spares. The experiment expendables include all recording media such as photographic film and plates, magnetic tapes, photoelectric sensor coolants, and developers. The subsystem expendables consist of attitude control and propulsion fuels and atmospheric control supplies. The spares requirement includes not only the subsystems spares such as the electronics, propulsion, communications, and mechanisms components but covers the sensors and optics spares for the experiment equipment.

A matrix, Figure 4 - 15, indicates the scientific experiment logistics required for both modes to support the astronomical program for one year. The volumes and weights for the film and plates have been calculated based on the number of exposures of a determined format. Individual cassettes are considered and sized to be compatible with the frequency of trips for replacements. For that equipment using magnetic tape, two 12-pound Gemini-type recorders with tape will be provided. Each recorder includes 2400 feet of tape which is adequate for the data recording requirements for each complete experiment. The data being recorded in the MOT is also being telemetered to the MORL so there is no necessity for tape replacement in the MOT during the conduct of each experiment. After completion of an experiment, the recorder will be replaced and returned to the MORL for transmission of data to Earth. When assured of receipt of the data, the magnetic tape is erased and the recorder checked for use again.

In the remote mode the subsystem expendables consist of attitude control and propulsion propellant and ECS/atmosphere gases. These require a total weight of 504 pounds for a 90-day period. This is based on transfer of the attitude control and propulsion propellant being done at the scheduled maintenance periods. The weight items include:

o MORL/MOT docking	=	177 pounds
o MOT orbitkeeping	=	144 pounds
o MOT attitude control	=	175 pounds
o O ₂ pumpdown coss.	=	369 pounds
TOTAL	=	865 pounds

The entire logistics requirements for the MOT is dependent on the total number of trips between MORL and MOT (including those for unscheduled maintenance), the spares and replacement requirements for all of the subsystem components, and the spares and replacement requirements for structural components and mechanisms, and cannot be defined at this time.

SCIENTIFIC INSTRUMENT	RECORDING MEDIA			FILM FORMAT	NO. OF EXPOSURES		APPROXIMATE SIZE		APPROXIMATE VOLUME		TOTAL WEIGHT/ PER CASSETTE	
	FILM	PLATES	TAPE		PER CASSETTE	PER YEAR	PER CASSETTE	NO. OF CASSETTES	PER CASSETTE	PER YEAR	PER CASSETTE	PER YEAR
WIDE FIELD PHOTOGRAPHY	X			16 x 16"	45	720	3x3x16	16	144 IN ³	2304 IN ³	4	04
LOW DISPERSION SPECTROGRAPH	X			0.6 x 0.6"	18	117	1x1x2	6	2 IN ³	12 IN ³	---	2
LOW DISPERSION SPECTROMETER			X	△	--	39	----	---	----	400 IN ³	---	12
HIGH DISPERSION SPECTROGRAPH	X			1.4 x 21"	24	180	3x3x1.5"	8	14 IN ³	112 IN ³	2.5	20
HIGH DISPERSION SPECTROMETER			X	△		61	---	---	----	400 IN ³	---	12
PHOTOELECTRIC PHOTOMETRY			X	△	--	17	---	---	----	---	---	--
LARGE SCALE PHOTOGRAPHY	X	X		2 x 2"	15	4,830	2.5x2.5x16"	33	100 IN ³	3300 IN ³	5	165
HIGH DISPERSION IR			X	△	171	---	-----	---	----	---	---	--
THERMOELECTRIC MEASUREMENT			X	△	23	---	-----	---	----	---	---	--
SUBTOTAL					296	5964			260	6528	11.5	275
GROWTH ALLOWANCE (100%)					296	5964			260	6528	11.5	275
TOTAL					592	11,928			520	13,056	23	550

△ 2 RECORDERS INCLUDING 2400 FT OF 1/2" TAPE WILL BE USED ALTERNATELY

Figure 4-15: Scientific Experiment. Logistics Requirements
(One Year)

4.6 DEFINITION OF SHUTTLE REQUIREMENTS

For the remote mode, a shuttle is utilized to accomplish the frequent short-duration transfer requirements between MORL and MOT. The shuttle is an independent vehicle sized to accommodate two men, logistics, and supporting subsystems. In addition to the requirement for a separate vehicle, the shuttle includes additional subsystems for propulsion, electrical power (batteries), communications, control, and environmental control. Spares and maintenance would also be required to support its operation.

In the remote mode, the MOT cabin is pressurized from the shuttle subsystem but does not create an added pressurization gas requirement over the attached mode other than the tankage provision on the shuttle. Approximately 150 pounds of pressurization gas is provided on the shuttle and is sized for 30-day capacity with capabilities to accomplish a transfer every 2 days. In addition, approximately 500 pounds of propulsion propellant is required by the shuttle to support the 30-day resupply period.

The spares and replacement requirement for the shuttle subsystems and mechanisms are a function of operation time, frequency of use, and design factors and cannot be defined at this time.

4.7 CREW REQUIREMENTS

The MORL crew complement will include crewmen having specialized skills associated with the optical program in addition to the normal MORL operation requirements. It is not necessary, however, that all crewmen qualify as experts in optics, astronomy and photography. Each crewman will be thoroughly trained in the extravehicular activities required for the setup and maintenance of the telescope. Mockups and simulators will be used to train the crew for the activities associated with the MOT system. The MORL crew complement will then include the capability for accomplishing all of the following tasks:

- o Initial Setup, Checkout and Alignment
 - o Perform rendezvous and docking operation
 - o Remove launch-support structure
 - o Attach orbital supports for sensitive optical elements
 - o Perform optical alignment
 - o Activate and check out thermal control system
 - o Activate and check out electrical power system
 - o Check out all electrical and electronic subsystems, e.g., computers, lighting, and communications
 - o Check out MOT cabin environmental control system
 - o Align and adjust prime focus equipment
 - o Work in a pressure suit, utilizing special space tools
- o Experiment Control
 - o Replace film slides, and tapes
 - o Service, and adjust automatic film and tape transports
 - o Monitor star patterns, focus, exposure reading, stability and thermal controls
 - o Remotely advance film and change film and exposure times
 - o Change primary and secondary mirrors, focus and align
 - o Manually slew equipment for gross orientation
- o Data Interpretation and Processing
 - o Plate and film development in MORL

- o Examine negatives and evaluate quality
- o Make enlargements of selected areas
- o Transmit portions of images to ground for "quick look"
- o Prepare data for return to ground via data capsule or ferry vehicle
- o Overall Program Monitoring
 - o Interpret program changes from the ground and interject in orbital operations
 - o Remotely monitor WOT for proper operation
 - o Perform periodic inspections and checkout
 - o Perform unscheduled maintenance involving equipment repair and replacement
- o Maintenance
 - o Perform fault isolation of modular packages
 - o Replace failed part

4.8 EVALUATION OF TWO FINAL CONCEPTS

The purpose of the evaluation was to assess the soft gimbal (948-41C) and shuttle (948-43D) concepts and to recommend the concepts which rated best using selected evaluation criteria. The criteria were identified during the first half of the study and served as a basis for comparing the various modes of operation. The two concepts which are assessed in this portion of the study differ primarily in mode of operation; therefore, the previously identified criteria are used. A discussion of each of the criteria and its measure is contained in the following paragraphs.

4.8.1 Technical Risk

Technical risk is defined as the probability of systems not meeting design or operational requirements by the specified operational date. In this evaluation, technical risk is measured by assessing new and unsolved design problems which are required for each concept.

The shuttle concept requires four areas of development which are different from the soft gimbal concept; a shuttle vehicle and separate electrical power, propulsion, and stability systems. Shuttle vehicle development should be relatively routine since it can be similar to the Apollo or Gemini vehicles. Electrical power and propulsion systems are also anticipated to be well within the state-of-the-art. In addition, MOT studies have shown that the separate stability system will be within the state of the art. For these reasons, the shuttle concept is assessed as having low technical risk.

The soft gimbal concept requires development in the attachment of the MOT to the MORL, and the stability system must cope with MORL motions which are transmitted through the springs and the gimbal limits. A requirement for an angular fine pointing error no greater than 0.01 arc seconds was established for the telescope. General Electric performed an analysis of the stability control system which indicated that performance is only slightly degraded. Additional pointing errors of less than 0.003 second of arc are introduced by the soft gimbal. The attached mode stabilization was assessed to be within the 0.01 second of arc requirements. There are some problem areas associated with the development of the soft gimbal and therefore the technical risk is considered higher than the attached mode. The technical risk of this system was assessed to be moderately low, compared to low for the shuttle concept.

4.8.2 Available Observation Time

Efficient utilization of available observation time is a fundamental requirement in order to obtain the maximum amount of data from the Manned Orbital Telescope. Available observation time has been defined as the night time of each orbit, thus providing a maximum of 12 hours per day for actual observations. All of the orbital night times cannot be utilized for observations because of the requirements for equipment changes, maintenance operations, routine inspections, and servicing. Other factors affecting the observation time are travel from the MORL to the MOT, docking and undocking requirements, and pressurization and depressurization of the MOL cabin.

In order to assess the effect of these factors on the two modes, a sample astronautical observation program was established. Estimates were made of the pre-experiment preparation requirements for each type of observation, based on a shirtsleeve environment. The total night hours for one year were assumed to be 4,380 for this analysis. A maintenance analysis indicated that 29 maintenance entries would be required for the soft gimbal concept and 31 entries for the shuttle concept. The two additional entries are considered for unscheduled maintenance of the solar cells. This results in slightly fewer hours being available for observations for the shuttle concept than for the soft gimbal concept. Figure 4-16 shows the effect of number of entries on the available observation time for each concept. As shown, both concepts have high availabilities and the differences between the two are not considered significant.

4.8.3 Reliability

Overall system reliability was measured in this study by the probability that the vehicle will be available for operations. The reliability of competing MOT concepts is a variable which may be increased by the investment of in-orbit weight, power and maintenance, and by increased preflight development effort. Since booster payload and flight schedules are relatively inflexible quantities, preflight development is limited and the primary reliability trade is one of MOT reliability versus the logistics requirements and experiment objectives. The primary limitation to the amount of experimental data obtained is, therefore, the total time required to repair MOT equipment. In other words, if sufficient payload is afforded to provide the necessary spares to make the ultimate reliability practically unity, the only limitation to completing experiments is the availability of the experiment and support equipment.

The unscheduled maintenance requirements for the two modes have been assessed to be approximately the same, with the primary exception being the solar panels in the remote mode. Figure 4-17 shows the relative reliability levels for one year's operation. These differences are not considered to be significant.

The reliability decrement associated with the operation of the shuttle is reflected primarily in the safety analysis. Failures will generally result in either the need for spares or abandonment of the shuttle. This will be quite feasible since extra-vehicular movement is being developed in existing programs.

4.8.4 Safety

Safety is measured as the probable number of fatal accidents per year of operation. The major safety hazards result from docking the MOT and the shuttle, radiation and micrometeoroids, and handling propellants, gases, and electrical equipment.

With minor variations, the latter two hazards will be common to both of the competing modes.

4.8.4.1 Docking

The docking of space vehicles is a fundamental requirement for all space programs of more than minimal objectives; therefore, considerable development of equipment and techniques can be expected. However, the problems of orbital mechanics and the

PERCENT OF TOTAL NIGHT
HOURS AVAILABLE FOR OBSERVATION

AVAILABLE OBSERVATION TIME FOR ONE YEARS OPERATION

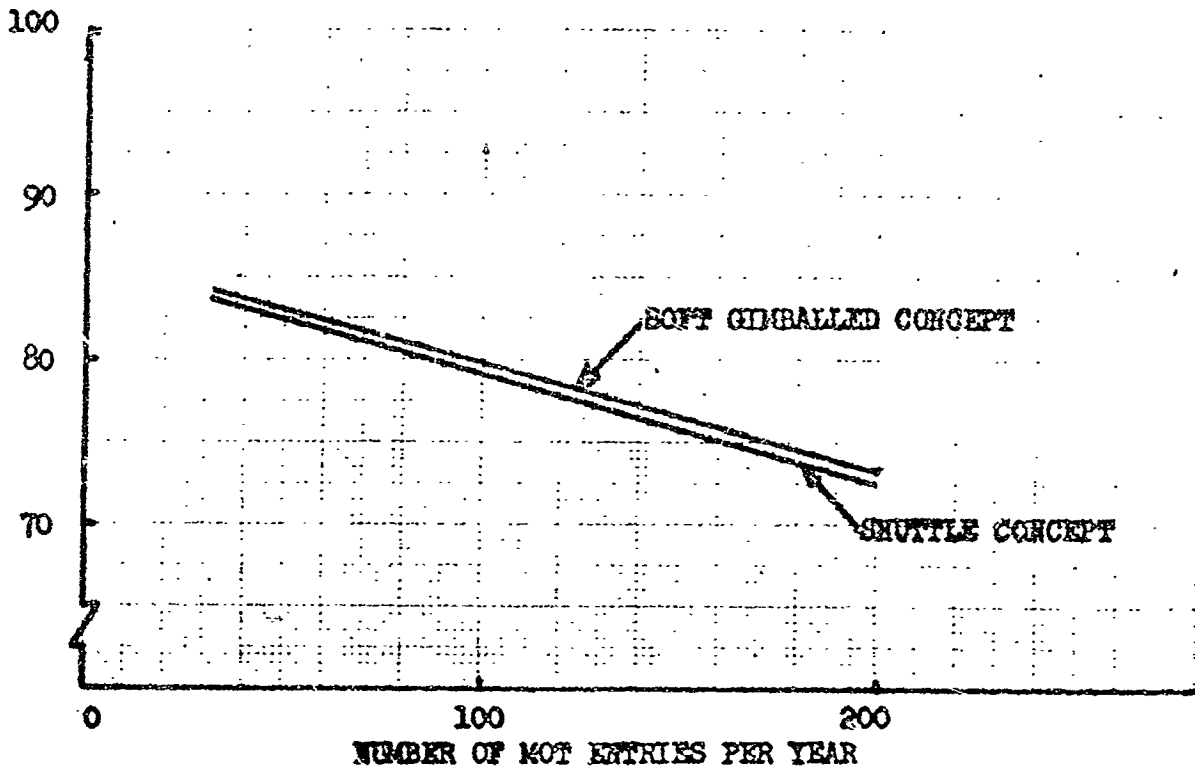


FIGURE 4-16

PROBABILITY MOT WILL BE AVAILABLE FOR
OPERATIONS

PROBABILITY MOT WILL BE
AVAILABLE FOR OPERATIONS ~ PERCENT

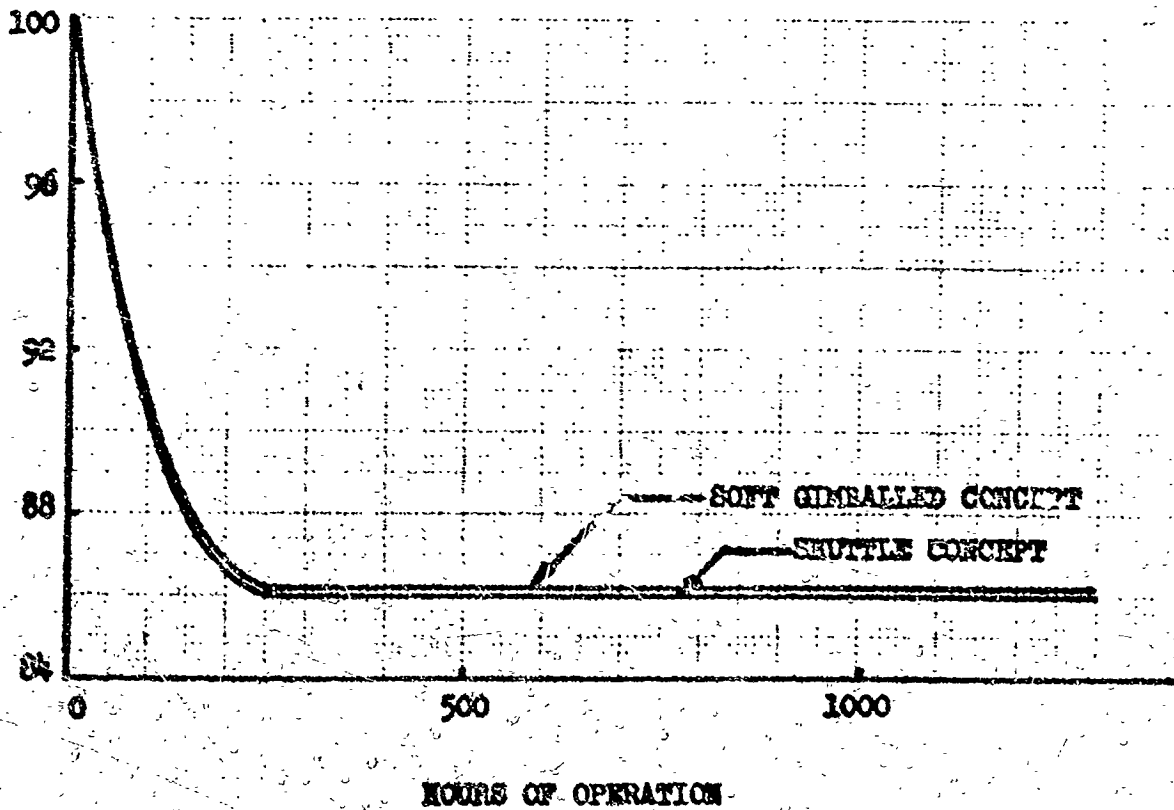


FIGURE 4-17

relatively complex equipment that is required will result in a significant probability of errors and accidents; at least within the foreseeable future. Present docking concepts rely on the astronaut to a large extent, and human error is the primary cause of potential failures. Whether an automatic servo control can be developed to satisfactorily replace the astronaut remains questionable, but until the weight limitations imposed by existing booster payload capabilities are less stringent, it appears likely that the astronaut will remain the primary docking controller.

Considering the incidence of major landing accidents with fighter aircraft, a level of serious accidents of 0.0001 might be expected. However, by proper design it should be possible for the shuttle to equal or improve the performance experienced with KC-13 aircraft of 0.00002.

Tests have shown that the human error probability of trained operators exceeds 0.001 per action. Considering that there must be at least one action per docking sequence which cannot be reversed (i.e., he is committed and cannot correct a mistake), this level could well represent the upper limit of docking accidents.

4.8.4.2 Radiation and Micrometeoroids

The hazards resulting from radiation and micrometeoroids become significant only when the astronauts must go outside of the MORL, OT cabin, or the shuttle vehicles, and consequently this hazard is related to the reliability of equipment such as the MOT doors, the reaction controls, and the repair of any docking damage. It was assumed that a suit similar to the Apollo suit would be used; and, therefore, the safety will be dependent on the Apollo suit requirement of 0.9999 probability of no serious hazard in 12 hours.

4.8.4.3 Handling Equipment

It was assumed that two consecutive errors must be committed before a safety hazard would arise from handling propellants, gases, etc. Assuming that the incidence of human errors in the spacecraft and space environment is 0.001 or 0.002, the probability of two consecutive errors will be 0.000001 to 0.000004 per reprovisioning or repair action.

4.8.4.4 Safety Comparison

In order to compare the competing concepts, it is necessary to estimate the probable level of each activity in order to determine the relative hazards.

The number of trips required for the one-year program plus approximately 17 trips for unscheduled maintenance resulted in 98 two-way trips or 196 separate docking operations. This would result in a cumulative potential hazard probability of 0.004 (0.00002 X 196) for one year.

Outside maintenance is estimated to require about four man-hours per month, which results in a safety hazard of approximately 0.0004 per year.

Equipment handling is estimated to require about ten potentially hazardous operations per month, which results in a hazard of 0.0001 to 0.0005 per year.

Figure 4-18 shows the hazard levels for the two modes as a function of number of entries into the MOT per year. The shuttle concept has five times the hazard of the gimballed concept.

4.8.5 Flexibility

Flexibility is defined as the ability of a concept to perform alternate missions without major modifications to the vehicle or equipment. Since both of the MOT concepts use the MORL as the primary vehicle, the flexibility of the two concepts was assessed in terms of the excess capability of the MORL equipment and manhours, and the ability of the concept to perform unscheduled MOT experiments. A review of the Douglas MORL reports shows that an excess of capability exists for the MORL vehicle under its normal operating mode. The criteria used to measure this capability are crew time, electrical power, storage volume, active volume, and weight. A summary of the available capability and the percent utilization of each parameter is tabulated in Figure 4-19.

FIGURE 4-19

MORL EXPERIMENT CAPABILITY AND AVERAGE FIRST-YEAR UTILIZATION

<u>Support Parameter</u>	<u>Available</u>	<u>Average Use</u>	<u>Percent Utilization</u>
Crew Time (manhours/day)	45.8	31.8	69.5
Electrical Power (watt-hours/day)	48,000	12,217	25.4
Storage Volume (cu ft/day)	1,100	787	71.6
Active Volume (cu ft/day)	3,700	183	4.9
Weight* (pounds mass)	79,300	20,850	26.3

* Based on the 6,300 pound laboratory discretionary payload plus the cargo delivery capability of six logistics launches scheduled during the first year, less 21,000 pounds of facility support requirements.

The shuttle concept requires only a small amount of MORL storage space for spares or propellant, electrical power, and weight. However, the shuttle will use more of the available manhours than the gimbal concept. The soft gimbal concept may require more storage capability than the excess available from the MORL requirements since all spares must be stored in the MORL. In addition, the soft gimbal concept will use more MORL electrical power and weight, but it is doubtful that all the excess capability of the MORL will be required. The ability of the two MOT concepts to perform unscheduled MOT experiments was assessed on the basis of two considerations; changing equipment to perform another experiment (change from tape to film, etc.), and slewing the telescope from one target to another. It was concluded that the soft gimbal concept offered greater flexibility in terms of making equipment changes, and the shuttle concept greater flexibility to slew from one target to another since less mass is involved and the slewing can be accomplished remotely.

The two concepts were rated good in terms of flexibility, since neither was considered to be significantly different. More detailed analyses are required before it can be

determined whether the concepts will require more electrical power and volume than the excess capability of the MORL.

4.8.6 Accessibility to Man

The accessibility of the MOT to the crew members was considered to be an important criterion, since it reflects the ease with which the crew can accomplish their servicing, checkout, and maintenance tasks. The shuttle concept requires approximately one hour for the crew to travel from the MORL to the MOT. In addition, maintenance tasks may require spares that are stored in the MORL, and an additional trip may be required before the maintenance can be completed. If several skills are required to repair and check out the equipment, it may be necessary to make more than one round trip with the shuttle just to transport men. The soft gimbal concept rates best in terms of this criterion since all men and spares are at a close proximity to the MOT. The soft gimbal concept is given a rating of good and the shuttle concept a rating of fair.

4.8.7 Man's Ability to Perform Assigned Tasks

The man hours required to perform the MOT servicing, setup and checkout, and maintenance operations are used as the measure for this criterion. A typical year's operation of the telescope will require 110 entries into the telescope cabin for the soft gimbal concept. An extra two entries will be required for unscheduled maintenance for the shuttle concept, due to the complexity of the electrical power system. A comparison of the manhours for each concept is tabulated in Figure 4-20.

FIGURE 4-20

MOT MANHOURS FOR ONE YEARS OPERATION

<u>Telescope Entry Requirement</u>	<u>Number/Year</u>	<u>Elapsed Time/Entry (Hours)</u>	<u>Manhours/Entry</u>	<u>Total Manhours/Year Gimbaled</u>	<u>Shuttle</u>
Servicing	71	3	6	426	426
Setup and Checkout	10	7.5	15	150	150
Maintenance (unscheduled)	15	24	48	720	720
	10	96	196	1960	1960
Maintenance (short duration)	4	72	144	432	432
	2	1.5	3	---	6
Shuttle Travel	98	2	4	---	392
Shuttle Maintenance	98	1	2	---	196
Shuttle Loading & Checkout	98	0.75	0.75	---	74
TOTAL				3688	4356

CREW SAFETY FOR ONE YEAR'S OPERATION

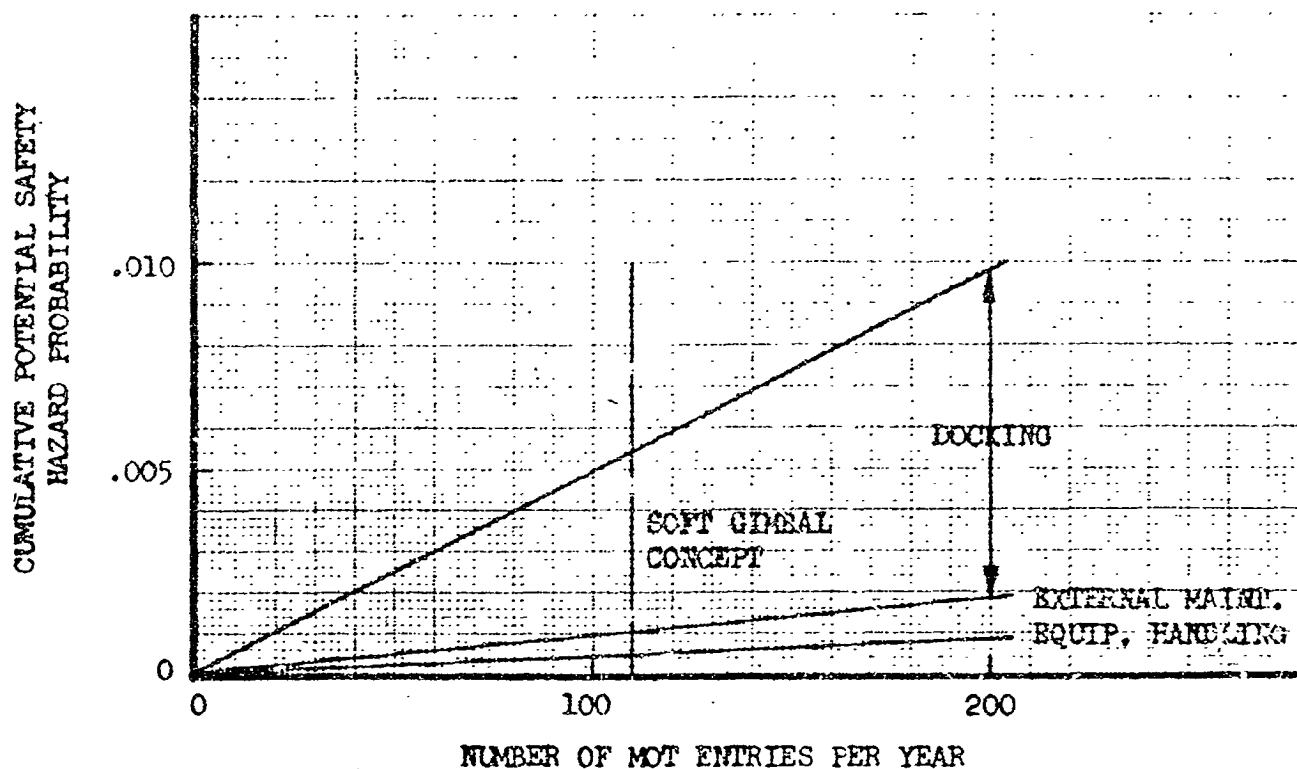


FIGURE 4-18

MANHOURS REQUIRED TO PERFORM MOT OPERATIONS FOR ONE YEAR

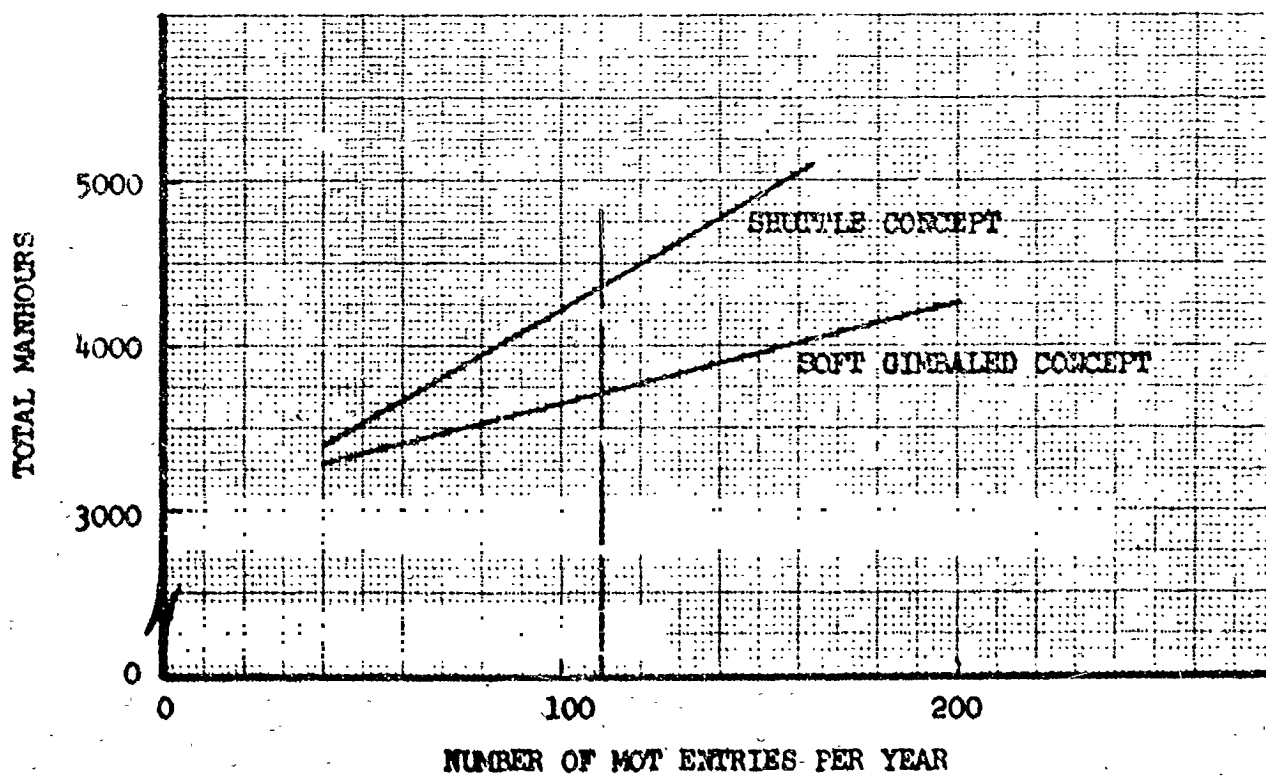


FIGURE 4-21

A comparison of the effect of number of MOT entries on the manhours required for each concept is shown in Figure 4-21. As shown, the gimbal concept requires the fewest total manhours for a year's operation. If a crew of six is used, the MORL experiments can be accomplished leaving an excess of 5,110 manhours per year. Since both concepts require considerably less than this excess, the difference between the two may not be significant.

4.8.8 Logistics Weight

The logistics weight required to support the MOT concepts is an important criterion because it is a factor in determining the frequency and mode used to resupply the concepts. The two concepts are compared on the basis of the weight required for spares and propellant to sustain operations for a one year period as a function of the number of entries into the MOT. Figure 4-22 shows that the shuttle concept rates better in terms of this criterion since it requires 1000 pounds less weight for the estimated 110 entries per year. However, if the number of entries exceed 140 per year, the soft gimbal concept will require less weight.

4.8.9 MORL Interface Constraints and Requirements

The interface between the MOT concepts and the MORL is evaluated in terms of the ability to perform MORL experiments in addition to the MOT experiments. The MORL experiments were reviewed and analyzed to determine whether they could be performed in conjunction with the MOT experiments. The MORL mission has the following required categories of experiments.

- o Biomedical
- o Behavioral
- o Biological
- o Orbital Environment Measures
- o Astronomy
- o Space Sciences
- o Physics Experiment Environment
- o Materials and Structures
- o Communications
- o Navigation
- o Gas and Liquid
- o Space Technology
- o Orbital Launch Operations

LOGISTICS WEIGHT REQUIREMENT FOR ONE YEARS OPERATION

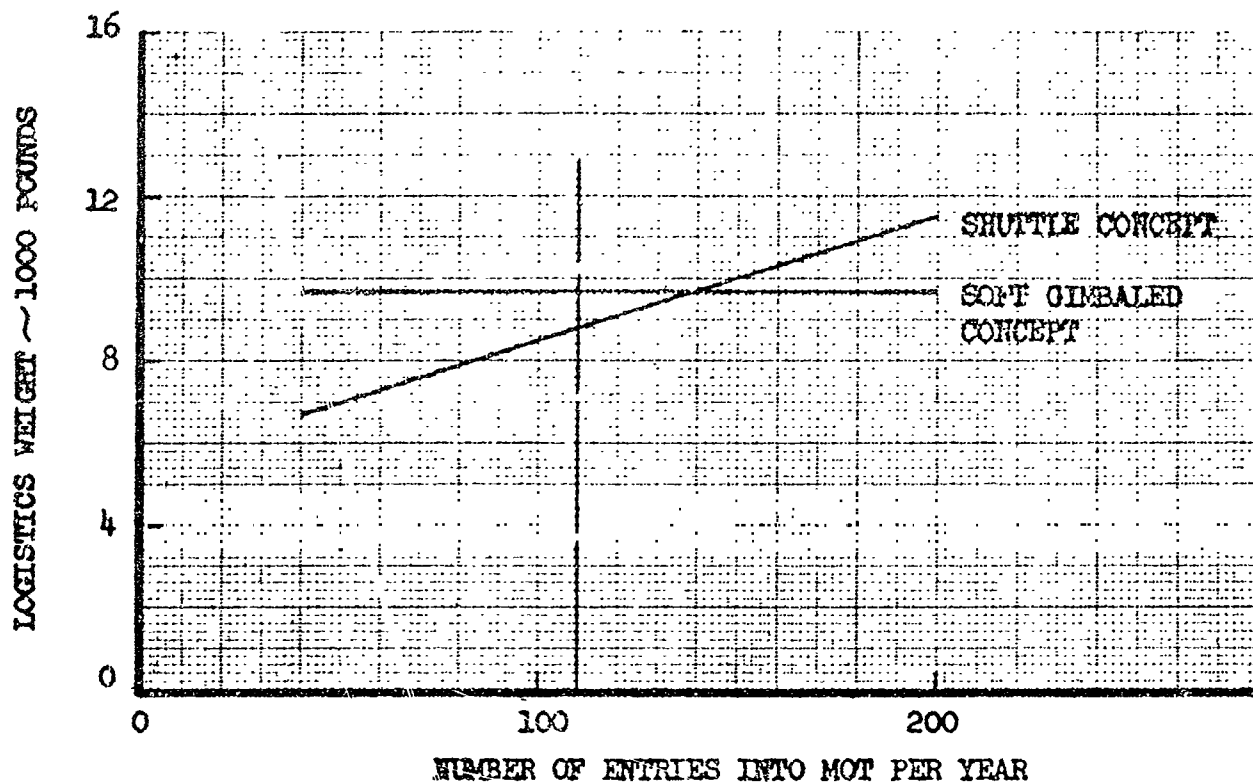


FIGURE 4-22

MORL EXPERIMENT ACCOMPLISHMENT FOR ONE YEARS OPERATION

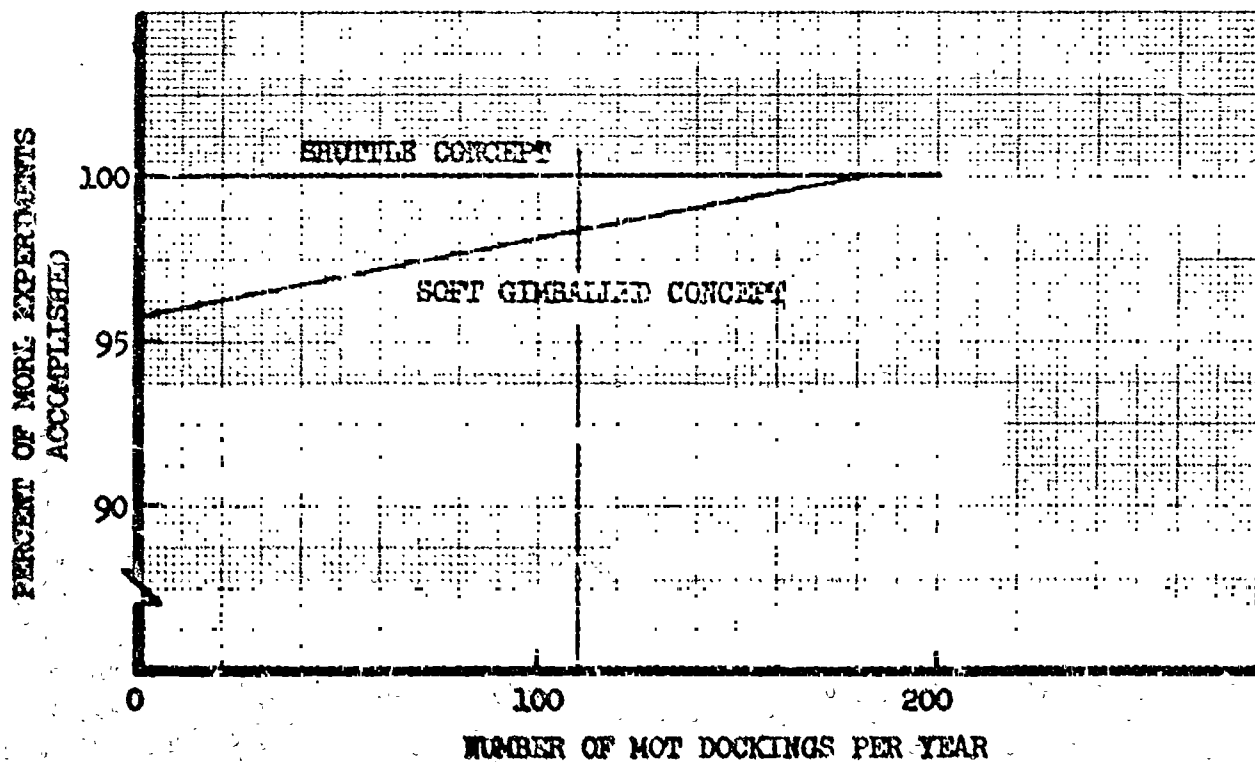


FIGURE 4-23

It was decided that only two categories of experiments required a specific orientation of the vehicle; astronomy and space sciences. Since the astronomy experiments can be accomplished with the MOT, the flexibility of the two concepts was evaluated in terms of the ability of each concept to perform the space science experiments.

The shuttle concept does not require a specific MORL orientation, therefore, it can accomplish all of the MORL experiments as long as there are sufficient manhours available. The soft gimbal concept requires that the MORL concept be oriented to the attitude required for the MOT experiments except when the MOT is being serviced, maintained, or repaired. If it is assumed that the space science experiments can be accomplished in short periods of time (three hours to four days), the flexibility of the concept can be evaluated. Utilizing the hours during MOT maintenance and setups, approximately 98 percent of the MORL experiments can be accomplished with the soft gimbal concept as shown in Figure 4-23. Therefore, the shuttle concept rates better in terms of this criterion.

4.8.10 Recommendations

A comparison of the concepts is shown in Figure 4-24. Each concept was assessed for one year's operation using the criteria shown, and the resulting values tabulated. As shown, the soft gimbal concept rated best in terms of available observation time, reliability, safety, accessibility, and man's ability to perform assigned tasks. The differences between the two concepts are not considered to be significant except for safety, accessibility, and man's ability to perform assigned tasks. The shuttle concept rates significantly better than the soft gimbal concept in terms of technical risk and logistics weight. Since the two concepts are essentially equal for many of the criteria, a recommendation is difficult. However, the soft gimbal concept rates better for more criteria than the shuttle concept. In addition, the trends shown in Figures 4-18 through 4-23 favor the soft gimbal concept with increasing number of entries into the MOT cabin. Since arrangements of the observational program other than that used in the timeline analysis could result in a greater number of entries, these trends demonstrate a significant advantage. Therefore, the soft gimbal concept is recommended as the best mode of operation.

FIGURE 4-24

CONCEPT COMPARISON SUMMARY

CRITERIA	CRITERIA MEASURE	MOT CONCEPTS		PERFECT SYSTEM (REFERENCE)
		SOFT GINBALED	SHUTTLE	
TECHNICAL RISK		MODERATELY LOW	LOW	NONE
OPERATIONS				
AVAILABLE OBSERVATION TIME	PERCENT OF NIGHT HOURS AVAILABLE	79.6	79.3	100
RELIABILITY	PROBABILITY OF CONCEPT BEING OPERATIONAL	85.2	85.0	100
SAFETY	POTENTIAL SAFETY HAZARD ACCIDENTS/1000 YEARS	1	5	0
FLEXIBILITY		GOOD	GOOD	EXCELLENT
ACCESSIBILITY		GOOD	FAIR	EXCELLENT
MAN'S ABILITY TO PERFORM ASSIGNED TASKS	MANHOURS REQUIRED TO PERFORM MOT OPERATIONS	3,683	4,356	576
LOGISTICS WEIGHT	RESUPPLY WEIGHT IN POUNDS	9,723	8,703	0
MORL INTERFACE				
CONSTRAINTS AND REQUIREMENTS	PERCENT OF MORL EXPERIMENTS ACCOMPLISHED	98	100	100

4.9 SUMMARY OF PROBLEM AREAS

At present one of the major problem areas is the dexterity limitations of man in a pressure suit and zero-g environment. It is anticipated that considerable improvement will be made by 1980 in these areas.

These limitations affect the design of structures for assembly and disassembly in space. Adjustment and alignment devices, as well as maintenance and replacement of components, are also affected. Man and equipment must be protected from damage due to dexterity limitations for suited and shirtsleeve man in a zero-g environment. Adequate hand and foot holds, restraints and padding must be provided to afford protection for both man and equipment. Every effort must be made to reduce maintenance problems. Spares components must be designed and packaged for most efficient removal and replacement.

Man must become proficient in the use of space tools and restraint devices. Considerable time on ground training simulators must be acquired to obtain optimum proficiency.

Slight temperature variations will introduce gross errors in the various telescope subsystems. Detection of these errors may be very difficult and time consuming. Therefore, the installation and mounting of the mirrors, optics, spectrometers, spectrographs, cameras, and photometers must be controlled to virtually eliminate temperature differentials.

The MORL will be modified to provide tail docking with the MOT, access hatch and tunnel from MORL to MOT, pressure cabin and interior arrangement changes. The changes in the MORL interior will include provisions for visual docking, film processing, and inspection. Remote controls and displays will be provided for MOT maneuvering, film transport, filter changes, monitoring focus, exposure reading thermal control, communications, etc. In addition, the MORL will provide pressurization capabilities for the MOT cabin.

5.0 DESIGN & SUBSYSTEM INTEGRATION

5.1 APPROACH & DESIGN DEVELOPMENT

A baseline telescope configuration was developed, including all basic optical and scientific subsystems and associated structural support. It was used to examine all methods of operation and the various design requirements of these methods. Development of this baseline configuration is described in detail in Section 4.1. The remainder of this Section details the operational configurations considered and developed, structural considerations, subsystems, controls, thermal considerations, and other operational systems.

5.2 CONFIGURATIONS

5.2.1 General

Conceptual vehicle configurations were generated to provide the design data necessary to establish technical feasibility and to select the best operational method and design of the observatory. Study requirements and design areas in which the conceptual configuration data presented in this section contributed to the study objectives are:

- 1) Definition of a feasible structural arrangement of the basic telescope mirrors, cabin, and scientific equipment, and supporting subsystems;
- 2) Definition of vehicle geometry and mass characteristics for analyzing and determining solutions for attitude control, thermal control, and optical geometry control. The vehicle configuration used is also required to be compatible with the launch vehicle and operational functions; and
- 3) Provision of an engineering basis for analyzing design problems associated with man's role, design and installation of major subsystems, and operational functions for astronomical observations.

Many design requirements of the MOT are relatively independent of the method of orbital operations. In general, these requirements are associated with basic telescope elements such as the primary and secondary mirror, experiment equipment, the cabin, and the primary structure which ties these elements together. This part of the MOT vehicle is called the "baseline telescope configuration." The design requirements associated with orbit functions vary with the different modes of operation. These design requirements are handled by the addition of interface structure and subsystems to the baseline configurations. The complete MOT observatory system is called an "operational concept." Design features of the two most promising operational concepts are presented in Paragraphs 5.2.2 and 5.2.3. The data includes conceptual drawings and brief descriptions denoting differences in both the launch and orbital configurations.

The baseline telescope configuration which was generated in the last phase of study and which was utilized in defining the final two operational design concepts is presented in Figure 5.2-2. Design of this vehicle is based upon the geometry fixed by the f/4 primary mirror optical system and upon the requirements for a structural support arrangement that can satisfy launch loads and provide acceptable thermal and dynamic characteristics for orbital operation. The optical system geometry is defined in Section 3. The significant dimensions are noted in Figure 5.2-1, which is an optical schematic depicting the mirrors and focus planes for both the F/15 and f/30 systems. Configuration design studies influenced the selection of the optical system geometry by imposing the following requirements:

- o The size of the secondary mirror and its mounting structure is restricted to a permissible light blockage of the primary mirror. For the purposes of this study, a 39.6-inch diameter was used as the maximum acceptable for the secondary mirror and housing. This diameter corresponds to an obscuration ratio (secondary dia./primary dia.) equal to 0.33.

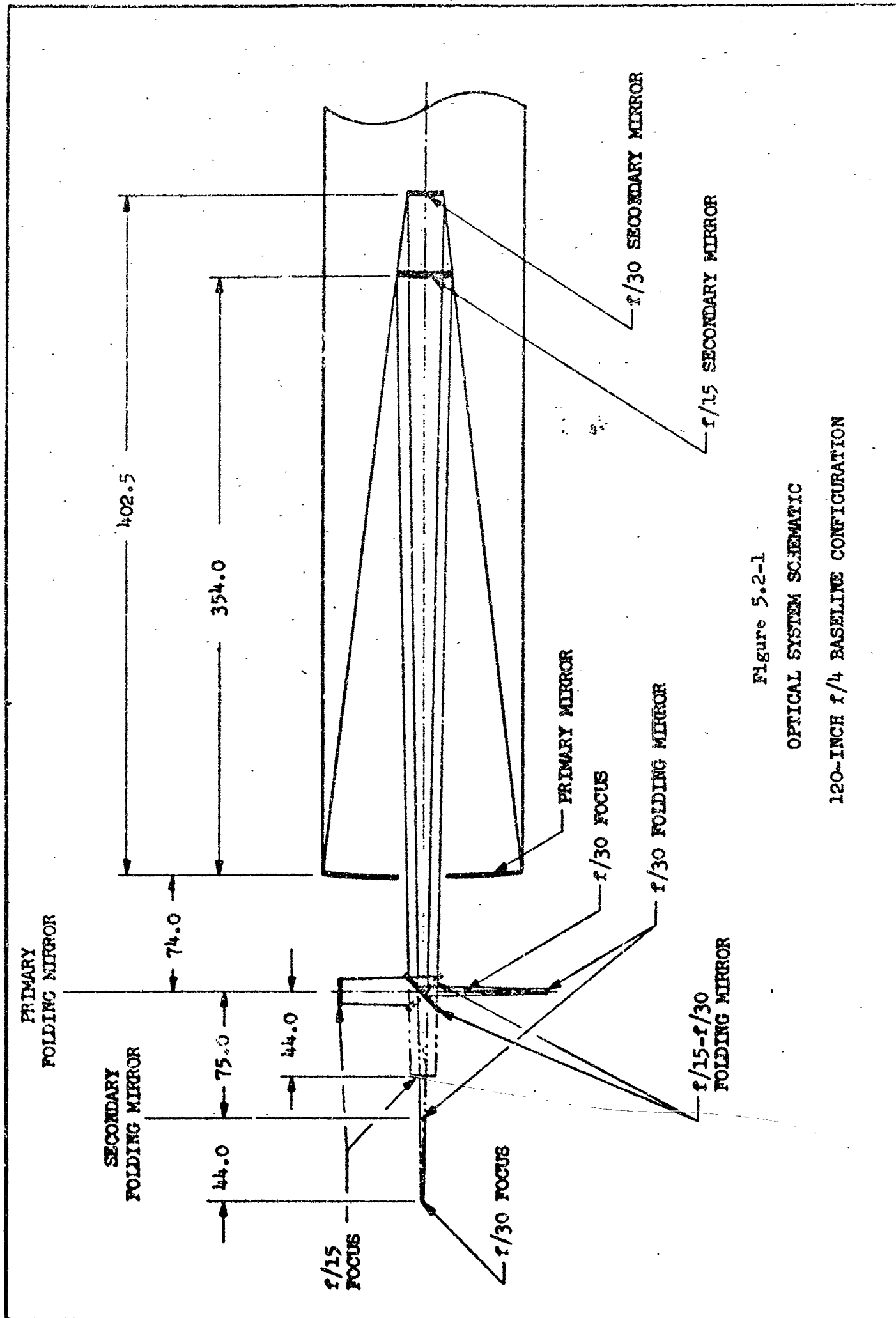


Figure 5.2-1

OPTICAL SYSTEM SCHEMATIC

120-INCH $f/4$ BASELINE CONFIGURATION

- o Folded light paths of the $f/15$ and $f/30$ mirror systems at the Cassegrainian focus have to be compatible with a folding mirror and experiment equipment installation arrangement.

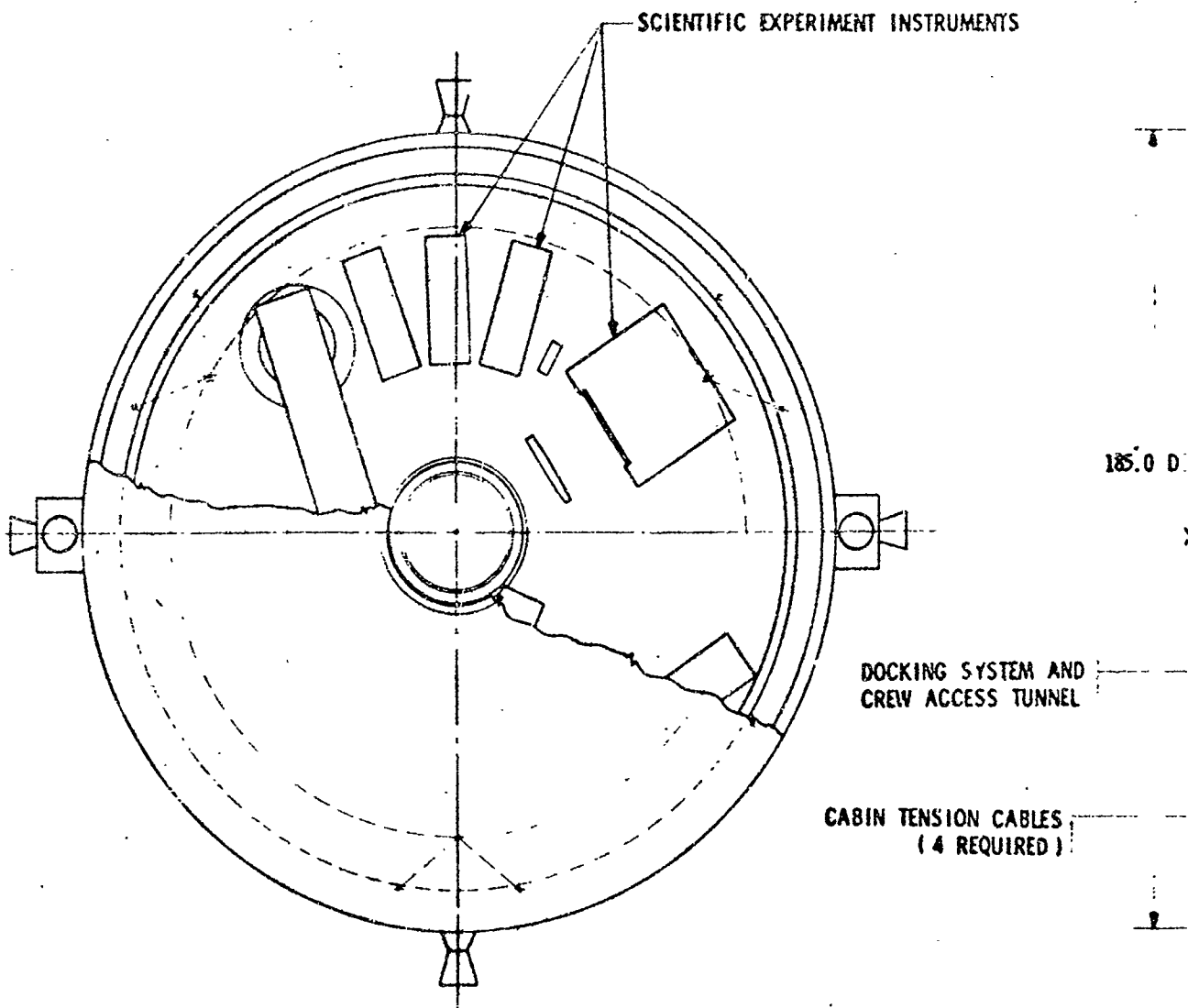
The lengths of the folded light paths that could be handled within the cabin determined the final location of the secondary mirrors relative to the primary mirrors. Selection of an experiment equipment arrangement and folding mirrors were also the dominating factors in determining the shape and size of the cabin.

The cabin is a cylinder with flat, pressure-type bulkheads on both ends. This shape provides volume and space in which a feasible arrangement can be provided for mounting the scientific equipment and for accommodating crew requirements. A double shell tubular structure is used for housing the telescope mirrors. The exterior shell is attached to the forward end of the cabin and extends the full length of the telescope.

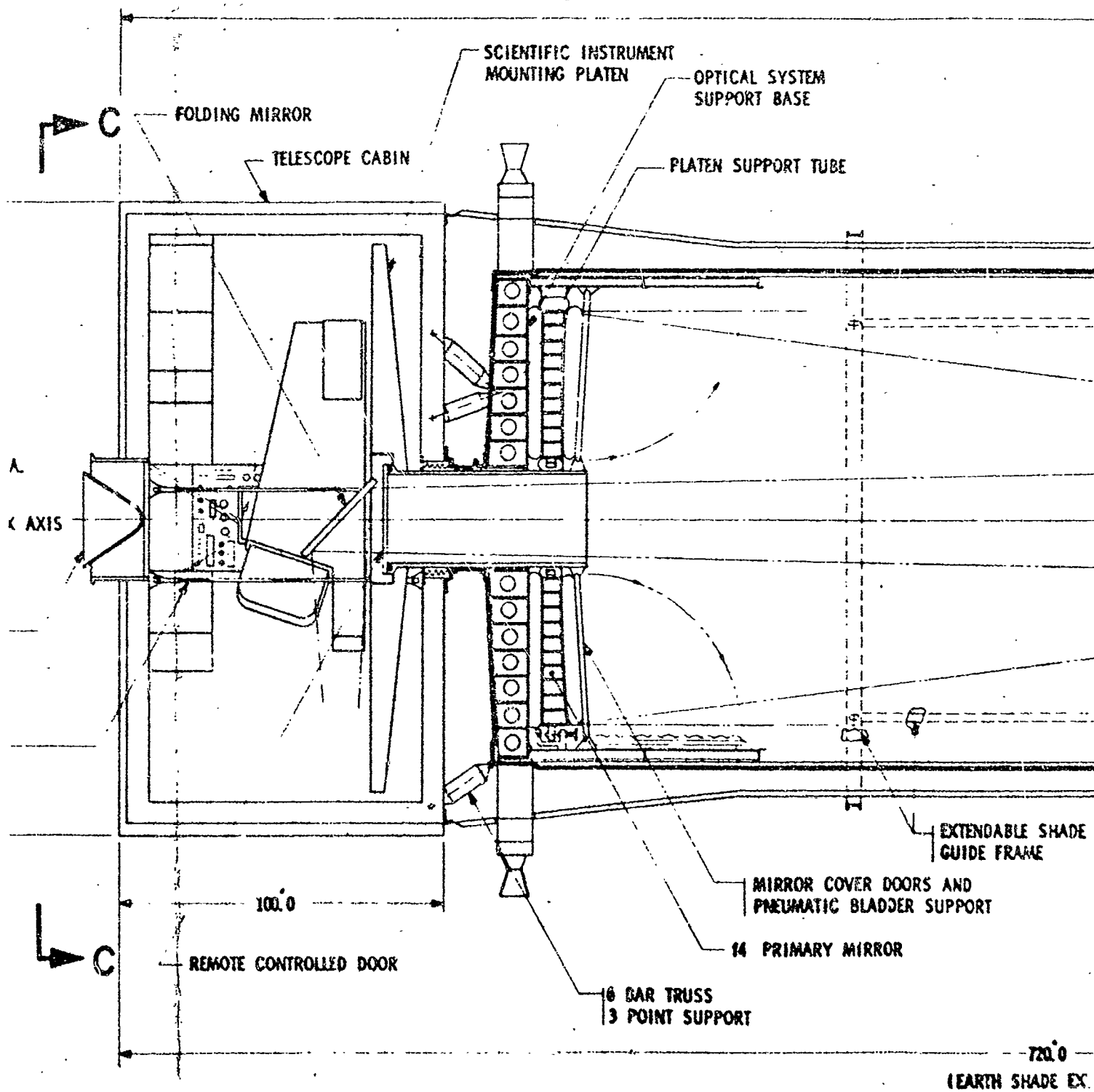
To obtain the desired shading from Earth radiation while keeping within a reasonable height for the launch configuration, a telescoping section, which is called an "Earthshade", was used at the forward end. This telescoping section is extended and fixed into position after the vehicle is in orbit. The Earthshade, which is sometimes referred to as the heatshield, was incorporated in the baseline configuration as a result of the thermal analysis. Purpose of the shade is to place the secondary mirrors and doors inboard of the end of the telescope shell which is exposed to Earth radiation. The doors in the open position should be in a uniform temperature zone so that when they are closed they have little thermal effect on the primary mirror. In the closed position, the doors also require thermal insulation to control their heat transmission when their outer surfaces are exposed directly to the Earth emitted and reflected radiation in the daylight half of orbit. The baseline drawing depicts a method for deploying the extendable Earthshade which utilizes four track and rollers spaced 90 degrees apart on the periphery of the fixed outer shell. An open frame structure is added to the aft end of the shade to provide increased L/D for guiding during deployment.

The inner shell of the double wall design is the main structure which supports or ties together all elements of the optical systems. The complete inner shell, mirrors, mirror support structure, and platen for mounting the scientific equipment are attached to the cabin by a six-bar cantilever truss design, in which the entire assembly is suspended on three structural attachment points. The overall arrangement of the two shells and three point mounting is used to decouple the optical system from the outer shell and cabin for thermal isolation and to minimize mechanically-induced structural distortions. The three-point mounting also permits the plane of attachment points to tilt without inducing stresses into the optical support structure. Since the platen to which the experiment equipment is mounted is located inside the cabin, a flexible bellows is shown between the platen tubular support and the cabin bulkhead. This permits the cabin bulkhead to be deflected by pressure and temperature variation without producing strains on the optical system structure.

A remotely operated door in the aft end of the platen support tube is used for pressurization of the cabin. Both of the two final operational concepts utilize a docking system; therefore, the combination docking mechanism and crew transfer

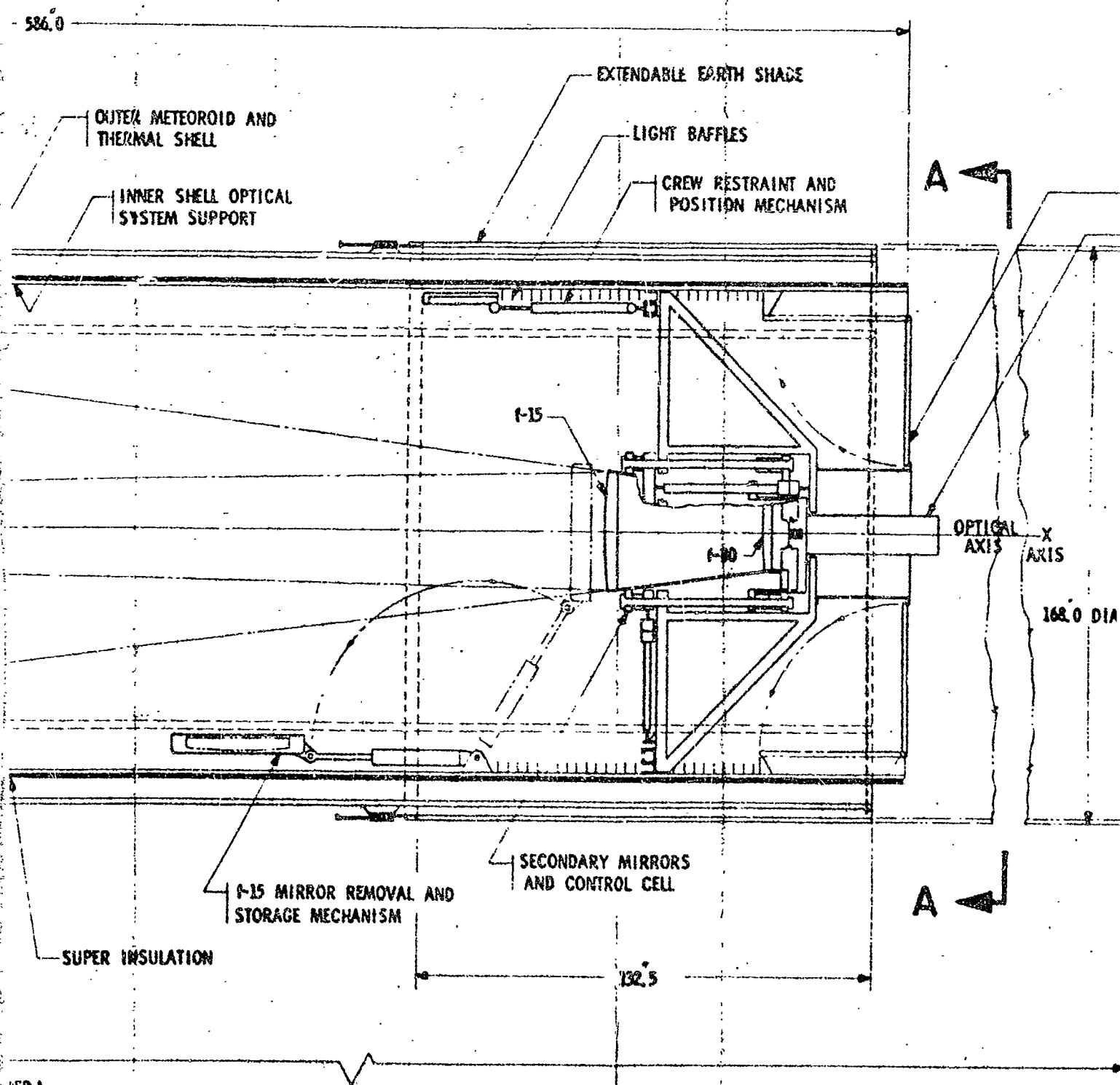


SECTION C-C



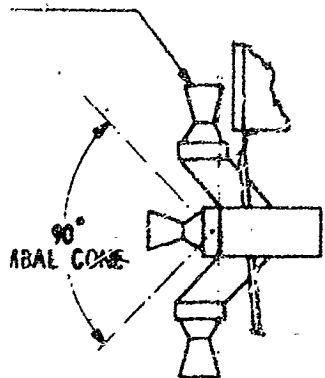
(EARTH SHADE EX.

STAR TRACKERS
8 REQUIRED
TOTAL FIELD OF VIEW
4 π STERADIAN



(ED 1)





SECTION B-B

TELESCOPE DOORS (CLOSED)

-INTERMEDIATE GUIDANCE SENSOR

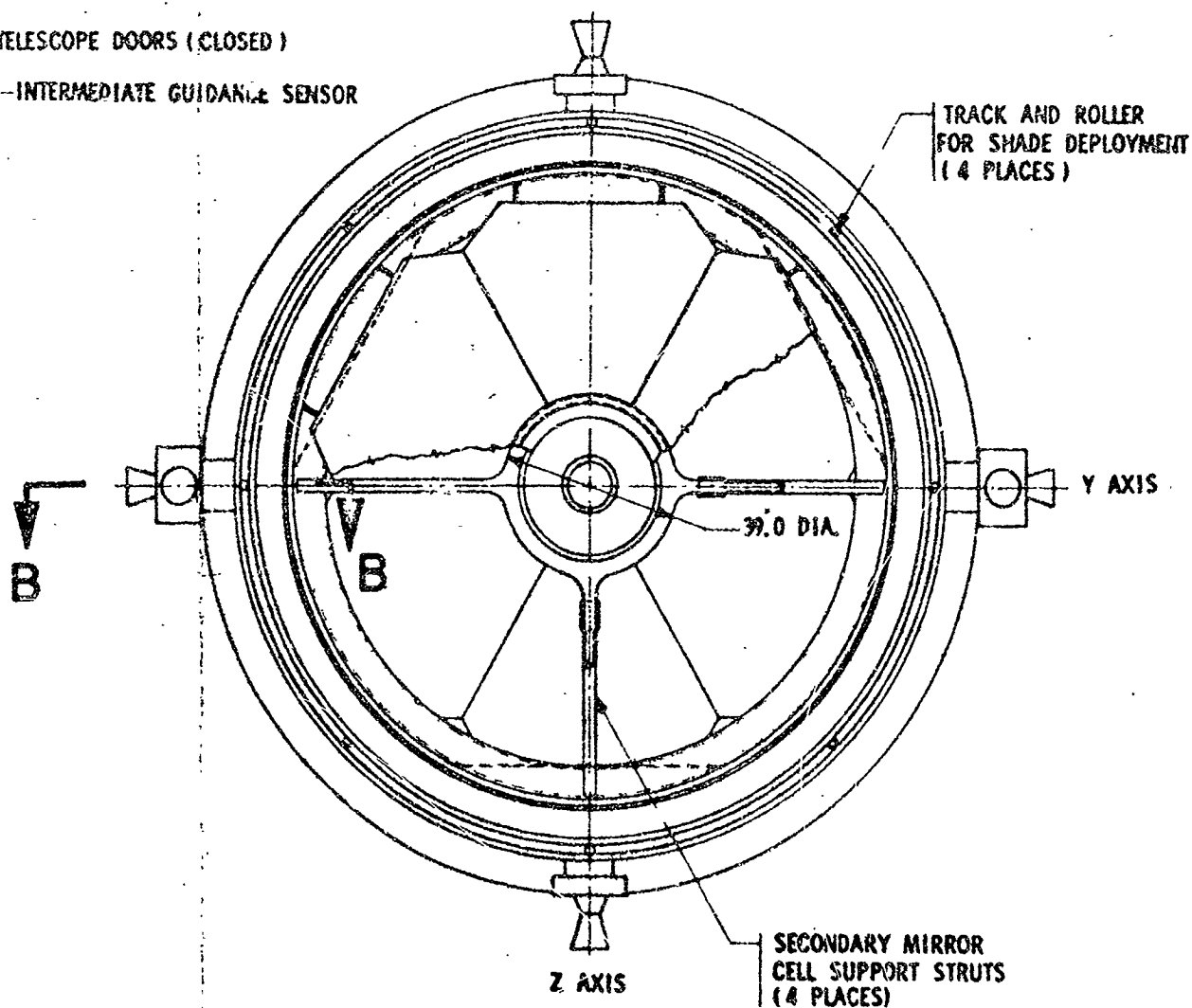


Figure 5.2-2

BASELINE CONFIGURATION
120 INCH MANNED ORBITAL TELESCOPE

tunnel is shown as part of the baseline. This design will be the same as that used on the MORL for Apollo-type logistic vehicles.

The primary mirror is mounted on three-point tangent bars, designed to minimize heat shorts and structural distortions. During boost to orbit, the primary mirror is structurally decoupled from the tangent bar mounting and floated on pneumatic bladders to insure that the mirror will retain its figure. Doors on the front side of the mirror serve a dual purpose in that they are used to protect the delicate optical surface from foreign material and also to provide structural support for the pneumatic bladders.

Secondary mirrors located at the forward end of the telescope are mounted in a control cell, which in turn is supported by four radial truss type spokes attached to the inner shell structure. Control cell design provides a five axis automated control for aligning the secondary mirrors. On the aft side of the mirror support struts, a crew constraint mechanism is shown in a stowed position. This mechanism is mounted in a track which runs around the inner diameter of the wall structure. A combination of motorized mechanical joints, an extendable arm and movement around the track provides crew positions for work on the secondary mirror while constrained to the seat of the device. The drawing also depicts the mechanism used for removing and stowing the f/15 secondary mirror. The doors located forward of the secondary mirrors are for these operational periods when it is desired not to have the optical system exposed to the external environment. More detail descriptions of the optical system's design and installations are presented in paragraph 5.2.5.

The star trackers required by the guidance system are basically the same for all operational concepts; therefore, they are included in the baseline configuration. Installation requirement for star trackers on the MOT calls for an arrangement of individual trackers having a 90-degree field of view to cover a total spherical field. Each star tracker should be mounted to structure on which its dimensional alignment can be maintained with the optical axis of the telescope. Careful attention was given to decouple the telescope optical mirrors and supports from the outer thermal protective shell. In the case of the star trackers they should be mounted to optical structural elements and their mounting structure must extend beyond the exterior surfaces of the MOT to accommodate the field of view needed. These requirements establish limited locations for mounting of the trackers. The first choice is to mount the trackers directly to the primary mirror and the second choice is the primary mirror support cell. The first choice creates a direct thermal short to the primary mirror which must be avoided. The second choice was, therefore, selected for the baseline configuration and the installations. The minimum number of trackers required would be six if the vehicle could accommodate an installation at the ends of the telescope for pointing fore and aft along the optical axis. However, there is structural blockage of the field of view of these trackers when mounted on the primary mirror cell; therefore, two additional trackers are required for total spherical coverage, increasing the total number required to eight. In the case of the soft gimbal concept, Model 94S-41C, the total field of view is still less than desired due to the view blocked out by the MORL structure, the solar panels being the largest offenders.

5.2.2 Operational Concept Mode, Model No. 94S-41

Operational concept Mode I is a design in which the baseline 120-inch telescope is

docked and then permanently coupled to the MORL. The conceptual design shown in Figure 5.2-3 is an orbital configuration of Model No. 948-41 which utilizes a structural attachment consisting of an open frame type support, manually attached to the MORL, and a soft spring suspension gimbal design. The telescope is shown attached to the end of the MORL opposite that used for docking and storing logistic vehicles. This location was selected so the telescope would not interfere with the MORL logistic operations and other experiments.

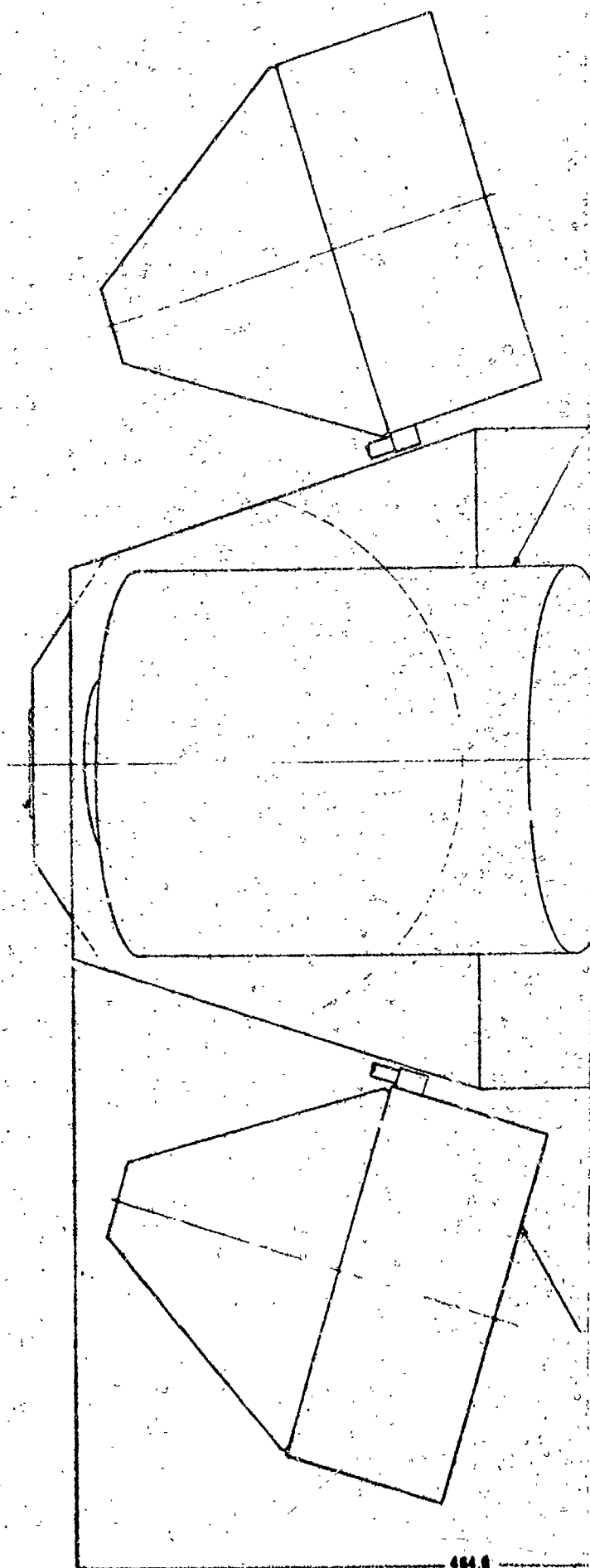
The MOT is docked to the MORL in essentially the same manner as an Apollo logistic vehicle is docked, except the MOT is unmanned and must be remotely controlled by the MORL. Similarly, the same combination of docking mechanism and crew transfer tunnel used between the Apollo and the MORL is shown for the MOT. In this particular application, the crew tunnel and docking structure is a telescoping design to accommodate decoupling of the docking interface during periods of astronomical observations.

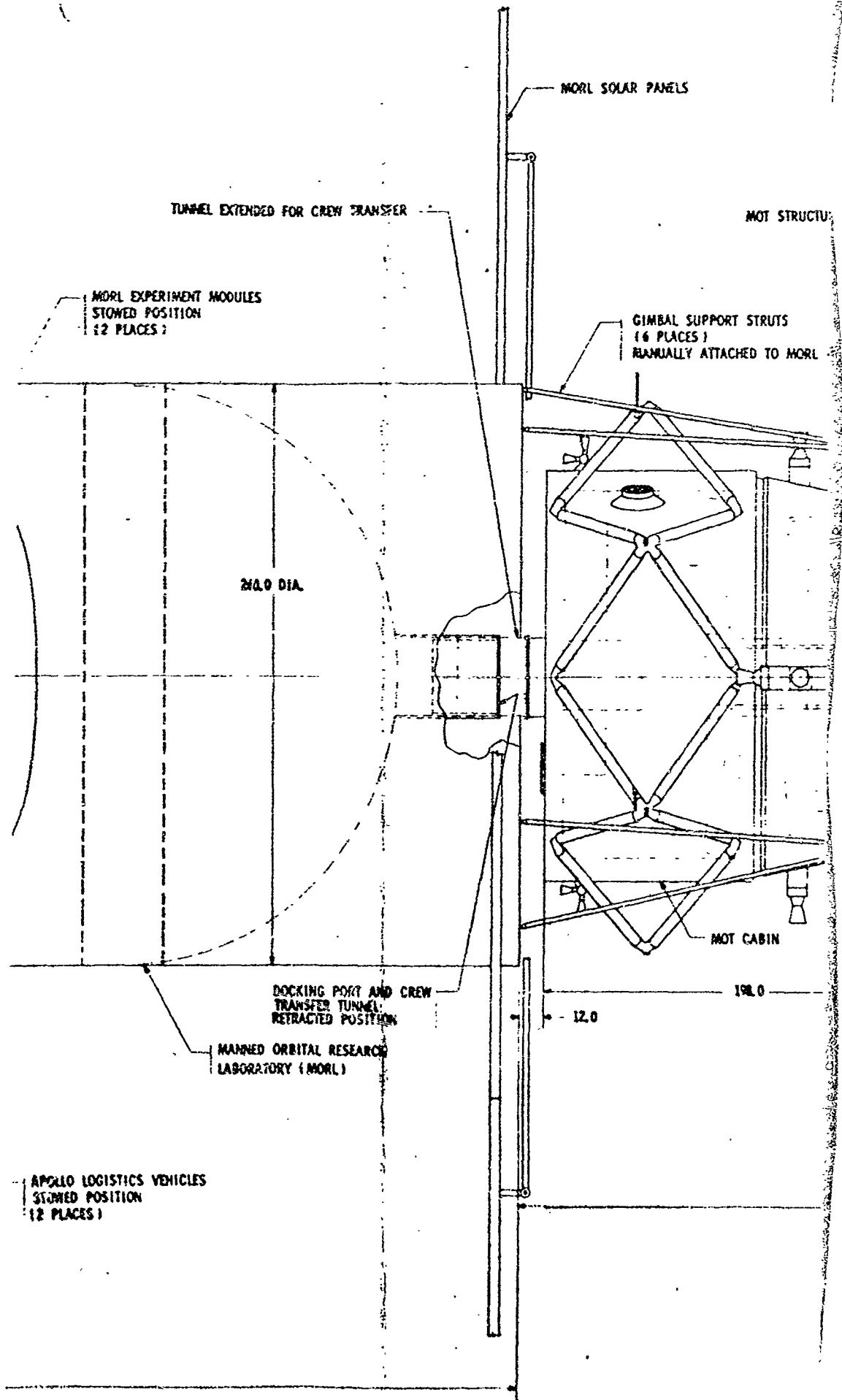
Sections of the gimbal support structure required to be permanently attached to the MORL are hinged for stowage during launch and can be swung into place and fastened to the MORL by crew members working in spacesuits. The gimbal assembly is located at the center of gravity of the MOT, with the outer ring attached to the end of the gimbal support structure by three sets of springs located around the periphery, 120 degrees apart. There are also three sets of position actuators mounted on the gimbal support structure which straddles the springs. These position actuators will acquire the MOT and position it for engaging the crew transfer tunnel. They are also structurally capable of supporting the MOT when the total observatory is slewed to acquire new astronomical targets, when the MORL is thrusting for orbit keeping, and when logistic vehicles are docking to the MORL. With the telescope in operation, the position actuators are retracted and the MOT floats on the spring suspension system. Clearance is provided between the MOT and the MORL structure to accommodate rotational and translational displacement of the MORL relative to the MOT. Displacements are based on man's disturbance and on the limit cycle of the assumed attitude control system for MORL. The design principle of the soft gimbal is to reduce the MORL disturbance forces to a level in which the resulting torques imposed on the MOT can feasibly be handled by a fine stabilization control system, while still transmitting the small forces necessary for orbit keeping.

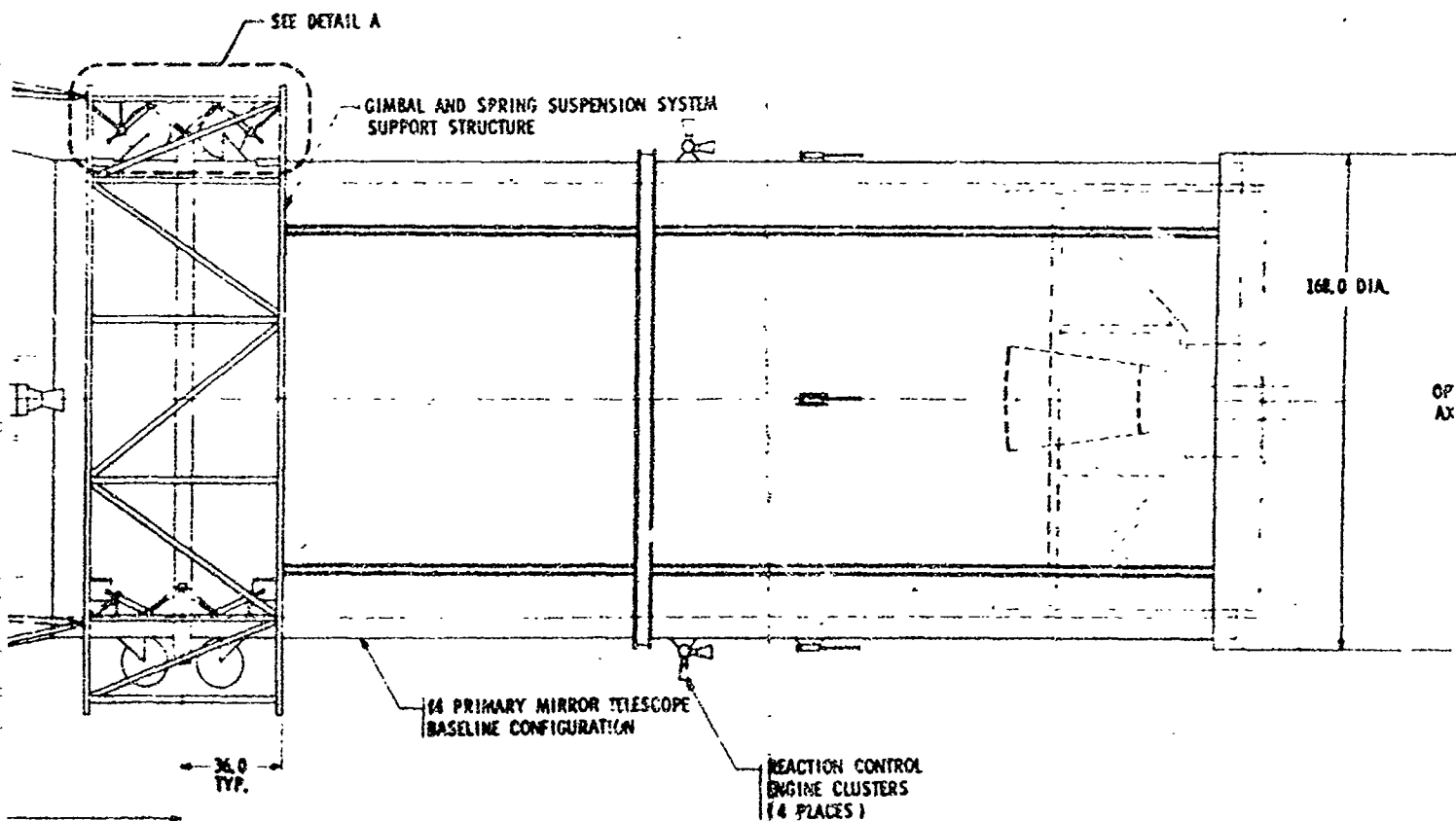
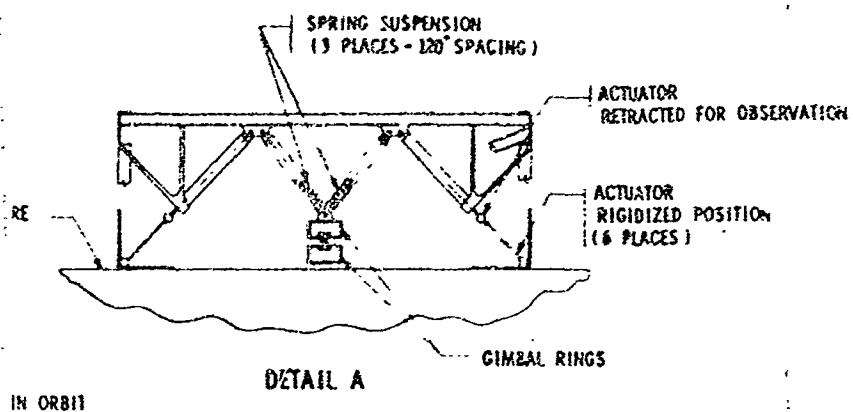
Inertial attitude differences between the two vehicles are handled by a two-axis gimbal, but an attitude change of the MORL results in a displacement at the gimbal location or CG of the MOT. This displacement, along with pure translational displacement, is handled by mounting the gimbal in a spring suspension system which has four degrees of freedom and spring rates that give the required amount of force attenuation. Spring rates are basically governed by the stroke associated with maximum displacement, the distance between the point of applied force and the MOT CG, the maximum permissible torque, thereby induced, and a requirement that the springs must accommodate gravity gradient forces and the forces due to differences of aerodynamic drag between the MORL and the MOT. Design analysis of the spring suspension system is described in Section 5.3.2.4.

The above description of the soft gimbal design concept denotes the structural interface requirements imposed on the MORL. MOT operations, in addition, impose system interfaces and modifications to the MORL subsystems. For purposes of this study, it was assumed that electrical power and atmosphere for life support would

DOCKING SYSTEM
MDRL LOGISTICS VEHICLES







132.0

A

GIMBAL SUPPORT STRUTS
(120° SPACING)

MORE SOLAR PANELS

TICAL
:15

X AXIS

A

Z-AXIS

Y-AXIS

SECTION A-A

Figure 5.243
ORBITAL CONFIGURATION
120 INCH MANNED ORBITAL TELESCOPE
OPERATIONAL CONCEPT 948-41C
(SOFT GIMBAL SUSPENSION)

be piped into the MOT from the MORL thru umbilical connections. A final design selection that may differ from this assumption would alter the operations analysis and possibly vehicle designs but would not affect the prime operational characteristics of the concept or feasibility. Other MORL subsystems that would require modifications are communications and data management, attitude control, orbit keeping, resupply equipment handling, environmental control, and possibly crew systems.

The only significant effect this operational concept has on the observation performance of the MOT is in the area of attitude control. An analysis of the control problem is presented in Section 5.4. Installation of the star trackers required by attitude control is affected because the MORL, with its large solar panels, causes considerable blockage of the total field of view desired for the trackers. Feasibility of using trackers mounted on the MORL structure for coarse acquisition of an astronomical target has not been evaluated.

A launch configuration with MOT Model No. 948-41C installed on top of the S-IV stage of the Saturn IB booster is shown in Figure 5.2-4. The MOT is packaged within a jettisonable boost shroud, similar to the Apollo LEM Adapter design concept. The boost shroud, which includes the nose cone section, is jettisoned after Saturn IB first stage burnout. By this technique, the payload to orbit is only penalized by approximately 12 percent of the boost shroud actual weight and the MOT primary structure need only satisfy the boost inertial loading and the orbital operation design requirements. At present, it appears more efficient to jettison the boost shroud and use the weight in orbit for selective structural design, selective insulation, and to provide an exterior surface coating protected from launch environment.

The MOT is supported on top of the S-IVB by a truss-type structure which transfers the flight inertial loads into the outer booster structure at six hard attachment points. Separation of the MOT from the S-IVB is also affected at these attachment points, which are located at the same separation plane as that used for the jettisonable boost shroud.

In the flight to orbit, the S-IVB (2nd stage of the Saturn IB) places the MOT in a phasing or holding orbit. The S-IVB is then separated from the MOT, and the two 1,000 pound thrust rocket engines shown near the aft end of the MOT cabin are used to perform the orbit transfer associated with the rendezvous maneuvers. Propulsion requirements for the terminal docking maneuver are handled by the reaction control jets, which are also used for attitude control and desaturation of the MOT control moment gyros. Noted on the launch configuration drawing are special designs and removable boost structure used to protect telescope systems during launch. The primary mirror is supported on pneumatic bladders and structure is added to remove loads from the gimbal bearings and spring suspension system. Additional removable boost structure, not shown on the drawing, will be required to protect the experiment equipment and platen-type support within the cabin and to protect the secondary mirror control cell. The extendable section of the telescope outer shell is in the retracted position for launch and remains in this position until after the MOT is docked to the MORL.

5.2.3 Operational Concept Mode III. Model No. 948-43D

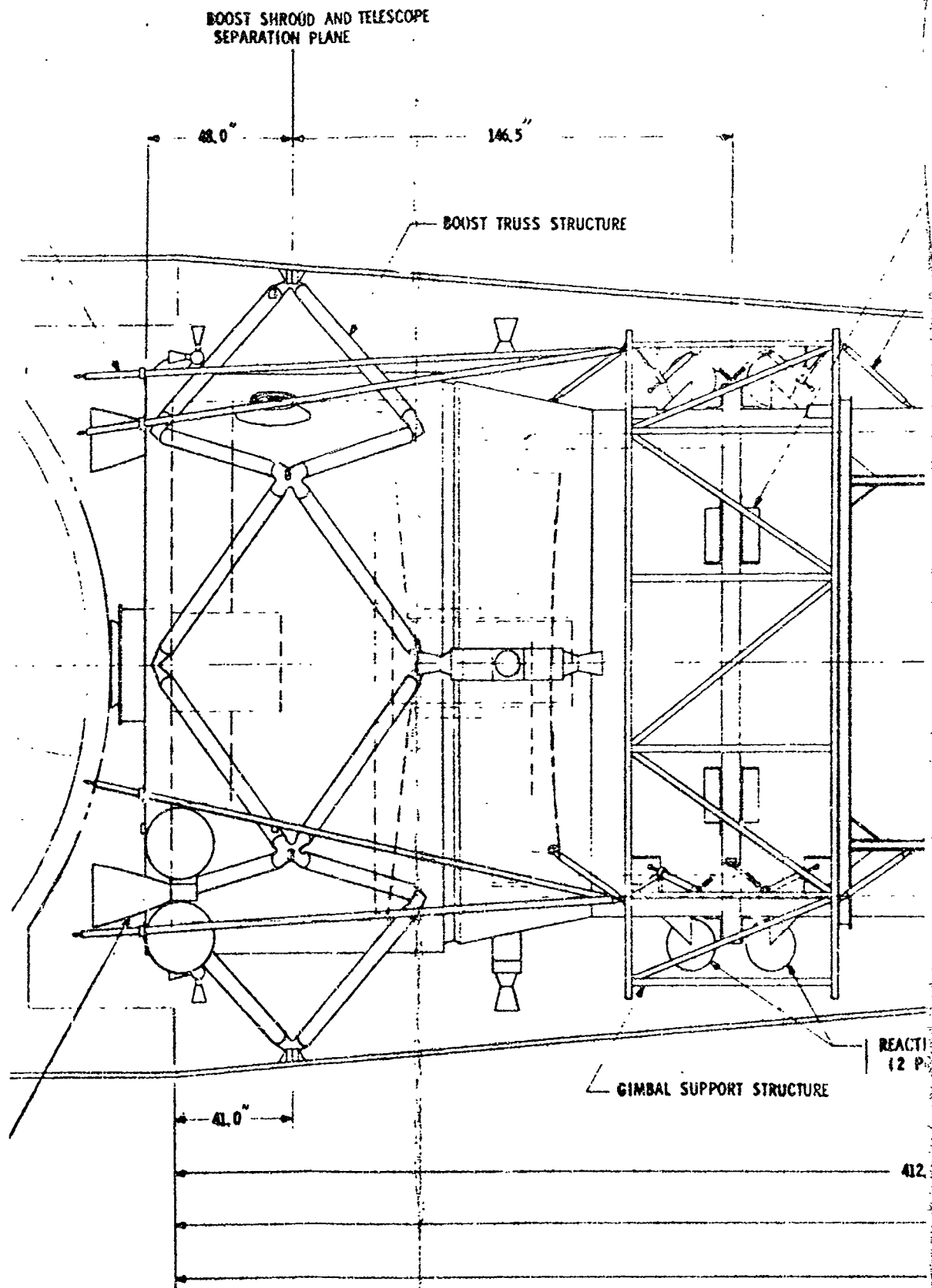
Operational concept Mode III is a design in which the baseline 120-inch telescope

GIMBAL SUPPORT STRUTS FOR ATTACHMENT
STOWED POSITION FOR LAUNCH TO MORL
(6 PLACES)

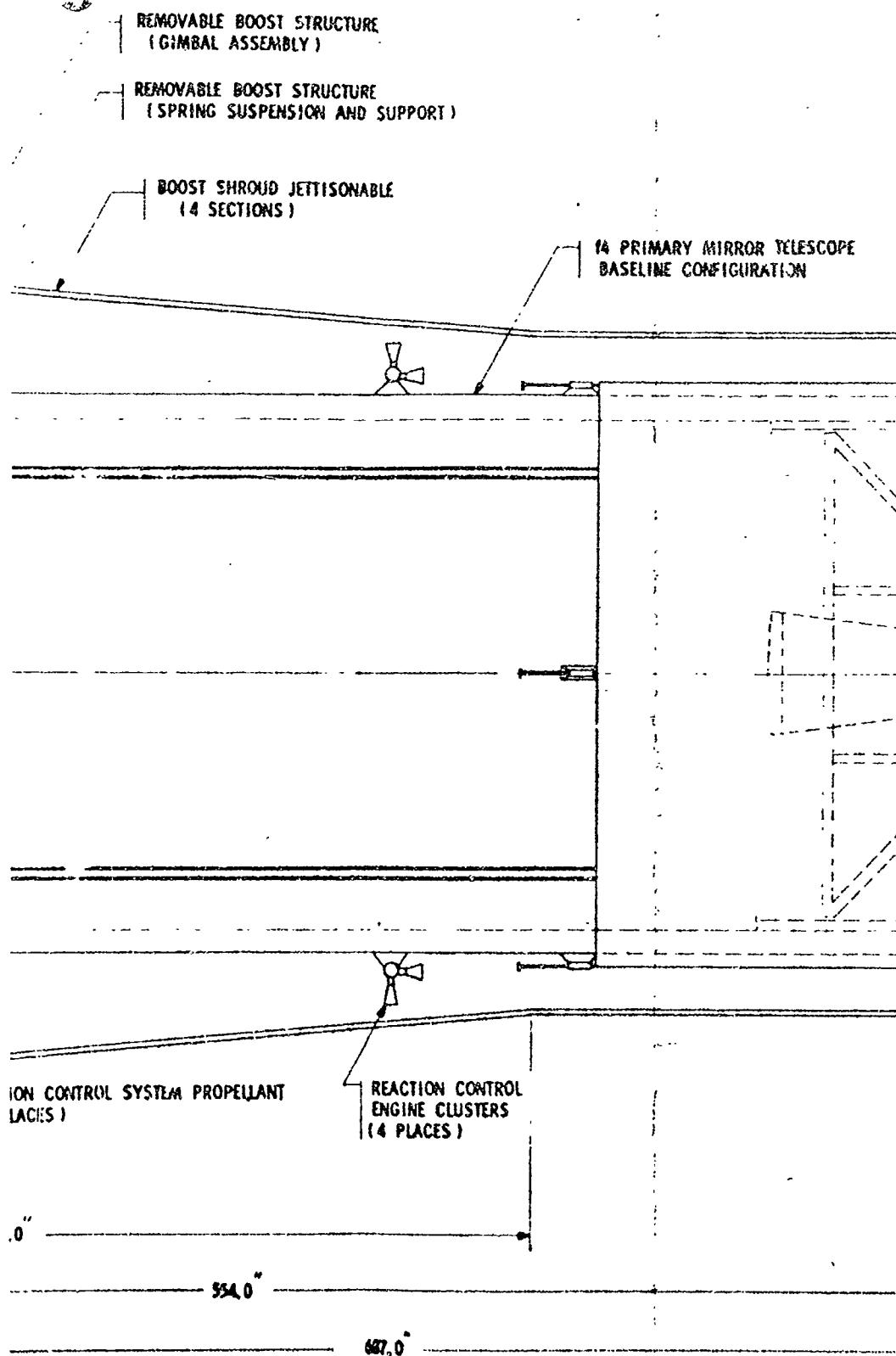
260.0 DIA.

SIV B STAGE SATURN
IB LAUNCH VEHICLE

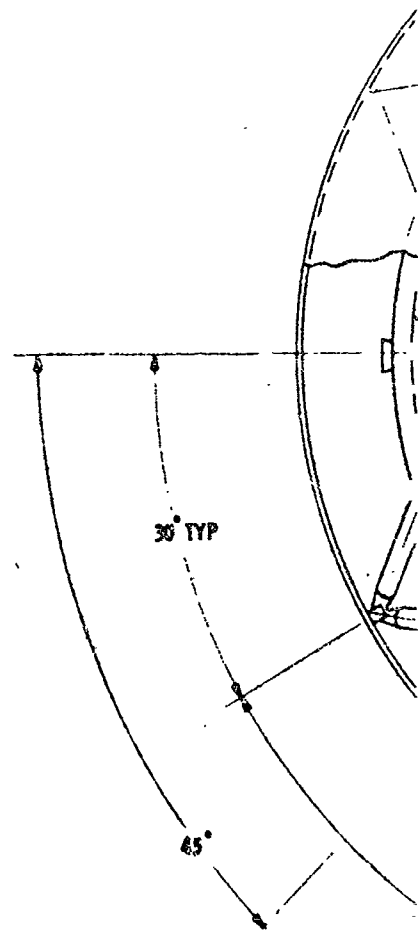
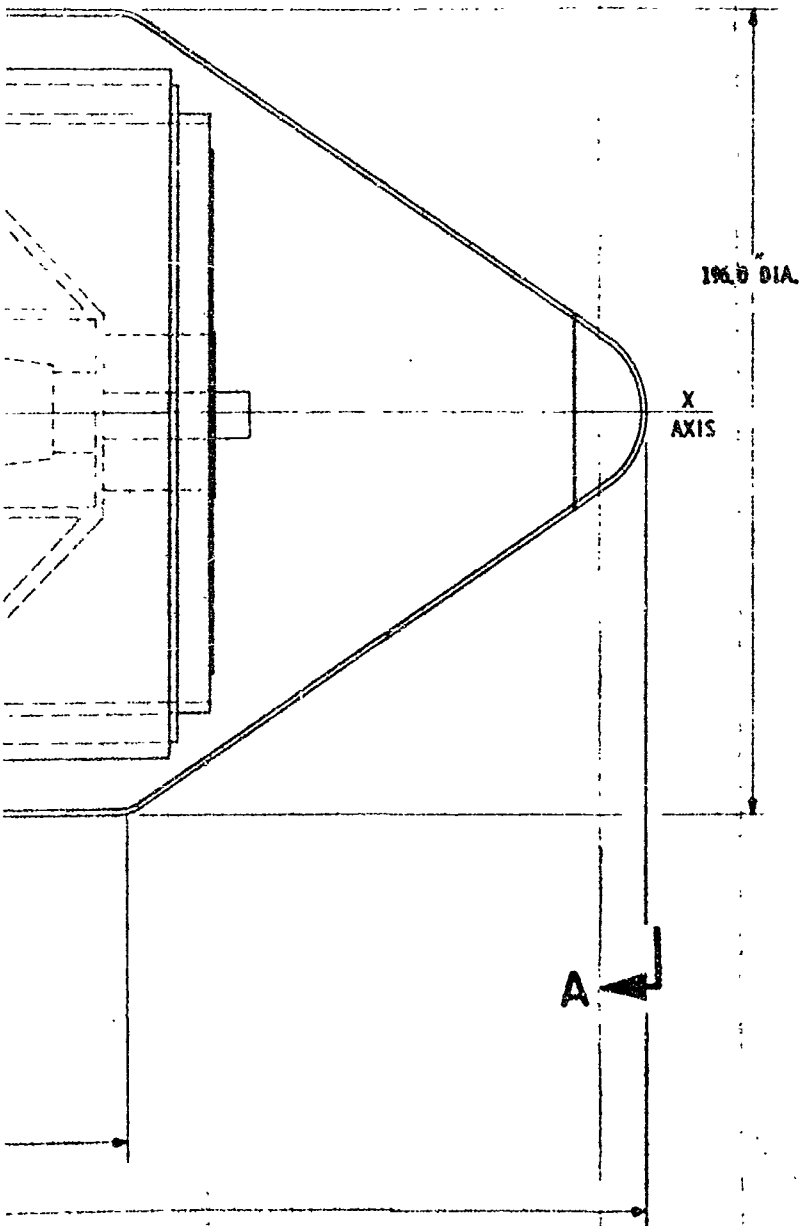
ORBIT II
RENDEZVOU
1000 ft
AND
12 PLACES



SECTION AND
OUS PROPULSION
B. THRUST ENGINE
PROPELLANT SUPPLY
S 1



A



196.0 DIA.

30° TYP

45°

196.0 DIA.

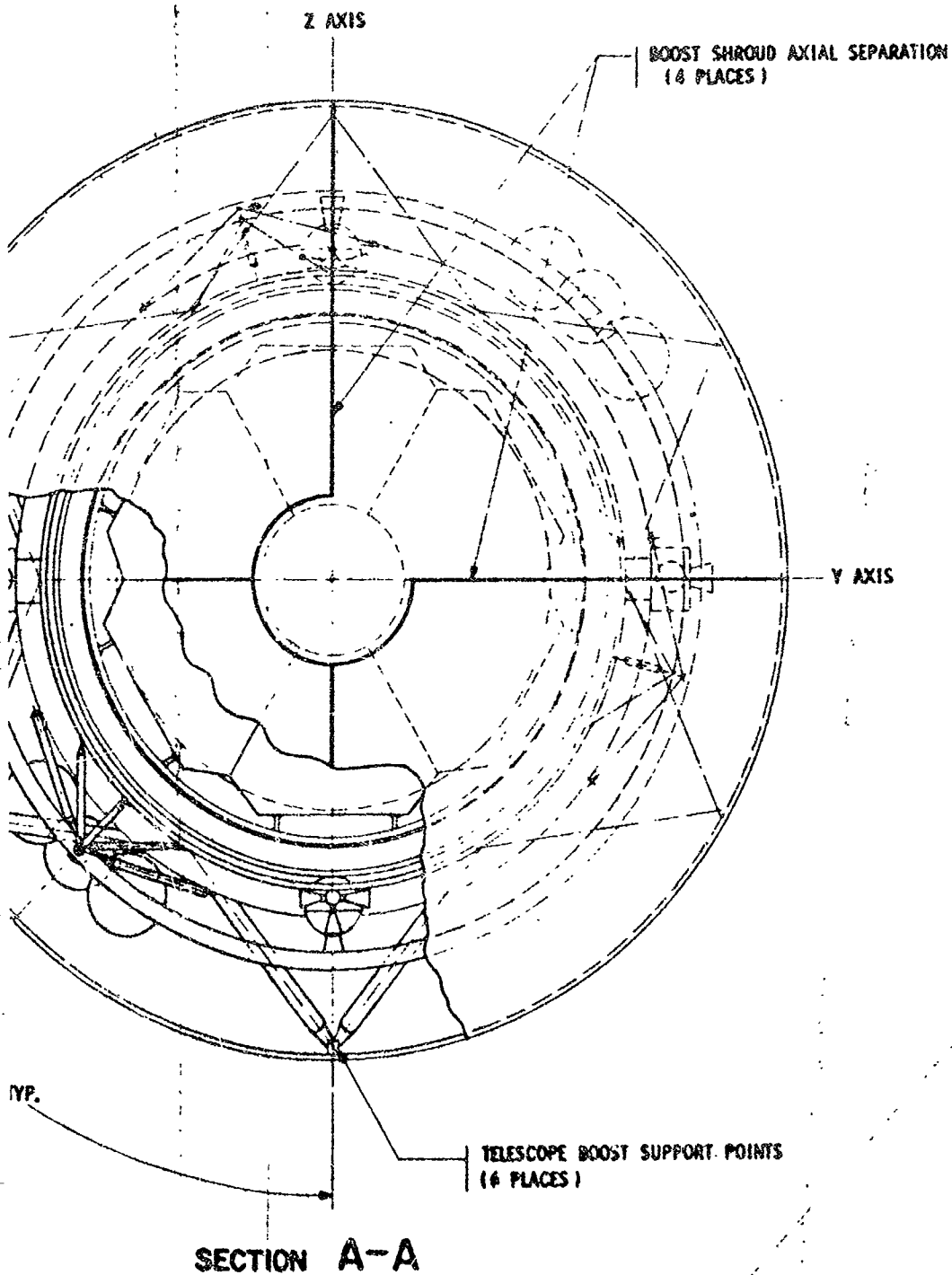


Figure 5.2-4

LAUNCH CONFIGURATION
120 INCH MANNED ORBITAL TELESCOPE
SOFT GIMBAL MODE
MODEL NO. 943-41C

is provided with subsystems for operation in orbit decoupled from the MORL. The complete MOT observatory system designated Model 948-43D utilizes a shuttle vehicle to ferry crew and equipment between the MORL and MOT for routine servicing. The MOT also has maneuvering and guidance capability to dock with the MORL, which provides the operational concept with long period direct access for crew participation which is considered important for initial activation of the telescope and for major maintenance or repair. The initial setup and checkout of the optical systems may require weeks in orbit due to the time required to stabilize temperatures in the mirrors and supporting structure.

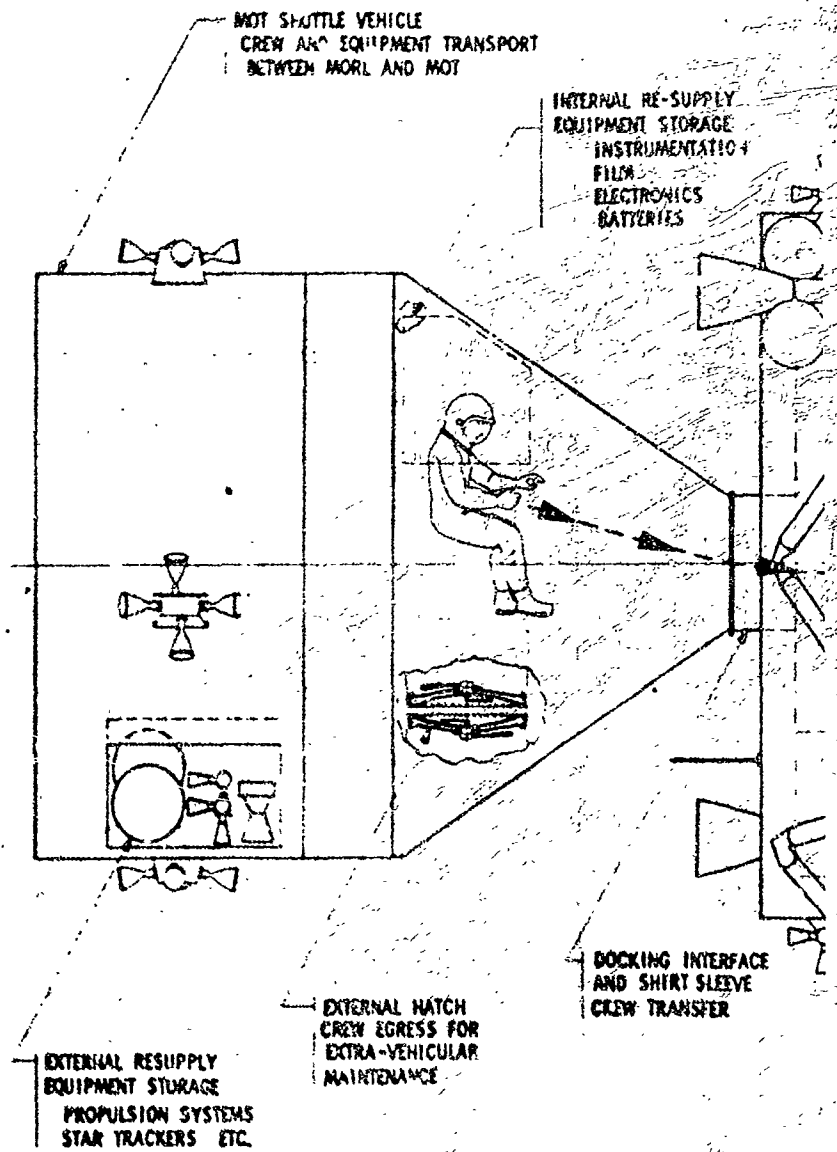
The conceptual design shown in Figure 5.2-5 is the orbital configuration of the MOT when it is detached for astronomical observation. Included on the drawing is an illustration depicting a shuttle vehicle docked to the MOT cabin. An Apollo type shuttle design was used to show concept feasibility. The docking and crew transfer designs used in the Apollo/logistics vehicle concepts developed for MORL are also shown for the MOT. By using a common design, the shuttle would be docked and stored on the MORL the same as the logistic vehicles. On the other hand, if the same basic structural design is used, the shuttle can be delivered to orbit simply by interchanging it with a command module in the logistics launch configuration.

The MOT orbital configuration, for operating separated from the MORL, is required to have the following onboard subsystems: reaction jet subsystem to supplement the control moment gyro system used for target pointing; propulsion for orbit keeping or maintaining its orbital position relative to MORL and for docking maneuvers; electrical power supply; and electronic systems for communications, data handling, and attitude control.

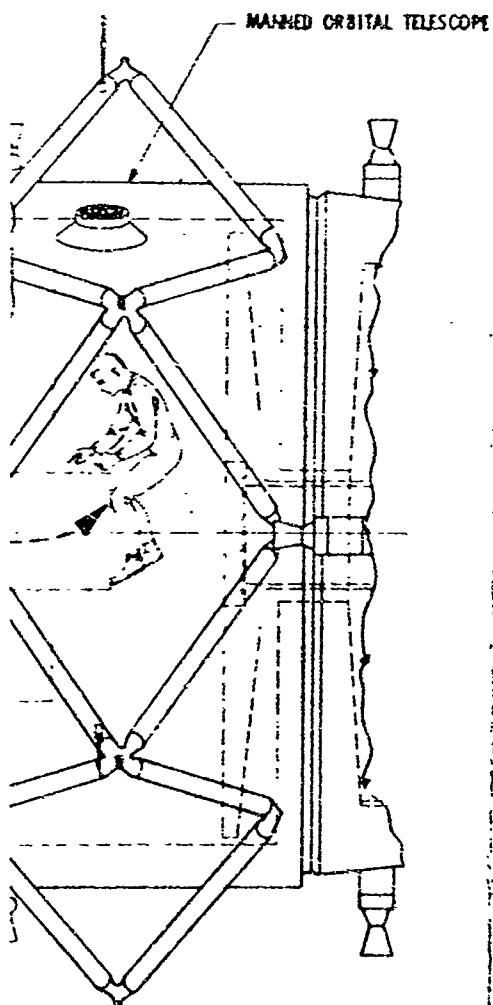
The orbital configuration (Figure 5.2-5) depicts only those subsystems which are added externally to the baseline configuration. The other subsystems are packaged within the telescope cabin.

The electrical power supply is a solar cell/battery system. Two foldout-type solar panels are shown which are sun-oriented by articulations of the panels about one axis and rolling the telescope for the second axis of control. The panels are locked in a fixed position for astronomical observations.

Four clusters of variable-thrust reaction jet subsystem are used for all propulsion requirements associated with attitude control and space maneuvering functions except initial rendezvous. A throttling ratio of approximately 10:1 is required to cover the range between low torque thrusters for control moment gyro desaturation and thrust levels used for docking. The propellant tanks for the reaction control system are located midway between the jet clusters and on the CG of the vehicle's pitch and yaw control axis. This location minimizes the CG shift with propellant usage. Two 1,000-pound-thrust rocket engines located at the aft end of the cabin are used for the orbit transfer maneuver associated with initial rendezvous. These engines and tank can be either jettisoned or retained for further use. Some of the antennas required for communication and guidance are also noted on the referenced drawing.



ORBITAL CONFIGURATION
(TELESCOPE MANNED FOR EXPERIMENT
SET-UP AND MAINTENANCE)



RENDEZVOUS PROPULSION
1,000 POUND ROCKET ENGINE
(2 PLACES)

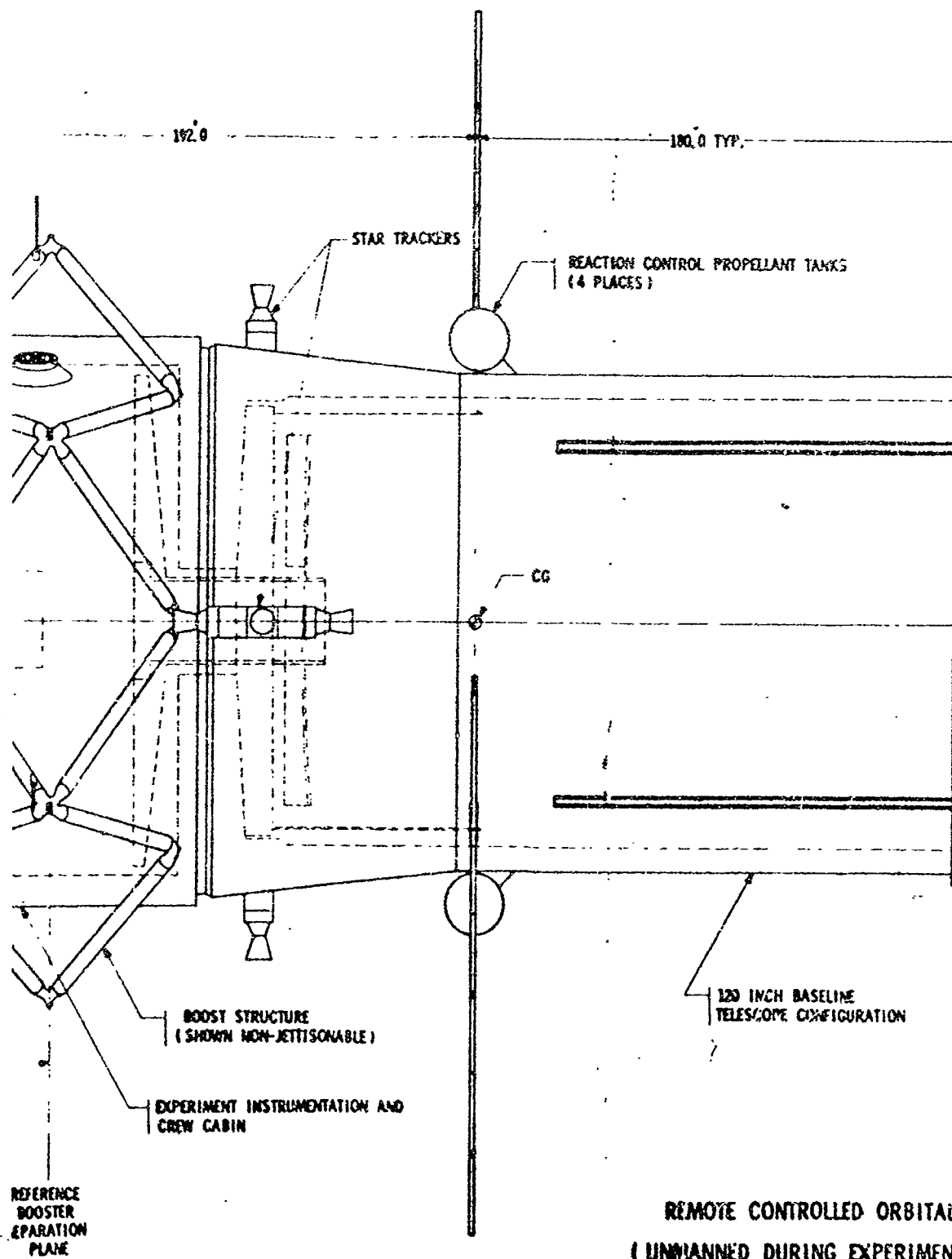
185.0 DIA.

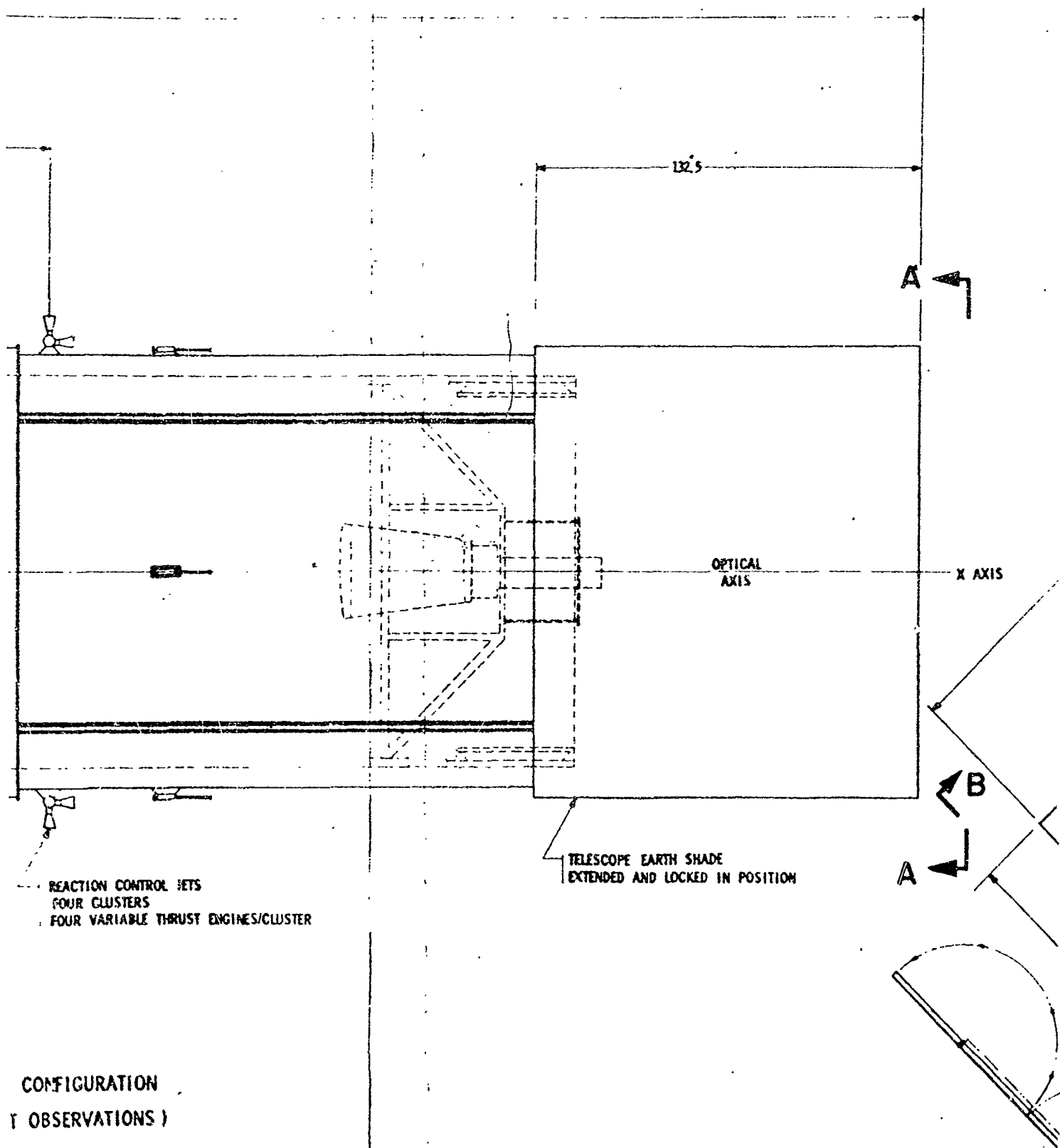
DOCKING PORT AND
CREW ACCESS

RADAR ANTENNA

51.0

720.0





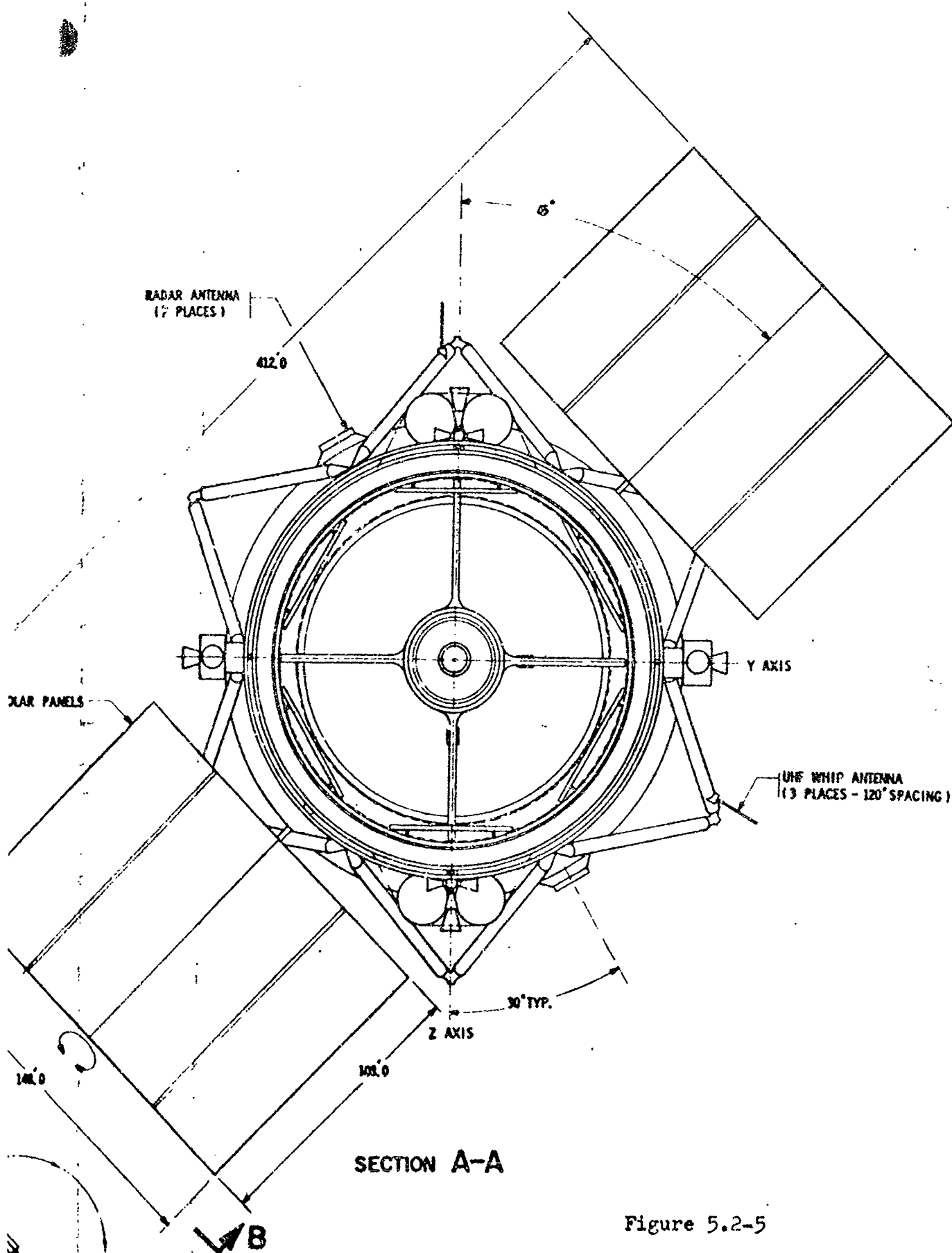


Figure 5.2-5

ORBITAL CONFIGURATIONS
120 INCH MANNED ORBITAL TELESCOPE
OPERATIONAL CONCEPT MODEL NO. 948-43D

Figure 5.2-6 is the orbital configuration of the MORL and the MOT docked together. Compared to Model No. 948-41C this concept utilizes the existing docking port on the MORL for docking the MOT which is normally used for logistic vehicles. It is assumed that the times MOT would be docked can be scheduled so as not to interfere with the MORL logistic operation. This approach minimizes the structural design changes required on the MORL but the operation requires a special docking mechanism design.

Probe and drogue design used on the MORL concept requires the probe section to be installed on the shuttle; therefore, the MOT must have a drogue cone section the same as MORL. Using the same docking ports for docking the MORL and MOT together thus requires one of the cones to be replaced with a probe unit. Launch configuration of this operational concept is shown in Figure 5.2-7. The only changes in this launch configuration compared to Model No. 948-41C (Figure 5.2-4) are those in the boost shroud. Removal of the soft gimbal structure permits the conical section of the shroud to be slightly smaller.

484.0

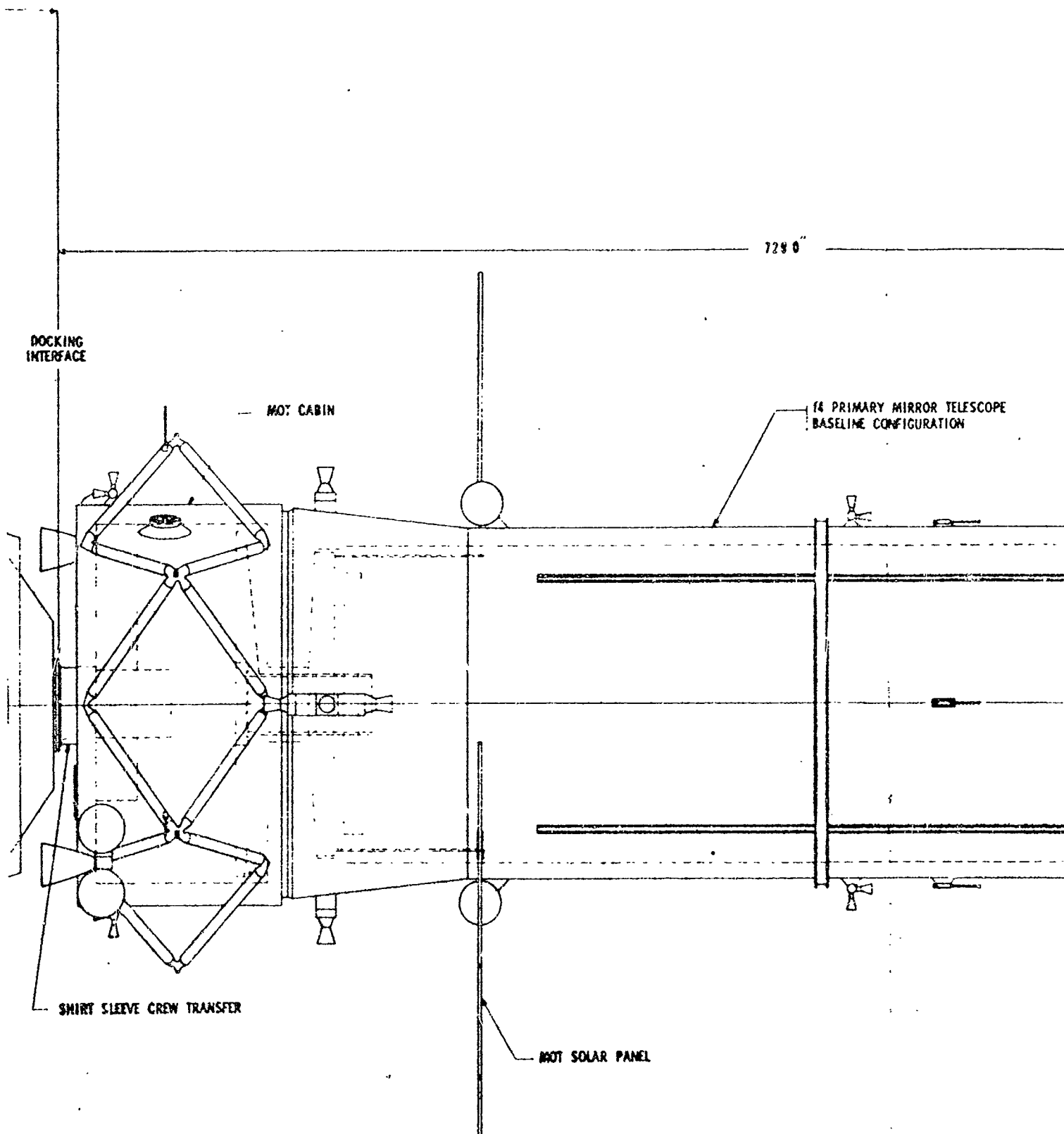
APOLLO LOGISTIC VEHICLES STOWED POSITION
(2 PLACES)

MAINED ORBITAL RESEARCH LABORATORY

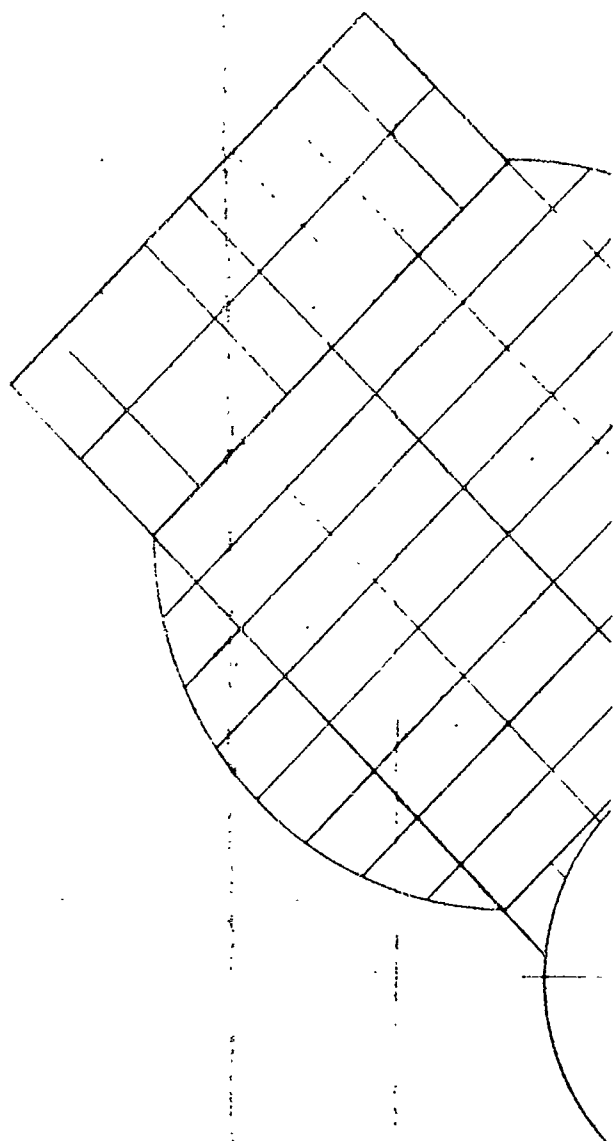
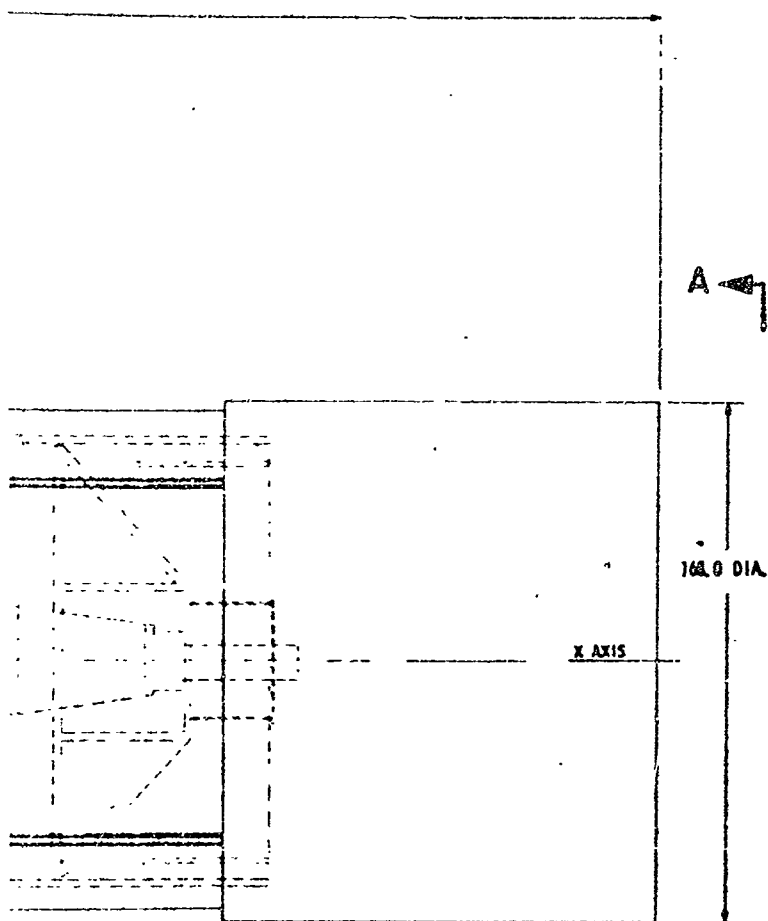
100.0 DIA.

MOEL EXPERIMENT MODULE

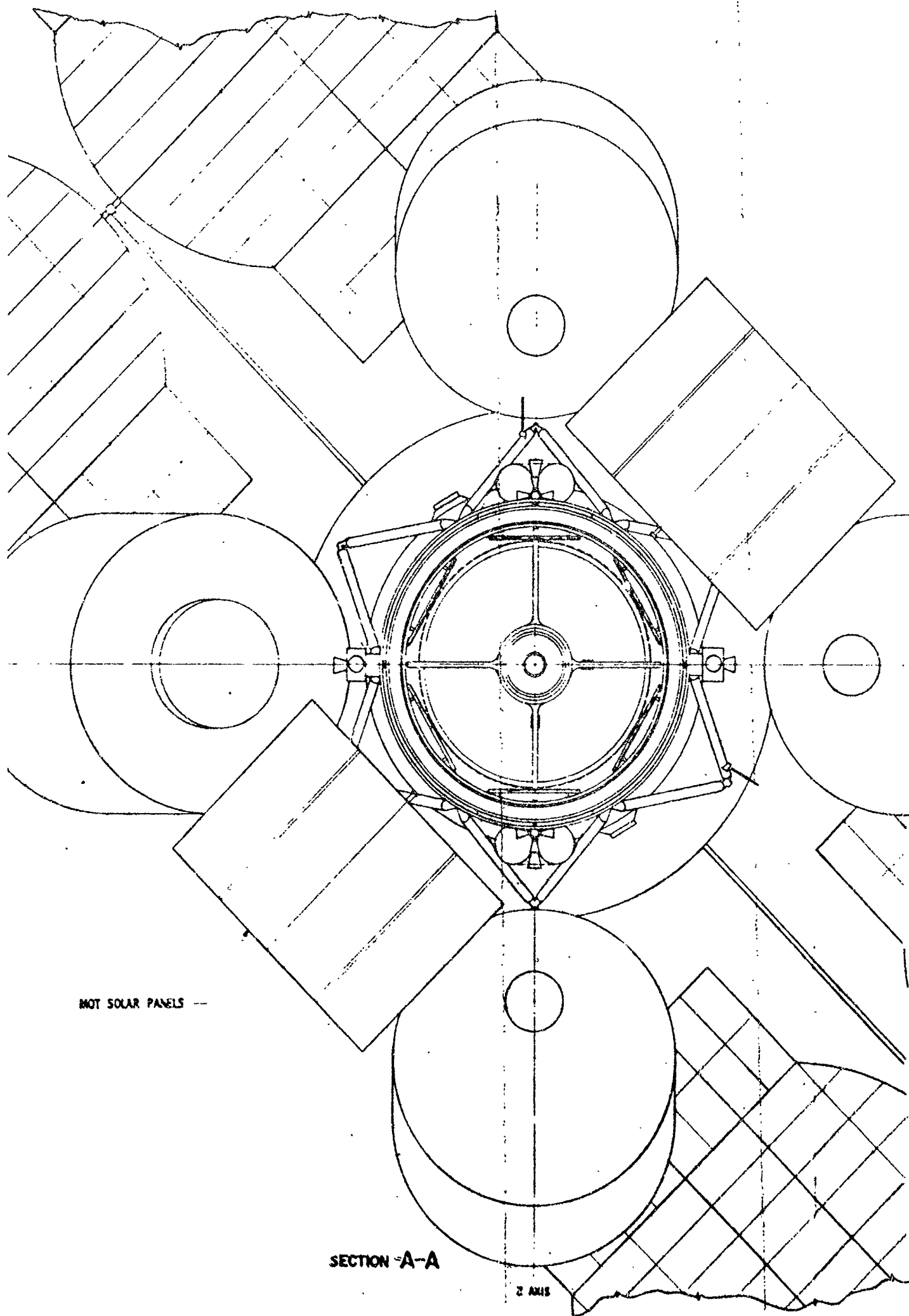
MOEL SOLAR PANELS



SHUTTLE



A



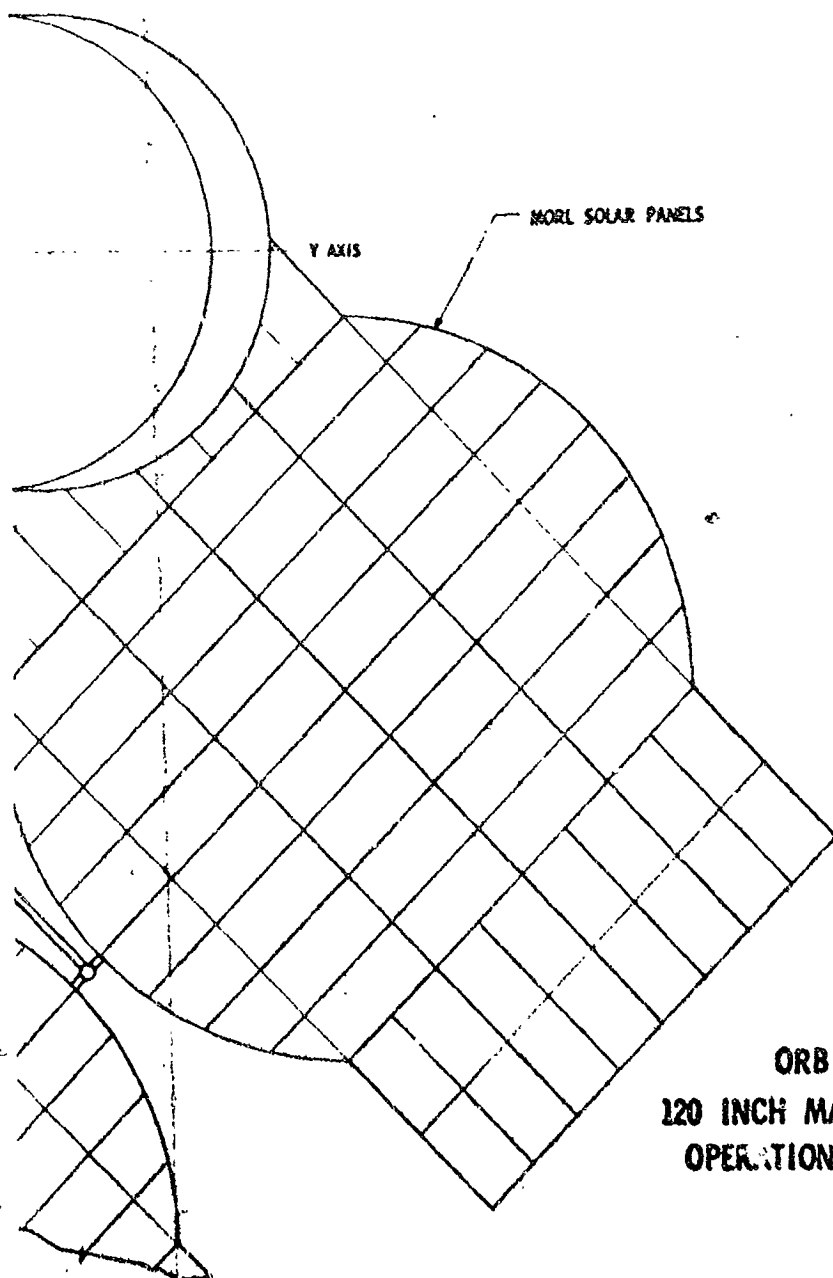


Figure 5.2-6
 ORBITAL CONFIGURATION
 120 INCH MANNED ORBITAL TELESCOPE
 OPERATIONAL CONCEPT NO. 948-43D

BOOST SHROUD
SEPARATION

260.0 DIA.

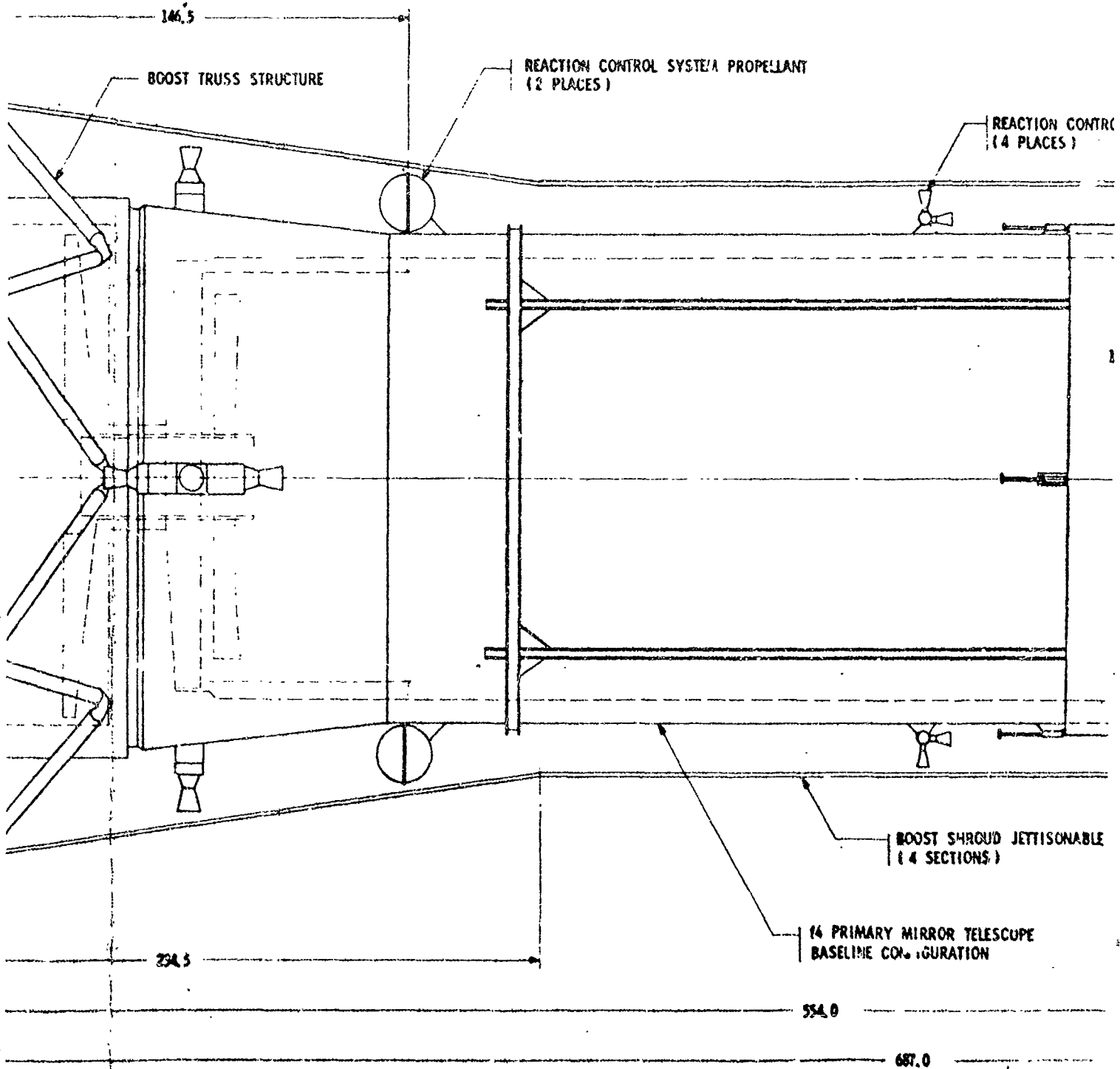
48.0

S IV B STAGE
SATURN IB LAUNCH VEHICLE

ORBIT INJECTION AND
RENDEZVOUS PROPULSION
1000 LB. ENGINE AND
PROPELLANT SUPPLY
(2 PLACES)

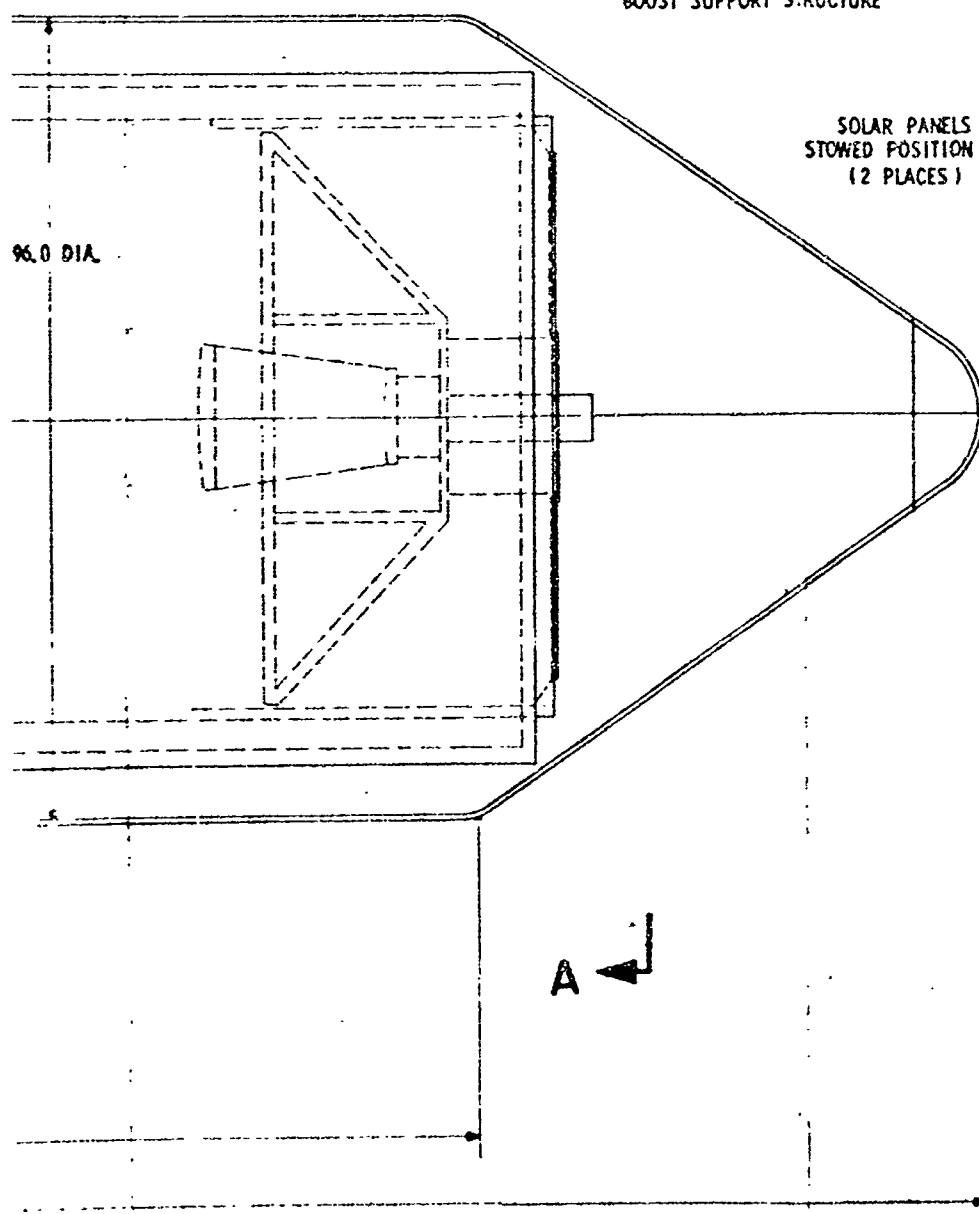
41.0

TELESCOPE
PLANE



135 (2)

DL ENGINE CLUSTERS



A

BOOST SUPPORT STRUCTURE

SOLAR PANELS
STOWED POSITION
(2 PLACES)

SECTION B-B

X AXIS

30° TYP.

45° TYP.

136 ①

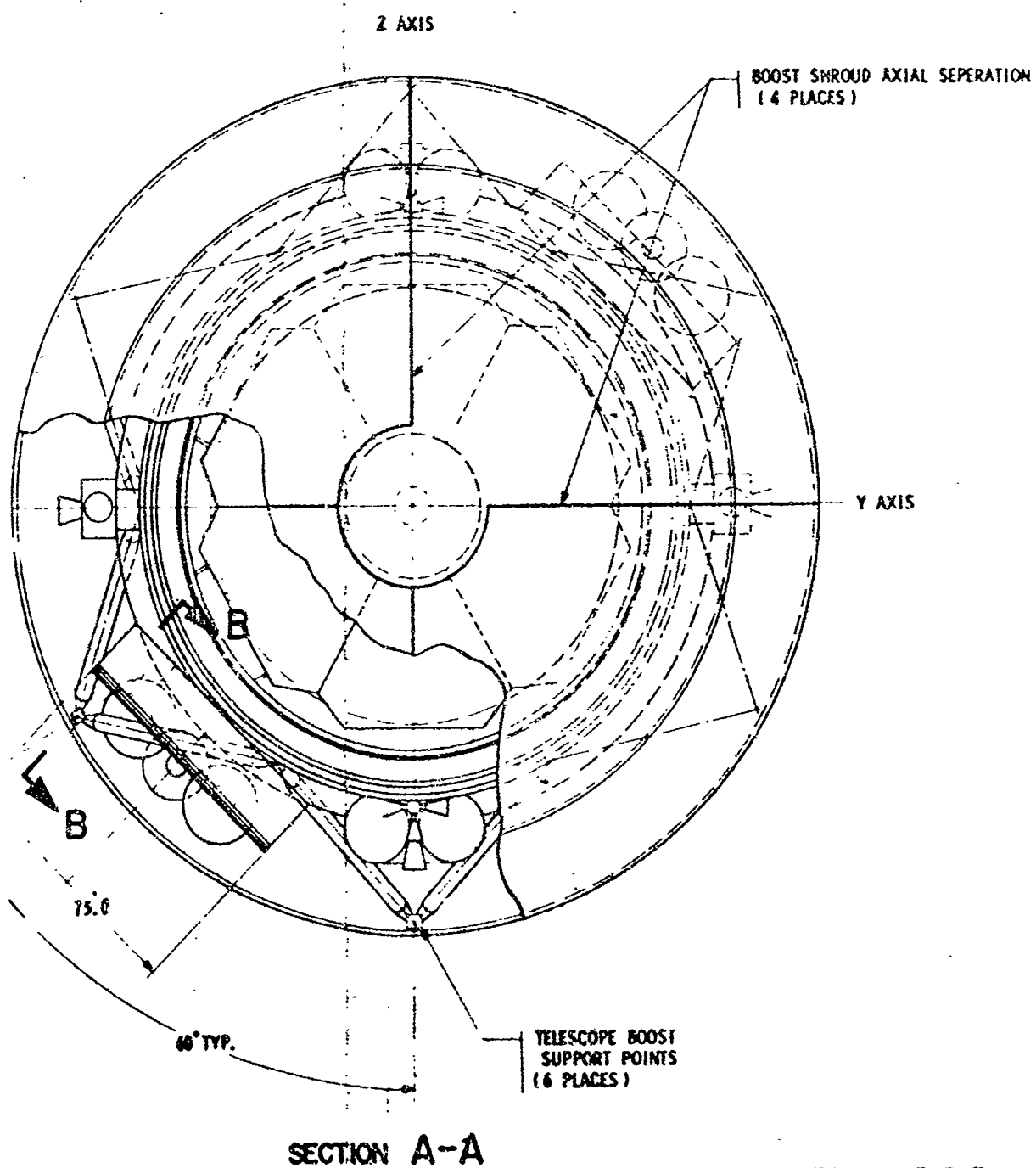


Figure 5.2-7
LAUNCH CONFIGURATION
120 INCH MANNED ORBITAL TELESCOPE
MODEL NO. 948-43D

5.2.4 Configuration Mass Analysis

This section contains an analysis of the mass properties of the MOT and the shuttle vehicle, including the integrated logistics requirements for the two proposed modes of telescope operation.

The mass of the MOT itself has been functionally divided between the optics, structures, mechanisms, thermal control, and operating subsystems. The interface between optics, structures, and mechanisms cannot be sharply defined. For convenience in reporting, those structural items and mechanisms associated with direct control or support of the telescope optical surfaces have been included with optics. Thermal control includes passive insulation and radiation exchange surfaces. The active temperature control components are included with the environmental control/life support (EC/LS) subsystem. Experiment packages are grouped as a separate subsystem.

The two shuttle configurations selected for detailed mass analysis are shown on Figures 5.2-3 and 5.2-5. The total mass of Model 948-41C, the gimbal concept, is less than the shuttle concept due to fuller utilization of the MORL subsystems. However, the gimbal concept will require MORL weight increases due to structural modifications. Model 943-43D, the shuttle concept, requires mass transfer by shuttle to sustain it during its operational periods away from the MORL. Many components are common to both concepts, but because of differences in the mass of interdependent items, the two modes have been analyzed separately.

5.2.4.1 MOT Mass Analysis Parameters

Spatially, the MOT can be divided between the telescope and the cabin. The telescope mass analysis is based upon the following major parameters:

- o Inner, outer, and Earth-shade tubes of one-inch aluminum honeycomb
- o Probability of no telescope meteoroid penetration of 0.95 for 3 years
- o Thermal protection of 1-inch super insulation over inner tube
- o Beryllium primary mirror--cell construction
- o Quartz secondary mirrors--solid construction
- o Main supports of titanium
- o Thermally insulated supports of fiberglass
- o Auxiliary boost structure and bladders are removed after initial rendezvous

The structure of the telescope consists of the inner tube, outer tube, telescope doors, extendable shade, and attachments not directly associated with control of the optics. The inner, outer, and extendable shade tubes are of the same sandwich construction, having 0.010-inch aluminum faces with a one-inch core of 3.0 lbs/ft³ honeycomb. Unit mass of each, including rings, bond, and closures is 0.89 psf. Cover doors are of similar construction, but have a unit mass of 1.10 psf due

to added closures and reinforcements. The hinges, hinge ring, and mechanisms are also included in the cover door total mass of 151 pounds.

The cabin is a pressure cylinder with flat heads. This configuration has evolved from Boeing studies of the Multipurpose Mission Module (MMM) for the NASA-AES. These studies indicated that for the same usable volume, a flat head design using tension ties between the two heads is comparable in weight to designs using spherical segment domes. Wall construction and thermal protection are essentially the same as that proposed for the MMM, with the exception that the meteoroid bumpers are removed from all but the aft head on the Model 948-43D cabin. A removeable head feature, designed for the MMM to allow removal of the aft flat head, has been retained. The following parameters used for the cabin mass analysis are common to both the gimbal and shuttle modes:

- o Flat heads are 0.071-inch aluminum waffle skin supported by 12 radial beams attached to 12 peripheral columns
- o Cylinder is 0.056-inch aluminum
- o Thermal insulation is 0.5-inch super insulation inside cabin walls
- o Experiment packages are mounted on the instrument platen
- o Subsystem packages are mounted on the aft flat head radial beams
- o Propellants and tankage for 180 days operation are included at launch
- o Initial rendezvous propellants are stored separately in a removable tank/engine assembly
- o Cabin is unpressurized when not occupied
- o Cabin atmosphere when occupied is 50 percent O₂ - 50 percent N₂ at 7.0 psi
- o Auxiliary boost structure is removed after initial rendezvous
- o Silver-zinc batteries removed after initial rendezvous

The following telescope and cabin design parameters are peculiar to the gimbal mode of operation (Model 948-41C) only:

- o Inner and outer gimbal rings of aluminum
- o Spring suspension by six 128-coil springs of 0.10-inch wire
- o MORL structural truss to gimbal mount carried aboard NOT at launch
- o Electrical power for operation provided by the MORL
- o Atmosphere supply, purification, and pumpdown provided by the MORL
- o Docking structure and rendezvous batteries removed after initial rendezvous

The following parameters are peculiar to the shuttle mode of operation (Model 948-43D) only:

- o Direct entry from shuttle to the MOT cabin, without airlock
- o Pumpdown power shared with shuttle
- o Pumpdown system and cooling supplied by the MOT
- o Pumpdown gaseous storage at 500 psia provided by shuttle
- o Electrical power by articulated solar panels of 216 square feet--fixed in position during telescope operation plus silver cadmium batteries providing 3430 watt-hours at 35 percent depth-of-discharge
- o Expendables and storage capability for 180 days operation--resupplied by docking to the MORL

5.2.4.2 MOT Mass Analysis Details

Mass analysis of major components are discussed below:

The main thermal protection insulation placed on the inner tube is one inch of laminated super insulation with a unit mass of 1.34 psf, including 20 percent laps and two 0.005-inch aluminum cover sheets. Shade insulation is 0.4-inch thick with a unit mass of 0.66 psf.

Electrical power solar panels have a unit mass of 1.05 psf, including substrate and closures for boost stowage. Including beams, actuators, extension system and supports, the unit mass is 1.50 psf. The silver cadmium batteries unit mass is 7 watt-hours/lb at 35 percent depth-of-discharge, not including installation, charging, and overcharge provisions.

Reaction control propellants are split between two tanks each for oxidizer and propellant, located at 180 degrees from each other. The mixture ratio is assumed to be 2:1, which results in N_2O_4 tanks that are slightly larger tanks than those for Aerozene 50. Propellant storage pressure is 350 psia. To be compatible with the MORL systems, nitrogen pressurant is used, at 1650 psia. Operational rendezvous and orbit keeping are also accomplished with the reaction control system. The large 1000 lbf engines and tankage for the initial rendezvous are removed after initial MOT-MORL coupling. The tanks required for the initial rendezvous are two of 23.2-inch diameter and two of 21.0-inch diameter for oxidizer and propellants, respectively, plus two 6.6-inch diameter helium tanks.

The masses of the attitude control and stabilization system components are considered to be conservative estimates. These components are subject to considerable development in view of the stringent pointing accuracy requirements. Communications, tracking, and data management components, on the other hand, are more closely identified with present state-of-the-art equipment and are a small fraction of the total electronics equipment mass.

The values for the MOT environmental control system are based upon a minimal system with the primary carbon dioxide removal and humidity control being accomplished by

the MORL or shuttle vehicle systems. Trace contaminant sensors are located on the MOT, but contaminate removal must be by the MORL or shuttle systems, or by atmosphere dump. A 500 psia shuttle storage is provided for recovery of the MOT atmosphere during unpressurized operation in the shuttle mode. Although the compressor mass and power requirements are high for pumping to this pressure, it is deemed necessary to lower the storage requirements aboard the shuttle. The compressor and intercoolers have been tentatively located onboard the MOT to save shuttle vehicle propulsion mass. In addition, more effective thermal coupling to the available MOT radiator surface can be made to dissipate the high energy involved in the compression cycles and the peak power conversion during pumpdown. The MOT power supply is augmented by the shuttle batteries during pumpdown. For the gimbal mode, the MORL pumpdown system is utilized.

Heat transfer from the experiments and subsystems during their operation is by cold plate and coolant loops. One loop is located at the experiment platen and the other on the periphery of the cabin between the subsystem support beams, which are integrated with the cold plate. Temperature control of experiment sensors requiring subcritical cooling is accomplished by connection of CO₂ or cryogenic containers to the sensor coolers prior to each experiment. The external radiator has a glycol solution coolant to prevent freezing. Redundant radiator loops are not provided due to the very low manned occupancy period. Meteoroid penetration or other failure of the radiator will require automatic shutdown of the power production units. Due to the high heat loads during cabin pumpdown, as opposed to normal operating heat loads, two separate radiators are provided. The combination requires all of the cabin outer cylinder wall for radiator surface, at about 70 watts/ft², due to the low radiation temperature average.

The mass of the experiments is based upon layouts of each package and the provision of adequate material to lower thermal gradients. The average unit mass of the spectrometers varies from 20 lb/ft³ to 28 lb/ft³, while that of the photometers is 30 lb/ft³. The vidicon cameras are similar to present state-of-the art units characterized by compactness and reduced mass.

As with the attitude control components, the experiment control sensors are conservative estimates based upon future development of components with almost no tolerances or thermal gradient distortions.

The onboard expendables are based upon the following 180-day supplies for the MOT:

	<u>Model 945-41C</u>	<u>Model 945-43D</u>
Orbitkeeping (Includes Station keeping)	By MORL	287 lbs
Attitude Control	350 lbs	350
Rendezvous (7 Times)	---	84
Docking Maneuvers and Control	---	245
	-----	-----
Total	350 lbs	966 lbs

Propellant for initial rendezvous is based on providing a total of 380 fps velocity change. Unused propellant is removed with the tanks and engines when the MOT is prepared for operation.

5.2.4.3 Mass Reserves, Allowances, and Contingencies

Mass Reserves are provided for off-nominal performance or mass usage rate variances. These include manufacturing tolerances, propulsion thrust variations and unexpected propulsion, attitude control, metabolic usage rates, and atmosphere loss rates. An example is the atmosphere stored aboard the MOT and shuttle vehicle for emergency repressurization. Another example is the period for which metabolic oxygen is provided, which includes 100 minutes for each rendezvous, although 10 to 20 minute rendezvous are possible by using propellant reserves. All reserves are included directly in the design quantities and do not appear as separate reserve tabulations. They vary from less than 1 percent in the optical structures to over 100 percent in the combined maneuver and altitude control propellant supplies.

Allowances must be included for undefined mass requiring conservative assumptions, component weight increases during development, additional components not previously identified, and mass associated with load changes due to refined design analysis.

It is also desirable to provide for the contingency of subsystem, operational mode, or structural configuration changes due to mission or method changes. A NASA-recommended 20 percent was used as a contingency on the MOT. Since this factor appears more than adequate, it is also assumed to include the allowances itemized above.

5.2.4.4 MOT Mass Properties

Summary mass statements are shown in Figure 5.2-8 for the gimbal Model 948-41C and in Figure 5.2-9 for the shuttle Model 948-43D. Center of gravity and moment of inertia values for both modes of operation are summarized on Figure 5.2-10. A launch mass summary for both modes is shown on Figure 5.2-11. This summary shows the mass of the MOT at various times between launch and operational readiness in orbit, after MORL rendezvous. Most components required for the launch period but not for telescope operation are removed and deorbited. The nose cone and boost shroud are jettisoned at first stage burnout. Their effective payload mass in orbit is thus only about 12.5 percent of their launch mass. Initial rendezvous components are also removed in orbit. For the gimbal mode, all detachable navigation components of sizeable mass are removed since no further rendezvous or docking is required. In general, the MOT launch mass, with contingencies, is well within Saturn IB capability for launch and transfer to a 250 N Mi orbit.

5.2.4.5 Shuttle Mass Analysis

The separated mode of operation, Model 948-43D, requires the use of a shuttle vehicle for experiment setup, optical changes, maintenance and spares, and expendables replacement. A modified Apollo crew module is proposed, with a permanently-attached 100-inch cargo module. The mass of the shuttle vehicle is divided between those subsystems and components in the Apollo crew module and those in the cargo module. The mass of the Apollo vehicle is modified by removal of all components required for sustaining a crew during launch and for sustaining the vehicle itself during reentry and landing. The heat shield and landing capability components are removed, leaving

FIGURE 5.2-8

OPERATIONAL MASS - MODEL 948-41C
(GIMBALED MODE)

		MASS (LB _m)	
TELESCOPE OPTICS			4343
Primary Mirror		2205	
Mirror	1936		
Inner and Outer Cylinders	164		
Attach Bases and Tangent Bars	105		
Support Base		479	
Floor	129		
Rings	44		
Beams	306		
Platen Support Tube		314	
Tube	97		
Insulation	127		
Flanges, Rings, and Door	90		
Folding Mirror Assembly		171	
Support Bladders		61	
Primary Mirror Doors		345	
Cover Doors	264		
Frames, Hinges, and Attachments	81		
f/15 Secondary Mirror		290	
f/30 Secondary Mirror		99	
Secondary Support Truss and Sleeve		86	
Secondary Positioning Systems		53	
f/15 Removal Mechanism		90	
Alignment Control		150	
Autocollimators	80		
Interferometer	25		
Sensors and Alignment Unit	45		
STRUCTURE - TELESCOPE			3864
Inner Tube		1413	
Honeycomb	1115		
Rings and Fittings	218		
Outer Ring and Door Fittings	114		
Light Baffles	26		
Outer Tube		1558	
Honeycomb	1290		
Rings and Fittings	268		
Telescope Doors		151	
Extendable Shade		523	
Honeycomb Sandwich	430		
Actuators and Mounting	60		
Rings and Fittings	33		
Shade Guide Frame		119	
Crew Restraint and Positioning		40	

FIGURE 5.2-8 (CONTINUED)

	MASS (LB _m)	
STRUCTURE - CABIN		2694
Cabin/Telescope Interface		393
Outer Wall Attachment	52	
Six Bar Truss	27	
Support Tube Connection	14	
Platen and Fittings	228	
Indexing Structure and Mechanisms	72	
Bulkheads		1351
Waffle Structure	713	
Radial Beams	244	
Intermediate Ring	82	
Inner Ring and Tunnel	63	
Seal Ring and Seal	99	
Fittings and Attachments	150	
Cylinders		503
Cylinder Skin	310	
Internal Columns	163	
Central Head Ties	30	
Penetrations and Seals		85
Subsystem Support Beams		72
Console Structure		35
Seat, Locomotion, and Restraint		40
STRUCTURE - GIMBAL MECHANISMS		581
Gimbal Mechanisms		279
Outer Gimbal Ring	103	
Inner Gimbal Ring	99	
Gimbal Bearings	36	
Coil Springs	12	
Actuators and Guides	29	
Gimbal Truss Structure		178
Support Rings	105	
Truss Members	41	
Support Frames	22	
Attachments	10	
NOT-MORL Support Truss		124
Truss Structure	62	
Fittings and Attachments	42	
THERMAL PROTECTION		2912
Inner Tube Insulation		1922
Shade Insulation		352
Primary Mirror Insulation		372
Platen Support Tube Insulation		92
Cabin Insulation		84
Thermal Coatings		90

FIGURE 5.2-8 (CONTINUED)

	MASS (LB _m)	
ELECTRICAL POWER		295
Battery Installation		17
Ag-Zn Batteries	*	
Installation Provisions	17	
Regulators		23
Inverters		60
Distribution System		195
REACTION CONTROL SYSTEM		161
Engines		40
N ₂ O ₂ Tanks and Residuals		22
Aerozene 50 Tanks and Residuals		19
Pressurization System		10
Valves, Plumbing, and Fittings		55
Wiring		15
ATTITUDE CONTROL & STABILIZATION		882
Trackers and Attitude Sensors		148
Tracker Control		165
Computer		50
Signal Processing		38
Gyros and Control		34
Control Moment Gyros		360
Yaw Gyros	165	
Pitch Gyros	165	
Roll Gyros	30	
CMG Controllers		45
Wiring		42
COMMUNICATION, TRACKING, & DATA MANAGEMENT		58
Telemetry		21
Vidicon Cameras		12
VHF System		19
Voice Transponder		6
ENVIRONMENTAL CONTROL/LIFE SUPPORT		238
Atmosphere Control		37
Heat Transport		66
Pumps, Accum, and Controls	10	
Cold Plates and HX	30	
Plumbing and Coolant	26	

*Removed in Orbit

FIGURE 5.2-8 (CONTINUED)

	MASS (LB _m)	
Emergency Repressurization		90
Gaseous Oxygen Tanks	39	
Gaseous Nitrogen Tanks	38	
Plumbing and Controls	13	
Radiator		45
Tubes and Headers	21	
Fluid System	24	
EXPERIMENTS - f/15		454
Low Dispersion UV Spectrometer		49
Low Dispersion Spectrograph		54
High Dispersion UV Spectrometer		122
Wide Field Camera		218
Vidicon Camera		11
Wiring		20
EXPERIMENTS - f/30		912
Thermoelectric Photometer		24
Photoelectric Photometer		63
High Dispersion IR Spectrometer		188
High Dispersion Spectrograph		440
Large Scale Camera		186
Vidicon Camera		11
Wiring		35
EXPERIMENT CONTROL SENSORS		495
Pointing Sensors		305
Intermediate Pointing	100	
Photometry Pointing	55	
Low Dispersion Pointing	60	
High Dispersion Pointing	90	
Photo Sensors		110
Star Field Photo	40	
Planetary Photo	30	
Planetary Spectrography	40	
Translation Mechanisms		35
Wiring		45
EXPENDABLES		415
Propellant		350
EC/LS Expendables		55
Sensor Coolants (Average)		10
CONTINGENCY (20%)		3661
TOTAL OPERATIONAL MASS		21,965

FIGURE 5.2-9

OPERATIONAL MASS - MODEL 948-43D
(SHUTTLE MODE)

	MASS (LB.)	
TELESCOPE OPTICS		4343
Primary Mirror		2205
Mirror	1936	
Inner and Outer Cylinders	164	
Attach Bases and Tangent Bars	105	
Support Base		479
Floor	129	
Rings	44	
Beams	306	
Platen Support Tube		314
Tube	97	
Insulation	127	
Flanges, Rings, and Door	90	
Folding Mirror Assembly		171
Support Bladders		61
Primary Mirror Doors		345
Cover Doors	264	
Frames, Hinges, and Attachments	81	
f/15 Secondary Mirror		290
f/30 Secondary Mirror		99
Secondary Support Truss and Sleeve		86
Secondary Positioning Systems		53
f/15 Removal Mechanism		90
Alignment Control		150
Autocollimators	80	
Interferometer	25	
Sensors and Alignment Unit	45	
STRUCTURE - TELESCOPE		3840
Inner Tube		1413
Honeycomb	1115	
Rings and Fittings	218	
Outer Ring and Door Fittings	114	
Light Baffles	26	
Outer Tube		1534
Honeycomb	1290	
Rings and Fittings	244	
Telescope Doors		151
Extendable Shade		523
Honeycomb Sandwich	430	
Actuators and Mounting	60	
Rings and Fittings	33	
Shade Guide Frame		119
Crew Restraint and Positioning		40

FIGURE 5.2-9 (CONTINUED)

	MASS (LB _m)	
STRUCTURE - CABIN		2847
Cabin/Telescope Interface		393
Outer Wall Attachment	52	
Six Bar Truss	27	
Support Tube Connection	14	
Platen and Fittings	228	
Indexing Structure and Mechanisms	72	
Bulkheads		1389
Waffle Structure	792	
Radial Beams	244	
Intermediate Ring	82	
Inner Ring and Tunnel	63	
Seal Ring and Seal	58	
Fittings and Attachments	150	
Cylinders		503
Cylinder Skin	310	
Internal Columns	163	
Central Head Ties	30	
Hatch, Penetrations, and Seals		105
Docking Structure		195
Subsystem Support Beams		123
Console Structure		35
Seat, Locomotion and Restraint		40
Meteoroid Bumper		64
THERMAL PROTECTION		2932
Inner Tube Insulation		1922
Shade Insulation		352
Primary Mirror Insulation		372
Platen Support Tube Insulation		92
Cabin Insulation		84
Thermal Coatings		110
ELECTRICAL POWER		1437
Solar Panels		324
Cells, Wiring, and Cover Glass	166	
Substrate Structure	62	
Beams and Actuators	57	
Extension System and Supports	39	
Battery Installation		593
Ag-Cd Batteries	545	
Installation Provisions	48	
Regulators		75
Inverters		180
Battery Chargers		15
Distribution System		250

FIGURE 5.2-9 (CONTINUED)

	MASS (lb _m)	
REACTION CONTROL SYSTEM		210
Engines		40
N ₂ O ₄ Tanks and Residuals		48
Aerozene 50 Tanks and Residuals		40
Pressurization System		12
Valves, Plumbing and Fittings		55
Wiring		15
ATTITUDE CONTROL & STABILIZATION		936
Trackers and Attitude Sensors		172
Tracker Control		193
Computer		50
Signal Processing		38
Gyros and Control		34
Control Moment Gyros		360
Yaw Gyros	165	
Pitch Gyros	165	
Roll Gyros	30	
CMG Controllers		45
Wiring		44
COMMUNICATION, TRACKING, & DATA MANAGEMENT		123
Telemetry		21
Vidicon Cameras		12
VHF System		19
Voice Transponder		6
Rendezvous Radar		30
Antennas, Cables, and Wiring		35
ENVIRONMENTAL CONTROL/LIFE SUPPORT		523
Atmosphere Control		22
Atmosphere Recovery		148
Compressor	120	
Coolers and Plumbing	28	
Heat Transport		81
Pumps, Accum, and Controls	12	
Cold Plates and HX	35	
Plumbing and Coolant	29	
Emergency Repressurization		90
Gaseous Oxygen Tanks	39	
Gaseous Nitrogen Tanks	38	
Plumbing and Controls	13	
Radiator		182
Tubes and Headers	84	
Fluid System	98	

FIGURE 5.2-3 (CONTINUED)

	MASS (LB _m)	
EXPERIMENTS - f/15		454
Low Dispersion UV Spectrometer	49	
Low Dispersion Spectrograph	54	
High Dispersion UV Spectrometer	122	
Wide Field Camera	218	
Vidicon Camera	11	
Wiring	20	
EXPERIMENTS - f/30		912
Thermoelectric Photometer	24	
Photoelectric Photometer	63	
High Dispersion IR Spectrometer	188	
High Dispersion Spectrograph	440	
Large Scale Camera	186	
Vidicon Camera	11	
Wiring	35	
EXPERIMENT CONTROL SENSORS		495
Pointing Sensors	305	
Intermediate Pointing	100	
Photometry Pointing	55	
Low Dispersion Pointing	60	
High Dispersion Pointing	90	
Photo Sensors	110	
Star Field Photo	40	
Planetary Photo	30	
Planetary Spectrography	40	
Translation Mechanisms	35	
Wiring	45	
EXPENDABLES		1041
Propellant	966	
EC/LS Expendables	65	
Sensor Coolants (Average)	10	
CONTINGENCY (20%)		4019
TOTAL OPERATIONAL MASS		24,112

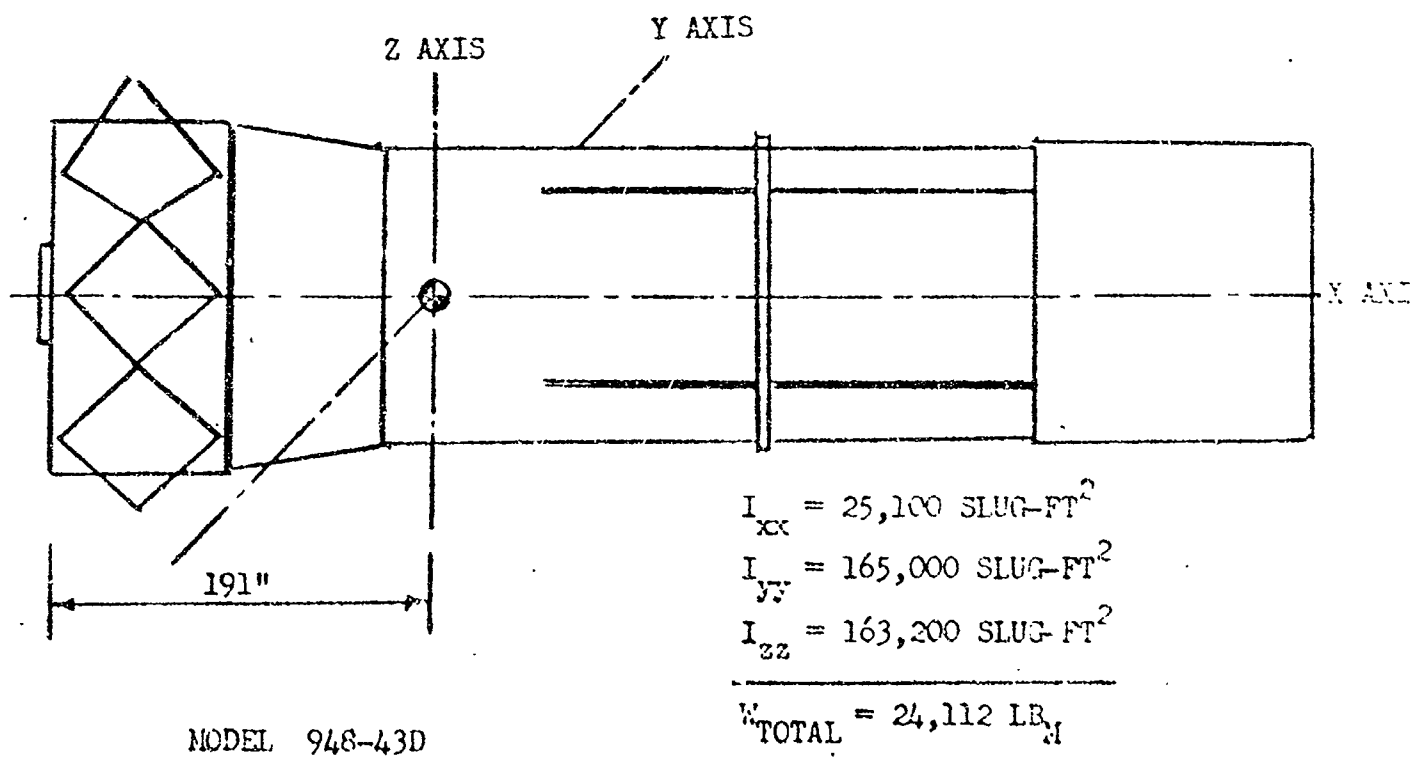
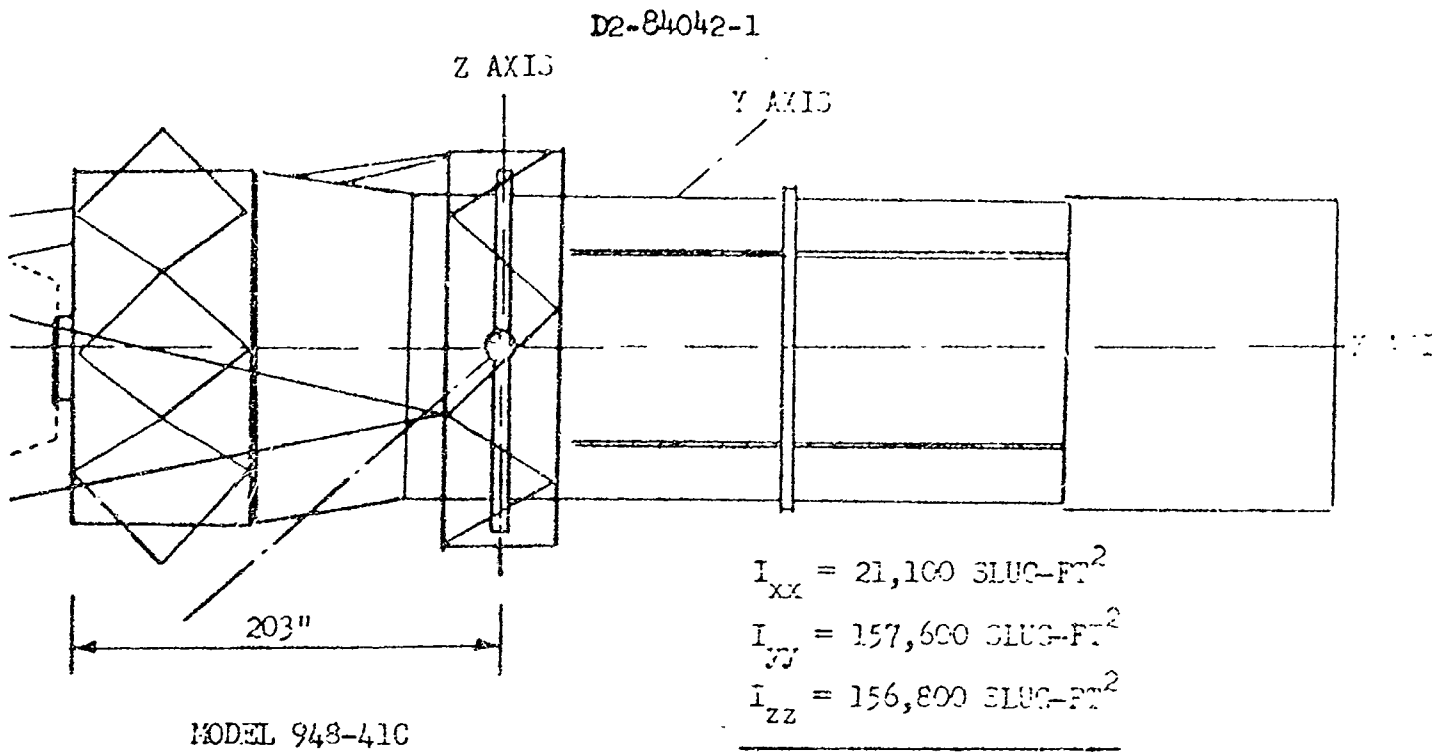


FIGURE 5.2-10: Center of Gravity and Moments of Inertia

FIGURE 5.2-11

LAUNCH MASS SUMMARY

	Model 948-41C (Gimbal) (Lb _m)	Model 948-43D (Shuttle) (Lb _m)
Telescope Optics	4,343	4,343
Structure - Telescope	3,864	3,840
Structure - Cabin	2,694	2,847
Structure - Gimbal System	581	-----
Thermal Protection	2,912	2,932
Electrical Power	295	1,437
Reaction Control System	161	210
Attitude Control and Stabilization	882	936
Communication, Tracking, & Data Management	58	123
Environmental Control/Life Support	238	523
Experiments - f/15	454	454
Experiments - f/30	912	912
Experiments Control Sensors	495	495
Expendables	415	1,041
Contingency (20%)	3,661	4,019
Total Operational Mass	21,965	24,112
(Removed in Orbit)		
Auxilliary Structure	208	153
Batteries	110	-----
Rendezvous Propulsion	160	162
Initial Docking Mass	22,443	24,427
Docking Propellant	35	35
Rendezvous Propellant	935	1,017
Start Rendezvous Mass	23,413	25,479
SIV-MOT Interstage	1,569	1,592
Staging Orbit Mass	24,982	27,071
Effective Fairing Mass*	808	631
Effective Nose Cone Mass*	117	117
EFFECTIVE LAUNCH MASS	25,907	27,819

*Removed at SI Stage Burnout--Effective Mass to Staging Orbit Assumed to be 12.5% of Actual Launch Mass.

the basic primary structure intact. This reduces the total mass considerably, while still retaining a large portion of off-the-shelf structural and mechanical items. It should be noted that a complete redesign using reduced boost load factor limits and eliminating the reentry factors would reduce the mass further. It is felt that the mass values presented represent a logical use of only about 30 percent of the existing Apollo structure. Since most of the Apollo subsystems must be modified anyway, further reduction of shuttle vehicle mass can more efficiently be accomplished by a new specific shuttle mission design. Mass values for the shuttle vehicle are shown on Figure 5.2-12.

The shuttle is used periodically at varying intervals, ranging from daily to every three or four days. Personnel manhour requirements analysis indicates that when the shuttle is refurbished at the MORL, it should be supplied with provisions for more than one roundtrip to the MOT. For purposes of volume and mass analysis, a conservative assumption of providing storage capability for 15 roundtrips is used. Since the MOT itself also docks to the MORL vehicle in the mode considered, the largest resupply mass and major repairs or changes are assumed to be accomplished with the MOT docked to the MORL.

The following major parameters have been used to determine the mass requirements of the shuttle, as well as the logistics requirements of the MORL to service the shuttle

- o 15 round trips, MORL to MOT to MORL, requiring 15 repressurization cycles of the MOT
- o Maximum of one mile MOT/MORL separation
- o Nominal two-man crew, with overload capability of three
- o Maneuver and attitude control by cargo module system only
- o Crew module atmosphere of 50 percent O_2 - 50 percent N_2 at 7.0 psia
- o Cargo module unpressurized
- o One emergency repressurization of crew module stored onboard
- o Storage capability for 90 percent of MOT recovered atmosphere at 500 psia
- o Atmosphere makeup for 10 percent MOT atmosphere makeup, stored at 3500 psia, for each repressurization cycle
- o No MOT propellant resupply capability, since this is a requirement of MOT/MORL docking operation
- o Cargo module cylindrical wall integrated with redundant tube radiator
- o Batteries sized for providing a total of 4000 watt-hours at 80 percent depth of discharge

FIGURE 5.2-12

SHUTTLE VEHICLE MASS PROPERTIES

<u>SHUTTLE VEHICLE</u>		<u>MASS (LE_m)</u>
CREW MODULE (4200)		
Structure		1860
Forward Section	210	
Center Section	660	
Aft Section	240	
Airlocks and Hatches	170	
Thermal Protection	120	
Subsystem Support	220	
Docking Support	90	
Cargo Storage	80	
Reinforcements	70	
Crew Systems		230
Electrical Power		410
Communications		120
Environmental Control/Life Support		360
Controls and Displays		160
Navigation and Stability Control		110
MOT Maintenance Provisions		30
Docking System		190
EC/LS Expendables*		110
Penetrations and Leaks		50
Crew and Equipment		570
Crew	370	
Suits	70	
Backpacks	130	
CARGO MODULE (2300)		
Structure		1220
Cylinder**	780	
Secondary Structure	190	
Thermal Protection	60	
Subsystem Support	80	
Cargo Storage	50	
Reinforcements	60	
Reaction Control/Propulsion		160
Atmosphere Storage System		270
Shuttle Propellant*		500
N ₂ O ₄	333	
Aerozene 50	167	
MOT Stored Atmosphere*		150
CONTINGENCY (20%)(1300)		1300
TOTAL SHUTTLE VEHICLE		<u>7800</u>
*Expendables Loading for 15-Trip Capacity. **Includes Radiator Tubes & Headers		

5.2.4.6 Logistics Mass Analysis

Logistics requirements are estimated for the two modes of operation. The Logistics presented are those pertaining to operation of the MOT only. The primary difference between the gimbal mode and the shuttle mode, from the logistics standpoint, is the mass of the shuttle vehicle, with its expendables and spares requirements, and the mass of expendables and spares that must be carried by shuttle or transferred directly through the MORL hatch to the MOT.

The shuttle mode, Model 948-43D, uses two logistics supply methods; that of the shuttle vehicle and that of coupling to the MORL. The number of trips that the shuttle makes and the number of MOT-MORL coupling periods is derived from the one year timeline analysis presented in Section 4.4.

The following parameters have been used to derive the mass of the 1-year logistics requirements for each mode:

Parameters Common to Both Modes

- o 71 film replacement periods of 3 hours each
- o 10 setup and checkout periods of 7.5 hours each
- o 4 scheduled maintenance periods of 3 days each
- o 1 scheduled 4-day period for f/15 to f/30 changeover
- o 10 unscheduled maintenance periods of two days or more
- o 15 unscheduled maintenance periods of one day or less
- o 0.30 lb/hr MOT atmosphere leakage rate
- o 2.5 lbs per man-day metabolic oxygen rate
- o Ecological requirements of food and water not included

Parameters for Model 948-41C (Gimbal Mode) Only

- o No food, water, and sanitation provisions - MORL facilities used as required
- o Emergency atmosphere repressurization by MORL, four per year estimated, required for high leak loss (dump) of cabin atmosphere

Parameters for Model 948-43D (Shuttle Mode) Only

- o 2 hours average shuttle travel time per docking cycle - two men
- o 1 hour average shuttle checkout and maintenance time per docking cycle - one man
- o 1 hour shuttle holding time for MOT pumpdown - two men

- o Spares replacement mass increased by electrical power equipment and by orbit control equipment
- o Emergency atmosphere for one complete repressurization stored in both the MOT and the shuttle, four replacements per year estimated for MOT plus one while coupled to MORL - two replacements per year for shuttle
- o Shuttle atmosphere leakage rate of 0.25 lb/hr
- o One year battery lifetime, replacement has not been included in the one-year logistics provisions

These parameters result in the total yearly expendables and spares requirements shown on Figure 5.2-13 for the two models.

5.2.5 Optical Systems Design and Installations

The major elements of the telescope optical system are the primary mirror, secondary mirrors, scientific experiment instruments, and the structure which ties these together. Each piece of optical equipment is sensitive to structural distortion and requires installation in which its physical positions relative to other equipment be maintained within very small tolerances. The general design approach taken is to provide concepts that minimize loads and thermal conditions which cause geometric distortions. In addition, the mounting for each element are provided with adjustment design features for aligning the optical system in orbit. Special attention was also given to the development of conceptual designs that can accommodate man for the major telescope functions which rely on his role to attain reliable and successful operation.

5.2.5.1 Scientific Instrument and Cabin Arrangement

The cabin as shown in Figure 4-6, is arranged with all the scientific optical instruments mounted to a rigid base or platen located in the forward section adjacent to the telescope. MOT supporting subsystems are located around the periphery in the aft section. The platen is a cantilever structure physically supported from the optical system support base by a tubular section extending thru the cabin bulkhead. The only physical attachment between the platen structure and cabin is a bellows located around the platen support tube. This design feature is used to protect the alignment of the scientific instruments with the main telescope optics. Removable boost structure is required to support the platen during launch to orbit.

The scientific instruments are positioned radially around folding mirrors on an arc formed by the locus of the focal point as the mirrors are rotated. The light beam from the telescope proper is folded once for $f/15$ experiments and twice for $f/30$ experiments. The primary folding mirror folds the light 90 degrees making the

FIGURE 5.2-13

LOGISTICS MASS SUMMARY

LOGISTICS CYCLES (ONE YEAR)	MODEL	
	948-41C (Gimbaled)	948-43D (Separated)
TOTAL MORL-MOT DOCKING CYCLES	----	15
TOTAL TRIPS BY SHUTTLE	----	96
TOTAL REPRESSURIZATION CYCLES		
MOT Atmosphere to MORL	111	15
MOT Atmosphere to Shuttle	----	96
Shuttle Atmosphere to MORL	----	96
TOTAL EMERGENCY REPRESSURIZATIONS		
By MORL to MOT	4	1
By MOT to MOT	----	4
By Shuttle to Shuttle	---	2
TOTAL HOURS PRESSURIZED		
MOT-MORL	1512	864
MOT-Shuttle	----	648
Shuttle Only	----	288
TOTAL MANHOURS		
In MOT-MORL	1512	864
In MOT-Shuttle	----	1296
In Shuttle Only	----	480

MASS REQUIREMENTS (ONE YEAR)	Shuttle		
	Gimbal	MORL/MOT	Shuttle/MOT 1
Oxygen - 3500 psia	834 lb	299 lb	862 lb
Nitrogen - 2000 psia	609	188	614
N ₂ O ₄	466	1289	1920
Aerozene 50	234	644	960
Spares Replacement	360	200	252
Film and Tape	550	----	550
Added MORL Propellant	(6670) 2	(925)	

1 Includes Requirements for Shuttle Alone

2 Assumes Use of an Additional Control Moment Gyro in MORL

light rays parallel with the mounting platen. The mirror can be rotated about the telescope optical axis thus aligning the focal plane with a selected instrument for $f/15$ observations.

In addition, an initial alignment fixture and TV camera are located in the same focal plane. The TV camera is used for checking the telescope field of view remotely from the MORL.

A secondary folding mirror is used in conjunction with the $f/30$ secondary mirror in the telescope to provide for the $f/30$ instruments positioned radially with respect to the secondary folding mirror.

Clearance from the surface of the platen to the cabin ceiling is approximately 69 inches which provides an average of 40 inches clearance above the instruments for the crewmen to maneuver in the zero gravity environment. All subsystem components are arranged in the upper section around the periphery of the cabin to allow maximum accessibility to the optical instruments. The subsystems provided in the MOT include communications and data recording, electrical guidance and control, and emergency pressurization. Cold plate cooling is provided for electronic subsystems component thermal control. Storage provisions for spares and maintenance tools are also located around the cabin walls.

The display and checkout console allows a seated crewman to monitor and operate the displays and controls. In the immediate area of the console, the maximum floor-to-ceiling clearance of 69 inches is maintained and will include a seat and restraint provision. The console will contain those displays and controls required to check out the operation and status of the subsystems.

A docking cone and mechanism, identical to that included on the MORL for use with the Apollo logistics vehicle, is provided at the cabin end of the MOT. For either mode, this location provides ingress/egress to the cabin. A pressure hatch to seal the cabin at the interface with the telescope is incorporated within the platen envelope. It will be remotely actuated and the seal accomplished prior to cabin pressurization and crew entry. The hatch or door is guided in a track which has a cam-type action for engaging and breaking the pressure seal at the end of the platen support tube. A small 3.0 inch diameter optically flat window is located in the center of the pressure hatch to allow the passage of a beam of light for gross alignment of the scientific instruments when the cabin is pressurized.

For on-pad access, a bolted-type hatch is provided in the outer wall of the cabin. The hatch will be approximately 30 x 42 inches to allow clearance of the largest single item of equipment. Prior to launch, this hatch will be fastened and sealed. Consideration was given to utilizing this hatch for emergency exit. However, this results in additional weight and complexity to provide the necessary structure and mechanisms.

5.2.5.2 Primary Mirror

Primary mirror installation is considered a major design problem area. The optical qualities are very sensitive to thermal gradients in the mirror structure. Similarly, structural distortions resulting from applied loads are inadmissible. Until more

definite material structural criteria can be established for the design and fabrication of the mirror, precautions must be taken to provide an installation design that minimizes the possibility of boost loads destroying the optical figure. The installation criteria also have conflicting structural design requirements in that precision dimensional alignment between the mirror and its supporting structure is desired. For thermal and stress considerations, it is preferable to decouple the mirror from its supporting structure as much as possible.

Figure 5.2-14 depicts a primary mirror installation in which the primary mirror can be completely decoupled from its structural attachment and floated on a pneumatic bladder support during boost to orbit. The bladders are used to distribute the acceleration loads over large areas of mirror surfaces, thus preventing harmful stress concentrations. A segmented bladder design is utilized to provide restoring forces for mirror angular displacement and to facilitate attaching sections permanently to the mirror cover doors.

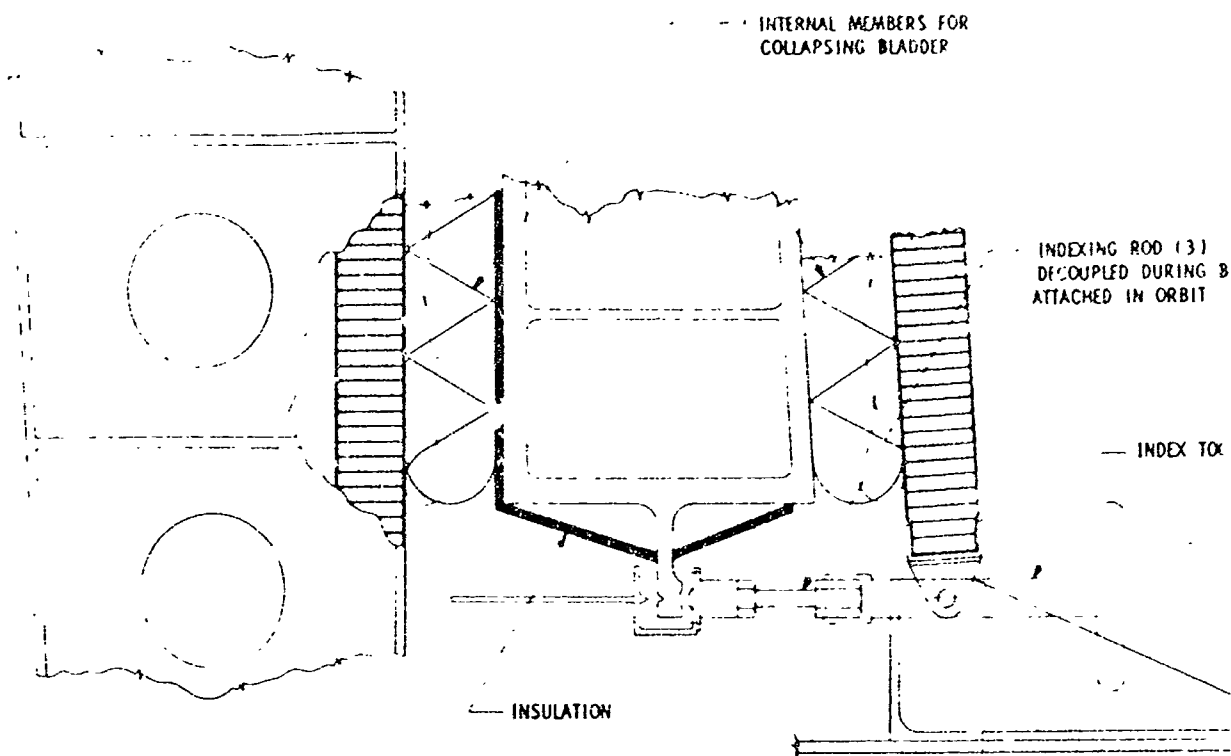
The concept requires internal elastic members which collapse the bladder wall nearest the mirror surfaces toward the support structure when the bladders are deflated. This disengages the bladders from the mirror for operations in orbit. Design precautions must also be taken to insure that the bladders do not harm the mirror surface due to vibrating movement during boost. Peel coat type materials can be used to protect the mirror surfaces from the bladders but this solution shifts the problem to one of developing methods for removing the coating in orbit without harming the mirrors.

The cover doors serve a dual purpose. They are the structural support for the pneumatic bladders on the forward side of the mirror and they are used to protect the delicate mirror surface from foreign materials and contamination from personnel working in the vicinity, both on the ground and in orbit.

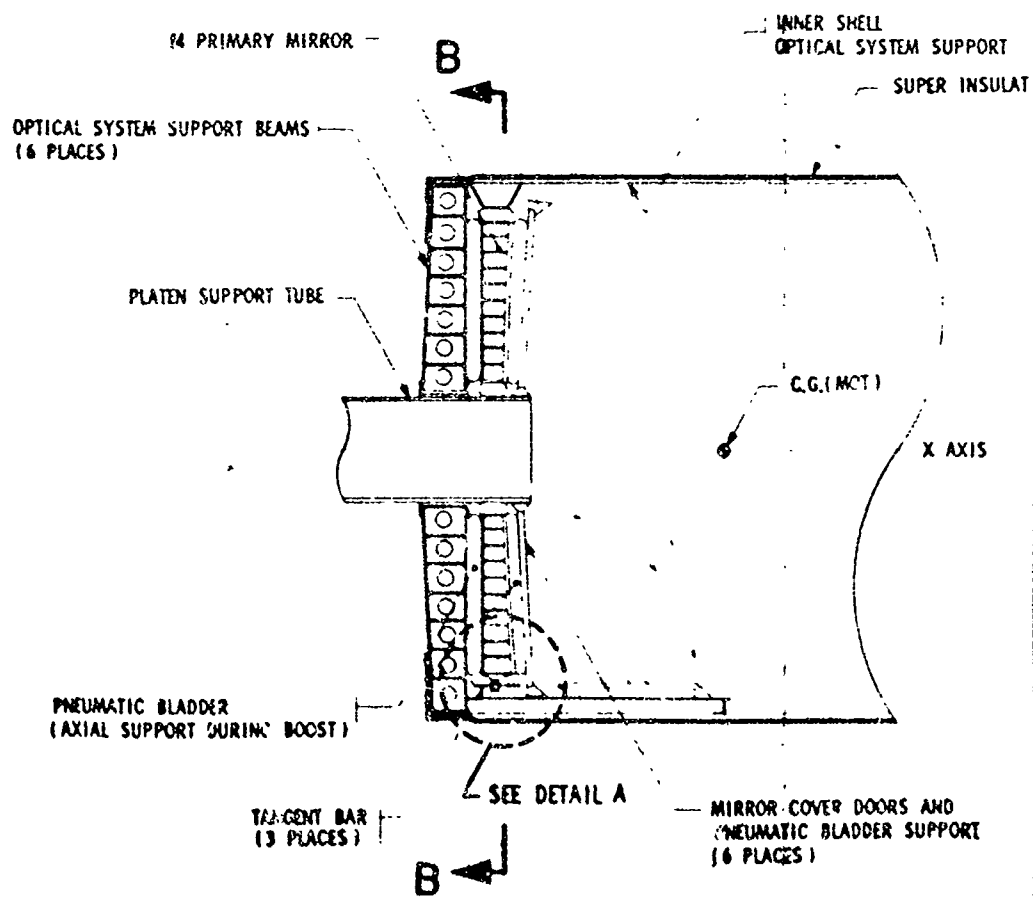
Mechanical attachment of the mirror to the optical system support structure is accomplished by a three point tangent bar mounting. The three attachment points are located on the outer rim of the mirror to make them more accessible. The tangent bar design is used to accommodate differential radial expansion between the mirror and the support structure without inducing loads into the mirror. The three point support also permits the plane of attachment to tilt without inducing stresses into the mirror. Index rods which hold the mirror on three conical seats of the tangent bars can be disengaged and retracted to allow for the necessary float of the mirror on pneumatic bladders. In orbit the index rods can be re-engaged either automatically or manually. Selective materials and fabrication methods are required in the designs of the tangent bar supports to minimize heat flow from the supporting structure into the mirror. The mirror alignment sensors mounted on the inner diameter of the primary mirror are used to position the secondary mirror relative to the primary mirror. Bladders on the inner and outer diameter are also segmented, with open areas provided for the sensors and attachment structure.

5.2.5.3 Secondary Mirrors

A conceptual installation of the $f/15$ and $f/30$ secondary mirrors was developed to establish feasibility of a design which reasonably satisfies the MOT operational and optical system design requirements. The MOT operational criteria requires



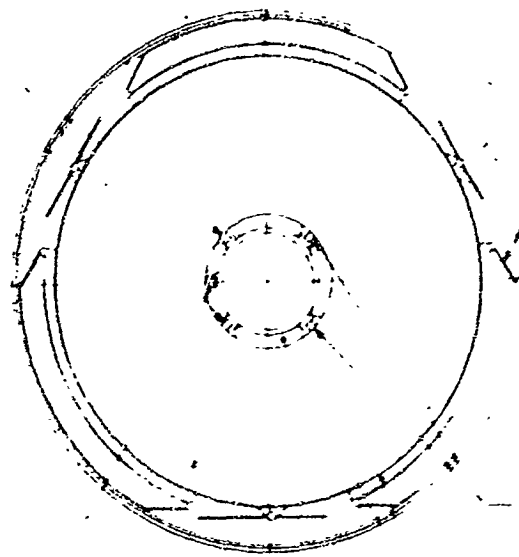
DETAIL A



SECTION A-A

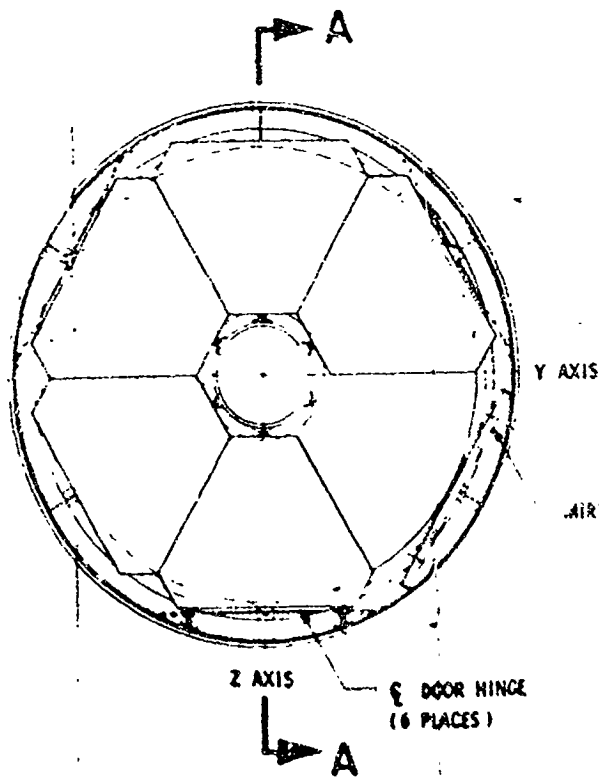
157

00ST

AUTOCOLLIMATOR UNITS
SENSING OFFSETPNEUMATIC BLADDER SUPPORT
(3 PLACES)AUTOCOLLIMATOR UNITS
SENSING TILTINTERFEROMETER
FOCUS SENSORPNEUMATIC BLADDER
(LATERAL SUPPORT DURING BOOST)

SECTION B-B

104



AIR COVER DOOR (DEPLOYED)

DOOR HINGE
(6 PLACES)

PLAN VIEW

Figure 5.2-14
PRIMARY MIRROR INSTALLATION
NOT BASELINE CONFIGURATION

the mirrors and associated mounting equipment to be accessible for man to perform setup with maintenance functions. In particular, the $f/15$ mirror has to be removed when experiments are being performed with the $f/30$ mirror system, and mechanical or electrical equipment subject to failure should be replaced by man. The optical system design criteria requires the mirrors to be positioned accurately relative to the primary mirror and the experiment instruments at the Cassegrainian focus.

Secondary mirror position tolerances are defined in the optical system study (Section 3). Mirror position disturbances which are primarily due to distortion of the supporting structure are evaluated in the structures study (Section 5.3). The initial structural thermal analysis indicates that, except for focus, the disturbances can be held below the allowable position tolerances once the telescope temperatures are stabilized in orbit. Although this implies that single degree of freedom control for the secondary mirrors may be feasible, the requirement for an automated secondary mirror position control for five axis of freedom was retained for initial alignment in orbit, realignment associated with reinstalling the $f/15$ mirror, and disturbances from repeated docking and other unforeseen causes.

Excluding the docking impacts, the disturbances affecting the secondary mirror alignment may be considered to be of sinusoidal character induced by differential radiant heating, and to be superimposed on initial errors induced by the removal of gravitational and thermal initial conditions. These initial errors are expected to be at least one order of magnitude larger than that induced by heating. The basic frequency content of the sinusoidal disturbance is at orbital frequency for all five degrees of secondary mirror freedom.

Position control of the secondary mirrors requires alignment sensors located on the primary mirror for each axis of control, and an alignment target element located on the secondary mirrors. Figure 5.2-15 schematically illustrates a position detecting system. Autocollimator-type sensors are used for two axes of translation and the two axes of tilt. An interferometer is used for the focus sensor. The target element is a small flat mirror with a reticle located at the center of each secondary mirror.

Initial alignment of the telescope is accomplished by using the sensors of the alignment unit, which is mounted on the main instrument support base. Upon alignment of tilt and lateral displacement, the folding mirror is indexed to the wide angle camera position. The telescope is slaved to a star and the auto-focus device of the camera is used to initially position the secondary mirror longitudinally. Thus, initial alignment and focus adjustment may be done either by full manual control or with the aid of automatic nulling circuits. Once initial aligning is accomplished, the primary control of these functions is switched to the sensors ringed the inside of the primary mirror aperture. The folding mirror may then be pivoted to one of the experiment packages. When the main camera is in use, the primary control of focus will be automatically shifted from the primary mirror interferometer instrument to an autofocusing instrument built into the camera package.

There are many design approaches for a position control system of the secondary mirrors and optimization is beyond the scope of this study. Studies were conducted to develop a five degree of freedom mounting and actuation system which has very small coupling between control axes and which can feasibly be packaged within the

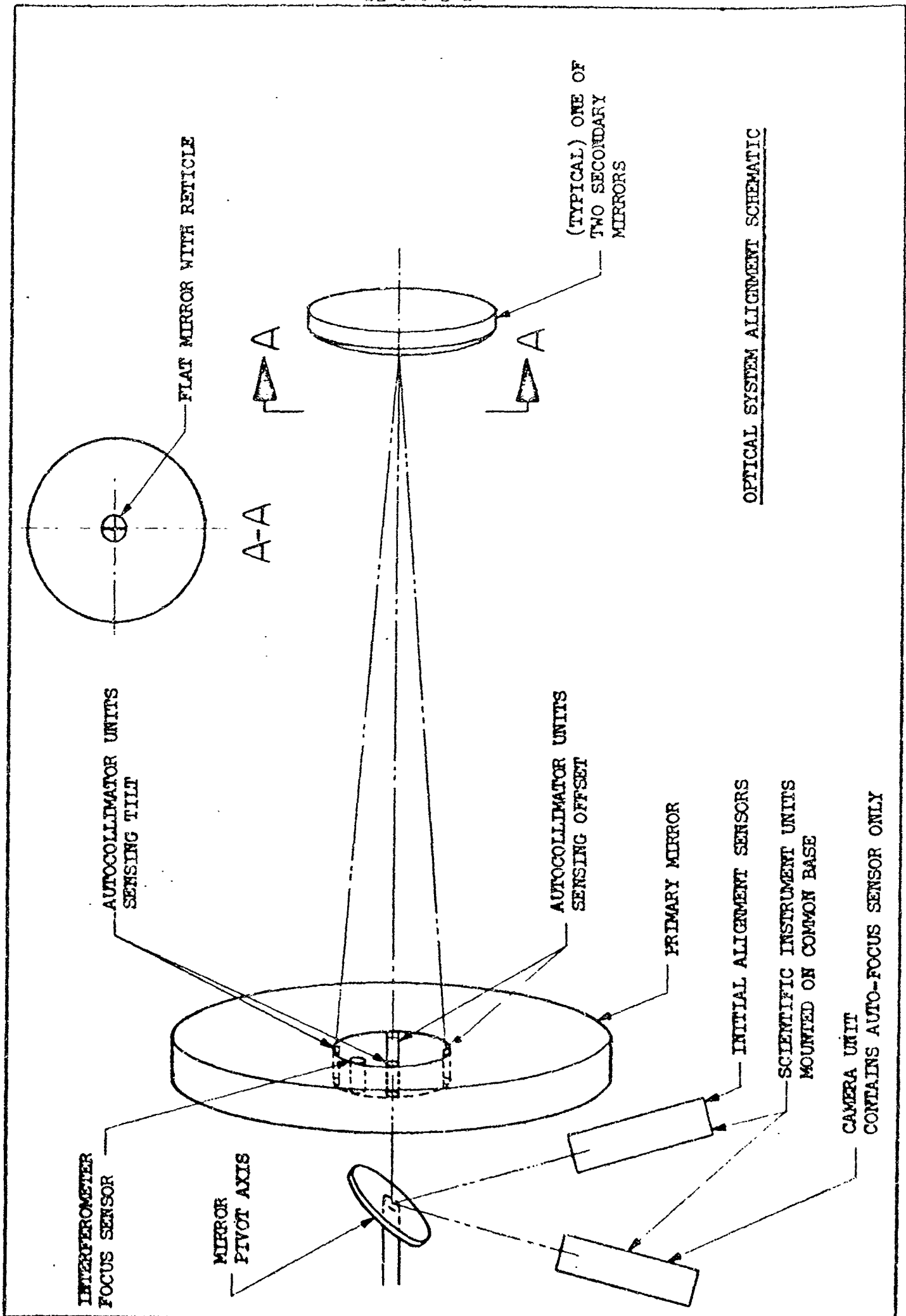


Figure 5.2-15

permissible light obscuration of the primary mirror. A system which does not have coupling between axes of control is preferred on the basis of utilizing displays and manual control for alignment functions. More coupling increases the requirements for an automatic control and synchronized actuation. No coupling and a single actuator for each axes of control are also desired for malfunction detection and maintenance. On the other hand, a mirror support that has five degrees of uncoupled movement, usually has more structural design complexity.

Since two secondary mirrors are being used, there is also the choice of controlling position of the mirrors individually or mounting them in a common control cell. The many factors involved point out that the secondary mirror installation is a major design trade area.

Figure 5.2-16 shows the conceptual design of a secondary mirror installation developed for the baseline telescope configuration. The main design features of the support and positioning are:

- o A four-legged rigid truss attaching the secondary mirror carriage to the inner telescope tube wall.
- o The $f/15$ and $f/30$ mirrors are mounted in a common control cell which has the five degrees of position control. The position target element required for alignment sensing is mounted on each mirror to eliminate position tolerances between the mirrors and cell structure.
- o A rotational and translational geometry consisting of three flexure pivoted struts aligned with the optical axis. Two of these struts can be extended to induce rotational motion of the mirror carriage. The entire three-strut flexure system can be translated by two additional strut actuators grounded on the inner telescope tube.
- o Focus adjustment is made by positioning of a single central actuator driving the mirror mounting structure along four ball-splined tubular ways.
- o A single electric motor driven jack screw is employed for positioning of each of the five degrees of mirror freedom provided. A minor degree of coupling is allowed between secondary mirror rotation, translation, and focus.

Each motor driven degree of freedom of the suspension receives an amplified signal command from one of the alignment sensors of a directional sense which drives the error seen by the sensor to a minimum threshold value. Thus, autocollimating sensors mounted on the inner aperture of the primary mirror detect angular misalignment between mirrors and furnish signals to the two flexure mounted actuators which then produce corrective rotations of the secondary mirror carriage.

Actuators consist of sealed packages, each containing a servo motor geared to a concentric differential jack screw drive incorporating a preload, spring to remove backlash from the differential thread.

5.2.6 Configuration Design Conclusions & Recommendations

Conceptual configuration design studies resulted in identifying many structural

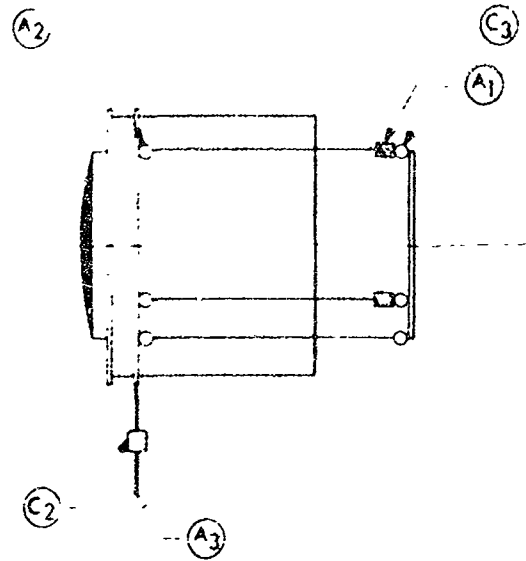
and installation problems which are very important in attaining an efficient or optimized design. None of the design problems, which could be identified at this level of detail, are considered insurmountable or beyond feasible engineering solutions. The most critical design problem areas are those associated with structural thermal requirements and protection of the optical systems during boost. A summary of the conclusions and recommendations of the structural thermal problems is presented at the end of the structures study (Section 5.3) and thermal control study (Section 5.5). In contrast to earth-bound telescopes or the OAO designs, the MOT requires a design interface between a pressurized cabin and the optical systems. This interface imposes constraints on the optical system design and constraints on man's functions in telescope observation. The baseline design concept requires remote operation of a cabin door and imposes fairly severe requirements on the atmosphere supply subsystem to make the experiment instruments accessible to man in a shirtsleeve environment. Additional studies are recommended of this problem area to determine if the constraints and complexity can be reduced.

The pneumatic bladder support for the primary mirror during boost imposes several fairly stringent design requirements. Pressure level control in many individual bladder segments, decoupling of the structural mounting and disposition of the bladders after the telescope is in orbit are all complexities that can possibly be reduced by further design refinement. Installation of the secondary mirrors is a definite trade area for further study and some of the possible design approaches are noted in paragraph 5.2.5.3.

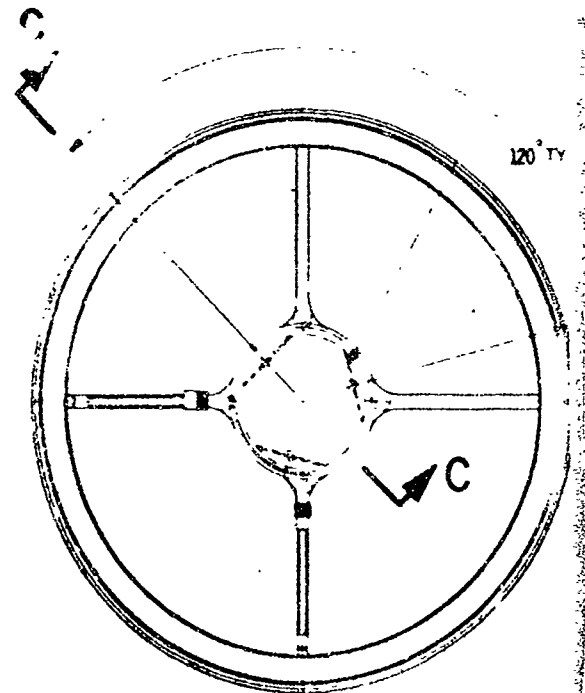
In the area of supporting subsystems, two installation problems in particular warrant further design studies, star trackers and expendables or movable equipment. The star trackers require installations in which accurate alignment can be maintained with the telescope optical axes, and they must be located externally of the basic protective thermal structure. The basic design philosophy used for the MOT was to decouple the optical systems from the outer protective thermal structure. In the case of the star tracker, a direct structural tie is required from the optical system structure to the external environment, thus making it difficult to obtain geometric stability.

Installation of expendables and movable equipment is critical in the soft gimbal operational concept (Model No. 948-41C), and to some extent on the separated concept (Model No. 948-43D). In the gimbal concept the torque transmitted to the MOT from the spring suspension system is directly proportional to the CG offset from the gimbal axes. The final design of the fine stabilization control system will, therefore, place stringent requirements on CG control. For example, the present studies are based on maintaining the CG within one inch of the gimbal axes, which limits usable expendables located at 70 inches from the CG to approximately 200 pounds.

The size of an $f/4$ 120-inch telescope relative to MORL indicates that structural interfaces and subsystem requirements imposed on MORL will necessitate long-range advanced planning to insure that the MORL will be compatible with MOT operations. For example, MORL attitude and orbit control systems will have to be sized for moments of inertial and ballistic coefficients for operation when the MOT is directly coupled to the MORL.

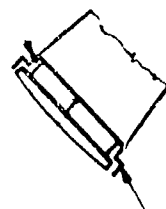


NEUTRAL POSITION



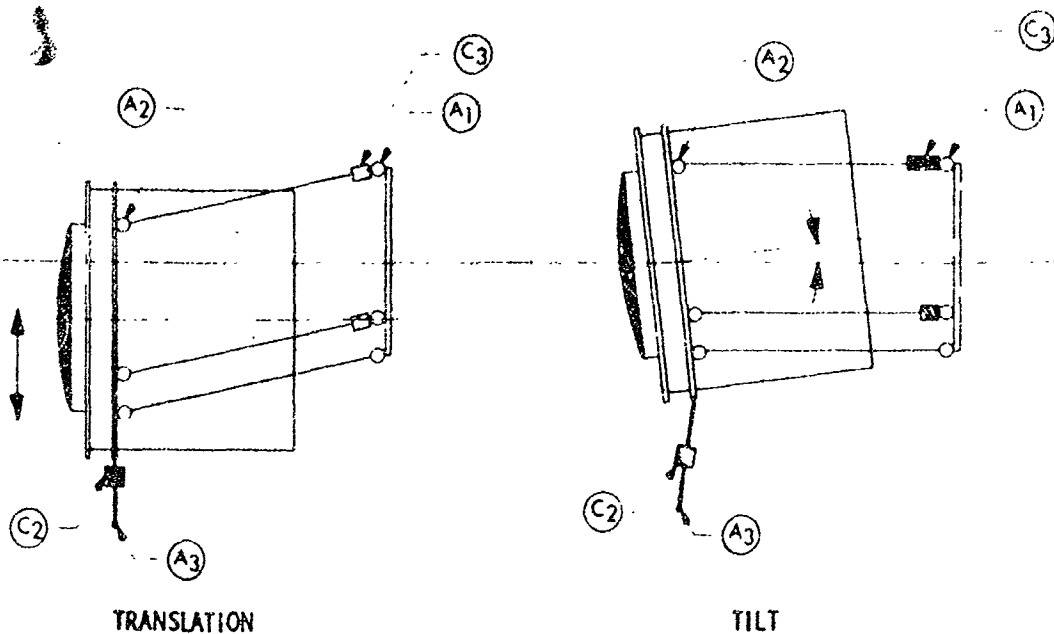
SECTION B-B

TAPERED PIN (3)
USED FOR DISENGAGING
MIRROR HOUSING FROM
CONTROL CELL

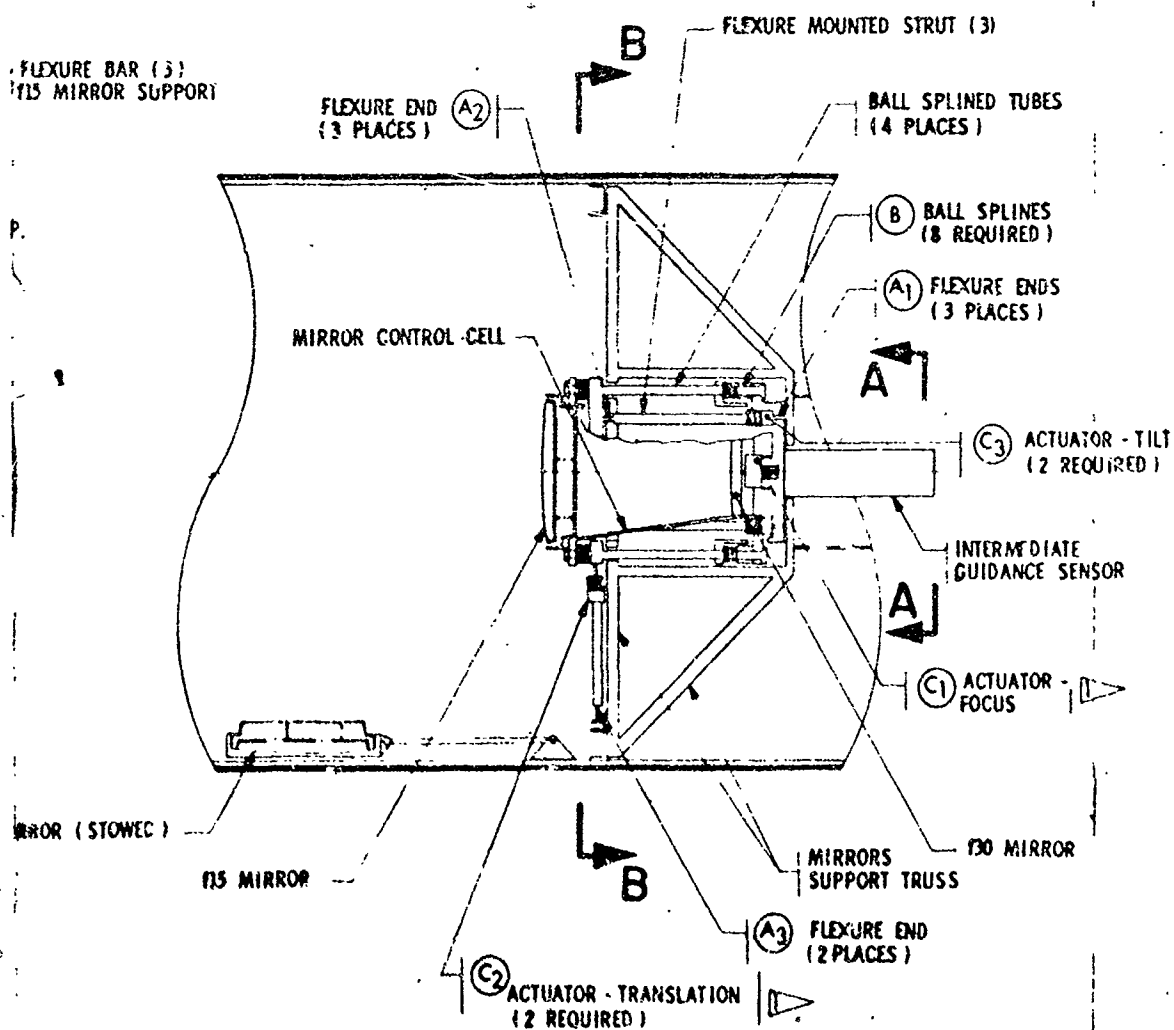


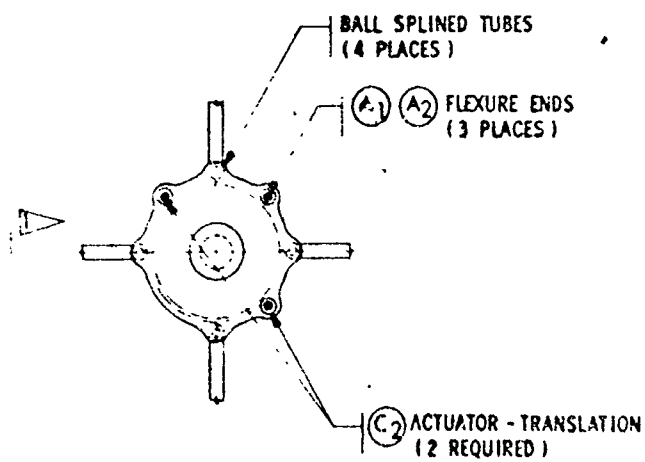
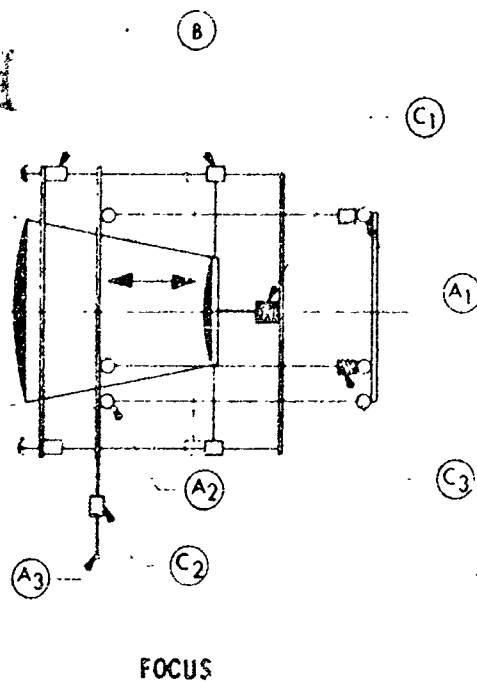
SECTION C-C

REMOVABLE SECONDARY
MIRROR HOUSING



ACTUATION SCHEMATIC





CODE:






-  - BALL SPLINE
-  - FLEXURE POINTS
-  - ACTUATOR
-  - ACTUATOR ACTIVATED
-  - PRELOADED BALL SCREW MOTOR ACTUATOR

Figure 5.2-16

SECONDARY MIRRORS INSTALLATION
NOT BASELINE CONFIGURATION

The spring suspension system for the soft gimbals design (Model No. 948-410) is purely conceptual, and further detail design studies, including spring design, gimbal design, and structural characteristics of the combined vehicles, are recommended to refine requirements.

5.3 STRUCTURES

Structural effort on the MGT was concentrated in five major areas of investigation, categorized by technological discipline:

- 1) Structural Design
- 2) Thermal Distortion Analysis
- 3) Meteoroids and Radiation
- 4) Direct Analog Dynamic Analysis, and
- 5) Launch Environment and Analysis

A baseline structural configuration (Figure 4-1c) was chosen having structural layout, optics, thermal characteristics, and mass distribution in common with other design studies. Where indicated, parametric variations were made around this baseline. The final configuration, Figure 4-1d, while it differs from the structural baseline by having a different cabin arrangement, does not deviate sufficiently in any respect to affect the conclusions of the structural studies.

5.3.1 Launch Environment and Analysis

Based on experience, it was considered necessary to assess the launch conditions, since they dictate critical load factors for telescope design and contribute to the environmental criteria. Time did not permit a complete flight vehicle analysis, so "handbook" values for boost load factors were adopted.

5.3.1.1 Acoustic and Vibration Environment

In anticipation of a detailed analysis of the mirror response to the environmental forcing functions, the acoustic and vibration environments were surveyed. However, little data could be obtained for the S-IB other than some measured data from the S-I/Apollo boilerplate flights. These data measurements indicate a maximum acoustic environment at booster station 1703 of sound pressure levels on the order of 135 to 140 db during the Mach 1/maximum q period of flight. The maximum vibration environment measured at the adapter ring, booster station 1571, was 1.23 grms laterally with a frequency of 825 cps.

Based on the amount of available data and the time involved, an analysis of mirror response was not considered feasible during this preliminary analysis.

5.3.1.2 Launch Analysis

A sketch of the air vehicle configuration and the matching dynamic model used for a launch release analysis are shown in Figure 5.3-1. This configuration was analyzed for axial vibrations, the so-called "pogo stick" mode. The solution of the applicable dynamic equations resulted in a vehicle axial modal frequency of 7.29 cps. Application of the associated modal data to the equation

$$\left| \Delta N_x \right|_{F/L} = 1 + \frac{T - W}{W} \left\{ 1 + \left| \sum_{i=1}^n \frac{\phi_{Ti} \phi_{F/L i}}{M_i / W} \right| \right\}$$

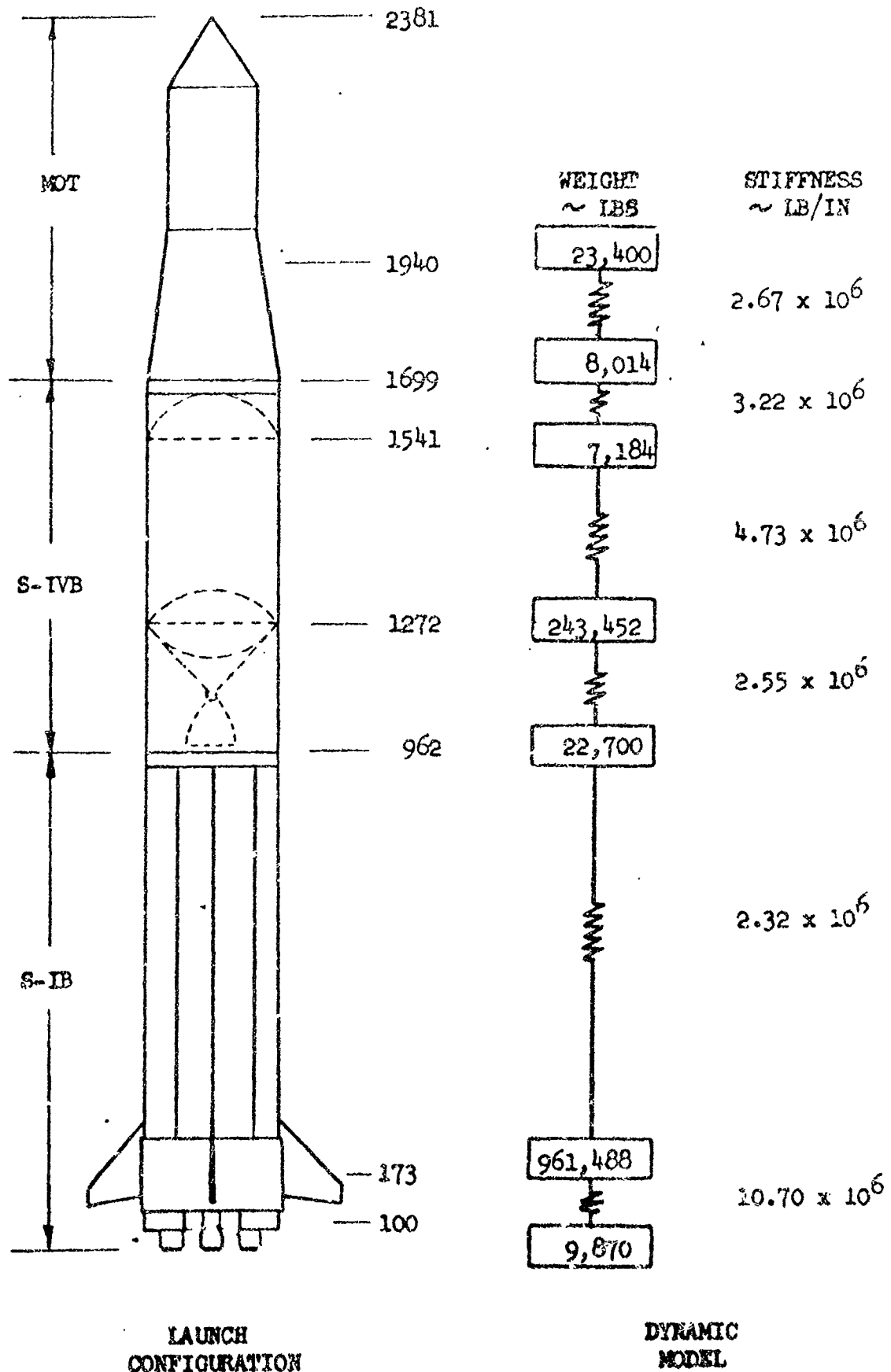


Figure 5.3-1: Launch Configuration Dynamic Analysis Model

with $|\Delta \ddot{u}_x|_{T/L}$ = axial load factor at payload, in g's

T = booster thrust, lbs

W = vehicle weight, lbs

M = vehicle mass, lb-sec²/in

M_i = ith mode generalized mass, lb-sec²/in

ϕ_{T_i} = ith mode displacement at nozzle, in/in

ϕ_{P/L_i} = ith mode displacement at payload, in/in

produces an axial load factor at the payload of 1.55 g, based on first mode response only.

To determine maximum design load factors, a brief investigation was made of other launch and staging events. A summary of events and the resulting load factors applicable to the telescope design is included as Figure 5.3-2.

CONDITION	LOAD FACTOR		LATERAL
	TENSION	COMPRESSION	
REBOUND	1.38	2.83	± 0.25
POST RELEASE	0.73	3.23	± 2.91
FLIGHT HIGH Q		1.95	± 0.41
THRUST CUT OFF	± 6.95		± 0.10
ENGINE HARD OVER, S-IVB		3.55	± 1.73

Figure 5.3-2

5.3.2 Structural Design

5.3.2.1 Primary Structure

At the initiation of primary structure sizings, it was recognized that stiffness requirements, as determined by servoelastic analysis, could be the design consideration for some of the primary structural elements. With this in mind, it was decided to proceed by sizing structural members on the basis of boost load conditions and make provision for parameterizing their stiffness characteristics in the dynamics studies.

Structural concepts and materials employed were chosen to arrive at the best compromise among the four requirements of structural stiffness, thermal isolation, optical alignment, and stress level. These considerations led to the following approaches being taken:

- 1) Determinate structure was used to minimize the transmission of stress-induced distortions where possible.
- 2) Structural configurations were chosen to maximize structural stiffness (i.e., tubes rather than rods; shells rather than frames) where possible.
- 3) Materials having highest stiffness with lowest heat conduction were used in critical areas such as primary mirror tangent bars.

The structural arrangement of the baseline is shown in Figure 5.3-3 with the individual structural elements identified by letter code. The element code is consistent with that used in the gimbal design, Section 5.3.2.4, and in the direct analog dynamic analysis, Section 5.3.5, as are the structural materials, concepts, and stiffnesses.

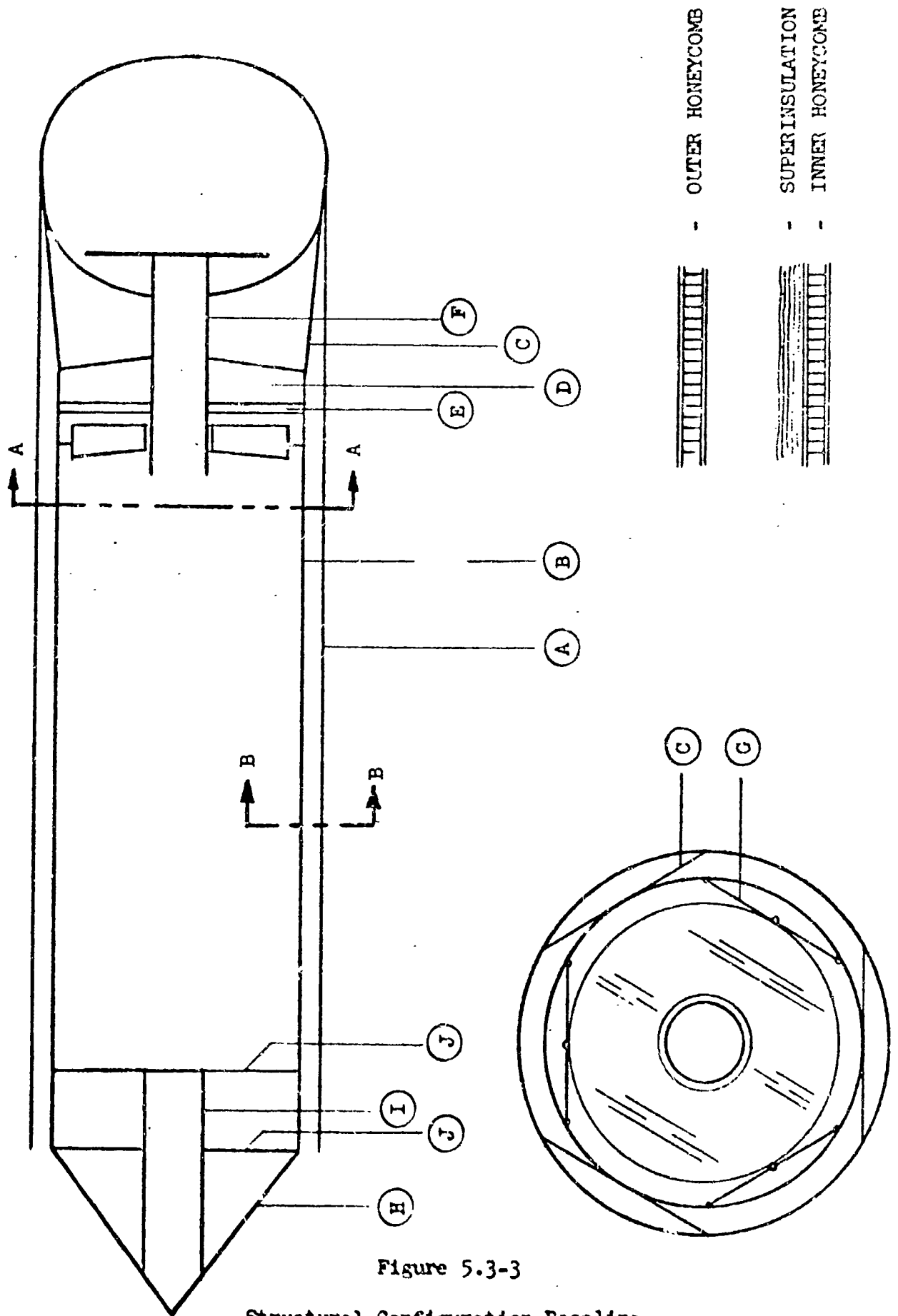
Structural sizings are based on the boost load conditions specified in Section 5.3.1, Launch Environment and Analysis. The design load factors are ± 6.95 axial and ± 2.91 lateral. The thermal protection afforded by the aerodynamic shroud is such that no significant heating will be experienced during the boost trajectory. The structure was thus sized at room temperature.

Generalized expressions for element stiffnesses were derived in terms of deflection axis, geometric parameters, and materials properties to facilitate parameterization of element stiffnesses and to permit parametric changes to be reflected in weight and thermal analyses.

Materials were chosen on the basis of ease of fabrication, thermal stability, structural stiffness and thermal conductivity where heat leak is important. In critical heat leak areas (Experiment Support Tube F, Cabin Support Truss C, and Tangent Bars G) material properties were traded to define the optimum. The parameter kA/K

where

k	= thermal conductivity
A	= cross-section area (based on boost load sizing)
K	= member stiffness (based on A)



was used to compare materials. As an example, the tangent bars produce the following material comparison:

MATERIAL	$\frac{k_A}{K} / \left(\frac{k_A}{K} \right)_{Ti}$
Aluminum	29.33
Titanium	1.00
Fiberglass	0.12

Fiberglass is therefore the best material choice on a theoretical basis. Because of its low bearing strength, fiberglass is at best a difficult material to attach; large end fittings become necessary and the fabrication problem is complicated. However, its obvious advantage in thermal isolation outweighs any manufacturing consideration and its use is dictated in critical heat leak areas.

Structural sizings proceeded along major load paths, and a running weight statement was prepared to reflect correctly the impact of inertial loads on the structural load levels.

The structural element code, the material used for each element, and the structural concept applied are displayed in tabular form in Figure 5.3-4. Figure 5.3-5 shows the important element geometric parameters and lists the associated stiffnesses. Since the direct analog simulation was concerned with deflections and rotations in a plane including the telescope optic axis, two stiffnesses are listed. The stiffness K_S applies to shear deflections; K_θ is associated with bending deflections.

Items in Figure 5.3-5 shown in parentheses represent the parameters which were changed to conform to the final configuration.

5.3.2.2 Mirror Dynamics

The dynamic characteristics of the primary $f/4$ mirror were investigated for two support conditions; first with the mirror supported on pneumatic bladders, and second with the mirror supported on the tangent bars.

For the bladder-supported case, the mirror was treated as a rigid body, unattached to the telescope structure and uniformly supported by the bladder. Using a typical cross-section and the coordinate system shown in Figure 5.3-6, the equations of motion were written in terms of the support spring constants. Thus:

$$m\ddot{h} = -(K_A + K_B)h + (K_A l_A - K_B l_B)\Theta$$

$$I\ddot{\Theta} = (K_A l_A - K_B l_B)h - (K_A l_A^2 + K_B l_B^2)\Theta$$

STRUCTURAL ELEMENT	CODE	MATERIAL	STRUCTURAL CONCEPT
Outer Tube	A	Aluminum	Ring-Stiffened Honeycomb
Inner Optics Tube	B	Aluminum (Titanium)	Ring-Stiffened Honeycomb
Cabin Support Truss	C	Fiberglass	Tubular Pin-Jointed Truss
Mirror Cell Beams	D	Titanium	Cantilever Beams
Mirror Cell Floor	E	Titanium	Honeycomb
Experiment Support Tube	F	Fiberglass	Monocoque Cylinder
Tangent Bars	G	Fiberglass	Hinged Rods
Secondary Support Structure	H	Titanium	Tubular Pin-Jointed Truss (Solid Vierendeel Truss)
Secondary Optics Tube	I	Aluminum	Ring-Stiffened Cylinder
Secondary Support Flexures	J	Titanium	Tension Straps (Solid Vierendeel Truss)

Figure 5.3-4

STRUCTURAL ELEMENT	GAGE IN	LENGTH IN	MEMBER AREA IN ²	HONEYCOMB DEPTH IN	K _S LB/IN	K _θ IN-LB RAD
A	0.01	63.7 Ring Spacing		1	39.2x10 ^{6*}	0.317x10 ^{12**}
B	0.01	63.7 Ring Spacing		1	35.2x10 ^{6*} (54.5x10 ^{6*})	0.228x10 ^{12**} (0.353x10 ^{12**})
C		56.1 (28.3)	2.057 (1.209)		79,400 (224,360)	1.995x10 ^{9**} (1.465x10 ⁹)
D		52.0	5.309		5.442x10 ⁶	1.062x10 ⁹
E	0.01			2	0.2763x10 ⁶	4.986x10 ⁶
F	0.27				30.54x10 ^{6*}	5.13x10 ^{9**}
G		32.4	0.93		301,400	---
H		133.5 (72.0)	0.391 (0.555)		29,690 (178,800)	---
I	0.03				10.56x10 ^{6*}	2.741x10 ^{9**}
J		45.0	0.02 (0.148)		18,990 (107,900)	---

K_S = Shear Stiffness

Figure 5.3-5

K_θ = Bending Stiffness

* = GA (LB)

** = EI (LB-IN²)

Assuming support symmetry with $K_A = K_B = K$ and $l_A = l_B = l$, and applying harmonic motion, the solution of the equations of motion produced uncoupled translation and rotation frequencies in radians per second of

$$\omega_h = (0.42598K)^{1/2}$$

$$\omega_\theta = (0.63620K)^{1/2}$$

Plots of ω_h and ω_θ versus the support bladder stiffness are shown in Figure 5.3-6. A rotational modal frequency of 10.5 cps is obtained for a spring rate determined by a bladder pressure of 320 psf.

For the second case, the flexible mirror was supported by the tangent bars which in turn were assumed to be rigidly attached to the telescope structure. The cellular mirror was divided into segments bounded by the radial ribs and circumferential rings. Nodes were assigned at the juncture of ribs and rings for both upper and lower surfaces, as detailed in Figure 5.3-7. Since the mirror is symmetric about a diametric axis passing through any of the three supports, one-half of the mirror structure was used in obtaining all the vibrational modes by imposing the proper boundary condition restraints along the symmetric axis.

The equations of motion used to determine the mirror natural mode shapes and frequencies are of the form:

$$[J] \{\delta\} + [K] \{\delta\} = \{0\}$$

where

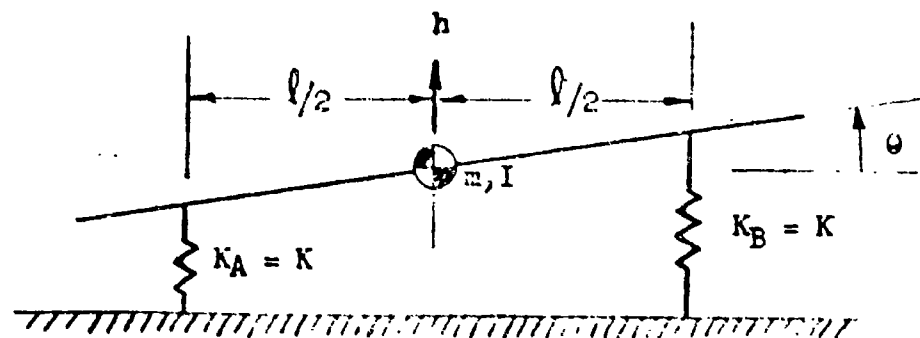
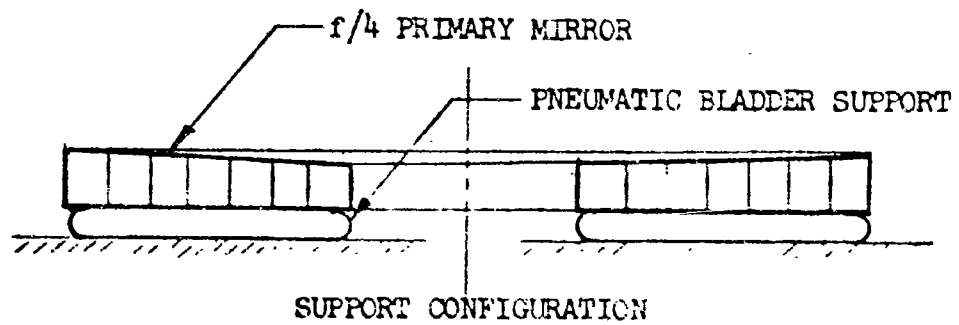
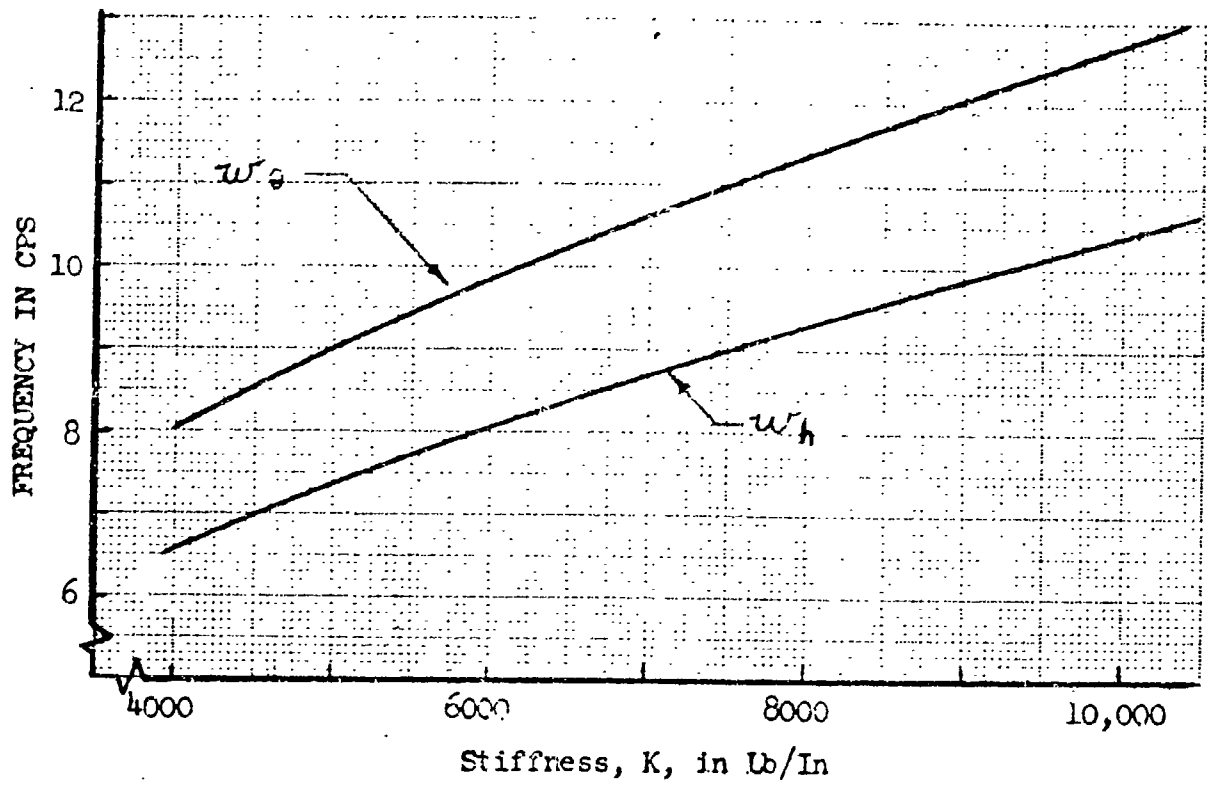
$[J]$ = mass matrix

$[K]$ = stiffness matrix

$\{\delta\}$ = degree of freedom of interest (in this case, displacement in z direction)

The stiffness matrix was obtained by formulating component stiffness matrices representing actual structural elements, and combining these submatrices at common nodes to form the complete structural representation of the mirror. The structural elements used in the mirror stiffness formulation are triangular flat plates representing the ribs, rings, and the upper and lower faces. Rectangular beams represent the tangent bar flexures.

An influence coefficient matrix was obtained for the symmetric and anti-symmetric cases by imposing appropriate boundary conditions on the stiffness matrix and applying an inversion routine. The influence coefficients were obtained for the Z-direction displacements at the nodes on the lower surface of the mirror; since vibration modes considered of interest were those characterized by Z displacements of the mirror's X-Y plane. The influence coefficient matrix, for the symmetric case, is a full matrix of 80 x 80 size. The antisymmetric matrix is a 64 x 64 due to additional boundary condition restraints.



COORDINATE SYSTEM

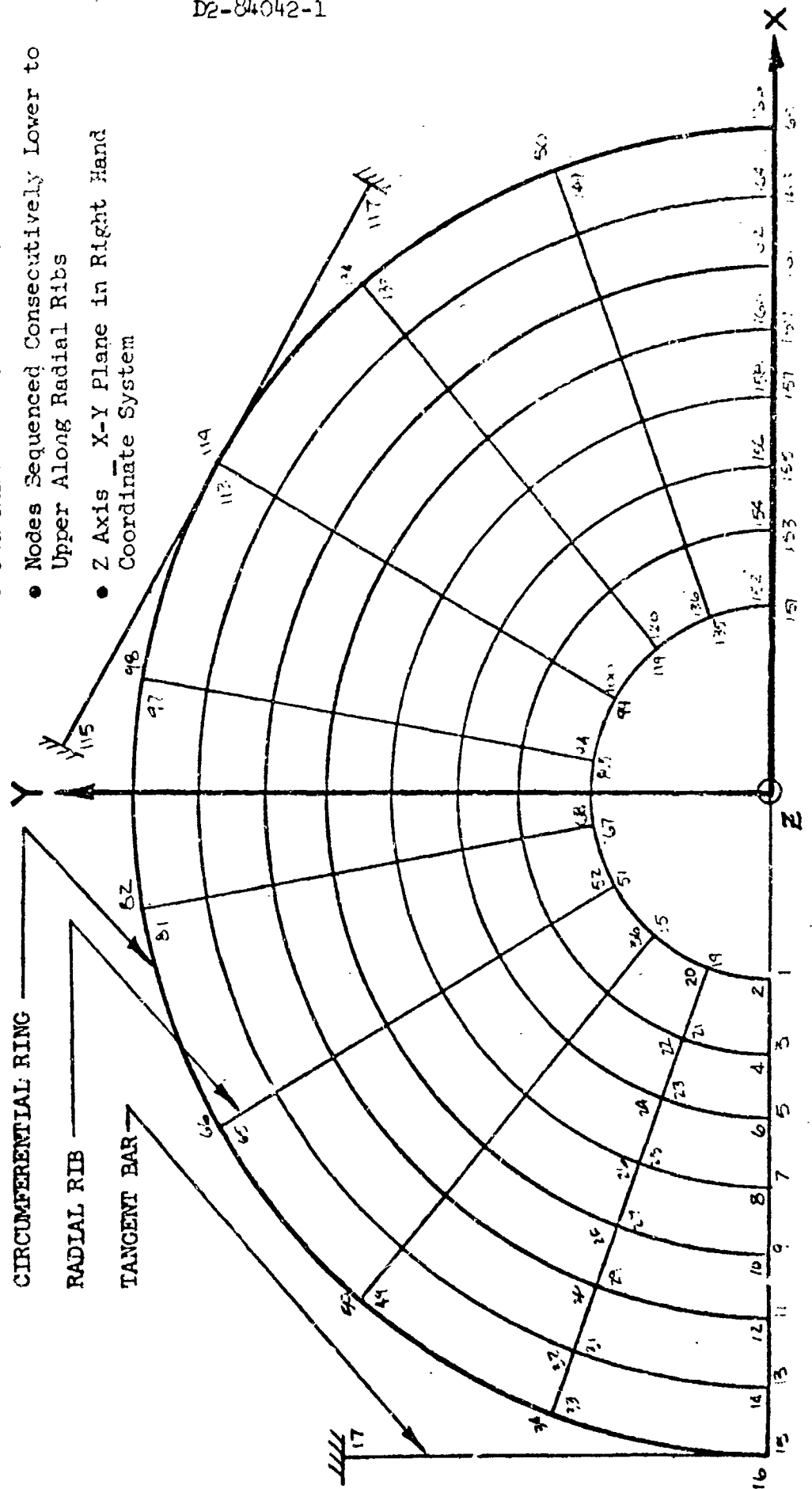
Figure 5.3-6

Primary Mirror Boost Dynamics

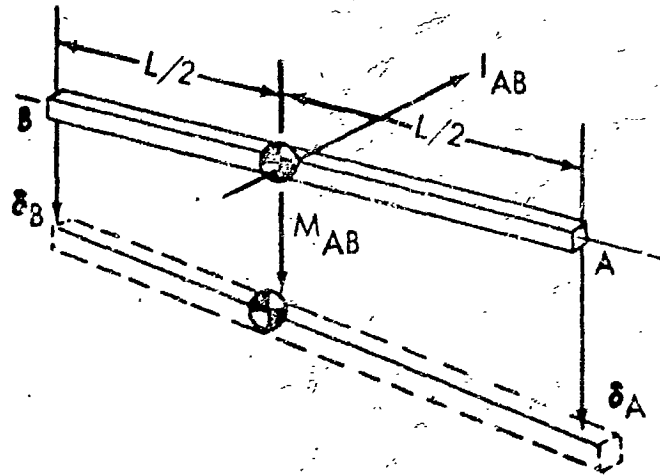
Figure 5.3-7

Primary Mirror Operational Dynamics Idealization

- Even Numbered Nodes on Upper Surface
- Odd Numbered Nodes on Lower Surface
- Nodes Sequenced Consecutively Lower to Upper Along Radial Ribs
- Z Axis - X-Y Plane in Right Hand Coordinate System



The mass matrix was formulated by lumping the mass properties of the structural segment between any two nodes at the midpoint of a rigid bar connecting those nodes as shown below.



Each lumped mass represents the mass properties, transformed to the plane of the lower surface nodes, of a mirror segment containing a portion of the upper and lower surface plates and the web of the rib or ring.

The kinetic energy for the single element shown may be expressed in terms of the displacements at each end as:

$$T = \frac{1}{2} m_{AB} \left[\dot{\delta}_A - \left(\dot{\delta}_A - \dot{\delta}_B \right) \frac{L/2}{L} \right]^2 + \frac{1}{2} I_{AB} \left[\left(\dot{\delta}_A - \dot{\delta}_B \right) \frac{1}{L} \right]^2$$

For the single lumped mass, the mass matrix may be written in terms of the node displacements as:

$$J \begin{Bmatrix} \ddot{\delta} \end{Bmatrix} = \begin{bmatrix} \left(\frac{m_{AB}}{4} + \frac{I_{AB}}{L^2} \right) & \left(\frac{m_{AB}}{4} - \frac{I_{AB}}{L^2} \right) \\ \left(\frac{m_{AB}}{4} - \frac{I_{AB}}{L^2} \right) & \left(\frac{m_{AB}}{4} + \frac{I_{AB}}{L^2} \right) \end{bmatrix} \begin{Bmatrix} \ddot{\delta}_A \\ \ddot{\delta}_B \end{Bmatrix}$$

Extending this single case to all the structural segments and summing terms at common nodes, the mass matrix J for the half mirror is generated.

The technique of matrix iteration is used to determine the natural mode shapes and frequencies. The equations of motion may be developed into a form suitable for iteration.

Substituting an assumed solution of the form

$$\delta = \delta_0 e^{i\omega t} \quad \text{or} \quad \ddot{\delta} = -\omega^2 \delta_0 e^{i\omega t} = -\omega^2 \delta$$

The equations may be rewritten to produce

$$[C] [A] \{\delta\} = 1/\omega^2 \{\delta\}$$

where

$[C]$ = Influence Coefficient Matrix
which is now in a suitable form for matrix iteration.

A tabulation of the first six symmetric and the first six antisymmetric modes for the f/4 primary mirror and a brief description of the characteristic motion is included as Figures 5.3-8. Contour plots of the mode shapes are included as Figures 5.3-9 through 5.3-16.

5.3.2.3 Primary Mirror Stress Analysis

The primary mirror geometry was taken from the Fecker report. Two changes were made from the referenced geometry; the focal length was changed from f/2 to f/4 as described in Section 3.7, and the radial ribs were made continuous. The second change has two advantages--fabrication of the mirror blank is simplified, and the configuration is made more amenable to computer analysis.

Only boost and operational load conditions were considered in the analysis. Not enough is known about fabrication, storage, and transportation conditions to permit their consideration in a study of this nature. However, certain conclusions can be drawn as to the allowable mirror load levels for any environment.

Two conditions of stress must be considered: first, overall mirror bending, and second, the bending of individual face panels. In general, these conditions will superimpose so that the maximum stresses will be directly additive.

The critical stress level is one which produces maximum permanent set in the mirror material corresponding to one microinch rms deviation. Permanent set data were obtained from tests of the precision elastic limit (PEL), defined as the stress required to produce plastic strain of 10^{-6} in/in. Communications with beryllium suppliers and a review of the metallurgical literature have revealed that the beryllium PEL is, on the average, 2500 psi or above, depending on surface conditions. Test data indicates that no observable plastic strain occurs at 80% of the PEL. Therefore, 2000 psi is taken as the allowable mirror stress in the following discussion.

Boost Conditions - During boost, the mirror is supported on pneumatic bladders. For static load conditions without rotations, the supporting load must be uniform across the contact surface. Dynamic conditions could exist which would, by establishing a pattern of strong shock waves within the bladders, cause nonuniformities in bladder pressure. However, for such a situation to occur, it would be necessary to develop compressible flow conditions; which, for the rigid body natural frequency discussed in Section 5.3.2.2, cannot occur at reasonable amplitudes. Thus mirror bending can only be induced by nonuniform inertial loads resulting from varying mirror thickness.

Rigid body rotations present a different problem. In order to generate restoring torques, the bladders must be segmented, preferably in both the radial and

MODE	FREQUENCY (CPS)	MODE DESCRIPTION
1	9.66	RIGID BODY TRANSLATION
2	17.86	RIGID BODY SYMMETRIC ROTATION
3	20.82	RIGID BODY ANTISYMMETRIC ROTATION
4	390.5	FIRST MIRROR RESPONSE - SYMMETRIC QUADRANT MODE W/TWO DIAMETRIC NODE LINES
5	565.9	FUNDAMENTAL DIAPHRAGM MODE W/ONE CIRCUMFERENTIAL NODE LINE
6	893.7	SECOND SYMMETRIC QUADRANT MODE W/THREE DIAMETRIC NODE LINES
7	932.8	DIAPHRAGM--QUADRANT COUPLED MODE W/ONE DIAMETRIC AND ONE CIRCUMFERENTIAL NODE LINE
8	1400.0	THIRD SYMMETRIC QUADRANT MODE W/FOUR DIAMETRIC NODE LINES

Figure 5.3-8

Figure 5.3-9
First Mirror Mode - Rigid Body Translation

$f_1 = 9.66 \text{ CPS}$

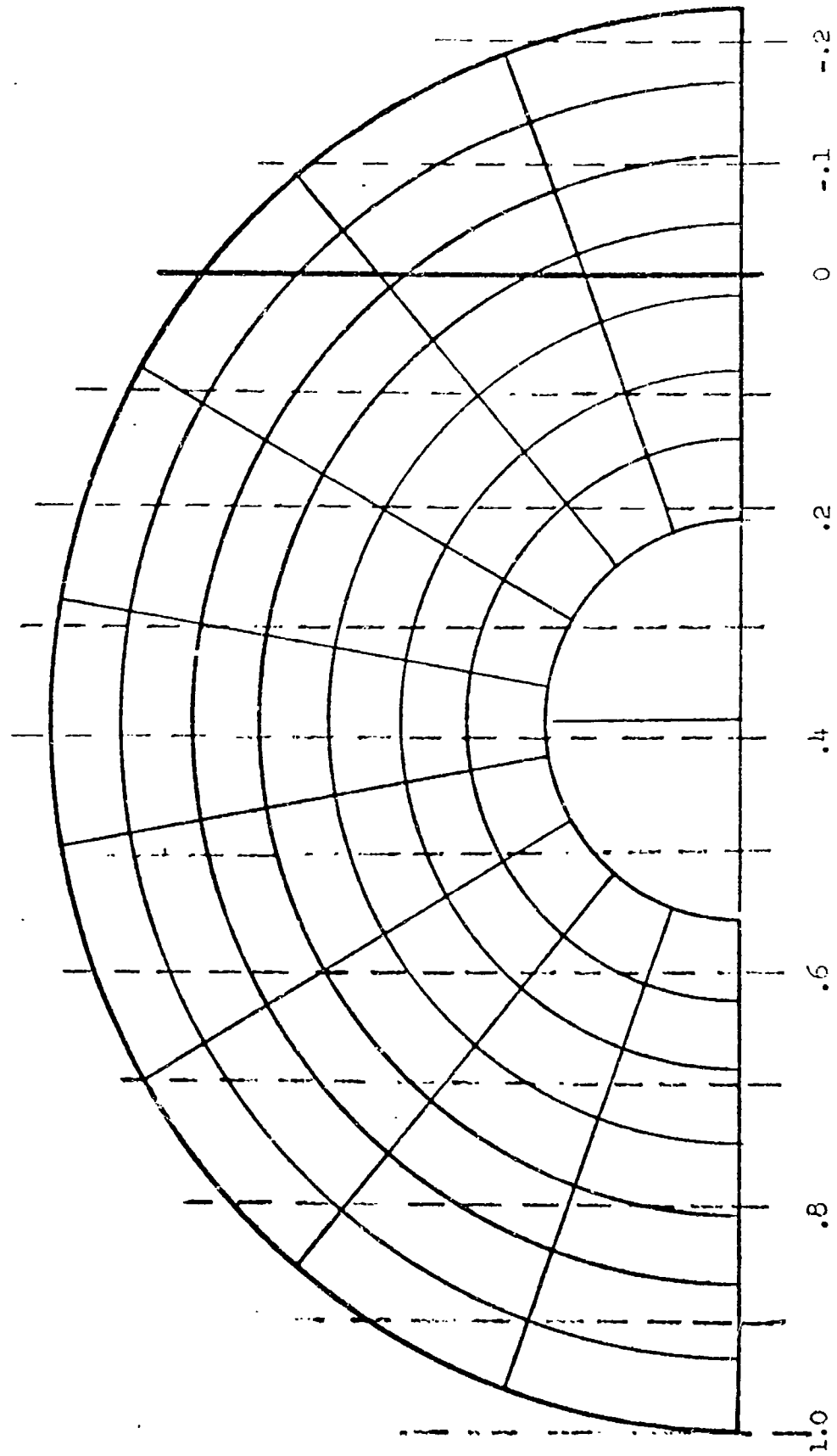
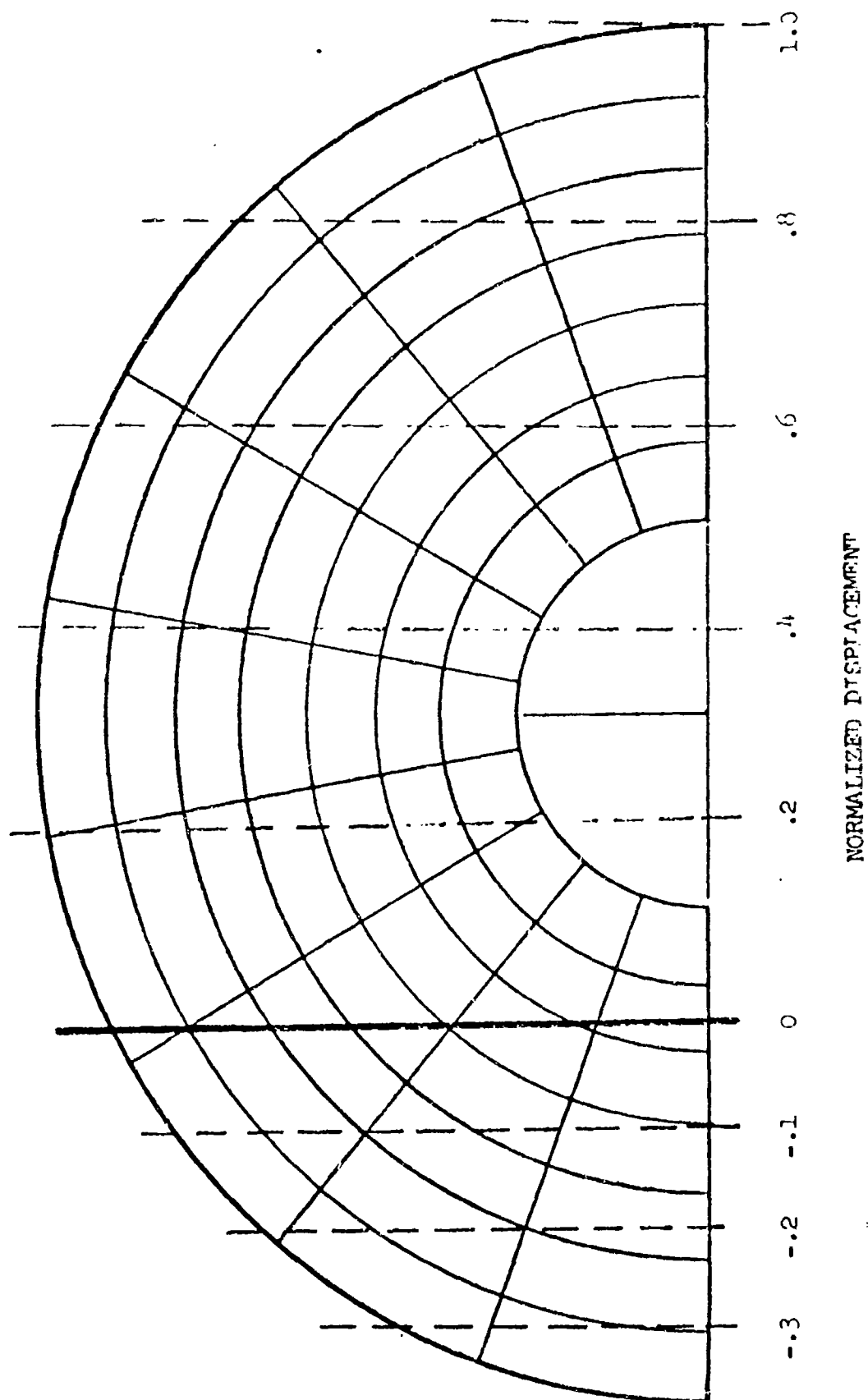


Figure 5.3-10
Second Mirror Mode - Rigid Body Symmetrical Rotation

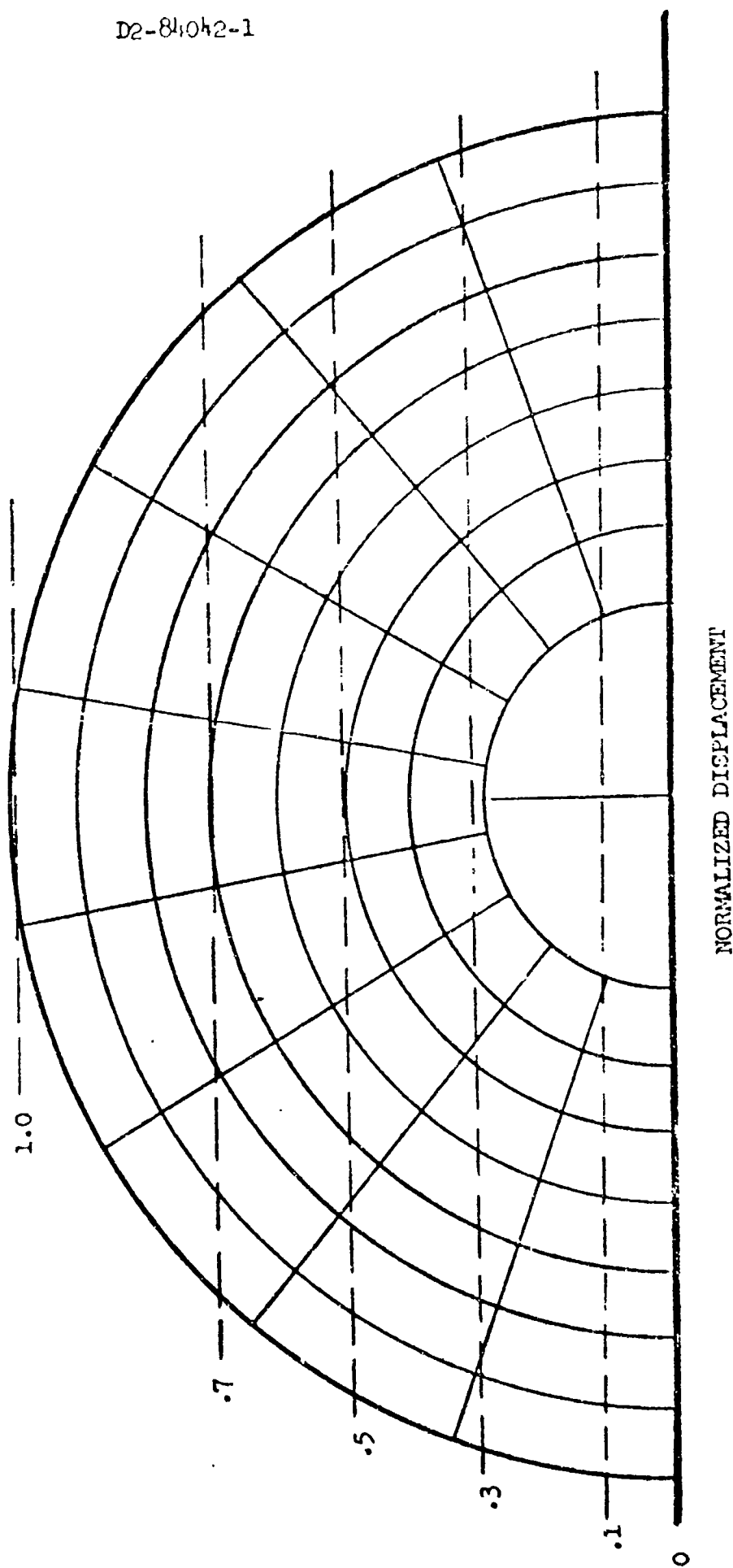
$f_2 = 17.86$ CPS



D2-84042-1

Figure 5.3-11
Third Mirror Mode
Rigid Body Antisymmetrical Rotation

$$f_3 = 20.82 \text{ CPS}$$



D2-84042-1

Figure 5.3-12
Fourth Mirror Mode - First Plate Mode

$f_4 = 390.5 \text{ CPS}$

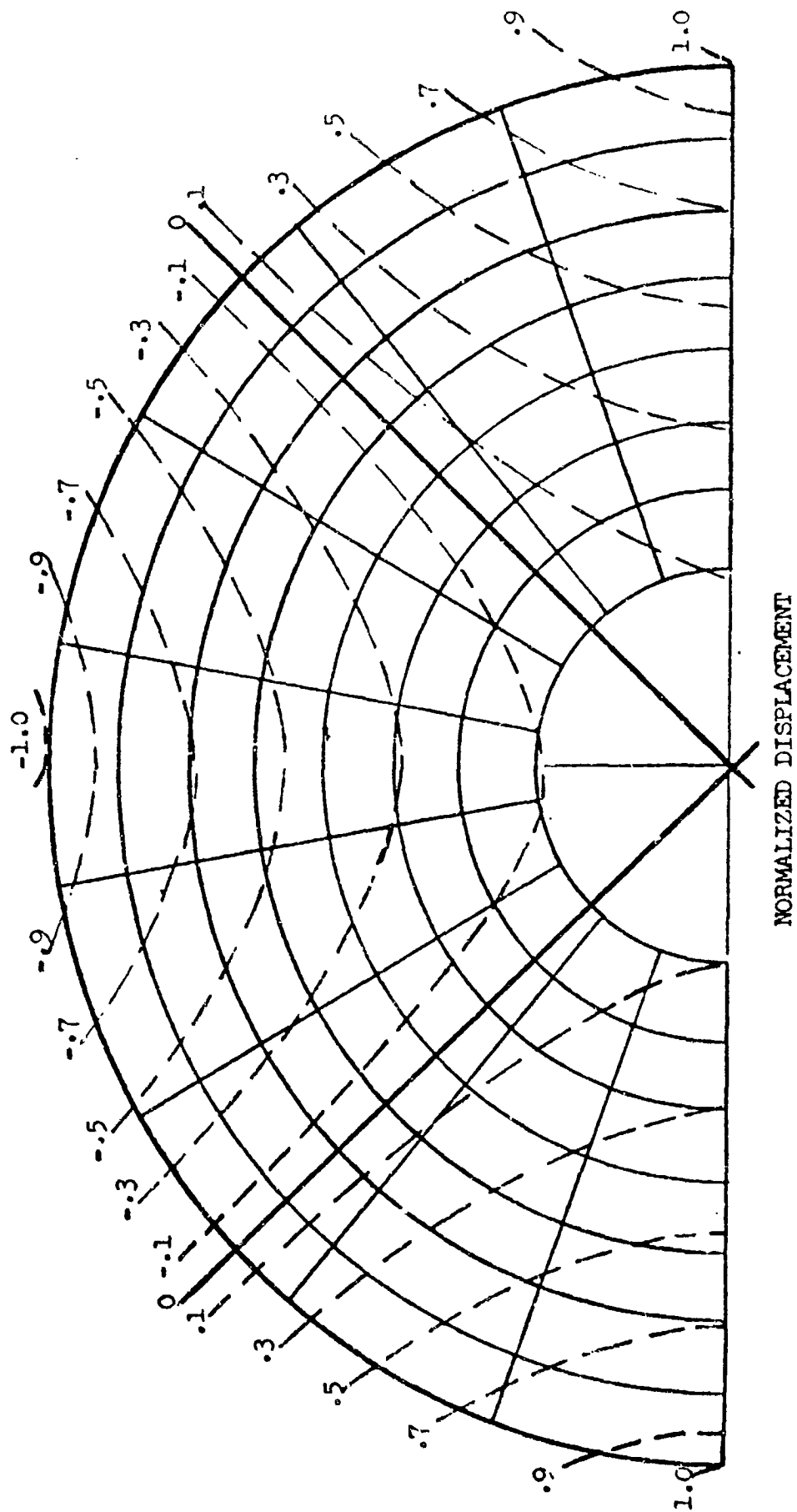


Figure 5.3-13

Fifth Mirror Mode - Second Plate Mode

$$f_5 = 565.9 \text{ CPS}$$

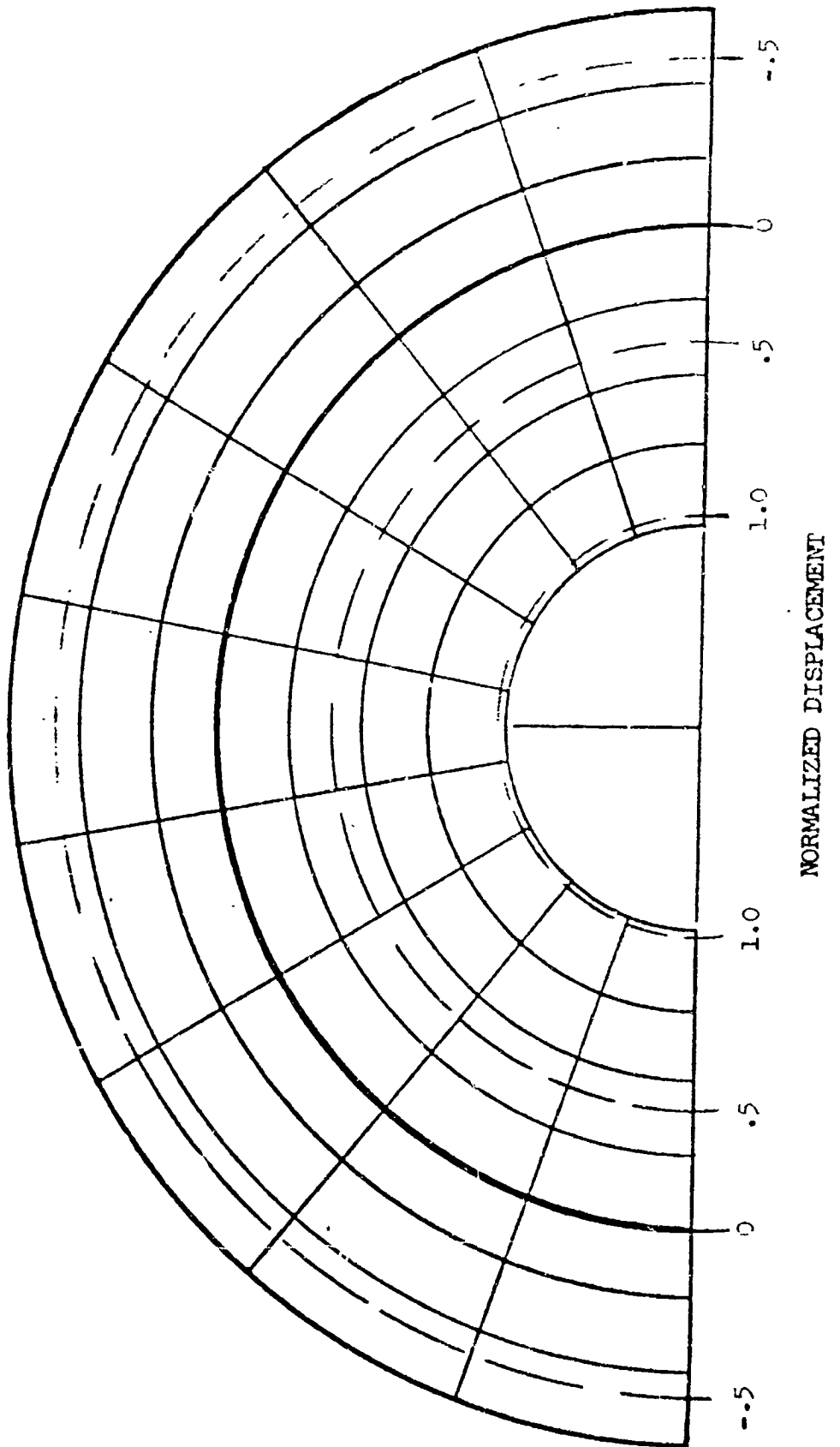


Figure 5.3-14

Sixth Mirror Mode - Third Plate Mode

$f_6 = 893.7$ CPS

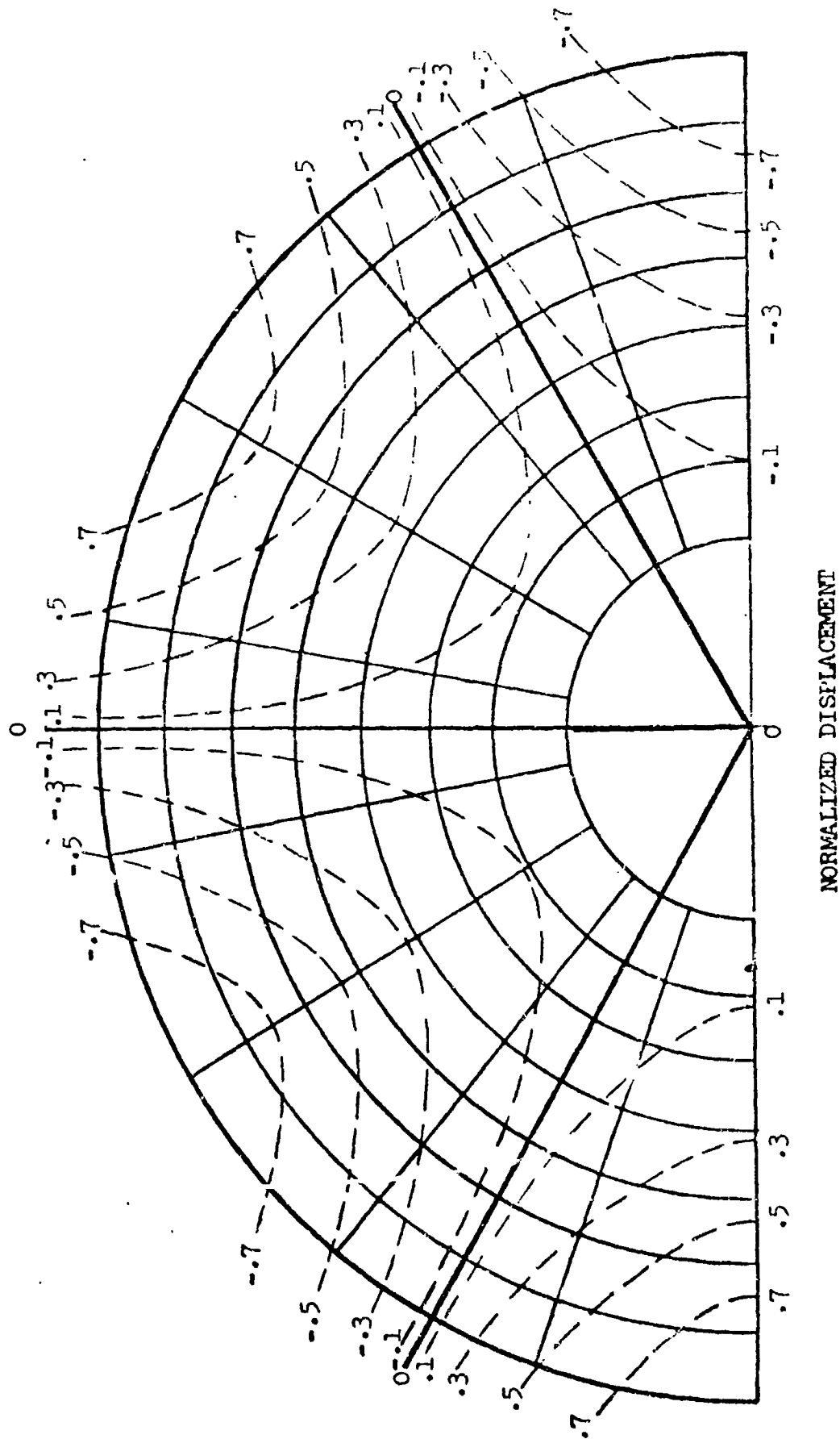
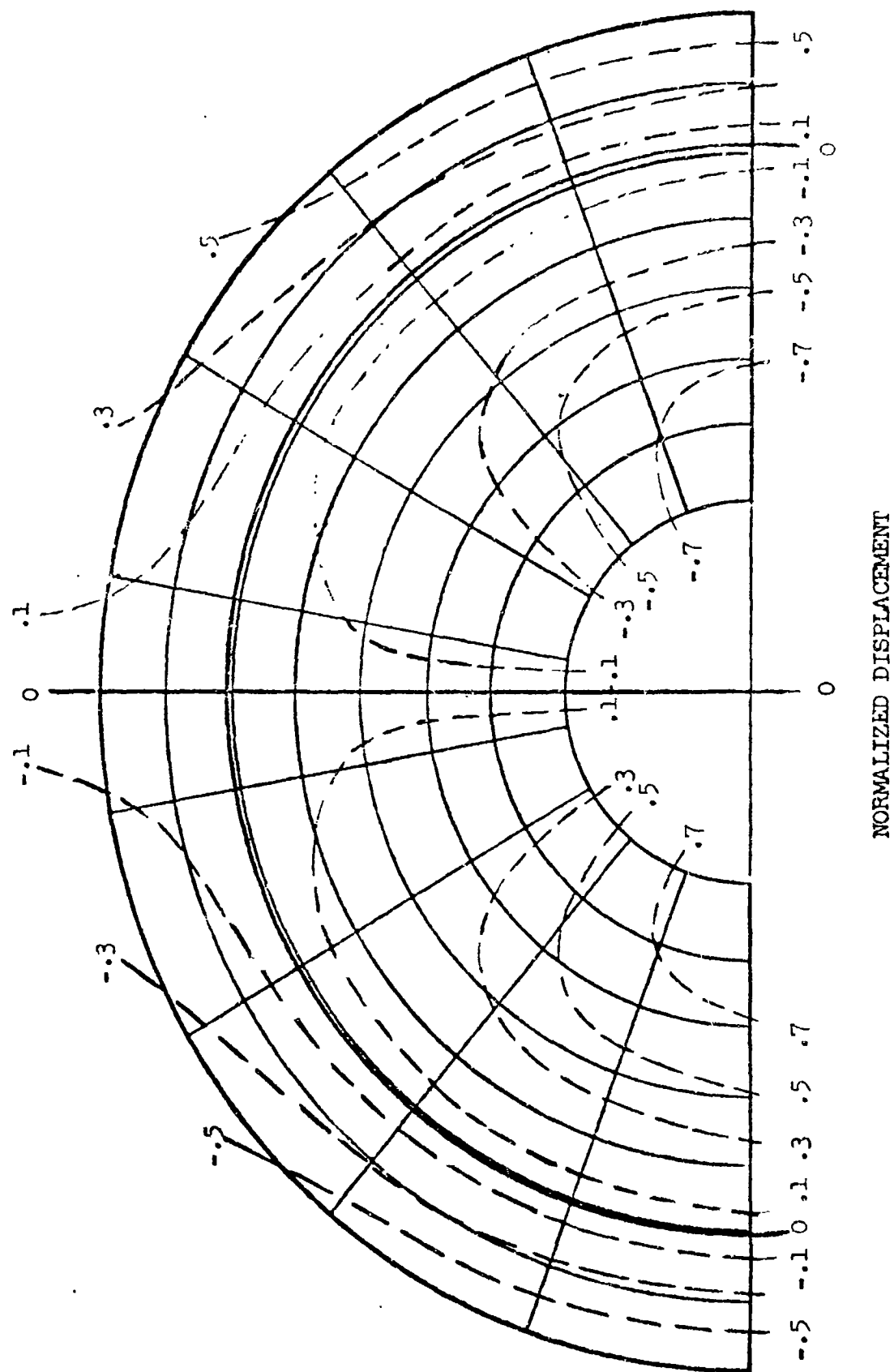


Figure 5.3-15

Seventh Mirror Mode - Fourth Plate Mode

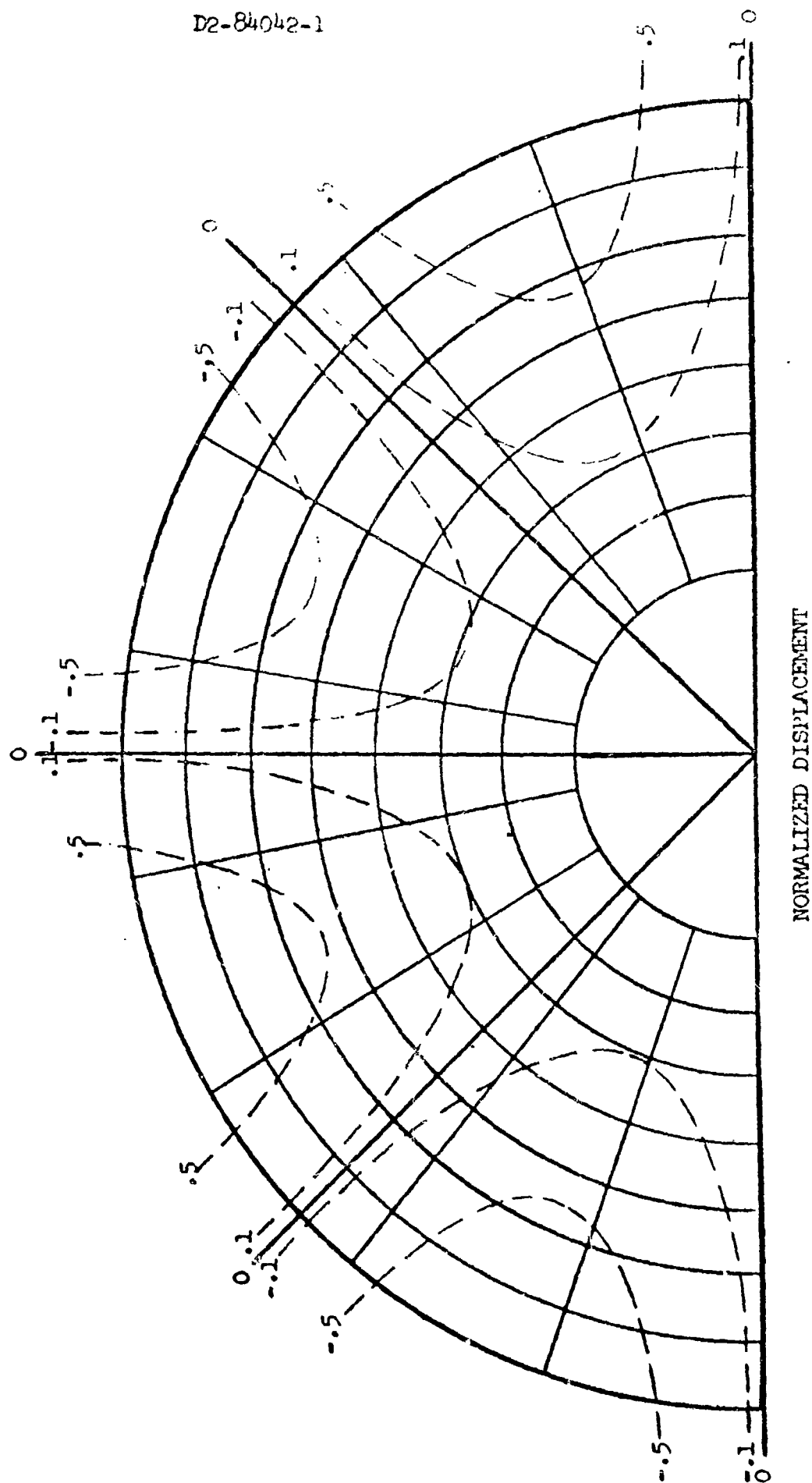
$f_7 = 932.8$ CPS



D2-84042-1

Figure 5.3-16
Eighth Mirror Mode - Fifth Plate Mode

$f_8 = 1400.1$ CPS



D2-84042-1

circumferential directions. Rotations will then produce nonuniform pressures from one bladder segment to another. These nonuniform pressures will induce bending in the mirror.

The nonrotational case was analyzed on the basis of loading shown in Figure 5.3-17. It was found that the mirror mass distribution can be approximated very closely by an expression of the form

$$m = a + b R^2$$

where m = mass per unit area
 R = radius

The values of the constants were found to be

$$a = 0.1771 \text{ lb}_m/\text{in}^2$$

$$b = 4.033 \times 10^{-6} \text{ lb}_m/\text{in}^4$$

The derived expression for the moment distribution and resulting stress level is extremely complex. The numerical solution for a load factor of 6.95 is shown in Figure 5.3-17. It can be seen from the figure that the maximum moment, 21.39 in-lb/in, occurs at the inner radius. This moment produces a maximum stress of 4.94 psi in the mirror faces. The face panel supporting the mirror is loaded by a net pressure at this point of 0.967 psi, which produces a bending stress of 27.71 psi. The maximum mirror stress level is thus 32.65 psi. The margin of safety for this condition is

$$MS = \frac{2000}{32.65} - 1 = 60.3$$

In the case of rigid body rotations, bladder restoring torque and total inertial reactions must be equal. As in the nonrotational case, bending arises essentially as a result of nonuniformities in the mass distribution. This load, shown in Figure 5.3-18, can be approximated conservatively by a linearly varying load and simple support at the mirror outer edge. In this case, the maximum value of the linearly varying load is given by

$$p' = \frac{b \alpha R^3}{12g} \quad (1)$$

where $b = 4.033 \times 10^{-6} \text{ lb}_m/\text{in}^4$

$$R = 60 \text{ in}$$

$$\alpha = \text{angular acceleration} - \text{rad/sec}^2$$

$$g = 386.4 \text{ in/sec}^2$$

Maximum bending moment for this case was found to be

$$M_{\max} = \frac{p' R^2 (5 + \mu)}{72 \sqrt{3}} \quad (2)$$

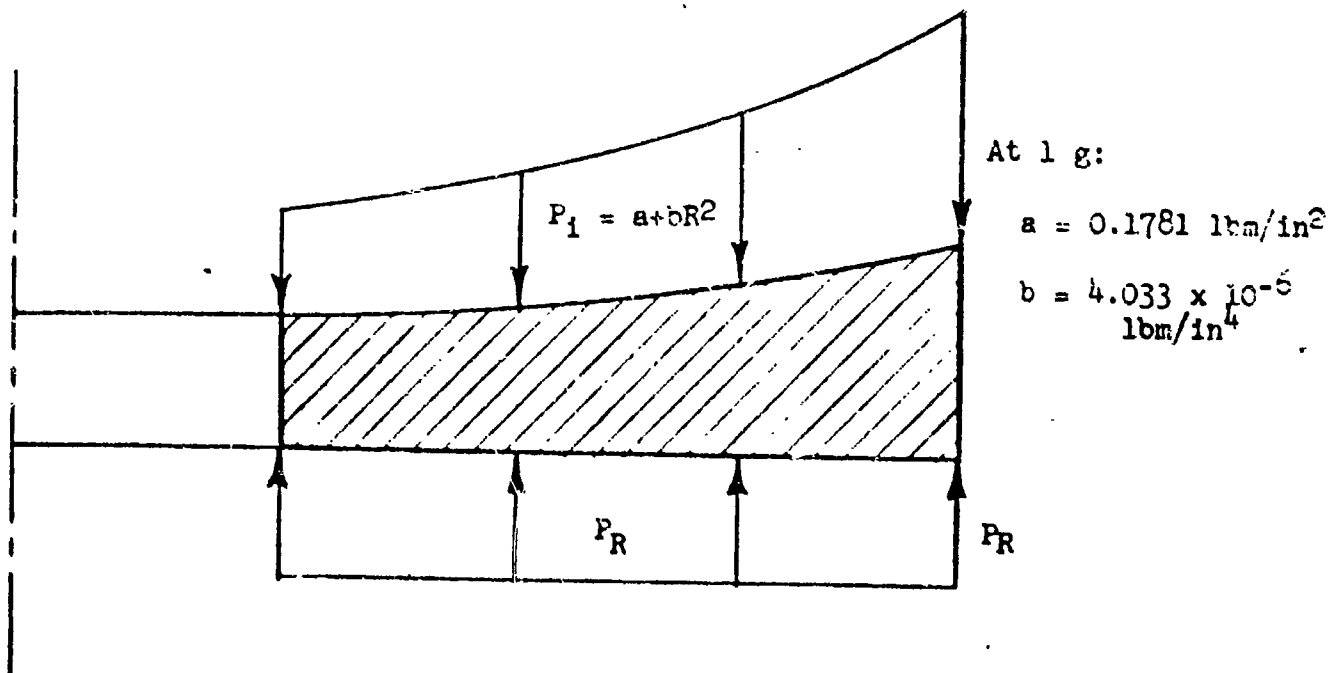
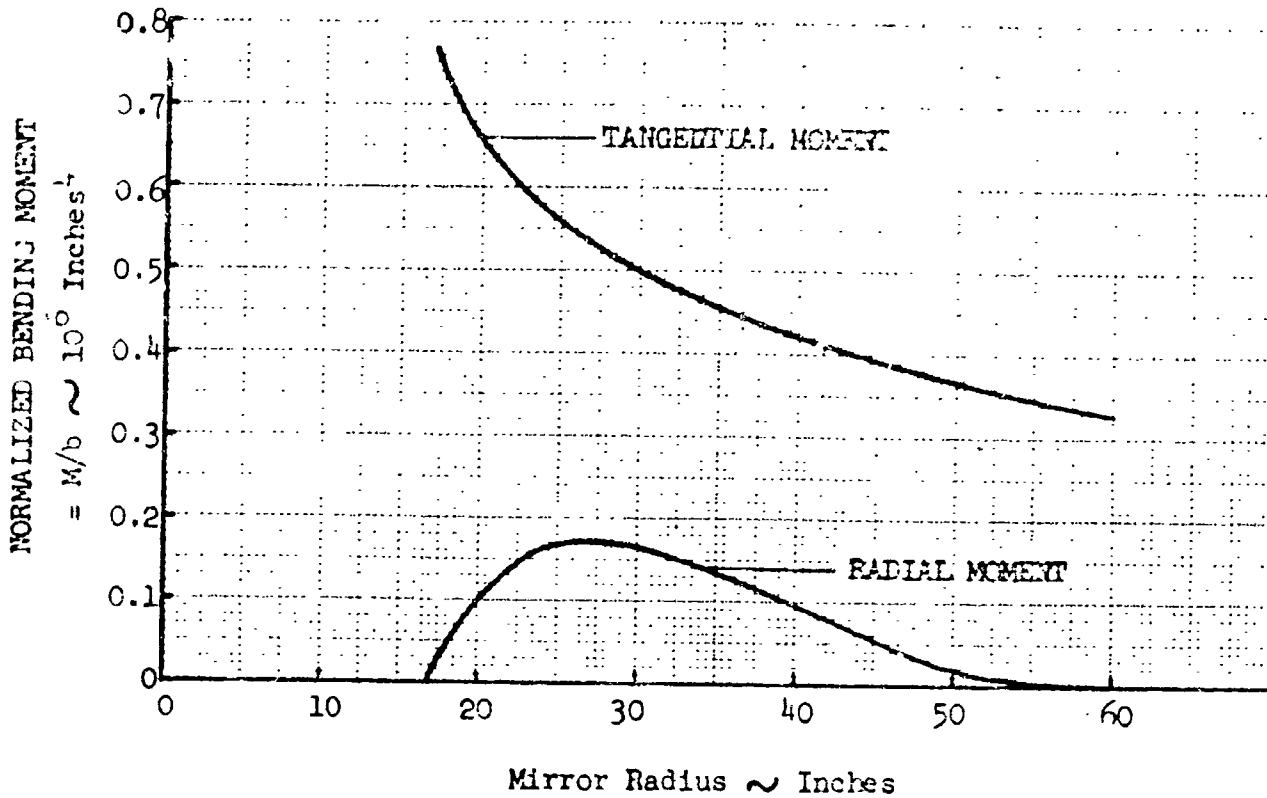


Figure 5.3-17

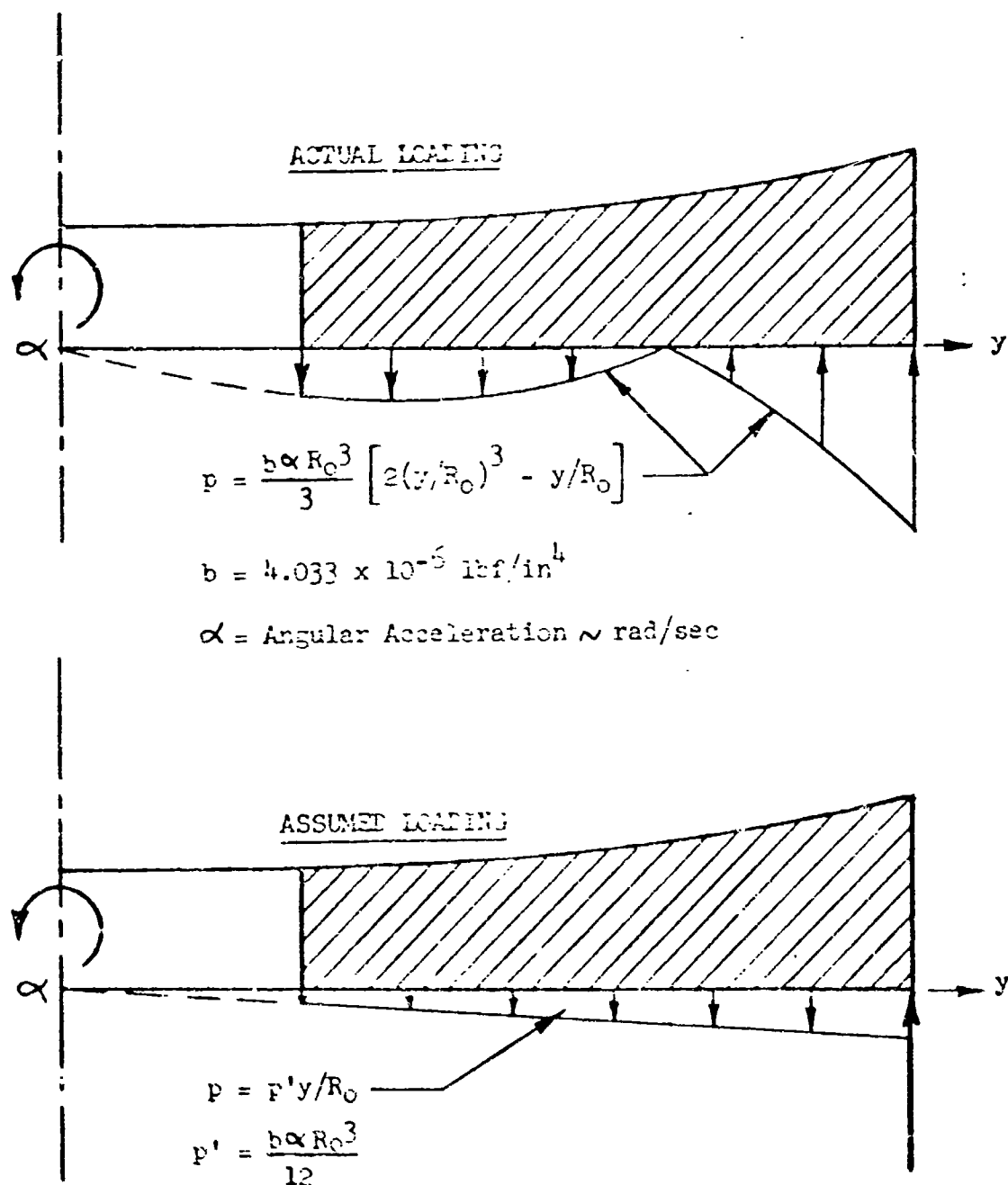


Figure 5.3-18

Boost Rotation Mirror Loading

at $R = 34.6''$

where $\mu = \text{Poisson's ratio} = 0.03$

If rotational motion of the mirror is assumed to be sinusoidally varying, the maximum angular acceleration is given by

$$\alpha = \frac{\delta}{R} \omega^2 \quad (3)$$

where $\delta = \text{edge displacement (assume } \delta = 1'')$

$\omega = \text{rotational frequency}$

$= 66.1 \text{ rad/sec (from Section 5)}$

Combining equations (1), (2), and (3):

$$M_{\max} = \frac{(5+\mu)bR^2 \delta \omega^2}{1496 g}$$

$$= 1.987 \text{ in-lb/in}$$

This produces a mirror bending stress of 0.443 psi. In the worst case, this stress is superimposed upon a 3.23 g axial load which produces 2.30 psi bending stress. Panel bending is 12.9 psi, and the margin of safety on combined stress is

$$MS = \frac{2000}{12.9 + 2.74} - 1 = 126.8$$

Operational Conditions - In operation, the mirror is supported by tangent bars at three attach points. Because of the discontinuous nature of the supporting loads, mirror stress levels are considerably higher than in the case of uniform supports. A general expression was derived for mirror bending moments as functions of R and θ for an annular disk of uniform weight. In this case, the gross effects of the point support loads will mask any nonuniformities in mass distribution, making the uniform weight assumption reasonable.

The resulting bending moments, both radial and tangential, are shown in Figure 5.3-19. Tangential moments were found to be more severe for all radial stations. The distribution of moment is approximately cosinusoidal with θ where $\theta = 3\theta$. Thus, both positive and negative moment maxima are plotted in the figure. The maximum moment occurs at $R = 60''$; $\theta = 0^\circ, 120^\circ, 240^\circ$, and is given by

$$M_{\max} = 2650 p \text{ in-lb}$$

where p is in psi. Using the mass distribution previously mentioned, with an allowable bending moment of 8970 in-lb, the maximum permissible acceleration of the mirror for a 50% margin of safety is 11.9 g's.

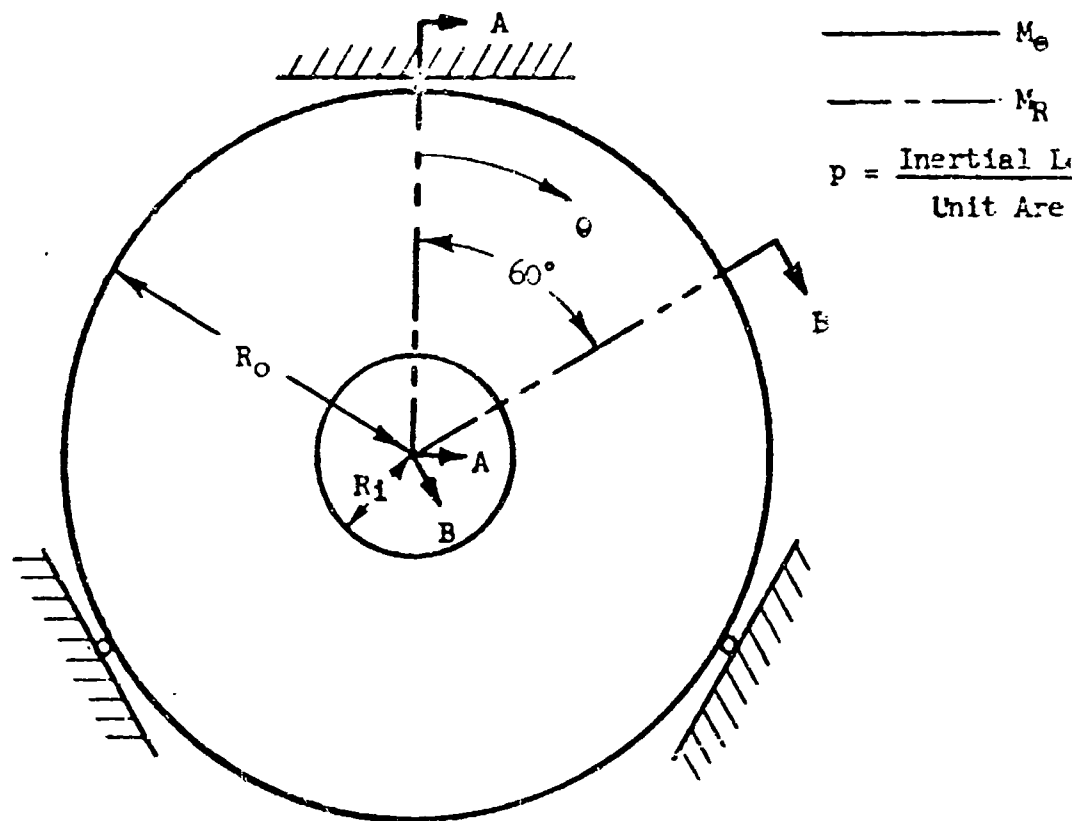
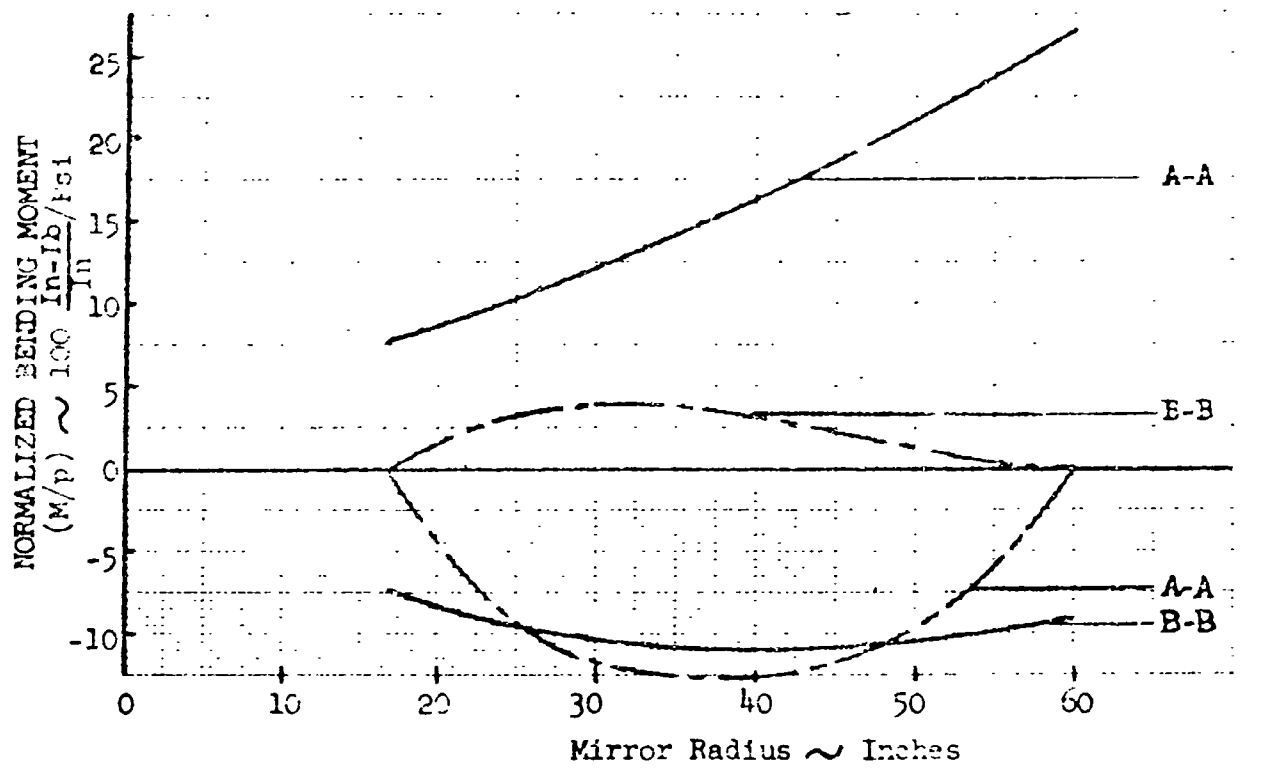


Figure 5.3-19

Mirror Operational Bending Moments .

5.3.2.4 Gimbal Design

A mode has been studied which combines features of the floating socket (IIB) and the gimbal (IP). In this concept, a soft spring suspension, as shown in Figure 5.3-20, was introduced between MORL and MOT which performs four functions. It serves to:

- 1) Attenuate high frequency components of disturbances such that a 3 cps control system is adequate.
- 2) Reduce the total level of force transmission.
- 3) Provide means to transmit the very low frequency orbital forces required to position MORL relative to MOT.
- 4) Provide positive location of the MOT so that it can be reattached to MORL for servicing and man transfer.

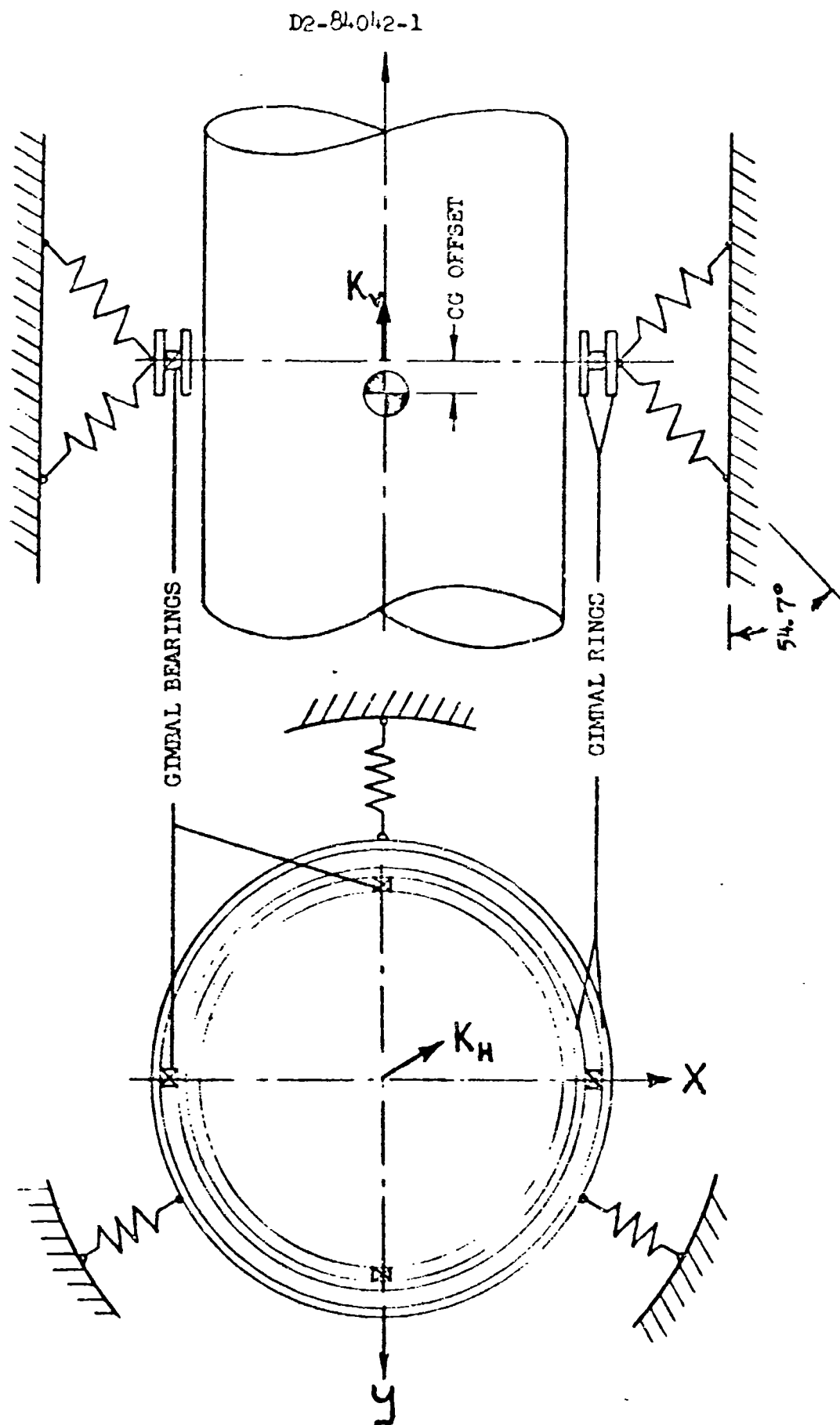
Study indicated a requirement for a gimbal between the spring suspension and the MOT to minimize the coupling of translational forces with torque inputs.

Design Criteria - The MOT design used in the gimbal concept is the same configuration used for Mode IIIC with the exception that it does not have solar panels for electrical power. The concept utilizes a two-axis gimbal located at the CG of the MOT and the outer gimbal ring is mounted in a spring suspension system that provides a soft spring rate for six degrees of freedom. The spring suspension system is mounted on an open frame truss-type structure which is permanently attached to the MORL. The design of the spring suspension system is schematically shown in Figure 5.3-20.

The design feasibility is based on the following data:

- o The allowable moment input to the MOT by the gimbal and spring suspension system is one inch-pound. This value is compatible with the control system used in MODE IIIC.
- o Gimbal and spring design torque allocation of 0.25 in-lb for bearing friction, 0.25 in-lb for electrical cable torque, and 0.50 in-lb for spring force x CG offset, giving a total of 1.00 in-lb.
- o The maximum MOT CG offset from the gimbal axis is 1.0 inch. The maximum spring force is therefore limited to 0.5 pounds. The one-inch CG travel is based on limiting the change in expendables on a 20-foot arm to 100 pounds or a shift of a 400-pound mass 70 inches.
- o The maximum displacement of the MORL and truss structure relative to the gimbal attachment point is ± 5.90 inches along the X and Y axes of MOT and ± 1.2 inches along the Z axis. The maximum angular attitude difference between the MORL and the MOT is 0.5 degrees. The 0.5 degrees is taken to be the control accuracy of the MORL.
- o Maximum lateral and longitudinal forces tending to separate the MORL and

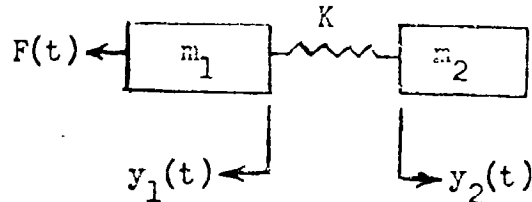
Figure 5.3-20
Soft Gimbal Suspension Schematic



MOT at the location of the spring suspension due to aerodynamic or gravity gradient forces are 0.071 pounds.

- c The maximum angular displacement in roll about the Z axis is ± 0.5 degrees.

Dynamic Analysis - The free motion of the system shown below was investigated.



Time did not permit an analysis with two degrees of freedom, so only the translational motion was considered. With the low coupling present, this assumption is realistic. The fundamental solution to the equation of motion (response to an impulsive forcing function $F(t) = I(o)$) was determined. It is:

$$S(t) = y_1(t) + y_2(t) = \frac{I}{m_1 \omega_n} e^{-\frac{\delta}{2} t} \sin \omega_n t$$

where: $y_1(t)$ = motion of MDRL

$y_2(t)$ = motion of MOT

I = impulse of disturbance

m_1 = mass of MDRL

m_2 = mass of MOT

$\omega_n = \sqrt{\sigma - \delta^2/4}$ = natural frequency

$\sigma = K/m'$

$\delta = \beta/m'$

K = spring constant

β = damping

$m' = m_1 m_2 / m_1 + m_2$

t = time

The corresponding expression for force transmission is:

$$F = I \sqrt{\sigma} \frac{m_1}{m_1} e^{-c/2 t'} \left[c \cos \sqrt{1-c^2/4} t' \right] \\ + \frac{1-c^2/2}{\sqrt{1-c^2/4}} \sin \sqrt{1-c^2/4} t'$$

where $c = \text{damping ratio} = \beta / \sqrt{k/m_1}$ ($c = 2$ for critical)
 $t' = \omega_n t / \sqrt{1-c^2/4}$

The force expression minimizes for $c = 0.55$.

Real Values of F(t) - To determine the vibration isolation characteristic of the system, transmissibilities were calculated. Transmissibility for the system shown is given by:

$$T = \frac{\sqrt{1 + (c \frac{\omega}{\omega_m})^2}}{\sqrt{\left[1 - (\frac{\omega}{\omega_m})^2\right]^2 + (c \frac{\omega}{\omega_m})^2}}$$

where: $\omega = \text{frequency of forcing function}$

$\omega_m = \text{natural frequency of MOT} = \sqrt{\frac{K}{m_2}}$

$T = \text{ratio of MOT to MORL displacement at the MOT CG}$

Transmissibility of the system is plotted in Figure 5.3-21 for $c = 0$ and $c = 0.55$ as a function of frequency ratio.

The direct analog dynamic simulation of MOT primary structure was utilized to establish the vibration environment of critical system components. By driving the telescope with normalized forcing functions at the CG position and performing a frequency sweep, the structural vibration transmission characteristics of the MOT structure were found. The results for critical elements are plotted in Figure 5.3-22. The response in deflection per unit force is plotted as a function of frequency.

Knowing the magnitude of vibrational disturbances arising in the MORL, the vibrational characteristics of critical elements in the MOT can be found by applying this data in conjunction with the transmissibility of the spring-gimbal system.

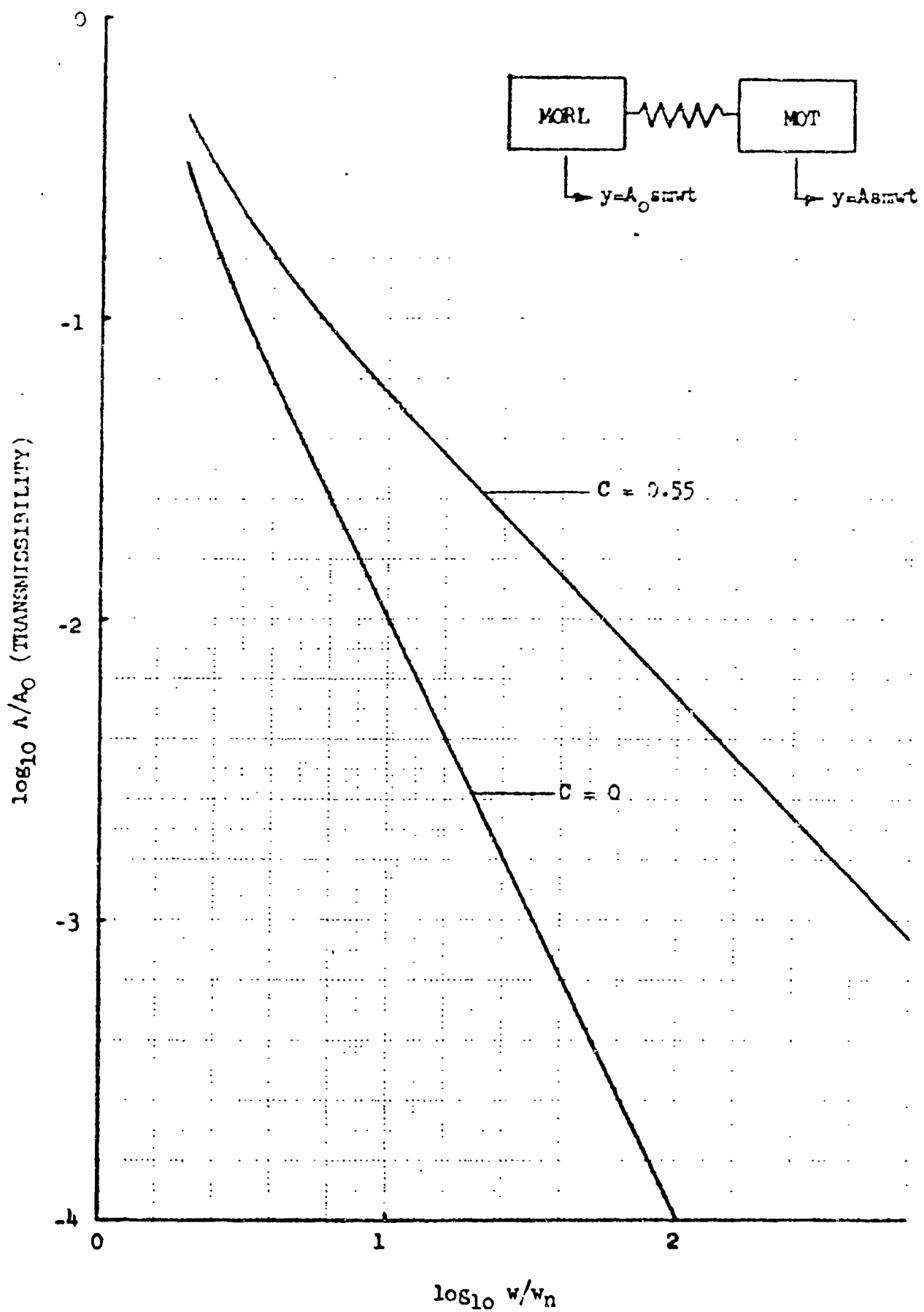


Figure 5.3-21

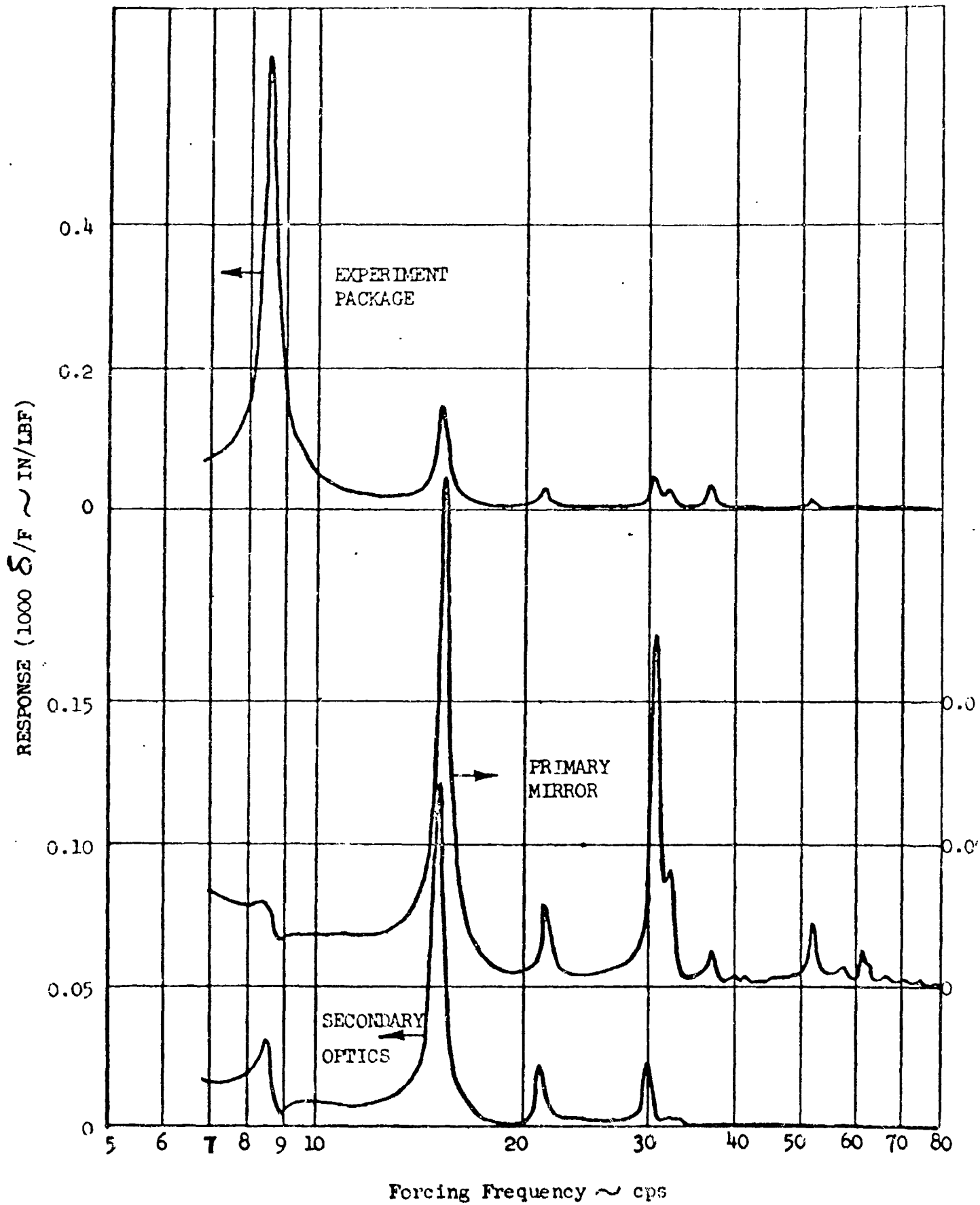
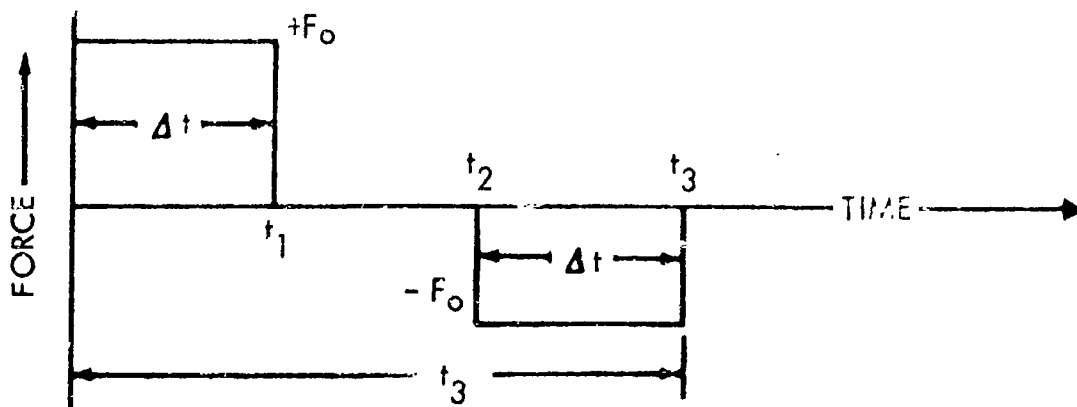


Figure 5.3-22

Optical Element Response
200

Man's Disturbance - The man disturbance used for evaluation has the characteristics shown below.



System response is evaluated by applying a superposition integral to the fundamental solution

$$y(t) = \int_0^{t_n} S(t-\tau) F(\tau) d\tau$$

where: $F(t) = +F_0 \quad 0 \leq t \leq t_1$

$= -F_0 \quad t_2 \leq t \leq t_3$

$t_n = t \quad 0 \leq t \leq t_1$

$t_n = t_1 = \Delta t = 0.5 \text{ seconds} \quad t_1 \leq t \leq t_2$

$t_n = t \quad t_2 \leq t \leq t_3$

$t_n = t_3 = 2.5 \text{ seconds} \quad t_3 \leq t$

Thus, four integrals were evaluated. For simplicity, only the case $c = 0$ is discussed.

The force transmitted to the MOT is given by:

$$F = K y(t)$$

But, since

$$\sigma = K/m^1$$

Then

$$F = m^1 \sigma y(t)$$

Based on the values:

$$m_1 = 1770 \text{ slugs}$$

$$m_2 = 775 \text{ slugs}$$

$$F_0 = 60 \text{ lbf}$$

$$m' = 539 \text{ slugs}$$

the peak forces for various suspension system frequencies are shown in the following table.

$\omega_n \sim \text{CPS}$	$F_{\max} \sim \text{Lbf}$
0.01	0.072
0.03	0.664
0.10	5.234

This variation is plotted in Figure 5.3-23.

Figure 5.3-23 demonstrates the desirability of low suspension system natural frequencies. If, for example, torque induced by man disturbance forces acting on a one-inch offset of the gimbal axis from the MCT CG is to be kept below 0.032 inch-pound, the natural frequency of the suspension system must be lower than 0.0060 cps. This dictates a system spring constant along any axis of 0.0847 pounds per inch.

MORI Oscillation - The characteristics of the MORI control system were assumed to be such that MORI will have an angular uncertainty of ± 0.5 degrees. This motion produces a driving function given by:

$$y = y_0 \sin \omega t$$

where: y_0 = deflection of spring supports induced by 0.5 degree rotation of MORI
 $= 4.695 \text{ inches}$

It was assumed that:

$$\omega = 1 \text{ cps} = 2 \pi \text{ rad/sec}$$

The ratio of spring force to static spring force, in other words the attenuation, is given by:

$$\frac{F}{F_0} = \frac{\frac{\omega^2 m_2}{K}}{\frac{\omega^2 m_2}{K} - 1}$$

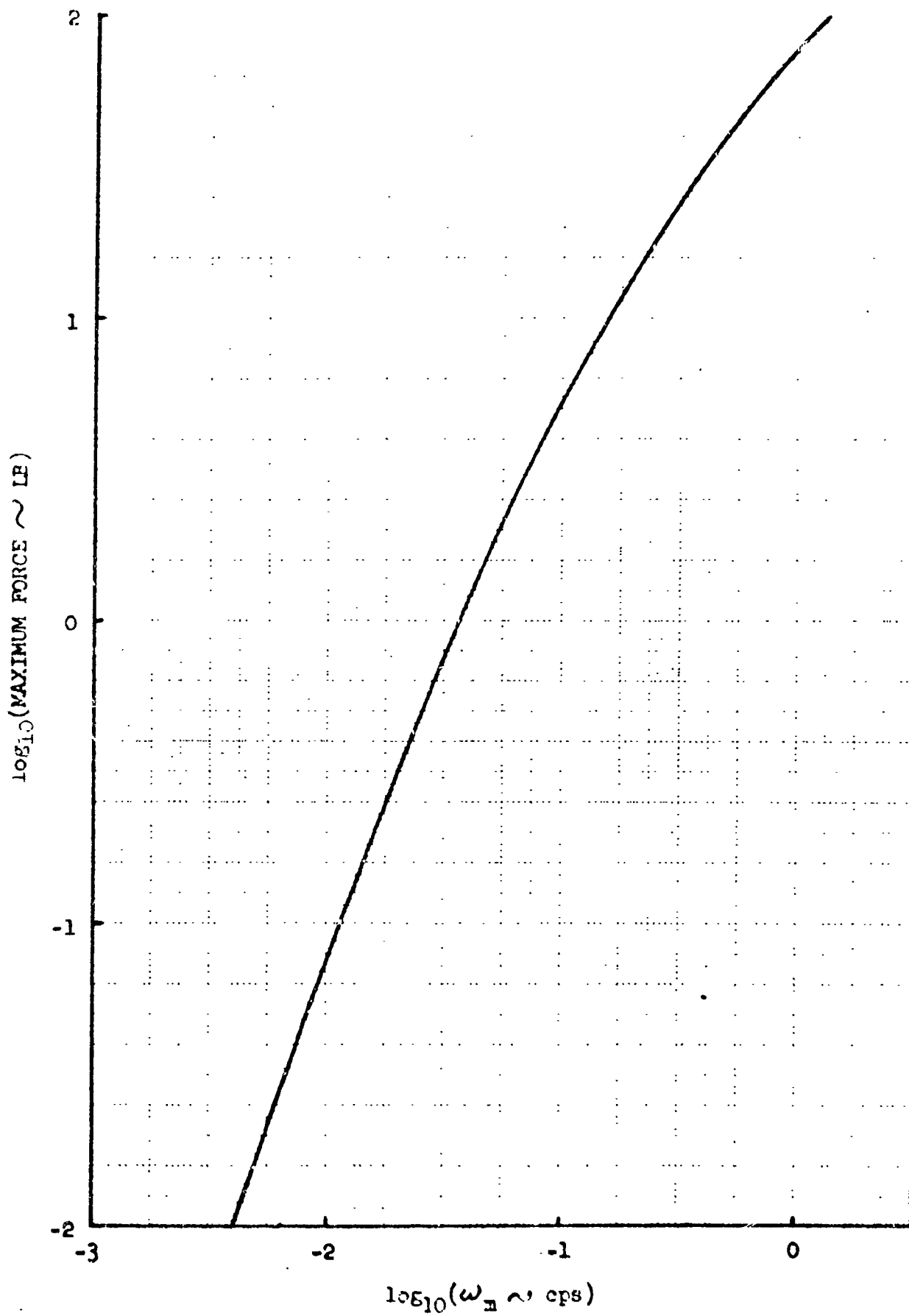


Figure 5.3-23

Transmitted Force Due to Man's Disturbance

For $\omega = 2\pi$ rad/sec,

$$\frac{F}{F_0} \approx 1 \quad \left(\frac{\omega^2 m_2}{K} \gg 1 \right)$$

Thus, the force induced by MORL rotations is unattenuated by the suspension system.

Combined Loads - The worst case of torque inputs to the MCT arises for orbital forces superimposed upon the man's disturbance and the MORL oscillation. For $K = 0.0847$ pounds per inch, the man's disturbance contributes 0.032 pounds of spring force and MORL oscillation produces

$$\begin{aligned} F_{\text{MORL}} &= K\delta = 0.0847(4.7) \\ &= 0.398 \text{ pounds} \end{aligned}$$

To these forces were added 0.001 pound for aerodynamic forces and 0.020 pounds for gravity gradient effects. Assuming a one-inch CG offset, the result is a torque of 0.50 inch pounds due to relative translations of the MORL spring supports and the MCT gimbal rings. This torque is applied at a mixture of frequencies from the orbital frequency for aerodynamic forces to the "frequency" which characterizes MORL oscillations.

Spring Geometry - For the spring layout shown in Figure 5.3-20, the vertical spring constant is

$$K_V = 6K \cos^2 \theta_0$$

where

K = stiffness of individual spring

The horizontal spring constant is

$$K_H = 3K \sin^2 \theta_0$$

For these to be equal,

$$\tan^2 \theta_0 = 2$$

or

$$\theta_0 = 54.7^\circ$$

If an effective spring constant of K_e is desired, the individual springs must have stiffness

$$K = \frac{K_e}{3 \sin^2 \theta_0}$$

For $K_s = 0.0247$ in/in, $\theta_0 = 54.7$ degrees

$$K = \frac{0.0247}{3(0.81647)^2} = 0.0424 \text{ lb/in}$$

The equation for designing coil springs with round wire is

$$K = \frac{G d^4}{64 R^3 n}$$

where: K = spring constant = 0.0424 lb/in

G = shear modulus

d = wire diameter

R = coil radius = 1 inch

n = number of active coils = 128

For aluminum springs, $G = 3.95 \times 10^6$ psi. The resulting wire diameter required is 0.097 inches. The solid height of these springs is 12.4 inches. For the maximum force condition, $F = 0.5$ pounds, the MOT translates 5.90 inches. Initial spring length is found by equating the solid height to the compressed spring length

$\sqrt{L^2 + (5.90)^2} - 2(5.90) L \sin \theta_0$, where L is the quantity sought. The result is

$$L = 16.7 \text{ inches}$$

These springs present no difficulties in fabrication or installation.

Because the suspension system geometry changes with stroke, the effective spring constants will vary. This effect is shown in Figure 5.3-24 for lateral and longitudinal motion. The effect of spring windup with roll displacements is to cause roll stiffness to develop. The resulting roll stiffness, K_R , is shown as a function of roll angle in Figure 5.3-24. It should be noted that spring constants, K_H and K_V , are shown normalized to their zero-displacement values.

The effects of geometric variations of spring constants on torque inputs to the MOT have not been included in the analysis. Their consideration would require a reduction of the 0.0424 pounds per inch baseline spring constant, because of nonlinearities and the presence of roll stiffness.

5.3.3 Thermal Distortion Analysis

One of the major problems associated with an orbital optical system is the variation of structural geometries due to temperature changes. Since no structural materials are available which possess absolute thermal stability (zero coefficient

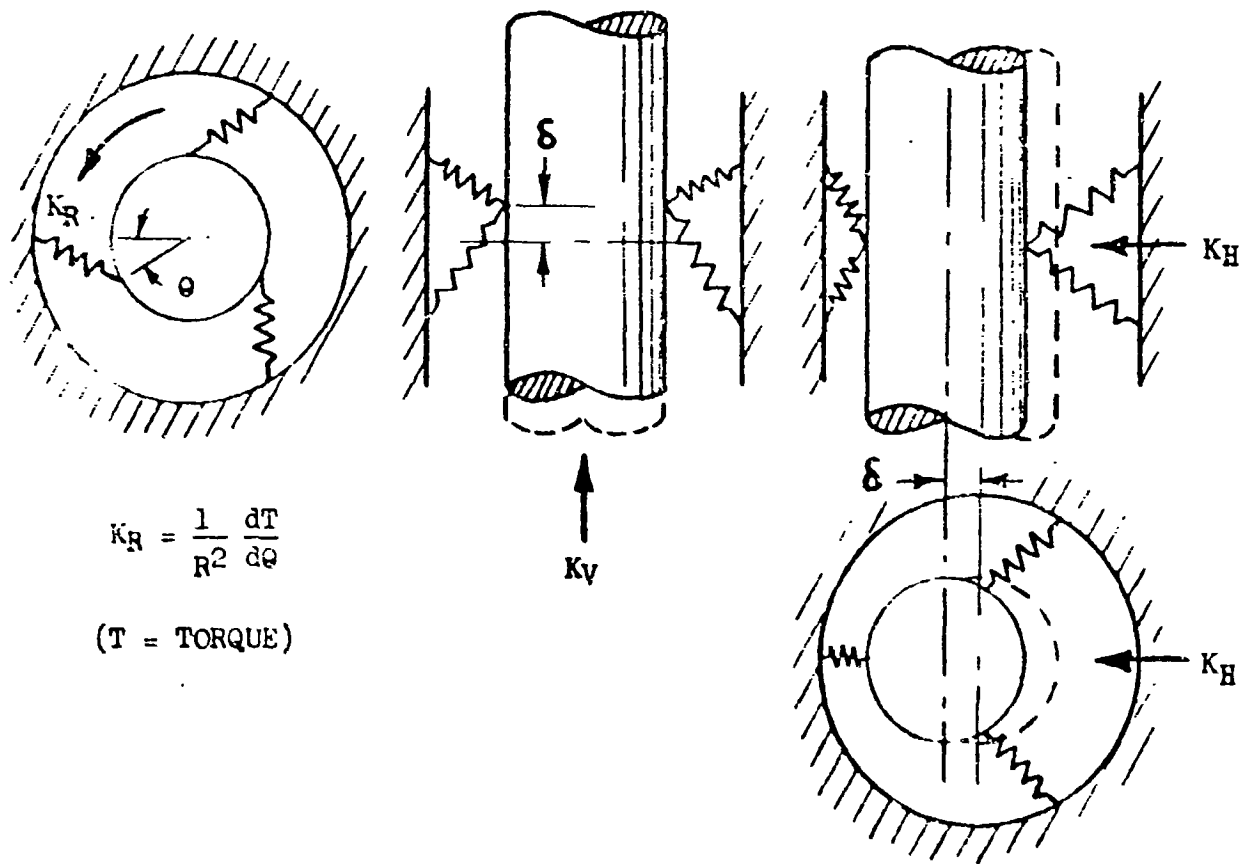
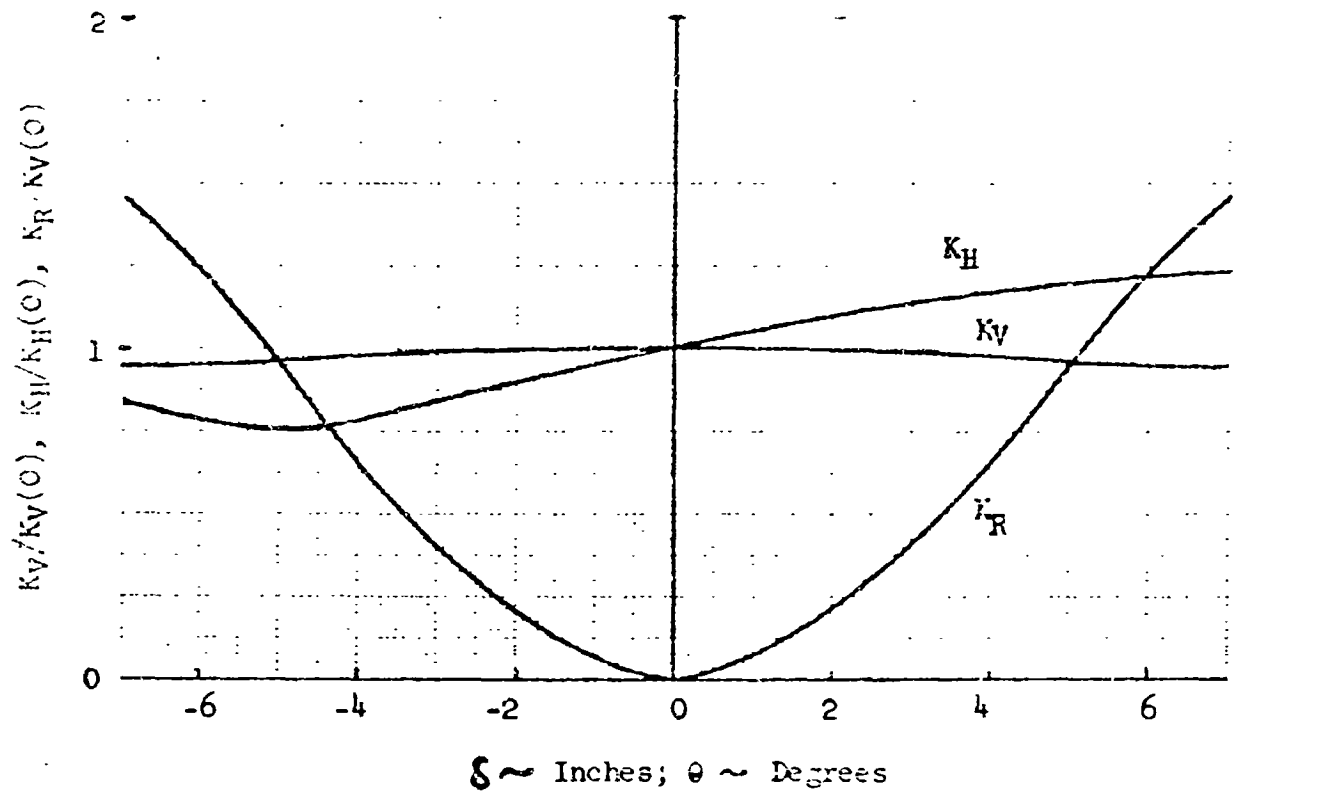


Figure 5.3-24

of linear expansion), the approach taken in MIT studies was to stabilize the thermal environment of critical components as much as possible and to design structures which would be affected as little as possible by the remaining temperature gradients.

Secondary Mirror Support - The structure connecting primary and secondary optical surfaces was found to be relatively critical. The tolerances which were applied are presented in Section 3.4.3.

Three structural concepts for secondary mirror support were studied. These include: a semi-monocoque cylinder, a three-tube linear support, and a six-bar determinate truss. The materials considered include 2029 aluminum and 5Al-2.5Sn titanium. The concepts and the appropriate materials are presented in Figure 5.3-25.

Analysis comparing these concepts was performed to determine the critical temperature gradient required to produce the permissible misalignment of secondary mirrors. A temperature gradient linear across the diameter was assumed. The allowable gradient is shown for the various concepts as a function of baseline operating temperature in Figure 5.3-25. Lateral misalignment was found to be critical for all concepts except the three-tube support, which is critical in tilt.

The final thermal data, Section 5.5, indicates that secondary alignment tolerances are exceeded by the baseline design. However, it is practical to hold the secondary mirrors within tolerance by making the inner tube of titanium, or by using the automated control system (Section 5.2.5.3).

Primary Mirror - Thermal distortions of the primary mirror were determined through the use of the Boeing-developed COSMOS machine program. This is a stiffness-method approach to structural analysis which is capable of computing thermal distortions in complex structures. The structural idealization applied in primary mirror analysis is shown in Figure 5.3-26. It consists of many triangular plate elements joined at nodes.

Temperatures were taken from the thermal analysis, Section 5, and interpolated to provide a temperature input for each node. The temperature case, for which data is presented, is shown in Figure 5.3-27. This is the case in which the primary mirror continuously views space and is the case which produces the least severe temperature gradients. Figures 5.3-28 and 5.3-29 show the other two temperature cases analyzed. It was assumed in the analysis that the mirror had been figured to $f/4$ at -54.9°F .

Distortions of the mirror reflecting surface for the continuous-viewing case are shown in Figure 5.3-30. To evaluate the consequence of these distortions in terms of optical performance, a least-squares paraboloid was fit to the data and the rms deviation evaluated. This paraboloid, represented by the equation

$$z = bx^2 - a$$

where $b = 0.520830766 \times 10^{-3} \text{ 1/in}^2$
 $a = 0.148754312 \text{ in}$

Figure 5.3-25
Secondary Support System Comparison

SUPPORT CONCEPT

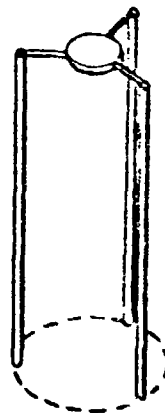
MATERIAL

PERMISSIBLE GRADIENT



① CYLINDER

T1 & Al



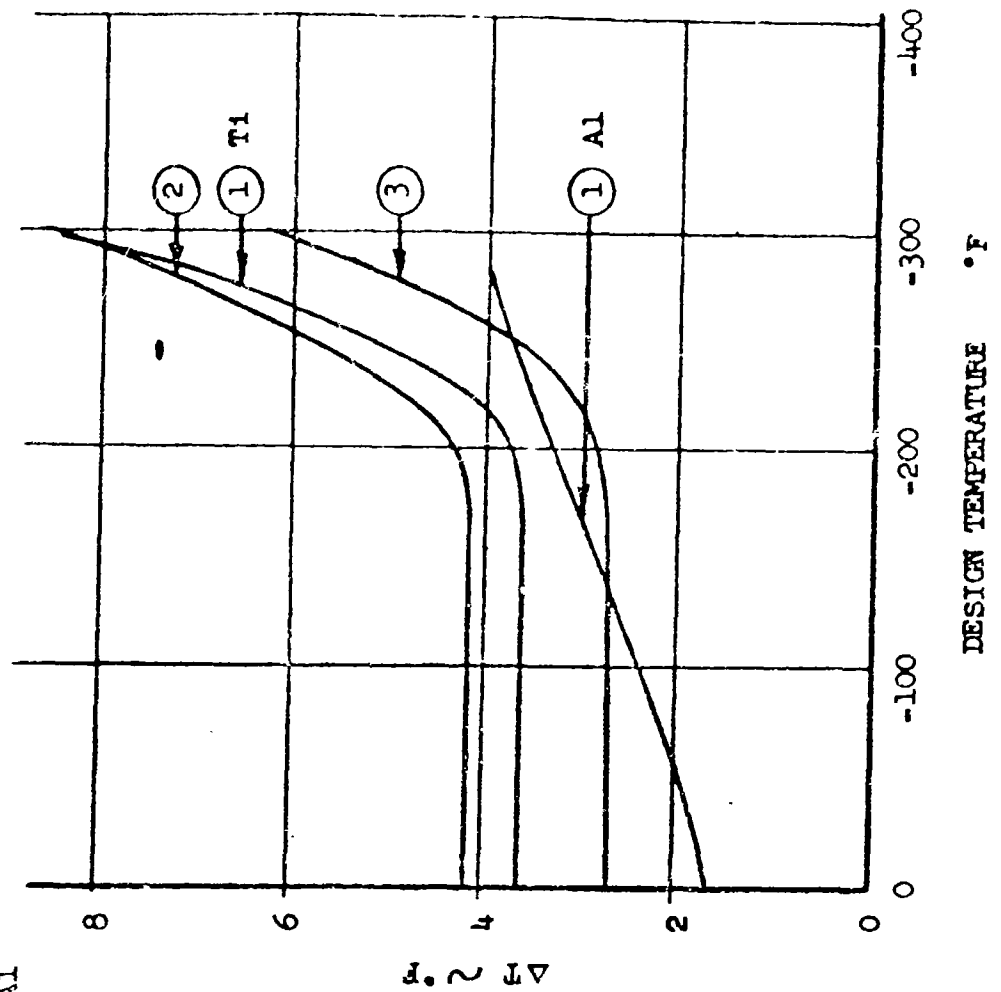
② THREE TUBE

T1



③ SIX BAR TRUSS

T1



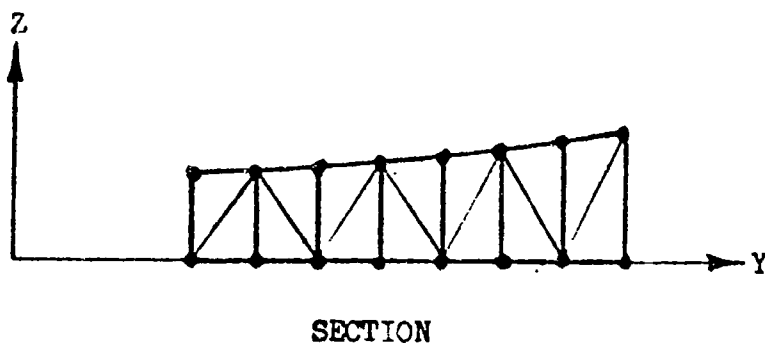
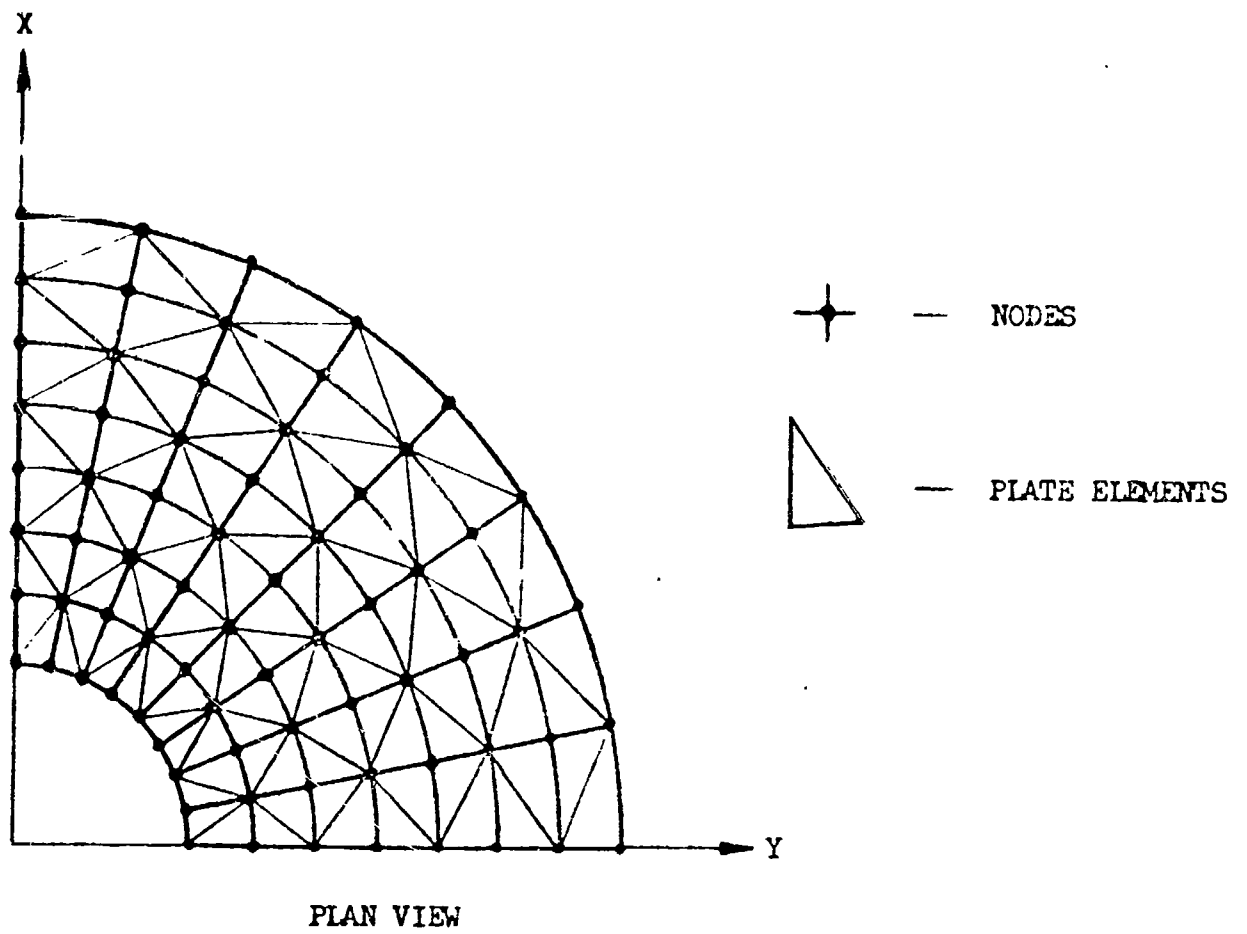


Figure 5.3-26

Primary Mirror Thermal Distortion Idealization

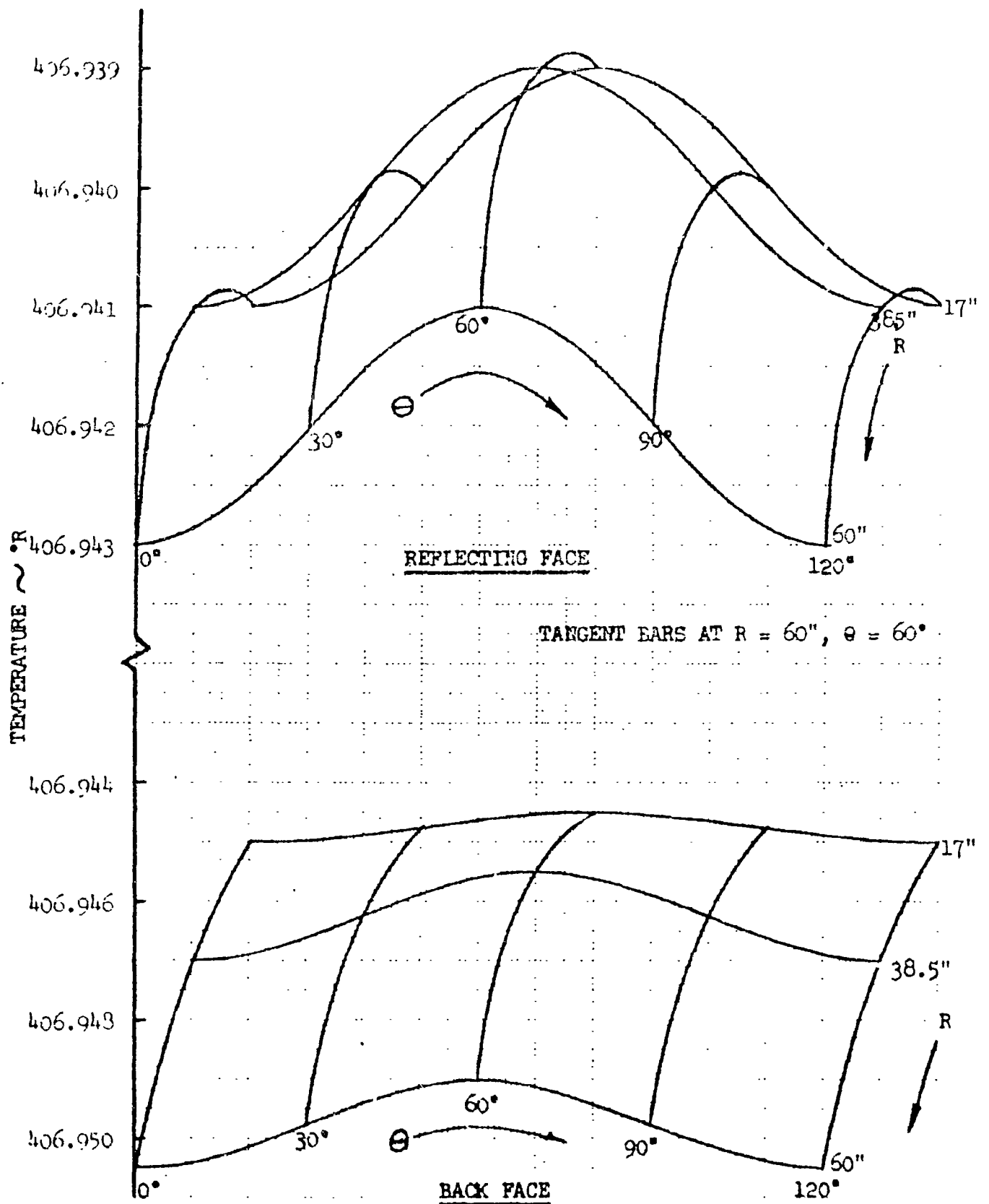


Figure 5.3-27

Mirror Temperature Distribution
Continuous Space Viewing
210

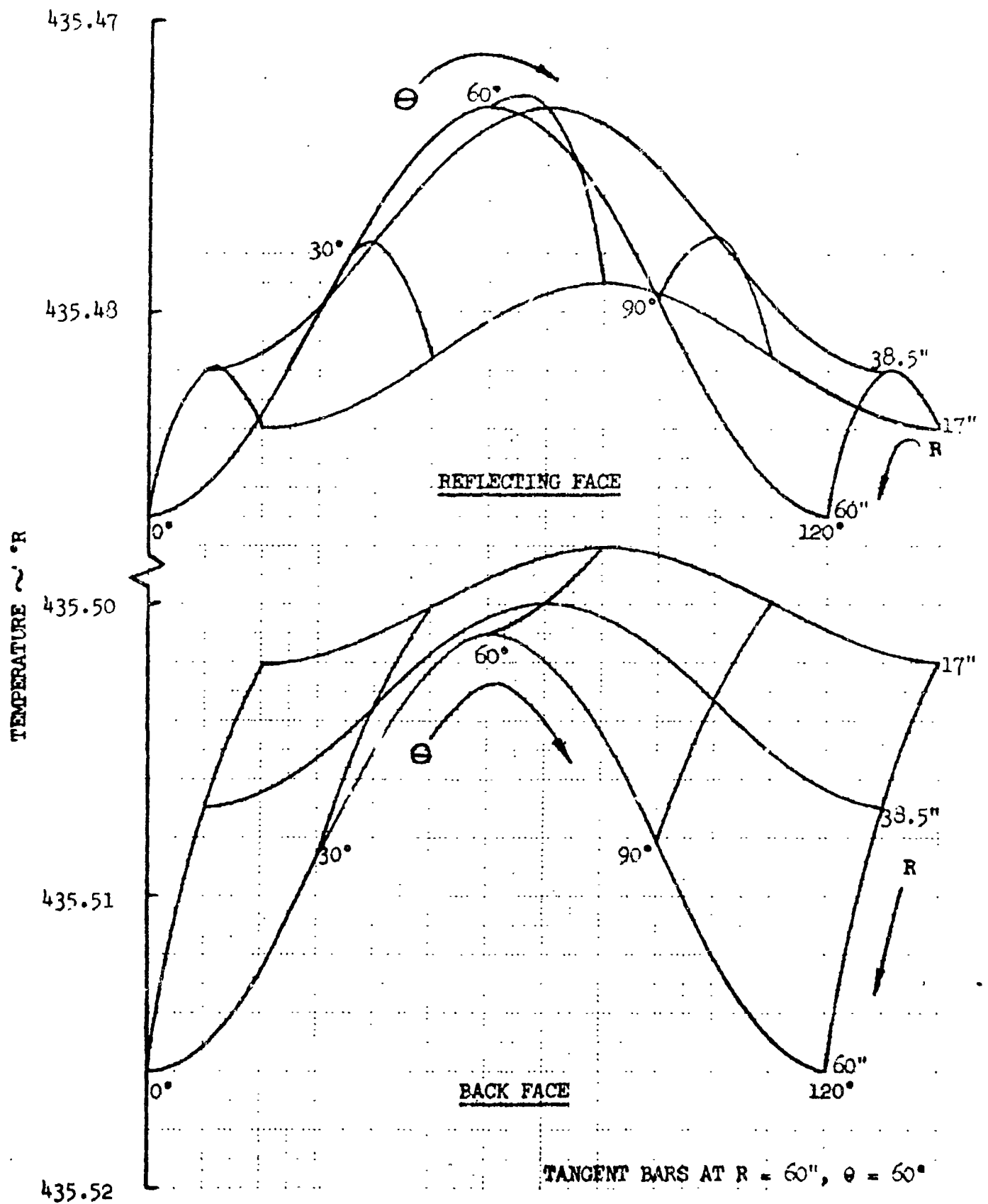


Figure 5.3-28

Mirror Temperature Distribution - Transient Case

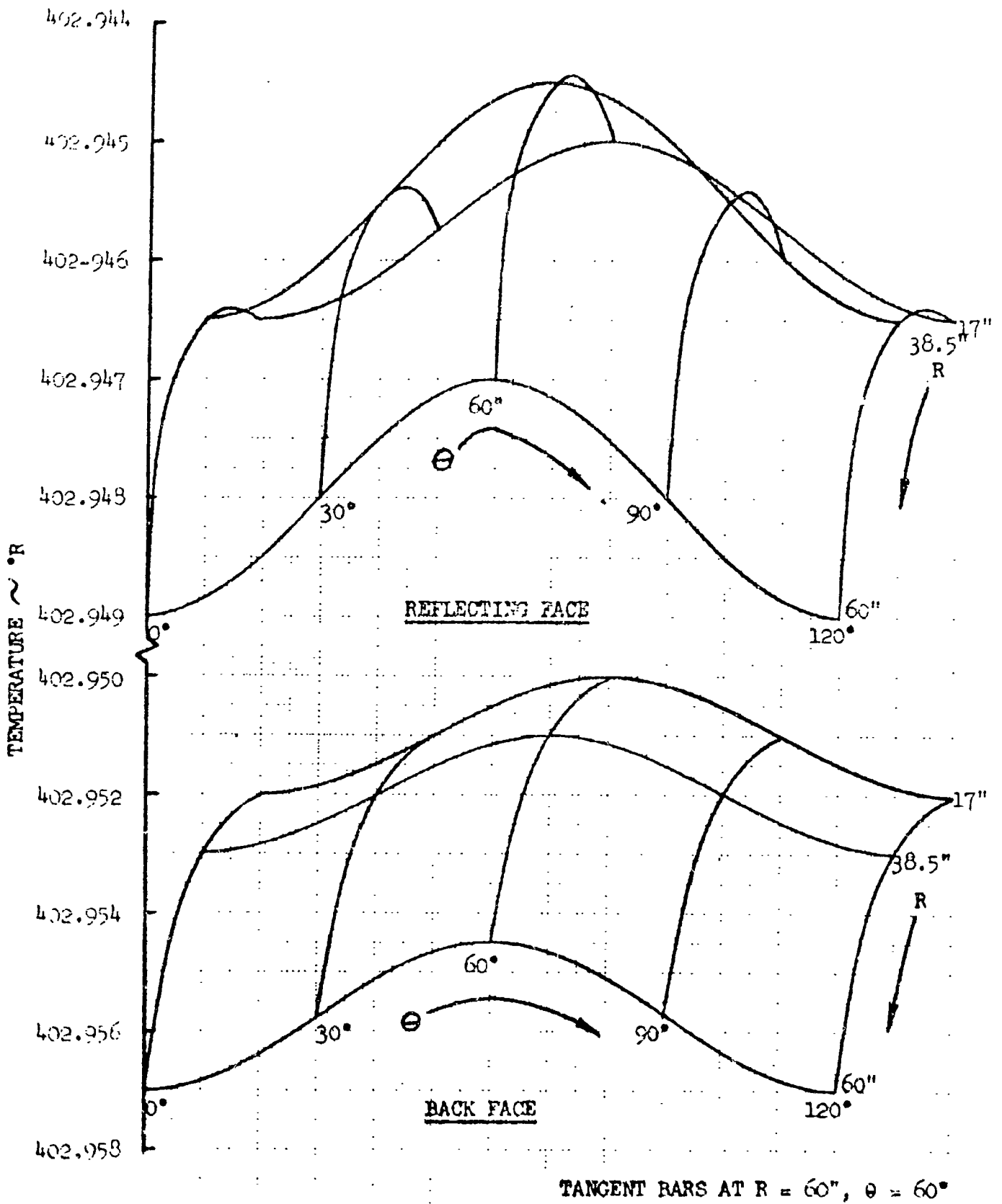


Figure 5.3-29

Mirror Temperature Distribution - Doors Closed

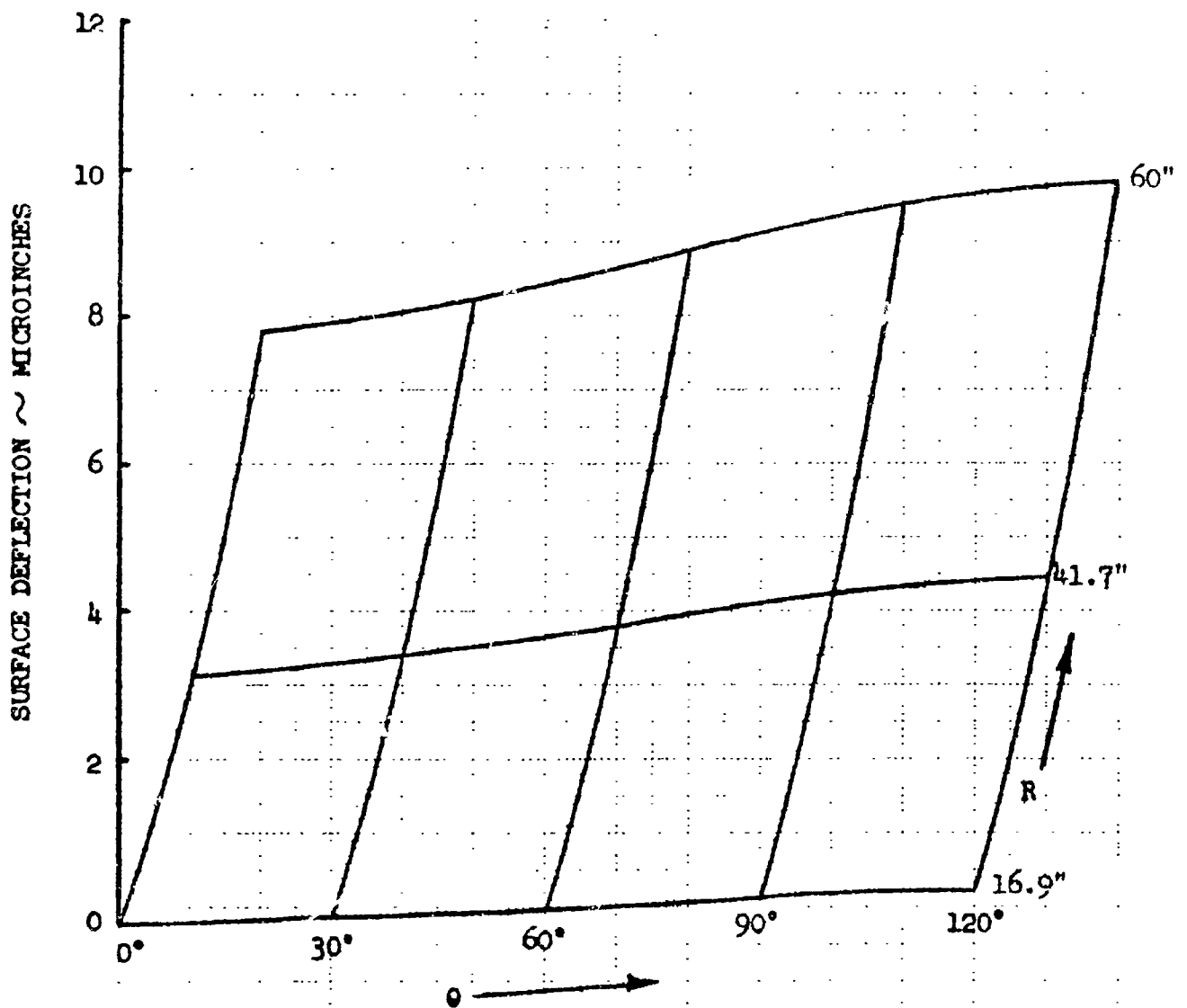


Figure 5.3-30

Mirror Thermal Distortions
Continuous Viewing Case
213

represents an increase in focal length of 0.00046 inch and change in position of the mirror surface of 0.00077 microinches. The resulting rms deviation is 0.042 microinches. For 5000 Å, this corresponds to a $\lambda/30.3$ mirror.

The deviation is large, despite the very small temperature gradients, because of the presence of circumferential gradients which force the mirror to depart from axial symmetry. Thus, entire angular zones of the mirror 20-40 degrees wide deviate as much as 1 microinch from perfect figure. The circumferential gradients appear to arise from tangent bar heat leaks. These heat leaks can be eliminated by improving the thermal isolation of the tangent bars or by actively controlling their attach point temperatures.

Theoretical analysis showed that, for an isotropic material, a bulk change in mirror temperature produces no distortion of parabolic mirror figure. However, a focal length change given by

$$\Delta f = f \alpha \Delta T$$

where f = focal length

α = coefficient of linear thermal expansion

ΔT = (Figuring temperature minus operating temperature)

results. This effect is shown in Figure 5.3-31. The change in focal length is shown as a function of the operating temperature for a mirror figured at 70°F. The thermal analysis shows the extreme of mirror operating temperature to be -54.9°F, which is reached for a continuous viewing of space. As can be seen from the figure, this produces a focal length change of 0.368 inch.

5.3.4 Meteoroids and Radiation

5.3.4.1 Meteoroids

Meteoroids present two problems in telescope design. First, since the primary mirror must view space directly, it cannot be shielded from meteoroid impacts, and particles of all sizes will cause damage. Second, meteoroids which impact and penetrate the telescope walls produce secondary fragments which can impinge upon the primary mirror.

Direct Damage - To compute direct damage to the primary mirror it is necessary to evaluate the damage from each increment of meteoroid mass and integrate over the mass range. The following assumptions were made in performing these calculations:

- 1) Flux is given by $\phi = 10^{-10.423} m^{-1.34}$ (ϕ in number/ft² day, m in grams)
- 2) Minimum meteoroid mass is 10^{-12} gm due to the sweeping effect of solar radiation pressure
- 3) An impact results in a hemispherical crater with depth given by the Summers & Charters equation, $d/D = 2.28 \left(\frac{\rho_p}{\rho_t} \right)^{2/3} (V/C)^{2/3}$, where D is meteoroid

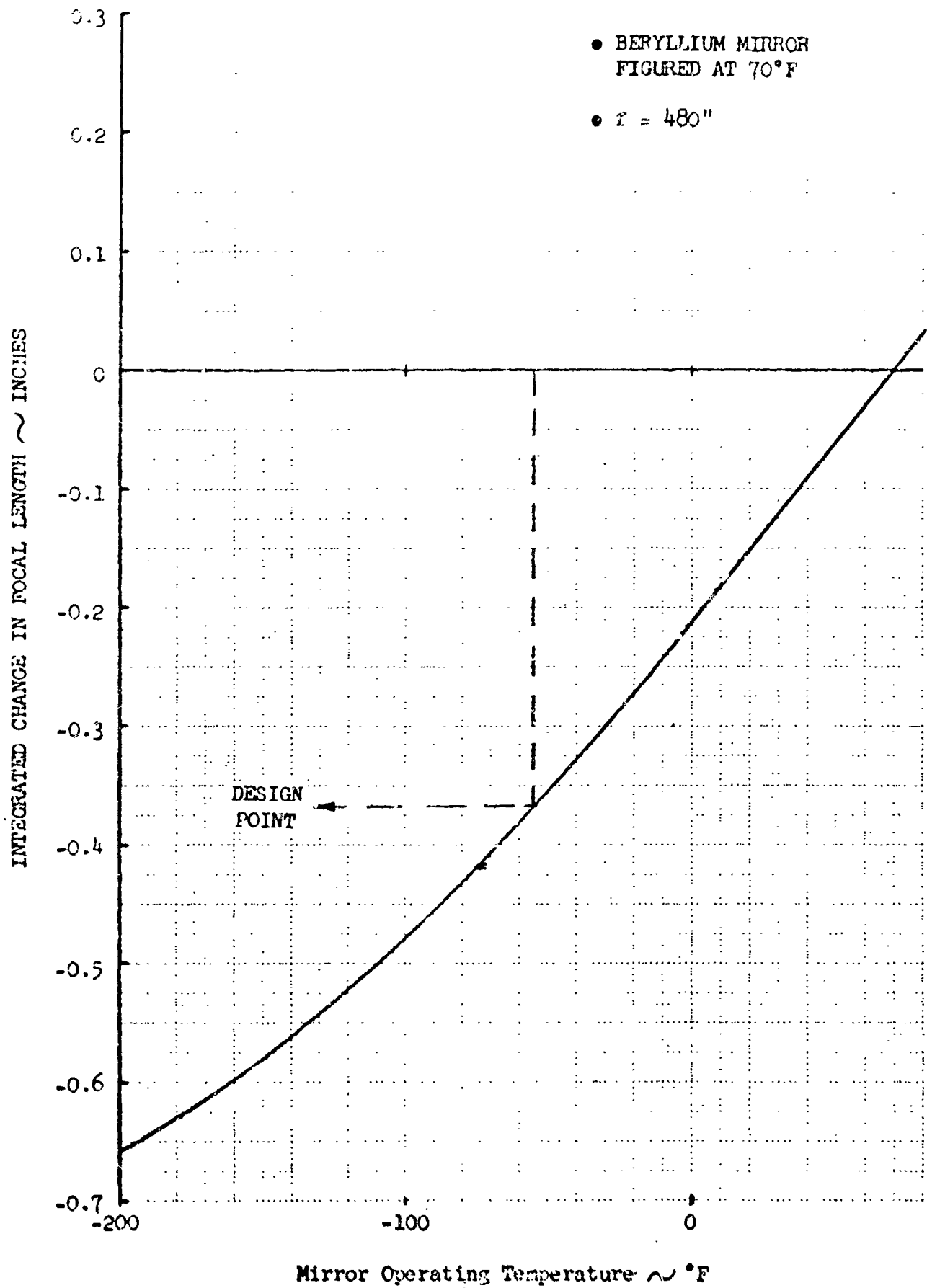


Figure 5.3-31

diameter, e , its density, e_t , the density of target, and V/C the ratio of meteoroid velocity to target far speed of sound ($\sqrt{e/e_t}$)

4) $e_p = 0.5 \text{ gm/cc,}$

$e_t = 8.9 \text{ gm/cc (Xanigen),}$

$C = 15,810 \text{ fps,}$

$V = \text{Whipple distribution}$

5) Average view factor for mirror surface is 0.16

6) During meteoroid showers, shower radiants are avoided. Shower flux is thus ignored

7) Mirror is exposed to space 40 percent of the total time in space.

The results of the integration are shown in Figure 5.3-32. In three years, 5.3 in² of the mirror have been destroyed. To reach the limit of 1.75 percent of the surface destroyed, the limit specified in the Fecker report, 101 years are required.

Secondary Damage - Damage produced by penetration residue cannot be predicted as such. Data is not available to support such a calculation, since little is known about the velocity or the nature of secondary fragmentation. It was considered sufficient for this study to compute the probability that no meteoroids will penetrate in such a fashion as to damage the primary mirror.

The work of Lundberg at Boeing was used to predict the size of meteoroid required to penetrate a specified wall configuration. For these calculations, shower flux was included, as was a correction for blockage of flux by the Earth. Tests have shown that, for all but the most glancing impacts, the resulting spray is included in a cone with a 45 degree half-angle having its axis normal to the penetrated wall. Therefore, it was assumed that only the first 140 inches of the tube wall is important to primary mirror damage.

The baseline wall geometry was evaluated, as were parametric variations of the honeycomb face sheet gage. Wall spacing, honeycomb depth, and insulation thickness were held constant. The results of the study are shown in Figure 5.3-33. The probability of no meteoroids penetrating in the sensitive area of the tube is shown as a function of honeycomb face gage. The baseline configuration, with 0.01-inch walls, has a probability of no penetrations of 0.947 for an exposure time of three years.

5.3.4.2 The Radiation Environment

The radiation environment encountered by the MCF space system includes geomagnetically trapped radiation (Van Allen Belts, Argus and Starfish radiation) and untrapped radiation (galactic cosmic radiation and solar particle event radiation). The flux, fluence (time integrated flux), and particle nature encountered in a given mission depends upon the mission parameters, i.e.,

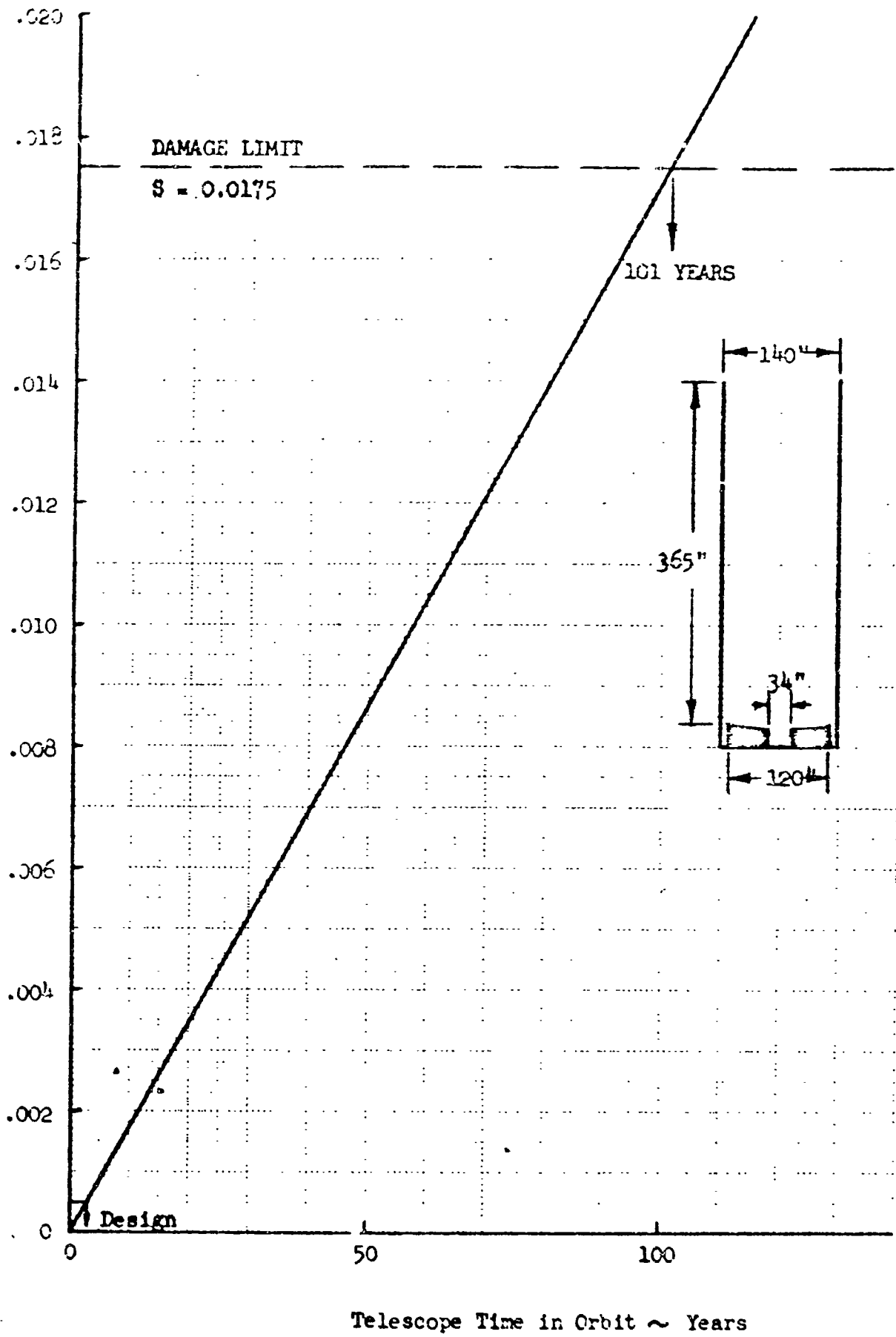


Figure 5.3-32

Direct Meteoroid Damage To Primary

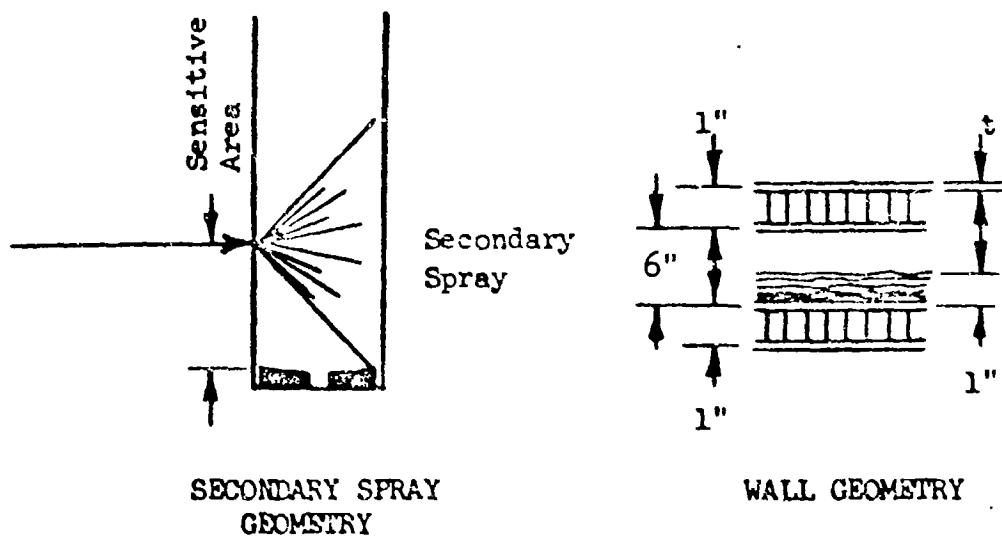
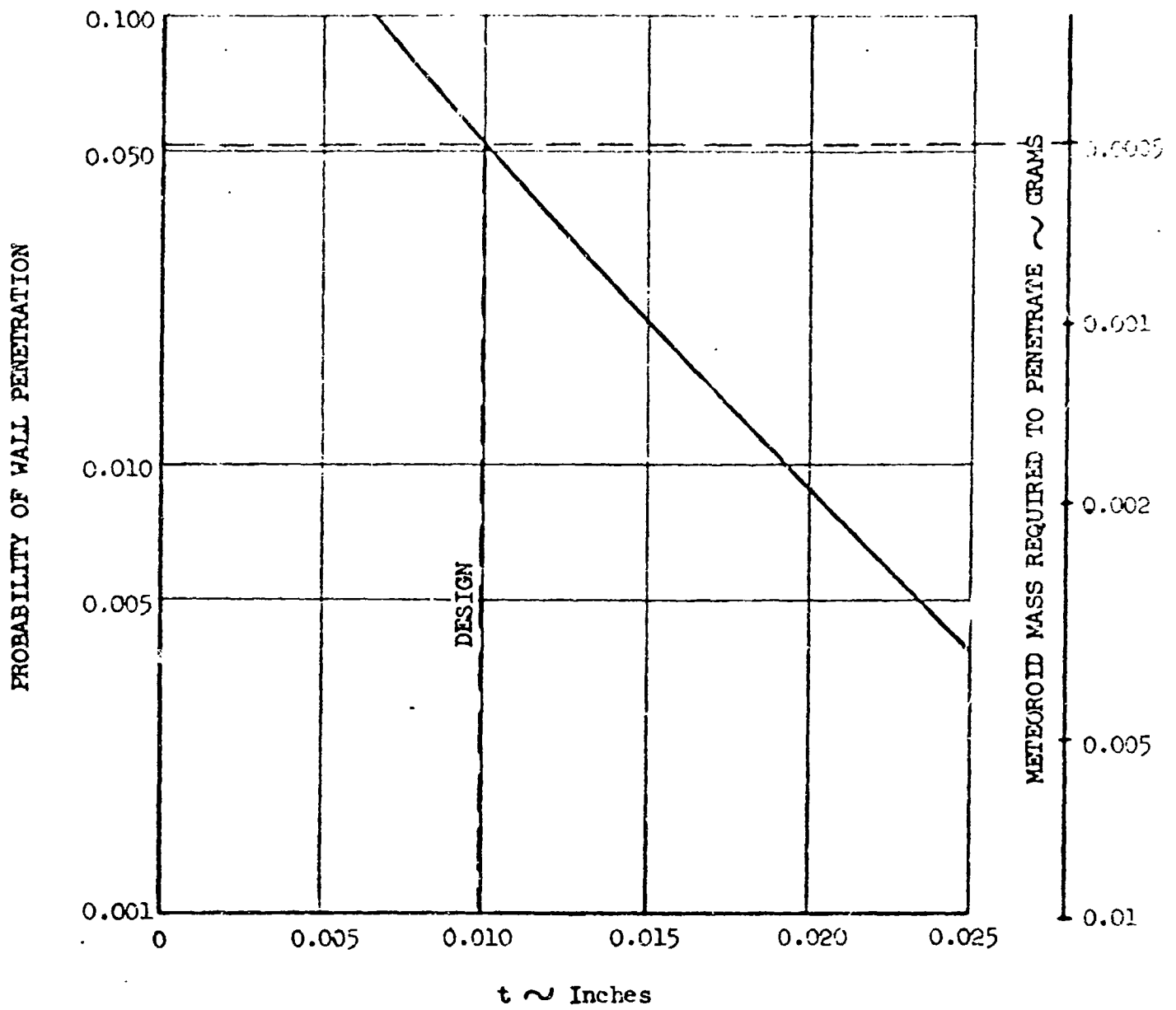


Figure 5.3-33

Indirect Meteoroid Damage to Primary

orbital altitude, inclination, eccentricity, and duration. A brief discussion of the model environments used to determine the radiation doses for the KILLNET missions follows.

Geomagnetically Trapped Radiation - The electron environment is provided by the electron grid compiled by Dr. James Vette of Aerospace Corporation. The proton environment is given by three grids; the MET & LEP compiled by Dr. Vette, and the P 1 compiled by Dr. Wilmet Hess of NASA Goddard. These grids are presented in Barton's report. The Aerospace grids are the best for the period extending up through 1966. To explain why this is so, the protons and electrons are discussed separately.

The flux of protons at low altitudes depends upon the solar activity. When the sun is active the atmosphere is heated and expands outward to increase the probability of scattering loss of the trapped particles. Hence the flux at low altitudes is greater from 1963 to 1967 than it could be from 1967 to 1972. The data compiled by Vette included the aerospace low altitude data of 1962 and hence reflects these increased fluxes.

The same argument would apply for the electrons were it not for the Starfish experiment in July 1962, which populated the inner belt with penetrating electrons. The remains of this belt of electrons are decaying principally by the scattering mechanism. Comparison at low altitudes between the Vette electron belt and Hess' predictions of the remains of Starfish place Vettes' flux at January 1965. The Vette flux map includes some of the softer natural electrons so that the penetrating dose from these electrons compares with dose predictions from Starfish at a date later than January 1965. Flux measurements are continuing so we expect the environment to be updated probably before the end of 1965. In the interim the aerospace environment is a reasonable natural belts model for low altitudes.

Untrapped Radiation - It has been determined experimentally at the Earth's surface, in high altitude balloons, and in satellites that the radiation background increases with increasing latitude and that there are large enhancements of this radiation which correlate with solar flares. This untrapped radiation consists of a galactic cosmic ray component which may be represented by the following analytic form:

$D_{\text{solar max}} = 0.192(L-1) + 0.072$	mrad/hour	$1 \leq L \leq 2.5$
0.36	mrad/hour	$L \geq 2.5$
$D_{\text{solar min}} = 0.54(L-1) + 0.072$	mrad/hour	$1 \leq L \leq 2.5$
0.88	mrad/hour	$L \geq 2.5$

where L is the McIlwain parameter

The solar particle event radiation is not significant for the low inclination of the KDT.

In summary, the principal components of space radiation, to their peak daily fluxes and their energy ranges at altitudes 250 N Mi, are as follows:

<u>Particles</u>	<u>Energy</u>	<u>Peak Daily Fluxes</u>
Protons	10-300 Mev	3×10^7
Electrons	0-10 Mev	5×10^{10}
Alpha particles	0-300 Mev	10^4

At a first approximation, the radiation fluxes given by the environmental models are assumed to be isotropic. To encounter an effective angular distribution which is significantly non-isotropic, the vehicle must be orientated with respect to the field line.

Vehicular and Space Suit Shielding - The critical dose points for this study are the film, crew members' eyes, and the optical surface coatings. Because of the extent to which space radiation interacts with material, it is important to consider the effect of any material between the environment and the dose point. Rather than performing a detailed sector analysis of the spacecraft to determine the mass distribution, an approximate MORL shielding of 2.0 gm/cm^2 of aluminum was assumed. The skin of the MOT can is 0.6 gm/cm^2 . While in the MOT, the space suit provides the astronaut with 0.4 gm/cm^2 additional shielding. Minimum local shielding for the film is also assumed to be 0.4 gm/cm^2 . The film storage compartment in the MORL is assumed to provide additional shielding for the film of 3.0 gm/cm^2 . Therefore, the analysis is concerned with dose and peak dose rates behind shielding of 0.4, 1., 2. and $5. \text{ gm/cm}^2$.

Radiation Effects and Tolerances - In order to provide a framework for the dose predictions to follow, a description of the effects upon (or tolerances of) the sensitive materials is given.

Film Radiation Sensitivity - Incident charged particles transfer energy to the sensitized photographic grains mainly by excitation and ionization. This energy transfer can cause reduction of the grains to atomic silver in a manner similar to light quanta exposure. Radiation also breaks chemical bonds of various long chain emulsion molecules important to film characteristics. Detailed effects resulting from this type of interaction are not completely understood at this time. Therefore, the assumed tolerances are based upon the film darkening effect. Radiation tolerances for widely used films covering a large range of optical sensitivities are shown below. These tolerances were determined as the radiation exposure which would produce a net density change of 0.3 above fog.

Radiation Tolerances for Films of Various Optical Sensitivity

<u>Film Type</u>	<u>Optical Sensitivity</u> (Relative)	<u>Tolerance (Rad)</u>
Micro-file	5	100
Kodachrome	10	50
Panatomic-X	60	8
Plus-X	160	3

Plus-X aeracron	210	2
Tri-X	400	1
Polaroid	3000	0.1

Requirements imposed by a given experiment may be more stringent on some characteristic of the film other than density, i.e., resolving power. Complete engineering data on all proposed films must include the effects of radiation upon these characteristics. Controlled temperature and humidity experiments indicate that some of the fog damage caused by the radiation can be repaired before exposure. Complete data on this effect for all films will also be required.

Human Tolerance - For the purpose of this study, radiobiological tolerances levels used are:

<u>Organ</u>	<u>Tolerance (Rad)</u>
Eye	27
Blood Forming	54
Skin	233

Optical Surface Effects - The characteristics of interest for MORL/MCT missions are the reflectivity, transmission, and fluorescence properties of the optical materials and mirror surface coatings, and the latter's ability to protect the polished mirror surface. Under moderately high energy radiation tests (Gamma rays ~ 1 Mev, Protons > 10 Mev), significant loss of these characteristics has been obtained at $\sim 10^4$ rad. Radiation effects on transmission and fluorescence of optical materials have proven troublesome on every satellite containing optical experiments launched to date. Complete data will be required to properly design the optical systems. A systematic approach to providing engineering data for radiation effects on optical materials to be used in space radiation environment has not yet been undertaken.

Although much remains to be known on the effects of radiation on reflective coatings, the high UV reflectivity of MgF_2 overcoated aluminum mirrors appears to be relatively less sensitive to UV or moderately high energy particle radiation. The effects of lower energy particles on the thin coatings of MgF_2 are still unknown.

Radiation Dose - Radiation dose encountered by MORL/MCT missions at inclination angles of 28.5 degrees to 30 degrees is primarily due to the protons and electrons trapped in the geomagnetic field. The geomagnetic field shields the untrapped radiation to a level of .0025 to .0035 rad/day, due to the galactic cosmic rays. The solar events dose is below this galactic background at these inclination angles, even during the largest events. The galactic dose is insensitive to the shielding thicknesses considered, so it represents a minimum yearly dose of 0.9 rad/year at solar maximum and 1.3 rad/year at solar minimum. The daily dose and peak dose rates for MORL/MCT missions are shown in Figure 5.3-34.

Daily Dose and Peak Dose Rate for MORL/MOT Missions

Alt. N Mi 200	TYPE Inclination X(gm/cm ²)	Daily Dose (Rad)					Peak Dose (Rad/Hr)						
		Protons		Electrons		Total*	Protons		Electrons		Total		
		28.5	30	28.5	30		28.5	30	28.5	30			
	0.4	0.5	0.7	3.4	9.3	3.9	10.0	1.7	2.3	11.0	32.0	13.0	34.0
	1	0.4	0.55	0.67	2.0	1.1	2.6	1.3	1.8	2.8	7.3	4.0	9.0
	2	0.27	0.36	0.05	0.16	0.33	0.53	0.9	1.2	0.2	0.6	1.1	1.8
	5	0.16	0.2	0.002	0.005	0.16	0.21	0.5	0.6	0.008	0.02	0.5	0.6
250	0.4	3.0	4.0	17	46	20	50	3.0	4.2	60	190	63	195
	1	2.5	3.3	3.5	11.7	6.0	15	2.6	3.5	19	48	22	52
	2	1.5	2.1	0.14	1.6	1.6	2.4	1.7	2.1	1.3	4.0	3	6
	5	0.8	1.4	0.01	0.03	0.81	1.5	1.0	1.5	0.06	0.1	1.05	1.6

*The galactic cosmic ray dose is not strongly dependent upon altitude, inclination, or shielding and is 0.0035 rad/day at solar minimum and 0.0025 rad/day at solar maximum for the entire range of this table.

Figure 5.3-34

Surface Dose - The surface dose is not shown because the low energy environment is not as well-known. An estimate of the surface dose can be taken as five times that inside, 0.4 gm/cm^2 . For example, the yearly surface dose at 250 N Mi would be $3.6 \times 10^4 \text{ rad/year}$ and $9 \times 10^4 \text{ rad/year}$ at inclination angles of 28.5 degrees and 30 degrees respectively. This represents an intolerable dose for all but high quality materials. Radiation effects data is urgently needed to properly assess the mission hazard.

Film Dose - With minimum protection the film dose is 6 rad/day at 250 N Mi in the MOT. Since up to ten days retention in the MOT is envisioned, this contributes a dose of 60 rad causing severe fogging to any of the sensitive films. This dose is received only while passing over the South Atlantic. The maximum dose received in any one pass is 2.5 rad. Assuming that the film is inside a camera in the MOT which supplies an additional 2.0 gm/cm^2 of shielding, the daily dose is reduced 1.3 rad/day, or less than a 13 rad contribution while in the MOT. Assuming a maximum storage of 180 days in the MORL at 0.8 rads/day before exposure, this would imply a maximum dose at 250 N Mi 28.5 degrees inclination of 149 rads. This far exceeds the tolerances given for all films considered. It would take five gm/cm^2 additional shielding for the storage compartment (bringing it up to 16 psf) to reduce this maximum dose to 55 rad. This dose is still damaging to most of the films that have been considered. Alternate means of reducing the radiation exposure or minimizing the effects of exposure on the film's role in the mission should also be studied.

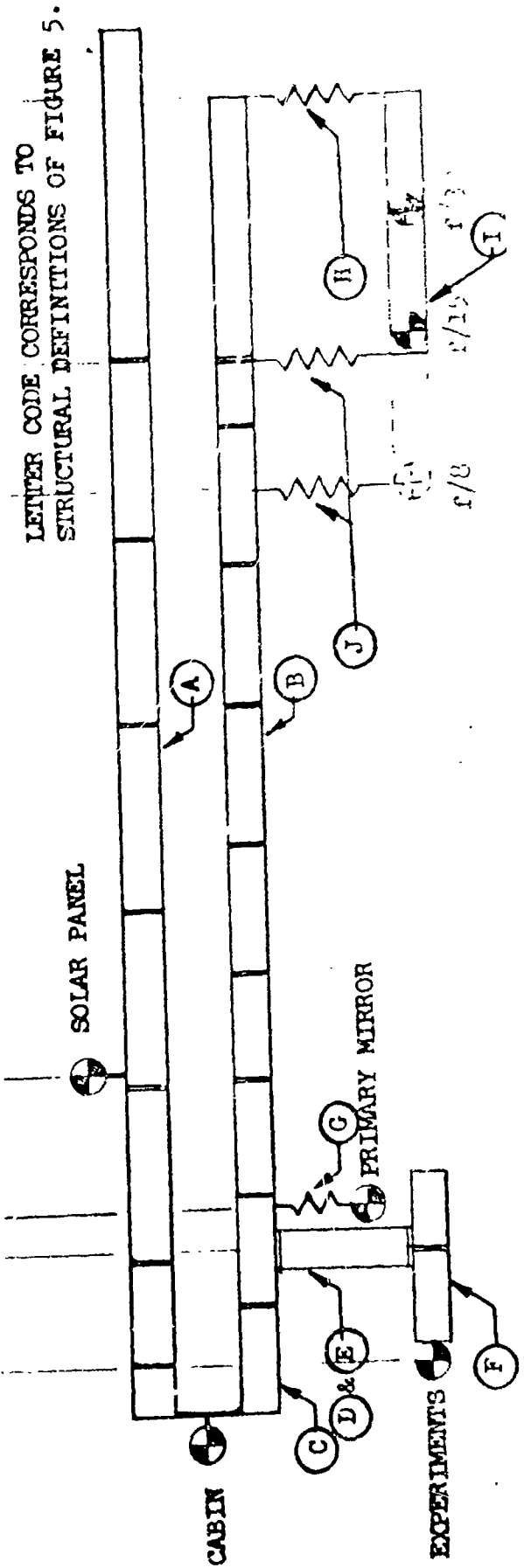
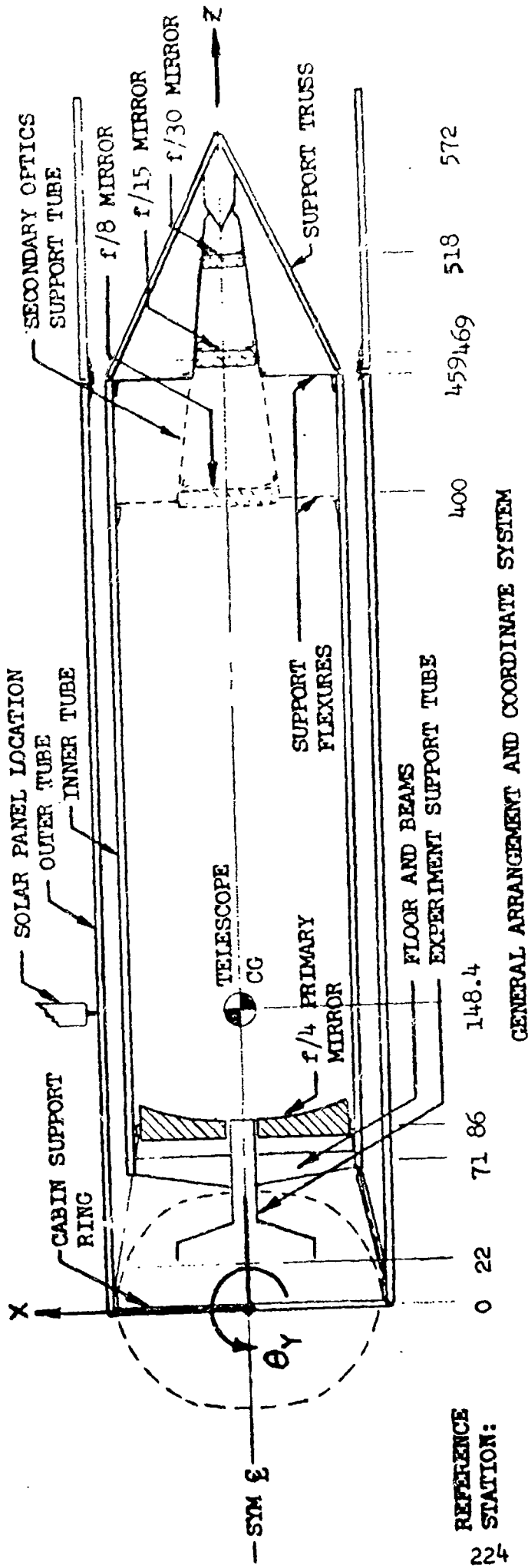
Human Dose - The most sensitive organ is the eye. The crew member's head shields the eye effectively over the half space. Hence the expected eye dose in the MORL is 50 percent of that shown in Figure 5.3-31. This gives a daily eye dose of 0.8 rad/day at 250 N Mi and 28.5 degrees inclination. The skin dose at the chest is nearly identical to the eye dose due to equivalent body shielding. Hence the skin dose is a tolerable 145 rad for each six-month mission. The eye dose exceeds the tolerance level. To bring the eye dose level down to 27 rads, about 15 gm/cm^2 (30 psf) local protection would be required during the passages over the South Atlantic. This radiation occurs in 10 to 20 minutes during 7 to 8 orbits per day. The crew member is scheduled to spend about 40 hours during each six months outside the MORL/MOT. This would nominally contribute about 15 rad to the eye in this mission. Another 350 hours is scheduled in the MOT, where nominally an additional 45 rad would be received. With random scheduling, the skin and eye dose would thus be 200 rad. By scheduling the extra-MORL activities away from the South Atlantic, the mission dose can be limited to 145 rad.

Summary - Photographic film is the most sensitive material to be subjected to the space radiation environment. Problems of image quality and contrast may dictate the use of the best available emulsions for the mission, independent of radiation sensitivity. In these cases, the sensitive emulsions must be provided adequate radiation protective shielding. The excessive shielding that would be required for the most sensitive films can be reduced by:

- o scheduling resupply to avoid any unnecessary extended storage of the film before exposure.
- o scheduling development of the film soon after exposure to avoid any unnecessary retention in the MOT.

Figure 5.3-35

Structural Dynamics Model



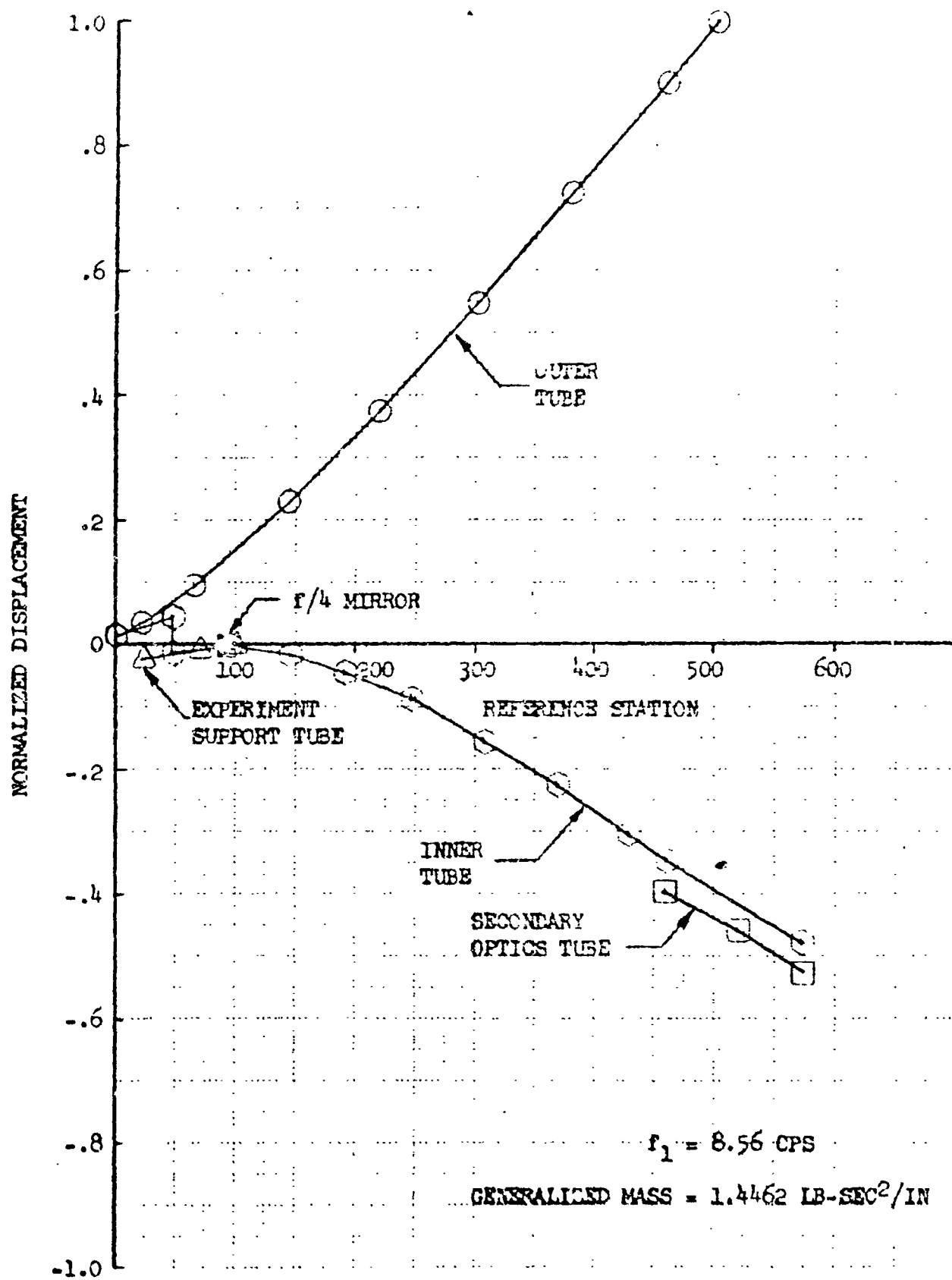


Figure 5.3-36

First MOT Bending Mode

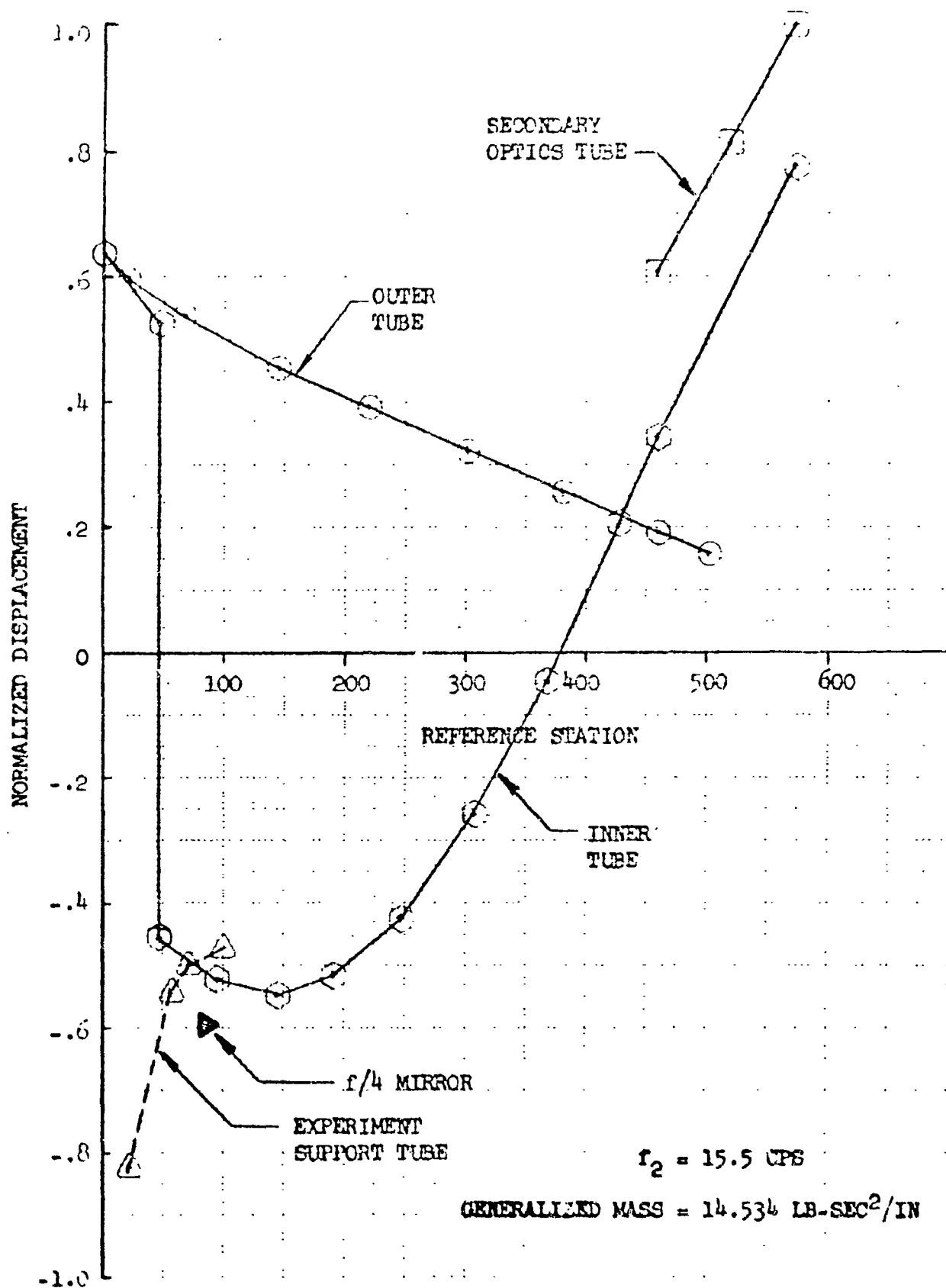


Figure 5.3-37

Second MOT Bending Mode

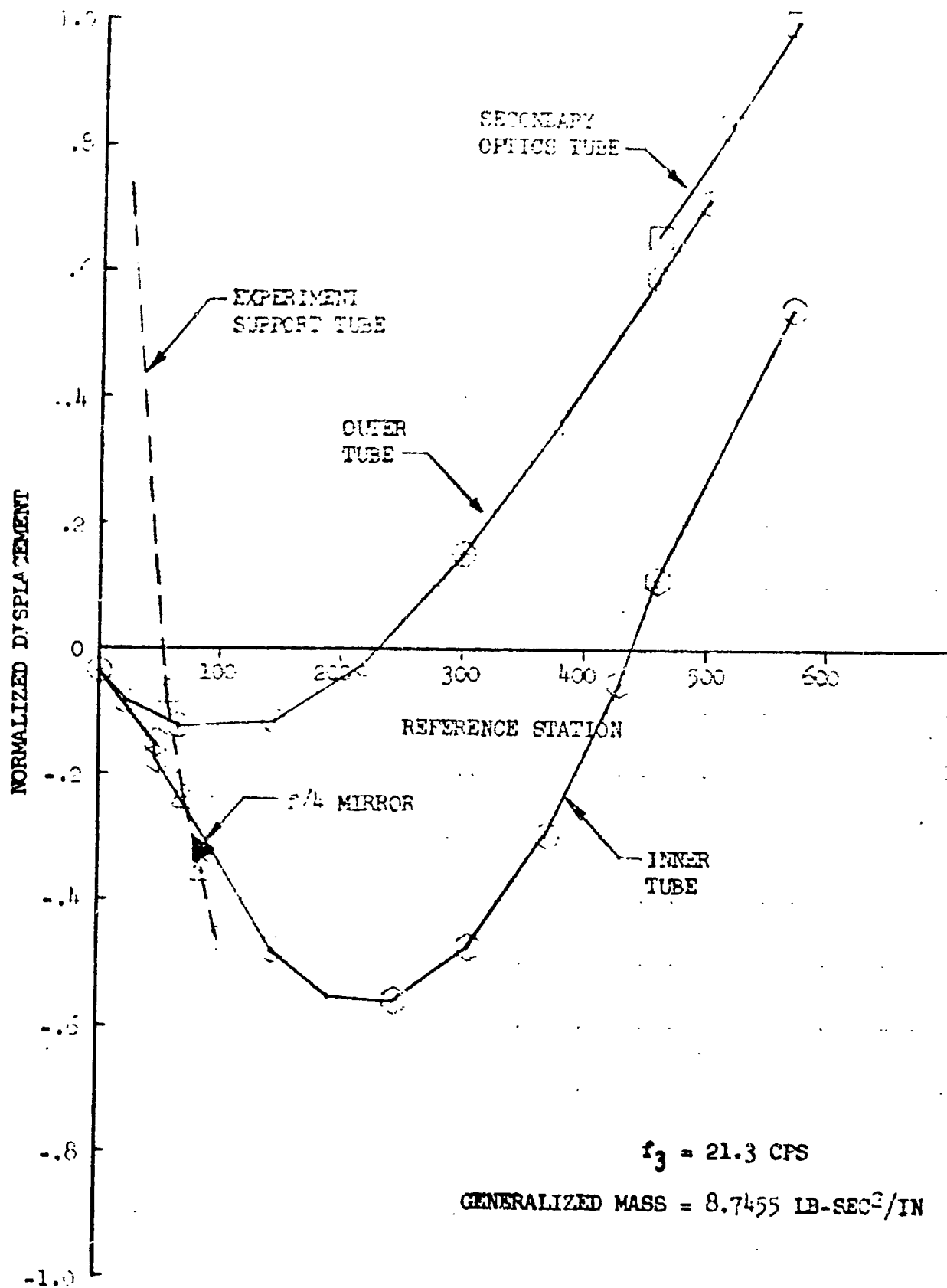


Figure 5.3-38

Third MOT Bending Mode

- o controlling the temperature and humidity of stored unexposed film to erase as much latent image caused by the radiation as possible without degrading its sensitivity and resolution characteristics.
- o lowering the altitude and/or inclination angle of the trajectory for the mission.

Scheduling and changing altitude or inclination should also be considered, along with eye shields, as alternate means of avoiding harmful dosage to the crew members' eyes.

5.3.5 Telescope Dynamic Analysis

The dynamic characteristics of the telescope in a free floating configuration were investigated by use of a direct analog computer, with voltage analogous to velocity, current to force, capacitance to mass, and inductance to spring flexibility. Objectives of this study were to determine mode shapes and frequencies of the baseline structure as required for the servoelectric analysis performed by General Electric, and to examine the effect on the telescope dynamics of structural parametric variations.

5.3.5.1 Structural Representation

For application to the direct analog computer, the telescope structure was assumed symmetric and idealized as a set of elastic beams and attached masses coupled together by linear springs. This idealization allowed motion in lateral translation and pitch rotation, the two motion sources considered of interest for this analysis. The general arrangement of the idealization and the coordinate system are shown in Figure 5.3-35.

The elastic properties of the beams used in the analogy were scaled to match the bending and shear stiffness values of the telescope tubes. Stiffness values of other structural elements were either made equal to equivalent beams or represented by translational springs, depending upon the element's orientation. Each beam used in the analogy was divided into the segments shown in the idealization sketch. This segmenting was necessary to achieve a lumping effect and to provide adequate description of the motion, since displacements and rotations were measured only at the centers of each segment.

By equating the component structural properties to the analogous electrical elements and applying appropriate scaling laws, an analog circuit was developed to represent the baseline telescope structure.

This circuit was modified when necessary for application of the structural parametric variations.

5.3.5.2 Baseline Configuration Mode Shapes

The natural free-free modal frequencies and the associated normalized mode shapes were obtained for the baseline configuration. The first three mode shapes are plotted in Figures 5.3-36 through 5.3-38. A summary of the normalized nodal displacements and slopes are included with the lumped mass characteristics in Figure 5.3-39.

DYNAMIC ANALYSIS - MASS & MODAL DATA

REFERENCE STATION	MASS LB- SEC ² /IN	INERTIAL LB-IN ² - SEC ² /IN	1ST MODE		2ND MODE		3RD MODE	
			Displ. ϕ	Slope ϕ'	Displ. ϕ	Slope ϕ'	Displ. ϕ	Slope ϕ'
		$\times 10^{-3}$		$\times 10^2$		$\times 10^2$		$\times 10^2$
<u>OUTER TUBE</u>								
0	12.3333	91.200	.0130	.099	.6380	-.191	-.0454	-.206
33.0	.3436	1.169	.0498	.138	.5815	-.132	-.0940	-.092
105.5	.4113	1.465	.1624	.171	.4960	-.106	-.1220	.008
182.0	1.0589	3.167	.3015	.193	.4230	-.084	-.6725	.126
260.0	.4270	1.537	.4600	.212	.3570	-.085	.0571	.215
340.5	.4113	1.465	.6350	.223	.2900	-.081	.2555	.267
419.5	.4113	1.465	.8110	.223	.2255	-.082	.4745	.287
501.5	.1014	.230	1.000	.237	.1590	-.080	.7150	.289
<u>INNER TUBE</u>								
35.5	.0735	.012	.0374	.069	.5525	.243	.1228	.240
86.0	2.7889	8.719	-.0043	.022	-.5092	-.142	-.2990	-.323
168.0	.7680	1.965	-.0300	-.058	-.5330	.069	-.5170	-.157
219.0	.9359	2.465	-.0662	-.082	-.4770	.168	-.5565	-.013
277.0	1.0002	2.679	-.1216	-.108	-.3410	.273	-.5175	.142
337.5	1.0180	2.750	-.1845	-.116	-.1503	.356	-.3855	.293
400.0	1.1538	2.679	-.2635	-.128	.0817	.411	-.1747	.404
443.5	.6162	1.286	-.3225	-.132	.2725	.435	.0198	.472
<u>SECONDARY OPTICS</u>								
<u>TUBE</u>								
469.0	1.258	.200	-.4070	-.108	.6520	.336	.7080	.275
518.0	.542	.041	-.4580	-.113	.8040	.349	.8170	.307
572.0	.129	.012	-.5220	-.119	1.000	.363	1.000	.339
<u>EXPERIMENT</u>								
<u>SUPPORT TUBE</u>								
22.0	5.440	2.904	-.0028	.032	-.8230	.821	.7310	-2.387
71.0	2.220	.908	-.0078	.026	-.4990	.200	-.2390	-.797
<u>f/4 MIRROR</u>								
86.0	4.6950	Incl. Above	-.0046	.022	-.5950	-.142	-.4110	-.323

Figure 5.3-39

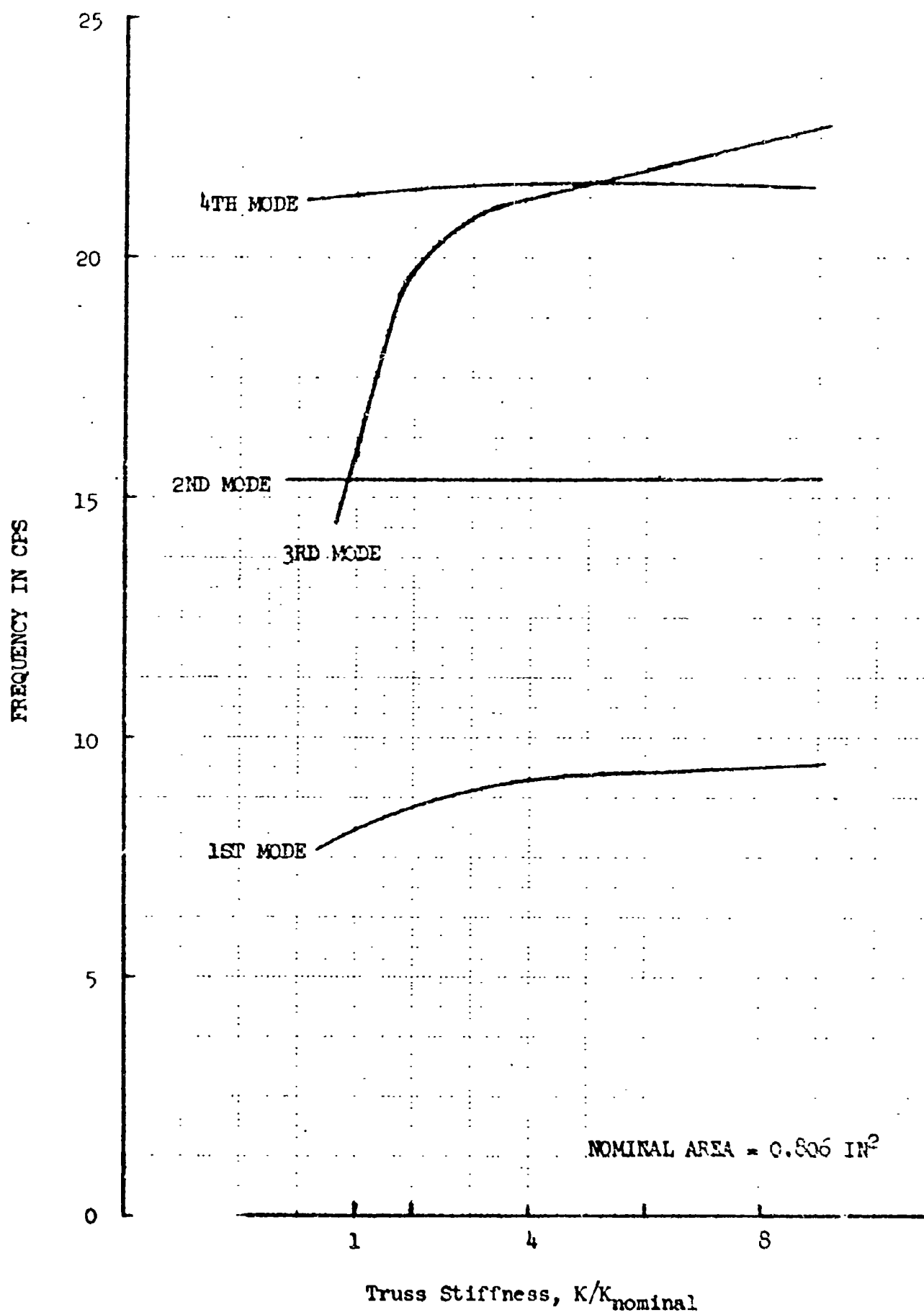


Figure 5.3-40

Effect Of Cabin Support Truss Stiffness

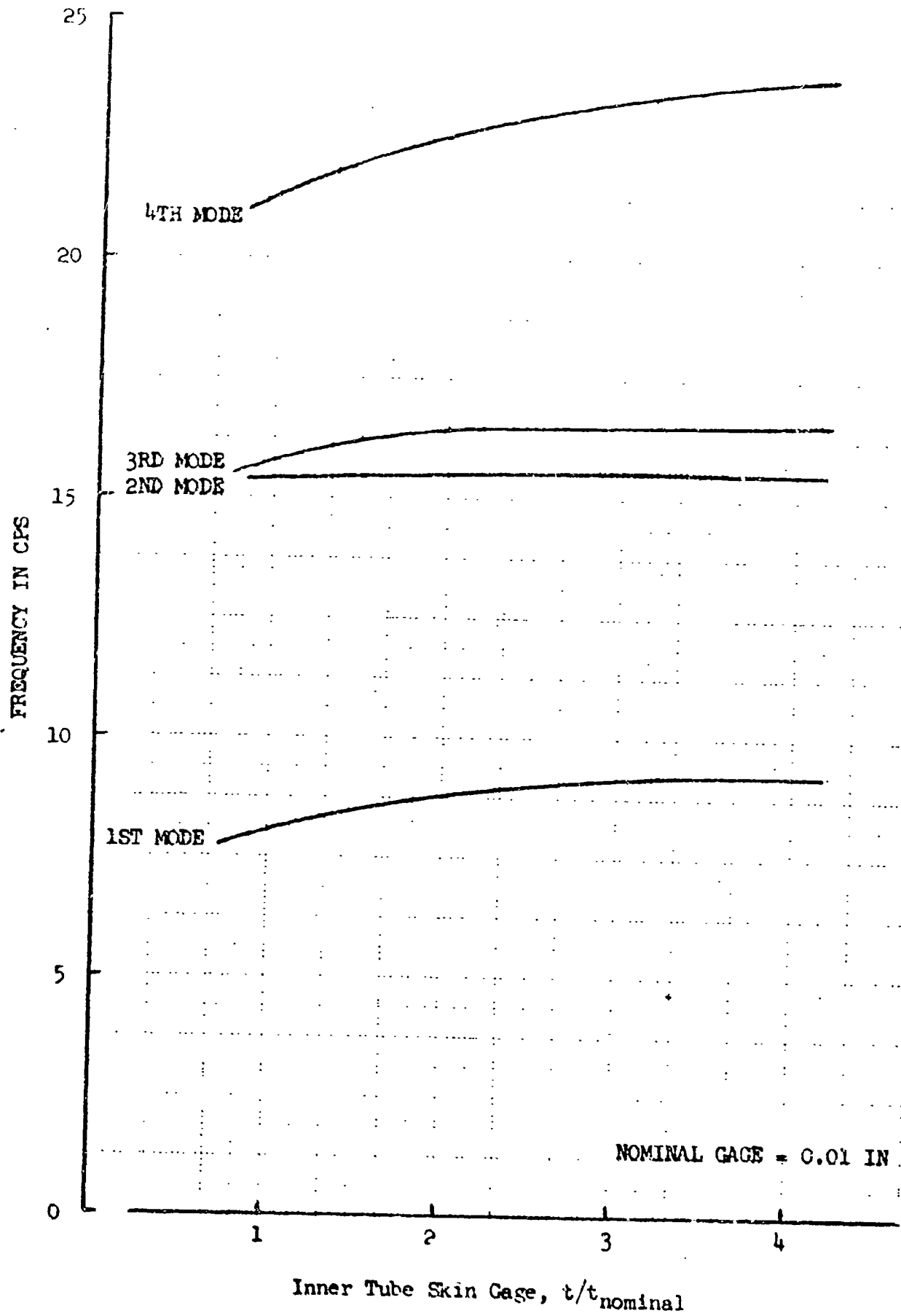
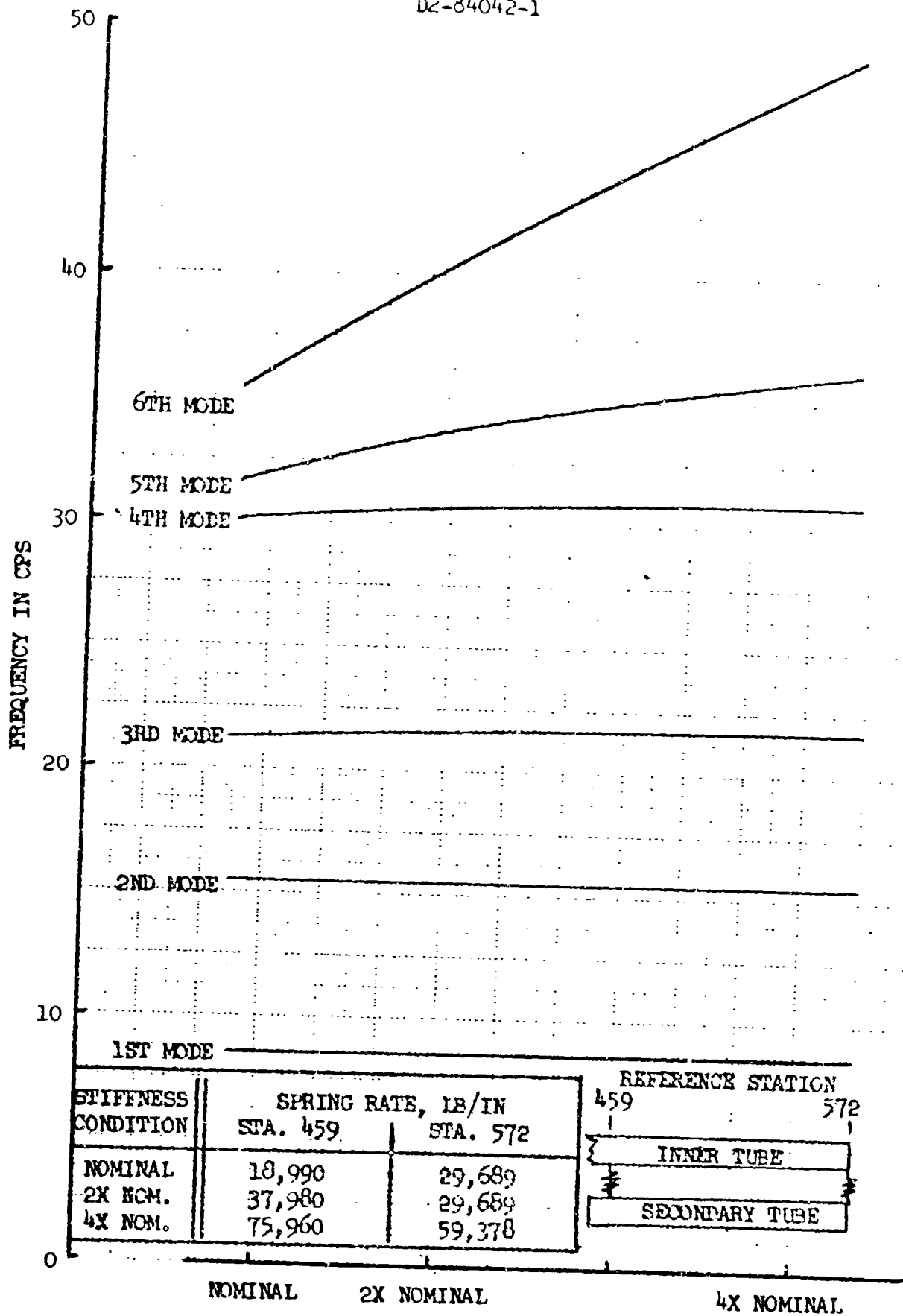


Figure 5.3-41

Effect Of Inner Tube Stiffness
231



Secondary Tube Support Stiffness Condition

Figure 5.3-42

Effect Of Secondary Support Strap Stiffness
Two Support System

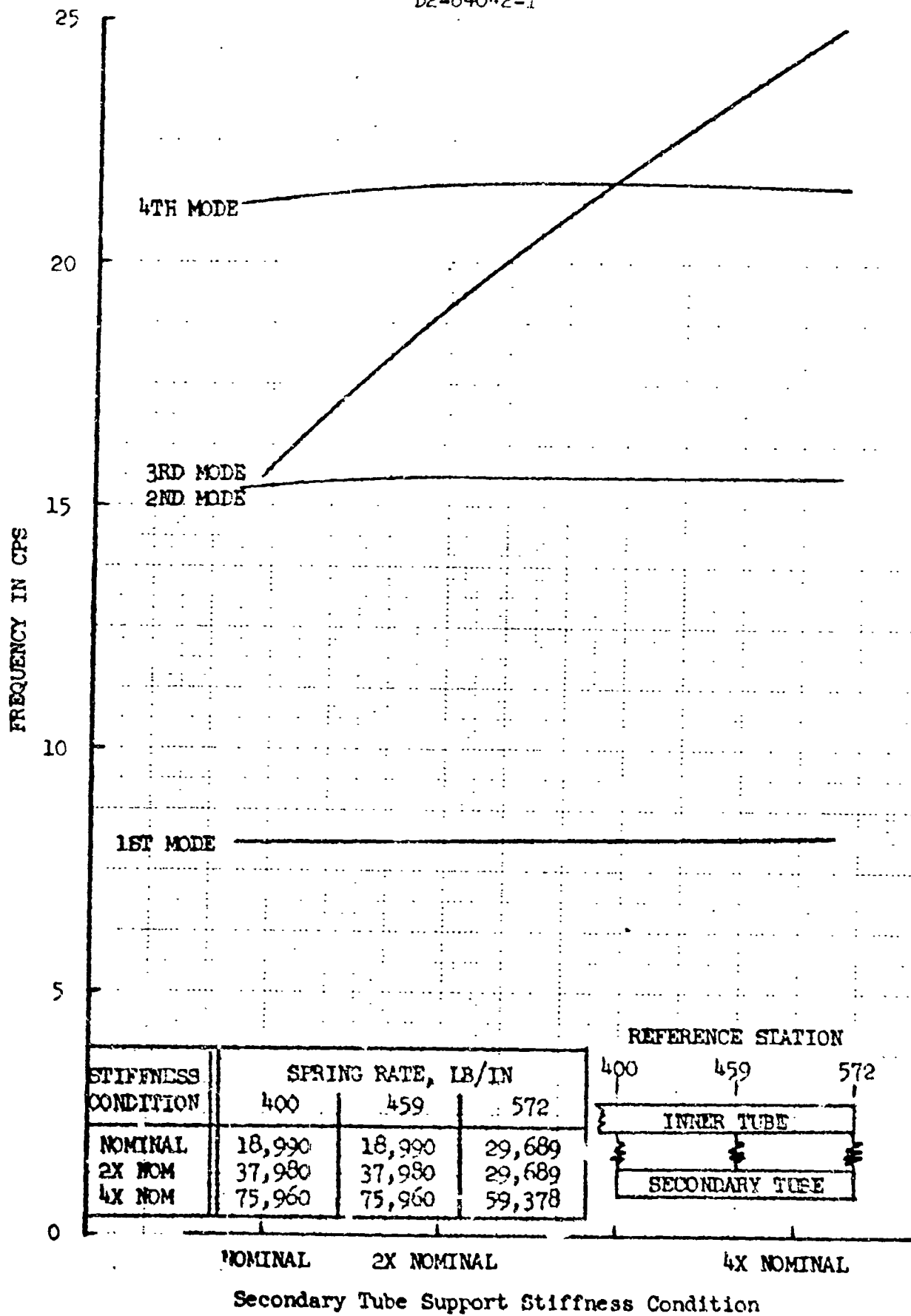


Figure 5.3-43

Effect Of Secondary Support Strap Stiffness
Three Support System

5.3.5.3 Parametric Variations

To evaluate the effect of a structural component stiffness change on the overall dynamic characteristics of the telescope, the stiffness of major elements was individually varied. The shift in modal frequencies was noted, and taken as an indication of the effect on dynamic properties for that parametric variation. When stiffness variations involved a major weight change, corresponding adjustments were made for the mass and inertia elements of the analog circuit.

Figure 5.3-40 shows the frequency shift of several modes for changes in the stiffness of the six-bar truss tie between the cabin and inner tube structure. A significant decrease in its displacement for the second mode was noted as the shear stiffness of this truss was increased.

The effect of increasing the skin gage of the inner tube is shown in Figure 5.3-41. Variation of stiffnesses for the flexure tie bars and the tripod supporting the secondary optics tube produced frequency shifts as shown in Figure 5.3-42, for a system with two supports, and in Figure 5.3-43 for a three-support system.

Results of varying the bending stiffness for the secondary optic tube and experiment support tube are shown in Figure 5.3-44.

The addition of a third mirror to the secondary optics package at station 400 resulted in a first mode frequency reduction to 8.04 cps from the baseline value of 8.56 cps.

An increase in insulation weight and a shift in placement from the exterior of the inner tube to the interior surface of the outer tube resulted in an additional reduction of modal frequency. For this case, the fundamental frequency dropped from 8.04 cps to 5.76 cps.

5.3.5.4 Structural Response

The structural response to a step input force was determined at several points on the telescope. The input unit force was applied to the outer tube at the location corresponding to the telescope center of mass. The response, in terms of acceleration, was measured at the f/4 mirror support, at the outboard ends of the inner and outer tubes, at the experiment package support, and at the f/15 secondary mirror support. The time history responses of the f/4 and f/15 mirrors are shown in Figure 5.3-45 for a unit input forcing function.

These time histories are typical of the responses measured at the other locations. The maximum acceleration response was 0.00145 g's/unit force measured at station 501.5 on the outer tube. Response frequency for all cases was approximately 30 cps.

5.3.6 Conclusions and Recommendations - Structures

Studies of telescope primary structure, dynamics, thermal distortion, and response to the launch and meteoroid environments revealed certain important facts about the structural design of the MOT. These are discussed in detail in the following paragraphs.

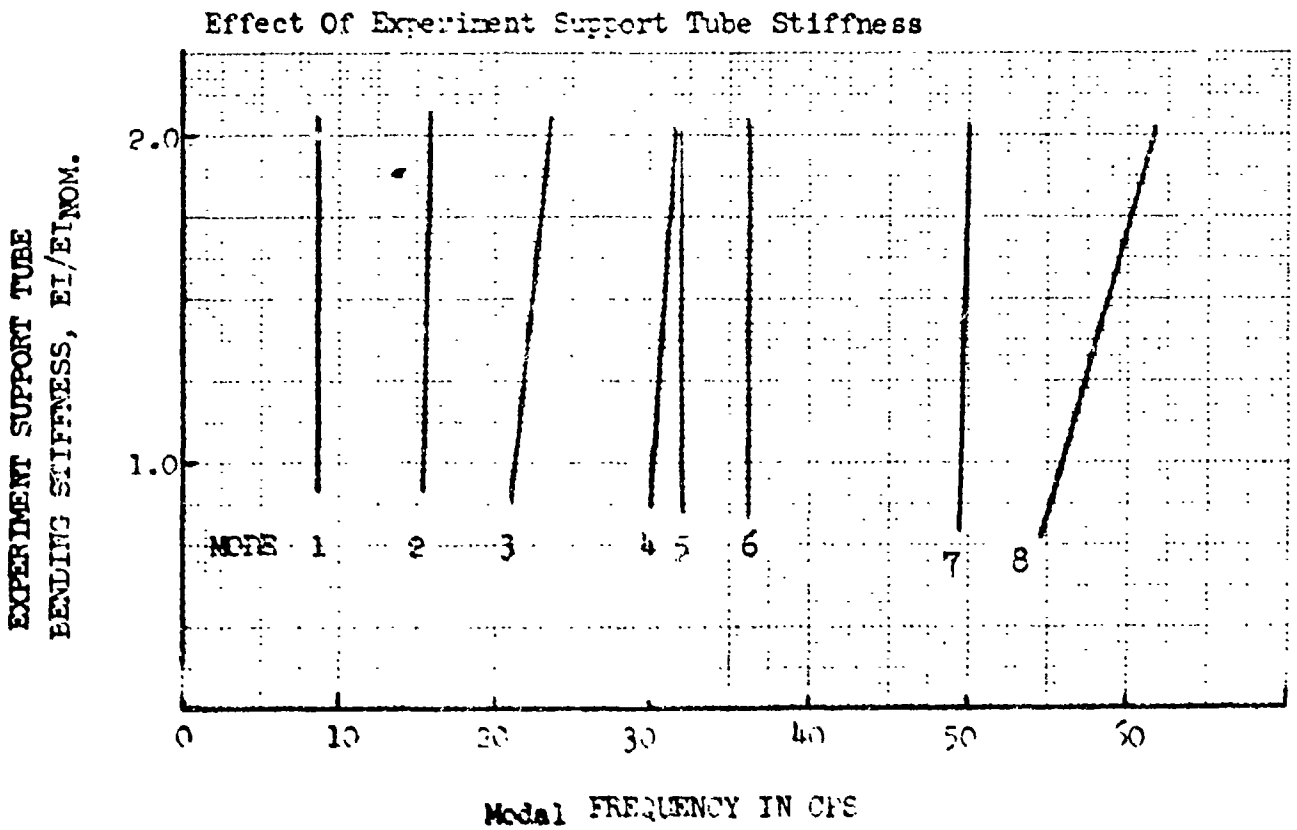
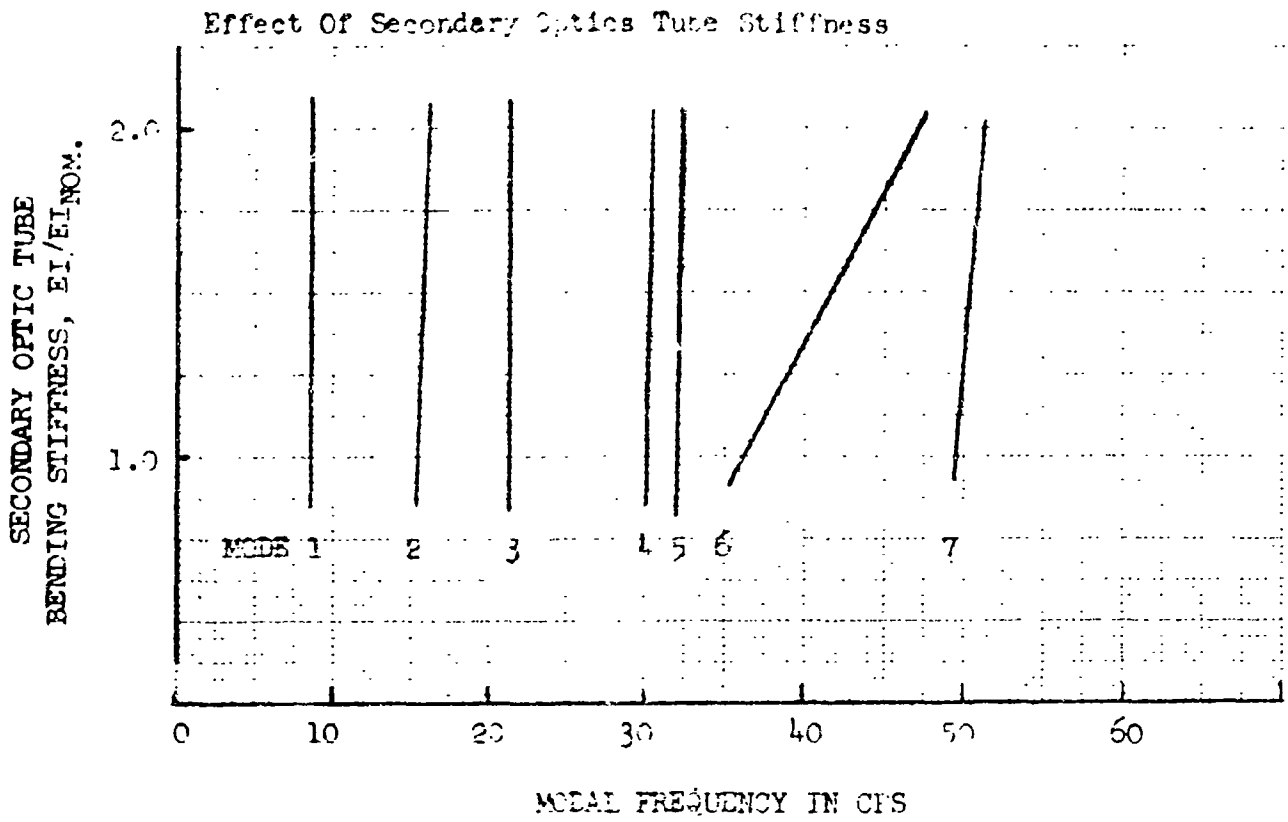


Figure 5.3-44
235

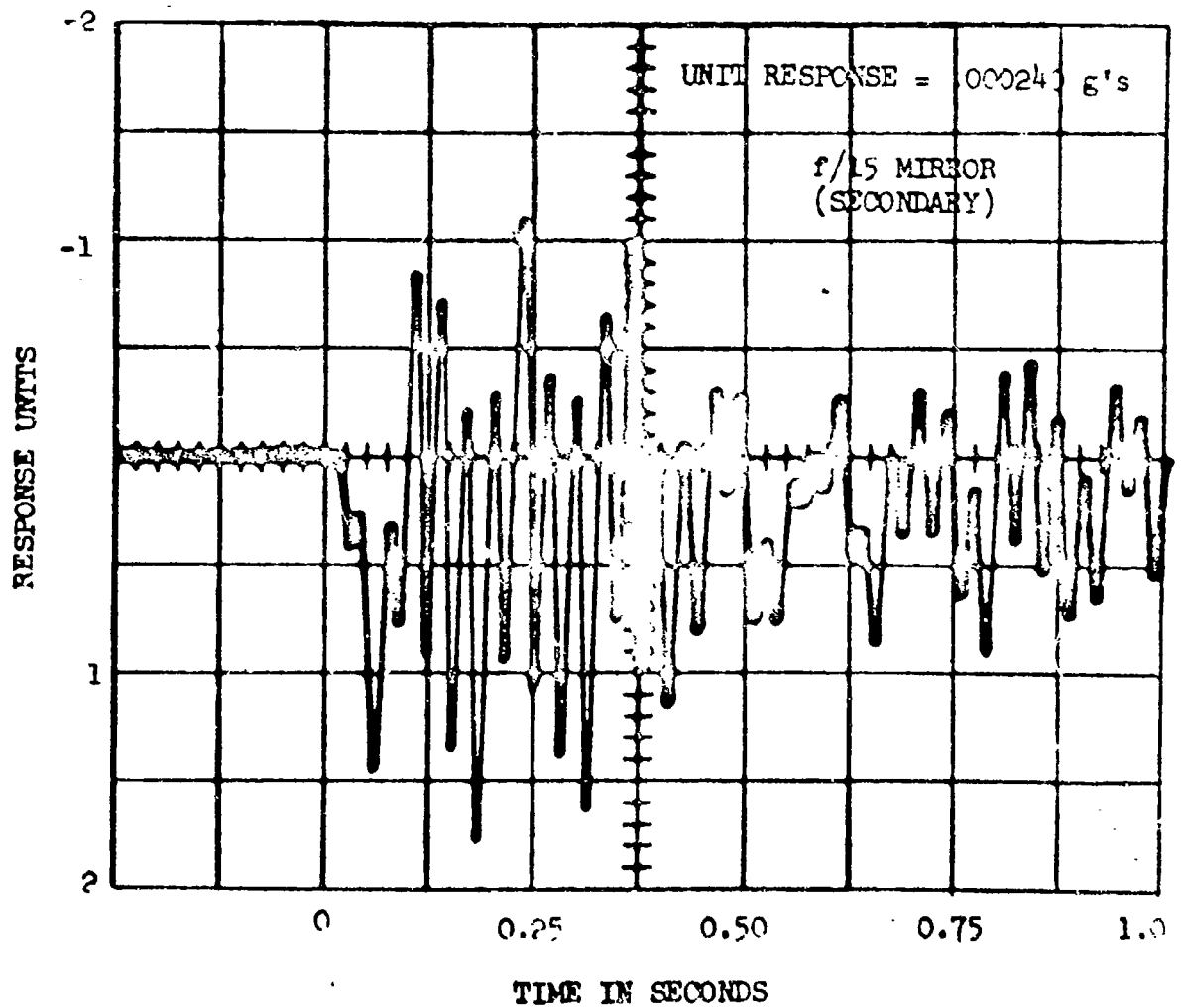
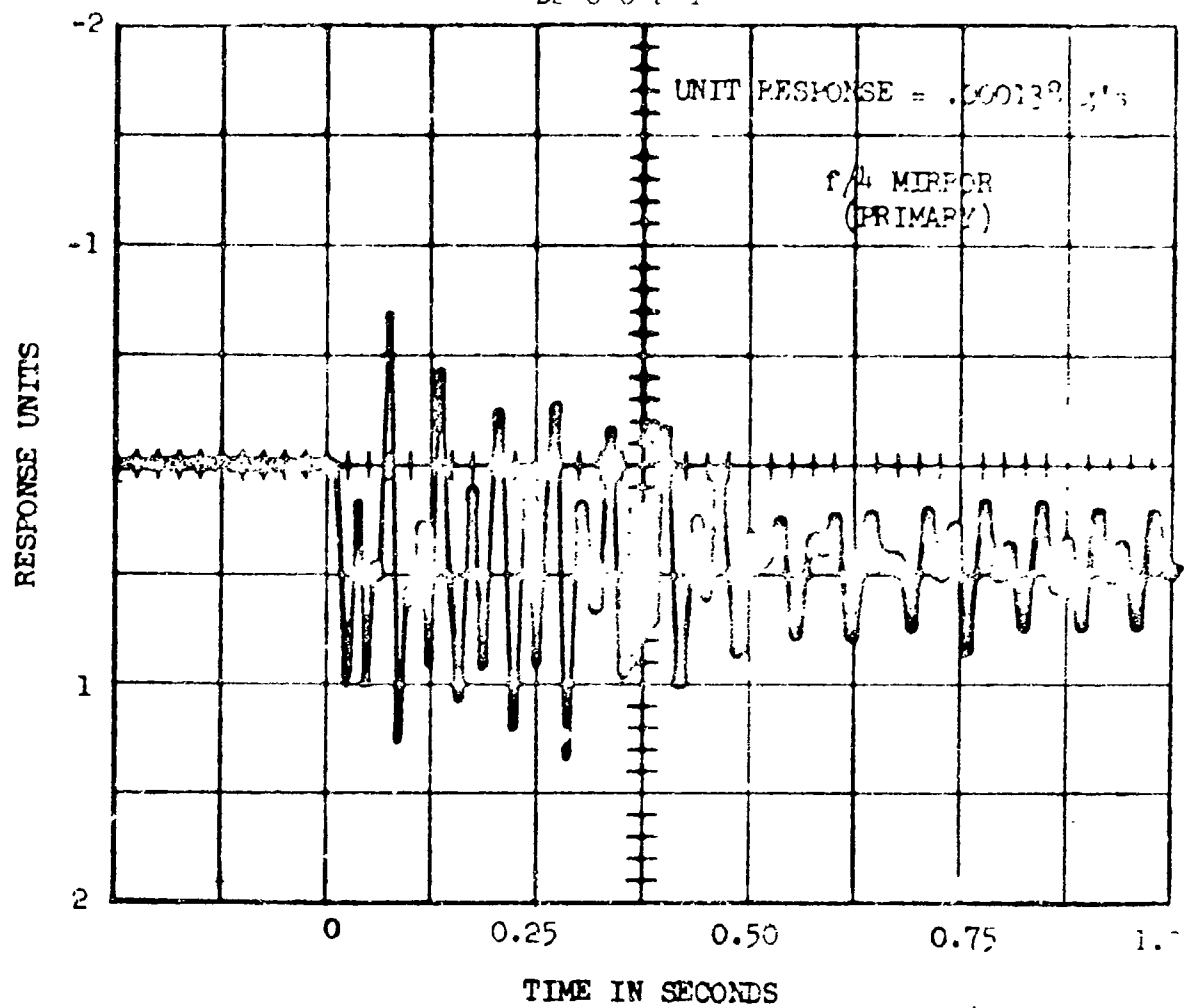


Figure 5.3-45
MOT Response To Step Input At C.G.

5.3.6.1 Launch Environment

Based on measured data available, the maximum acoustic environment will be on the order of 135 to 140 db, and the expected vibrational environment will be about 1.23 g_{rms} laterally at a frequency of 225 cps. In conjunction with an analysis of structural attenuation, an evaluation of mirror and equipment response to these environments should be conducted to determine the requirements for a boost isolation system.

5.3.6.2 Boost Load Factors

The maximum load factors used for sizing the telescope structure are ± 6.95 axially and ± 2.91 laterally. A detailed analysis of the complete air vehicle will be required to determine the boost loads and prove compatibility between the telescope structure and the S-IB booster.

5.3.6.3 Primary Structure

Materials - Materials trades indicate that:

- 1) Fiberglass should be employed in areas where minimum heat leak combined with maximum stiffness and structural strength are desirable;
- 2) Titanium should be used in structural areas where maximum strength and stiffness with minimum thermal deflection are required.

Structural Concepts - Investigation of structural concepts has indicated that determinate structural ties should be employed in the support of critical optical elements to eliminate the transmission of stress-induced distortions. However; since such structures are inherently weak in shear, their use must be tempered with considerations of vehicle flexibility as it affects the servoeelastic problem.

5.3.6.4 Mirror Dynamics

The rotational response frequency of the f/4 primary mirror supported on segmented bladders with an internal pressure of 2.64 psig is 10.5 cps. A detailed analysis of the f/4 mirror supported at three points by the tangent bars shows the rigid body rotation frequency to be 17.8 cps, well separated from the first mirror mode of 390.5 cps. The tangent bars and bladders are flexible enough to allow the vibration modes of the supported mirror to approach free-free conditions.

5.3.6.5 Mirror Stresses

Analyses of stress distributions in the primary mirror during boost and in operation have revealed that large margins of safety exist between applied stresses and the 2000 psi limit which prevents microyield. These results indicate that, for the conditions studied, the mirror is overstrength. It appears that the mirror will be sized for manufacturing or figuring conditions or for thermal performance.

5.3.6.6 Gimbal Design

Investigation of the soft gimbal concept demonstrated, within the study constraints of a limited control investigation, use of existing gimbal bearing data, and linearized equations of motion, that the concept is feasible. Specifically, the study demonstrated that:

- o Disturbances arising in the MORL can be acceptably attenuated by a spring system having an effective spring constant of 0.0847 pounds per inch
- o The springs required to produce this spring rate are physically practical, being 2 inches in diameter, 16.7 inches long, and wound with 10 gage aluminum wire to a pitch of 8 coils per inch; and,
- o The supporting structure necessary to couple the spring-gimbal system to the MORL is adaptable to the boost payload envelope constraints.

5.3.6.7 Thermal Distortion Analysis

Analysis of structural concepts for connecting secondary optics to the primary mirror have shown that secondary mirrors remain within optical tolerance if the diametral temperature gradient is less than 2.0°F for aluminum structure or 3.6°F for titanium structure. Thermal analysis of the structure using aluminum reveals the actual gradient to be about 3.0°F. In consequence, a passive system using aluminum does not meet the optical requirements. Titanium structure would result in a suitable passive system if its use did not aggravate the diametral temperature gradient through titanium's reduced transverse conductivity.

The alternative, use of automated secondary alignment control, is applicable to the secondary design shown in Figure 5.2-16 and is the suggested method of this study.

Figure deviation due to thermal distortions of the primary mirror is, at best, $\lambda / 36.3$, which occurs when the primary mirror is protected from any transient temperature changes. This deviation results largely from circumferential gradients induced by tangent bar heat leaks. The deviation exceeds that demanded by optical performance. Thus, further study should concentrate on methods of 1) designing a mirror which is less sensitive to temperature gradients or which produces lower gradients from given heat inputs, or 2) achieving reduced heat leaks through the tangent bar supports.

5.3.6.8 Meteoroids

Meteoroid studies associated with the MOT indicate that the meteoroid environment does not present a problem to the feasibility or operation of the telescope, showing that:

- 1) Damage to the primary mirror from direct meteoroid impacts is insignificant in a three-year period. In this time, 0.05 percent of the mirror surface is destroyed. A period of 101 years is required to destroy the mirror's function of diffraction limited performance by direct impacts;

- 2) Any damage to the primary mirror by secondary spray resulting from impacts on the telescope wall has less than a 5.3 percent chance of occurring in a three-year period.

5.3.6.9 Telescope Flexibility

The fundamental modal frequency of the baseline telescope structure, as determined by analog simulation, is 8.56 cps. This frequency may be raised or lowered by appropriate changes in the stiffness of structural components.

5.4 ATTITUDE CONTROL

5.4.1 Summary and Technical Approach

The MOT attitude control system study was accomplished primarily to demonstrate the feasibility of meeting the high accuracy attitude control requirements (0.01 arc sec) and secondarily, to optimize the design of the system. Chronologically, the efforts supporting these objectives were transposed.

In attempting to determine the optimum MOT configuration, eight concepts were generated at the initiation of the study. The control effort until program midterm was predominantly spent in assessing the relative feasibility of these concepts. The effort consisted mainly of:

- o Establishing pointing requirements for each observational experiment
- o Establishing internal (crew motion) and external (gravity gradient) disturbance torques for each operational configuration
- o Translating the above into control system performance requirements on each operational mode and assessing the feasibility of meeting these requirements using extrapolated state-of-the-art control hardware

These comparisons were then used to select two of the eight modes, the floating socket and the detached mode. Since these modes were very similar from the control aspect, the effort was easily narrowed into a detailed investigation of the expected performance, in which realistic control hardware and telescope characteristics were considered. These studies indicated that the requirements could be met. With feasibility established, future studies can proceed into a more detailed examination of the potential problem areas uncovered (see Section 5.4.6).

Observational Program Pointing Requirements

The nature of the fine pointing task requires a very close interface with the telescope and scientific instrumentation design, since the observational program dictates fine pointing requirements, and because the fine pointing sensor is an integral part of the instrumentation and utilizes the collection aperture of the primary mirror. Each of the observational programs was thus reviewed to determine the various possible fine pointing sensor configurations, and the advantages and disadvantages of each. No single program is clearly more difficult or demanding than all others, rather each is complex in its own way. A summary of sensor considerations for the six observational programs is shown in Figure 5.4-1.

Figure 5.4-2 tabulates the most stringent of these requirements, as well as the requirements for the other functions the attitude control system must perform. A detailed discussion of these requirements is contained in Section 5.4.2.

System Description

The proposed attitude control system for the MOT is shown in block diagram form in Figure 5.4-3. This system makes maximum utilization of experience obtained from the Orbiting Astronomical Observatory program and the advanced concepts resulting from

Type of Observation	High Resolution Stellar Spectrometry	Low Resolution Stellar Spectrometry	Photometry/Polarimetry	Stellar Photography	Planetary Photography	Planetary Spectrometry	Specialized Types of Observations
Relative Priority (% Observation Time)	25 to 30%	15 to 20%	5 to 10%	28 to 30%	5%	10%	5 to 10%
Wavelength Region & Star Magnitude of Object	Vacuum Ultraviolet to intermediate and far infrared. +10 visual magnitude or brighter	Vacuum ultraviolet to far infrared. Fainter than +20 magnitudes if possible	Vacuum ultraviolet to far infrared. Fainter than +28 magnitude if possible	Both wide and narrow field photography. Wavelength region and star magnitude limited only by film plates.	Narrow field photography of planets and their satellites. All planets with exception of Mercury accessible.	Intermediate and far infrared. Planets and their principal satellites	
Duration of Observation Exposure Time	Multiple-orbit observations of single star	Multiple-orbit observations of single source	Multiple-orbit observations of single source	Multi-orbit exposure of single plate. Limited by background noise.	Limited by planet rotation to fractional orbit	A few orbits maximum. Limited by rotation rate of planet. Spot tracking of a given area of planet required.	This category left open for specific observational programs to be defined at later date
Highest Pointing Accuracy and Stability Requirement of Telescopes	Diffraction limit of telescope 0.04 arc sec at 5000 Å. Accuracy and stability of point of 0.01 arc sec desirable	Not operating diffraction limited, but as large aperture telescope capable of multi-orbit exposure time. Small entrance slit (1 arc sec) necessary to minimize background noise.	Not operating diffraction limited, but as large aperture telescope capable of multi-orbit exposure time. Small entrance slit (1 arc sec) necessary to minimize background noise.	Diffraction limit 0.04 arc sec at 5000 Å. Stability of point for given plate of 0.01 arc sec desirable	Diffraction limit 0.04 arc sec at 5000 Å. Stability of point with respect to planet or object of 0.01 arc sec desirable during time of exposure	Not operating diffraction limited. Instantaneous field of view defined by spectrometer slit may be as small as 1 x 1 arc sec	
Flare Pointing Accuracy Requirement	Must guide & share energy of experimental star. Final alignment must be made in orbit by remote means.	Effect guidance required because of faintness of experimental source. Total effect field of view required in many minutes.	Effect guidance required because of faintness of experimental source. Total effect field of view required in many minutes.	Effect guidance desirable. At least one star in total field must be sufficiently bright to permit high stability pointing. Reproducibility of point from orbit-to-orbit critical.	Effect pointing using star field with some form of image motion compensation is required. Total field of view required is many minutes	Accuracy and stability of point of 0.05 to 0.1 arc sec desirable. Direct assistance of man to select pointing location of planet may be necessary.	
Flare Pointing Accuracy Requirement	Must guide & share energy of experimental star. Final alignment must be made in orbit by remote means.	Effect guidance required because of faintness of experimental source. Total effect field of view required in many minutes.	Effect guidance required because of faintness of experimental source. Total effect field of view required in many minutes.	Effect guidance desirable. At least one star in total field must be sufficiently bright to permit high stability pointing. Reproducibility of point from orbit-to-orbit critical.	Effect pointing using star field with some form of image motion compensation is required. Total field of view required is many minutes	Accuracy and stability of point of 0.05 to 0.1 arc sec desirable. Direct assistance of man to select pointing location of planet may be necessary.	Effect pointing using star field with some form of image motion compensation is required. Total field of view required is many minutes

Figure 5.4-1

OBSERVATIONAL PROGRAM

FIGURE 5.4-2

ATTITUDE CONTROL REQUIREMENTS

INITIAL RENDEZVOUS

Pitch, Roll, Yaw	+0.5 degrees
Thrust Duration	2.3 minutes

SUN ACQUISITION

Pitch and Yaw	+0.25 degrees
Pitch, Yaw, and Roll Rate	+0.09 degrees/sec
Acquisition Time	6 minutes

ORBIT AND STATION KEEPING

Pitch, Roll, Yaw	+0.5 degrees
Maximum Frequency	Every 9 hours

DOCKING - MOT TO MORL

Pitch, Roll, Yaw	Manual control
Control Authority	0.1 ft/sec ² - 1.0 deg/sec ²
Maximum Frequency	5 per year + 10 for unsched maintenance

STAR ACQUISITION

Coarse Pointing - Pitch, Yaw, Roll	+3 arc minutes
Initial Star Acquisition Time	15 minutes
Reorientation in Coarse Mode	5 degrees in 2 minutes, 90 degrees in 30 minutes
Intermediate Pointing	+2 arc seconds

FINE POINTING - Performed on dark side of Earth onlyON AXIS - MOT optical axis coincident with fine error sensor null axis

Pitch	+0.03 arc seconds
Yaw	+0.15 arc seconds
Roll	+3 arc minutes
Star Magnitude	10th magnitude or brighter
Maximum duration	10 half-orbits

OFF AXIS - MOT optical axis has angular offset from fine error sensor null axis

<u>Absolute Pointing</u>	
Pitch, Yaw	+0.2 arc seconds
Roll	+30 arc seconds
<u>Stability and Repeatability</u>	
Pitch, Yaw	+0.01 arc seconds
Roll	+4 arc seconds
Star Magnitude	+11 to +13
Maximum Duration	10 half-orbits

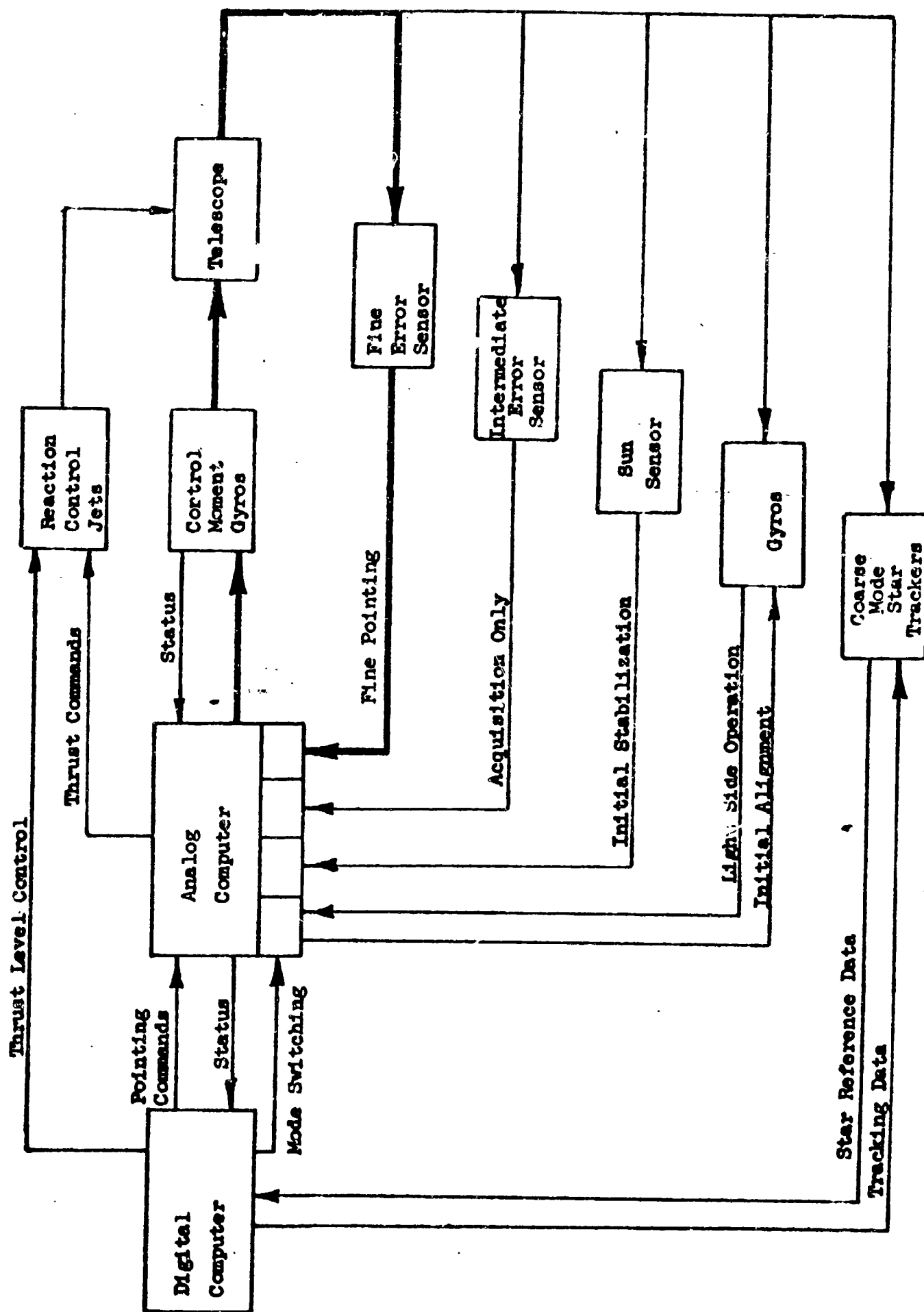


Figure 5.4-3

ATTITUDE CONTROL FUNCTIONAL DIAGRAM

it. It provides automatic stabilization of MOT residual angular rates upon separation from the booster. It provides control through the initial rendezvous with the MORL. During these periods, the gyro reference system and the reaction jets are used. After rendezvous, a stellar reference is acquired through a programmed roll search procedure to establish the coarse pointing mode in which the attitude reference is obtained from star trackers and control torques are generated by control moment gyros. In this mode, the MOT may be reoriented to any predetermined celestial attitude with an accuracy of 3 arc minutes.

An intermediate star tracker is required to permit transition from the spacecraft coarse pointing mode to the fine pointing mode. A direct transition from the coarse to fine pointing modes would require a highly accurate coarse pointing mode, with attendant penalties on spacecraft thermal and structural design, and would require a very wide linear range on the fine pointing sensor. The intermediate pointing sensor should employ its own small (6- to 12-inch diameter) objective and be independent in operation of the main telescope, but boresighted to it. Attitude hold is maintained by the intermediate pointing sensor reference until suitably low pointing errors and error rates are achieved, at which time the control is switched to the fine pointing sensor.

A gyro reference package provides the required inertial reference during occultation of the fine pointing sensor. Large angle slews will also be accomplished with this gyro reference system and the CMG's. During the coarse, intermediate, and fine pointing, the MOT is controlled by torques generated by a control moment gyro. These modes involve holding inertial attitudes over long periods of time, during which the effects of external disturbances must be countered. The CMG's will counter them over a single observation period (one-half orbit) but over a longer period of time will require desaturation. This will be provided by a low thrust reaction jet subsystem.

An additional function required in the detached mode is the docking of the MOT to the MORL for major repairs or refurbishment. This will be accomplished using the gyro reference system and the reaction jets. The MORL-based crew will command the MOT to perform the docking. The angular degrees of freedom will use rate command loops, the linear degrees of freedom will use acceleration commands. All the above items except the fine pointing are felt to be within the state of the art; consequently, most of the analyses were restricted to that mode.

As a result of the program midterm recommendation for a completely detached MOT, a control philosophy was adopted which favored a high static accuracy and low bandwidth.

For the purpose of conceptual design of the attitude control system, the 0.01 arc sec performance requirements derived from study of the desired experiments were assumed. A nominal apportionment of the total error allowed 0.001 arc seconds each for electronics null offset, sensor mechanical and electrical null offset, and error equivalent due to sensor noise. The remainder of the allowable errors are allotted to residual control equipment inaccuracies and overcoming the disturbances to the system. Since the system as conceived exhibits a steady state offset that is proportional to the input torque disturbance, a high gain is required to minimize this error. A low bandwidth was desired to minimize the high noise levels inherent in high response systems and interactions with the vehicle bending mode frequencies. The final bandwidth chosen was 10 radians/second. To obtain the low response, high gain system, an elaborate lag compensation network was required. For the fine pointing mode the studies indicate the control moment gyro to be more suitable than

inertia wheels or reaction jets for the bandwidth selected. Twin rotor, single-degree-of-freedom control moment gyros were selected as torquers for the study, because they offered the best probability for demonstration of control system feasibility. With a twin CMG for each axis, the gyroscopic cross coupling inherent in a single gyro system is eliminated. Also the twin CMG approach is suitable for the advanced design concepts utilizing brushless gimbal torquers and internal eddy current damping.

Two basic sensor types have emerged as desirable for the MOT fine pointing sensor. These are a null-type sensor using photomultiplier detectors capable of a very narrow linear transfer function range, and an image tube sensor using an image orthicon detector with a wide linear transfer function range, and serving the dual role of spacecraft control sensor and TV pickup for visual observation. The specific sensor requirements vary with the observational programs, but the overall similarity in basic sensor characteristics is great. In many cases the same sensor type with minimum modification will be adaptable to several observational programs.

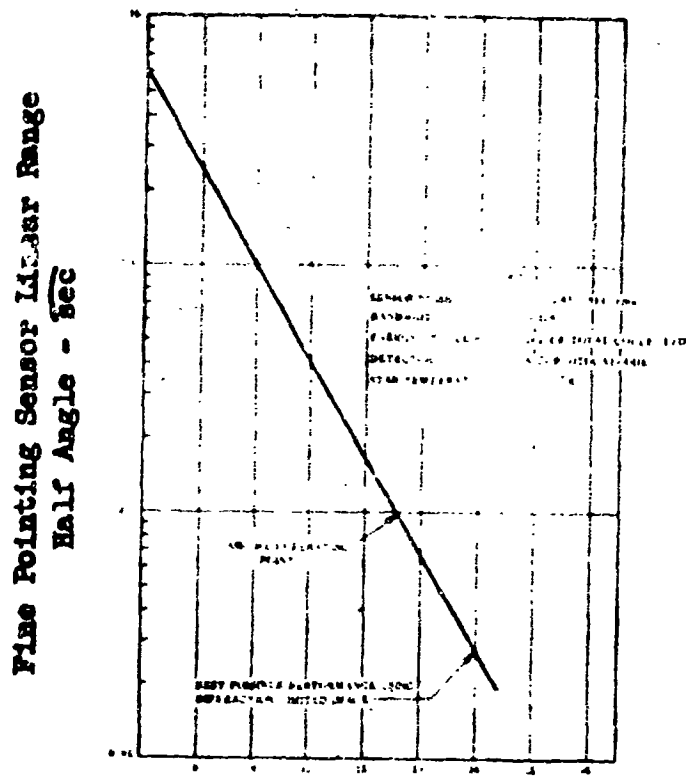
An estimation of the MOT fine pointing sensor characteristics for the 1975 time period has been made. Figure 5.4-4 summarizes the results for a null-type sensor employing a photomultiplier detector. For the conditions specified, guide stars brighter than 12.5 visual magnitude are suitable for a sensor linear range of 0.1 seconds of arc. This is based on an off-axis star, for on-axis stars where light sharing is necessary, this reduces to 10-15", depending on the optimum light sharing ratio between the experiments and the fine error sensor. The effect of using a guide star of higher magnitude is to increase the sensor noise for the same linear range. This nominal combination was considered the best compromise between control system performance and availability of guide stars to permit off axis pointing to any location in the celestial sphere.

Analysis

A considerable amount of analysis was performed on the disturbance environment for the MOT. The external disturbances contribute mainly to determining the size of the required control hardware. For example, the comparison of the relative external disturbance torque impulse as a function of vehicle size, is shown in Figure 5.4-5. This illustrates the smaller momentum storage requirement and therefore the smaller momentum transfer devices required by the separated MOT, a factor to be minimized for minimum internal disturbances.

Unless counteracted, the internal (i.e., crew motion) disturbances in the attached mode will induce pointing errors larger than permissible. Since these disturbances may be applied rapidly, they require a fast acting control system to counteract them. One method of minimizing these disturbances is to gimbal the MOT. Even with frictionless gimbals, offset between the CM and gimbal axis will cause disturbances which in turn require large control bandwidths as shown in Figure 5.4-6. An exception to the above is the soft gimbal mode which replaced the floating socket mode in an attempt at a simple solution to the station keeping problem without introducing appreciable crew disturbance coupling.

Knowledge of the disturbance environment permits the synthesis of a system to satisfy the requirements. The actual performance of such a system cannot be analytically predicted however, because the system non-linearities normally determine this performance. An analog simulation was thus resorted to as described in the following section.

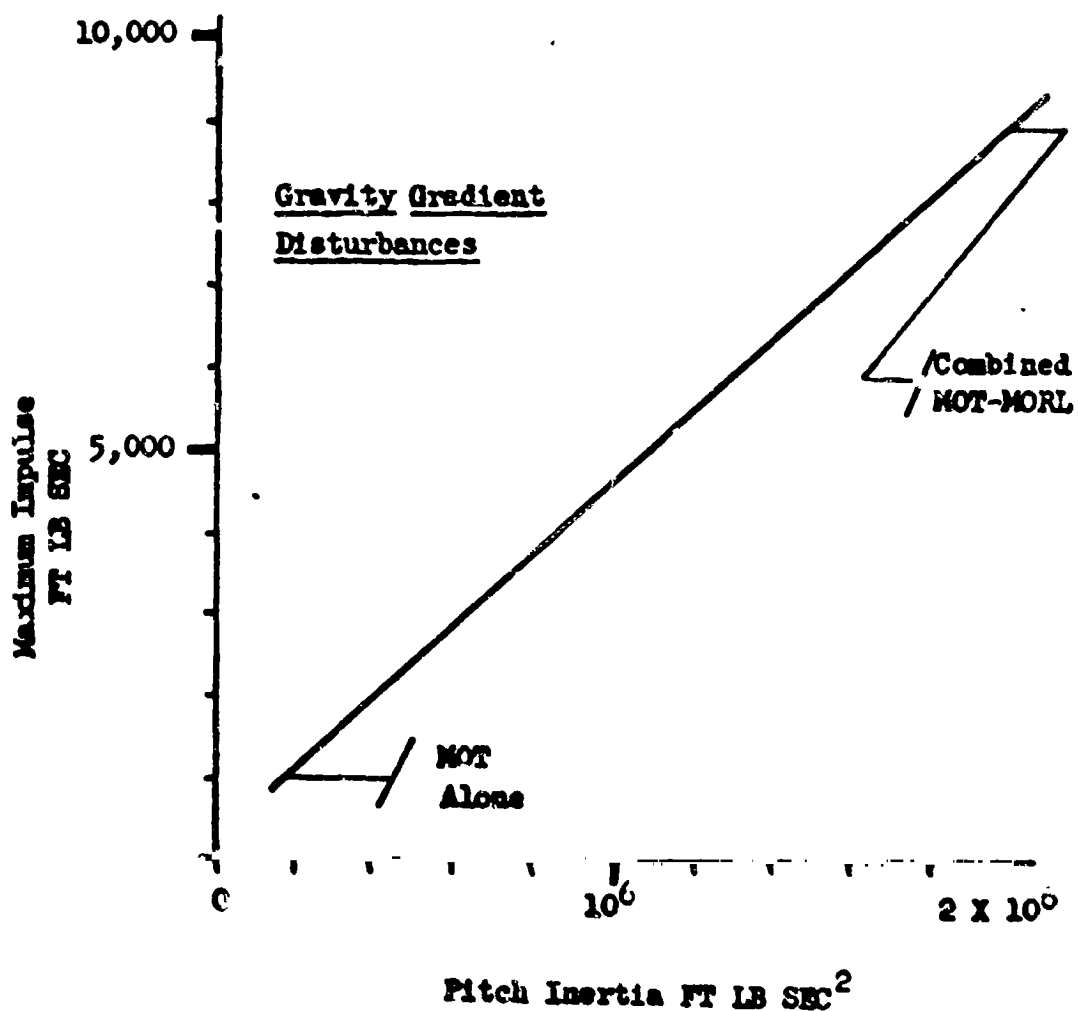
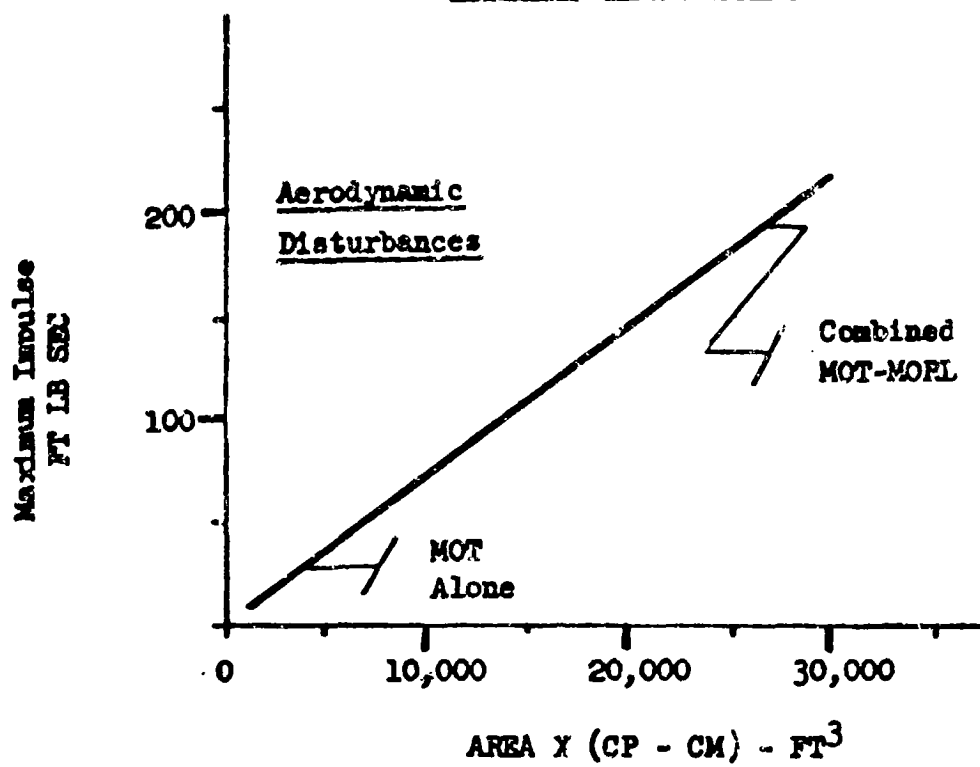


Limiting Guide Star Magnitude

Figure 5.4-4

PHOTOMULTIPLIER FINE POINTING SENSOR

EXTERNAL DISTURBANCES



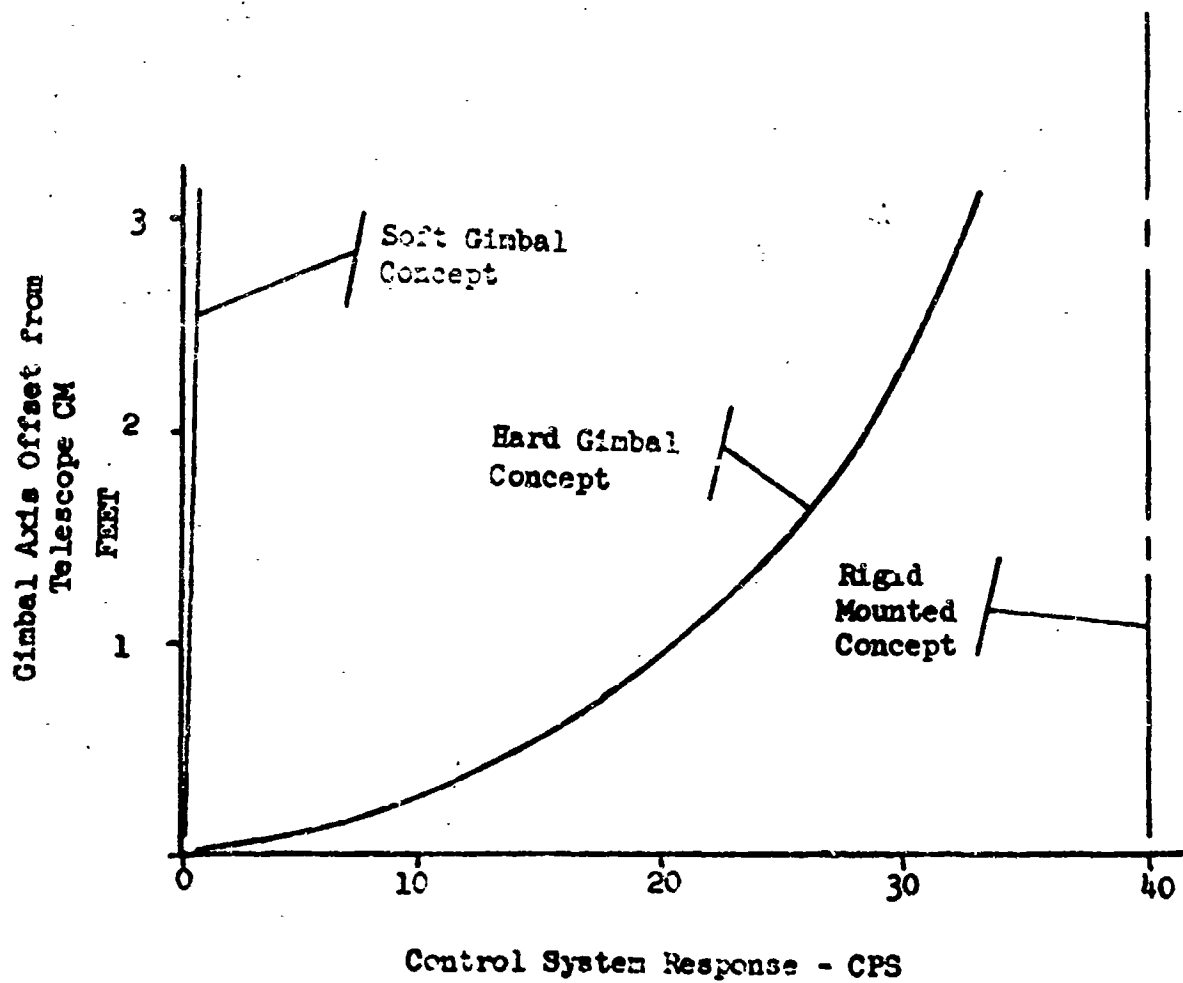


Figure 5.4-6

CONTROL FREQUENCY REQUIREMENTS

Performance Verification

In accordance with the desire for conclusive proof of feasibility, an in-depth servo elastic study of the fine pointing attitude control loop concept was accomplished. This included a computer simulation of the loop complete with component non-linearities and the flexible vehicle transfer function.

Computer simulation was limited to the study of the fine pointing since coarse and intermediate pointing are essentially state of the art. The simulation demonstrated the feasibility of attaining better than the 0.01 arc sec stability. These studies indicated that the major error source was due to the CMG gimbal friction. This quantity causes a characteristic oscillation in the system. The amplitude of this oscillation can be diminished by increasing system bandwidth (thus the increase from the original 1 rad/sec bandwidth). Figure 5.4-7 shows some typical results from this study. They indicate the worst case oscillation is ± 0.007 arc sec, while the effects of sensor noise and external torques tend to reduce the oscillation amplitude. This is due to their linearizing effect on the CMG. The effects of disturbances and noise will be beneficial only so long as the basic error they induce is less than the friction induced oscillation. This is shown in Figure 5.4-8. The reason that the noise initially increases performance is that it acts as a dither on the CMG gimbal. This dither essentially reduces the effect of the stiction by keeping the gimbal continuously in motion. The reason that external disturbances initially increase performance is that the CMG must continuously precess to absorb the disturbance momentum. This motion makes the frictional effect only a steady offset, the value of which, for low level disturbances, is rather small. An important item in the latter case is that the disturbances vary sufficiently slowly, external disturbances such as gravity gradient and aerodynamic torques qualify, internal disturbances such as crew disturbances do not. As expected, biases from control components cause the control limit cycle to be unsymmetrical about null. It should be noted that the value of CMG gimbal friction (0.05 oz m) used in the simulation was approximately twice the value considered to be achievable.

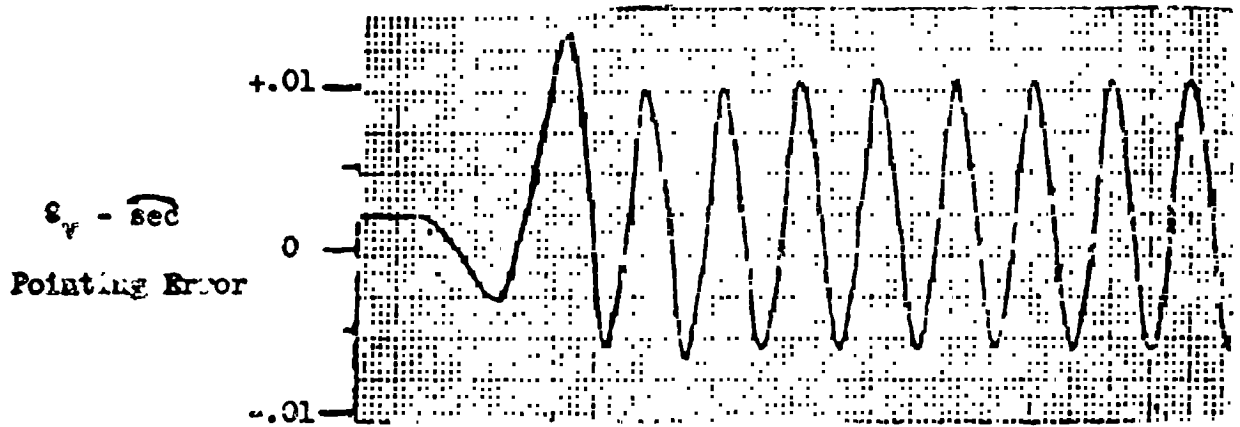
Man's presence will be an invaluable aid in carrying out certain attitude control tasks for the MDT. Man's role in fine pointing breaks down logically into two categories--those functions he will perform at the telescope, and those he will perform remotely. His functions at the telescope involve mainly maintenance, setup and subsequent coarse realignment. The remote functions of man include both equipment fine alignment and target acquisition. The alignment of the fine pointing sensor to the scientific instrumentation and telescope must be done to within a few hundreds of an arc second (spectrometry). This alignment will have to be made and checked frequently, hence it is a function for which man must become adept. Man will also participate remotely in the observational program. For example, in planetary spectrometry it will be necessary for man to orient the telescope to selected portions of the planet with higher precision than can reasonably be achieved with an automatic system.

Conclusions

A general conclusion derived from this study is that, disregarding the absolute pointing, it is feasible to stabilize the telescope to within 0.01 arc seconds. If, in addition, it is desired to point the telescope within 0.01 arc seconds of a particular star, this is feasible based on light sharing of that star. In like manner, it has been shown feasible to point the telescope to any arbitrary direction to

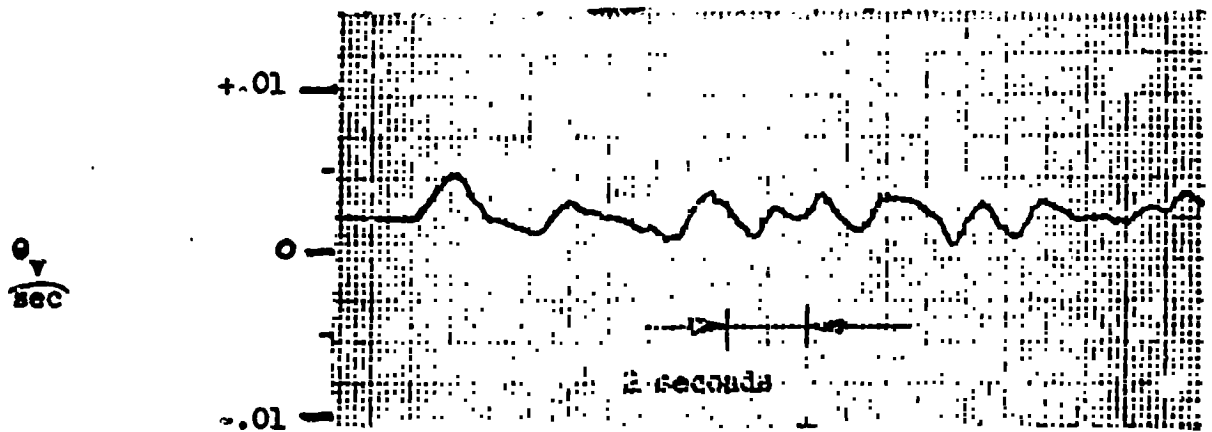
PREDICTED PERFORMANCE *

Without Sensor Noise or
External Disturbances



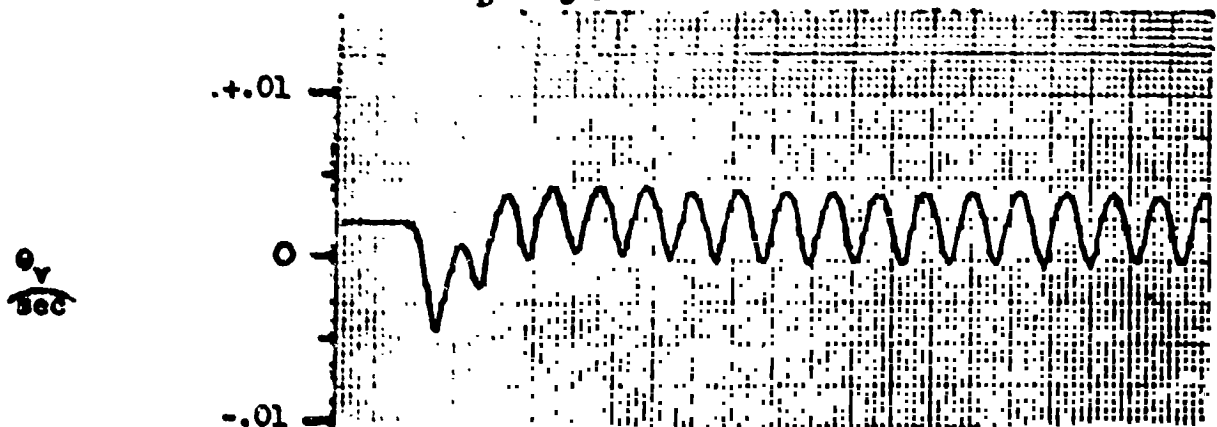
With Sensor Noise

$$\theta_n = .005 \text{ sec}$$



With External Disturbances

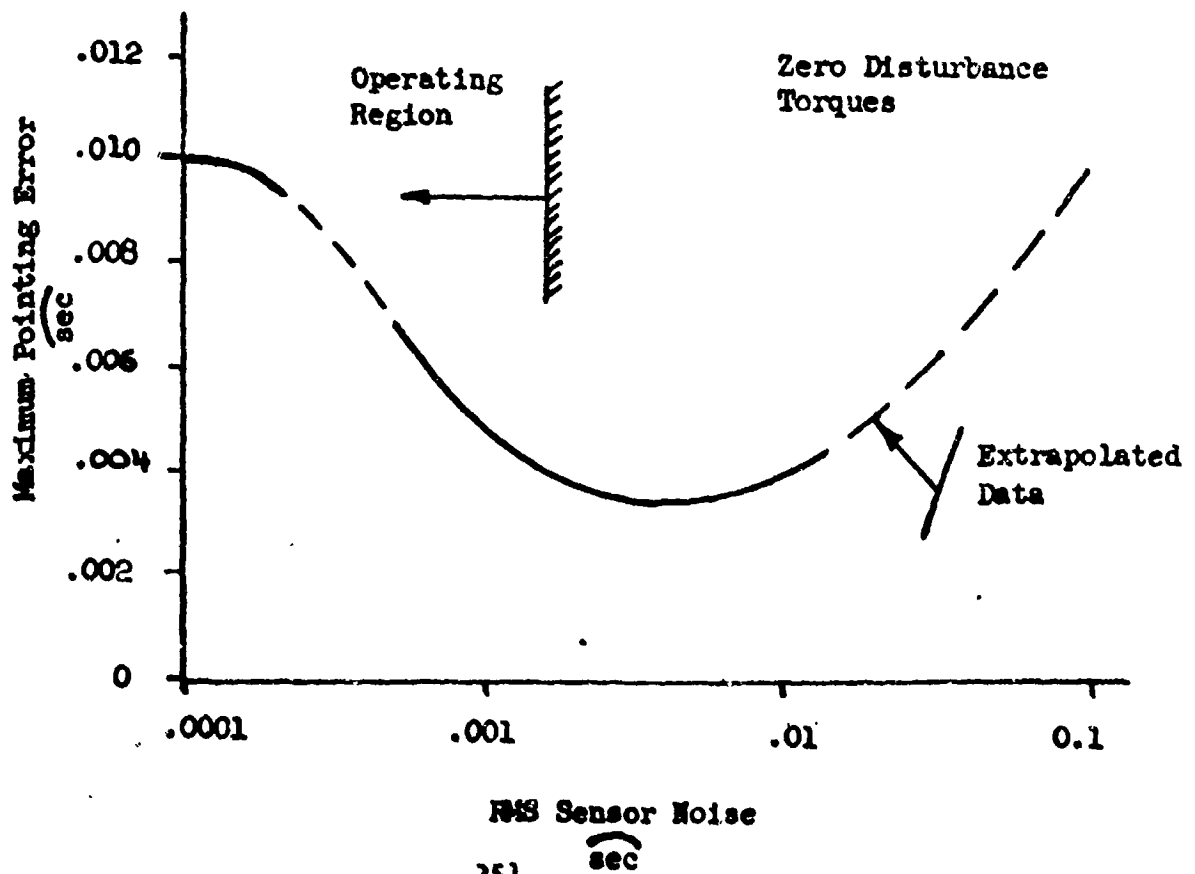
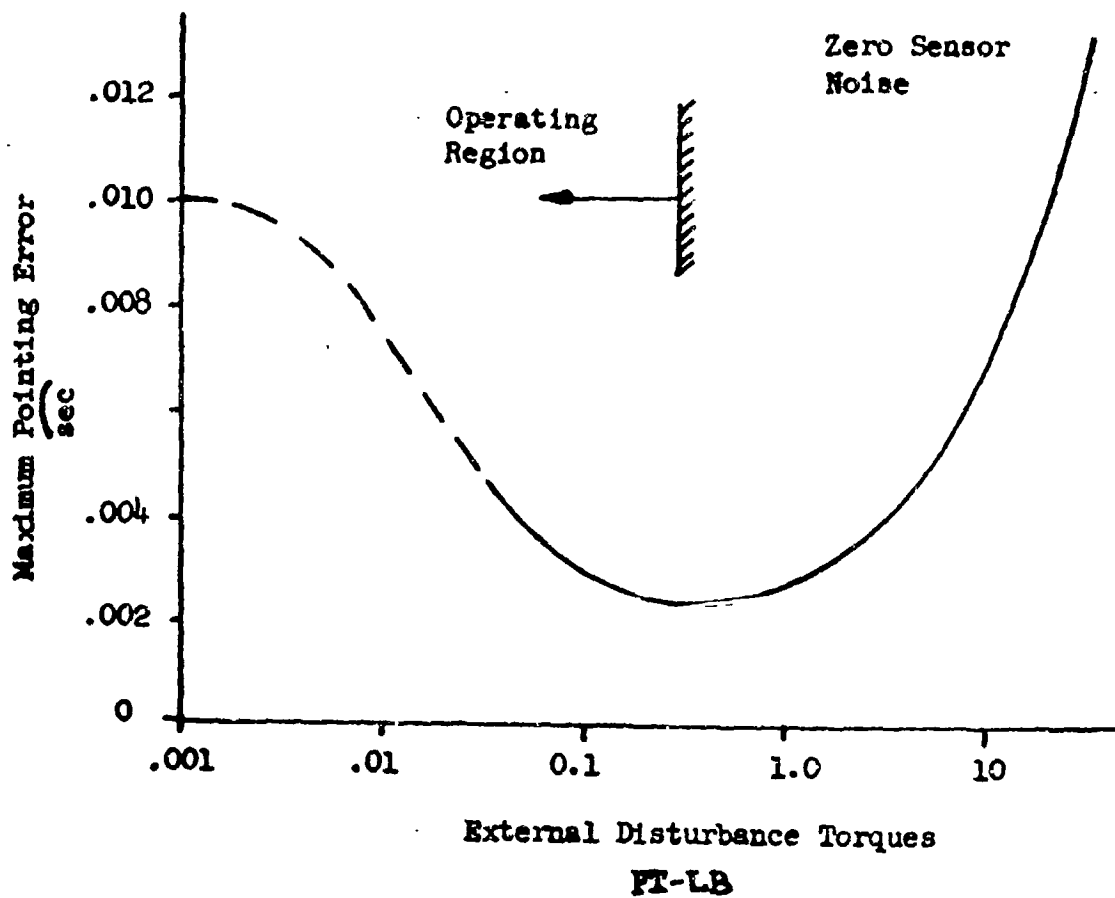
$$T_D = .03 \text{ FT LB}$$



* with .05 in oz gimbal friction

D2-84042-1
Figure 5.4-8

PARAMETRIC POINTING PERFORMANCE



within 0.2 arc second. In addition to proving feasibility, a substantial amount of performance trade data was developed, and, to a limited extent, used in this study.

A high probability of feasibility has been determined for the soft gimbal concept. Present studies indicate a pointing error of about 0.003 arc second greater than that of the detached mode.

All fine pointing sensors should share the primary telescope collecting aperture with the scientific instrumentation. This is necessary not only to provide sufficient light gathering power and small diffraction pattern images, but also because it would be an extremely complex task to boresight separate telescopes to the required accuracy and maintain this alignment for extended periods of time. The fine pointing sensor design should not rely on diffraction limited images for diffraction limited operation of the main telescope. This is a necessary condition for those observational programs where the sensor is offset a significant distance from the telescope axis.

The best present day detectors (highest detectivity) for the fine pointing sensors use an S20 response photoelectric cathode in the form of photomultipliers or image orthicon detectors. Significant improvement in detectivity, particularly in the image-type detector, can be expected in the next ten years. A solid state analog of the photomultiplier is currently in development and offers promise of detectivity improvement by a factor of two or three. Assuming minor advances in these detectors, the basic technical feasibility of providing fine pointing sensors to meet the scientific objectives of MOT has been established. There are no fundamental problems related to sensor development that will compromise telescope/instrumentation performance.

The most likely control system torquer is the control moment gyro. It emerges on top due to its inherent mechanical torque gain and small size, weight, and power. These, in turn, enable it to be constructed with extremely large dynamic ranges in its output torque (easily over one thousand to one).

Recommendations

A very important area of required activity involves the breadboard fabrication of the fine pointing sensors and control moment gyros. These items must be built and laboratory tested to provide the experimental data to keep the analytic studies realistic. The present state of knowledge as to their realistic characteristics is not adequate, and since these items are by far the most critical in the control system, this program is very important.

A complete analysis of the MOT-MORL soft gimbal control system taking into account the active non-linear control system must be performed to further demonstrate feasibility of this concept. This concept is very promising since changes in the soft gimbal concept may be made to enhance the control system feasibility (e.g., addition of a roll gimbal or softer springs).

The trades existing between subsystems have made it apparent that the final design criteria for the MOT will emerge only after repeated iteration of the scientific program, scientific instrumentation, fine pointing sensors, control loop, and all other facets of the spacecraft. Closely associated is the need for a detailed definition of the observational program, including the consideration of the

subsystem capabilities developed in this program.

The fine pointing sensor study discovered several areas of fruitful further study on the sensor problem.

- 1) Thermally induced structural/electronic instability.
- 2) The in-orbit optical alignment of sensors to the scientific instrumentation and telescope.
- 3) The conflicting sensor requirements of large linear range for acquisition and narrow linear range for tracking.
- 4) Very accurate image motion compensation techniques (introduced at spacecraft or scientific instrumentation) must be developed for planetary observations.

5.4.2 Requirements

The main functional modes of operation required of the MOT attitude control system are rendezvous, orbit and station keeping, docking, maneuvering and target acquisition, and fine pointing.

Rendezvous

Attitude control is required during the initial rendezvous of the MOT with the MORL. Coarse attitude control (-0.5 degree) is required during the propulsion phase of this maneuver, which is 380 feet per second of incremental velocity. The active propulsion phase will last only a few minutes followed by a long coast period.

Orbit and Station Keeping

During the detached mode, the MOT and MORL will tend to separate due to differences in their ballistic coefficients. Since it is desirable to maintain their separation within one mile, the vehicle whose orbit is decaying faster will be continuously station kept. Eight hours is estimated as the minimum time between these orbital corrections. Low performance attitude control must be maintained during these corrections to insure the proper inertial orientation of the resultant velocity correction vector. In the attached modes, the orbit keeping is assumed to be exclusively a MORL function.

Docking

In the detached mode, it will be necessary to dock the MOT to the MORL for major repairs or refurbishing about fifteen times per year. It is required that the MOT perform the actual docking since it is the lighter vehicle. This docking is anticipated to be controlled by the MORL crew commanding the MOT attitude and orbit control subsystem. The MOT control authorities must be suitable for the pilot to remotely perform the docking function. Although most of the data on this subject available to date is with the pilot in the maneuvered vehicle, it is expected to be applicable. This is due to the ability of the pilot to work with very low control authorities, and at these levels, his own physiological feedbacks are negligible. The required uncoupled control authorities are thus

Linear Acceleration = 0.1 ft/sec^2

Angular Acceleration = 1 deg/sec^2

Maneuvering and Target Acquisition

To permit accomplishing the observational program, the NOT must be maneuvered to any desired orientation in the celestial hemisphere facing away from the Earth-Sun line of sight. A maneuver and acquisition time of two minutes for 5 degrees is required. Time for larger angle maneuvers is not as critical because they will be infrequent and during light side operation. The small angle acquisition time is critical however, since this may occur on each orbit.

Fine Pointing - Observational Program

The basic requirement of the NOT attitude control system is to provide a stable platform that can be oriented precisely to any portion of the celestial sphere with the pointing and stability performance required by the astronomical observations. Fine pointing requirements for each of the observational programs will be discussed in the following paragraphs. These requirements vary widely, depending on the observation being made. They are summarized in Figure 5.4-9. A definition of spacecraft and instrumentation axes are given in Figure 5.4-10 as they apply to Figure 5.4-9. A rotation about the spacecraft pitch axis corresponds to a wavelength change of the spectrometers. The yaw axis is perpendicular to the wavelength sensitive axis of the spectrometer, and the roll axis is coincident with the telescope optical axis.

Two basic ground rules were defined for the scope of the NOT observational program. First, it should be extremely versatile so that observational programs conceived at some later date may reasonably be implemented, and second, the primary observational programs should be limited to those that cannot be accomplished by ground based observatories, or at least, can be done far better in orbit. This does not exclude the possibility, however, that certain measurements will be made (e.g., high dispersion spectrometry in the visual region) to compare NOT performance against ground measurements if these experiments do not impose major design constraints.

Within these guidelines, an outline of observational programs has been formulated. Specifically, the six observational programs that have been defined will constitute perhaps 90 percent of total observational time. These are:

- o High dispersion stellar spectrometry
- o Photometry and polarimetry of stars and extended sources
- o Low dispersion spectrometry of stars and extended sources
- o Stellar photography
- o Planetary photography
- o Planetary spectral and total radiance measurements

Mission Requirement (1)	High Dispersion Stellar Spectrometry	Low Dispersion Stellar Spectrometry (2)	Photometry and Polarimetry	Stellar Photography	Planetary Photography	Planetary Spectrometry
Absolute mean pointing accuracy Pitch Yaw Roll	± 0.01 ± 0.1 None Required	± 2 ± 2 ± 30 (3)	± 0.2 ± 0.2 ± 30 (3)	± 10 ± 10 ± 180	± 10 ± 10 ± 180	± 0.05 to 0.1 ± 0.05 to 0.1 ± 180
Repeatability of initial pointing direction for succeeding orbits	Within above tolerance up to 10 orbits	Within above tolerance for up to 10 orbits	Within tolerance above for 5 to 10 orbits	Pitch & Yaw ± 0.01 Roll ± 4	None-Limited by planet rotation rates	Not determined. Man in loop. Usually one or-bit only. Spot tracking required
Pointing Stability Pitch position 70% of time 95% of time Yaw position 70% of time 95% of time Roll position 95% of time (or equivalent roll rate over 30 minutes of time)	± 0.02 ± 0.03 ± 0.1 ± 0.15 ± 180 from initial position	± 0.2 ± 0.3 ± 0.2 ± 0.3 ± 30 from initial position (3)	± 0.2 ± 0.3 ± 0.2 ± 0.3 ± 30 from initial position (4)	± 0.01 ± 0.01 ± 0.01 ± 4 from initial position at start of each orbit	± 0.01 ± 0.01 ± 0.01 ± 15 from initial position	± 0.05 to 0.1 ± 0.05 to 0.1 ± 0.05 to 0.1 ± 15 from initial position
Magnitude of Guide Star	± 10 or brighter	± 13 or brighter	± 13 or brighter	± 11 or brighter	± 11 or brighter	± 12 or brighter
Comments	Limiting star magnitude will be determined by scientific instrumentation; ± 10 is assumed as guideline. Guide star & exportment star are one and the same.	14th magnitude stars desirable if permitted by acquisition considerations	14th magnitude of guide star desirable	11th to 12th magnitude stars desirable to permit greater experimental program flexibility	11th to 12th magnitude desirable to minimize main telescope field of view for off-axis pointing	A unique requirement is that the location of the actual pointing direction of the telescope axis to be determined to 0.05 to 0.1 arc sec. Man in loop

1. Angular values specified in arc seconds.

2. This experimental program has pointing requirements that are a compromise of high dispersion spectrometry for bright experiment stars (tenth, eleventh magnitude) and photometry/photometry for the stars fainter than fourteenth to sixteenth magnitude. Characteristics of scientific instrumentation will dictate pointing requirements. Estimates at this time are: tenth magnitude - 0.05 ; twelfth magnitude, 0.2 ; fourteenth magnitude - 1.0 ; sixteenth magnitude and fainter - 2.0 . Roll axis control requirements are dependent on above. Typically, will not be more stringent than photometry/photometry. The values specified in the table apply to the case where offset pointing is used.

3. These quantities can be traded if desired, the important consideration being the sum should not exceed ± 60 arc sec.

Figure 5.4-9
FINE POINTING REQUIREMENTS

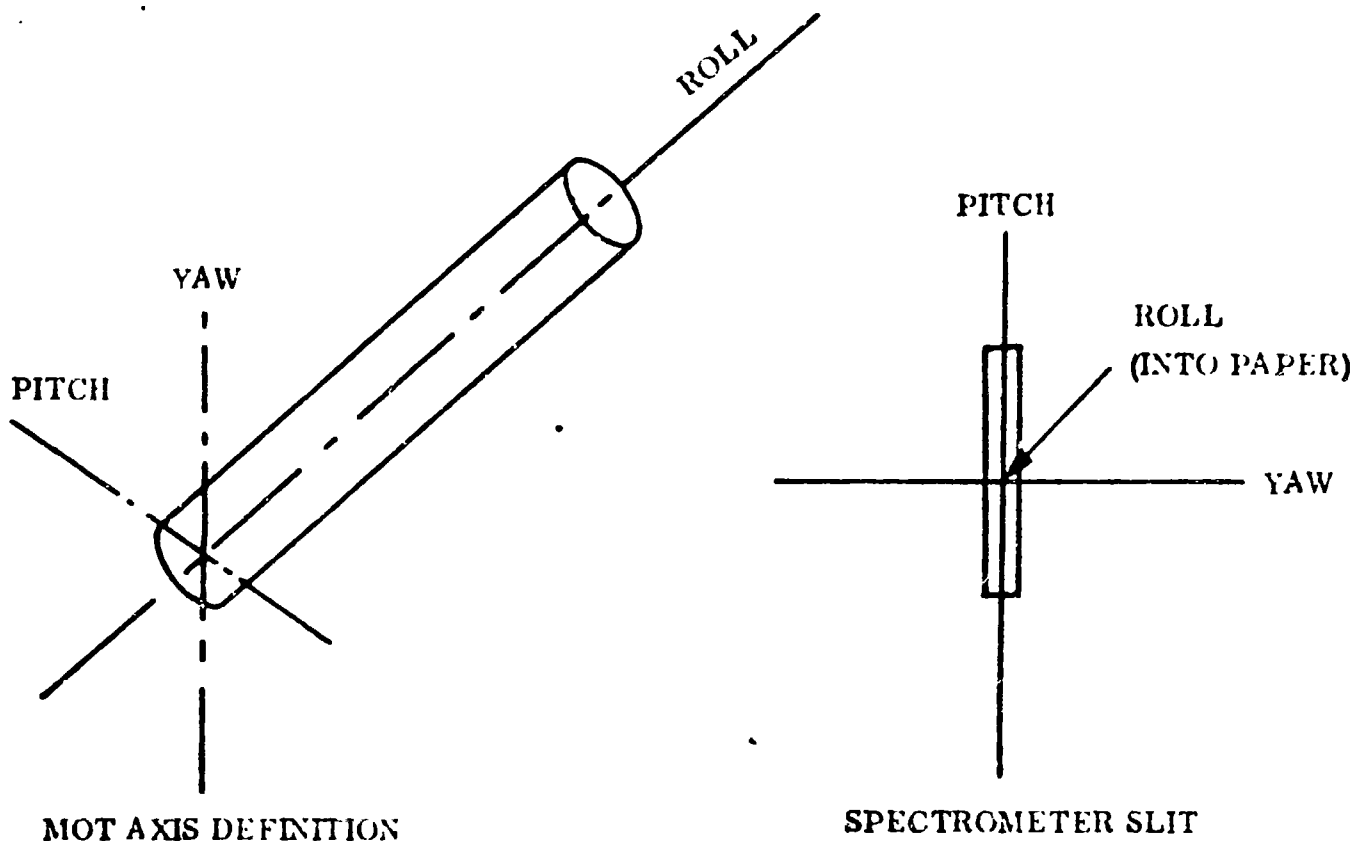


Figure 5.4-10

MOT AXIS DEFINITION

That these requirements vary down to ± 0.01 arc second emphasizes the importance of the attitude control problem. In the following paragraphs the source of these requirements are described.

High Dispersion Stellar Spectrometry

High resolution measurement of stellar spectra is a fundamental requirement for MOT because of the inherently high resolving power and large wavelength coverage of the 120-inch diameter diffraction limited telescope. Observation will generally be limited to stars of tenth visual magnitude or brighter and would use the f/30 telescope configuration. The total f/30 field-of-view will be limited to a few minutes of arc by mirrors used to fold the beam. The principal wavelength interval of interest is the vacuum ultraviolet (1000 \AA) to the intermediate infrared (few microns).

The very wide wavelength region of coverage will require a variety of spectrometers each capable of having detectors and gratings changed. Detectors will include film, photoelectric devices, and supercooled photoconductors and bolometers.

The Airy disk of a diffraction limited 120-inch aperture has a size of about 0.01 arc second at 1000 \AA and one arc sec at 10 microns. Since the entrance slit of the spectrometer is used to define the angle of incidence to the grating, it should be on

the order of the Airy disk in width at the wavelength being monitored. This imposes an absolute pointing accuracy on the order of 0.01 arc second worst case. Angular instability in excess of this figure will not degrade the data with this small entrance slit, but imposes longer observation time to compensate for time lost in not "filling the hole." Since it is not practical to check for correct exposure continuously (at least with film), a knowledge of actual exposure time is needed. This implies both an absolute pointing accuracy and stability of about 0.01 or 0.02 arc second worst case. A second consideration is that even if it were possible to monitor exposure continuously, it is desirable to always keep the entrance slit filled because of the very long exposure times required.

Control of the spacecraft attitude with respect to image motion along the length of the spectrometer slit (perpendicular to the wavelength axis) is less critical than along its width. Some motion of the image (~ 0.1 arc sec) along this axis is actually desirable when using film in order to elongate the spectra, but this also increases exposure time. Accurate roll position control is not particularly significant, and could be dictated by other observational programs. Rate control of this axis could also be employed.

A summary of the fine pointing requirements for high dispersion stellar spectrometry is as follows:*

Absolute Mean Pointing Accuracy, Up to 10 Orbits

Pitch	± 0.01 arc second
Yaw	± 0.1 arc second
Roll	None Required

Pointing Stability

Pitch Position	70 percent of time ± 0.02 arc second
	95 percent of time ± 0.03 arc second
Yaw Position	70 percent of time ± 0.1 arc second
	95 percent of time ± 0.15 arc second
Roll Position (or equivalent roll rate)	95 percent of time ± 180 arc second from initial position

The faintest star for which these requirements apply will depend on the practical energy limited resolution of the spectrometer, and the ratio of energy sharing between the experiment and fine pointing sensor. These more detailed studies have not yet been accomplished, hence no firm basis exists for establishing the faintest star at this time. For working purposes it was assumed to be about the tenth magnitude, although this probably is conservative. For fainter stars, reduced pointing accuracy and stability can be permitted, because the spectrometer will be energy limited for reasonable exposure times, and wavelength resolution must suffer.

*These are worst case conditions, taken at the shortest wavelength. At longer wavelengths, the Airy disk is correspondingly larger, and greater instability can be permitted without degrading resolution

Low Dispersion Spectrometry of Stars, Galaxies, and Nebulae

This experiment is similar to the high dispersion spectrometry previously described, except that in this case the amount of energy from the fainter objects will not be sufficient to permit measurement of spectra with high wavelength resolution. The spectra of objects as faint as the eighteenth to twentieth magnitude would be measured. The wavelength resolution will vary with star magnitude, star temperature, and the wavelength region being examined. The total wavelength region of interest will cover the vacuum ultraviolet to far infrared.

The total observation time for a single star may vary from a fraction of an orbit to many orbits, thus reacquisition is required. The f/15 telescope configuration would be used. Low resolution spectral measurements will constitute 15 to 20% of total observation time.

It is clear that the pointing requirements for these low dispersion spectra measurements will vary widely. The transition from high-to-low dispersion measurements is not abrupt even though we have classified it as such. If, for example, a pointing stability of 0.01 arc sec is required for high resolution for a ninth magnitude star, then at 11.5 magnitude (low dispersion work), a pointing stability of about 0.1 arc sec should be provided. This factor is very important in determining the optimum light-sharing ratio. On very faint objects, pointing accuracy and stability will be limited by the desire to minimize the spectrometer entrance slit size to avoid noise background problems, rather than from considerations of resolution degradation due to image motion. The net result of these considerations is that the requirements for spacecraft pointing accuracy and stability cannot realistically be established until the expected performance of the spectrometers is evaluated as a function of star magnitude and temperature. As a working figure, one should consider always filling the spectrometer slit for slit sizes of the following:

- o Tenth magnitude - 0.04 arc sec
- o Twelfth magnitude - 0.1 arc sec
- o Fourteenth magnitude - 1 arc sec
- o Sixteenth magnitude or fainter - 2 arc sec

It is obvious that many of the experiment objects will be too faint to permit their use as a guide star. In this case, offset pointing of a brighter guide star will be required. A preferred roll axis attitude and roll axis control will thus be required for the fainter stars, e.g., the thirteenth magnitude or fainter. The general range of the control requirements is calculated to be about $3/4$ arc min based on image motion of less than 0.1 arc sec for the experiment star. This is several times less stringent than that required for the photographic observations, hence not critical. Roll rate control would be equally suitable, rates up to 0.01 degrees/hour would be satisfactory.

Photometry and Polarimetry of Stars and Extended Sources

Broadband photometry and polarimetry will constitute approximately 5 percent of the observational time and will be performed at f/30. Primary emphasis now is on the UV and visible region where photoelectric detectors can be used. The capability of covering the near and immediate IR may be desirable. The total observational

time per star or other object would be as long as 5 to 10 orbits. Fine pointing requirements are similar to those of low dispersion spectrometry--it is only necessary to position and maintain the source image in the instrumentation field stop aperture.

The field stop size can be arbitrarily selected since its sole function is to limit the instrumentation field-of-view to minimize background noise input. Ideally it should be sufficiently small to exclude companion stars and to make background corrections unnecessary except for the extremely faint objects. On the other hand, if the aperture stop is made too small, a very difficult fine pointing requirement would exist for both absolute pointing direction and stability. A field stop size of perhaps 2×2 arc sec would seem to be a suitable compromise, leading to a pointing requirement of perhaps $\pm 1/2$ arc sec. The actual field stop will be remotely variable over a wide range of values. An aperture smaller than a two-arc sec diameter is required for remotely calibrating the fine pointing sensors to remove fixed bias errors. A larger aperture will be required when viewing objects of extended size.

On the brighter objects, it may be possible to reduce the aperture size to perhaps a one-arc diameter to take full advantage of the high pointing stability with the brighter sources.

As in the case of low dispersion spectrometry, many of the stars to be observed will be sufficiently bright (e.g., thirteenth to fourteenth magnitude) to permit direct guidance on the guide star. Others, however, may be as faint as the eighteenth to twentieth magnitude, and will definitely require offset guidance on a star other than the experiment star. An auxiliary pointing requirement for this application is that the telescope be capable of being off-set a few seconds of arc to an adjacent part of the sky to permit a check of the detector zero (background). This looking-at-nothing may require one or more orbits (depending on the magnitude of the experimental star) and hence constitutes a definite offset guidance requirement.

Noise background seen by the telescope emanates from several sources. These include the emissions of the upper atmosphere, the galactic and zodiacal light, and the extremely faint star background. The last three of these sources are reported to have an equivalent total radiance of between 2×10^{-11} to 5×10^{-11} watts/cm²-steradian, with the bulk of this energy in the visible portion of the spectrum. Assuming a uniform background, this corresponds to an irradiance of approximately three times 10^{-21} watts/cm² per (arc sec)² field of view. This is approximately equivalent to the power received from a +23 visual magnitude star.

The spacecraft fine pointing requirements are derived from the desire to operate the experiment star on-axis to minimize its size due to telescope aberrations. This implies the guide star will be off-axis, hence position control about the spacecraft roll axis will be required. The maximum angle off-axis that it will be necessary to work depends on the limiting guide star magnitude for which the required spacecraft stability can be maintained. The approximate half-angle field-of-view required for 100 percent sky coverage for a given limiting star magnitude determined by star population charts is:

- a. Twelfth magnitude - eleven arc min
- b. Thirteenth magnitude - eight arc min
- c. Fourteenth magnitude - six arc min

If the limiting magnitude determined by the fine pointing sensor is the eleventh or twelfth magnitude, the large offset angle may require the use of field correcting optics to obtain a suitable image size for guidance. The scientific instrumentation does not require these optics, and should not employ them. For the polarimeter, in particular, it is undesirable to insert any optical element that may increase the instrumental polarization.

Allowing a maximum pointing error of 0.1 arc sec at eight arc min off-axis due to an uncertainty in roll position permits a roll position uncertainty of about ± 20 arc sec and a maximum roll axis instability of about ± 30 arc sec. The combination of ± 60 arc seconds for position uncertainty and position instability can be apportioned other than on a 50/50 ratio if it is advantageous to do so.

A reasonable limit on absolute pointing accuracy and pointing stability are each about ± 0.25 arc sec in pitch and yaw, and approximately ± 30 arc sec in roll. These requirements hold for an indefinite number of orbits.

Star Field Photography

Two basic photographic missions are envisioned--wide angle (between $1/2$ and 1 degree total field) with the f/15 telescope, and narrow angle (perhaps 10 arc min total field) with the f/15 telescope. Both configurations would require field correcting optics. Observation will be made for one orbit or longer--possibly five or even more. The exposure time will be dependent on photograph purpose, and the limiting exposure time will depend on sky background noise or the failure in film time-intensity reciprocity.

Based on the above description of the stellar photographic mode, and the desire not to degrade the inherently high angular resolution possible with this diffraction limited telescope the pointing requirements become fairly obvious. With an image size on the order of 0.03 to 0.05 arc sec on axis, image position should be held to 0.01 arc sec maximum on the photographic plate on this region. This would hold for all astrometric work (small field) and over the central portion of the astrophysical work (wide field). At the outer edge of the wide angle plate, where image quality is degraded by telescope aberrations to something on the order of tenths-of-seconds, greater image motion can be tolerated. This affects roll control primarily, and indicates something near 0.05 arc sec image smear would be permissible at the edge of the field. Image smear would be proportionately less for stars near the telescope axis, and would be less than 0.01 arc sec for all stars in narrow field work. This requirement leads to a roll control stability of about six arc seconds, since

$$\theta_R = \frac{\text{angular smear}}{\text{field of view}} = \frac{(0.05 \text{ arc sec})}{(1/2 \text{ degree})} = 6 \text{ arc sec}$$

The limiting magnitude of the star to be used for control should be as faint as possible in order not to seriously restrict the observational program. Star population density charts show that near the galactic pole (worst case), an average of about two stars of the tenth magnitude or brighter will be present in a one

degree square field. This indicates that it would be desirable to have the capability of control with stars of at least the tenth magnitude, and then an eleventh to twelfth magnitude capability would be necessary to more effectively cover all regions of the sky with small corrected fields of view.

The requirement on absolute pointing direction about any axis is not critical, since it merely determines the starting point for the film plate. The absolute pointing accuracy will be determined by the total range of the fine pointing sensor, and hence should be held to about 10 arc sec or less for the axes controlled by the fine sensor, and about two or three arc min for the roll axis. Once a particular pointing direction is selected, however, it must be held very stable during all exposure time, and possibly repeated from orbit to orbit up to about 10 orbits depending on the film capabilities.

Planetary Photography

Photographs of the planets at the $f/30$ focus will be made. Mercury will not be accessible because of its close angular proximity to the Sun. Venus may be accessible for a few minutes per orbit during certain times of the year when Earth acts as a sun shield between sunset and Venus-set (or between Venus-rise and Sunrise). Total planetary photographic work will probably not exceed 5 percent of the total observation time of the telescope.

Depending on the speed of the film being used, and whether filters are being employed, exposure times will vary from tenths of seconds or seconds on the nearby planets to nearly a half-orbit for Pluto. Like starfield photography, the absolute direction of pointing is not critical, and generally can be 10 percent to 20 percent of film plate size—that is, about 6 to 12 arc sec for a one minute photographed field. To avoid image smear once the telescope pointing direction has been established and the camera shutter has been opened, stability with respect to the planet being photographed should be on the order of 0.01 arc sec, as with star field work.

Unlike starfield photography, where objects remain fixed in inertial space, all the planets are sufficiently near the Earth to have significant relative angular motion with respect to the stars. This motion is made up of two parts, parallax due to the motion of the telescope in Earth orbit, and the angular change induced by the relative motions of the Earth and the other planets in their solar orbits. Generally speaking, these quantities are comparable in magnitude and vary as a function of telescope position in Earth orbit and relative solar orbit position. Figure 5.4-11 shows the approximate magnitude of these two quantities when the Earth-planet distance is minimum. As is apparent from the Figure, a telescope attitude fixed with respect to the stars would limit exposure times by image motion to a few seconds of time for most planets, and even less for both Venus and Mars. Since ideal exposure time will generally exceed these figures, attitude control must always be referenced with respect to a point on the planet itself. The planets are extended sources, hence, roll axis control is required. Since the size of the planets is fairly small, the roll axis pointing requirement is less severe than for the star field photographic work. A roll stability of ± 15 arc sec will provide insignificant image motion due to roll motion of the telescope.

	VENUS	MARS	JUPITER	SATURN	URANUS	NEPTUNE	PLUTO	EARTH MOON
Angular size from Earth orbit (arc sec)	60	18	45	18	4	3	0.2	1800
Angular motion with respect to Stars $\left(\frac{\text{arc sec}}{\text{sec}}\right)$	Spacecraft Orbital		0.001	0.0005	0.0002	0.00015	0.0001	2
	Solar Orbital		0.005	0.002	0.001	0.0006	0.0005	1/2
Stellar Magnitude	- 4.4	-2.8	-2.5	-0.4	+5.7	+8.8	+15	-12.7
Relative Photographic Exposure Time Based on Planet Radiance ⁽²⁾	0.1	1	10	10	120	1000	1500	1
Maximum Exposure time (seconds), not to exceed 0.01 arc sec motion with respect to stars without image motion compen- sation	0.2	0.5	2	5	10	16	20	0.005
Maximum Exposure time not to exceed 0.02 arc sec smear due to planet axial rotation	3000	50	9	20	90	190	Half-orbit for axial rotation period greater than 16 hours	-

Notes: 1. All quantities are approximate for earth/planet distance at a minimum.
2. Relative exposure time based on providing equal energy per unit area at the film plate.

Figure 5.4-11

Planetary Spectral and Total Radiance Measurements

The concept of this experiment is similar to that being considered by NASA/Ames for a future OAO mission. Basically, the emission and reflection spectra of the principal planets (Venus to Saturn) would be measured over as wide a wavelength interval as possible (say 1 to 100 μ), with the smallest instantaneous field of view practical (e.g., 1 x 1 arc second) and with a wavelength resolution limited by input energy available. The telescope would operate at $f/30$, and a variety of spectrometers and detectors would probably be necessary to cover the full scientific objectives. In addition to spectrometric measurements, total energy measurements would also be made. Differences in these two types of measurements would primarily affect the scientific instrumentation. From the standpoint of the control system and fine pointing sensors, there is no significant difference and these will be considered as a single mission. An observation time of about 10 percent of the total is allocated to these measurements.

The requirements for absolute pointing accuracy, stability of pointing, and duration that the pointing must be maintained are not fully determined at this time. They will depend on the specific nature of the various instrumentation, the wavelength interval being examined, and the purpose of the measurement. For example, if it is desired to point to a given area of planet surface for a significant amount of time (on the order of seconds or minutes), it will be necessary to change the pointing direction of the telescope continuously (with respect to planet center) to compensate for planet rotation. Near the equator of Mars, for example, this rate of change of position is about 0.1 arc sec per four minutes of time. Jupiter's rate is nearly three times higher, and is a maximum for any of the planets.

Even if it were possible to very precisely point and hold the direction of the telescope to a value in the neighborhood of 0.01 arc sec, it is not entirely clear that this would be more beneficial than a larger value of perhaps 0.05 arc sec. This follows because one must know where the telescope is pointing with the same precision as the stability of the point; otherwise it is hard to envision the usefulness of the very high stability. A second criteria useful in establishing pointing stability is spectrometer slit size. With a minimum slit size of about 1 x 1 arc sec determined by energy considerations and the large diffraction limit in the IR region, a pointing stability of 0.01 arc sec would change the area of the planet being viewed by only 0.01 percent, an insignificant amount compared with the overall precision of the spectrometer measurement. A pointing stability as poor as 0.05 arc sec would still lead to an area change of only 0.25 percent, hence even a larger instability could probably be tolerated without any significant degradation of experimental data.

The worst case requirements are as follows:

Point to any desired location on the surface of the principal planets (Venus to Saturn)	± 0.05 arc sec
Stability of point on a given area for 45 minutes of time	± 0.05 arc sec
Repeatability of point on successive orbits	unspecified

Determine where the telescope axis is pointed		± 0.05 arc sec
Roll axis orientation		± 4 arc min
Roll stability	position or rate	± 5 arc sec $\pm 0.004 \frac{\text{arc sec}}{\text{sec}}$

5.4.3 Description of the Attitude Control System

Operational Description

The block diagram of the control system proposed for MDT was shown in Figure 5.4-1. This system provides the capability to perform initial rendezvous, orbit and stationkeeping, docking (MDT to MCR), initial stabilization, reorientation, and target acquisition and fine pointing. The first three items will not be discussed in detail since they are considered to be within the present state of the art. They may be accomplished with the gyro reference system and the reaction jets. Interesting sidelights are that the orbit and stationkeeping should be done without requiring major MDT reorientations: the 16 jet concept can accomplish this by selectively firing jets to realize the desired velocity correction vector. In addition, the docking is accomplished with the reaction jet subsystem set of high thrust levels to accommodate the required control authorities (see Section 5.6.3). A 10 to 1 throttleable reaction jet subsystem satisfies both the docking high thrust requirements while providing reasonably small thrusts for desaturation of the CMGs. The latter three items are discussed in considerable detail in the following paragraphs.

Description of Initial Stabilization

The initial stabilization will be with the telescope optical axis (roll axis) facing directly away from the Sun. After separation, the intense energy from the Sun makes it the easiest reference to detect and identify. An arrangement of a solar sensor distributed around the vehicle allows acquisition from any initial attitude.

The requirements for an efficient acquisition and the removal of residual angular separation rates are not compatible with the stabilization momentum requirements for the fine pointing mode. Thus a "high thrust" reaction control jet (RCJ) subsystem is used. During this phase of operation the signal flow in pitch and yaw channels is from the rate gyros and coarse solar sensors to analog electronics, to the appropriate high thrust RCJs. Signal flow is the same in the roll channel except that no solar sensors are used. Using the coarse sun sensor, the spacecraft roll axis aligned to within less than ten degrees of the Sun, with residual rates less than 0.1 degrees per second, at which time control is switched to a fine sun sensor. The roll channel continues to use only the roll rate gyro. Completion of this operation with the MDT roll axis to within one degree of the sun line within less than twenty minutes is reasonable. Pitch and yaw control authority is then switched to the CMGs to align to the Sun LOS within ± 0.25 degrees. Automatic star acquisition may be accomplished by a roll search procedure. A biased roll rate command is introduced into the roll channel to establish a roll search rate. The

rate of rotation shall be compatible with the spacecraft's dynamics and the ability of the star trackers to acquire and track guide stars. The gimbal angles of each tracker shall be pre-positioned such that at some roll attitude about the sun line, each tracker will have a preselected guide star in its field of view. The gimbals remain locked until a minimum of two coarse pointing star trackers simultaneously acquire guide stars. When this star pattern acquisition occurs, the gimbals of the trackers which have acquired stars are unlocked and the star trackers allowed to track. When the star acquisition has been obtained the biased roll rate command is removed, causing the vehicle to stop rolling. The reference is then switched from the gyros and fine sun sensors to the star trackers.

Description of Target Acquisition and Fine Pointing.

Since the telescope must have the capability of pointing anywhere on the celestial sphere within very high accuracies, three types of star trackers are necessary. Through the use of externally mounted gimballed star trackers, initial coarse orientation to accuracies of 3 arc min is known to be feasible. This coarse accuracy is determined mainly by the thermally induced structural deformations of the MOT, and secondarily, the star tracker characteristics.

Accomplishment of coarse pointing requires reference signals furnished by two or more star trackers. The reference for determining inertial attitude will be a set of selected guide stars. The required star tracker gimbal angles for these guide stars is precomputed for any orientation desired.

The individual trackers are pre-positioned to this orientation and the trackers are switched to the "track mode", the trackers then track their celestial references. Thus the difference between the commanded and actual gimbal angles can be transformed to derive pitch, yaw, and roll attitude error signals. A central digital computer performs this transformation and any averaging necessary. These signals are sent to the appropriate CMG's for each axis (switchover point for roll axis). Desaturation of the control moment gyros is provided by the low thrust RCJ subsystem. Thus a known spacecraft inertial orientation in the celestial coordinate reference system has been established in the coarse pointing mode.

To transfer control to the intermediate pointing sensors, predetermined guide stars of sufficient magnitude are brought into their field of view by the coarse pointing mode. The pitch/yaw intermediate sensor is boresighted to the telescope LOS and the roll intermediate sensor is aligned normal to this LOS. If a gimballed tracker is used for the pitch/yaw intermediate pointing sensor, a two axis predetermined angular offset is commanded. Upon receipt of star presence signals from the intermediate pointing sensors, and vehicle rates lower than 60 arc seconds per second attitude control reference is commanded from the star trackers to the intermediate sensors. If image tube intermediate sensors are used the procedure is similar except that the two axis outputs of the image tube are summed with "electronic gimbal" commands to obtain the attitude reference error signals. Once control is switched to the intermediate sensor the MOT pointing accuracy is improved to a predicted spacecraft absolute pointing accuracy of 4 arc seconds. This is sufficient accuracy about the roll axis for all requirements. The pitch and yaw control in the intermediate pointing mode is accomplished by processing intermediate pointing sensor error signals in the analog computer and sending them to the CMG controller. During occultation of the intermediate pointing sensor, control reference will be switched to the 3 axis

gyro reference updated during the dark period from difference signals between gyro and intermediate sensor outputs.

To acquire the fine pointing sensor, the sensor is offset about the pitch/yaw axis at the prescribed amount in order to acquire a preselected guide star (magnitude +10 to +13 or brighter in the field of view of the sensor. When a star presence signal, acceptable vehicle rate signals (10 arc sec/sec) and a positive signal from the astronomer are received, the pitch and yaw attitude control reference is switched to the fine pointing sensor.

In this mode, the fine pointing sensor utilized for the particular experiment provides the inputs to fine pointing channel of the CMG and jet controller. The controller provides control torques to the CMG gimbals. The CMG's magnify this torque many times and apply it to the telescope. Roll control is achieved in a similar manner using the roll intermediate pointing sensor. During occultation of the guide star, the control reference is switched to the 3 axis gyro reference, updated during the "dark period" to the fine pointing sensor and roll intermediate pointing sensor.

Description of Reorientation

Reorientation of the MOT through relatively large angles requires selection of a new guide star. This requires reverting to the coarse pointing mode to perform the required vehicle rotations to acquire the new guide star. A typical concept for vehicle orientation limited to several degrees is a closed loop method in which, prior to their being used as references, the star trackers acquire the new guide stars. The star trackers are then placed in the track mode and gimbal angle commands are introduced into the computer. The differenced commanded and actual gimbal angles are then transformed to derive pitch, yaw, and roll error signals.

These error signals command the appropriate CMG's to maneuver the vehicle to the desired orientation.

An alternate method for controlled reorientation for large reorientation angles up to 90 degrees, would make use of the three axis gyro reference during slewing. Using the CMG's the vehicle would be rotated in response to error signals developed by the difference between the commanded angle and the angle obtained from quantized torque pulses to the gyro. In this case, reorientation would be accomplished about the roll axis and one other to minimize disturbances to the vehicle.

Prior to the maneuver, precomputed star tracker gimbal angles are commanded to enable the trackers to acquire their new guide star. The trackers are then put in the track mode during the maneuver, in order not to relinquish the celestial reference. If the angular slew exceeds the gimbal freedom of trackers other trackers and guide stars are used so that at least two trackers are always operating.

Description of the Altitude Control Components

Referring again to the block diagram of figure 5.4-3, the following control components are required.

For sensing the telescope's orientation, the system includes the following equipment:

Sun Sensors	- used for initial orientation only
Rate Integrating Gyros	- used as prime angular reference in light side of the orbit. Used in rate mode for initial stabilization
Star Trackers	- used in coarse pointing mode, coverage of complete celestial sphere
Intermediate Pointing Error Sensor	- used as interface between coarse and fine pointing modes - smaller range and high accuracy than star trackers
Fine Error Sensor	- used as pointing mode

To actuate the control system commands, the following equipment is available:

Control Moment Gyros (CMG's)	- used as the prime actuator for pointing and maneuvering
Reaction Control Jets (RCJ's)	- used for initial stabilization, high control authority maneuvers (i.e., docking) and CMG desaturation

The interface between sensors and actuators is handled by computers, signal processors, amplifiers, etc. Electronics are predominantly analog to circumvent signal conversion problems. The telescope digital computer is used in the coarse mode because of the extensive computation required for commanding and processing the star trackers and their data. This computer also handles the mode control for the system, switching between components to accomplish the function at hand.

The two most critical items in the control loop are the CMG and the fine pointing sensor. Each uses approximately one third of the total allowable error. These two components will thus be discussed in considerable detail.

Control Moment Gyros Description

Figure 5.4-12 shows a block diagram of the twin-gyro control system. The main components of the system include the fine error sensor, two CMG's, a compensation network, desaturation electronics and power amplifiers for driving each gyro torquer. The control system consists of four functionally separate control loops. The main feedback loop consists of the vehicle position sensor, compensation network, power amplifiers and gyros. This loop generates the major attitude control torques on the vehicle. In parallel with the compensated position feedback loop, the inherent vehicle rate feedback through the gyros furnishes additional but minor vehicle feedback.

The remaining three control loops shown are primarily concerned with controlling the position of the gyros. All three loops make use of resolved gyro gimbal position to perform their function. The gyro tracking loop compares the position of each gyro and generates a signal for torquing each gyro to an equal gimbal angle. This loop compensates for differences in gyro damping, inertia and friction and serves to minimize control cross-coupling into another vehicle axis.

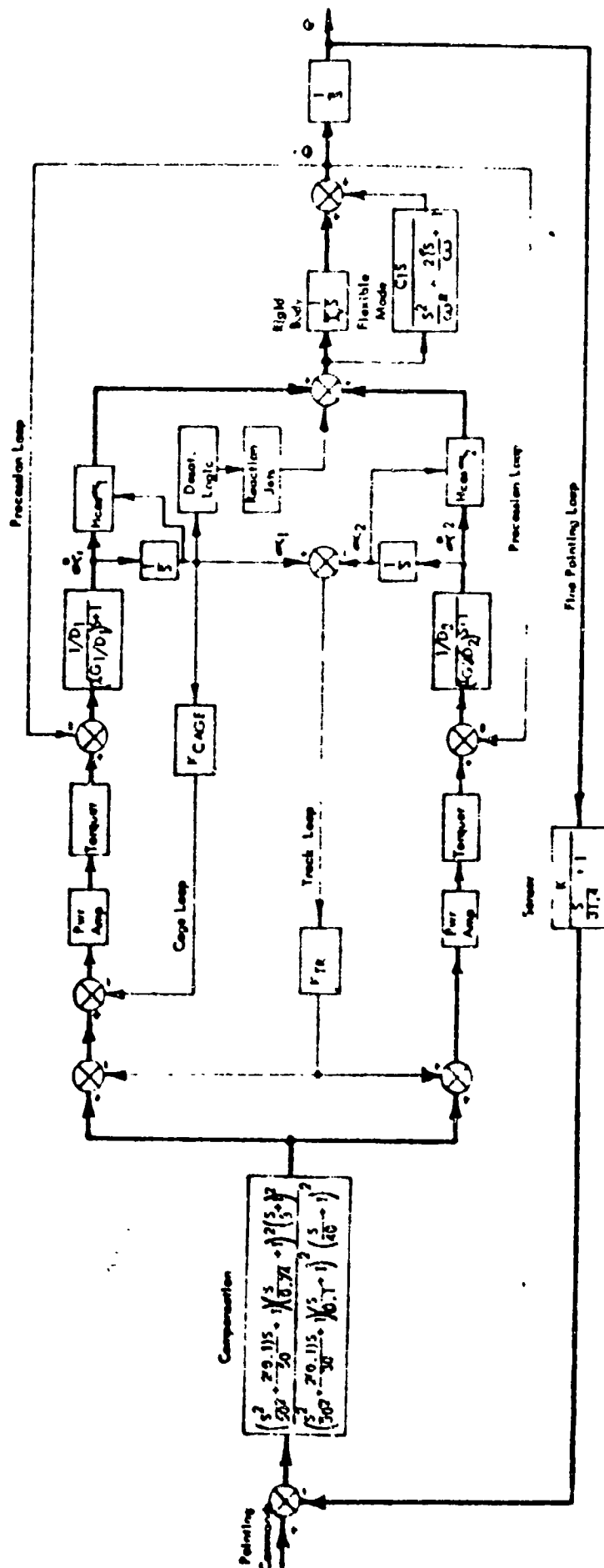


Figure 5.4-12

FINE POINTING BLOCK DIAGRAM

Like all momentum transfer controllers, the gyros require desaturation when they have absorbed a momentum magnitude close to their maximum capacity. The desaturation loop performs this function by actuating the RCJ's for a predetermined time period. This is done twice per orbit in order that no desaturations are required during an observation period. The amount of desaturation is determined by the digital computer.

The remaining control loop, the caging loop, is used to electrically restrain the gyros to a zero gimbal angle. The caging switch serves to drive gyro 1 to zero gimbal angle and the tracking loop requires gyro 2 to follow gyro 1.

A selection of the magnitude of gyro momentum was made on the basis of the worst case gravity gradient and aerodynamic torque characteristic. Using this characteristic, the gyros would be required to absorb 353 ft-lb-sec of momentum over the worst 50-minute span. For 45 degrees of maximum gyro angle, each gyro absorbs 250 ft-lb-sec of momentum. In order to include a safety factor, $H = 300$ ft-lb-sec was assumed to be the gyro momentum required. For this size gyro, the momentum to gimbal inertia ratio is approximately 2000 to 1. Gimbal inertia I_g is therefore 0.15 ft-lb-sec^2 .

The basic vehicle rate loop is a second order system. Assuming gyro angles zero, gyro damping D equal to $0.63 \text{ ft-lb/rad/sec}$ sets the damping factor at 0.7 and frequency at 3 rad/sec . For this size gyro, a D of 2 ft-lb/rad/sec with eddy current damping is within practical limits. Therefore, the damping required should present no design problems.

For this system, maximum torquer capability is required only during maneuvering. For the 5-degree-in-2-minute maneuver rate specified, a torquer size of 42 in-oz is required. To include a safety factor, 50 in-oz was specified. The maneuver rate is generated with 9.4 degrees of gimbal angle, thus no jet assist is required.

Because of the tight attitude accuracy specifications on the control system, the gyro units are constrained to have a friction level of 0.05 inch ounces. This low friction level can be attained by using a brushless torque motor, unpreloaded gimbal bearings and spiral leads to supply gimbal and resolver signals.

With the worst case disturbance torques predicted, it is anticipated that the gyro gimbal angles should not have to exceed plus or minus 45 degrees. Over this operating range, a d'Arsonval type torquer has a low enough torque gain variation to be acceptable. If this is not practical, it is feasible to consider (1) servoing the torque motor stator to follow the larger gimbal motions or (2) to use an electrically commutating brushless torquer with skewed poles to reduce reluctance torques.

Figure 5.4.-13 shows a typical friction plot for the size gimbal bearings required on a 300 ft-lb-sec gyro. Minimum bearing friction can be attained by using a pair of unpreloaded bearings with one bearing having its inner race nonrigidly attached to the gimbal shaft. This would allow the gimbal to expand or shrink freely with temperature changes and keep thrust loading to a negligible level.

In a zero gravity environment, radial loading would only be caused by gimbal rate, and is proportional to this rate. Thus radial loading causes a friction which essentially adds linear damping to the gyro. The linear damping due to friction is

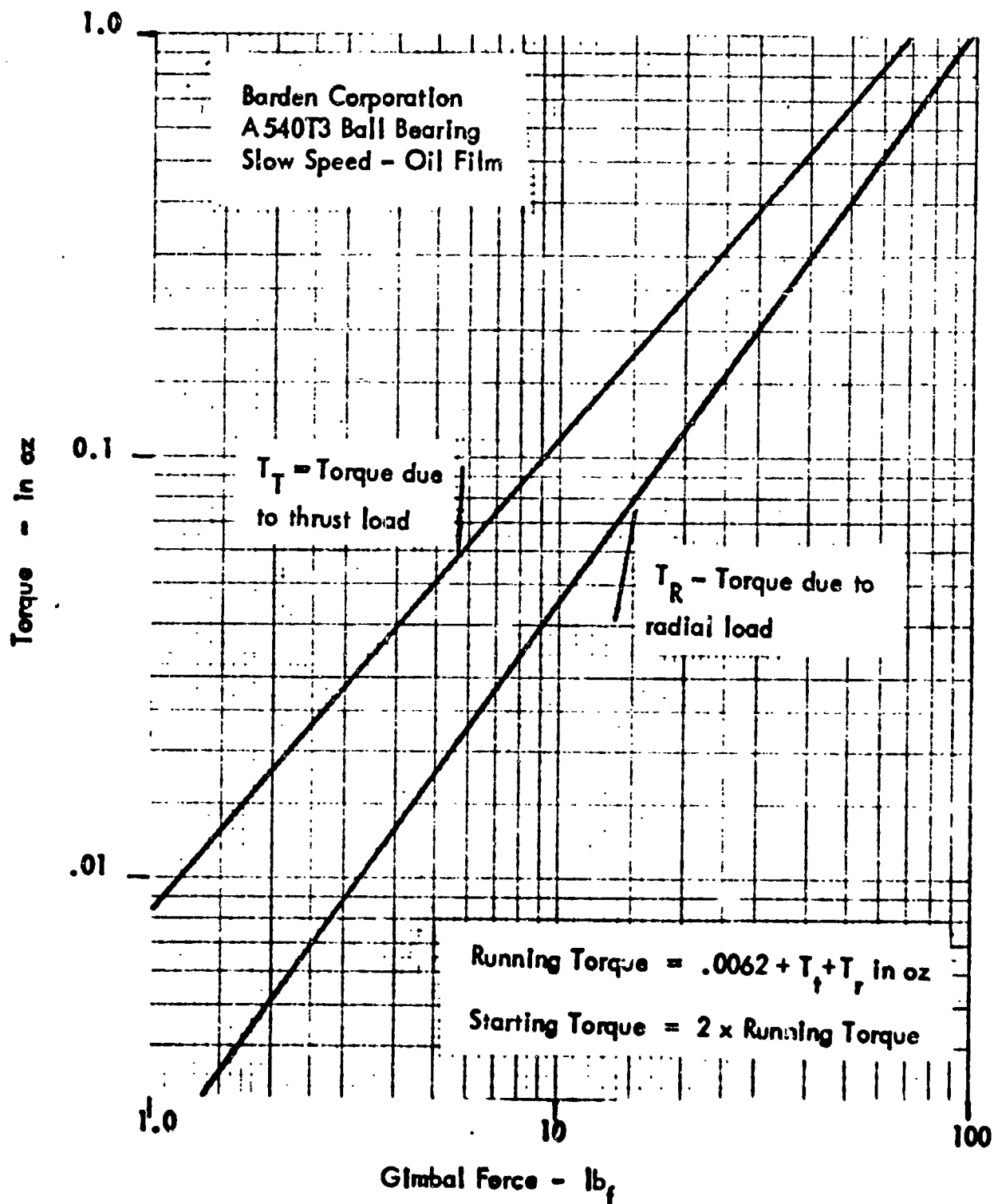


FIGURE 5.4-13

CMG GIMBAL FRICTION

calculated to be 0.03 ft-lb/rad/sec of gimbal rate. This damping is relatively small compared to the 0.63 ft-lb/rad/sec eddy current damping which must be used in the gyro.

From the equation in Figure 5.4-13, the bearing friction with no thrust loading is 0.0062 inch ounces, and is mostly due to retainer drag.

With the bearing mount design discussed above, the bearings would, therefore, cause a running and static friction of:

$$f_r = 2 \times 0.0062 = 0.0124 \text{ in-oz}$$

$$f_s = 2 \times 0.0124 = 0.0248 \text{ in-oz}$$

Using spiral leads rather than slip rings would not add to the friction levels calculated above. Spiral leads have been used in applications where 190 degrees of motion was required; therefore, 145 degrees should be an entirely feasible range of operation. The gyro gimbal assembly, however, may require fluid floatation in order to protect the leads in the vibration environment encountered during launch.

As discussed later, 17 leads are the maximum required between gimbal and outer structure. The worst case restoring torque per lead is 2×10^{-4} in-oz at a gimbal angle of 60 degrees, for a total of 34×10^{-4} inch ounces. This restoring torque when divided by the 166.7 inch ounce/arc sec of feedback gain required in this position feedback loop causes a negligible position offset.

Two types of flywheel spin motors have been investigated; both having a synchronous speed of 12,000 rpm. A 400 cycle, 3-phase spin motor would require 24 watts of running power, for a total of 40 watts with a d.c. to a.c. conversion efficiency of 60 percent. A brushless type d.c. motor operating synchronously at 12,000 rpm would require 13 watts of running power, and would be driven by a time ratio controller having 4 watts loss, for a total of 17 watts input power. The 400 cycle motor would require a minimum of 3 leads, and the d.c. motor would require 11 leads. If power leads are made redundant, the a.c. motor would need 6 leads and the d.c. motor, 15 leads.

The resolver on each gyro needed for reset, tracking and caging loops requires 400 cycles, but at a small power level. Each resolver requires 2 input leads.

Each single-axis power gyro unit is made up of the following subassemblies:

- o Gimbal
 - 300 ft-lb-sec flywheel
 - synchronous flywheel motor
 - gimbal supporting structure and bearings, and flywheel bearings
- o Brushless Torque Motor
- o Eddy Current Damper
- o Resolver
- o Spiral Leads

Preliminary specifications on the pitch or yaw axis control moment gyros are:

		<u>Per Gyro</u>	<u>Total</u>
Flywheel Momentum	ft-lb-sec	300	600
Weight	lbs		168
Volume	cu ft		2.75
Input Power*	watts	17	34
Torque Motor Saturation	in-oz	50	
Gimbal Inertia	ft lb-sec ²	0.15	
Damping	ft lb/rad/sec	.63	
Gimbal running friction	in-oz (max)	0.025	
Gimbal static friction	in-oz (max)	0.05	
Soft Stops	degrees	±60	
Hard Stop	degrees	±65	

*Applies to d.c. Motors driven by time ratio controllers with 76 percent efficiency.

Fine Pointing Sensor Descriptions

The item of the control system most sensitive to the observational program is the fine pointing sensor. Two main sensor types have evolved, an on-axis sensor, buried in the high dispersion spectrometer, and a general purpose off-axis sensor used for all other experiments. Sensor concepts and requirements are discussed in the following paragraphs for each of the observational experiments.

Fine Pointing Sensor Concepts For High Dispersion Stellar Spectrometry

A fundamental choice exists on whether to control spacecraft attitude with the star whose spectra is being measured, or whether to guide on a separate star (offset pointing). An evaluation of the advantages and disadvantages of each possibility indicate the penalties of offset pointing are too severe to permit this choice. The one clear cut advantage to offset pointing is that 100 percent of the energy of the experimental star is available for the scientific instrumentation. The disadvantages of offset pointing are:

1. Absolute stellar separations are not known to 0.01 arc sec, hence man would be required to acquire the experiment star by controlling its position relative to the spectrometer entrance slit. Preslected guide stars would then be used to hold that attitude. Both an internal sensor for the spectrometer and an external offset fine pointing sensor would be required.
2. A large corrected total field of view would be required (about 20 arc min diameter) to provide sufficiently bright guide stars for 0.01 arc sec spacecraft stability. (Only one arc min field of view is required by the observational experiments)
3. A preferred roll attitude with difficult requirements (4 arc sec) would be required. This accuracy is difficult due to a lack of a large collection aperture for roll axis sensors.
4. With respect to the experiment star, the system operates open-loop. Man or instrumentation would probably be required to continuously monitor the slit to determine that no changes in attitude have been induced by relative motion

between the fine pointing sensor and spectrometer slit (180 microinches - 0.01 arc sec at $f/30$).

5. The overall objective is to minimize the total experiment observation time. Giving 100 percent of the light to the experiment does not accomplish this. This is due to the loss in pointing accuracy inevitable if the control system does not receive some of the experiment starlight. The pointing error in turn, results in an apparent loss in light because of a higher percentage of the time spent not "filling the slit". A more detailed study is required to determine the optimum energy sharing ratio.

Based on these considerations, the choice is fairly clear. The guide star and experiment star should be identical unless there are very compelling reasons not to do so. There are two basic approaches to guidance possible, as exemplified by the "outside" sensor type of the OAO Princeton experiment, and the "inside" sensor of the OAO Goddard experiment. By outside and inside we mean that the fine pointing sensor is external or internal to the spectrometer.

Consider first the Princeton approach. Here, the spectrometer entrance slit is sized at about one-half the size of the Airy disc in the visual spectrum. A comparison is then made of the energy on either face of the slit jaws and error signals are generated if the energy distribution is unequal. The scheme has the very great advantage that is foolproof, i.e., if the star doesn't fill the spectrometer entrance slit, error signals are generated to correct attitude. An overriding disadvantage for the MOT mission, however, is the fact that using this concept the spectrometer entrance slit cannot be significantly varied from one fixed opening. This is a prohibitive restriction based on MOT requirements of wide star magnitude and wavelength coverage. Beyond about one micron, for example, the spectrometer slit width will be larger than the visible Airy disc, the portion used by the fine pointing sensor. The concept is feasible only for the condition that the spectra measurements be made at shorter wavelengths than those used by the fine pointing sensor. From a practical detector standpoint, this means only an ultraviolet spectrometer can employ this concept.

A second important factor that must be considered is that a fixed slit spectrometer (even in the UV) predetermines the ratio of energy sharing between the spectrometer and the sensor. This will be the optimum ratio for only one star magnitude, since in general, the optimum ratio is a function of star magnitude.

A second outside sensor concept (see Figure 5.4-14) that does have merit employs a mirror to share energy between the spectrometer and sensor.

The beam splitter can be a neutral density filter, or may be tailored to reflect UV or IR, for example, while transmitting visual for sensor operation. In this mode it could not only be used to optimize the amount of energy to both spectrometer and sensor, but also would serve to eliminate unwanted higher or lower ordered reflections from the grating. If a variable neutral density filter were used it could have the capability of being rotated to change the reflectance/transmittance ratio to a value that is optimum for the particular star being observed. For example, with a bright fourth or fifth magnitude star, a 90/10 experiment to sensor ratio may be desirable to minimize exposure time, while for a tenth magnitude star, a 50/50 ratio may be necessary to achieve the required pointing stability at the sacrifice of longer exposure time.

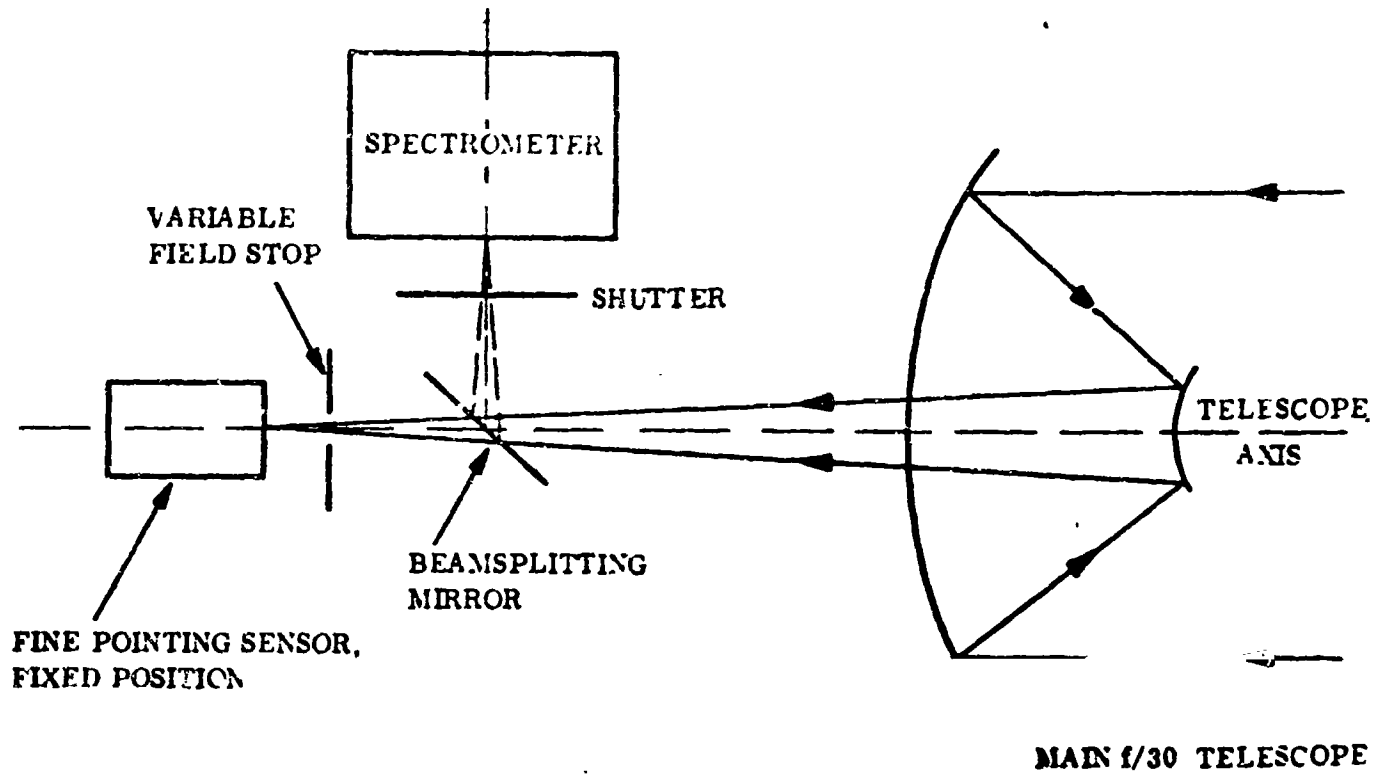


Figure 5.4-14

OUTSIDE SENSOR - HIGH DISPERSION SPECTROMETRY

A final alignment of this system will have to be made in orbit. This can be accomplished remotely from the MORL with a bright star by using successively smaller apertures on the spectrometer while offsetting the fine sensor electrically or mechanically, as decided by the sensor type. An auxiliary sensor within the spectrometer would be monitored while aligning to determine that the image is centered in the slit. For a spectrograph, a detector could be used to monitor the zeroth order reflection. For a spectrometer using electrical sensors, their output could be used for this purpose. In either configuration the appropriate detector could be monitored continuously while taking experiment data as a positive means of knowing the spectrometer slit is always being filled, and as a measure of exposure time when film is used as the detector.

It will be virtually impossible to rotate the mirror beam splitter (to change reflectance ratios for example) without adversely affecting sensor/spectrometer alignment. It will be necessary to do a fine realignment by remote means after every grating or spectrometer change. Thus it is a function for which the astronomer must become adept. It should be a fairly simple task if the sensor can be quickly offset electrically or mechanically.

Once a proper alignment is achieved, the system must be sufficiently mechanically and electrically stable to hold this alignment. This will be a difficult design job since the image plane angular sensitivity is quite large - 18 mils per arc sec at $f/30$. High thermal stability will be required and the overall thermal design will be critical.

During acquisition and when operation on the linear portion of the transfer function has been achieved, it may be desirable to stop down the fine pointing sensor ± 15 arc sec field to about one arc sec or less to reduce background noise and to eliminate any companion stars from the field of view. This could be a mechanized process using a logic signal generated by the fine pointing sensor to open or close the stop.

A special problem exists when the desired experiment star is a binary or other multiple star whose angular separations are less than a few seconds (depending on the use of a sensor field stop) and are comparable in magnitude. In this case, the fine pointing sensor will track the effective center of radiance and produce a null offset. In this event, the experiment star will not necessarily fill the spectrometer entrance slit. If the two stars are one magnitude apart, the offset for the brighter star will be $1/2.5$ of its diameter or about 0.015 arc sec. A separation of 4 magnitudes is necessary to keep the null offset smaller than 0.001 arc sec.

If the source is a nebula or other object of extended size (i.e., a tenth of an arc second or larger), special problems in tracking may exist if it is necessary to scan the object. These objects are considered to be of secondary importance to stellar sources, and the fine pointing sensor should not be compromised to accommodate them. If necessary, a modified fine pointing sensor could be provided for these high resolution spatial scans that has a precision small-increment angular offset capability.

The above described beamsplitter concept appears to be the most suitable method of fine pointing control when the sensor is placed outside the spectrometer slit. Consider now the application of the sensor inside the spectrometer entrance slit, and the possibility of combining an outside and inside sensor.

A fine pointing sensor located within the spectrometer housing, and viewing only that portion of the sky defined by the spectrometer slit is an obvious candidate for the fine pointing sensor concept. An optical pick-off to share energy with the spectrometer could take the form of a flat on the spectrometer collimating mirror as done in the OAO Goddard experimental package, or may be an auxiliary beam splitter similar to that discussed above for the outside sensor. For those spectrometers with non-scanning gratings, the zeroth order reflection could be used for guidance. The chief limitation of the method is its narrow acquisition range, as defined by the spectrometer slit. If the slit is opened sufficiently wide (say ± 15 arc sec) to accommodate the full transition range from intermediate to fine pointing, then essentially the situation previously described for the outside fine pointing sensor prevails -- the one difference being that the spectrometer itself is not stopped down to a few hundredths of an arc second during the acquisition phase. It can be stopped down after acquisition to some reasonably small value (say ± 0.1 arc sec) in order to eliminate background noise or companion stars. In this condition, any large disturbance would cause complete loss of the star image, and the spacecraft control would revert to the intermediate pointing control loop. It would then be necessary to open up the spectrometer slit and reacquire the guide star, with a resulting loss in exposure time and possible degradation in data.

A big disadvantage of this mode is that the spectrometer must be wide open during acquisition and settling time, with a ± 15 arc sec entrance aperture. Multiple star within this solid angle and exposure during acquisition time might seriously degrade the experimental data, particularly with film if the detector cannot be shut off.

The alternative to an inside-only sensor would be an outside/inside combination. The outside sensor could be identical to that previously described, and the spectrometer could be shuttered during acquisition and settling time. When the shutter is opened, the inside sensor would take command and center the image within the slit. The slit in this case could be held to about ± 0.1 arc sec as previously mentioned. In the event of a disturbance sufficiently large to lose control of the inside sensor (fine/fine pointer), control would revert to the outside sensor (fine pointer) for subsequent quick return to the operating mode.

The advantages and disadvantages of the inside/outside concept as compared to outside alone as follows:

Advantages

- o The extremely high gain of the inside sensor (linear range 0.05 to 0.1 arc sec) will provide very favorable signal to noise ratios for control, or could provide the margin of S/N necessary for a fast internal servo of an optical element for fine/fine pointing.
- o It is fail-safe in the sense that a positive indication of data taking would be available.
- o It is safer design concept in terms of the required thermal and electrical stability of the outside sensor alone.

Disadvantages

- o The in-orbit alignment procedure is more difficult.
- o Each spectrometer would require its own sensor, thus increasing overall cost. The two sensor types may be different thus requiring separate development programs.
- o More sensors mean more parts to fail, hence reducing overall reliability.

No choice will be made at this time between the outside sensor alone vs. the outside/inside combination. Both concepts should be pursued in greater depth to determine the advantages and disadvantages in terms of overall loop operation, and the complexity introduced when operating with multiple spectrometers.

All three of the basic sensor types considered (pyramid beam splitter, image dissector, and image tube) would be applicable to the outside sensor concept. The image tube is particularly appealing, however, since it has a linear acquisition range of ± 15 arc seconds, and excellent detectivity. Based on a 25 percent, 25 percent, 50 percent energy sharing ratio between the outside sensor, inside sensor, and scientific instrumentation respectively, stars as faint as 12.5 magnitude will yield noise error voltages of about 0.01 arc sec.

Depending on overall control loop characteristics, pointing stabilities of 0.1 arc sec or better should be realized, i.e., within approximately the linear range of the inside sensor. The image tube detector would have another very significant advantage as an alignment aid, since the raw video can be processed to present the astronomer with a picture of the telescope field of view.

The inside sensor would be either the pyramid beam splitter or the image dissector types, with no clear cut advantage to either. The pyramid beam splitter, with its potential to operate with virtually the diffraction limited image size linear range (± 0.02 arc sec) may be superior in terms of noise voltage for a given magnitude star. Stars as faint as 11.6 to 12.4 magnitude may be used for a linear range of 0.1 arc sec and a noise voltage of 0.001 to 0.002 arc sec.

In summary, it is apparent that fine pointing stability of 0.01 arc sec with stars as faint as the tenth magnitude is feasible, based on today's detector technology. With a 50/50 sensor/instrumentation energy-sharing ratio, stars fainter than the eleventh magnitude can be used with MOT based on anticipated detector improvements in the next decade.

Fine Pointing Sensor Concepts for Low Dispersion Spectrometry

Low dispersion spectrometry is essentially a continuation of the high dispersion work to fainter sources. The brightest of these sources, e.g., eleventh and twelfth magnitude, will require pointing accuracy and stability only slightly less stringent than those for the high dispersion work. In these cases it is practical to use the experiment star as the guide star as in the high resolution work since the reduction in pointing stability associated with lower fine pointing sensor signal-to-noise ratio will be commensurate with the lower pointing stability that is required. The concepts involved and perhaps the actual implementation would thus be similar or identical to those previously discussed for the high dispersion mode.

As the object whose spectra is to be measured gets fainter (e.g., thirteenth, fourteenth, or fifteenth magnitude), several factors change. First, the lower inherent energy limited resolution means that pointing stability can be relaxed without degrading the experimental data. Secondly, different types of lower dispersion spectrometers may be employed that could not previously be used on the brighter stars because of their relatively poor wavelength resolution. The variable interference filter, for example, may be more efficient than the grating spectrometer, hence a better choice in the energy region where its lower resolution can be tolerated. Finally on the fainter stars, a point is reached where the energy collected is insufficient to permit use with the fine pointing sensor, and it will be mandatory to rely on offset pointing on a star different (brighter) from the experiment star for control purposes.

The maximum angle for offset pointing, i.e., the largest angular separation between guide star and experiment star should ideally be made sufficiently large to permit complete freedom in selecting the experiment star. Because extremely high spacecraft stability is not required for the fainter experimental stars (e.g., 0.1 to 0.2 arc sec), guide stars as faint as the thirteenth to fourteenth magnitude should be usable for guidance, depending on the type of sensor and its linear range. With this freedom, a maximum offset angle of about eight arc min half angle would be adequate, based on the star population density. A wider range of perhaps 10 arc min would provide a margin of safety and probably would still not be so far off axis as to require a field correcting lens for the sensor.

A single fine pointing sensor, capable of being mechanically offset along one axis, is adequate when coupled with spacecraft roll axis control. Electrical offset, though desirable, is impractical both from the physical size and the precision of offset required (in excess of one part in 3000). The mechanically offset system should readily be capable of this precision. It may be desirable to add a transfer lens to increase the angular sensitivity in the sensor focal plane. This would increase the required sensor translation distance (plate scale), hence reducing the mechanical precision required for the offset.

This configuration is shown in Figure 5.4-15. It is similar to the high dispersion outside sensor concept, the major difference being the need to mechanically translate the sensor to accommodate the required offset pointing. The neutral density beamsplitter needs to operate over only the central diameter, thus allowing maximum energy to the fine pointing sensor for off-axis stars. The beam splitter could be mirror at the small expense of vignetting small angular offset guide stars.

To align this system in orbit, a bright star would be selected to permit real time use of the spectrometer detector as a go/no-go indicator. The spectrometer slit would be stopped down to some very small value (say 0.1 arc sec) and the fine pointing sensor would be mechanically offset until the slit is filled. Once alignment is made, the spectrometer slit would be opened up to its normal size for operation.

The fine pointing sensor noise voltage can be as large as about 0.01 to 0.02 arc sec leading to a spacecraft pointing stability of perhaps 0.1 to 0.2 arc sec. This is achievable with stars as faint as about the 12.5 magnitude based on a 50 percent beamsplitter and a linear sensor range of one arc sec. A smaller linear range (say 0.2 to 0.4 arc sec) would be desirable in order to reach stars of the 13.5 to fourteenth magnitude if this is compatible with acquisition requirements.

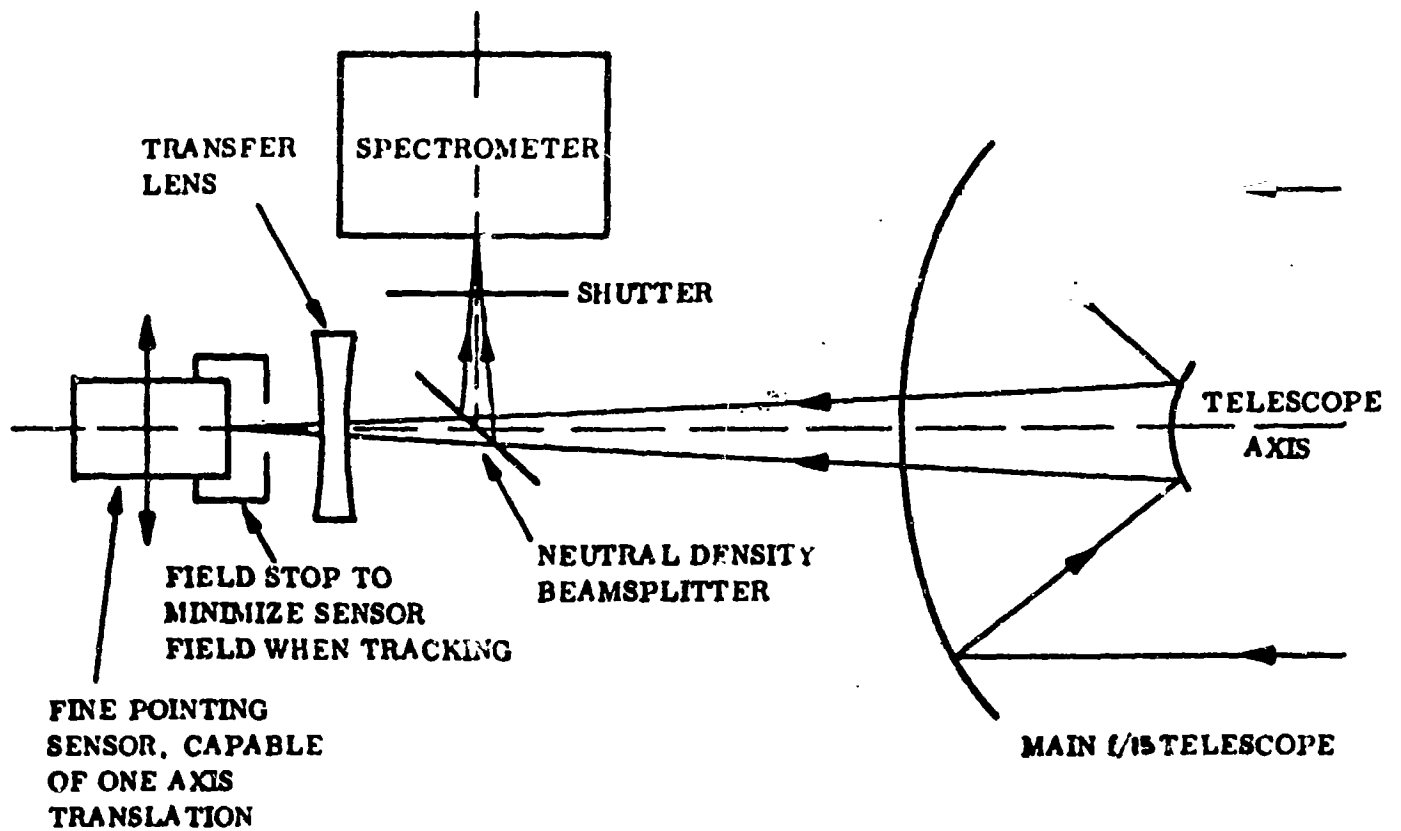


Figure 5.4-15

SENSOR - LOW DISPERSION SPECTROMETER

Fine Pointing Sensor Concepts for Photometry & Polarimetry

As in the low dispersion spectrometry mode, concepts for fine pointing sensors logically break down into two distinct categories, namely when the experiment star is sufficiently bright for guidance, and when a different off-set star must be used. In the former case, with stars as faint as perhaps the thirteen or fourteenth magnitude, the guidance scheme could be identical to the high dispersion case, where a beamsplitter is used to share the energy.

This concept has two distinct advantages. First, pointing accuracy and pointing stability will be high, and the field stop for the photometer/polarimeter could be significantly reduced in size (e.g., one arc sec diameter). Secondly, the sensor functions essentially only as a null detector, and no angular offsets are necessary.

This concept also has two disadvantages -- it takes roughly half the energy that would otherwise be available for the experiment, and it introduces an additional optical surface for the polarimeter that is otherwise not necessary. The additional surface in front of the polarimeter is probably the more serious of the two since the energy limitation is not critical for these brighter objects.

This fixed position sensor for on-axis operation with the brighter stars would have the capability of operating to at least the fourteenth magnitude. With an image tube detector and transfer lens of 1.5X to 2.0X, a total field of view of about ± 20 arc sec would be obtained. With a fine pointing sensor angular resolution of one part in 2000, a noise error voltage of about 0.02 arc sec would result. This would permit a pointing stability of the required 0.2 arc sec.

A further advantage of the image tube device is that raw video could be processed to provide a TV display for the astronomer. This could be employed to permit monitoring of the experimental star image position. Such a presentation would be very valuable when using the off-axis fine pointing sensor since it would permit direct verification that the very faint object was falling within the photometer field stop. By slowing down the frame rate of the image tube to perhaps one or even 0.1 frames per second, it should be possible to detect stars of eighteenth to twentieth magnitude with an image orthicon, that is, most stars to be observed. The image tube in this case is used only for a visual presentation of these stars, not spacecraft control, because the very low frame rates are inconsistent with control system requirements. This concept has the further advantage that by using the intelligence of man to determine whether the telescope is suitably pointed, a calibration of the absolute mechanical or electrical offset can be readily made.

For those objects that are sufficiently faint to require offset pointing (or for the bright objects if the increase in instrumental polarization is too serious), a different concept is required. Here, a sensor must be capable of very accurate continuous off-set (± 0.25 arc sec) over an angular range of 8 to 10 minutes, based on considerations developed in the previous description of low dispersion spectrometry. This is equivalent to about one part in 3000. The compensated focal plane scale is nine mils per arc sec, and the full 10 arc min half angle field corresponds to a linear dimension of 5.4 inches. This would appear to be an ideal application for a moniac detector consisting of 3000 to 4000 elements, each roughly 0.2 mils ($1/4$ arc sec) wide. Unfortunately, suitable detectors of this type and size are not

available at present. Image tubes come closest to this requirement, but they lack the required resolution (one part in 3000) except under the most favorable conditions. Even if a suitable single image tube were available with the required resolution, the absolute angular offset requirement would necessitate an extremely linear sweep of about ± 0.03 percent.

The best approach to the problem appears to be identical to that of low dispersion spectrometry. A detector operating as a null device would have to be mechanically offset with a precision of ± 2 mils in six inch total travel. The sensor in this case would require a total field-of-view that is commensurate with intermediate sensor/spacecraft pointing capability, that is, about 30 arc sec total field. This configuration is very similar to that described for low dispersion spectrometry.

The total configuration for the photometer polarimeter instrumentation might appear as shown in Figure 5.4-16 based on one fixed image tube detector for on-axis work, and one moveable sensor for off-axis work.

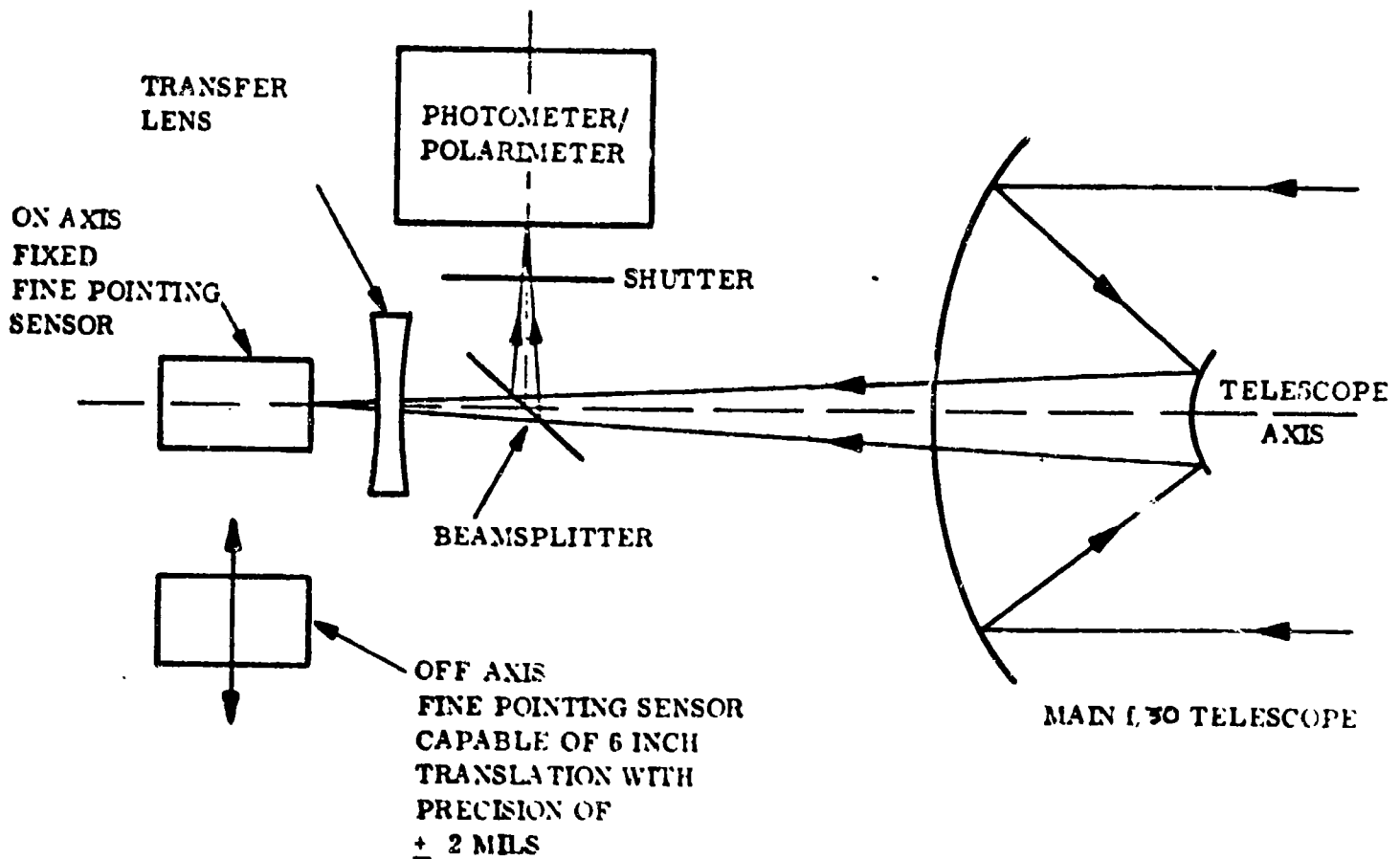


Figure 5.4-16

SENSOR - PHOTOMETRY/POLARIMETRY

In case it is not possible to employ any optical element between the telescope and the polarimeter, only off-axis guidance would be used.

Fine Pointing Sensor Concepts - Star Field Photography

Since the two modes (narrow field and wide field) are somewhat different, consider first the narrow-field case. Assume the total film plate field of view is 2×2 arc min. This corresponds to a film plate size of 2.2×2.2 inches for the $f/30$ camera. It would be extremely undesirable from the astronomical point of view to employ a fine pointing sensor in the film plane that would violate photographic field. On the other hand, the further off-axis the fine pointing sensor is moved, the greater the control problem becomes, since the image becomes larger and asymmetrical due to telescope aberrations. The obvious compromise in this case would be to locate the fine pointing sensor as close to the film plate as practical, without violating the prime field of view. It will then be necessary to determine sensor performance based on a ray trace of the optical system. As a working figure, assume an off-axis sensor location of 2 arc min.; i.e., one arc min separation from the edge of the film plate to the sensor null position. This corresponds to a mechanical clearance of 1.1 inches. The overall configuration in this case would appear as shown in Figure 5.4-17.

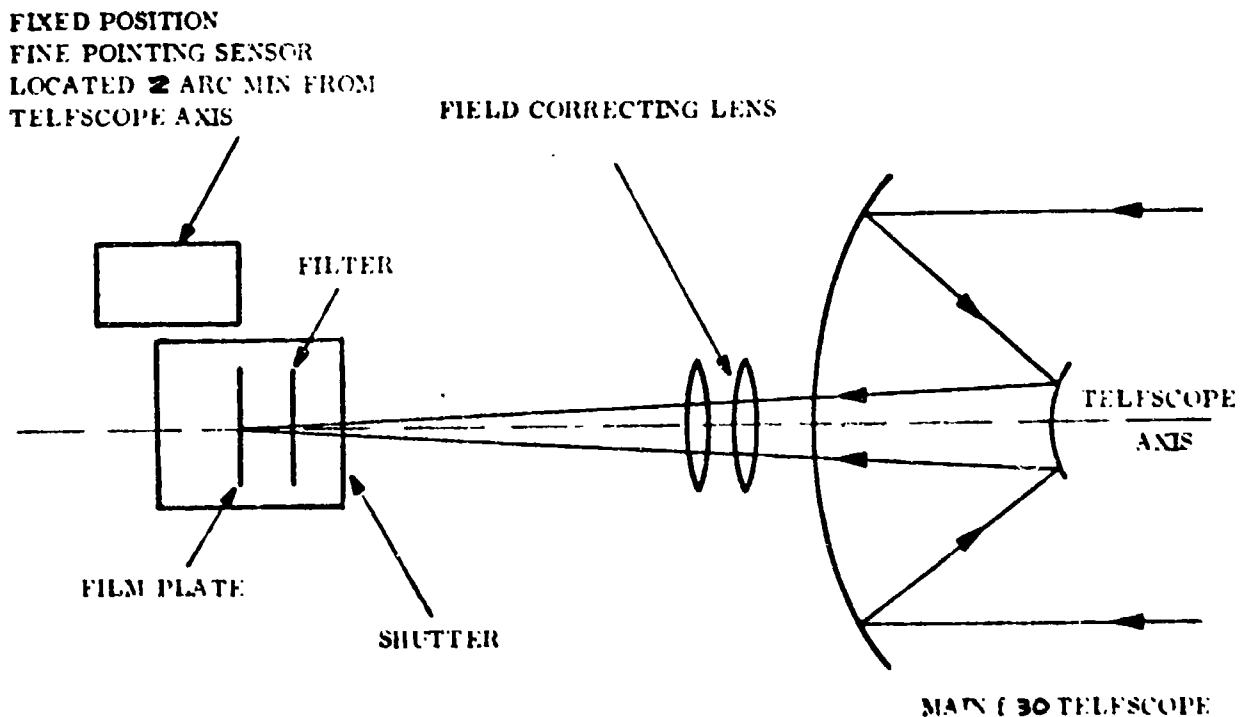


Figure 5.4-17

SENSOR - NARROW FIELD PHOTOGRAPHY

In this configuration, the fine pointing sensor could be located at one fixed position, and the entire spacecraft would be rolled to the proper orientation to image the guide star at the fine pointing sensor. The sky could then be photographed in the following pattern (see Figure 5.4-18) about the guide star.

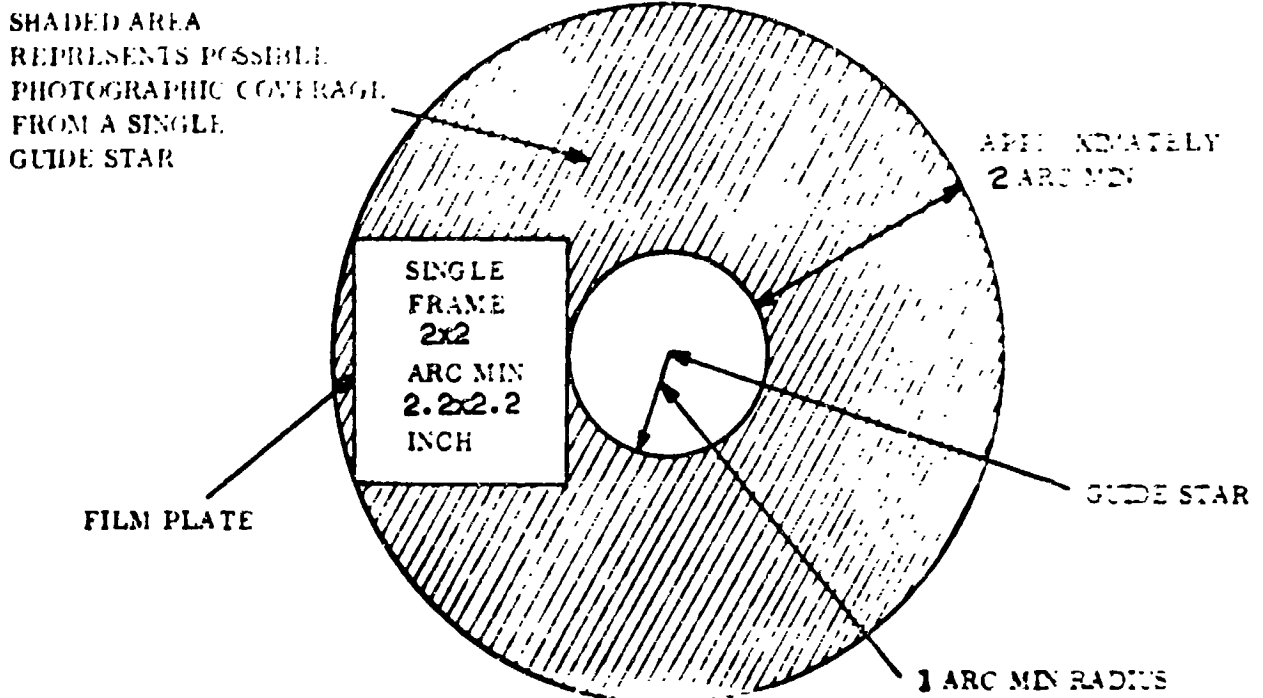


Figure 5.4-18

SKY PHOTOGRAPHY PATTERN

If the limiting magnitude of the guide star for proper sensor operation is +10 magnitude then from star population density curves, it is apparent that some portions of the sky near the galactic pole would not be accessible for photographing. If the limiting magnitude for guidance were between the eleventh and twelfth magnitude, the entire sky would be available except for the hole in the "boughman". The limiting star magnitude will be about +12 if a sensor linear range as small as ± 0.1 arc sec can be used. It is desirable from the standpoint of the fine pointing sensor, telescope design, and observational data to reduce the radius of the hole to the minimum consistent with mechanical interference limitations with the film plate holding and changing mechanism.

The great advantage of the previously described concept is that the total energy gathered by the telescope is available for both photographs and guidance; i.e., neither has to share the available energy from a single star with the other. The film plate can be shuttered independently of the sensor, and the sensor field can be independently stopped down after acquisition to reduce background noise. The effect on guidance of close neighbors to the guide star is not critical provided the center of radiance does not shift as a function of time.

The repeatability requirement of image position at the film plate from orbit to orbit will require a highly stable mechanical and electrical sensor/film plate system. The configuration described above would appear to be optimum from this standpoint.

with fixed mechanical positions and close mechanical proximity. Auxiliary active temperature control of the sensor/film plate assembly may be required.

From a control standpoint, if it becomes necessary to employ a two-step sensor to handle both the acquisition problem (large linear sensor range desirable), and the stability problem (very small sensor linear range desirable), the above concept is fairly readily adaptable to modification. A fixed position beam splitter could be used in front of the sensor alone (not the film plate) and the energy from the guide star could be shared by the two separate sensors. The second sensor would have a large linear acquisition range. In this case one of the two sensors must have the capability for small angular offsets (a few seconds) for initial remote alignment in orbit.

Should the telescope off-axis aberration problem be very severe, an alternate concept would be to use the fine pointing sensor on axis by using a beamsplitter and sharing the available energy with the film. Since this may double the time required to expose a given plate (depending on the energy sharing ratio), it would be a costly penalty, but one that could be accepted if absolutely necessary.

Consider now the wide angle stellar photographic mode and also any variation in fine sensor pointing concepts previously discussed. Assume the total corrected field-of-view as 1×1 degree for the $f/15$ telescope configuration. This leads to a film plate size of 34×34 inches.

Since the film plate will be sized to fully utilize that portion of the field that is fairly well corrected, any fine pointing sensor in the film plane must employ approximately a 30 arc sec cut-out in the film plate. Further, this cutout should not be near the edge of the field where image quality is poorest, but should be within perhaps 10 arc min of the telescope axis. This technique is not desirable but is not completely objectionable if there are no suitable alternatives.

The hole in the film plate would constitute a loss of less than 0.01 percent of the area of coverage. With this large a field of view, the entire sky could be covered with tenth magnitude or brighter guide stars. An eleventh magnitude capability would be more desirable, however, to permit more versatility in selecting that portion of the sky to be viewed on axis.

If the telescope aberrations are sufficiently low to permit fine sensor operation out to perhaps 20 arc min, the cut-out in the film plate could be slotted to permit more versatility in selecting that portion of the sky to be viewed on axis. This also increases the ratio of hole size to film size.

As an alternate to the cut-out in the film plate, a beamsplitter could be used as described for the narrow field mode.

The fine sensor in this case could be in an arbitrary fixed position near the x.c.s of the telescope. Some versatility in the experimental program would be obtained by mechanically translating the sensor (one axis only), or by having two or more sensors in fixed positions. Roll axis control would be required in all cases.

As discussed before, the disadvantages of this method are the increased exposure time required, the large beamsplitter required, and the greater risk of instability

Inherent in failure to monitor image position directly at the film plane. The compensating advantages are more experimental versatility, operation nearly onaxis, better shuttering arrangement, and no loss of field due to film plate cutout.

Fine Pointing Sensor Concepts - Planetary Photography

Although pointing requirements must be established in terms of the planet being photographed, it is apparent that direct planet tracking is not feasible to hold the pitch and yaw errors to a value even close to 0.01 arc sec. With Jupiter, for example, this corresponds to an angular resolution of about 1/4000 of its diameter, and probably closer to one part in 6000 of the sensor field of view. This is one to two orders of magnitude better than is feasible today, and is not considered practical for the 1980 time period. Secondly, the faintness of Pluto, Neptune, and Uranus compared to the other planets would not yield the high signal-to-noise ratios commensurate with extremely precise pointing. Finally, even if these basic engineering problems were soluble, it is not obvious that there is anything on the planet to track that is stable to 0.01 arc sec for the nearby planets; that is, it is not obvious that surface brightness or edges remain sufficiently well defined under the influence of planet rotation that they are stable to the required angular resolution.

These reasons indicate that the most fruitful approach to the planet tracking problem lies in the utilization of the star field as a frame of reference, and employing rate (image motion) compensation. In some cases, depending on the length of film exposure time, it will be possible to expose the planets in an inertial reference frame without image motion compensation. In most cases, particularly for the distant planets and when using filters, it will be necessary to modify the effective pointing direction in the inertial reference frame as a function of time. This can be introduced either at the film plate, or the entire spacecraft could be slewed. This fine pointing concept is the only suitable method for obtaining high quality photographs of faint moons of the planets, for example, or of asteroids and comets that are too faint for guiding on them directly.

If stars are to be tracked for the planet photographic mode, a suitably bright star must be within the telescope field of view. This requires that the f/30 telescope have a field of view far larger than would otherwise be necessary. For the photographs alone, a field of one minute in diameter would be adequate, whereas for the sensor a field of many minutes is required. The size of the field is indicated (in the general case) by the number of sufficiently bright guide stars near the ecliptic. The angular size of the field to ensure a suitable guide star most of the time is indicated below as a function of the faintest star with which the fine pointing sensor is capable of operating:

- . 5-minute half-cone angle - 12 magnitude
- . 10-minute half-cone angle - 10.5 magnitude
- . 15-minute half-cone angle - 9.8 magnitude

It is highly desirable from many aspects to limit the field to the smallest possible value. In any event, it is apparent that field correcting optics for the sensor may be required, and that a total field of 5 to 10 arc min half-angle will be necessary, depending on sensor characteristics.

The field can be significantly reduced (to less than five minutes) only at the expense of operational flexibility by photographing a planet only when a suitable guide star happens to fall within the limited telescope field of view. This is an undesirable alternative, since it means that the planets could be photographed only occasionally, and usually only one planet per equipment setup. It would be extremely restrictive with respect to Venus, since an extremely small window is available due to sun angle limitations.

The fine pointing sensor can be located in the film plane, or could be physically separated using a plane mirror if mechanical interference problems should exist. The plane mirror location is sketched in Figure 5.4-19.

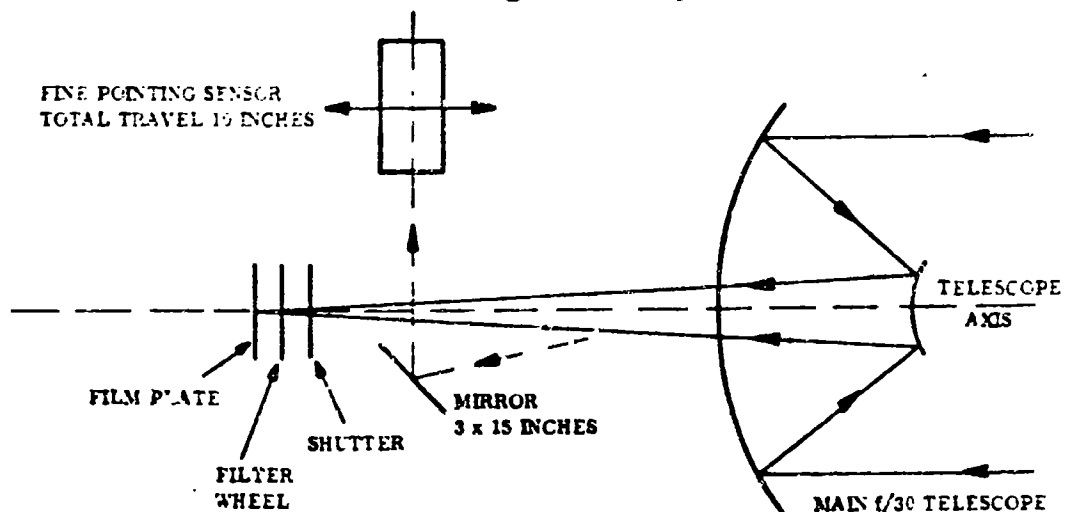


Figure 5.4-19

SENSOR - PLANETARY PHOTOGRAPHY

The plate scale of the $f/30$ telescope is approximately one inch per minute, or 17 mils per arc sec. This means the total mechanical travel of the fine pointing sensor must be about 5 to 10 inches. Precision of the offset can be crude, perhaps a few seconds of arc. This is roughly 0.1 inch if the plate scale at the sensor is identical to the film plate. This provides the reference direction of the telescope for exposing the film. A programmed rate compensation (image motion compensation) can now be inserted mechanically or electrically into the tracker or into the film plate. The image motion compensation would ideally be made continuously. The highest rate will be for Venus and Mars (0.04 arc sec/sec), and the largest total offset will be for Mars and Pluto, approximately 1.5 arc sec based on an exposure time not to exceed 0.02 arc sec due to planet axial rotation.

The required fine pointing sensor for this observational program will be very similar to that required for the stellar photographic modes. The two main differences are the need to provide a coarse single axis mechanical offset for initial acquisition, and a fine two axis offset for image motion compensation. As in the stellar photography fine pointing sensor, a limiting guide star of the eleventh to twelfth

magnitude will be achievable for a linear range of ± 0.1 arc sec. With this capability, a maximum offset angle of 10 minutes (10 inches) will be needed, and a field correcting lens probably can be avoided.

If image motion compensation were inserted by a mechanical translation of the sensor, a precision offset of 15 to 30 microinches would be necessary (0.001 to 0.002 arc sec) for the f/30 telescope plate scale. This is in the range where an interferometer would probably be necessary to measure the offset. Another means of achieving the same end result would be to leave the sensor in a fixed position, and offset the stellar image by means of optical wedges. The required offset precision (0.002 arc sec in 2 arc sec or one part in 1000) should be readily achievable. A third method of achieving the required precision of offset is with an electrostatically deflected image dissector photomultiplier detector. A deflection voltage linearity of one in 1000 or even one in 2000 should be possible with this detector, whereas the magnetically deflected version is an order of magnitude poorer. It is not clear however, that it will be possible to obtain the very small linear transfer function range with the image dissector, because of limitation on cathode aperture size. If this is true, the pyramid beamsplitter type detector with either sensor translation or image translation to provide the image compensation becomes the only choice.

Fine Pointing Sensor Concepts for Planetary Spectral and Total Radiance Measurements

As was discussed for the case of planetary photography, the relative motion of the planets with respect to the fixed stars is relatively large -- many seconds of arc during the orbital period of the MOT spacecraft. The telescope must either track the planet directly, or use rate (image motion) compensation with star tracking. Planet tracking to the required spacecraft pointing stability is within the realm of possibility in this mode because only the principal planets are involved. Nevertheless, because of the requirement that it must be known where the telescope is pointed, it is felt that this program cannot be carried out in the 1980 time period with direct planet tracking since more than an order magnitude improvement over planet trackers now under development would be necessary (the NASA Ames tracker). The star tracking concept with rate compensation is required for the photographic mode in any case, and it should be used here where the stability requirements are somewhat less stringent. This concept has the further advantage that it is more general, and could be extended to measure the spectra of the more distant planets, the principal planetary moons, and perhaps the larger asteroids or comets. Rate compensation in the general case must include the axial rotation rate of the planet under observation, otherwise the planet surface would actually be scanned as it rotates. One final advantage of the star tracking mode compared to planet tracking is that a star is then available for focus control of the main telescope.

These planetary spectral measurements are a case whereby man can remotely make a significant contribution to the overall process. He can select the specific area of the planet to look at, can guide the spacecraft telescope to that location, and monitor performance on a realtime basis.

Because of the wide wavelength region that must be covered by the spectrometers and bolometers, it is highly undesirable to employ any refractive elements in the optical train. The experiment itself does not need field correcting optics, since

its angular field is less than a minute. The fine pointing sensor will not have to operate more than 10 minutes off-axis (as in planetary photography), and probably will not need correcting optics. A knowledge of telescope off-axis aberrations is necessary to make a proper judgment in this matter.

The fine pointing configuration shown in Figure 5.4-20 is similar to the sensor arrangement discussed for the planetary photography mode. The basic differences are a high resolution TV camera is added to permit man to select and know which portion of the planet is being viewed by the spectrometer, and the system must be capable of accommodating image motion compensation for any planet under observation for extended periods, at least one half-orbit.

The TV camera images the mirrored spectrometric slit jaws. The camera should have the minimum field of view consistent with planet size, spacecraft initial pointing errors, and spectrometer-to-telescope alignment considerations. A value of about 60×60 arc sec would seem to be about the best compromise. A resolution of 2000 to 3000 lines would yield a planet resolution of 0.02 to 0.03 arc sec with the 60 arc sec field. This would be about the minimum that would be acceptable based on an 0.05 arc sec requirement for position determination. In order to achieve this high resolution on the planets it may be necessary to reduce the image tube frame rate to a much smaller value than is normally used - say something in the range of 1 to 10 frames per second. This is feasible since the device is not used in the spacecraft control loop. While it is desirable to have a very high sweep linearity of the image tube, it is not critical since the spectrometer slit is being imaged, hence planet pointing location is derived from resolution considerations alone.

The fine pointing sensor, for reasons discussed in the planetary photography section, may require a total mechanical offset capability of 5 to 10 arc min (5 to 10 inches) depending on the limiting star magnitude that is necessary to achieve the desired pointing stability. Since the stability requirement in this mode is less than that of photography by a factor of about five, stars as faint as the thirteenth to fourteenth magnitude may be used, thus reducing the total required mechanical offset. This is beneficial since it reduces the field correction requirements on telescope aberration and probably will eliminate the need for a corrector lens.

As discussed in the planetary photography mode, image motion compensation can be introduced in a variety of ways at the fine pointing sensor. The two axis position offset required is about 90 arc sec per half orbit for the worst case (Mars). This is more than an order of magnitude larger than for photography. The precision of the offset should be comparable to sensor noise when tracking the faintest guide stars: i.e., on the order of 0.005 to 0.01 arc sec. This corresponds to 0.1 to 0.2 mils mechanically at the $f/30$ plate scale. The 10^4 ratio of total offset to offset precision effectively rules out electrical means to accomplish the offset and implies a fine mechanical translation of the sensor (or spectrometer) should be made.

The basic system, as described above, would begin to function when the telescope is oriented toward the desired planet to within about 5 to 10 arc sec through the coarse pointing/intermediate pointing modes. Proper roll orientation has been established. The planet is then well within the field of view for the observer on the TV display. A suitable guide star has been selected and the fine pointing sensor is mechanically positioned with a precision of about 20 mils (one arc sec)

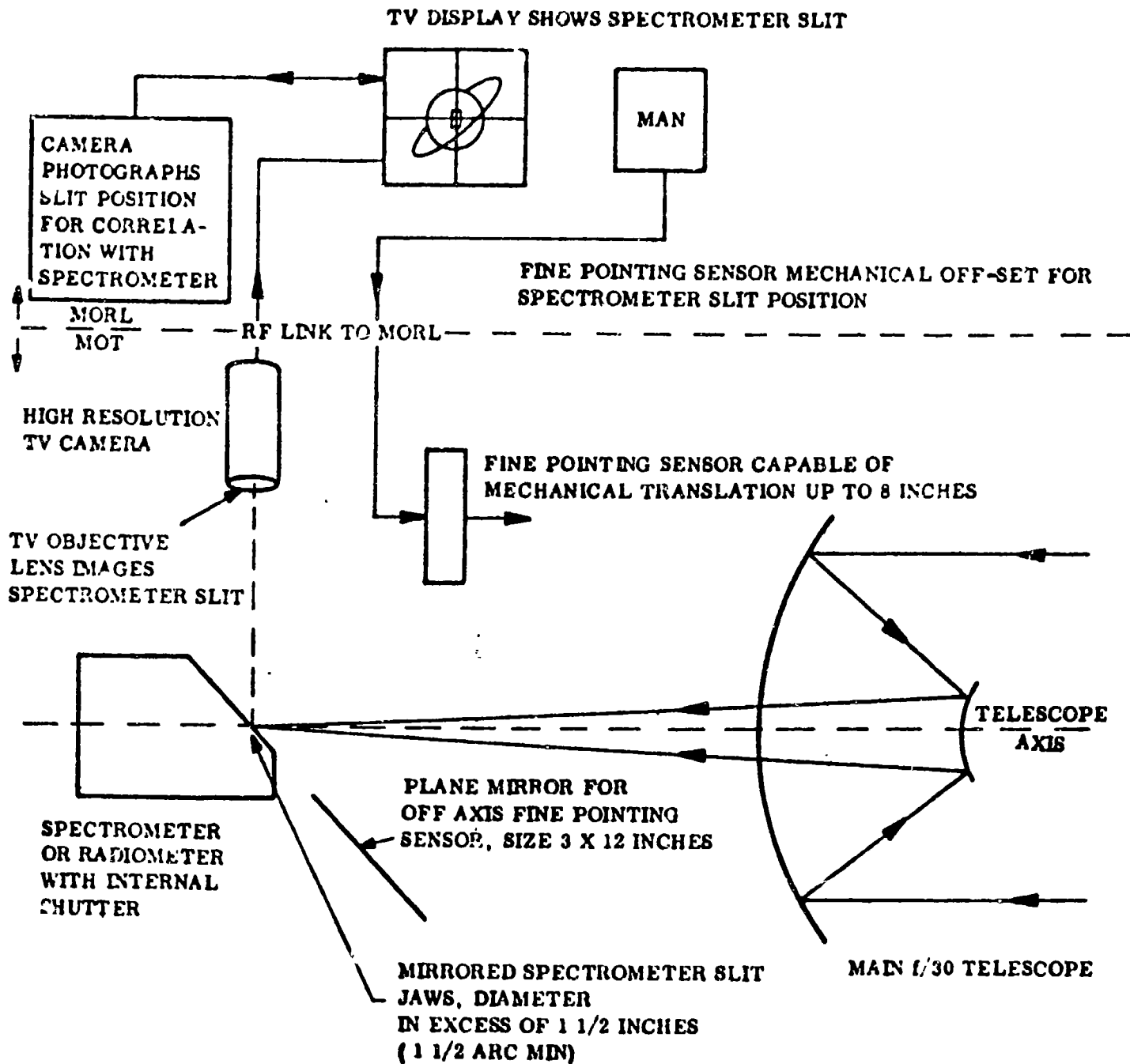


Figure 5.4-20

of the calculated offset. The guide star is now well within the field of view of the fine pointing sensor (± 15 arc sec, each axis total field), and spacecraft attitude control is switched to this sensor. The observer now locates the spectrometer slit position on his TV display and determines where on the planet he wishes to point. He inserts an electrical or mechanical offset to the fine pointing sensor (or other element of the system) until the spectrometer is viewing the desired location to within ± 0.05 arc sec. He now initiates the prepared rate (image motion) compensation program, and opens the shutter of the spectrometer. A series of photos are made of the TV display to make a permanent record of spectrometer slit position for later correlation with spectrometer data. The rate compensation program may or may not include the rate contribution of planet axial rotation, depending whether spot scanning or spatial scanning is desired. On successive orbits, the process can be repeated on the same spot on the planet or on a different point.

Physical Characteristics of the Attitude Control System

An estimate of the physical characteristics of the system components is summarized in Figure 5.4-21.

This estimate is based on pre ent day hardware with some improvement attributed to advanced techniques. A brief description of the component functions and constraints are given in the following paragraphs.

For MOT, four trackers are mounted equally spaced normal to the longitudinal axis of the telescope, each along a control axis, and in the vicinity of the primary mirror to provide maximum rigidity and accuracy of alignment. Two trackers cover the 90 degree field of view about the MOT anti-optical centerline. Two more trackers cover the 90 degree conical field of view about the MOT optical centerline are again mounted in the vicinity of the primary mirror. The two tracker pairs are required due to field of view interference from the MOT structure and a desire to take advantage of the accuracy of alignment afforded by mounting them at the primary mirror. These eight trackers are in order to cover the complete celestial sphere with state-of-the-art star trackers. If trackers with larger than ± 45 degree field of view become available, the number may be reduced and indeed, full celestial coverage itself is not a necessity.

For the soft gimbal mode some sacrifice in the coverage of the celestial sphere will result from the loss of the trackers looking aft (conical field of view about the antioptic axis) due to the occultation caused by the MORL.

The coarse sun sensors provide pitch and yaw attitude control signals for orienting the (antioptic) end of the MOT to the sun line.

The fine sun sensor provides position information about the pitch and yaw axes during the final phases of stabilization. It has a 10 degree half cone field of view.

A three-axis fully redundant gyro reference package provides rate and attitude information. Rate information is required during initial stabilization to the sun and star references and for logic signals to the computer as necessary inputs for switching to intermediate and fine pointing. As an attitude reference the gyros will be required to serve as an inertial reference during periods of occultation of celestial references or large angle maneuvers. During the MOT time period it is

<u>Components</u>	<u>No. Req.</u>	<u>Weight lbs.</u>	<u>Size Inches</u>	<u>Power Watts</u>	<u>Spares</u>
Star Tracker	7	24	11x17x16 ea	1.8	20
Star Tracker Control & Pickoff Electronics	7	27.5	12x16x8 ea	12	10
Intermediate Pointing Sensor	1	50	11x11x40	15	4
Fine Pointing Sensor: On axis	1	20	6x6x6	10	1
Off Axis	1	40	6x6x6	15	2
Analog Computer	5	85	2.8 ft ³	45	2
Fine Solar Sensor Pkg	1	2.3	3.5x3.5x1.2		1
Course Solar Sensor	2	1.0	1.5dia.x1.5ea		1
Pate and Postion Gyro Pkg	1	16	4x8x8	30	2
Gyro Electronics Pkg.	1	16	4x14x16	14	2
Twin Control Moment Gyro P	1	165	12x22x16	34	2
Twin Control Moment Gyro Y	1	165	12x22x16	34	2
Twin Control Moment Gyro R	1	30	5x6x4	8	2
Reaction Control S/S		180			
Propellant		350			
Digital Computer	2	307	6.5 ft ³	100	2

Figure 5.4-21

envisioned that long-life gas-bearing gyros with a short term trimmed drift rate down to 0.001 degree per hour will be available. The gyro trim may be obtained from the optical sensor during fine pointing experiments.

Three cmg's are used each with two counter rotating rotors in their own gimbal. This arrangement provides minimum cross coupling, that is, the control torques are always directed along a single axis independent of gyro gimbal angle.

A variable thrust reaction control system is used for both attitude control and minor orbit maneuvering. These functions are provided by a sixteen-jet system divided into four four-engine clusters located fifteen feet fore and aft of the center of mass. Each of these engines is throttleable over a ten to one ratio, from 4 to 40 pound thrust. By selecting proper combinations of engines, either pure couples or pure forces are available. Initial stabilization, large reorientations and CMG desaturation will be performed at low control authority, docking and rendezvous will be performed at high authorities.

The MOT computer will perform the following attitude control functions:

- o Establish and control the sequence of events (mode switching)
- o Perform all computations and data storage required by star trackers. (i.e., star map storage and tracker pointing commands)
- o Perform computations necessary for gyros (i.e., integration when they are used in the rate mode).

5.4.4 Analyses

In synthesizing a feasible attitude control system for the MOT requirements a necessary step is to define the external and internal disturbances to the control system and the control system hardware characteristics. This section discusses the analyses of these parameters as well as the syntheses of the fine pointing control loop. Since analytical studies cannot include the system nonlinearities and vehicle flexibility that realistically determine system performance, an analog computer study was performed. That study is reported in Section 5.4.5.

The orbit and vehicle parameters used for all these studies are given in Figure 5.4-22. The products of inertia were assumed to be the order of 100 slug ft.² maximum, but the later final configuration exceeded this somewhat due to solar panel location.

External Disturbance Torques

For the separated configuration in a 250-nautical-mile circular orbit, the major disturbance torques are due to gravity gradient and aerodynamic drag. Since both of these disturbances are a function of the vehicle inertial attitude, the maximum disturbance torque and momentum storage requirements for one half orbit were based on the worst case telescope orientation.

The maximum gravity gradient torque about an individual vehicle axis occurs when the gravity vector is 45° from the vehicle principle axes and is given by:

$$L_x \max = \frac{3}{2} \frac{GM}{R_o^3} (I_{yy} - I_{zz})$$

where G is the gravitational constant

M is the mass of the earth

R_o is the orbit radius

which for the values of the parameters given in the configuration selected yields maximum gravity gradient torques of:

$$L_x \max = 0.0013 \text{ ft-lb}$$

$$L_y \max = 0.212 \text{ ft-lb}$$

$$L_z \max = 0.210 \text{ ft-lb}$$

The aerodynamic disturbance torque about each vehicle control axis is the product of atmospheric drag and the offset of the vehicle CP from its CM. This can be expressed as:

$$T_{aero \max} = 1.1 P' R_o A r$$

where P' is the atmosphere specific weight at orbit altitude

R_o is the circular orbit radius

A is the projected area of the vehicle along the velocity vector with solar panels symmetrical about CM, if used

R is the CP-CM offset

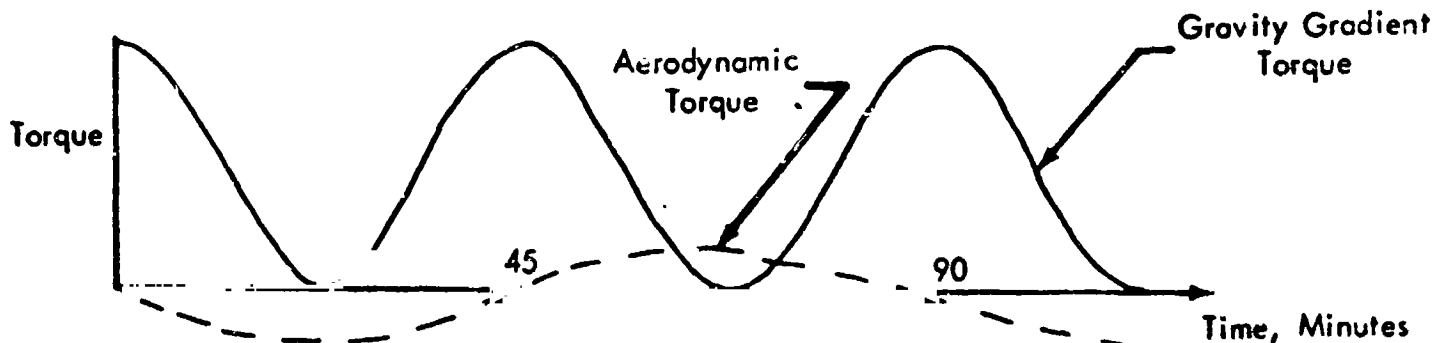
magnitude larger than the maximum aerodynamic torque, the orientation to produce the maximum gravity gradient torque will very nearly produce the maximum total disturbance torque.

$$\begin{aligned} T_{dx} &= 0.0013 + 0.001 = 0.0023 \text{ ft-lb} \\ T_{dy} &= 0.212 + 0.5 (0.021) = 0.222 \text{ ft-lb} \\ T_{dz} &= 0.210 + 0.5 \times (0.021) = 0.220 \text{ ft-lb} \end{aligned}$$

The maximum gravity gradient torque impulse about a given axis for a 3000 second fine pointing period occurs for an inertial vehicle orientation which maintains one control axis in the orbit plane and the two orthogonal control axes 45 degrees to the orbit plane. This produces a torque of one polarity about the axis in the orbit plane that attains a maximum value twice per orbit. For the MOT orbit and vehicle parameters, the maximum gravity gradient torque impulse for each axis is:

$$\begin{aligned} H_x \text{ max} &= 2.07 \text{ ft-lb/sec/half orbit} & (H_y = H_z = 0) \\ H_y \text{ max} &= 338 \text{ ft-lb/sec/half orbit} & (H_x = H_z = 0) \\ H_z \text{ max} &= 335 \text{ ft-lb/sec/half orbit} & (H_x = H_y = 0) \end{aligned}$$

The disturbance torque impulse about each vehicle control axis due to aerodynamic drag during inertial orientation of the telescope is cyclic with a period equal to the orbit period. The maximum momentum storage requirement during fine pointing is equal to the worse case combination of aerodynamic and gravity gradient torque impulse. This worse case occurs for the vehicle inertial orientation that produces the phase relationship between aerodynamic and gravity gradient torques as a function of time as shown below.



For the vehicle X axis, this worst case condition occurs for a vehicle orientation in which the X axis is maintained in the orbit plane and the Y and Z axes are at a 45 degree angle to the orbit plane. The maximum X axis aerodynamic torque impulse for the 3000 second interval indicated is:

$$H_x = 1.78 \text{ ft-lb/sec}$$

and the maximum disturbance torque impulse from gravity gradient and aerodynamic drag is:

$$H_{cx} \text{ max} = 2.07 + 1.78 = 3.85 \text{ ft-lb/sec}$$

Similarly, the total disturbance about the y and z axes is:

$H_y \text{ error} = 14.7 \text{ ft-lb/sec}$
 $H_z \text{ error} = 14.7 \text{ ft-lb/sec}$
 $H_{dy} \text{ max} = 338 + 15 = 353 \text{ ft-lb/sec}$
 $H_{dz} \text{ max} = 335 + 15 = 350 \text{ ft-lb/sec}$

Error Analysis

The MOT attitude pointing requirements fall into two general categories; one in which the experiment star is bright enough to allow on-axis pointing so the experiment star is the guide star, and the other where off-axis pointing is required because the experiment star or star field is not sufficiently bright to be used as a guide star, or in the case of a planet where a point source is required to obtain the required pointing accuracy. The most difficult requirement, which essentially determines the control design philosophy, arises from the combined requirements of stellar photography and photometry and polarimetry, each of which require off-axis pointing. The absolute pointing accuracy requirements in the photometry and polarimetry experiment are very tight, ± 0.2 arc seconds in pitch and yaw and ± 20 arc seconds in roll.

The initial error allocations to achieve the required performance are discussed below. For experiments that can be accomplished using on-axis guide star as a fine pointing reference, the estimated errors in imaging the experiment star at the null position of the experiment instrumentation are:

- o Mechanical and electrical null offset of
sensor null from experiment instrumentation null ± 0.001 arc sec
- o Sensor rms noise equivalent error ± 0.001 arc sec
- o Electronics null offset ± 0.001 arc sec
- o Servo loop standoff error due to
disturbance torques ± 0.001 arc sec
- o Torquer threshold error ± 0.003 arc sec

TOTAL ON-AXIS INACCURACY ± 0.007 arc sec

Considering this error on both the pitch and yaw axes and negligible cross coupling torque disturbance at the low vehicle rates (less than 5 arc sec/sec) in this mode, the angular error of the LOS from the star to experiment instrumentation package at null is estimated to be 0.01 arc seconds. The pointing stability would be slightly less, by an amount equivalent to the initial mechanical misalignment error between the fine pointing sensor and the instrumentation package.

For experiments requiring an off-axis guide star for a pitch and yaw reference, the derived pitch and yaw errors, not including telescope distortion errors due to thermal effects, are:

- Mechanical and electrical null offset of
sensor null from experiment instrumentation null ± 0.001 arc sec
- Sensor rms noise equivalent error ± 0.001 arc sec

Electronics null offset	± 0.001 arc sec
Servo loop standoff error due to disturbance torques	± 0.001 arc sec
Torquer threshold error	± 0.003 arc sec
Error due to open loop offset of fine error sensor	± 0.050 arc sec
Sensor cross coupling error into pitch axis due to 4 arc sec. roll error for 15 arc minute sensor offset angle	± 0.002 arc sec
Structure response to peak external disturbance torque	± 0.0002 arc sec
Inaccuracy of knowledge of stars in celestial coordinate ref. system	± 0.1 arc sec
Total off-axis inaccuracy	± 0.159 arc sec

Considering this error on both pitch and yaw axes and negligible cross coupling torque disturbances at the low vehicle rates in this mode, the angular error of the LOS from the star to the experiment instrumentation package would be of the order of 0.2 arc seconds. However, pitch and yaw pointing repeatability would be better since the inaccuracy in knowledge of star position, initial alignment error of roll intermediate pointing sensor and the open loop offset positioning error of the fine error sensor may be neglected. Assuming no telescope thermal distortion errors for the duration of the experiment, the pitch and yaw repeatability errors are estimated to be:

Sensor electrical null offset error of sensor null from experiment instrumentation null	± 0.0005 arc sec
Sensor rms noise equivalent error	± 0.001 arc
Servo loop standoff error due to external torque disturbance	± 0.001 arc sec
Torquer threshold error	± 0.003 arc sec
Sensor cross coupling error into pitch axis due to 2 arc sec roll error for 15 arc minute sensor offset angle (does not include initial alignment error)	± 0.001 arc sec
Electronics null offset	± 0.001 arc sec
Total off-axis stabilization errors	± 0.0075 arc sec

The angular repeatability error is thus less than the required ± 0.01 arc sec.

Error Analysis - Soft Gimbal Concept

The MOT soft gimbal configuration is a low pass mechanical filter coupling which provides positive location of the MOT relative to the MORL to overcome of orbit perturbations. The desired design of the gimbal would be such that only the extremely low frequency orbital perturbative forces would be transmitted through the soft gimbal.

A spring constant along any axis of 0.125 lb/in. (individual spring constant of 0.0625 lb/in.) resulting in a natural frequency of 0.0084 cps was investigated. This design value while small is still much stiffer than the minimum required to transmit orbital perturbative forces. As a result, induced forces produced by crew or equipment motions are partially transmitted from MORL through the soft gimbal to the MOT. Rough estimates of the effects of disturbances on MOT due to MORL indicate that the present controller only slightly exceeds the pointing error restrictions. The most troublesome disturbances being crew motion, MORL attitude control oscillations and gimbal bearing static torque.

It has been shown that the crew motion produces an equivalent torque on MOT of;

$$L_{\text{crew}} = 0.00189 \text{ t ft-lb}$$

acting for 2.2 sec. The gimbal bearing static friction produces an equivalent torque on MOT of;

$$L_{\text{friction}} = 0.021 \mu, (t-t_1) \text{ ft lb}$$

where t_1 is the time at breakaway and μ , is a unit step function. MORL attitude control oscillations produce an equivalent torque on MOT of;

$$L_{\text{morl}} = 0.0484 \sin \omega \text{ ft-lb}$$

where ω is 2π radians/sec. The primary self induced torque on MOT is estimated as;

$$L_0 = 0.11 (1 - \cos \omega_0 t) \text{ ft-lb}$$

where ω_0 is 0.00224 radians/sec. (0.00035 cps). The soft gimbal natural frequency was given as 0.0084 cps which is much greater than the frequency of orbital perturbative forces.

The nature of the disturbances are: sinusoidal due to self-induced torques at a frequency of 0.00224 radians/sec.; sinusoidal due to MORL motion at a frequency up to 6.28 radians/sec.; a ramp input due to crew motion; and a step due to gimbal bearing static friction.

The crew motion disturbance can be reduced by lowering the natural frequency of the soft gimbal but gimbal static friction disturbance occurring on the MOT side of the spring suspension can be reduced only by reducing the gimbal static friction itself.

The errors for MORL oscillations, electrical cable and bearing coulomb friction

are estimated below. The maximum induced pointing error due to the hypothesized crew motion would be 0.00009 arc sec. The bearing static friction induced pointing error would be a maximum of 0.0009 arc sec. The individual errors and the conglomerate error are shown below.

<u>Source</u>	<u>Magnitude (arc sec)</u>
MORL Attitude Control Oscillations	0.00200
Electrical Cable Torque	0.00004
Coulomb Bearing Torque	0.00004
Crew Motion	0.00009
Static Bearing Torque	0.00090
Conglomerate	0.00307

The MORL control oscillations of $\pm 1/2$ degree at 1 cps are considered to be extremely pessimistic. Thus, the soft gimbal induced errors are felt to be quite small and well under control.

It should be pointed out, however, that only the linear responses to deterministic input signals are treated. The conclusions should be qualified in that the magnitudes of the deterministic inputs are estimates and that these estimates bear directly upon the magnitude of the conglomerate error. In addition, roll control may present additional problems. These potentially would require either a roll gimbal or much softer springs.

The ten radian bandwidth controller defined for the detached MOT vehicle is thus proposed for the soft gimbal vehicle mode with those exceptions in control compensation that would become evident in a complete analysis of the MOT-MORL control system, including nonlinearities.

System Synthesis - Fine Pointing Sensor

In accordance with the above error analysis, the synthesis of a fine pointing sensor is described in this section. The background on the available performance of state-of-the-art detectors is first presented in order to illustrate the degree of depth in estimating the synthesized sensor characteristics.

The fine pointing sensors summarized here employ various principles of operation to transform star angular error into a useful electrical control signal. The basic scheme is always the same, however. If an image of a star is formed with a suitable optical system, the image will be displaced in the focal plane if the angle between the star and the axis of the optical system changes. The basic problem, therefore, is to sense this motion and convert its magnitude into suitable electrical signals. The supporting document, D2-84039-1, includes a detail discussion of following sensors:

- GE fine pointing sensor for simulating OAO sensors
- Stratoscope II fine pointing sensor
- OAO boresight star tracker
- Goddard experimental package fine pointing sensors
- GE/LMED vidicon system
- Princeton OAO experiment fine pointing sensor
- NASA Ames planet tracker

It is difficult to compare the performance of these various fine pointing sensors without some common basis. We cannot tell immediately, for example, whether the OAO fine pointing sensor is better than the Stratoscope II fine pointing sensor in performance, because they have different collecting apertures, different electrical bandwidths, operate with different magnitude stars, and have different linear ranges. To circumvent this, a figure of merit is developed whereby any two trackers may be compared by relating suitable parameters. Let

$$P = \frac{(\Delta f)^{1/2} I}{(2.5)^{7-m} J D^2} \quad \text{Figure of Merit}$$

where Δf - sensor electrical bandpass (cps)
 I - linear range of transfer function in arc sec (half angle)
 J - noise error voltage in rms arc sec for a star of magnitude m
 D - diameter of objective in inches.

The quantity P is not a rigorous concept in that it does not consider optical losses use of signal level to control photomultiplier gain, etc. In practice P will even vary somewhat for a given sensor as a function of star magnitude because of the use of gain control. Nevertheless, it is a useful quantity since it does permit approximate tracker-to-tracker comparison and permits rapid approximate calculation of expected tracker performance for a change in any given parameter. P has been calculated for various present day trackers which use photomultiplier detectors, and has a value between about 0.5 and 1.5 for different trackers, based on published or estimated data. A greater numerical value of P corresponds to better overall tracker performance.

The quantity P defined in the preceding equation is actually related to the quantum efficiency of the detector, and hence to its detectivity. This becomes apparent when one considers that ratio I/J in the equation is actually the

signal-to-noise ratio, and the quantity $(2.5)^{7-m} D^2$ is proportional to the total flux collected. Thus, the figure of merit equation can be compared to:

$$\frac{S}{N} = \frac{(\text{detector quantum efficiency})(\text{time rate of arrival of photons})^{1/2}}{2 \Delta f}$$

which is valid for the case where the photomultiplier dark current is much less than the signal current.

The number P is useful in evaluating MOT fine pointing sensor performance since it is based on actual present day tracker characteristics, rather than theoretical quantities. A value of P for the MOT sensors could probably not exceed 5 or 6, based on expected performance of 1975 photocathodes. As an example of the calculations that can be employed, let us determine the faintest star that can be tracked in a typical MOT application, assuming a collecting aperture of 23% of 120-inch diameter. For a linear range of ± 0.1 arc sec, a noise voltage of 0.001 arc sec, an electrical bandpass of 5 cps, and a figure of merit of 5 we have:

$$(2.5)^{7-m} = \frac{I \Delta f^{1/2}}{J P D^2} = \frac{(5)^{1/2} 0.1}{10^{-3} \times 5 \times .23 \times (120)^2} = 0.013$$

Hence, $m = 11.5$ magnitude.

This result is significant since, considering the star field density, stars as faint as the 11.5 to 12th magnitude are required for use as guide stars in the photographic modes to obtain full sky coverage. Since Δf , J , and P are essentially fixed to the values specified, improved performance must come through a better optical system efficiency (entirely possible in the photographic modes), or by a relaxation in the linear range of the transfer function. The second method may not yield large improvement because of the aberrations in the optical system off-axis where the sensor may be located. With a small improvement in sensor linear range, and requiring use of 50 percent of the total energy collected for guidance, the limiting magnitude of the guide star becomes between 12 and 12.5, a fully acceptable figure.

Such a limited linear range with the attendant large saturated range required (115 arc sec) means that no effective rate damping is possible during the acquisition phase with a single sensor. Throughout this region, no rate information and only gross position information is available. This situation tends to make the acquisition very oscillatory and inefficient.

This condition can be overcome in a variety of ways. One method would simply be to have two sensors; a fine pointing sensor and a fine/fine sensor. The former would be used for acquisition and the latter for tracking. A second method, employing only one sensor but two transducers, is exemplified by the Stratoscope II fine pointing sensor. Here, tracking is maintained by servoing the position of a transfer lens over a very narrow angular range (± 0.1 arc sec), while a transducer for the lens position with respect to the telescope optical axis has a range of ± 1 arc min for an adequate rate damping interval. For the MOT application the beam splitter itself could be servoed.

The need for a very small linear region of the transfer function and a long acquisition range may eliminate the possibility of using image type detectors (e.g., the image orthicon). This application would require a resolution in excess of 1 part in 10,000 which is not practical to obtain. The image dissector multiplier phototube (e.g. the ITT FM143) has a reasonable maximum limit of perhaps 5 to 10 on the ratio of total acquisition range to linear range. This is inadequate for the expected MOT requirements. The detector, however, through electrical offsetting is capable of being used in a separate acquisition mode, where a search for the guide star takes place. Once located, tracking could proceed normally. Because of limitations of photocathode hole size to image size, it may not be possible to achieve a linear range as small as 0.1 arc sec with this type detector. The only detector type where linear range can be as small as image size, and where the linear range and total acquisition range are independent, is the pyramid beam splitter or some modification of it.

Three principal types of star trackers will have application for the MOT fine pointing sensors. The selection of the configuration for each of the scientific programs will depend on the pointing requirements and peculiarities of each experiment. The three types are:

- 1) Pyramid beam splitter (e.g. Stratoscope II)
- 2) Image dissector phototube (e.g. OAO boresight tracker)
- 3) Image tube (e.g. image orthicon)

A fourth type using a conventional photo multiplier and electrical chopping (e.g., OAO Gollard experiment) is not considered since it is electrically similar to the image dissector, but does not possess many advantages of that type detector.

A comparison of the three types are as follows:

- . Detectivity—All use photoelectric operation. The performance of types 1 and 2 are comparable. Type 3 is superior, particularly at low frame rates.
- . Dynamic star magnitude range—Comparable in performance - A range of 5 to 6 magnitudes is reasonable. Type 3 is capable of 8 to 10 magnitudes in a single frame with automatic beam control on a point-for-point basis.
- . Effect of image aberration—A symmetrical aberration in all three cases leads to no null shift. A non-symmetrical aberration (the usual case) produces a null shift proportional to the shift in the light centroid of the image. For type 1, the gain of the sensor decreases for increasing image size. In types 1 and 3, the minimum detectable star gets brighter as image size increases.
- . Transfer function—All types are amenable to two-axis control. Type 1 has independent linear range/total range. Type 3 has identical linear range/total range. For type 1, the linear range can be as small as image size. The type 3 detector in itself is not suitable for use for missions requiring 0.01 arc sec spacecraft stability because of the identity of linear/total range. This follows from the fact that type 3 is a larger area (e.g., 1.5 x 1.5 inch) detector. To produce a linear range (total range) of one arc sec for example, would require the enormously large focal ratio of $f/2700$.
- . Acquisition mode—Type 2 is capable of an acquisition mode through an internal electrical servo. Type 1 is capable of an acquisition mode with an internal mechanical servo. Type 3 has the inherently large linear range required for an acquisition mode, but lacks the narrow range required for extreme tracking stability.
- . Error gradient—Type 1 is approximately linear near null. A Fraunhofer diffraction pattern of a point source is symmetrical in one axis but varies as a first order Bessel function perpendicular to this axis. A cursory examination of this effect indicates that such an energy distribution is not linear but will produce an error function whose maximum slope occurs at null. Type 2 is a nonlinear device that must be calibrated when used other than as a null device. The slope of the linear region is minimum at null. Type 3 is linear over the total field of view in digital increments.
- . Reliability—The detector of type 3 uses a hot cathode and is more complex than types 1 or 2. Mean time to failure of 10,000 to 20,000 hours should be realized for the MOT time period of operation.
- . Auxiliary—Type 3 sensor data can be processed to provide a TV format picture for visual viewing in addition to being used as a fine pointing sensor for control loop operation.

Possible candidates for detectors for the MOT fine pointing sensors are determined primarily by the wavelength region where typical target stars emit the largest quantities of energy.

As shown below, the ideal detector would have a significant response from the far ultraviolet (1500 to 2000 Å) to the near infrared (10,000 Å) to cover all spectral class stars. Thermal detectors are wavelength independent since they respond to total power, hence cover the full region above. No other single detector will cover the full region, but photoelectric detectors will cover a significant portion of this range. In D2-84039-1 a detail discussion is given of the capability of the following detectors:

- o Photomultiplier detectors
- o Photovoltaic solid state detectors
- o Avalanche solid state detectors
- o Bolometers (thermal detectors)
- o Image orthicon and related imaging devices
- o Photoconductive detectors.

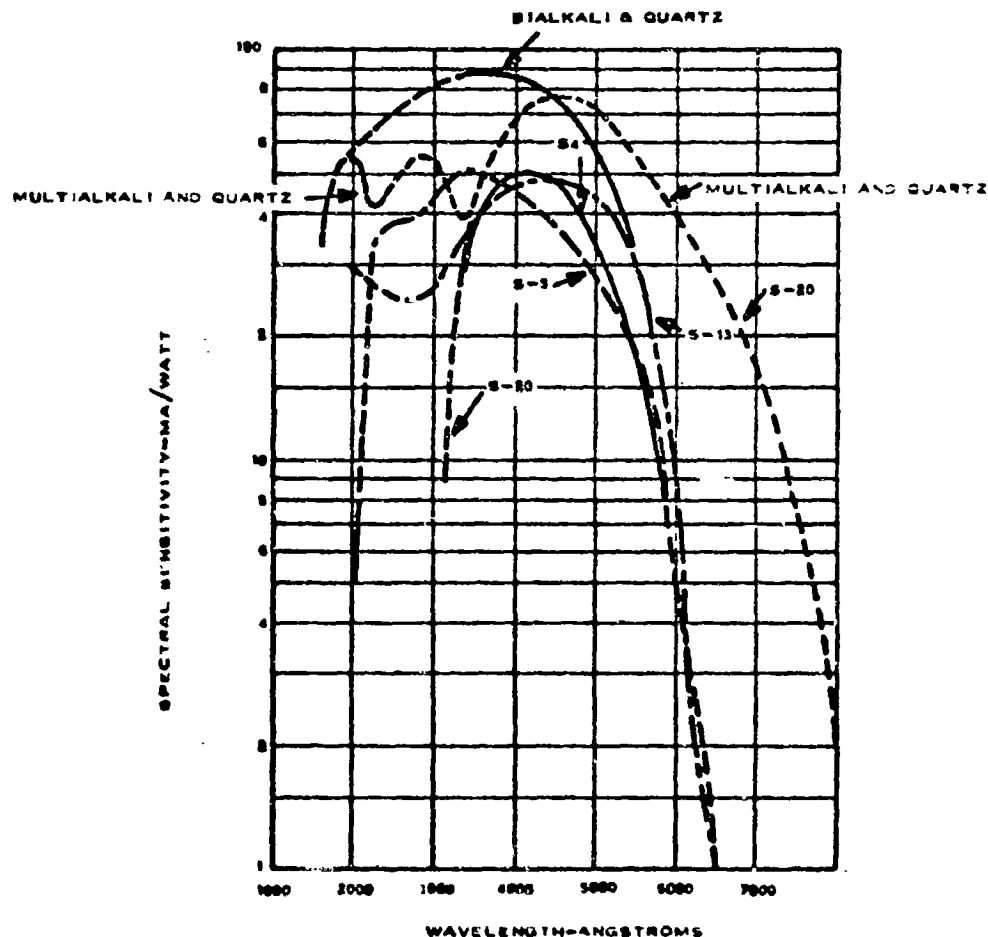


Figure 5.4-5 is a summary of the anticipated performance of the image orthicon and other detectors. It is apparent that the photomultiplier (7-20), image orthicon (7-21), avalanche detector, and the silicon photovoltaic detector all have reasonably good performance for the conditions specified.

The most dramatic improvement in performance over the next ten years is expected in the image tube category. The development and use of monoenergetic* electron scanning beams, for example, will lead to an improvement in detectivity of a factor of 5 to 10. Other improvements possible include the reduction of background scatter from the light transmitted by the multialkali photocathode, the use of channel electron multipliers, and the development of image intensifier stages.

From the standpoint of complexity, weight, and reliability, present day image orthicons leave much to be desired for the MOT application. Image tube development is expected to be rapid in the next few years, however, and most of these drawbacks will be reduced in severity. The image tube has a great advantage for the MOT application since it can provide a dual purpose detector. In addition to providing control system error voltages, the raw video may be processed to provide the astronomer with a view of the sky through the telescope. He thus will be able to visually monitor spacecraft pointing performance in essentially real time.

If the MOT fine pointing sensors had to be developed now, photomultipliers would have to be relied on very heavily for the detecting element. Even so, credible performance could be assured. Within the next two to four years, however, the designer may have photovoltaic detectors, the avalanche solid state detector, and image tube detectors of improved detectivity and reliability from which to draw, thus enhancing the performance to be expected today.

Based on the observational programs and the required fine pointing sensor characteristics, two basic sensor types emerge as desirable for the MOT application. These are: a null type sensor using photomultiplier detectors capable of very narrow linear transfer function range, and an image tube sensor using an image orthicon detector with a wide linear transfer function range, and serving the dual role of spacecraft control sensor and TV pickup. The former type sensor shows up in every observational program, and the latter in the high dispersion spectral measurements, photometry/polarimetry measurements, and as a position readout for planetary radiance measurements.

The specific sensor requirements vary with the observational program in terms of permissible noise level, star magnitude dynamic range, amount of electrical or mechanical offset required, etc. Nevertheless, the degree of similarity in the sensors is great, and in many cases the same sensor type with minimum modification will be adaptable to several observational programs.

The basic design of the required null type sensor using photomultiplier detectors is very similar to hardware in existence today, e.g., the Stratoscope II fine pointing sensor, and the GE simulated fine pointing sensor for OAO. Improved performance will come through use of detectors with improved quantum efficiency,

* The range of energy for electrons emitted for a hot cathode is quite large. Monoenergetic electrons are those with identical kinetic energy.

Detector	Operating Temperature	Element Area (cm ²)	Response Time (sec)	NEP (watt for 5 cps bw)	D* λ Peak	Spectral Response	Star Magnitude giving S/N = 100 with MOT (1)
1) RCA 7265 Photomultiplier or ITT FE 143 multiplier phototube	25°C	11	10 ⁻⁸	9(10 ⁻¹⁵)	2(10 ¹⁵)	S-20	11.6
2) Silicon Photovoltaic Cell	25°C	4(10 ⁻²)	10 ⁻⁵	6(10 ⁻¹⁴)	1(10 ¹²)	.6-1.1 μ	9.8
3) Cd S Photoconductive Cell	25°C	1	5(10 ⁻²)	1.6(10 ⁻¹⁴)	3(10 ¹⁴)	.3-.55 μ	10.6
4) Silicon Avalanche Detector	25°C	4(10 ⁻²)	10 ⁻⁸	7(10 ⁻¹⁵)	1(10 ¹⁴)	.6-1.1 μ	12
5) Thermistor Bolometer	25°C	4(10 ⁻²)	3(10 ⁻³)	2(10 ⁻⁹)	2(10 ⁸)	flat	1.0
6) NbN Superconducting Bolometer	15°K	4(10 ⁻²)	5(10 ⁻⁴)	8(10 ⁻¹¹)	5(10 ⁹)	flat	2.5
7) Ge:As Bolometer	2°K	4(10 ⁻²)	4(10 ⁻⁴)	5(10 ⁻¹³)	8(10 ¹¹)	flat	8.0
8) Z7806 Electromagnetic Image Orthicon, 20°C, S-20 Response	Element Area (cm) ²	Frame Rate (sec) ⁻¹	NEP per Element (watts)	Star Magnitude giving S/N=10 with MOT(1)			
4.8(10) ⁻⁴	1		2.2(10) ⁻¹⁶	18			
(300 TV lines per target inch) ⁽²⁾	30 100		7.2(10) ⁻¹⁶ 2.2(10) ⁻¹⁵	16.6 15.5			
4.3(10) ⁻⁵	30		6.5(10) ⁻¹⁵	14			
(1000 TV lines per target inch) ⁽²⁾	30		2(10) ⁻¹⁴	12.7			

(1) Assumes 23% utilization of total energy collected

(2) (1 line pair)² on photocathode at limiting resolution, 100% contrast

Figure 5.4-23

and by extension of the usable guide star energy to below 2000Å with reflective optical systems.

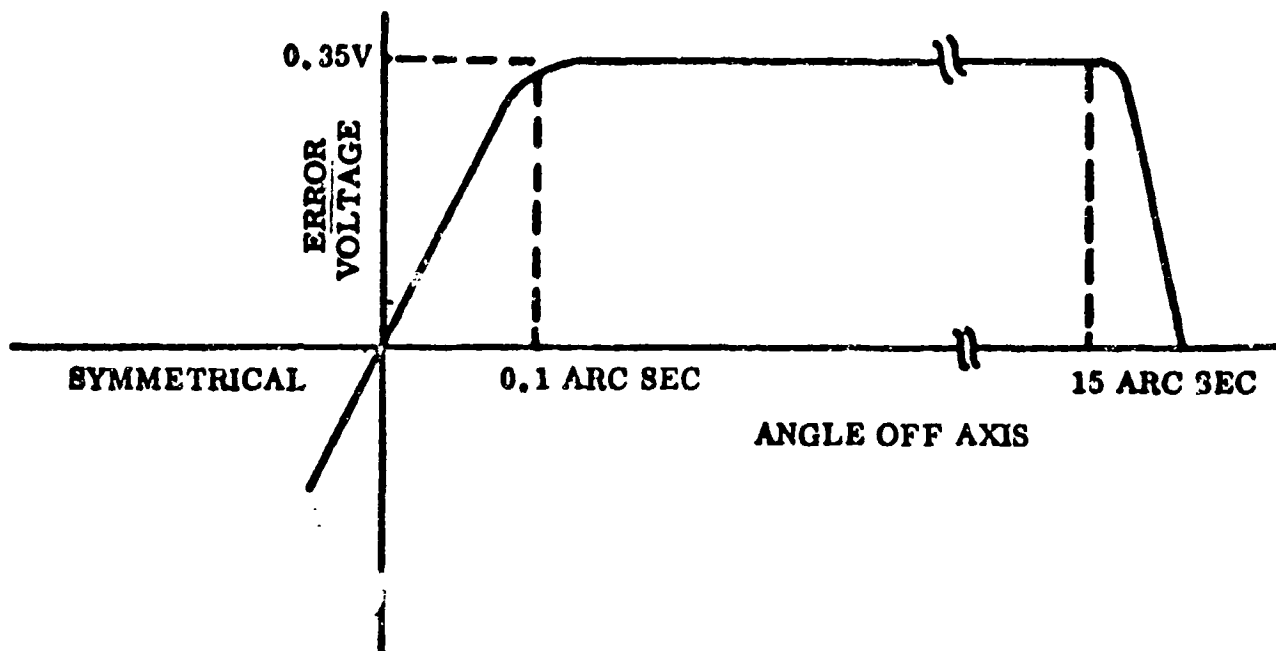
The required imaging type sensor using an image orthicon has not yet been developed for flight hardware, but an engineering prototype of similar characteristics and using a vidicon detector has been built. Rapid strides in development of both image tubes and sensors employing them are expected in the next several years.

For purposes of synthesizing a basic fine pointing sensor configuration, the high dispersion stellar spectrometry mode is selected since it may employ a sensor of each type described above. In this event the null type detector would be internal to the spectrometer housing and would be used for maintaining the stability of the telescope point with high precision. The image tube sensor would be external to the spectrometer and would provide a large acquisition range as well as a visual frame of reference through a TV link to assist the astronomer in remotely aligning his instrumentation.

System Synthesis - Null Type Photomultiplier Sensor

For this sensor inside the spectrometer housing we select the pyramid beamsplitter type. The image dissector type is also applicable, but the pyramid beam splitter has greater utility for the total program (considering all observations) since it has an independent linear/total range. The data presented below are considered representative for sensors to be built several years from now. The difference between 1965 and 1975 performance is estimated to be between 1 and 2 star magnitudes.

The noise equivalent power in a five cps electrical bandwidth of the best photomultiplier is about 9×10^{-15} watts for an A_0 type star. This leads to baseline condition of a signal to noise ratio of 100 from a 11.5 magnitude star with an effective collecting aperture of 23% of the energy from the 120 inch MMT telescope. This signal to noise ratio is equivalent to the ratio of linear transfer function range to noise error voltage expressed in equivalent angular range. The noise error voltage should be significantly less than the overall spacecraft stability of 0.01 arc sec. Allowing a reasonable margin of ten, gives a rms noise error voltage of 0.001 arc sec for a sensor linear range of 0.1 arc sec. The baseline fine pointing characteristics are shown in figure 5.4-24.



Linear Range	± 0.1 arc sec
Total Range	± 15 arc sec
Error Gradient	3.5 volts per arc sec nominal, can be varied to suit control loop
Error Gradient Linearity	$\pm 5\%$ 0 to .05 arc sec $\pm 20\%$.05 arc sec to remainder of linear region (should be relaxed if compatible with control loop)
Dynamic Response	5 cps
Noise Error Voltage	0.001 arc sec
Null Instability (drift)	0.001 arc sec
Noise Frequency Spectrum	White
Star Magnitude	+11.5 magnitude

Figure 5.4-24

System Synthesis - Image Tube Sensor

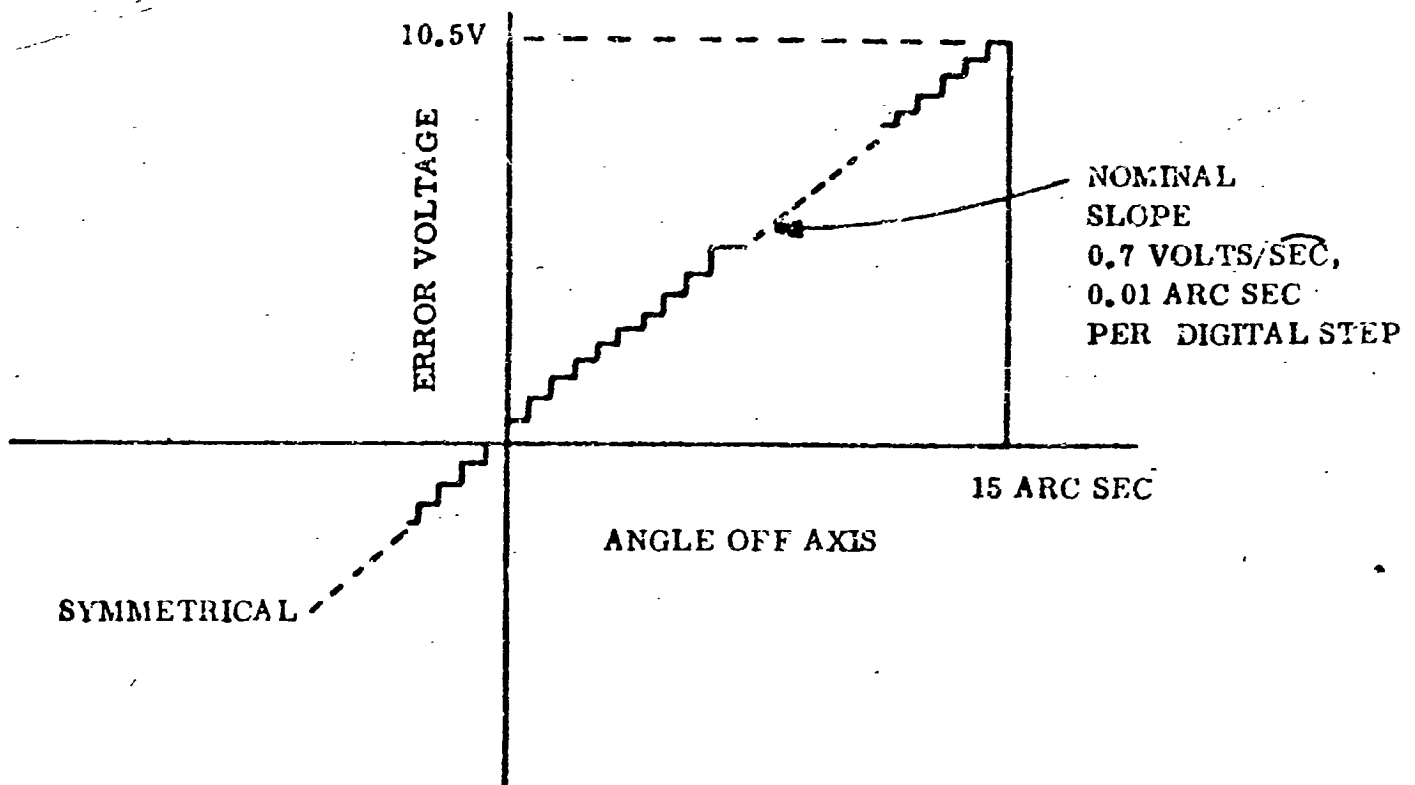
For the sensor outside the spectrometer housing in the high dispersion stellar spectrometry mode, was selected the image tube type with the image orthicon as the detector. As mentioned previously, it has the dual capability of providing control system error voltages for the acquisition phase, and a video readout for visual observation. The total field of view required is ± 15 arc sec in pitch and yaw. A transfer lens with a magnification of about three is required to reduce the effective speed of the telescope to f/90, based on a raster size of 1.5 x 1.5 inches. A frame rate of 100 per second is selected for the baseline case, and is a conservatively estimated figure based on estimated control loop characteristics.

Detection is assumed to occur if the signal to noise ratio for a discrete resolution element exceeds ten. This detector is essentially a threshold detector, and experience on similar type vidicon image tube sensors indicates a required S/N of 5 to 10 to permit consistent processing of the raw data. The limiting S/N depends to a large extent on the electronic processing methods, but a S/N of 10 is a reasonable minimum to demand.

Based on 3000 total line resolution, the noise equivalent power per resolution element of the image orthicon is approximately $2(10^{-14})$ watts at 100 frames per second. For a signal to noise ratio of ten, this gives a limiting guide star magnitude of about 12.7 based on utilizing 23 percent of the total energy collected by the 40T telescope, or 13.7 magnitude based on 58 percent utilization.

There is a trade between angular resolution and minimum guide star magnitude over certain limits. For the baseline case described above (3000 resolution lines per raster), the star image size is larger than the resolution element. The NEP per resolution element decreases (becomes better) as the element size increases, in proportion to the area change, until the star image size and the resolution element are equal in area. For the f/90 configuration described above, this occurs at approximately 2600 total raster lines, and hence about 0.3 magnitude fainter stars can be detected by reducing the angular resolution from 0.01 arc sec to $\frac{2}{3}$ (0.01) arc sec. There is also a reciprocity between exposure time (frame rate) and faintest detectable star. At a rate of one frame per second, for example, the improvement should be nearly 100 times that at 100 frames per second, i.e., about five magnitude fainter stars (18th magnitude) will yield the same signal to noise ratio. Although this is far too slow a frame rate to use for spacecraft control purposes, it is satisfactory for visual readout by an observer.

The estimated characteristics of the image orthicon fine pointing sensor are shown in Figure 5.4-26



Linear Range:	± 15 arc sec
Total Range:	± 15 arc sec (± 1500 digital steps)
Error Gradient:	0.7 Volt/sec nominal, can be varied to suit control loop
Error Gradient Linearity:	Step function
Null Offset (Drift)	.01 arc sec
Noise Error Voltage:	$\pm .01$ arc sec-digital step
Noise Frequency Spectrum:	100 cps or submultiple thereof, i.e. 50 cps, 25 cps, 12.5 cps, 6.25 cps, etc, with probability determined by star magnitude
Dynamic Response:	100 cps sampling rate
Limited Guide Star Magnitude	+12.7

Figure 5.4-26

IMAGE ORTHICON FINE POINTING SENSOR

System Synthesis - Intermediate Pointing Star Tracker

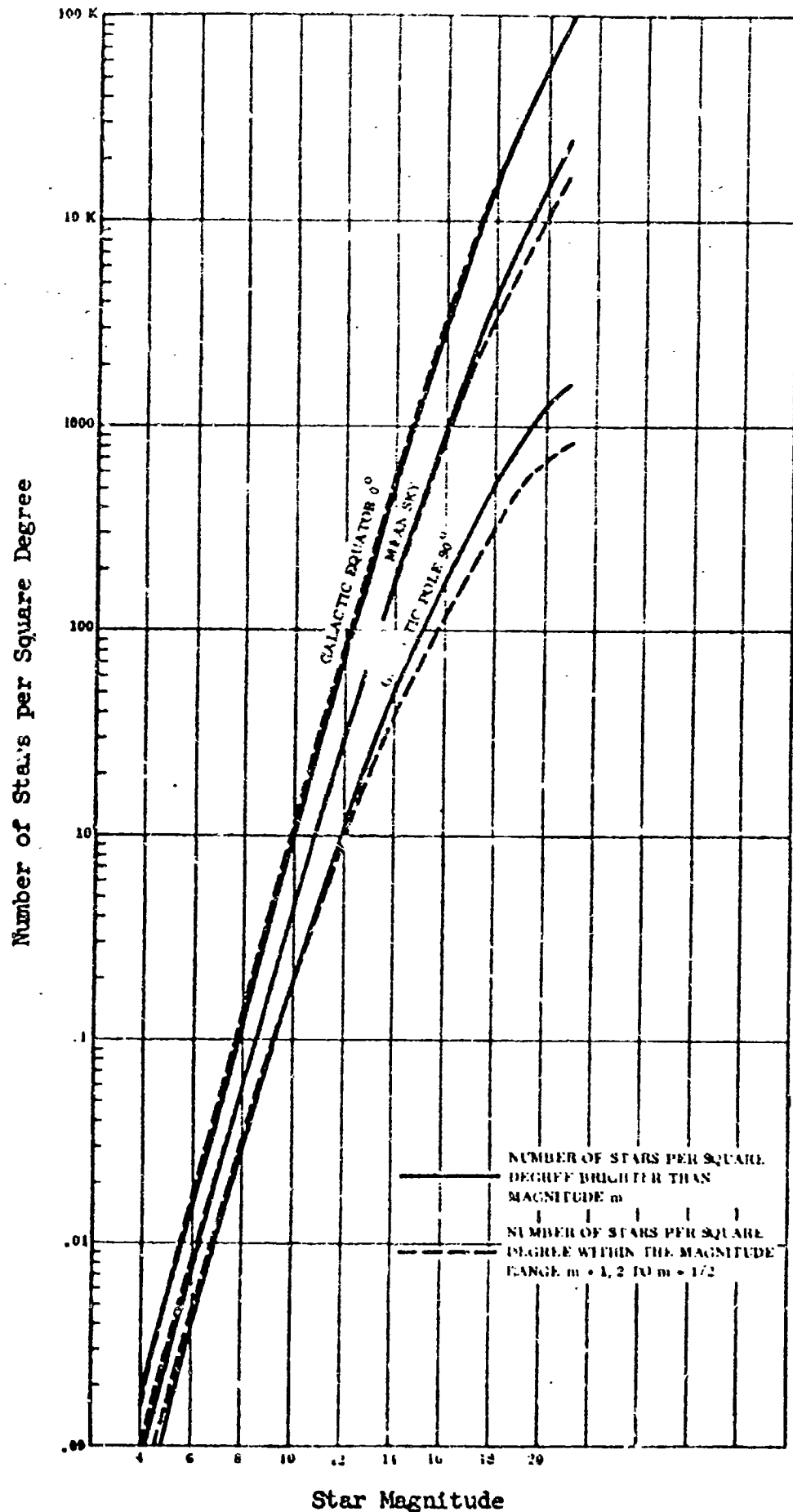
Overall stability and pointing accuracy as small as 0.01 arc second for the main telescope is required for some IOT observational programs. With no intermediate star tracker between the coarse and fine pointing modes, the ratio of fine pointing field-of-view to accuracy would be on the order of 2×10^4 . This is unrealistically high and can be avoided thru the use of an intermediate star tracker to control spacecraft pitch and yaw axes. Its nominal optical axis would be boresighted to be coincident with the optical axis of the main telescope.

The intermediate pointing sensor must improve spacecraft coarse pointing accuracy by more than an order of magnitude - preferably two orders - in order that the demands on the fine pointing sensor not be too severe. The intermediate sensor is completely independent of the main telescope in operation; hence the problem of spacecraft thermal and structural instability is still present. The problem is somewhat different, however, in that now only one star tracker is involved, and its nominal pointing direction is fixed. It can structurally be tied into the main telescope assembly, or be located in the instrumentation cabin looking along the main telescope structure, or can be located on the f/30 Cassegrain secondary mirror structure if necessary.

The intermediate pointing sensor must have an instantaneous field of view that overlaps the coarse pointing accuracy (approximately ± 4 arc min) if a tedious search process is to be avoided. Since the nominal point direction of the main telescope may be to a very faint star (to perhaps twentieth magnitude for some experiments), a brighter nearby star must be used for guidance. This will require the intermediate pointing tracker to have either a very large instantaneous field of view (tens of minutes to degrees) or be capable of being mechanically or electrically gimballed over this range.

The total offset field (or gimbal range) is determined by the star population density of brighter stars in conjunction with a given objective aperture size. Figure 5.4-27 is a plot of star population vs position in the galaxy. It is apparent that any part of the sky is accessible to a boresight tracker if it can track a fifth magnitude or brighter star, and if the gimbal freedom is at least ± 5 degrees. Near the galactic plane (± 30 degrees), this amount of gimbal freedom would permit use of fourth magnitude stars. Figure 5.4-28 is a direct plot of this data showing the required gimbal freedom required versus the minimum magnitude star suitable for guidance. A large angular offset capability (10 to 20 degrees) would permit use of guide stars in the third to fourth magnitude range, hence the use of a relatively small collecting aperture. This advantage is paid for in accuracy (the cross coupling between axes for a fixed misalignment) and electronic complexity (the required extra storage capacity for the same increment offset). A total freedom of about five degrees should thus be considered an upper bound since the required star magnitude (± 5) is not unreasonable. Smaller gimbal travel would be desirable, but must be paid for by a larger objective.

The required telescope pointing accuracy when using the intermediate pointing star tracker is determined by the maximum acquisition range of the fine pointing sensors. A typical mission in terms of fine pointing requirements is high dispersion spectra measurements for which absolute pointing and stability on the order of 0.01 arc



seconds are required. Current state-of-the-art star trackers exhibit characteristics such that the ratio of field of view to angular resolution is limited to a value of perhaps 500 to 1000. Assuming this quantity can be increased to about 1500 to 2000 for the time period of interest, this would establish the maximum

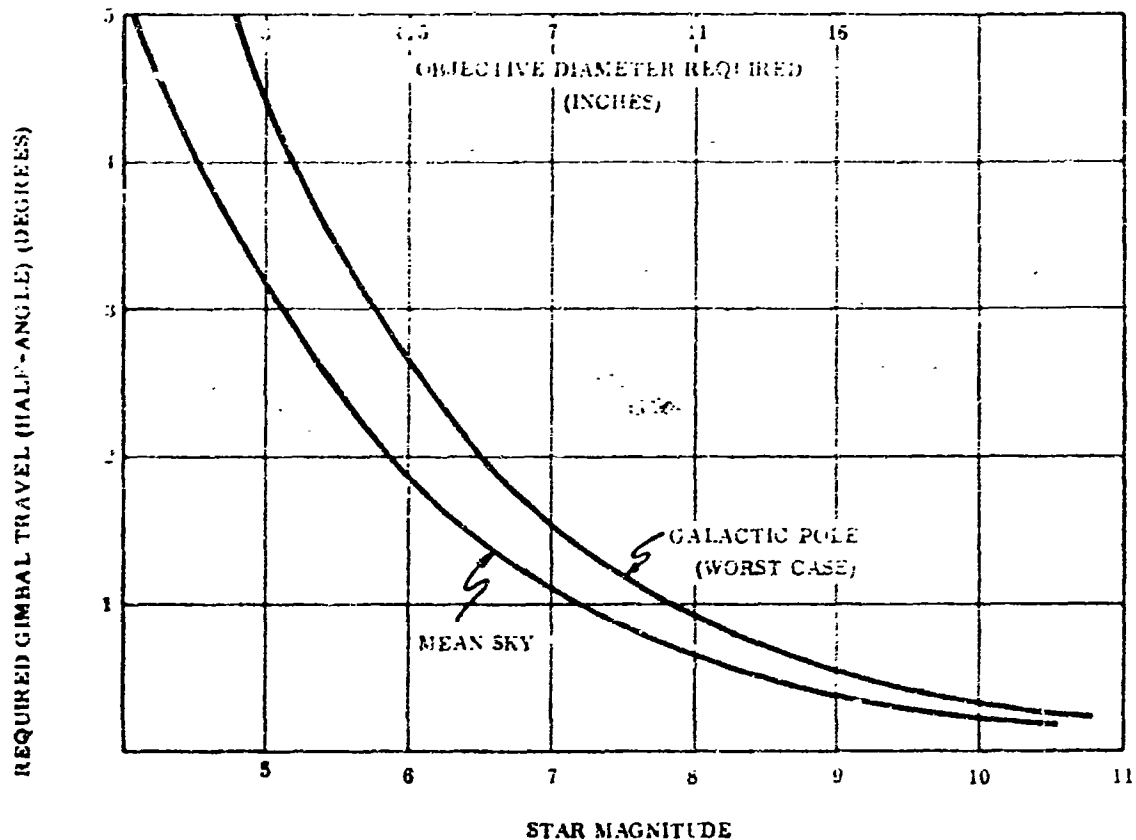


Figure 5.4-28

INTERMEDIATE SENSOR GIMBAL FREEDOM

field of view for the MOT high dispersion fine pointer at ± 15 to ± 20 arc seconds, or a total field of 30 to 40 seconds. In order to allow some measure of safety in the capture range of the fine pointing sensor, it is desirable that the intermediate tracker/control system overall accuracy be held to $1/3$ to $1/2$ the fine pointer field of view, that is, 5 to 10 arc seconds. Pointing accuracy of the intermediate tracker/control system is defined as the angle between the desired pointing direction of the main telescope and its actual pointing direction. Initial system bias errors are excluded since these can be removed by calibration in orbit.

There appears to be two different concepts of trackers for the intermediate pointing mode - each with its advantages and disadvantages. The first concept would employ a photomultiplier detector of either the image dissector type (as with the QAO boresight tracker) or the pyramid beam splitter type (as used with Stratoscope). Each would require an instantaneous field of ± 4 arcmin, and be mechanically

gimbaled over 15 degrees. The objective size would be five to six inches at about $f/20$, based on a $1/4$ inch detector. The required angular offset precision is on the order of one arc sec, hence a complex and costly dual angular transducer will be required.

The second concept employs an image orthicon detector with a sufficiently large objective (9 to 10 inches) to permit operation with a tenth to eleventh magnitude star. In this configuration, no mechanical offset is required, and the field of view is about 40×40 arc minutes. This requires an $f/15$ objective for a 1.5 inch detector face.

The overall length of the gimbaled telescope would be about 25 inches based on an $f/3$ primary, and about 40 inches for the image orthicon sensor with the same focal ratio. These values assume a Cassegrain configuration. Other configurations may be used to reduce the size somewhat, but it is assumed that size and weight are not a major limitation. The weight of the image tube concept would be somewhat more than the gimbaled type even though it has no moving parts or transducers.

The final decision between the two concepts should be made on the basis of the following considerations.

- Improvements in image tube reliability, and weight and size reduction in the next several years.
- The relative importance of size and weight for the intermediate pointing sensor.
- The decision as to whether a boresighted TV will be carried by MOT for other purposes.
- The complexity and cost of a 20-bit equivalent angular transducer for the gimbaled concept.
- Control system considerations for a large increment (1.2 arc sec) digital resolution of the image tube detector.
- The savings in weight and cost associated with permitting a coarse pointing mode accuracy of 5 to 10 minutes (image tube) rather than three to four minutes (gimbaled tracker).

Some of the more pertinent characteristics of the two sensor concepts are summarized below. These numbers are only rough estimates, and little can be gained in attempting to refine them at this stage of the feasibility study. Structural/thermal analysis and control system concepts must be pursued in the next iteration of the intermediate pointing sensor characteristics:

<u>Comparison</u>	<u>Gimbaled Star Tracker</u>	<u>Image Tube Star Tracker</u>
Instantaneous field-of-view	± 4 arc min	± 20 arc min
Total gimbaled field-of-view	± 5 degree	None

<u>Comparison</u>	<u>Gimbaled Star Tracker</u>	<u>Image Tube Star Tracker</u>
Accuracy of Offset	± 1 arc sec	± 1.2 arc sec
Sensor Linear Range	± 20 arc sec	± 20 arc min
Frequency Response	5 cps	50 frames/sec
Required Star Magnitude	+ 5	+ 10.5
Required Objective	6 -inch diameter, f/20	9 -inch diameter, f/15
Required maximum rms sensor noise	0.2 arc sec	1.2 arc sec
Estimated spacecraft pointing stability	± 2 arc sec	± 3 arc sec
Estimated weight	25 lbs	50 lbs
Estimated power required	10 watts @ 28 V	8 watts @ 28 V
Estimated size	9-inch dia x 25 inches long	12-inch dia x 40 inches long

Should subsequent thermal/structural analysis indicate major problems in maintaining alignment between the telescope axis and intermediate pointing sensor axis, it may be necessary to incorporate the boresight tracker within the main telescope, utilizing the 120 inch collection aperture. While at first thought this may appear advantageous because of the much greater light gathering power of the 120 inch primary, there are significant penalties associated with this approach. First, the total field of view of the f/30 telescope configuration will be limited to some small value - probably 10 to 20 minutes maximum - by the field stop in the primary mirror itself. With such a limited offset capability, the entire sky might not be accessible for high dispersion measurements even taking into account the much greater light gathering power of the main telescope mirror since only a small fraction of this energy can be taken for the intermediate tracker. This limitation can be fully assessed once the actual field limitation of the main telescope is known. Several additional disadvantages that are apparent are the large linear travel of the guide star image (10 inches for a 10-minute field) with its attendant need for large internal optics and/or detector; the addition in complexity to the experiment instrumentation caused by sharing the experiment objective with the intermediate tracker objective; the need to change the intermediate tracker (or at least its optics) each time the f-number of the main telescope is changed; and finally, the loss in light to the main experiment (perhaps 10 to 20 per cent) that is required to drive the intermediate tracker.

System Synthesis - Fine Pointing Attitude Control Loop

In this section, the previously discussed sensor and CMG parameters are combined into the fine pointing loop in a manner to achieve the pointing requirements. Figure 5.4-12 is a block diagram of this loop.

The primary consideration in designing the compensation network was to minimize the limit cycle caused by gyro friction. The final compensation network took into account the results being obtained from analog computer limit cycle tests using first cut compensation designs. The computer results indicated that the magnitude of the limit cycles could be decreased by increasing the compensation gain and pointing loop crossover frequency.

Referring to Figure 5.4.29, curves 1 and 2 show the uncompensated (forward loop) and compensated total pointing loop bode plots, and curve 3 shows the compensation network plot. With the sensor lag at 30 rad/sec and the flexible mode at 54 rad/sec, a 10 rad/sec crossover was selected as the maximum attainable. Maximum compensation gain was selected by stipulating that the first pair of compensation poles be no lower than 0.1 rad/sec. This permitted a compensation gain of 167 inch ounce/arc sec.

The transfer function of the compensation network not including the flexible mode filter was:

$$F(s) = \frac{167 \left(\frac{s}{0.74} + 1 \right)^2 \left(\frac{s}{3.0} + 1 \right)^2}{\left(\frac{s}{0.1} + 1 \right)^2 \left(\frac{s}{40} + 1 \right)^2} \quad \frac{\text{in-oz}}{\text{arc sec}}$$

The pointing loop bode plots of the previous figure are made with the compensation network above and do not include the flexible mode filter. The incorporation of a flexible mode filter into the attitude feedback loop was used to stabilize the flexible mode vibrations. The complex pole zero network below was cascaded with the compensation network to filter out the flexible mode.

$$\frac{\frac{s^2}{50^2} + 2\frac{(.1)s}{50} + 1}{\frac{s^2}{30^2} + 2\frac{(.1)s}{30} + 1}$$

This filter gave results that agree with the rigid vehicle over a ten percent frequency variation from the flexible mode. Figure 5.4-30 shows an open loop bode plot of the system incorporating this filter.

A brief paper analysis of the gyro tracking loops was undertaken to see the effects of non-identical gyros. The analysis indicated that the tracking loop would add a complex pole-zero combination to the system transfer function, much the same as a flexible vehicle mode with high damping. The location of the pole-zero combination, through variable with tracking loop gain, would lie close to the complex poles of the vehicle rate loop. With identical CMG's, the complex pole-zero combination cancels itself out.

System Synthesis - Non-Linear Analysis

The main purpose here is to explain why the previously described compensation network was chosen. The initial compensation network, designed and tested on the analog computer, produced a 1 rad/sec pointing loop crossover frequency. These

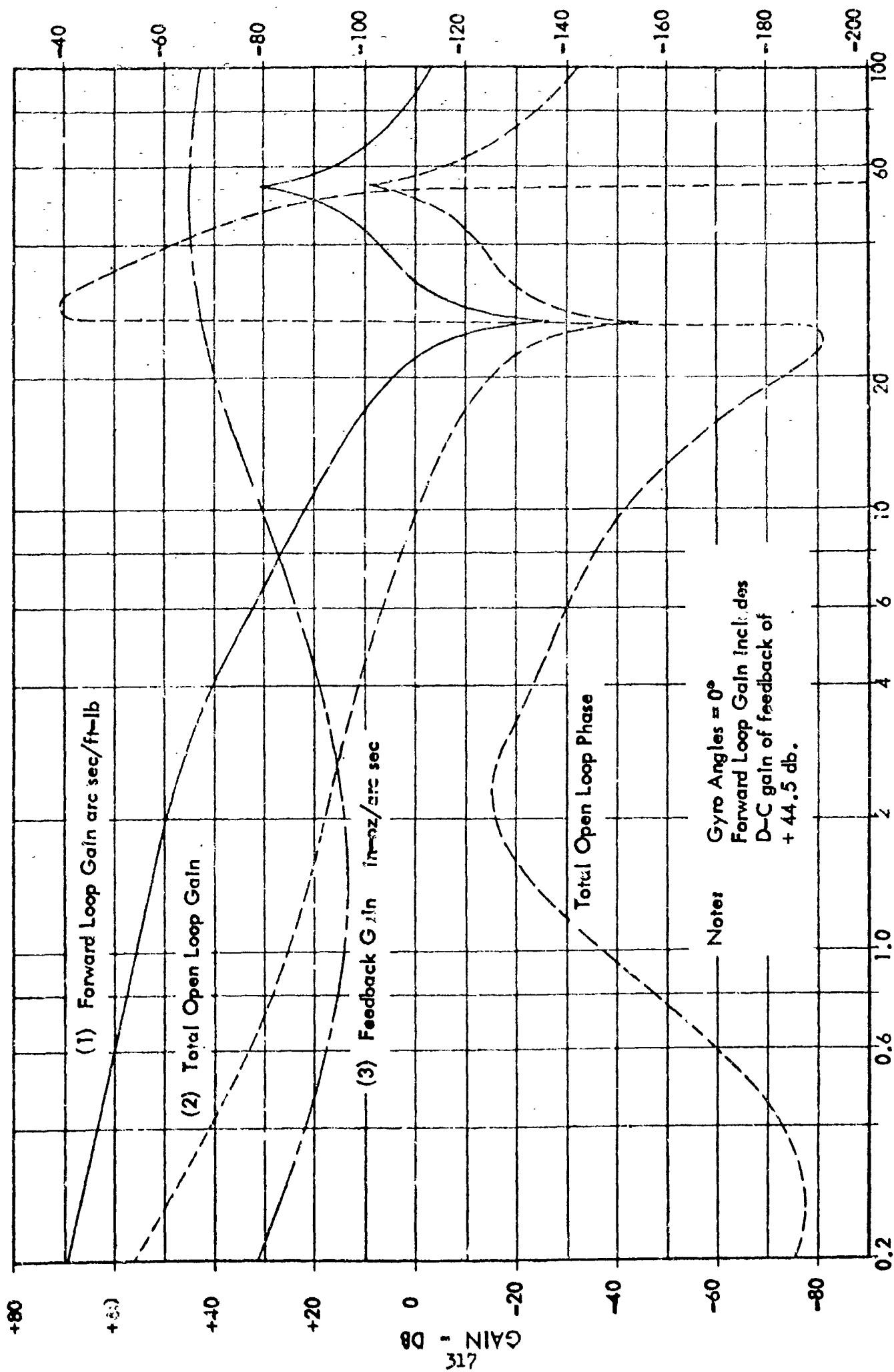


Figure 5.4-29

POINTING LOOP - BODE PLOT

816

GAIN - DB

+90
+60
+40
+20
0
-20
-40
-60
-80

Open Loop Phase

Open Loop Magnitude Response

$\gamma = 0$

0.2

0.6

1.0

2

6

10

20

60

100

FREQUENCY - RAD/SEC

Figure 5.4-30

PHASE SHIFT - DEGREES

-40
-80
-120
-160
-200
-240
-280
-320
-360

D2-840-12-1
1-2-048-20

tests showed that gyro friction caused limit cycling, and that a higher pointing loop response would be needed to meet the pointing specifications.

A phase plane paper study was then carried out to obtain an idea of what limit cycle frequencies would be required to meet the 0.01 sec of arc specification. The study indicated that limit cycle frequencies near 1 cps would be required as disturbance torque magnitude approached maximum. These conclusions were later borne by the computer results.

The compensation network was thus designed to produce a maximum pointing loop frequency response.

The frequency and magnitude of the limit cycle can be explained by referring to the describing function plot of Figure 5.4.31 and the previous bode plots of Figure 5.4.30. To limit cycle at a frequency of 3.2 rad/sec, the complete open loop including the gyro friction describing function must have a gain of 1 and phase of 180 degrees at this frequency.

The linear transfer function has a gain of 7.95 and phase of -158° at this frequency while the friction contributes -22 degrees of phase shift and gain of $1/5$ when the input magnitude is 0.05 inch ounce. Physically, this limit cycle can be explained as follows. The position limit cycle after being compensated must have a magnitude large enough to break gyro friction. For a limit cycle magnitude of 0.008 arc sec at a frequency of 3.2 rad/sec, the compensation network has a gain of 6.3 inch ounces/arc sec. The input into the gyro is therefore 0.0504 inch ounce, just enough to overcome gyro friction.

In summary, the compensation network must have a gain large enough at the limit cycle frequency to allow the vehicle oscillations to remain below specification and still break gyro friction. Since the compensation gain increases with increasing frequencies in the region of 3 rad/sec, a higher limit cycle frequency requires less position magnitude.

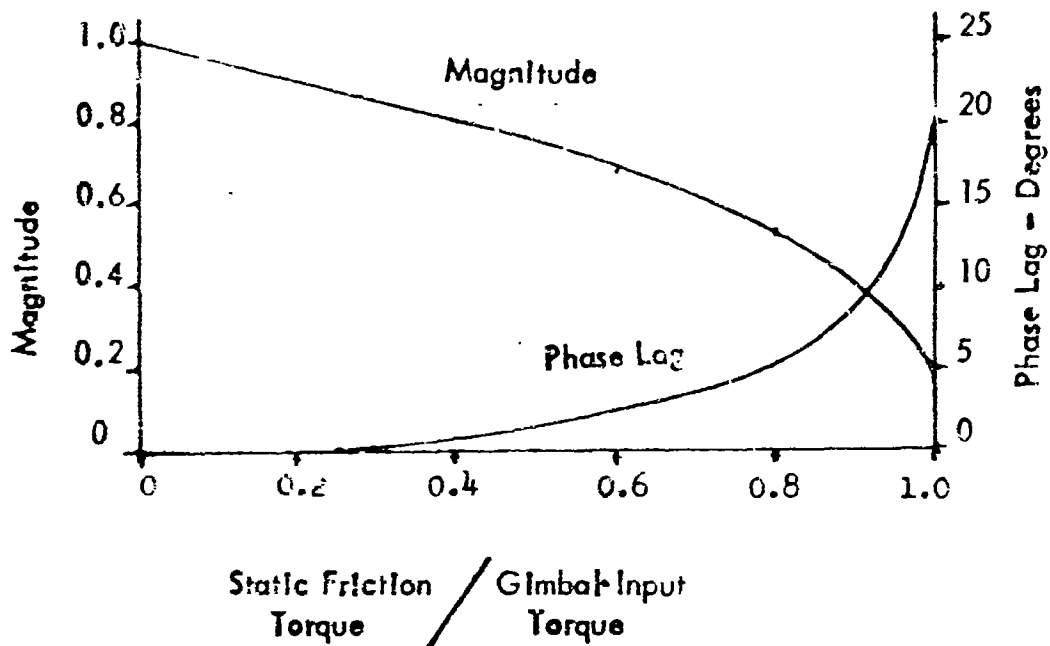


Figure 5.4-31

CMG DESCRIBING FUNCTION

5.4.5 Performance Verification

A detailed study including an analog computer simulation was performed to evaluate the single axis performance of the fine pointing attitude control loop. The simulation concentrated on the fine pointing mode, thus the acquisition and reorientation problems received only minor attention. The simulation assumed identical control moment gyros and included gyro friction, torque motor and sensor saturation, sensor noise, and the first flexible mode of the vehicle. Figure 5.4-32 shows a block diagram of the system simulated.

The gyro control torque is proportional to gimbal rate times the cosine of the gimbal angle and the vehicle rate feedback is proportional to the cosine of the gimbal angle, but during fine pointing gimbal angle variations are small. The cosine of gimbal angle multipliers present in the forward loop and rate feedback loop can therefore be considered constant for a given simulation run. The two extremes of magnitude for these multipliers, $\cos 0$ degrees = 1.0 and $\cos 45$ degrees = 0.707, were both simulated to obtain fine pointing performance. These gain variations were four to present no major problems.

The important quantity of gyro friction for this system is the static friction; i.e., the deadband presented to the torque motor at very small gimbal rates. The magnitude of f_s dictates the minimum gain required in the position feedback loop for a given position accuracy specification.

Definition of the friction characteristic near zero gimbal rate is extremely difficult, and was simulated as a worst case, constant f_s or deadband up to



FIGURE 5.4-32
ANALOG SIMULATION BLOCK DIAGRAM

breakaway gimbal rate. A more detailed description of the simulation and the results is contained in the backup documentation. The results of the study are summarized in the following paragraphs.

Analog Computer Runs

The analog computer traces made during the study were broken down into three categories: linear gyro; nonlinear gyro; $\alpha = 0, \alpha = 45$ degrees. A tabulation of the results is listed in Figure 5.4-33 for the majority of the runs. Some of the time histories of these runs are shown in Figures 5.4-34 and -35.

Linear Gyro Dynamics

In Runs 16 and 17 the linear gyro dynamics were utilized to serve as a comparison with the nonlinear responses. In the first 0.005 sec. rms noise was introduced into the sensor. The 0.0002 sec attitude offset was due to the amplified computer null offsets. The second consists of the linear response to an attitude initial condition.

In Runs 18, 19 and 20, the maximum attitude rate that would not exceed the sensor range was determined. In these cases the computer scaling was changed and the torquer and sensor saturation levels incorporated into the circuit. The criteria used consisted of introducing an attitude initial condition of 5.0 sec and increasing the attitude rate initial condition until the attitude peaked at 10.0 sec. This was done for each sensor saturation level. The results were:

<u>Sensor Saturation Level sec</u>	<u>Maximum Attitude Rate sec/sec</u>	<u>Time to Reach Steady State sec</u>
± 0.4	20.0	4.2
± 0.2	16.0	6.6
± 0.1	14.0	15.6

Nonlinear Gyro Dynamics, $\alpha = 0$ degrees

Runs 21, 22 and 23 show the effect of increasing the disturbance torque from zero to 0.22 foot-pounds. With increasing T_D , the limit cycle, with worst case at zero ft-lb, decreases until the system becomes linear. The second trace has a T_D approximately half way between zero and the linear region while the last shows the worst case disturbance in which the system was well into the linear region.

Runs 24 through 32 show the effect of 0.001, 0.002 and 0.005 sec rms sensor noise as the disturbance increases from zero to 0.22 ft-lb. Of particular importance was the reduction of the limit cycle at $T_D = 0$ ft-lb. A further reduction occurs as the disturbance torque increased to 0.22 ft-lb which was to be expected since the nonlinear effect was greatly reduced.

In Runs 33, 34 and 35, the effect of various initial attitudes to the system was studied with these responses. After the initial transient, the system returned to the limit cycle of Run 21.

Fig. #	System Type	Time Constant	Transfer Function	Initial Condition θ_{IC}	Peak 1	Peak 2	Peak 3	Peak 4
16*	Linear	1	$\frac{1}{s^2 + 1}$	Peak = 1.000 Steady = 1.000	Peak = 1.000 Steady = 1.000			
17	Linear		$\frac{1}{s^2 + 1}$	Peak = 1.000 Steady = 1.000	Peak = 1.000 Steady = 1.000	Peak = 1.000 Steady = 1.000	Peak = 1.000 Steady = 1.000	
21	Non-linear	1	None	Limit Cycle	Limit Cycle	Limit Cycle	Limit Cycle	Limit Cycle
22	Non-linear	0.1	None	Peak = 1.001 Steady = 1.000	Peak = 1.002 Steady = 1.000	Peak = 1.000 Steady = 1.000	Peak = 1.000 Steady = 1.000	Peak = 1.000 Steady = 1.000
23*	Non-linear	0.22	None	Steady State = 0	Steady State = 0	Steady State = 0	Steady State = 0	Steady State = 0
34*	Non-linear	1	Sensor Noise .001 sec RMS	Peak = 1.005 Steady = 1.000	Peak = 1.007 Steady = 1.000			
25*	Non-linear	1	Sensor Noise .002 sec RMS	Peak = 1.005 Steady = 1.000	Peak = 1.005 Steady = 1.000			
26*	Non-linear	1	Sensor Noise .005 sec RMS	Peak = 1.001 Steady = 1.000	Peak = 1.001 Steady = 1.000			
27*	Non-linear	0.03	Sensor Noise .001 sec RMS	Peak = 1.002 Steady = 1.000	Peak = 1.002 Steady = 1.000			
28*	Non-linear	0.03	Sensor Noise .002 sec RMS	Peak = 1.001 Steady = 1.000	Peak = 1.004 Steady = 1.000			
29*	Non-linear	0.03	Sensor Noise .005 sec RMS	Peak = 1.0025 Steady = 1.0015	Peak = 1.012 Steady = 1.006			
30*	Non-linear	0.22	Sensor Noise .001 sec RMS	Peak = 1.001 Steady = 1.000	Peak = 1.001 Steady = 1.000			
31*	Non-linear	0.22	Sensor Noise .002 sec RMS	Peak = 1.001 Steady = 1.000	Peak = 1.002 Steady = 1.000			
32*	Non-linear	0.22	Sensor Noise .005 sec RMS	Peak = 1.0015 Steady = 1.0005	Peak = 1.004 Steady = 1.0005			
33**	Non-linear	0	$\theta_{IC} = 1.1 \text{ sec}$	Peak = 1.007 Steady = 1.000	Peak = 1.002 Steady = 1.000	Peak = 1.003 Steady = 1.000	Peak = 1.115 Steady = 1.115	
34**	Non-linear	0	$\theta_{IC} = .15 \text{ sec}$	Peak = 1.03 Steady = 1.000	Peak = 1.1 Steady = 1.000	Peak = 1.45 Steady = 1.000	Peak = 17.0 Steady = 17.0	
35**	Non-linear	0	$\theta_{IC} = .25 \text{ sec}$	Peak = 1.15 Steady = 1.000	Peak = 1.5 Steady = 1.000	Peak = 1.50 Steady = 1.000	Peak = 27.5 Steady = 27.5	
36**	Non-linear	0	$\theta_{IC} = .20 \text{ sec}$	Peak = 1.215 Steady = 1.000	Peak = 1.10 Steady = 1.000	Peak = 1.25 Steady = 1.000	Peak = 1.25 Steady = 1.25	
39	Non-linear	0	None	Limit Cycle	Limit Cycle	Limit Cycle	Limit Cycle	Limit Cycle
40	Non-linear	0.03	None	Peak = 1.005 Steady = 1.000	Peak = 1.012 Steady = 1.000	Peak = 1.0 Steady = 1.000	Peak = 1.0 Steady = 1.0	
41*	Non-linear	0.22	None	Steady State = 0	Steady State = 0	Steady State = 1.03	Steady State = 1.03	
42*	Non-linear	0	Sensor Noise .001 sec RMS	Peak = 1.0020 Steady = 1.0015	Peak = 1.005 Steady = 1.000			
43*	Non-linear	0	Sensor Noise .002 sec RMS	Peak = 1.0020 Steady = 1.0015	Peak = 1.006 Steady = 1.000			
44*	Non-linear	0	Sensor Noise .005 sec RMS	Peak = 1.0015 Steady = 1.0015	Peak = 1.004 Steady = 1.000			
45*	Non-linear	0.03	Sensor Noise .001 sec RMS	Peak = 1.0020 Steady = 1.0015	Peak = 1.004 Steady = 1.000			
46*	Non-linear	0.22	Sensor Noise .005 sec RMS	Peak = 1.001 Steady = 1.001	Peak = 1.001 Steady = 1.001			
47***	Non-linear	0	$\theta_{IC} = .01 \text{ sec}$	Peak = 1.007 Steady = 1.000	Peak = 1.072 Steady = 1.000	Peak = 1.004 Steady = 1.000	Peak = 1.15 Steady = 1.15	

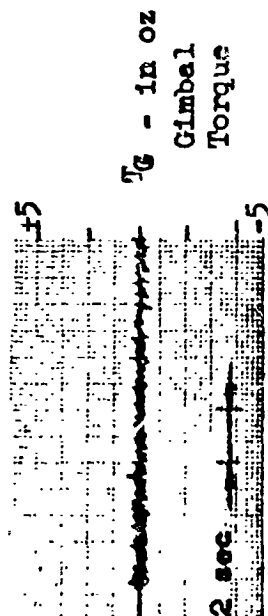
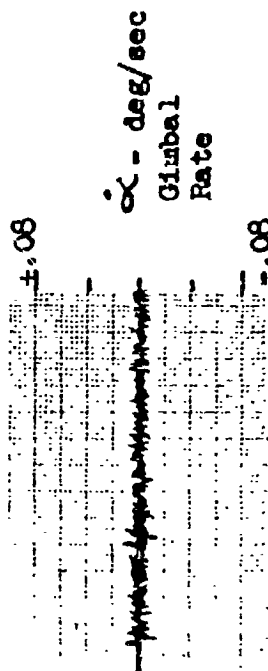
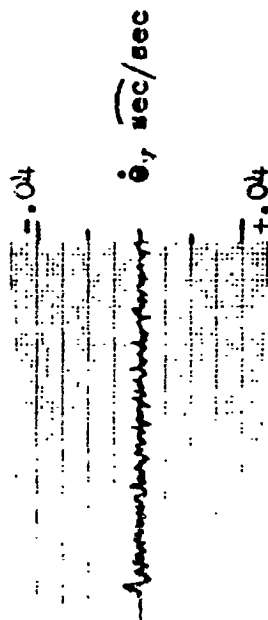
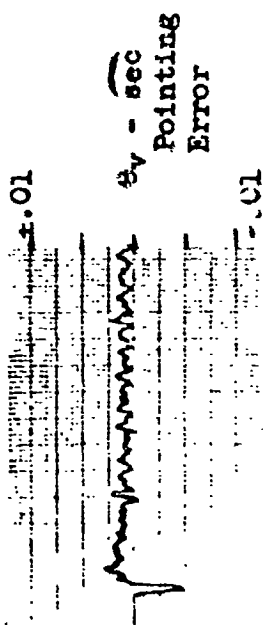
* Amplitudes for sensor noise listed for values after initial transient decay

** Returns to limit cycle of Figure 5-9 after initial transient decay

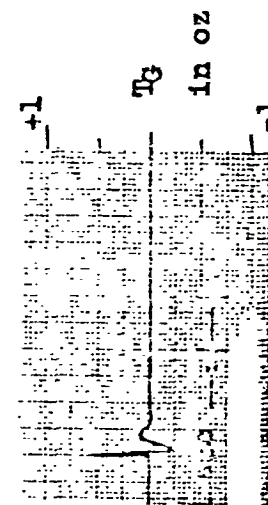
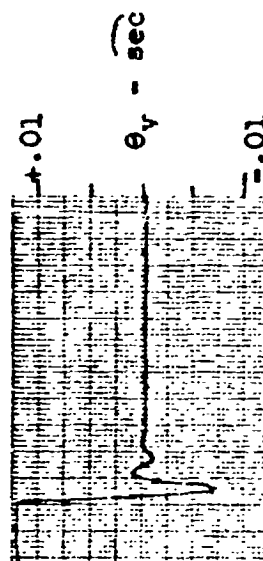
*** Returns to limit cycle of Figure 5-27 after initial transient decay

Figure 5.4-33

RUN 16



RUN 17



RUN 23

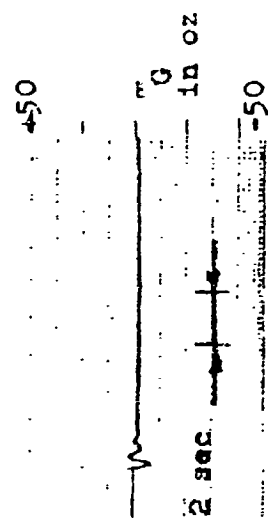
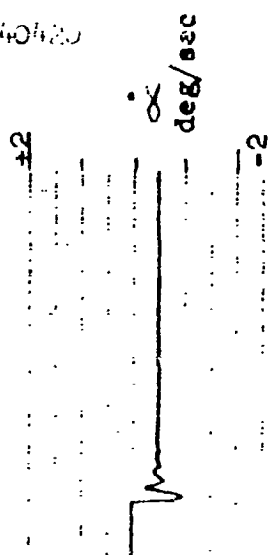
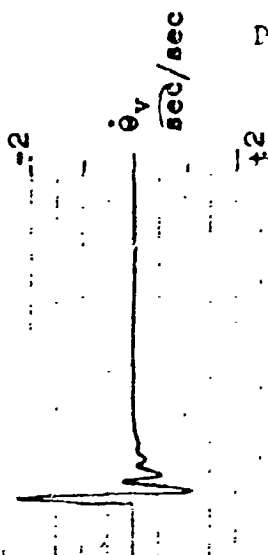
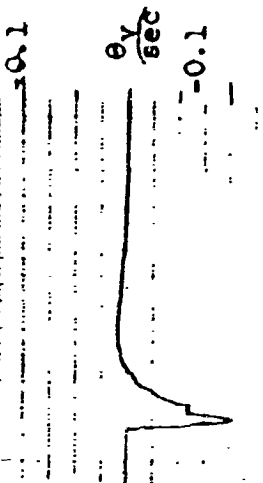
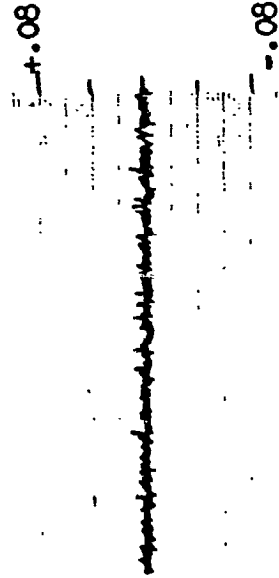
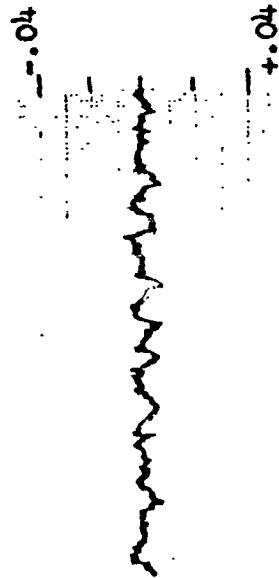
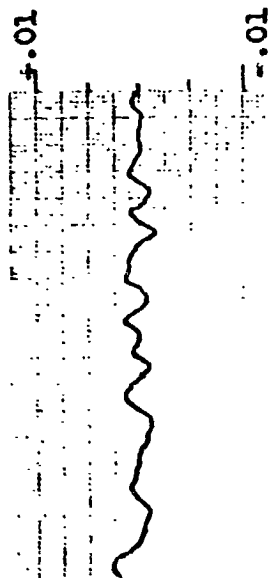
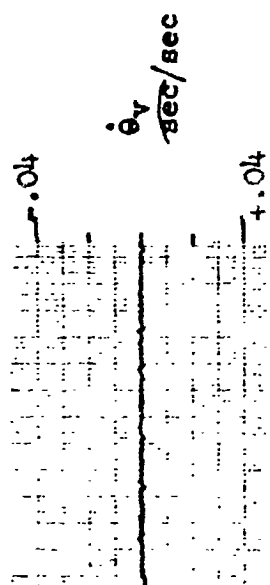


Figure 5.4-34

RUN 26



RUN 30



RUN 35

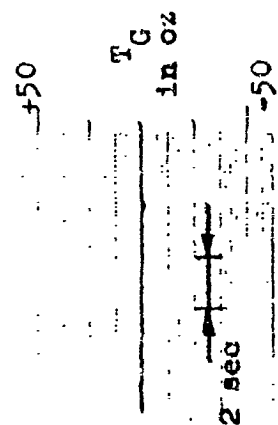
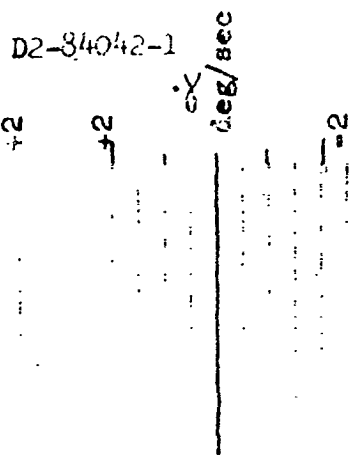
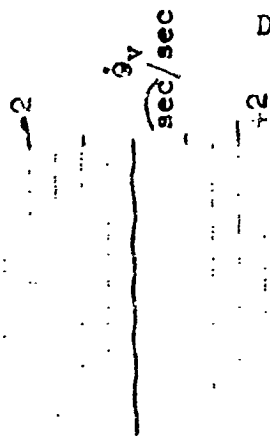
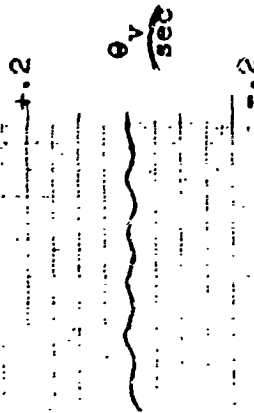


Figure 5.4-35

In Run 36, the effect of an initial attitude rate was established. Here again the system returned to the limit cycle of Run 21 after the initial transient decay.

Run 37 showed the effect of a torque ramp of 0.002 ft-lb/sec. The result was a reduction of the limit cycle as was to be expected from the foregoing responses.

Nonlinear Gyro Dynamics, $\alpha = 45$ degrees

Runs 39 thru 47 indicated the response variation when the gimbal angle reaches 45 degrees which was the design maximum. An insignificant increase in the responses can be seen as compared to the zero gimbal angle condition.

The effect of null offsets in the sensor and electronics was not simulated during the study; however, as an example of a null offset consider the zero disturbance limit cycle of Run 21. An offset would shift the limit cycle up or down an equivalent number of sec but would not change the limit cycle amplitude.

Conclusions

Initial computer results showed the limit cycle caused by gyro friction was above specifications using an initial compensation design. The results indicated that the limit cycle magnitude could be decreased by a combination of increasing the position loop crossover frequency and minimizing gyro friction. A second compensation network was designed to produce a position crossover at 10 rad/sec, the maximum permitted by the sensor response and the flexible mode of the vehicle. The above changes were incorporated into the computer simulation and limit cycle tests were run. The results showed that the system met specifications over the total range of disturbance torques, sensor noise and gimbal angles that would be experienced.

Realistic worst case limit cycles of ± 0.0025 second of arc were attained with 0.002 seconds of arc rms sensor noise. With no sensor noise, an unrealistic case, the limit cycle increases to ± 0.0083 seconds of arc.

The above realistic worst case result was obtained with gyro angles of 45 degrees and zero disturbance torque. Neither a decrease in gyro angles or changes in sensor noise appear to effect the magnitude of the limit cycle significantly. An increase in the disturbance torque, however, decreases the limit cycle magnitude appreciably. With the maximum disturbance of 0.22 ft-lb there is essentially no limit cycle and a position offset of approximately 10^{-4} arc seconds.

As shown above, because of the high position loop gain required, disturbance torques in addition to electronic offsets generate negligible position offsets. The compensation network passes most of the sensor noise, and with the magnitude of noise specified, helps to decrease the effects of gyro static friction.

Radial loads on the bearing due to gyro motion would effectively add a small amount of damping, but would not increase the static friction level quoted above. To achieve the required pointing accuracy, the gyro gimbal friction is the most critical factor. Other system components are within the state of the art.

The performance indicated by this study is in excess of the specifications, which leads to more confidence in the results. This study, while quite detailed for this level of system definition, has established feasibility, but in so doing, has uncovered several critical areas, requiring further study as discussed in the next section.

5.4.6 Critical Areas

Breadboard Studies of Control Hardware

Breadboard studies of control hardware are required at an early date to support development of an intermediate size orbiting telescope. One purpose for this telescope will be to verify design concepts for the attitude control system for the MOT.

The design of control moment gyros to meet the requirements imposed by the high accuracy fine pointing control loop is within the framework of known technology. The gimbal friction needed is lower than found in conventional gyros of this size. It is predicted that this low friction level can be attained by using a brushless torque motor, unpreloaded bearings, and spiral leads rather than slip rings. Breadboard designs are required to substantiate these predictions, as well as uncover any unacknowledged problem areas.

Design criteria for the MOT fine pointing sensors are such that no need for inventions are anticipated. Sensors similar to existing hardware types should be adequate, with improved performance to be achieved primarily through improved detector performance. This does not imply that sensor design will be easy or inexpensive, as this has not historically been the case. It is also true that severe development problems can be induced by demanding a high performance system in a small size, low weight, low power package. For the MOT sensors, where other design criteria can take preference over size and weight, these induced problems will be minimized.

Star trackers employing photomultiplier detectors are in a higher developed state than image tube sensors. An image orthicon star tracker has not yet been orbited. Vidicon systems, however, have been developed. The primary problem with today's image orthicon is its large weight and relatively low reliability. These problems, as well as additional improvements, are soluble when subjected to an orderly development cycle. If the MOT sensors were required within the next 2 or 3 years, this would have to be classified as a problem area. Over a long period of 5 to 7 years, many of the disadvantages of the image orthicon system will have been solved if an orderly development program is initiated at an early date. A logical first step in this program would be laboratory investigations of breadboarded sensors.

Detailed Analysis of MOT-MORI Soft Gimbal Mode

From the limited time available during the latter part of the study to investigate the vehicle mode in which the MOT is coupled to the MORL by means of a soft gimbal concept, a high probability of feasibility has been determined. A complete three-axis nonlinear analysis and simulation of the MOT-MORL control system stability, taking into account an active control system on the MORL and structural flexibility of both vehicles, should be performed. Determination of the optimum spring rate and suspension technique should result from this study.

Spacecraft Roll Axis Control

The need for fairly accurate absolute roll axis position and roll axis stability is required for several of the observational programs. By "fairly accurate" is meant seconds of arc or tens of seconds of arc. The problem arises from the fact that a star tracker for roll attitude control should nominally be directed at right angles to the telescope axis. This poses a thermal/structural stability problem between the axis of the main telescope and that of the roll star tracker.

The roll star tracker does not pose any problem of special significance. It can, in fact, be virtually identical to the intermediate boresight tracker described in Section 5. The heart of the problem lies in the thermal/structural stability of the spacecraft structure, and the resulting time variation of the angle between tracker/telescope axis.

Sensor Setup and Alignment

The MOT will have eight or more separate observational programs, with each program requiring one or more separate assemblies of scientific instrumentation. The total number of instrumentation assemblies will thus total 15 or 20 or more. Since it is probably not practical to hold the extremely tight optical alignment tolerances through the launch environment, and since it will be necessary to make changes of instrumentation/sensors in orbit, an in-orbit optical alignment of the sensors to the remaining system is required. Alignment accuracies will vary with different observational programs, but generally will be on the order of one to three seconds of arc for the "coarse" manual adjustment.

Man's capability to perform the required alignment using conventional Earth-based techniques is uncertain. Complete prealigned assemblies, containing both sensor and scientific instrumentation, may be necessary, for example, to reduce the magnitude of the in-orbit alignment function.

Thermally Induced Structural/Electronic Instability

A design problem inherent in all systems that require high mechanical/electrical stability is that of thermally induced electrical drifts or mechanical distortion. This applies not only to the sensor as an entity, but to the short-term thermal distortions of the structure that maintains the sensor/instrumentation/telescope alignment. This problem is associated with the intermediate pointing sensor as well as the fine pointing sensors. A short-term temporal instability in excess of 2 to 4 seconds of arc between the boresight directions of the intermediate pointing sensor and the main telescope will be cause to reevaluate the entire intermediate tracker design concept, as has previously been discussed.

The thermal design problem is felt to be less severe for the sensor itself than for the relative alignments between sensor/scientific instrumentation. A direct extrapolation of sensor temperature sensitivity for the MOT sensors from the OAO Goddard Experiment fine pointing sensor indicates a sensitivity on the order of 0.001 sec/°C. By making thermal stability a prime design criteria for the MOT sensors, even better performance can be expected.

The associated problem of maintaining the relative alignment between the sensor and scientific instrumentation may require an active temperature control system or a

closed-loop servo. For the narrow field photographic mode, for example, a lateral displacement of 17 micro-inches between the film plate and sensor corresponds to 0.001 arc sec angular change ($f/30$ focal plane). Since stabilities on the order of 0.01 arc sec over ten orbits are desired, the complexity of the materials/thermal/structural design becomes apparent.

Acquisition Problem

The general problem of large angle slewing and reacquisition, while not considered beyond the state of the art, requires detailed study to determine the optimum trade offs. Large angle closed loop slews about an arbitrary axis, not possible in the CAO implementation due to the compromise made in favor of equipment simplification should be studied for MOT. These studies would determine the digital computer requirements, the number required and the linear ranges of the optical sensors, etc. Some of these items interface quite closely on the feasibility problem of fine pointing. For example, the fine pointing sensor linear range (determined from acquisition requirements) has a strong effect on the sensor noise.

Alternate slewing methods include open loop slewing about one axis at a time using the gyro reference. A somewhat different approach would be to use attitude gyros as the principle inertial reference and update the gyros with error signals derived from the star trackers. The processed tracker error signals would be inserted into gyro torquers, thus slaving the gyros to the trackers. This method would place the cross coupling and gain variations in the gyro updating loop rather than in the vehicle control loop.

Image Motion Compensation

The required image motion compensation for planetary photography and planetary radiance measurements must be listed as a potential problem area that will require additional effort. It has not been determined what the effects of such rate compensation will be on the spacecraft control system, or whether the compensation should be introduced at the film plate rather than in the telescope point. This is not foreseen as a major problem area with respect to the fine pointing sensor per se, only as a source of additional complexity.

5.5 THERMAL CONTROL

5.5.1 Approach

A thermal analysis was conducted to determine temperature distributions in the TCT. The Boeing Engineering Thermal Analyzer (BETA) Program (AS 0915)* which makes use of the IBM 370 computer for the finite difference solution of heat transfer problems, was used for making a three dimensional time dependent thermal analysis. Temperature gradients in the telescope structure and in the primary and secondary mirrors were determined. Heating due to incident solar, Earth reflected, and Earth emitted radiation as functions of orbital position was first calculated using a Planetary Environment Computer Program (AS 2116). Script F view factors were then calculated using a generalization of a Mussett Double Projection Computer Program (AS 2034), which treats combined specular and diffuse reflecting surfaces to determine the radiant heat exchange between nodal points on the inner telescope tube wall, the secondary mirror support structure, and the primary and secondary mirrors. Internal reflections resulting from the presence of mirror surfaces and the blocking effect of the secondary mirror structure were included.

5.5.2 Assumptions

- o The telescope configuration assumed for conducting the thermal analysis is that shown in Figure 5.5-1. The telescope shell and the rear surface of the primary mirror are insulated with one inch of multilayer vacuum insulation having a nominal conductivity of 7.0×10^{-5} Btu/hr-ft. °R. The primary mirror is supported from the telescope structure with tangent bar supports.
- o Material properties assumed for the thermal analysis are given in Figure 5.5-18.
- o Cabin temperature is assumed to be 530°R.
- o Telescope altitudes and orbit assumed are shown in Figure 5.5-2.
- o The solar constant is taken to be 443 Btu/hr-ft².
- o Assumed Earth temperatures, taken from TIROS data, are given in Figure 5.5-19.

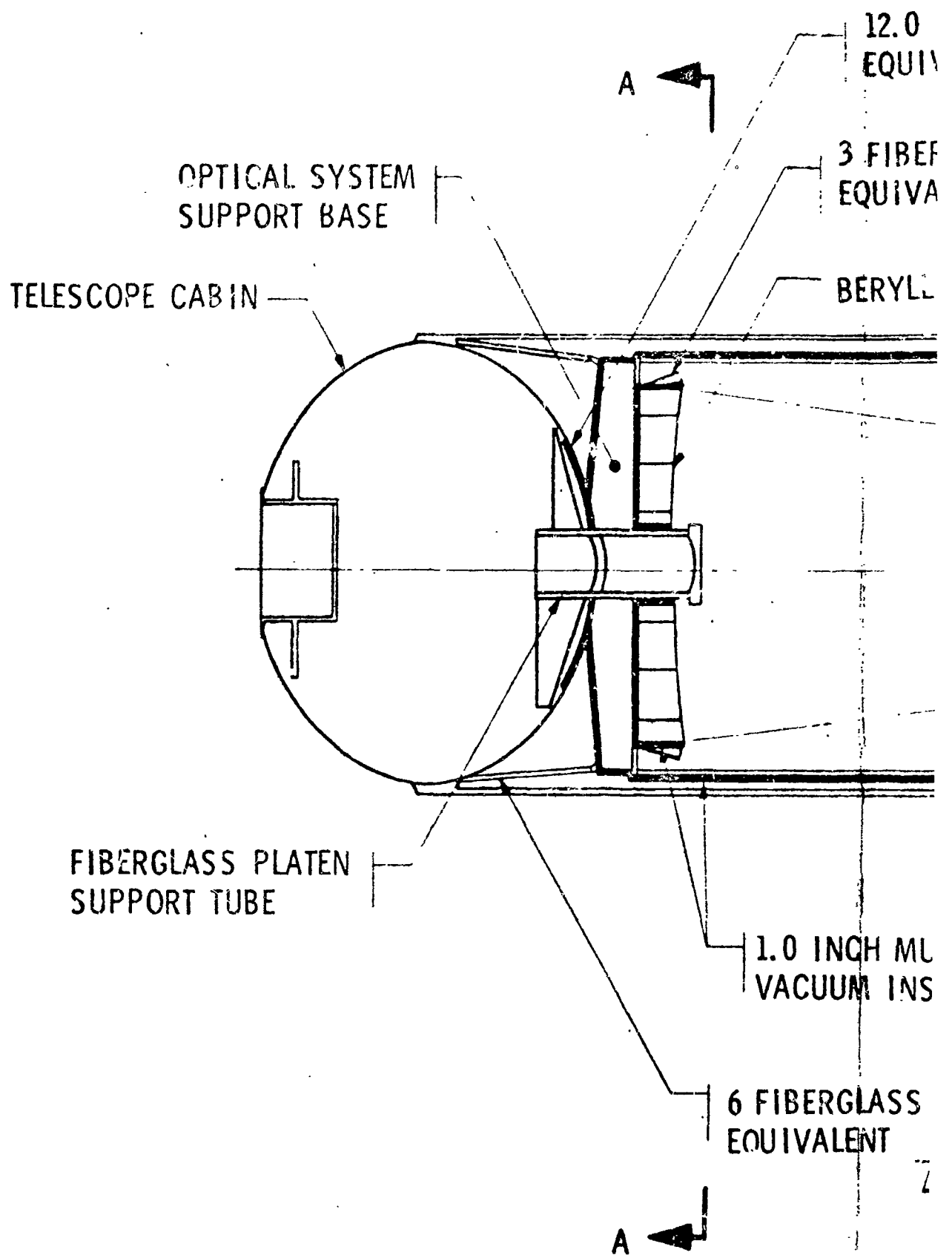
5.5.3 Analysis Method

Thermal balance of the telescope is a function of the incident solar radiation, Earth emitted radiation, Earth reflected radiation, radiation from the telescope structure to space, radiant interchange with other telescope structure, and heat conducted through the telescope structure. The thermal balance for unit areas of structure gives:

$$\epsilon_{DS} \alpha_S + \epsilon_{ET} \alpha_S + \epsilon_{ET} \alpha_{IR} = \sigma \epsilon_{IR} F_{SP} T_1^4 + \sigma \mathcal{F}_{1,2} (T_1^4 - T_2^4) + \dots$$

$$\sigma \mathcal{F}_{1,n} (T_1^4 - T_n^4) + \frac{k_{1,2} A_{1,2}}{\Delta x_{1,2}} (T_1 - T_2) + \dots \frac{k_{1,n} A_{1,n}}{\Delta x_{1,n}} (T_1 - T_n) + W_1 C_1 \frac{dT}{dt} \quad \text{(See Section 5.5.4.3 for nomenclature)}$$

*Number designates Boeing Computer programs



1/2 INCH RADIUS FIBERGLASS COLLAR

EQUIVALENT $A = 4.91 \times 10^{-2}$

ΔX

2 GLASS MIRROR SUPPORTS

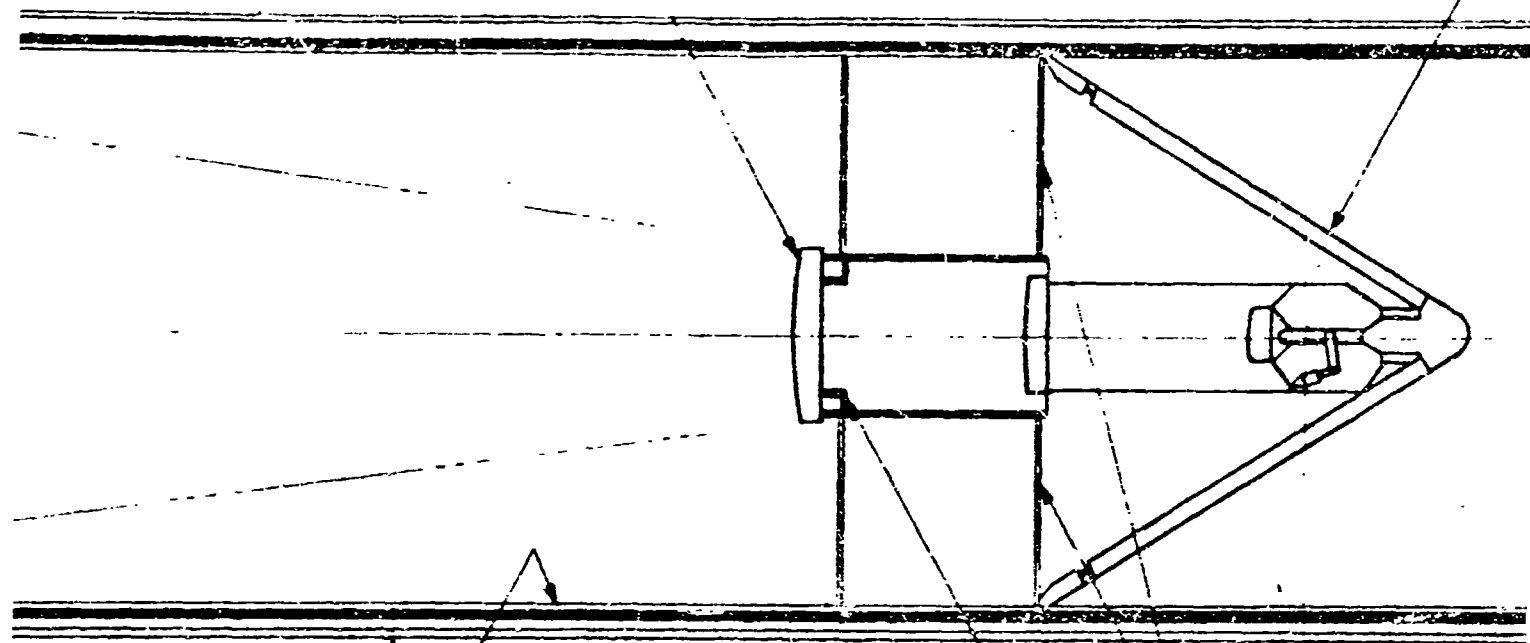
EQUIVALENT $A = 4.78 \times 10^{-3}$ EACH

ΔX

ALUMINUM PRIMARY MIRROR

FUSED SILICA

SECONDARY MIRROR



MULTILAYER
INSULATION

0.50 INCH ALUMINUM HONEYCOMB
0.010 INCH FACE SHEETS
4.0 PCF CORE

6 TITANIUM F
EQUIVALENT

SUPPORT TUBES

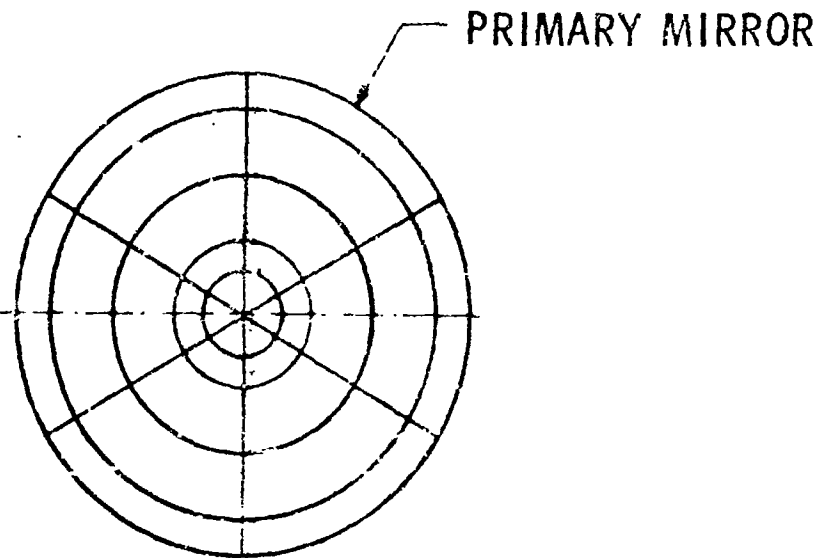
$A = 3.05 \times 10^{-3}$ EACH

ΔX

3 FIBERGLASS
EQUIVALENT

Δ

3 TITANIUM SUPPORTS
EQUIVALENT $\frac{A}{\Delta X} = 2.71 \times 10^{-4}$ EACH



X STRAPS
= 2.32×10^{-5} EACH

SEC. A-A

MIRROR SUPPORTS
= 4.78×10^{-3} EACH

DIMENSIONS IN FEET
EXCEPT AS NOTED

FIGURE 5.5-1
**BASELINE CONFIGURATION
USED IN THERMAL ANALYSIS**

A three-dimensional finite element analysis of heat transfer through the telescope structure was conducted on an IBM 7094 Computer. A discussion of computer programs used in the analysis is presented in Working Document 15-1462-1.

To insure a controlled thermal environment for the telescope mirrors, it was assumed that direct solar radiation is never permitted to fall on the inner surfaces of the telescope tube; that is, the telescope viewing axis is never less than 10 degrees with respect to the solar vector. This restriction permits astronomical observations to be made in any direction in the hemispherical portion of the universe that is oriented away from the Sun. Two critical attitudes considered to produce extremes in thermal environment are telescope axis parallel to the solar vector, and telescope axis perpendicular to the solar vector, as defined by Figure 5.5-2.

The BETTA computer program used in the heat transfer analysis solves heat flow problems that have been converted to thermally analogous electrical networks. Radiative and conductive heat paths are simulated by assigning appropriate conductance values to a conductor network. The telescope structure is broken into nodes; each node being assumed to have a uniform temperature throughout its mass. Increasing the number of nodes increases the accuracy, but at the expense of increasing complexity.

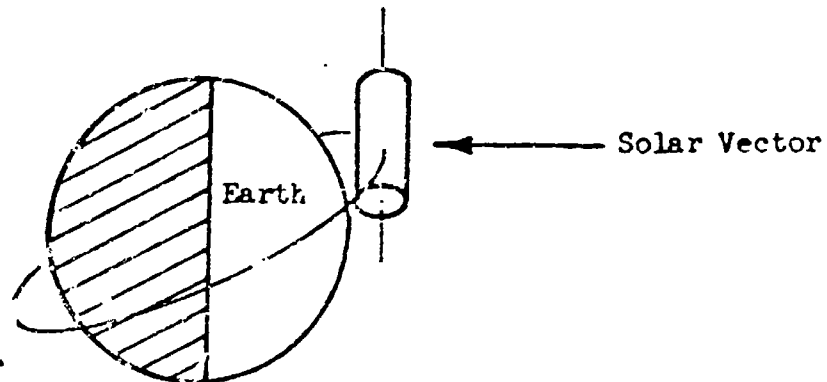
The thermal model of the AOT is relatively complex; therefore, a fairly fine nodal mesh was considered necessary to simulate accurately incident radiation from the Earth and Sun and radiant exchange between elemental areas of telescope structure with other structure and space. Outer and inner telescope shells were each broken into nine equal nodal areas and the primary and secondary mirrors were broken into 36 and 7 nodal areas, respectively. Other nodes were required to account for other structural elements, making a total of 88 nodes. Figures 5.5-3 and 5.5-4 show the nodal network and structural thermal conduction paths employed in the analysis. In addition, view factors for 365 radiant transfer paths (not shown) were determined. Incident Earth and solar heat loads on 40 nodal areas were determined by linear interpolation between calculated values at 20 positions in orbit. The variation in thermal conductivity with temperature of all materials was considered, as well as the variation with temperature of the specific heat of beryllium. Heat loads calculated as a function of orbital position were calculated using a Planetary Environment Computer Program, and Script F view factors were determined with a generalized Russell Double Projection Computer Program. These data were then input to the BETTA Program.

5.5.4 Results

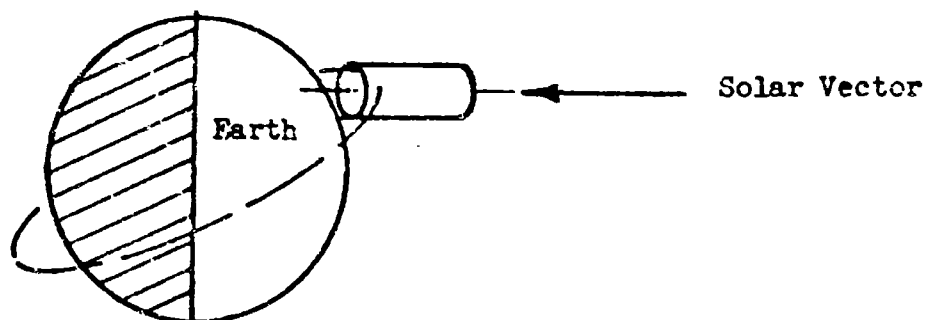
Thermal time constants of the mirrors and telescope structure can be seen in Figure 5.5-5, which shows the transient temperature history after an initial launch temperature of 530°K. Outer wall temperatures (not shown) reach equilibrium after a few minutes in orbit, because the outer wall has a relatively small thermal capacitance and is well insulated from the internal structure. Inner wall temperatures also stabilize within about 10 to 15 hours, due to low thermal capacitance of the walls. The primary and secondary mirrors require a much longer time to reach equilibrium temperature, which, depending on telescope attitude and thermal insulation effectiveness, varies from 380°K to 450°K. In general, the equilibrium temperature of the secondary mirror is 10 to 20°K colder than the

250 N.M. CIRCULAR ORBIT

ORBITAL INCLINATION: 28.7°



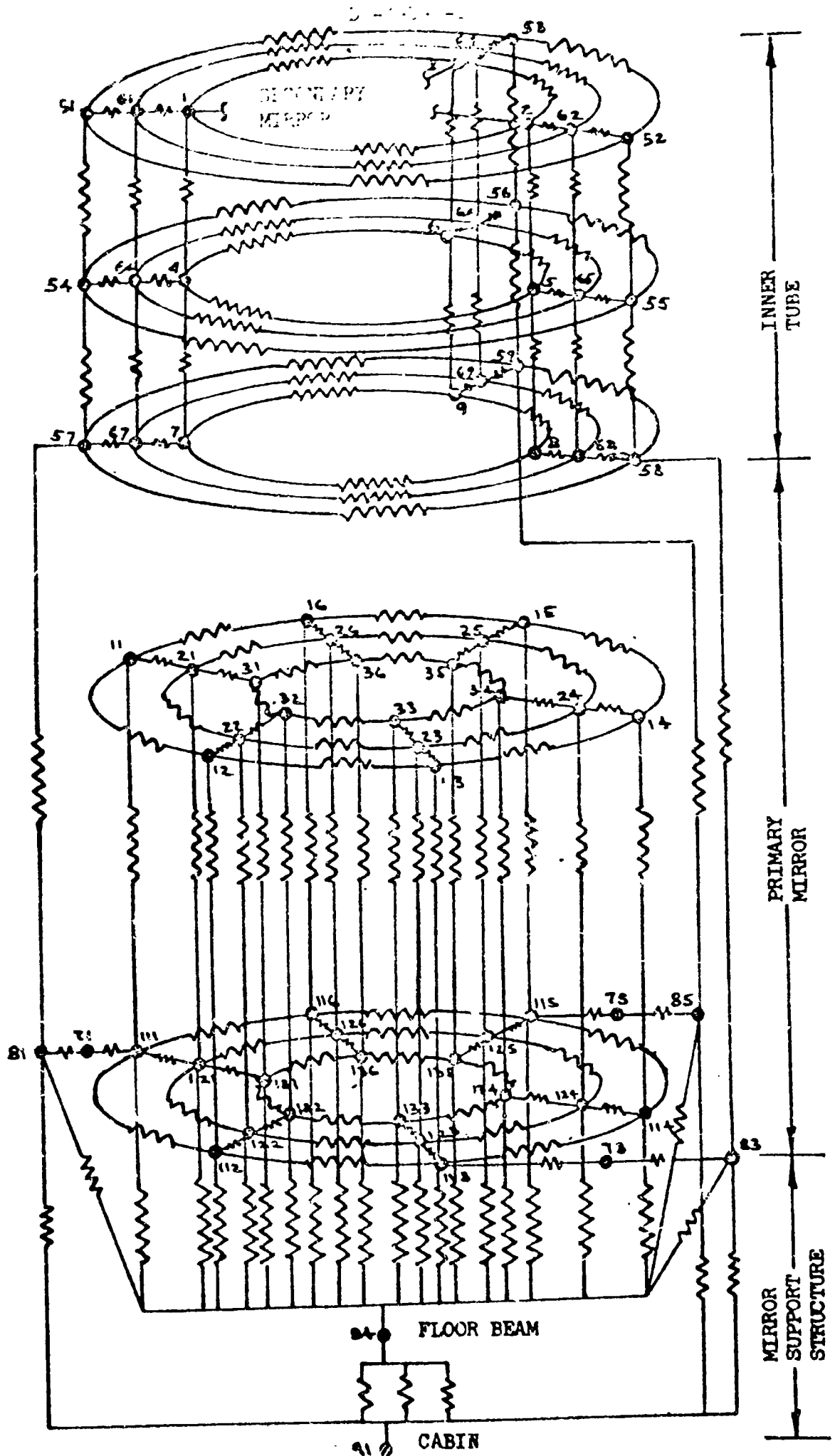
Telescope Axis Perpendicular
to Solar Vector
Continuous Viewing



Telescope Axis Parallel to Solar Vector
Alternate Viewing

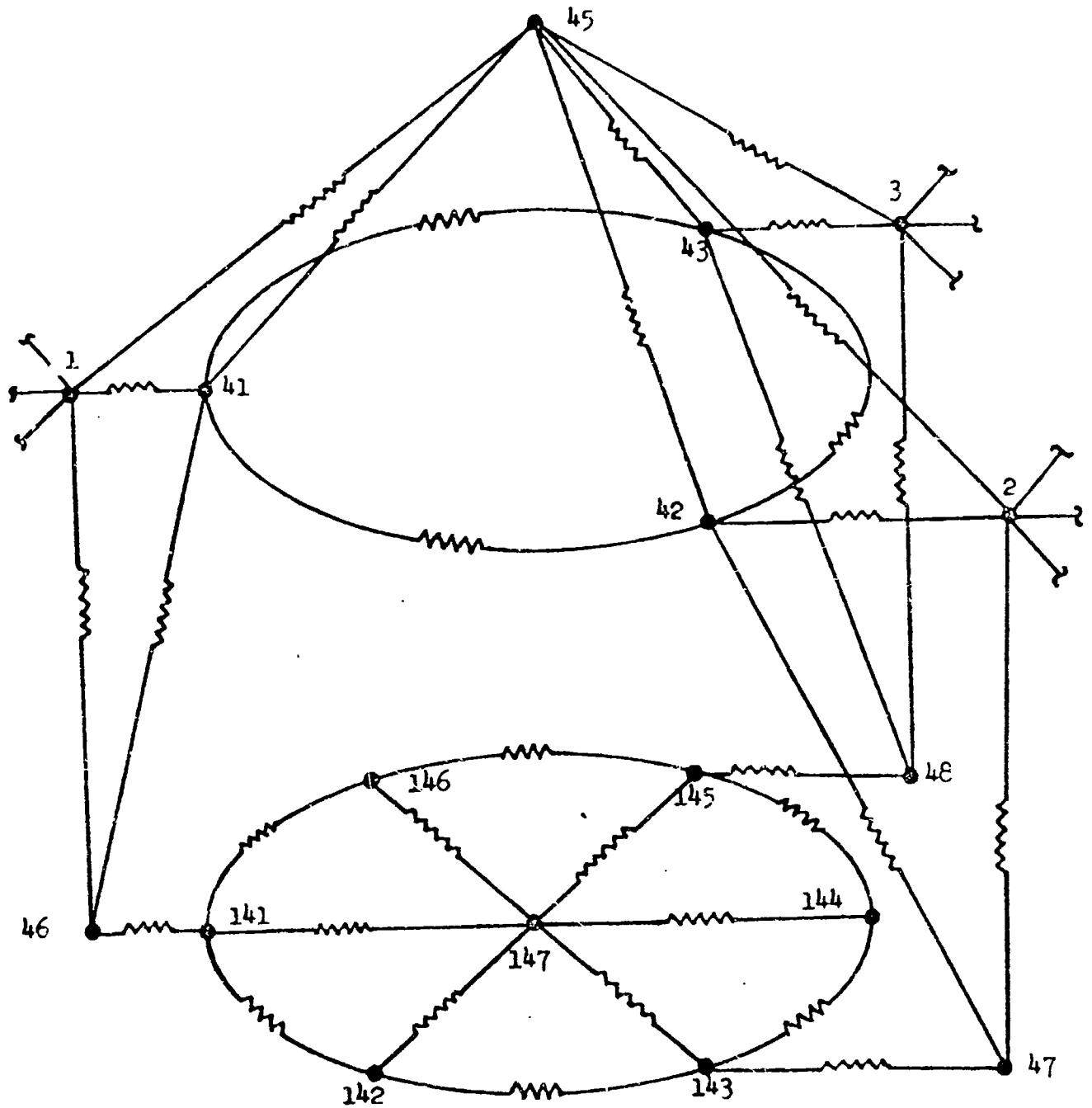
MOT THERMAL ANALYSIS ORBIT DEFINITION

FIGURE 5.5-2



PRIMARY MIRROR THERMAL NETWORK

FIGURE 5.5-3



SECONDARY MIRROR THERMAL NETWORK

FIGURE 5.5-4

Initial Temperature: 530°R
 Outer Coating: $\alpha_s = .2$; $\epsilon_{ir} = .9$

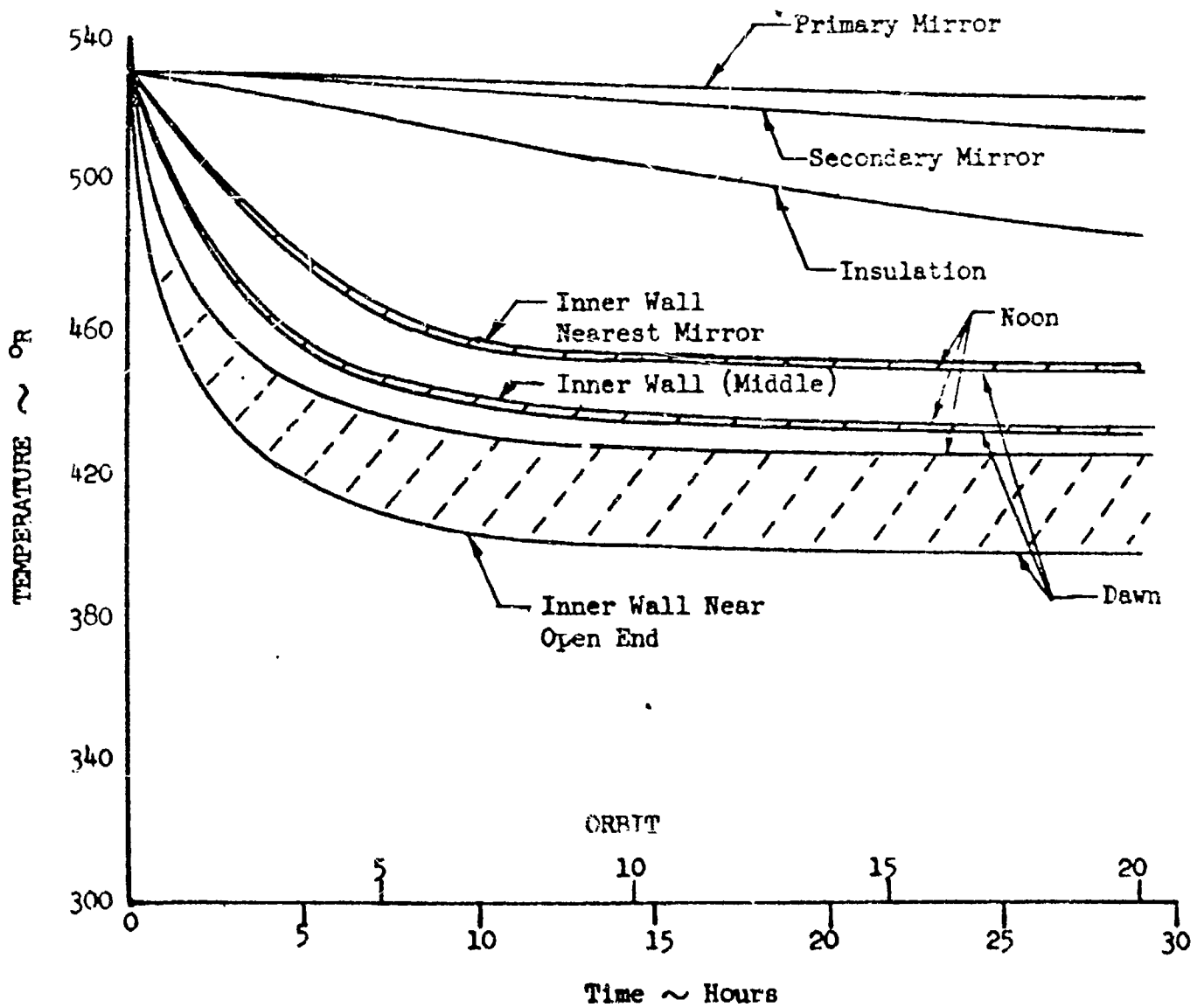


FIGURE 5.5-5 : TRANSIENT TEMPERATURES AFTER LAUNCH TELESCOPE AXIS PARALLEL TO SOLAR VECTOR

primary mirror because the secondary mirror is more completely isolated from the cabin. Maximum mirror thermal gradients occur during this cool-down phase, due to heat conduction from the mirror to the tangent bar supports. Maximum temperature gradients occur about 15 hours after launch, with the following temperature differences between adjacent nodes: circumferential, 0.17°R ; radial, 0.03°R ; and axial, 0.13°R .

Figure 5.5-6 shows the effect on outer-wall temperature of changing the outer surface coating α_s/ϵ_{IR} when the telescope axis is perpendicular to the solar vector. The upper curves represent average nodal temperature of a 120° segment of the outer wall that is always oriented toward the Sun. Figure 5.5-7 shows that surface coating α_s/ϵ_{IR} has considerably less effect when the telescope axis is parallel to the solar vector.

Figure 5.5-8 shows quasi-steady state inner tube wall temperatures for the two telescope attitudes studied. Variations in outer coating α/ϵ were found to exert only a minor influence on inner wall temperature, due to the relatively small heat flux through the super insulation with either type coating. Hence, selection of either a high or low α/ϵ coating appeared to offer no particular advantage, and all subsequent analyses were therefore based on a white coating having an $\alpha_s/\epsilon_{IR} = 0.2/0.9$.

Inner wall temperatures are seen to be somewhat higher when the telescope attitude is parallel to the solar vector, due to the heating effect when viewing the sunlit Earth. It may also be seen that greater circumferential gradients occur at portions of the inner tube represented by the three nodal areas near the open end and that the gradient is quite small for nodal areas nearest the primary mirror.

The importance of maintaining small circumferential gradients in the inner tube wall near the mirror may be seen from Figure 5.5-9. In this figure, the effect of varying the reflectance and emittance of the nodal areas nearest the mirror (represented by nodal areas 7 to 9 inclusive) is clearly shown. The nodal areas 1 to 6 inclusive, corresponding to the outer $2/3$ of tube wall, were assumed to be coated with flat black paint ($\rho_{\text{specular}} = 0$, $\rho_{\text{diffuse}} = 0.1$, $\epsilon = 0.9$) in each case. Making the near wall nodes highly specular, as represented by the polished aluminum configuration, is undesirable because it diminishes the view factor to the wall surface nearest the mirror, where the wall temperature is uniform, and increases the view factor to the wall surface near the open end, where the wall temperature variation is much greater. The use of sandblasted aluminum near the mirror would provide some advantage if the wall temperature near the mirror was nonuniform because it tends to equalize the view factors. However, because the wall temperatures near the mirror are quite uniform (see Figure 5.5-8), the use of flat black paint for the entire inner wall surface is recommended as it provides the smallest view factor to the wall surface near the open end.

Figure 5.5-10 shows quasisteady-state primary and secondary mirror temperatures when the telescope axis is perpendicular to the solar vector; i.e., the telescope views only space. The terms defining the curves may be better understood by referring again to nodes 11 to 36 and 111 to 136 inclusive in the nodal network (Figure 5.5-3). The primary mirror quasisteady-state gradients are less than 0.01°R , due to the nearly isothermal mirror environment and the relatively high

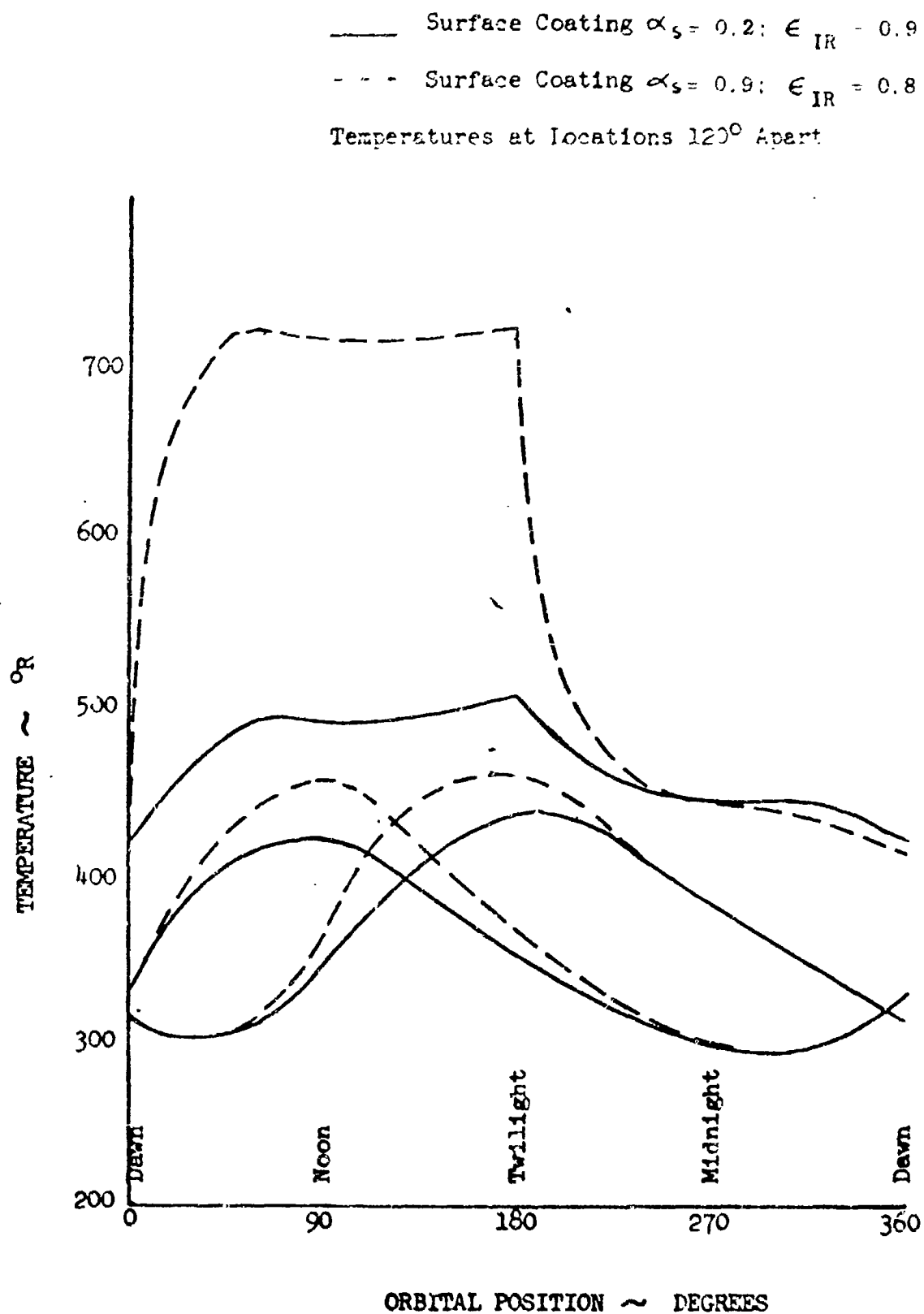


FIGURE 5.5-6 ; OUTER WALL TEMPERATURES TELESCOPE AXIS PERPENDICULAR TO SOLAR VECTOR

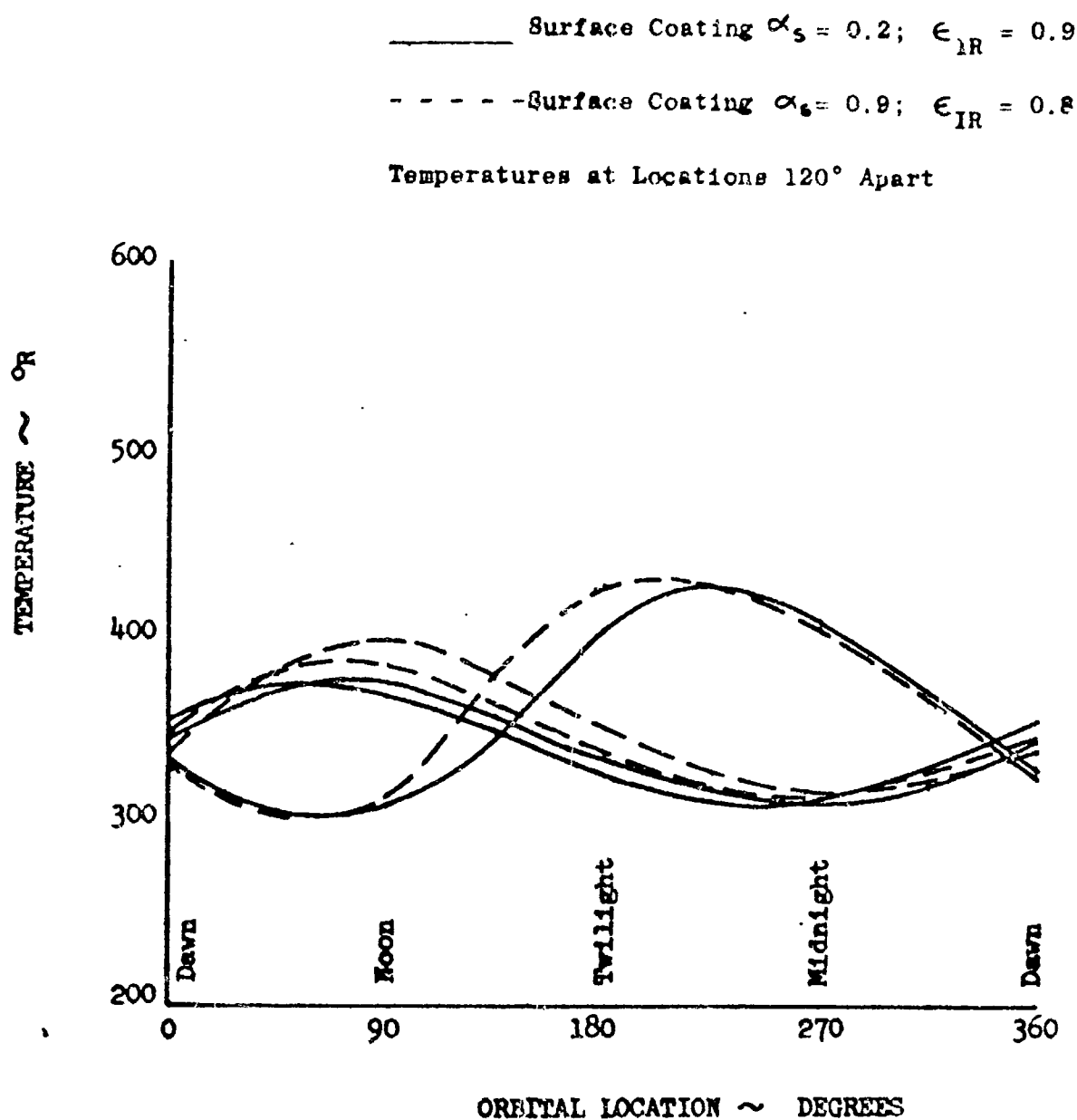


FIGURE 5.5-7 : OUTER WALL TEMPERATURE; TELESCOPE AXIS PARALLEL TO SOLAR VECTOR

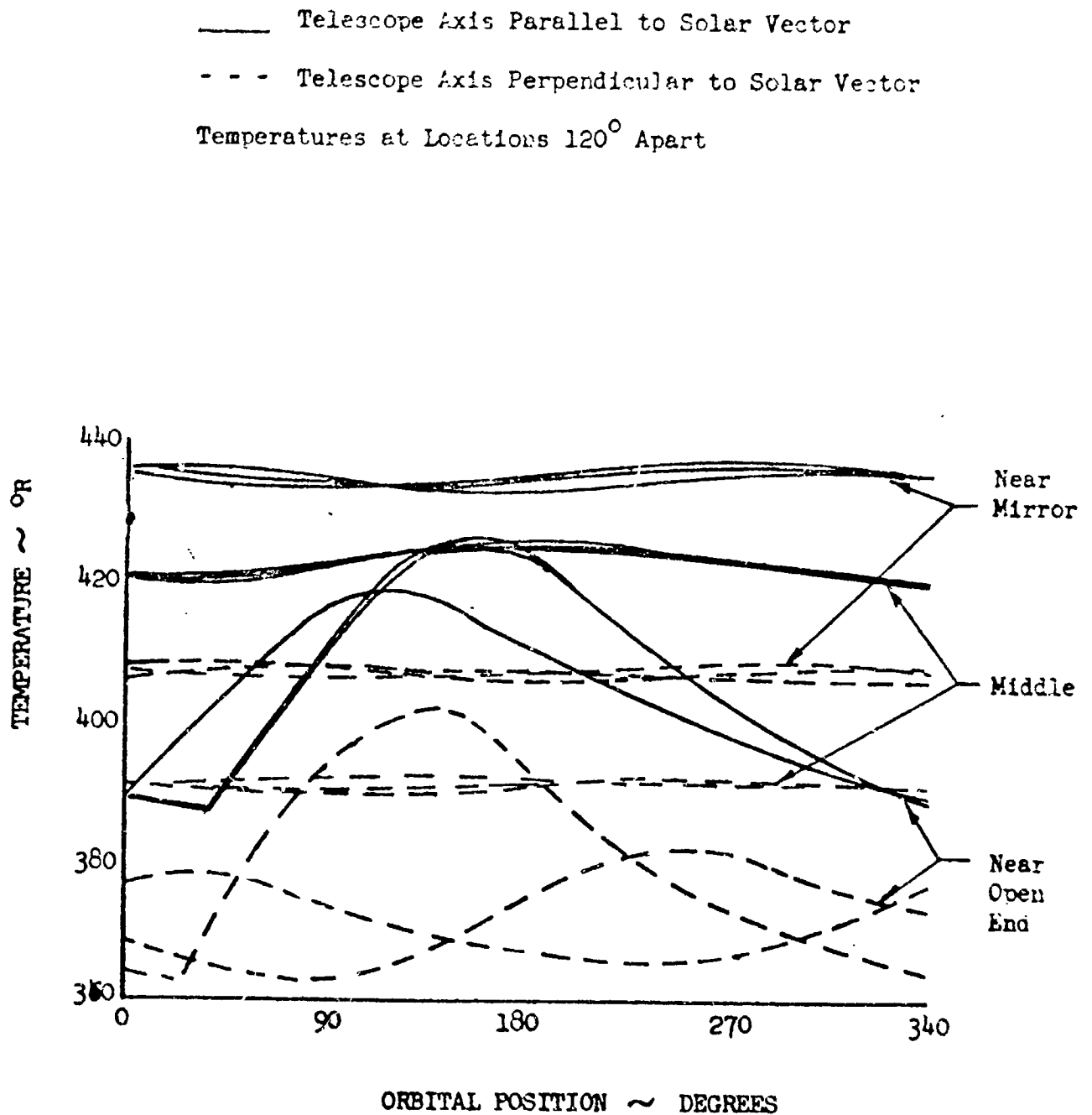


FIGURE 5.5-8 : INNER WALL TEMPERATURE

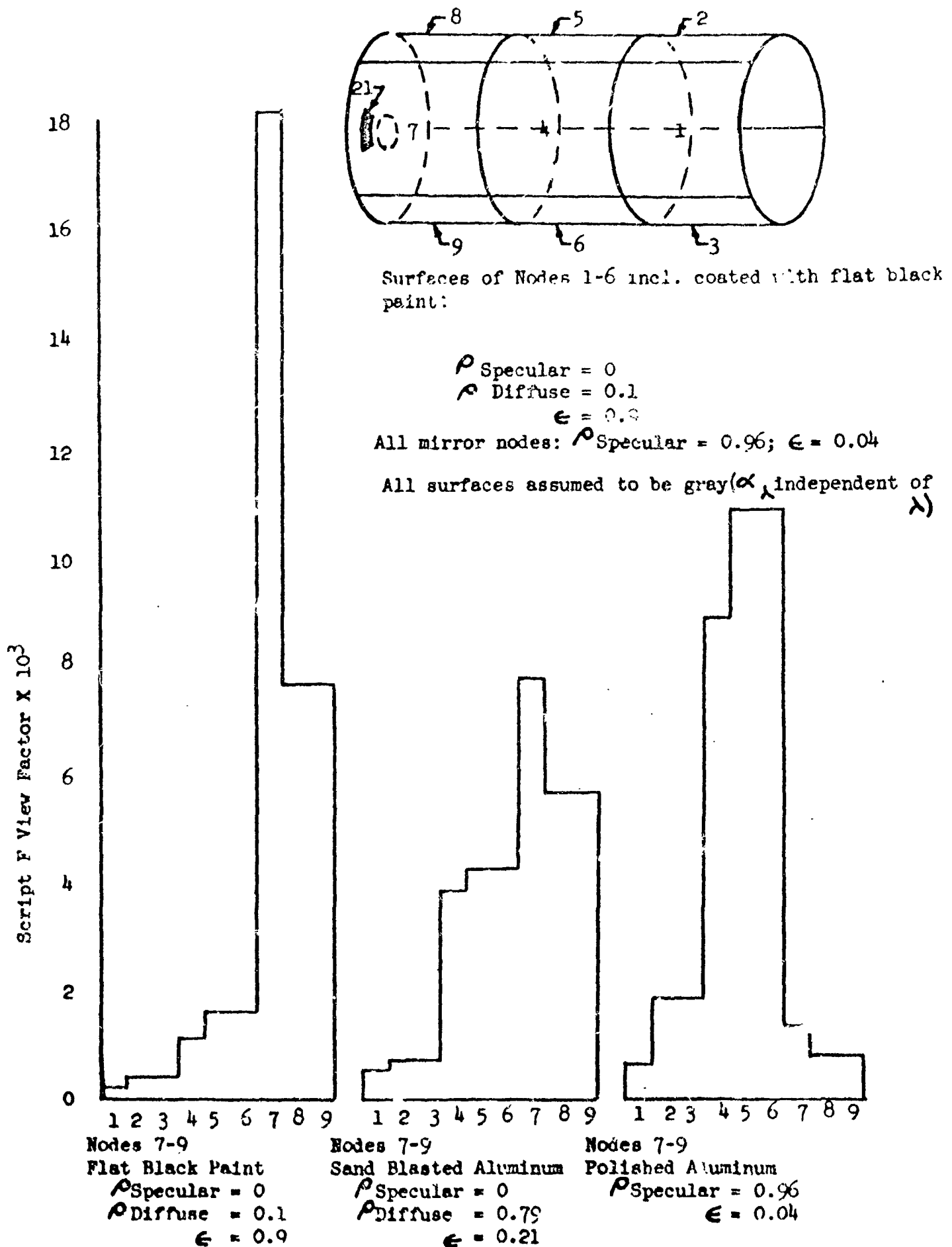
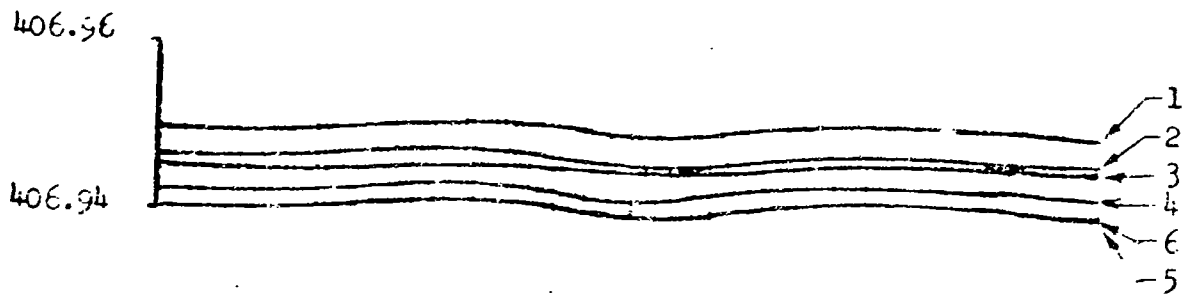


FIGURE 5.5-9 : VIEW FACTORS FROM MIRROR NODE 21 TO INNER TUBE SURFACE NODES 1-9 INCLUSIVE

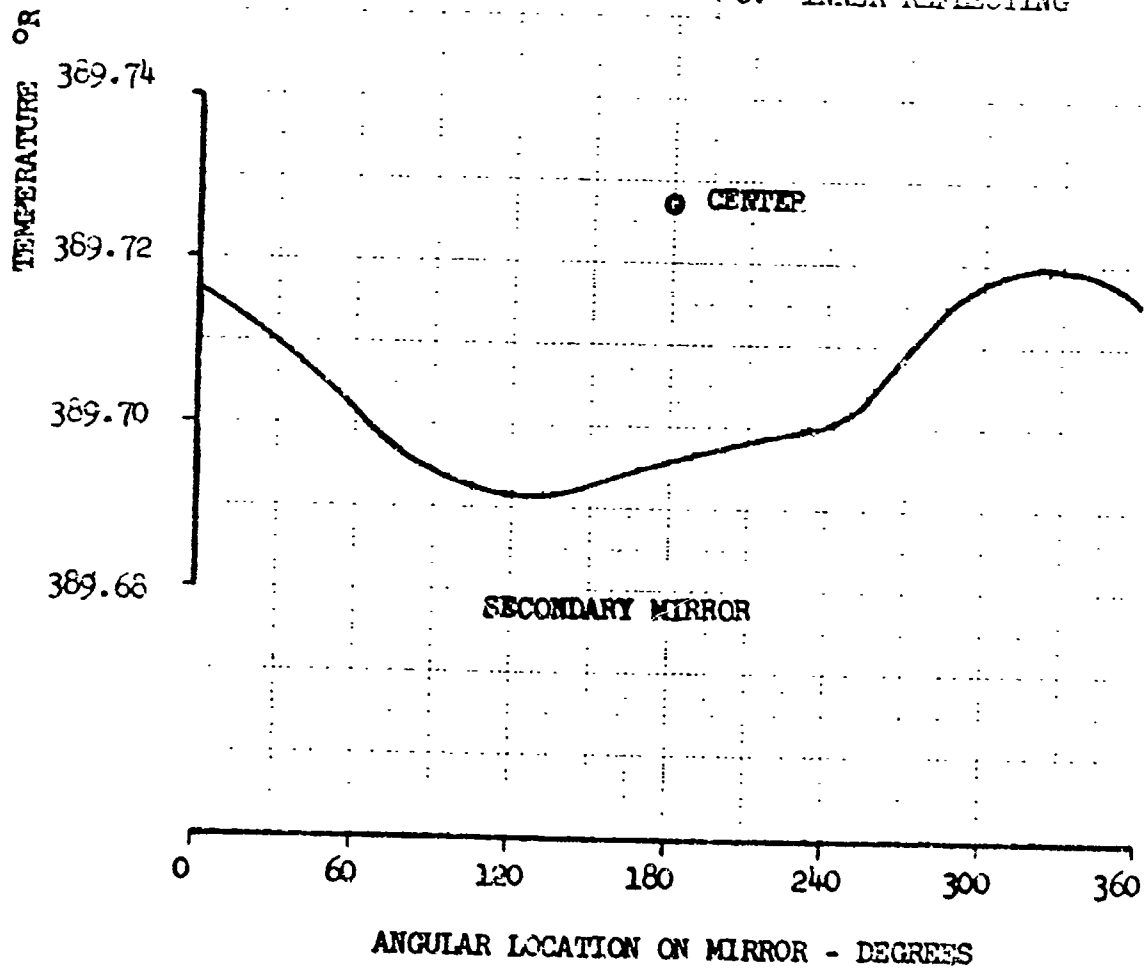
DAWN CONDITION



PRIMARY MIRROR

AIRZULI

1. OUTER BASE
2. MIDDLE BASE
3. INNER BASE
4. OUTER REFLECTING
5. MIDDLE REFLECTING
6. INNER REFLECTING



QUASI-STEADY STATE MIRROR TEMPERATURES
TELESCOPE AXIS PERPENDICULAR TO THE SOLAR VECTOR
FIGURE 5.5-10

thermal conductivity of the beryllium used in the mirror construction. Because of the small view factor between the mirror surface and the tube wall surface near the open end, the nonuniform wall temperatures in this region have very little effect and the circumferential mirror temperature gradient is therefore quite small.

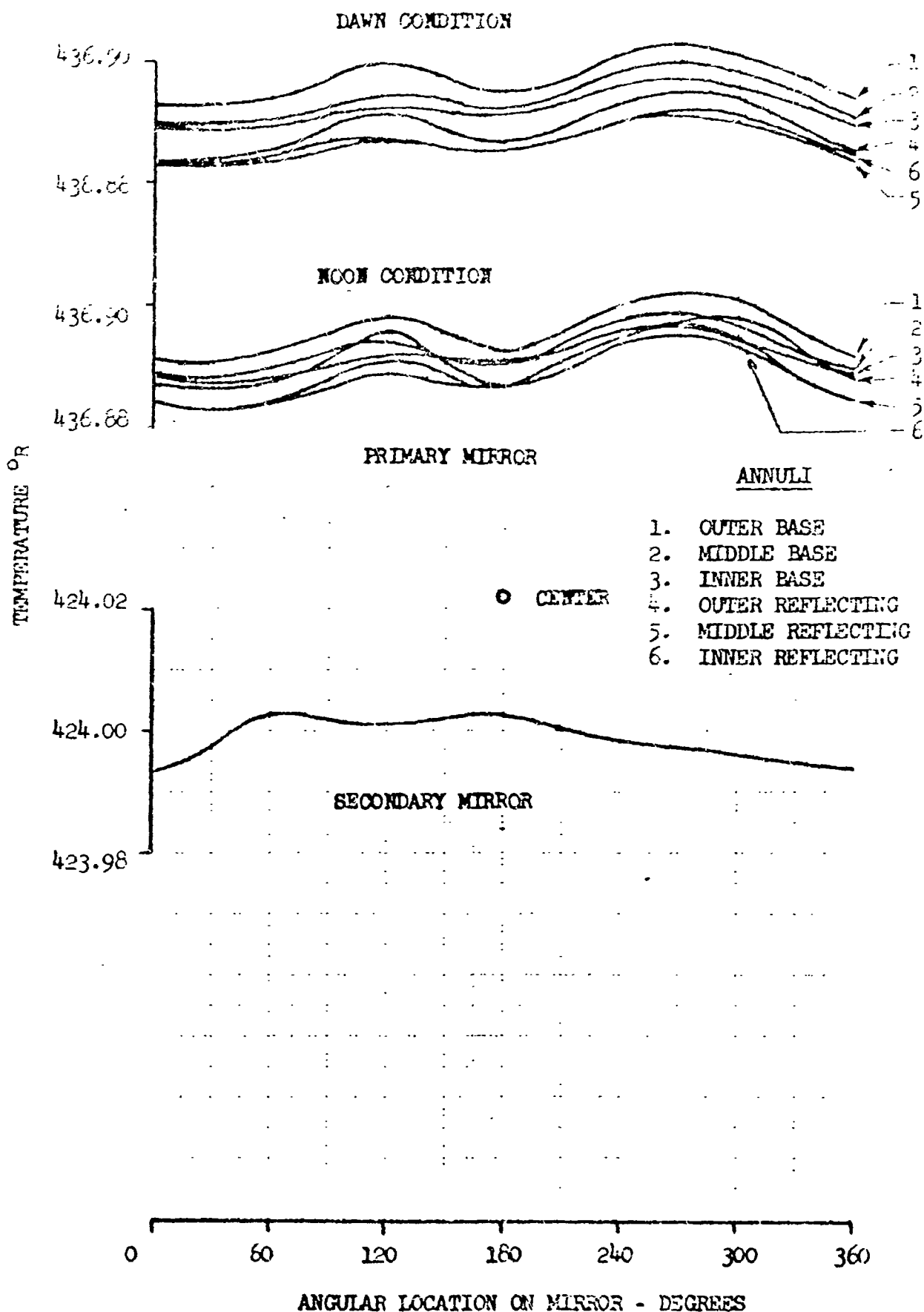
The temperature gradients in the secondary mirror are considerably larger, due to the lower thermal conductivity of the fused silica material and the directional nature of the incident heat loads on the secondary mirror support structure. Larger gradients are permissible with fused silica, however, because of a lower thermal expansion coefficient.

Figure 5.5-11 shows quasisteady-state primary and secondary mirror temperatures when the telescope axis is parallel to the solar vector, so that the inner wall and primary mirror alternately view sunlit Earth and space during each orbit. Increased circumferential gradients in the primary mirror result from incident Earth reflected and emitted radiation on the primary mirror surface, and the shadow pattern cast by the secondary mirror structure and tube wall. The circumferential gradients in the secondary mirror are less severe for this case, because the incident heat flux is more uniform around the circumference of the secondary mirror support structure.

Figure 5.5-12 shows the mirror temperature gradients that can develop as a result of an orbital attitude change. The telescope structure and mirrors were first permitted to reach equilibrium temperature with the telescope axis parallel to the solar vector so that the primary mirror alternately views sunlit Earth and space. From Figure 5.5-11, it may be seen that the equilibrium primary and secondary mirror temperatures are 437°R and 424°R , respectively. The telescope attitude was then assumed to rotate 90 degrees to another viewing position, such that the telescope axis is perpendicular to the solar vector and the telescope continuously viewed space. The new mirror equilibrium temperatures for this telescope position are seen from Figure 5.5-10 to be 407°R and 389°R . After approximately 20 hours, the inner telescope wall temperatures decrease approximately 30°R to a new equilibrium temperature (see Figure 5.5-8), whereas the mirror temperatures have only dropped about 1.4°R . This produces a maximum temperature difference between the mirrors and supporting structure that causes an appreciable circumferential and radial gradient to occur in the mirror near the tangent bar supports.

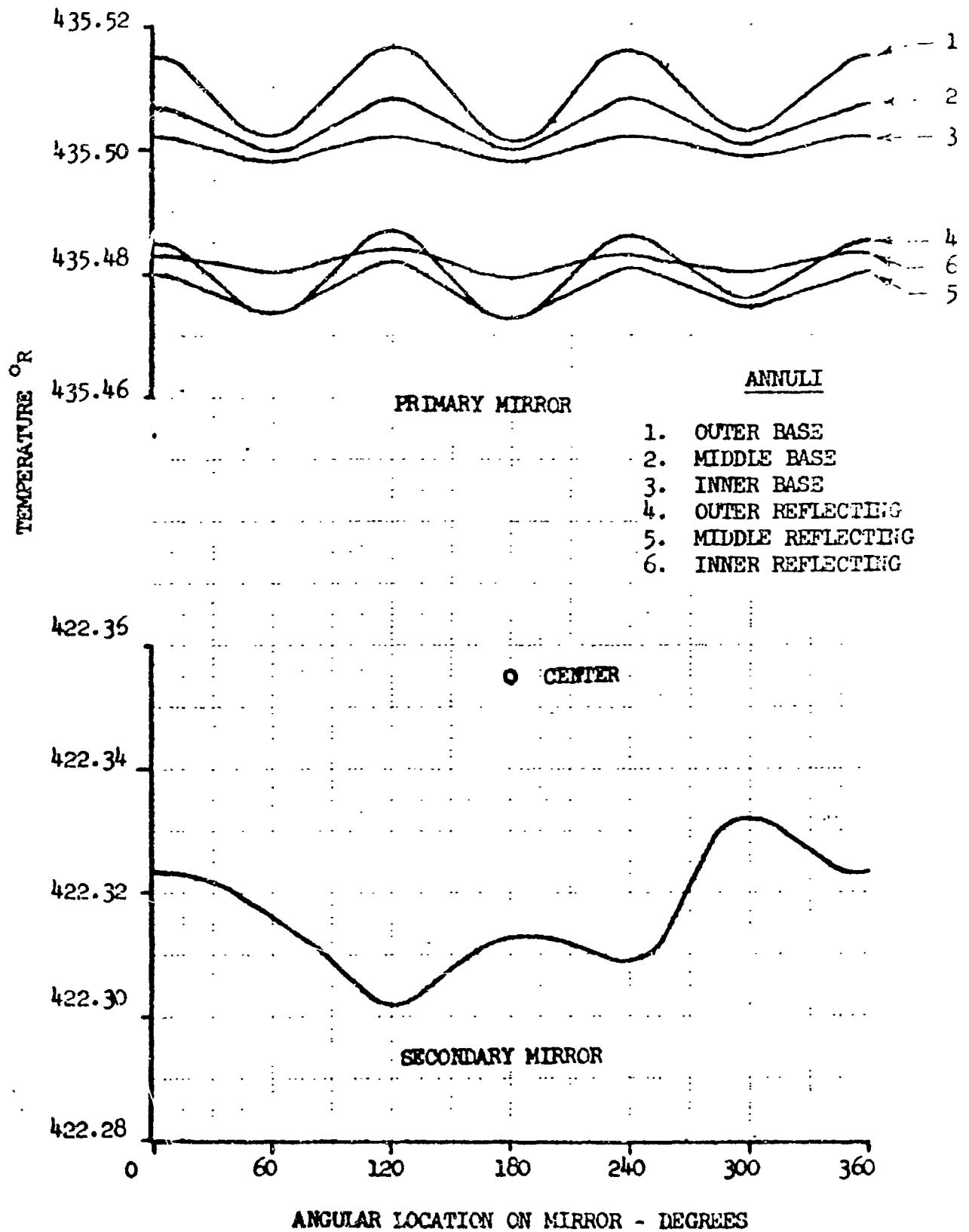
Figure 5.5-13 is a cross plot of the data of Figure 5.5-12 to show radial temperature gradients. It is apparent from these plots, that objectionable gradients can occur during periods when the mirrors and surrounding structure are undergoing transient temperature changes to a new equilibrium temperature. These gradients can be almost eliminated if the mirror and structural equilibrium temperatures are made nearly equal for all telescope attitudes. This can be achieved by the use of doors that are closed whenever the telescope views sunlit Earth. These doors are located in an isothermal environment provided by the earthshade, as described in Section 5.2.1.

Figure 5.5-14 shows quasisteady-state mirror temperatures that occur when the telescope is oriented parallel to the solar vector with the doors closed when viewing sunlit Earth. Comparison with Figure 5.5-11 shows that the doors



QUASI-STEADY STATE MIRROR TEMPERATURES
TELESCOPE AXIS PARALLEL TO THE SOLAR VECTOR

FIGURE 5.5-11



TRANSIENT MIRROR TEMPERATURES 20 HOURS AFTER CHANGING ATTITUDE FROM PARALLEL TO PERPENDICULAR TO SOLAR VECTOR

FIGURE 5.5-12
346

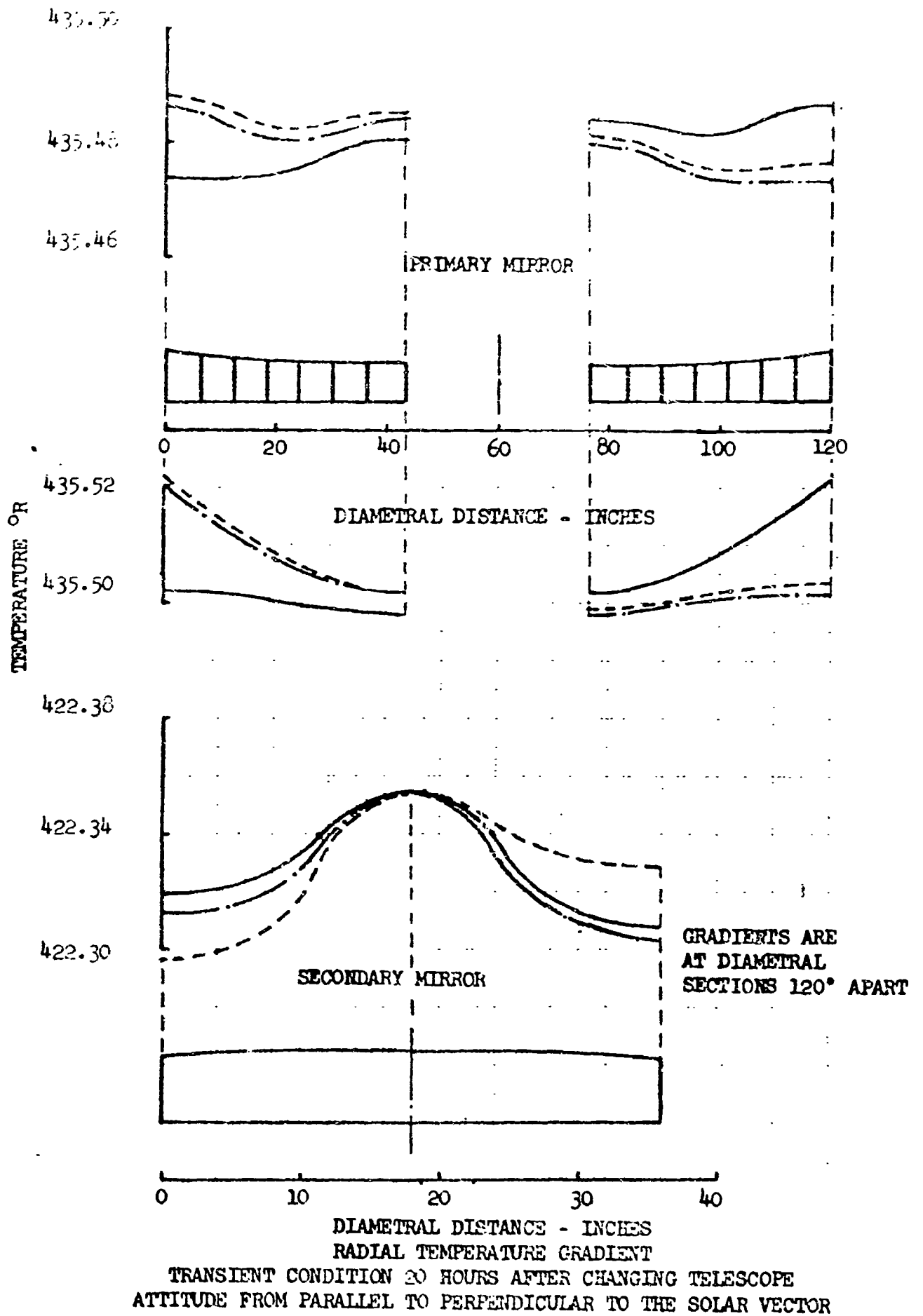
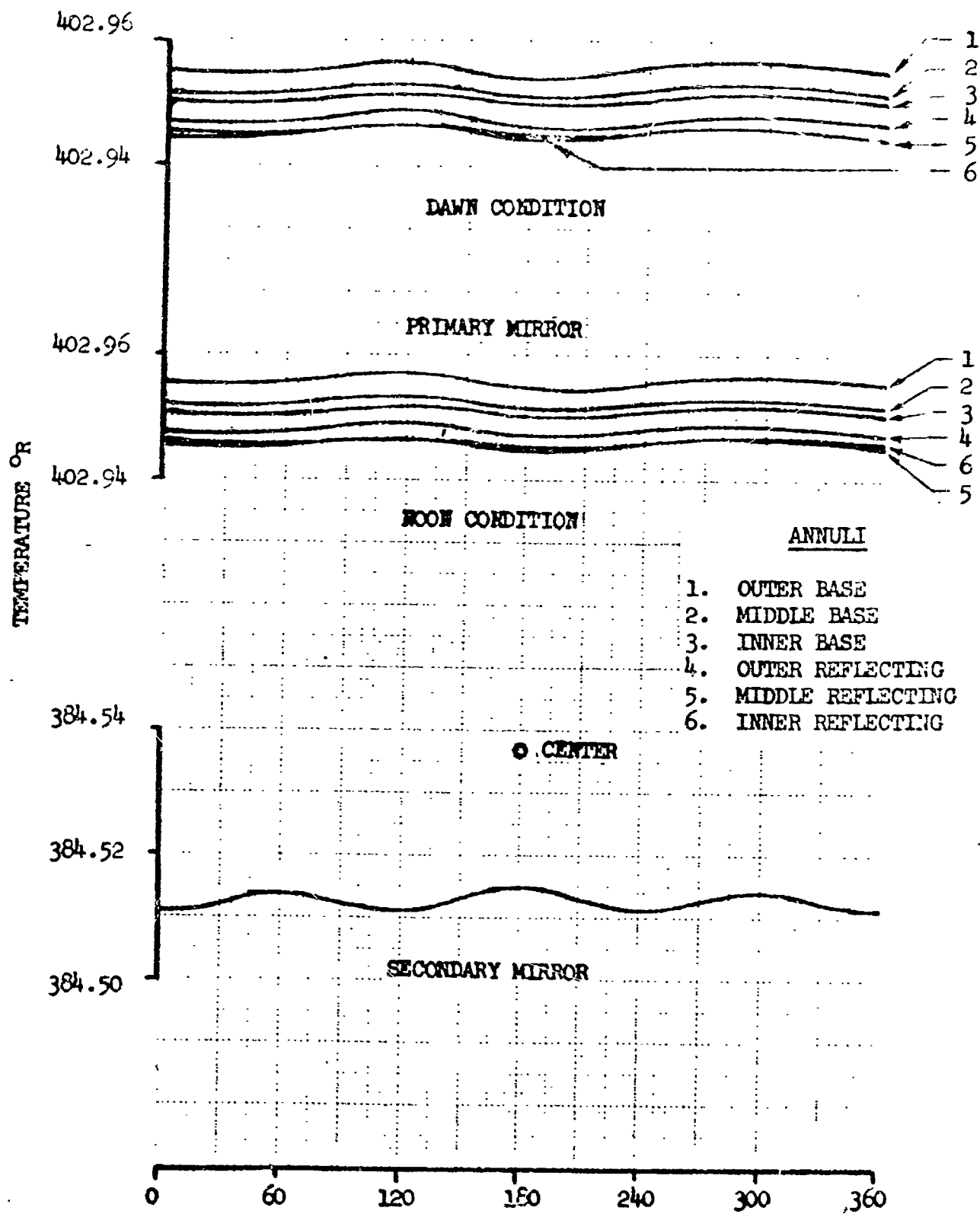


FIGURE 5.5-13



effectively reduce the mirror temperature gradient. They also reduce the primary mirror equilibrium temperature from 427°K to 403°K, which is much nearer the 407°K equilibrium mirror temperature for a telescope orientation perpendicular to the solar vector.

Figure 5.5-15 shows that when doors are used, the objectionable gradients that develop with changing telescope attitude are largely eliminated.

The validity of the mirror gradients presented in this study are clearly dependent on the ability to manufacture a telescope structure having insulation and tangent bar thermal conductance of magnitude comparable to those assumed in the analysis. Insulation installed between the primary mirror and floor beam will be compressed while the mirror is supported by the floor beam assembly during boost. Boeing test data for an insulation consisting of alternate layers of 0.00025-inch aluminum foil and grade "A" Dexiglass paper, which was compressed and then allowed to recover, were used in the analysis. These data were used to develop constants for an equation of the form derived by Fraunhofer. Effective insulation conductance is expressed as a function of temperature:

$$K = \left[1.52 \left(\frac{T_w}{100} \right)^3 (1+R+R^2+R^3) + 0.0837 \frac{T_w(1+R)}{\frac{\text{Btu}}{\text{ft hr} \cdot R}} \right] 10^{-7} \quad (2)$$

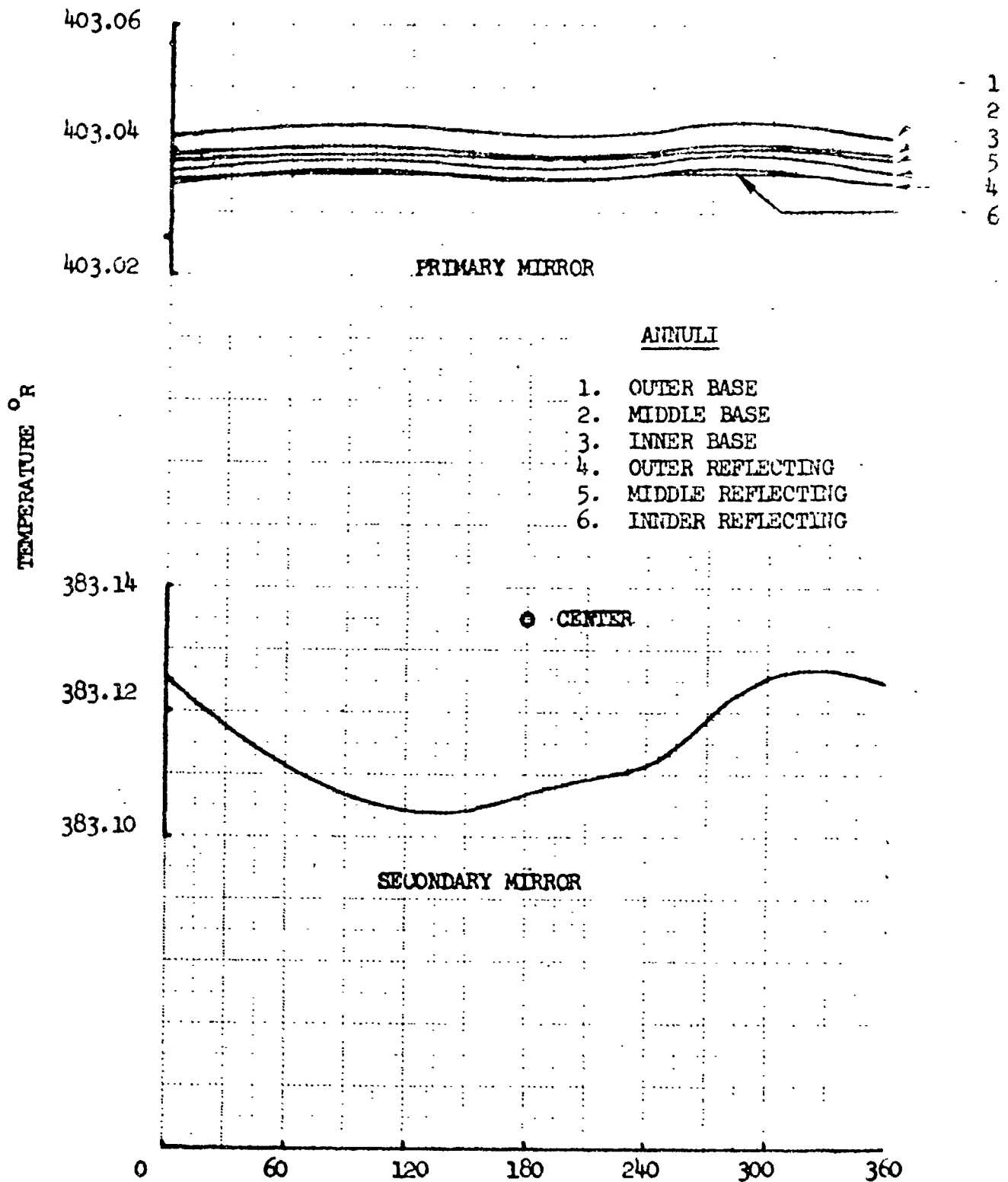
where $R = \frac{T_c}{T_w}$

To establish the sensitivity of mirror temperature gradients to insulation system effectiveness, the same tangent bar conductance was assumed, but the insulation conductance determined by equation (2) was increased by a factor of 10. Figure 5.5-16 shows that a large increase in axial mirror gradient can result from increasing the insulation conductance. If the assumed conductance cannot be met in practice, it may become necessary to increase the insulation thickness from the nominal one inch value. To explore the potential of different mirror construction, a brief investigation was made of a solid mirror. In this event, Figure 5.5-17 shows the quasisteady-state temperatures for a 2.0 inch thick solid beryllium mirror for a condition similar to that of Figure 5.5-11, in which the telescope alternately views sunlit Earth and space and doors are not employed.

The results just presented indicate that with further design improvements, it should be possible to obtain short term thermal control of optical mirror geometry by passive means. The effect of long term stress relaxation and operation at temperatures other than the temperature at which the mirrors were manufactured has not been established and may require some form of active control.

5.5.4.1 Materials Properties

A summary of the thermal properties of materials used in the thermal analysis is presented in Figure 5.5-18. Only nominal properties at a specified temperature are presented, although in the thermal analysis the dependence of thermal conductivity and specific heat on temperature were considered.



TRANSIENT MIRROR TEMPERATURE 20 HOURS AFTER CHANGING
ATTITUDE FROM PARALLEL TO PERPENDICULAR TO THE SOLAR VECTOR
(DOOR CLOSED WHEN VIEWING SUNLIT EARTH DURING PARALLEL OPERATION.)

FIGURE 5.5-15

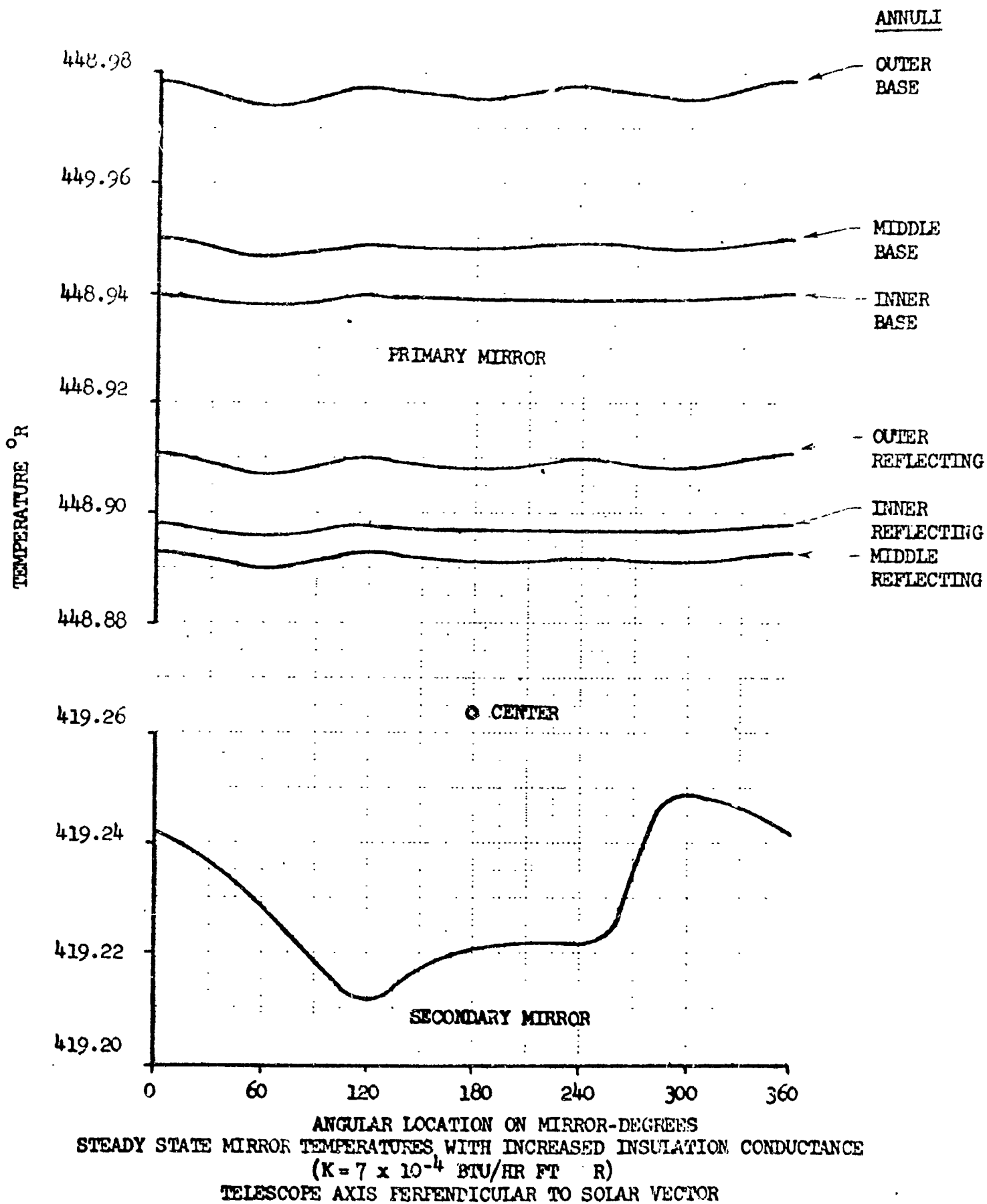


FIGURE 5.5-16

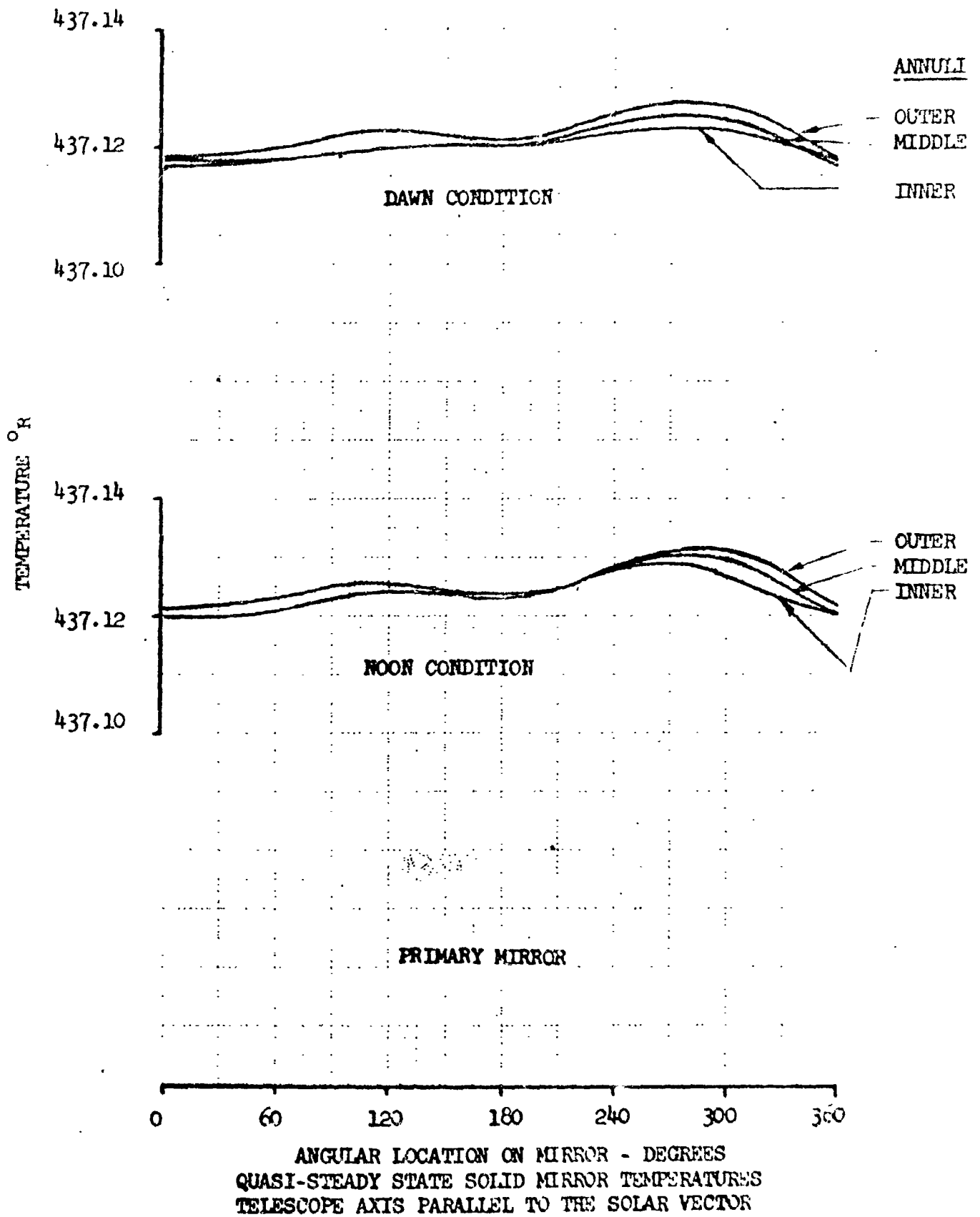


FIGURE 5.5-17

MATERIALS PROPERTIES USED IN THERMAL ANALYSIS

Figure 5.5-18

STRUCTURAL MEMBER	MATERIAL	DENSITY lb_m/ft^3	SPECIFIC HEAT $\text{Btu}/\text{lb}_m\text{-}^\circ\text{R}$	THERMAL CONDUCTIVITY $\text{Btu}/\text{hr ft-}^\circ\text{R}$	RADIATION PROPERTIES
Telescope Shell	Aluminum 2219-T62	176	0.204	74.4	Outer α_s/ϵ IR = 0.2/0.9 Inner α_s/ϵ IR = 0.9/0.9
Primary Mirror	Beryllium	115	0.40	96.4	$e = 0.94$ $\epsilon = 0.04$
Secondary Mirror	Fused Silica	137	0.145	1.02	$e = 0.94$ $\epsilon = 0.04$
Thermal Insulation	Multilayer Aluminum Foil-Dexiglass	12	0.20	7.42×10^{-5}	
Primary Mirror Support Secondary Mirror Support	Resin Impregnated Fiber-glass	114	0.30	0.0064	
Secondary Mirror Tube Support	Titanium 6Al4V	276	0.128	5.62	

*Nominal Value at 460°K

**For the mirror surfaces the assumption was made that $e_s = e_{IR}$ and $\alpha_s = \alpha_{IR}$

5.5.4.2 Planetary Thermal Environment

The incident thermal radiation on nodal areas of the telescope structure and mirrors were determined with Planetary Thermal Environment Computer Program (AS 2116). Effective Earth temperatures from TIROS data, in accordance with Figure 5.5-19, were assumed. Values of effective Earth temperature as much as 30°R lower than the values used in the analysis have been proposed by some investigators. The results of the analysis showed, however, that because of the effectiveness of the superinsulation used in the telescope wall structure, the effect on the inner wall and mirror equilibrium temperature is small. This applies particularly when a door is used to prevent direct viewing of sunlit Earth.

5.5.4.3 Nomenclature

- A = area normal to heat conduction path
- C = specific heat
- F = geometric view factor
- \mathcal{F} = script F view factor (calculated by Computer Program AS 2034)
- K = thermal conductance
- \dot{q} = incident heat flux on nodal area (calculated by computer program AS 2116)
- R = ratio
- T = absolute temperature
- ℓ = length between nodes in direction of heat conduction path
- W = mass
- α = absorptance
- ϵ = emittance
- θ = time
- σ = Stefan-Boltzmann constant = 0.17123×10^{-8} Btu per hr-sq ft-°R⁴
- ρ = reflectance

Subscripts:

- c = cold side
- DS = direct solar
- ER = Earth reflected
- ET = Earth emitted
- H = hot side
- IR = infrared
- S = solar
- SP = space
- l,n = node numbers

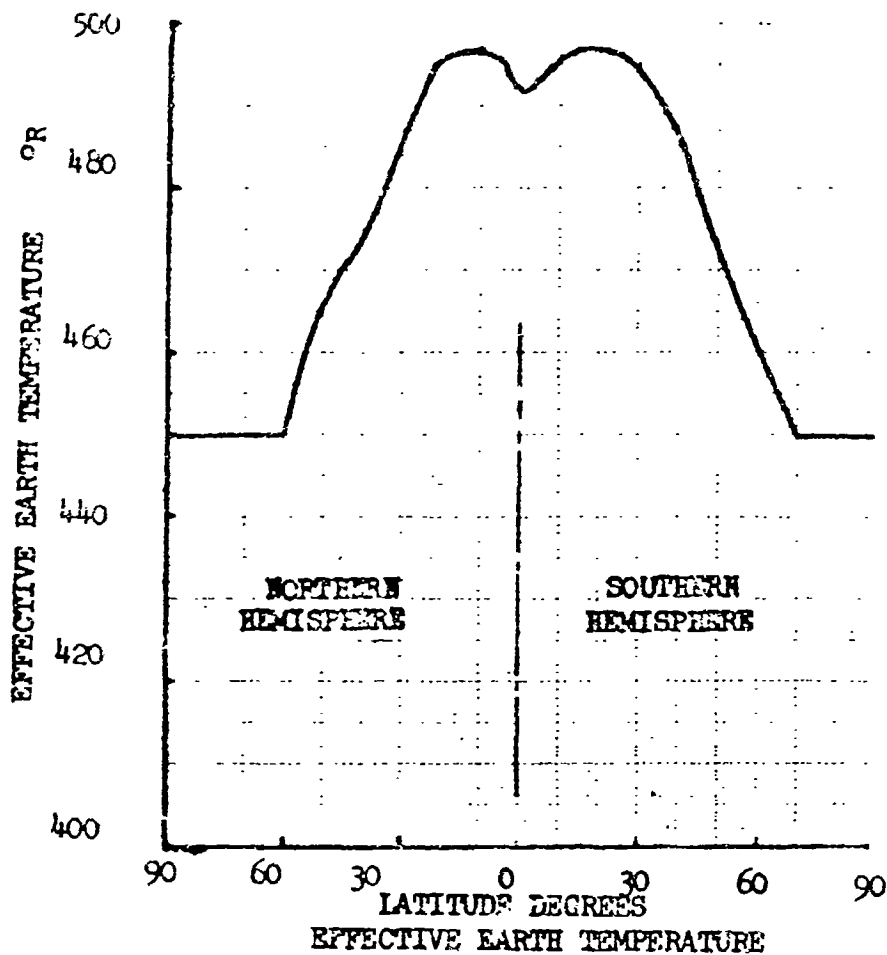


FIGURE 5.5-19

5.5.5 Conclusions

Thermal control of primary and secondary mirror optical geometry by passive means appears to be feasible for short term operation. Long term effects such as stress relaxation, which could cause mirror distortions requiring an active system, have not yet been evaluated. The effective thermal insulation of the primary mirror from the floor beam and use of low conductive tangent bars to the inner telescope tube structure are of prime importance for preventing the occurrence of excessive mirror temperature gradients. Employment of doors which are maintained isothermal by means of an earthshade, proved beneficial and is recommended. Recommended surface coatings are low α_s / ϵ_{12} white paint for the exterior tube wall and flat black paint for interior wall and secondary mirror support structure. A 2-inch-thick solid mirror could be employed which has smaller axial temperature gradients than the honeycomb construction.

Further investigations of the thermal problems associated with optical geometry are needed, but should be deferred until second generation trade studies have been performed in the following areas:

- Primary mirror materials, constructions, and fabrication
- Secondary mirror cell design
- Telescope configuration

5.6 OTHER SUBSYSTEMS

Supporting subsystems for the MOT that are similar to the systems being developed for current space programs and that do not affect the operational feasibility are defined in the following paragraphs. These systems are defined only for the purposes of completing descriptions of typical requirements for a MOT operational concept. In general, the data were only used to develop installation requirements for configuration drawings and weight statements.

5.6.1 Communications and Data Handling

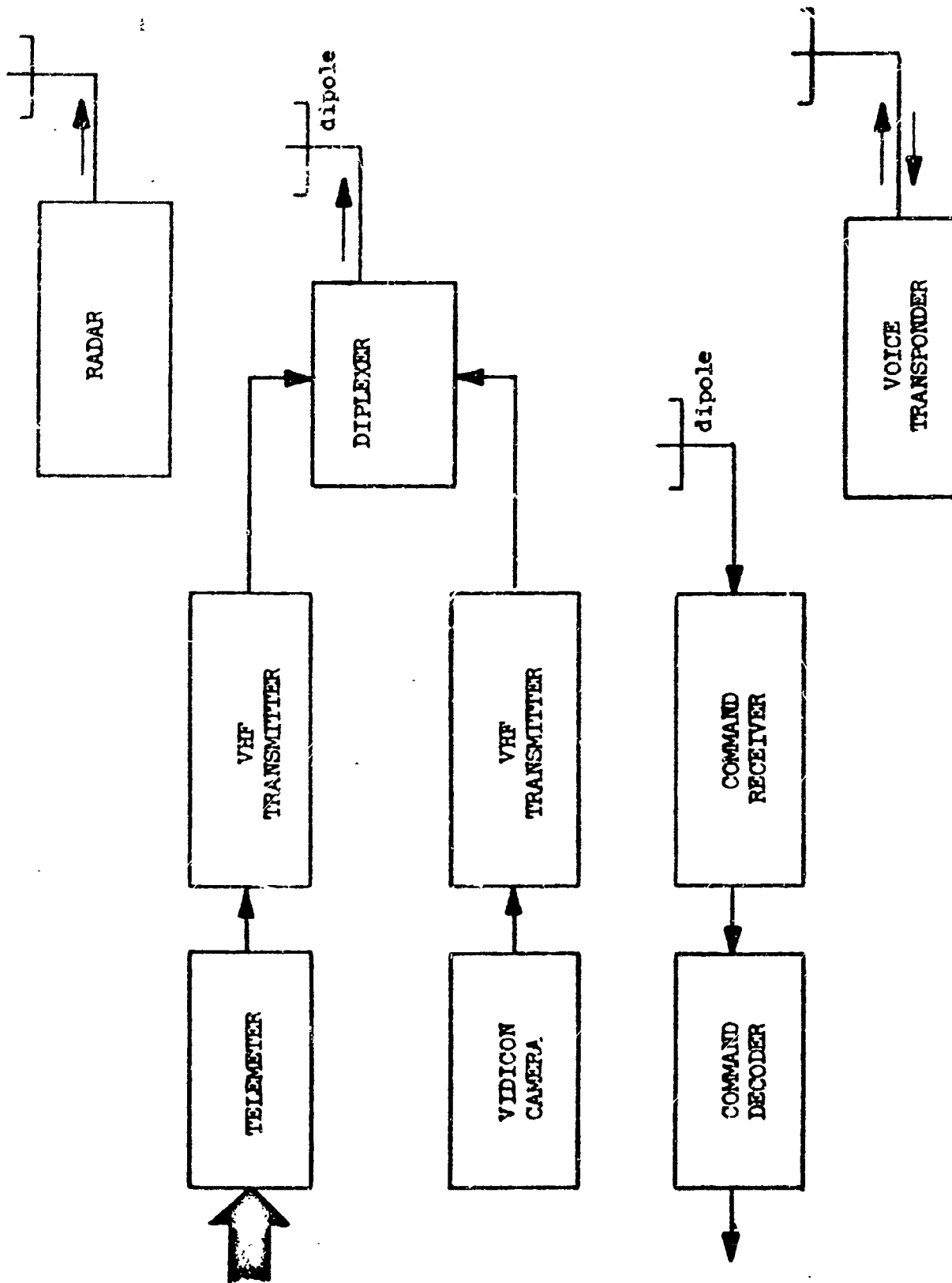
Subsystems required to support the orbiting telescope mission include the communications, data handling system, and the guidance electronics associated with rendezvous and docking operations. Inasmuch as the rendezvous mission is so intimately supported by the communications system, the rendezvous and docking subsystem will be covered under the communications and data handling system.

The detached mode of operation described in Section 4 necessitates the use of R-F links for monitoring attitude control, and communications purposes. The coupled mode lends itself to the use of flexible cables. In either mode the number and type of functions are essentially the same. Only the decoupled mode will be described in detail since it has the greater requirements. In the gimbaled mode, the receiver and transmitter functions for telemetry, command, and imagery data can be handled with cables.

The communication and data handling subsystem provides all transfer of command and control data and mission related information to and from the MOT. This subsystem supports and provides such functions as tracking, voice communication, reception and distribution of commands, formatting and transmission of data for the monitoring and control of the MOT subsystems, and acquisition and transmission of imagery data for visual monitoring. A block diagram of the communications and data management subsystem which identifies the equipment needed to perform the necessary functions is shown in Figure 5.6-1. Figure 5.6-2 defines the centerline equipment (without spares) in terms of weight, volume, and power.

FIGURE 5.6-2
COMMUNICATIONS AND DATA HANDLING EQUIPMENT CHARACTERISTICS

<u>Component</u>	<u>Weight (lbs)</u>	<u>Power (w)</u>	<u>Size</u>
Telemetry	21.0	0.5	7.5 x 16.5 x 3.5 in
Vidicon Camera (2)	6.0 (ea)	11.0 (ea)	2.5 x 7.8 x 6 in (ea)
VHF Transmitter (0.5w)*	0.4	7.0	2.3 x 3.3 x 1.0 in
VHF Transmitter (2 w)*	0.9	18.0	2.3 x 3.3 x 2.0 in
Command Receiver	4.0	2.0	3.9 x 7.6 x 3.4 in
Command Decoder	12.0	8.0	250 cu in
Rendezvous Radar Transponder	15.0	12.0	0.75 cu ft
Antennas	6.0	-	4 cu ft (est)
Cables	15.0	-	
Diplexer	1.0	-	1.9 x 5.8 x 2.7 in
Voice Receiver and Transmitter	3.0		2.8 x 7.7 x 2.4 in
*(Transmitter Power)			



BLOCK DIAGRAM - COMMUNICATION & DATA MANAGEMENT

FIGURE 5.6-1

The telemetry system provides the data required to monitor the status of the MGT vehicle and its subsystems by transmissions to the MORL. The data are used as the basis for control and operation of the telescope and its subsystems. A PCM system using magnetic logic, which needs little power, is recommended as a candidate telemetry system. The number of functions estimated to be monitored for each of the basic scientific experiments and each of the major subsystems are shown in Figure 5.6-3. The analog and discrete channels needed to perform the monitoring functions listed in Figure 5.6-3 are estimated to be as follows:

40 analog channels at a rate of 2 samples/sec

247 analog channels at a rate of 1 sample/sec

100 discrete channels at a rate of 1 sample/sec

FIGURE 5.6-3

MONITOR FUNCTIONS

Camera	5
Spectrograph	8
IR Spectrometer	8
Optical Spectrometer	13
Polarimeter	13
Binary Detector	13
Power	35
Attitude Control	210
Thermal Control	20
Communications	33
Rendezvous	11
Contingency	18
Total	387

Some of the scientific data lends itself to transmission by an RF link from the telescope to MORL. Since the monitoring data requires only a narrow bandwidth, the scientific data can be transmitted with the monitoring data over the same link. The data may be digitized and multiplexed as pulse code modulated (PCM) data with the monitoring data for transmission to MORL. Postulated sampling rates are:

Binary Detection (16-bit word)	- 1 sample/sec
Polarimetry (analog)	- 1 sample/sec
Spectrography (analog)	- 1200 samples/sec

Synchronization is also required and may be accomplished by using a 31-bit word transmitted once per second. All analog data may be digitized and formatted into 8-bit words, which provides sufficient accuracy for both monitoring and scientific data.

The primary data to be obtained from the MGT will be in the form of photographic plates. The photographs will require such detailed analysis that it is presently

impractical to transmit the data by radio links. Hence, the photographic plates will be physically recovered and returned to Earth. There is provision, however, in the communication and data management subsystem for a video link which permits remote monitoring of the camera image. The image is derived from a slow-scan vidicon having a resolution capability of 1150 TV lines which provides a 400-line-pair image when the Kell factor is introduced. A frame rate of one image every 6 seconds is considered adequate for monitoring purposes when combined with a long persistence viewing screen. By limiting the frame rate, it is possible to utilize a reasonably narrow solid state transmitter. It is assumed that six grey levels will be adequate and that analog transmission may be employed with a bandwidth of about 100 kc.

VHF transmitters may be used to transmit both telemetry and imagery data since solid state transmitters are available with relatively high efficiency and the antennas are conveniently small in size. The narrow bandwidth needed for the PCM telemetry permits the selection of a 0.5-watt transmitter while the wider bandwidth of the video link needs a 2-watt transmitter for transmission for distances of about a mile. A diplexer permits the use of a single antenna system which consists of three whip antennas equally spaced around the circumference of the MOT base, thereby assuring coverage at all times. The whip antenna may be of the type used on Gemini which can be stored inside a retaining drum and latched in position. When released, the antenna would form an element about 12 inches long and 0.5 inch in diameter.

Recording of scientific data from experiments other than high resolution photography can best be done on magnetic tape, with the recorder installed with the other instrumentation in the orbiting telescope. A recorder similar to the one designed for Gemini would be very appropriate. This weighs about 12 pounds with a 2400-foot reel of 1/2-inch tape and has a volume of about 400 cubic inches. At the low record speeds necessary to accommodate the data rates, the power to operate the recorder would be less than 5 watts. The MTBF of the recorder and tape is about 7000 hours. It is advisable to have at least two recorders, so that a replacement recorder and tape could be installed in the telescope instrument package when the tape on the other recorder had been used up. This is preferable to replacement of tape at the telescope because the operation would be awkward and tedious. The used tape with its recorder could then be played back to a MORL recorder or directly to a ground station recorder via the MORL communication link. The tape can then be erased and it is then ready (along with its recorder mechanism) for subsequent replacement in the telescope.

The scientific data to be recorded, and subsequently transmitted to the ground stations, amounts to about 3,200,000 bits, which occur over a period of 48 days, or 700 hours of recording time. The breakdown of the data is:

- o High dispersion spectroscopy in 0.1 Å increments over a range of 1000-4000 Å to an accuracy of 10 percent. . . .1,900,000 bits
- o High dispersion IR spectroscopy in 0.2 micron increments over a range of 1-15 microns to an accuracy of 10 percent 600,000 bits
- o Low dispersion spectrometer in 50 Å increments over a range of 1000-4000 Å to an accuracy of 10 percent. 10,000 bits

- o Photometry to 1 percent accuracy. 600,000 bits
- o Thermoelectric (IR detector) measurements to 2 percent accuracy. 60,000 bits

For the above data, the recorder can be operated at 0.04 in/sec tape speed, meaning a 2400-foot reel of tape would last about 200 hours. Accordingly, it would take about four reels to accommodate the 700 hours of recording, which is equivalent to three recorder (plus reel) changes.

Scientific data accumulated by MOT must be processed and transmitted by the MORL data handling system. A preliminary analysis of the MORL communications and telemetry system capability indicates:

- o Channel "F" designated for PCM experimental data, has a capacity of 76,800 bits per second.
- o Total contact time per day over Cape Kennedy and Corpus Christi ground stations is 77 minutes.
- o Total transmission capability over Channel "F" is 355,000,000 bits per day.
- o Experiment data accumulated from MORL experiments is 304,000,000 bits per day.
- o Data handling capacity available for additional data, as for example from MOT, is 51,000,000 bits per day.

Hence, adequate capability exists on MORL to accommodate the MOT data. It is highly probable that many of the MORL experiments will have been completed prior to MOT, and additional capability will be available which might be used to scan specific areas of the high resolution photographs.

Control signals are received from MORL through a command receiver and are decoded and distributed by a decoder. The number of control commands and the equipment or function that requires the commands are listed in Figure 5.6-4.

Commands may be encoded on the MORL into a serial PCM pulse train and transmitted over a single carrier to MOT. The receiver can be a narrow-band receiver which demodulates the pulse train and presents it to the decoder. The decoder identifies the intended equipment and sends pulses or analog signals to it as required. A command rate of once per second for each item of equipment or function is believed adequate.

The command receiver operating in the UHF band is available off the shelf with only minor modification. The decoder must be designed to fit MOT requirements. The antennas that serve the receiver would be similar to those used with the VHF telemetry and imagery transmitter. A frequency of about 400 mc is selected because receivers exist and antennas are small in size.

Voice communication between crewmen on MOT and MORL, when required, will be accomplished with a two-way low-power voice transceiver, since the expected range will be

FIGURE 5.6-4

CONTROL COMMAND FUNCTIONS

<u>Equipment or Function</u>	<u>Number of Commands</u>	
	<u>Discrete</u>	<u>Analog</u>
Camera	15	
Spectrograph	30	
IR Spectrometer	15	
Optical Spectrometer	5	
Polarimeter	4	
Binary Detector	5	
Power	6	
Attitude Control	20	20
Thermal Control	6	
Communications	6	
Rendezvous	8	
Contingency	3	
	<hr/>	<hr/>
Total	123	20

about a mile. The transceivers may also be on VHF and use antennas similar to the video and telemetry transmitter. A second camera can provide visual monitoring of the crewmen and their activities while they are in the MOT. If such a camera is used, transmission of the imagery data should be shared with the camera imagery monitoring since it is not proposed to provide two video links.

Interfaces need to be provided in MORL to operate with the communication and data management subsystem of MOT. Those interfaces are:

- o Receivers, demodulators, and data presentation devices for the telemetry and video link. Also appropriate antennas.
- o A command coder and transmitter (with appropriate antennas) to communicate with the command receiver and decoder on MOT.
- o Data storage provisions for the telemetry data.
- o Voice transceiver for communicating with crew while on MOT.

MOT-MORL Rendezvous and Docking

Rendezvous of MOT with MORL may be accomplished in a manner similar to the Gemini-Agena technique. Inasmuch as MORL is scheduled to be equipped with a rendezvous radar, it is necessary to equip MOT with the radar transponder. The radar and transponder could be interchanged between MOT and MORL, but such other considerations as the availability of a computer, manual data insertic unit, and incremental velocity display unit in MORL make it desirable to have the radar in MORL. This will necessitate attitude orientation of MORL in order to permit the radar antenna beam, which is a 70 degree cone, to be directed at the MOT.

The transponder antenna system would consist of a dipole mounted on a boom, two spiral antennas, and selector switches. The dipole has a doughnut-shaped pattern with the dipole located in the center. The patterns of the spiral antennas, pointed in opposite directions, would provide spherical coverage by operating in the space above and below the dipole pattern. The antenna switches would cycle between antennas, sample signals on each, and lock on the antenna with the strongest signal. A circulator permits the same antenna system to be used for transmission and reception.

The transponder has appropriate bandpass filters to discriminate against unwanted radar frequencies and also has attenuators to permit operation at close ranges. The transponder responds to a predetermined interrogation pulse from the rendezvous radar at an offset frequency with a 2-microsecond delay and expands the 1-microsecond pulse received from the radar into a 6-microsecond retransmitted pulse. The retransmitted pulse provides the source of information for azimuth, elevation, range, and range rate data. The data is then provided to the computer which operates on the data and presents it for use to the appropriate indicators and displays used by the crew in obtaining a successful rendezvous. Desired commands for maneuvering MOT may be transmitted over the command link. The command receiver will probably be turned on at launch and left on at all times. It can also be used for turning on the rendezvous transponder.

Tracking of MOT from the ground for purposes of commands for coarse and fine phasing orbit maneuvers may require a beacon and appropriate antenna. It is quite likely that skin tracking will be adequate. If not, additional equipment weighing 22 pounds and antennas and boom weighing about 6 pounds should be added. The beacon requires about 35 watts of power.

Tracking information about the position of MOT can be transmitted to MORL over their ground-to-space link and such information can be used for preparation of rendezvous activities.

For final docking maneuvers, and possibility of docking in the dark, two 25-watt beacon lights should be installed on opposite sides to assist the MORL crew in maneuvering MOT in the docking phase. The lights can also be used by the shuttle crew in approaching MOT. The lights may be turned on and off through the command link.

5.6.2 Electrical

The electrical power subsystem is required to provide the MOT subsystem electrical power requirements, upon demand, from the launch through the operational mission phases. The electrical subsystem concepts selected for each of the MOT concepts, Mode IC-Configuration 948-41C, and Mode IID-Configuration 948-43D, were based on the following requirements and assumptions.

- o Operational life is 3 to 5 years.
- o MORL electrical subsystem can supply MOT power requirements with no additional power sources or conditioning equipment required during docked periods.
- o Periodic maintenance and resupply will be provided.

o Power Requirements:

MOT Operational, - (see Figure 5.6-5 and Figure 5.6-6)
 Launch & Rendezvous - 300 watts, average
 4800 watt-hours

- o The roll axis of the MOT may be used to sun-orient solar panels in the Mode IIID concept.

5.6.2.1 System Selection and Description

The Mode IC, Configuration 948-41C, electrical power subsystem concept utilizes primary silver-zinc batteries (weight--110 pounds) to supply the MOT electrical requirements (4800 watt-hours) during launch, rendezvous and docking. After docking, the

FIGURE 5.6-5
 ELECTRICAL POWER REQUIREMENTS
 (Operational Phase)

	AVG. POWER (Watts)		PEAK POWER (Watts)**	
	Mode IIID	Mode IC	Mode IIID	Mode IC
Attitude Control	320	320	620	620
Communications	35	35	57	57
Experiments	50	50	50	50
Environmental Control				
Telescope	50	50	50	50
Cabin Manned*	20	20	200	200
Cabin Unmanned*	90	90	100	100
Depressurization*	65	---	3250	----
Miscellaneous Actuators	---	---	200	200
Electrical Power	290	35	1200	70
	---	---	---	---
TOTALS	920	600	5000	1350

* Assumptions: Cabin is manned 4 hours per 1.5 days. Depressurization requires 2.25 average for 1 hour at the end of each manned period. Depressurization while docked is accomplished by the laboratory subsystems. Cabin pressurization power requirements were estimated on the basis of Configuration "C" in Figure 4-1. A two hour pumpdown time will be required to be compatible with the final configuration. This will have a negligible effect on the timeline analysis.

**Total peak power reflects diversification of the loads.

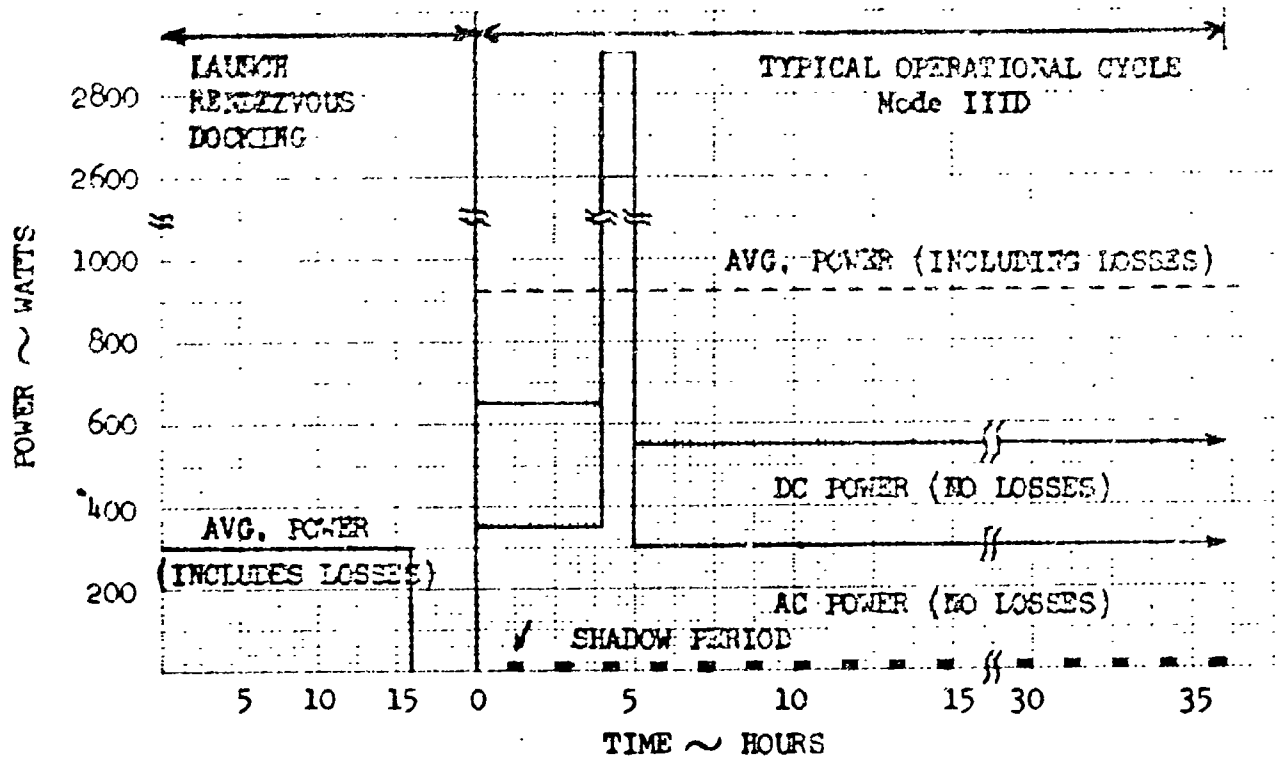


FIGURE 5.6-6 MODE IIID POWER PROFILE

MOT buses (28 volts d.c. and 400 cycle, 3 phases, 115/200 volts a.c. buses) are connected directly to the laboratory electrical subsystem. The connecting electrical wiring will be designed with enough flexibility at the MOT gimbal point to prevent imposing significant disturbing torques to the MOT regardless of attitude. The individual MOT electrical loads are connected to their respective buses, through manually-activated circuit breakers for control and protection. If a more detailed analysis indicates a need for either peaking or additional power sources located in the MOT, it is anticipated that the primary batteries used for launch and rendezvous may be replaced by rechargeable batteries which can be recharged periodically from the laboratory electrical subsystem.

The Mode IIID, Configuration 948-43D, electrical power subsystem center line concept selected is a solar cell/battery electrical power subsystem. Figure 5.6-7 shows a subsystem weight summary. The solar cell panels supply the average power requirements of the loads and the batteries during sunlight portions of the orbit. Silver cadmium batteries are used to supply power demands during the shadow portion of the orbit, during peak demand periods, and during the launch, rendezvous, and docking phases. Voltage regulators connected to the solar panels and the batteries provide regulated 28 volt d.c. power to the d.c. loads and to the inverters. The d.c.-to-a.c. converters supply 400 cycle, 3-phase 115/200 volt a.c. power to the a.c. loads.

The solar cell panels are oriented to the Sun by articulation of the panels with respect to the MOT pitch axis and by rolling the MOT about its roll axis. After orientation of both the MOT and the solar panels, the panels are locked in position so as not to affect the MOT stability during an observation period. This will result in only a small reduction in solar panel power output as MOT orientation is maintained. Fixed panels would require as much as five times the solar panel area to supply the required power. The solar panels are sized to provide 1.515 kilowatts at end-of-mission with no maintenance or resupply. A panel degradation of 30 per cent due to micrometeoroids, radiation, and thermal cycling was assumed.

Sealed, rechargeable, silver-cadmium batteries operated to 35 per cent depth of discharge was selected to provide energy storage capable of supplying the power requirements during shadow periods. In addition, the batteries will supply peak demands which are above the power capabilities of the solar panels during sunlight and supply all power requirements during the launch, rendezvous and docking phases. The batteries are sized to supply 3430 watt-hours required during one shadow period (cabin-manned) and including a one hour depressurization cycle. Backup power requirements will be provided by the batteries in the shuttle to support frequent repressurizations during large scale photograph experiments. Two batteries are installed and both are required to supply the maximum energy requirements; however, it is assumed that only one is required to supply the energy requirements during an emergency or maintenance period such as for replacement of batteries at the end of their one-year design life or in the event of a random failure, or during replacement of a failed battery charger. Two battery chargers are installed, one for each of the silver-cadmium batteries with interconnections such that in the event of a failure the remaining charger may be used to charge either battery. The batteries can be charged to full capacity between periods of manned occupancy.

Two voltage regulators are installed, one operating and one non-operating standby. These regulators are "step-down", non dissipative type and are sized to regulate

FIGURE 5.6-7

MODE IIID ELECTRICAL SUBSYSTEM SUMMARY

ITEM	RATING	SIZE (Total)	WEIGHT (Total) (Lbs.)
Solar Panels (2)*	1515 W	216 ft ²	324
Batteries (2)	3430 WH	4.5 ft ³	545
Regulators (2)**	5000 W	2140 in ³	75
Inverters (2)**	4500 W	5150 in ³	180
Battery Chargers (2)	745 W	430 in ³	15
Distribution System	-----	-----	250

*Number in (2) is the number of units installed.

**One unit operating, one unit stand-by

Basic Assumptions:

- o Solar Cell Panels
 - 7 watts/sq ft at end of mission.
 - 1.5 lbs/sq ft including extension and orientation mechanisms and support structure.
- o Batteries
 - Sealed, rechargeable silver-cadmium
 - 18 WH/lb nominal rating.
 - 35 percent depth-of-discharge maximum.
 - 1 year operating life.

the d.c. power output (no load to full load) from 26 to 30 volts with input voltages which vary from the end-of-discharge battery voltage (27 volts) to the solar panel output voltage at the end of battery charge (42 volts). Two d.c.-to-a.c. static inverters, one operating and one non operating standby, are connected to the regulated d.c. bus. These inverters provided regulated 400 cycle, 3-phase, 115/200 volt a.c. power.

All switching for control and protection of the electrical subsystem is automatic with manual override capability. The individual loads are connected to the buses through manually activated circuit breakers.

Although the solar cell/battery electrical subsystem has been tentatively selected for the Mode IIID concept, a more detailed subsystem optimization and trade study may show that a system utilizing a radioisotope energy source is the optimum choice. Preliminary estimates indicate that the RCA thermionic system using a PU-238 radioisotope heat source (PU-238 has a half-life of 90 years) would have the following advantages:

An estimated system weight of 200 pounds less than the solar cell/battery concept. The isotope/thermionic source would weight approximately 375 pounds including shielding to limit radiation levels to 10 millirem per hour at one meter. Rechargeable batteries used to supply peak power are estimated at 300 pounds. The remainder of the subsystem would be approximately the same as the solar panel concept.

The isotope system does not require orientation and does not require external components such as large solar panels. This will minimize disturbing torques on the IXT and appreciably reduce the stability problem.

The greatest disadvantages of the radioisotope concept are handling, safety, and availability of sufficient quantities of the radioisotope.

5.6.3 Propulsion

Propulsion subsystems are used on the MOT for initial rendezvous, docking, orbit keeping, station keeping, and control moment gyro desaturation.

The initial rendezvous requires propulsion to maneuver the MOT from a phasing orbit to the 250 NM orbit of the MORL. The Saturn IB launch vehicle is used to place the MOT in the elliptical phasing orbit which has an apogee of 250 NM. The ΔV required for this Hohmann transfer or orbit injection maneuver is 380 fps. The docking maneuver requires propulsion for both attitude control and small orbit changes. The ΔV required for this maneuver is 20 fps which is sufficient to perform a terminal rendezvous and docking for vehicle orbital separations of one nautical mile. Orbit keeping and station keeping propulsion requirements are the same, except for the frequency of applied impulses. Station keeping is required in a two-vehicle system and the vehicle with the lower ballistic coefficient is boosted periodically to keep within a mile distance of the other. The propellant required to orbit-keep the MOT for one year is 575 pounds based on a propulsion efficiency of 300 I_{sp} . The operation performance analysis for establishing the rendezvous, docking, and orbit-keeping propulsion requirements are presented in the Operations section of this report. The Propellant requirement for desaturation

of the MOT control moment gyros, defined in the studies on attitude is 700 pounds per year.

Except for the initial rendezvous, all other propulsion requirements can be handled by a reaction control jet (RCJ) subsystem using variable thrust engines (4-40 lb thrust). The initial rendezvous ΔV of 380 fps requires a higher thrust to weight ratio than the other requirements and the thrust must be high enough to keep the engine burn time within reason. Two 1000-pound-thrust engines were selected for this function.

Similar propulsion systems are used for both operational concepts of the MOT. Model No. 948-41C (Soft Gimbal Concept) requires initial rendezvous, docking, and control moment gyro desaturation. Model No. 943-43D, in which the MOT normally operates separated from MORL, has these same requirements except the number of dockings are increased and MOT must perform its own orbit keeping function.

5.6.3.1 System Selection and Description

The following are the propulsion systems used in the MOT configurations and weight statements for each of the operation functions.

Initial Rendezvous

Rendezvous Engines	2 -- 1000-lb-thrust units
Rendezvous Propellant	1000 lbs
Attitude Control Propellant	20 lbs
Acceleration Capability	2.75 ft/sec ²
ACS Authority	1°/sec ²
Rendezvous Burn Time	2.3 minutes (within present SOA)
Rendezvous Engine Weights	20 lbs ea.
Reaction Jet Burn Time	45 sec/engine

Rendezvous From One Mile

This maneuver can be feasibly handled by either the initial rendezvous engines or the RCJ subsystem. The estimated propellant is 12 lbs/rendezvous.

Docking

For major repairs the MOT is to be cooperatively docked to the MORL. Control is to be initiated by the MORL-based crew, but the docking actuation is aboard the MOT. This is not expected to cause difficulties as it is substantially the same situation as when the pilot is aboard the maneuvered vehicle when low control authorities are used. Figure 5.6-8 shows a plot of useable control authorities as developed and reported in Boeing docking studies, based on uncoupled control and equal authority in all angular and linear degrees of freedom. In order to maximize the compatibility between the docking, orbit maneuvering and CMG desaturation requirements, the MOT-RCJ authority is selected as shown in Figure 5.6-8. For this type system, the worst case docking conditions are as follows:

Pitch angle	+10°
Pitch rate	1.5°/sec

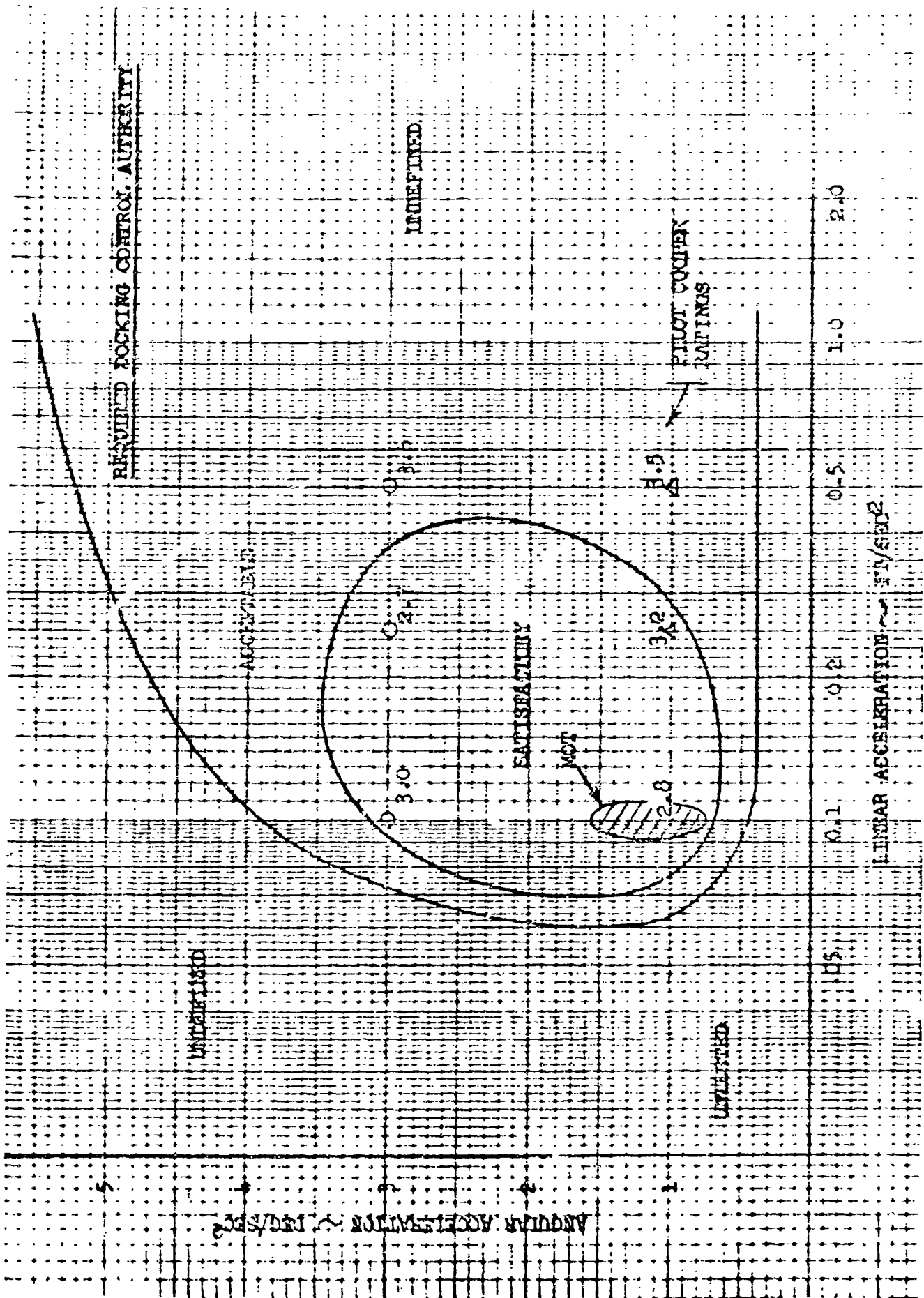


FIGURE 5.6-8 HANDLING QUALITIES REQUIRED CONTROL AUTHORITY

Yaw angle	+10°
Yaw rate	1.5°/sec
Roll angle	+10°
Roll rate	1.5°/sec
Y axis offset	12 in
Y axis rate	0.75 ft/sec
Z axis offset	12 in
Z axis rate	0.75 ft/sec
X axis rate	1.5 fps

Figure 5.6-9 shows the implementation of these requirements. The engines are 10:1 throttleable type which meet all RCJ requirements except rendezvous. The details on this system are:

Engine size	4-40 lb variable
	16 required
Weight/engine	2.5 lbs
I_{sp}	300 sec.
Propellant required	35 lbs/docking
3 ft/sec	
60°/sec	
Lever arm pitch	15 ft
yaw	15 ft
roll	7 ft
Total burn time	60 sec/engine/year (pulsed mode)
Control authority	per Figure 5.6-9

Orbit Keeping

Orbit keeping propellant, 575 pounds for one year, can be supplied entirely by the MOT-RCJ subsystem. The operation can be performed without reorientating the MOT by the MORL computer resolving the required velocity correction vector onto the MOT control axes, and determining the proper thrusting times.

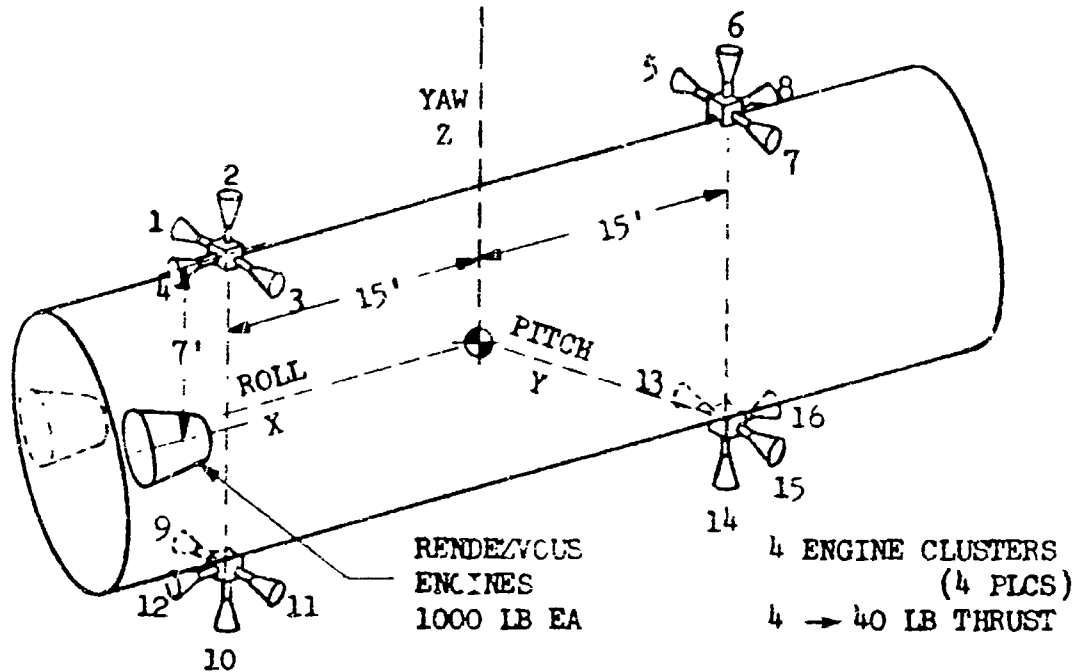
Station Keeping

To keep the MOT and MORL within one mile of one another, periodic corrections must be made. Performance analysis indicates, as a worst case, these will be 0.29 fps corrections every 9 hours. Since the vehicle decaying fastest is to be corrected, no additional fuel over that for orbit keeping is required. This essentially means the orbit keeping corrections will be made in small increments. With the small control authorities available (0.01 ft/sec²), this is favorable to system operation (high engine life and I_{sp}).

CGM Desaturation

The thrust levels of the low authority (4 pounds) system are adequate for this task, and the propellant (700 pounds/year) can be supplied by the MOT-RCJ subsystem.

Propellant Supply



	ENGINES FIRED	<u>DOCKING</u> Control Authority	<u>STATION KEEPING</u> Control Authority	<u>DESATURATION</u> Control Authority
+ ROLL	3, 13	1.59°/SEC ²	---	0.159°/SEC ²
- ROLL	5, 11	1.59°/SEC ²	---	0.159°/SEC ²
+ PITCH	2, 8, 12, 14	0.76°/SEC ²	---	.076°/SEC ²
- PITCH	16, 10, 4, 6	0.76°/SEC ²	---	.076°/SEC ²
+ YAW	1, 9, 7, 15	1.03°/SEC ²	---	0.103°/SEC ²
- YAW	3, 11, 5, 13	1.03°/SEC ²	---	0.103°/SEC ²
+ X	8, 16	0.11 FT/SEC ²	0.011 FT/SEC ²	---
- X	4, 12	0.11 FT/SEC ²	0.011 FT/SEC ²	---
+ Y	1, 13	0.11 FT/SEC ²	0.011 FT/SEC ²	---
- Y	3, 15	0.11 FT/SEC ²	0.011 FT/SEC ²	---
+ Z	10, 14	0.11 FT/SEC ²	0.011 FT/SEC ²	---
- Z	2, 6	0.11 FT/SEC ²	0.011 FT/SEC ²	---

FIGURE 5.6-9 NOT CONTROL AUTHORITIES

The entire MOT-RCJ subsystem can thus be supplied from a central propellant storage supply. The total requirements for 180 days are tabulated below:

<u>Propellant Required/Year</u>	<u>Model No. 948-41C</u>	<u>Model No. 948-43D</u>
Rendezvous (Initial)	935 lbs	1017 lbs
Rendezvous (From 1 mile) 1 req'd	12	(4 req'd) 48
Docking (5 req'd)	35	(5 req'd) 175
Orbit Keeping	----	287
CMG Desaturation	350	350
Total	1332	1877
Required Storage Volume		
Fuel	14 ft ³	
Oxidizes	17 ft ³	
Tankage and Pumping Estimate	210 lbs	
Engine Weights	80 lbs	

The above propulsion propellant requirements are shown for 180 days to coincide with an assumed resupply cycle and sizing tankage that could reasonably be installed on the MOT configurations. It should be noted that the propellant weights represented for the first 180 days of operation includes that used only in the initial rendezvous. The propellant tankage for this initial rendezvous was divided into two modules and mounted adjacent to the 1000-pound thrust rocket engines.

The propellant tanks for the RCJ subsystems were also divided into two modules and located at the CG of the MOT. This arrangement locates the tanks midway between RCJ engine clusters and results in minimum CG shift with propellant usage. Minimum CG shift is a very important factor for Model No. 948-41C as increased displacement of CG with respect to gimbal axis increases the disturbance torque imposed by the spring forces. All propellants were assumed to be N₂O₄/Aerozene 50 and the I_{sp} = 300.

Propellant weight requirements established for the shuttle in Model No. 948-43D are based on the same propellants and the rendezvous & docking ΔV's used for MOT.

5.6.3.2 Conclusions

No major problem areas are anticipated in either of the propulsion systems. The burntime requirements (23 hrs/year in pulsed mode) are outside the present state of the art. Materials advances are expected to overcome this limit, however. Should these advances not take place, this simply implies more frequent engine replacement.

5.6.4 Environmental Control

5.6.4.1 General Description

In the environmental control system description which follows, references to the MORL system apply also to shuttle vehicle ECS except as noted. Means will be provided for pressurization of the MOT cabin during periods when manned occupancy is

necessary for equipment adjustment. The MOT cabin will be openly interconnected with the MORL during this operation and the MORL pressurization system will be employed. A cooling system on board the MOT will provide a controlled temperature environment for instruments and equipment.

The principal ground rules for the environmental control system:

1. The MOT shall contain its own independent temperature control system.
2. Pressurization during manned occupancy shall be provided by the MORL (or shuttle vehicle) atmosphere supply system and the MOT cabin shall operate unpressurized during observational periods.
3. The MOT cabin atmosphere shall match the MORL atmosphere; namely, 50% oxygen; 50% nitrogen; 7.0 psia; $535 \pm 5^{\circ}\text{R}$; 50% relative humidity; CO_2 partial pressure, 4 mm Hg nominal, 8 mm Hg maximum.
4. The MORL carbon dioxide, moisture, and contaminant control systems shall be utilized for atmosphere conditioning.
5. Emergency gaseous atmosphere supply for one pressurization shall be provided in the MOT cabin.
6. The MOT cabin volume is 1400 cu. ft.
7. The leakage rate shall not exceed 0.25 lb. per hr. at 7.0 psia.
8. The MOT cabin shall be depressurized for making observations.
9. For the 948-41C MORL soft gimbal concept, provision will be made for access approximately 100 times per year from the MORL to the MOT cabin through a transfer tunnel located on the MORL. For the shuttle vehicle configuration, access will be provided 15 times during each shuttle vehicle mission through an airlock on shuttle vehicle; and the MOT may dock with MORL 4 to 8 times each year for major maintenance.

5.6.4.2 Pressurization System

Provision should be made to recover the cabin gases since otherwise approximately 47.3 lb of expendables would be required for each repressurization. A system employing a three stage compressor with jacketed compression stages and intercooling between stages is proposed to compress the gases to 500 psia. Assuming a one hour repressurization time, the compression flow is approximately 56 CFM, the estimated peak compressor power is 7.25, and the total energy required is 4.5 Kw hr. The cabin is pumped down from 7.0 psia to 0.7 psia and the compressed gas stored in an 18.0 cu. ft. accumulator at approximately 500 psia. An oversized compressor and accumulator on the MORL could be employed which would serve this requirement as well as other MORL airlock operations. To conserve weight on the shuttle vehicle, the compressor and accumulator for this application could be located in the MOT cabin.

For the 948-41C MORL soft gimbal concept, access to the MOT cabin is achieved as follows: The transfer tunnel flange is coupled to the MOT cabin hatch. The transfer tunnel is then pressurized. The MORL hatch is opened allowing access to the transfer tunnel interior. The MOT cabin vent to space is closed. Coupling is made with the MOT pressurization line and the MOT cabin is pressurized from the accumulator with the addition of 10 per cent make up gases to bring the MOT cabin pressure to 7.0 psia. The MOT hatch is then opened allowing access to the pressurized MOT cabin. Egress from the MOT cabin is achieved by a reverse sequence of operation.

A cabin fan is provided to maintain circulation in the MCT cabin and the MCT cabin exhaust gases are then ducted to the MORL air purification system.

During depressurization and repressurization special precautions must be taken to prevent moisture condensation in the instrumentation and optical system. A replaceable silica gel dehumidification canister may be required in the vent passage between the interior of the instrumentation console and the cabin.

For unpressurized operation, the maintenance of pressure levels that will preclude corona discharge problems or the cold welding of faying metal surfaces must be studied.

5.6.4.3 Cooling System

Conditioning and temperature control of the MCT cabin atmosphere is provided by the MORL cabin atmosphere conditioning system. Precise temperature conditioning of instruments and equipment in the MCT cabin is achieved by thermally insulating the instruments from the cabin and regulating the equipment temperature with liquid-cooled cold plates installed on the instrument platen. Additional temperature regulation may be obtained with thermostatically controlled heaters; if required. Instruments that will require close temperature control ($530 \pm 0.1^\circ \text{R}$) are the high dispersion spectrograph and the high dispersion ultraviolet and infrared spectrometers. Other instrumentation such as the photomultiplier tube will require special cooling provisions because it operates most efficiently at about 350°R . Infrared sensors may require refrigeration to temperature levels as low as 8°R . A closed cycle helium system employing regenerative cooling with a multistage expansion turbine is under development for achieving this temperature level with flightweight equipment.

The liquid coolant would be cooled in a space radiator installed on the cylindrical portion of the cabin exterior. Approximately 70 sq. ft. of radiator surface per KW of heat dissipation is required. For better temperature regulation of the electrical equipment coolant loop it appears desirable to provide a separate radiator loop for the compressor coolant system. The use of redundant coolant loops would also provide added meteoroid protection. A suitable coolant such as an ethylene glycol - water mixture that will not freeze during periods of low heat rejection must be used.

5.6.4.4 Conclusion

The cabin pressurization and thermal control systems for the MCT cabin appear to be well within the projected state of the art for the MCT launch date. However, the transient effects of the operation of such control systems on attitude stability should be studied. The precise dimensional control required for the instrument platen and optical system will warrant a more detailed thermal and distortion analysis when the design configuration is better defined. The developmental program may also include the laboratory testing of an instrumented platen for a final pre flight verification of the optical system.

6.0 BIBLIOGRAPHY

American Optical Company, Fecker Division, "Final Report, Feasibility Study of a 120-inch Orbiting Astronomical Telescope," AF-1143, Prepared under NASA-Langley Contract NAS1-1305-18.

Code, Arthur D., Stellar Astronomy From a Space Vehicle. The Astronomical Journal, Vol. 65, No. 5, June 1960 pp. 273-284.

Frainier, R. J., Advances in Cryogenic Engineering, Vol. 6, Plenum Press, New York (1961), p. 20.

Fredrick, Laurence W., editor, Final Report for Applications in Astronomy Suitable for Study by Means of Manned Orbiting Observatories and Related Instrumentation and Operational Requirements, Volume I and II. Supported by NASA Grant NSG-460.

Hufnagel, Robert E., "Random Wavefront Effects," The Practical Application of Modulation Transfer Functions, Perkin-Elmer Electro-Optical Division, Norwalk, Connecticut.

Liller, William, "Concave Gratings for Astronomical Spectrographs and Spectrometers," Applied Optics, Vol. 2, No. 2, February 1963, P. 187-192.

Lundeberg, J. F., P. H. Stern, and R. J. Bristow, "Meteoroid Protection for Spacecraft Structures," Final Report, NASA-Lewis Contract NAS 3-2570.

Pond, C. R., "Photo Reconnaissance 1964 Research Summary - Optical System Analysis" Boeing Document D2-36209-1

"Preliminary Studies and Supporting Data for a Manned Orbiting Telescope Study," Boeing Document D2-84041-1.

Schulte, D. H., "Auxiliary Optical Systems for the Kitt Peak Telescopes," Applied Optics, Vol. 2, No. 2, February 1963, P. 141-151.

Selwyn, E. W. H., Photography in Astronomy, Eastman Kodak Company, Rochester, N. Y. 1950.

Summers, J. L. and A. C. Charters, "High Speed Impact of Metal Projectiles on Targets of Various Materials," presented at Third Symposium on Hypervelocity Impact, 1958.

"Supporting Data for the Attitude, Stability, and Control Study of a Manned Orbiting Telescope" Boeing Document D2-84039-1